

The [1,2]-Stevens Rearrangement of Oxonium Ylides: Synthetic Applications and  
Mechanistic Studies

by

Seyedeh Nargess Hosseini

A thesis submitted in partial fulfillment of the requirements for the degree of

Doctor of Philosophy

Department of Chemistry  
University of Alberta

© Seyedeh Nargess Hosseini, 2016

## Abstract

The Stevens [1,2]-rearrangement of onium ylides has been employed as a valuable synthetic method to construct new C-C bonds. Oxonium ylides are reactive intermediates that undergo facile Stevens rearrangement under mild conditions. In the last several decades, the Stevens rearrangement of oxonium ylides has been extensively employed in synthesis of important core structures, heterocycles and natural products. Despite significant synthetic applications of the Stevens [1,2]-rearrangement, its mechanism has remained ambiguous. Different mechanistic pathways including the presence of either radical or zwitterionic intermediates have been proposed based on the product distribution or CIDNP spectroscopy. However, these mechanistic studies have mostly been performed on ammonium ylides.

In Chapter 1, I will describe the Stevens rearrangement of cyclic oxonium ylides and its application in synthetic chemistry. I will also discuss mechanistic studies that have been performed on the Stevens rearrangement of the onium ylides since its discovery.

It is known that cyclic oxonium ylides can undergo ring contraction via endocyclic [1,2]-shift. In Chapter 2, I demonstrate the ability of the cyclopropylcarbonyl migrating group to generate cyclobutanones through a [1,2]-shift. The generality of the cyclopropylcarbonyl migration will be demonstrated in this chapter. I will also discuss the importance of strained four membered rings in natural products and synthetic chemistry. [1,2]-Migration of the cyclopropylmethyl group provides more strained structures possessing both cyclobutanone and intact cyclopropane moieties.

The presence of the intact cyclopropane in the structure of the cyclobutanones resulting from the Stevens rearrangement, delivers an important message related to the reactive intermediates involved in the reaction mechanism. A fast cyclopropane ring opening is

expected in the case of radical intermediates. In Chapter 3, the nature of the reactive intermediates will be described, employing ultrafast radical clocks as differentiation tools to determine the nature of the actual intermediates present during the Stevens rearrangement.

The last chapter will describe the design and synthesis of broad-spectrum antivirals which inhibit viral entry. Inspired by the antiviral activity of the epigallocatechin gallate (EGCG), an extracted catechin from green tea, against a large group of unrelated viruses, we designed and synthesized a library of molecules possessing polyphenolic moieties which have been known to be the active site in the EGCG viral inhibition. The effect of the central scaffolds as well as the importance of the functional groups and the number of the polyphenolic structures will be discussed.

## Preface

Chapter 3 and parts of Chapter 2 of this thesis will be published as S. N. Hosseini, J. R. Johnston and F. G. West, “Mechanistic Studies of the [1,2]-Stevens Rearrangement of the Cyclic Oxonium Ylides Employing Hypersensitive Radical Clock”, *Manuscript in preparation*. I was responsible for the experimental work, characterization of compounds and preparing the manuscript. J. R. Johnston performed the preliminary studies including the synthesis of compounds **80a**, **80a'**, **73** and **74** (numbering from Chapter 1). F. G. West was the supervisory author and was involved with concept formation and manuscript composition.

Chapter 4 of this thesis will be published as S. N. Hosseini, D. J. Schatz, C. C. Colpitts and F. Mukhtarov, F. G. West and L. M. Schang, “Synthesis and Development of the Small Molecules Acting as Broad Spectrum Antivirals”, *Manuscript in preparation*. I was responsible for the chemistry experimental work including synthesis, data collection and characterization of compounds. A part of the experimental work and data collection was performed by D. J. Schatz during his undergraduate research experience. The virus infectivity assays were done by C. C. Colpitts and F. Mukhtarov in the L. M. Schang group from the department of biochemistry. F. G. West and L. M. Schang were the supervisory authors and were involved with concept formation and manuscript composition.

**Dedication**

*To my husband*

*For his unconditional love and support*

*And to my parents*

*Who believed I could do everything*

*And to my grandmother*

*For the first words she taught me to read & write*

## Acknowledgements

First and foremost, I would like to express my special appreciation and deep gratitude to my supervisor, Dr. Frederick. G. West for all his support and guidance during my PhD journey. He helped me a lot to overcome difficulties and challenges during my research by his priceless advice and comments. I am very grateful for all his help during the last five years and also for his support to get the postdoctoral fellowship.

It was a great opportunity for me to be a member of the West group in which I learnt a lot and had so much fun with the people who loved chemistry and were eager to help. During the last five years, I made very good friends from the present and past group members which is a great achievement in my life.

To Olivier: thanks for listening to me when I was tired, stressed out and frustrated and also for discussing chemistry. Without your help, working in the lab was incredibly hard.

To Yong: I have missed those days we were drinking coffee when we were tired of lab work. Thanks for all your advice on how to write my thesis and of course, for buying me coffee!!

I would like to thank Dr. Hayley Wan for encouraging me to teach. Working with her provided me with valuable experience on teaching and lots of fun during the last five years.

I also like to express my appreciation to all of the NMR, IR, mass spec, X-ray service labs and support staff. It was not possible to finish my PhD without their help and support.

I would love to thank my family. My mother, who was my hero. She always expected me to be kind and helpful to other people and was always encouraging me to become a better person with learning and teaching. My father, who was always believing me and provided the best condition for me to grow up and achieve my goals.

To my husband, Amirhossein: You know how hard it is to find proper words to thank you. Without your love and support, I could not pass any steps of the way. You've been always there listening to me and giving me confidence whenever I needed. You put up with me when I was disappointed, angry and tired. On those days, nothing could be better than you and your warm embrace. I Love you!

## Table of Contents

Chapter 1 The Stevens [1,2]-Rearrangement of the Cyclic Oxonium Ylides .....	1
1.1 The Chemistry of Onium Ylides .....	1
1.2 Cyclic Oxonium Ylides.....	5
1.2.1 The Stevens [1,2]-Rearrangement.....	6
1.2.1.1 Discovery of the Stevens [1,2]-Rearrangement .....	6
1.2.1.2 Mechanism of the Stevens [1,2]-Rearrangement.....	7
1.2.1.3 Synthetic Applications of the Stevens [1,2]-Shift in Cyclic Oxonium Ylides.....	13
1.2.1.4 Important Factors in the [1,2]-Stevens Rearrangement of the Cyclic Oxonium Ylides .....	21
1.2.1.5 The Application of the Stevens Rearrangement in Total Synthesis.....	27
1.2.2 [2,3]-Sigmatropic Rearrangement of Cyclic Oxonium Ylides .....	29
1.2.3 The [1,4]-Rearrangement of Cyclic Oxonium Ylides.....	35
1.3 Conclusion .....	38
Chapter 2 Construction of Substituted Cyclobutanones via [1,2]-Stevens Rearrangement of Oxonium Ylides.....	40
2.1 Introduction .....	40
2.1.1 Ring Strain .....	40
2.1.2 The Chemistry of Cyclopropanes .....	42
2.1.3 The Chemistry of Cyclobutanes.....	43
2.1.4 Synthesis of Cyclobutanones .....	48
2.1.4.1 [2+2]-Cycloaddition of Ketenes and Alkenes.....	48
2.1.4.2 Cyclopropyl Ring Expansion to Cyclobutanones .....	49
2.1.4.3 Transition Metal Catalyzed Synthesis of Cyclobutanones .....	52
2.2 Results and Discussions.....	53
2.2.1 Background .....	53
2.2.2 Substrate Synthesis .....	56
2.2.3 Formation of the Cyclobutanone Derivatives .....	59
2.2.4 Mechanistic Proposal .....	63
2.3 Conclusion .....	65
2.4 Future Directions.....	66

2.5 Experimental .....	67
2.5.1 General Information .....	67
2.5.2 General Procedure for Construction of Diazo Ketones <b>76a-e</b> : .....	67
2.5.3 General procedure for Decomposition of Diazo Ketone <b>72a-e</b> with Cu catalysts:...	77
2.5.4 General procedure for Decomposition of Diazo ketone <b>76a</b> with Rh <sub>2</sub> (OAc) <sub>4</sub> :.....	77
Chapter 3 Mechanistic Studies of the Stevens [1,2]-Rearrangement of the Cyclic Oxonium Ylides Employing Hypersensitive Radical Clock .....	83
3.1 Introduction: Free Radicals .....	83
3.2 Radical Clocks .....	84
3.2.1 Cyclopropylcarbinyl Radical Clock .....	85
3.2.2 Ultrafast Cyclopropylmethyl Radical Probes .....	86
3.2.3 Application of Cyclopropylmethyl Radicals in Mechanistic Studies .....	87
3.2.4 Hypersensitive Radical Probes to Distinguish between Radical and Carbocation Intermediates .....	90
3.3 Background .....	91
3.3.1 The Migratory Aptitude of Cyclopropylmethyl Moiety in Exocyclic [1,2]-Shift ....	92
3.3.2 Employing 2-Methoxy-3-phenyl-cyclopropylcarbinyl .....	97
3.3.3 Characterization of Products .....	99
3.3.4 Proposed Mechanism .....	101
3.4 Conclusion .....	103
3.5 Future Directions.....	103
3.6 Experimental .....	105
3.6.1 General Information .....	105
3.6.2 Procedures and Characterizations .....	105
3.6.3 General Procedure for the Synthesis of Esters <b>45</b> and <b>46</b> .....	106
3.6.4 General Procedure for the Synthesis of Carboxylic Acids <b>47</b> .....	107
3.6.5 Procedure for the Synthesis of Diazo Ketone <b>37a</b> and <b>37b</b> .....	108
3.6.6 General Procedure for the Reaction of Diazo Ketones <b>37a</b> and <b>37b</b> with Cu(hfacac) <sub>2</sub> : .....	110
3.6.7 Procedure for the Formation of Alcohols <b>59a</b> and <b>59b</b> .....	112
3.6.8 Procedure for the Formation of Esters <b>60a</b> and <b>60b</b> .....	113
3.6.9 Procedure for the Formation of Carboxylic Acids <b>61a</b> and <b>61b</b> .....	115
3.6.10 Procedure for the Formation of Diazo Ketones <b>62a</b> and <b>62b</b> .....	116



3.6.11 Procedure for the Treatment of Diazo Ketone <b>62a</b> with Cu(hfacac) <sub>2</sub> .....	117
Chapter 4 Design and Synthesis of Broad-Spectrum Antivirals .....	119
4.1 Introduction: Virus Structure and Infectivity.....	119
4.2 Viral Attachment.....	121
4.3 Broad-Spectrum Antivirals .....	123
4.4 Results and Discussions.....	126
4.4.1 Background.....	126
4.4.2 Synthesis of Polyphenolic Derivatives Possessing Ester Linkers.....	130
4.4.3 Antiviral Activities of the Synthesized Polyphenolic Compounds.....	139
4.4.3.1 Digallates with Flexible Linkers .....	139
4.4.3.2 Digallates with Rigid or Less Flexible Linkers .....	140
4.4.3.3 The Effect of the Number of Gallate Moieties .....	142
4.5 Polyphenolic Compounds Possessing Other Functional Groups.....	143
4.5.1 Polyphenolic Molecules Possessing Amide Linkers .....	143
4.5.2 Polyphenolic Molecules Possessing Ketone Linkers.....	146
4.5.3 Studying the Impact of the Functional Group.....	150
4.5.4 Construction of Ether Functional Group.....	151
4.5.5 Antiviral Activities of Compounds <b>32</b> and <b>47</b> .....	152
4.6 Conclusion .....	152
4.7 Future Directions.....	155
4.8 Experimental .....	156
4.8.1 General Information.....	156
4.8.2 Procedure for the Construction of the esters <b>19a-b</b> .....	157
4.8.3 General Procedure for Construction of Compounds <b>22a-m</b> Possessing Ester Linkers: .....	158
4.8.4 General Procedure for Construction of Compounds <b>25a-c</b> possessing Amide Linkers: .....	165
4.8.5 General Procedure for Deprotection of Benzyl Group .....	167
4.8.6 General Procedure for Deprotection of MOM Group.....	173
4.8.7 Procedure for the Formation of Ketone <b>32</b> .....	175
4.8.8 Procedure for the Formation of Compound <b>47</b> .....	179
References.....	181

Appendix I: Selected NMR Spectra (Chapter 2) .....	194
Appendix II: Selected NMR Spectra (Chapter 3) .....	223
Appendix III: Selected NMR Spectra (Chapter 4) .....	256
Appendix IV: X-ray Crystallographic Data for Compounds <b>61b</b> (Chapter 3) .....	283

## List of Tables

Table 2-1: Optimization of Cyclobutanones Formation .....	61
Table 2-2: Substrate Scope .....	62
Table 3-1: Copper Catalyzed Decomposition of Diazo Ketone <b>37a</b> .....	95
Table 4-1: Formation of Protected Gallate Derivatives Possessing Ester Linkers .....	133
Table 4-2: Deprotection of Benzyl Group .....	136
Table 4-3: Deprotection of MOM Group .....	138
Table 4-4: Formation of Polyphenolic Compounds Possessing Amide Linker .....	144
Table 4-5: Deprotection of Benzyl Group in Compounds <b>25a-c</b> .....	145
Table 4-6: EC <sub>50</sub> against HSV-1, IAV and HCV .....	154

## List of Figures

Figure 1-1: Common Onium Ylides .....	1
Figure 1-2: Proposed Mechanism for the Formation of Cyclic Oxonium Ylides .....	6
Figure 1-3: The Structure of Gambierol .....	32
Figure 2-1: The Strain Energy of Cycloalkanes .....	40
Figure 2-2: Eclipsed C-H Bonds in Cyclopropane Resulting Torsional Strain.....	41
Figure 2-3: Torsional Strain in Cyclobutanes.....	41
Figure 2-4: The Strain Energy of the Bicycloalkanes .....	42
Figure 2-5: The First Synthesis of a Cyclopropane by Perkin.....	42
Figure 2-6: Walsh Cyclopropane Molecular Orbitals .....	43
Figure 2-7: Stabilization of Cyclopropylmethyl Cation by Hyperconjugation .....	43
Figure 2-8: Complex Natural Compounds Containing Cyclobutanes and Cyclobutanones .	44
Figure 2-9: Orbital Symmetry For the [2+2]-Cycloadditions .....	49
Figure 2-10: TROESY Correlations of Cyclobutanones <b>80d</b> and <b>80d'</b> .....	63
Figure 3-1: Rapid Radical Inversion Bearing both Pyramidal and Planar Geometry .....	83
Figure 3-2: Stability of Free Radical .....	84
Figure 3-3: Captodative Long-Lived Free Radicals .....	84
Figure 3-4: Examples of Radical Clocks Proposed by Ingold.....	85
Figure 3-5: Cyclopropylcarbinyl Radical .....	85
Figure 3-6: The Rate of the Ring Opening of the Phenyl Substituted Cyclopropylcarbinyl Radicals.....	86
Figure 3-7: Increasing Ring Opening Rate of the Strained Radicals.....	86
Figure 3-8: Ultrafast Radical Probes .....	87
Figure 3-9: ( <i>trans, trans</i> )-2-Methoxy-3-phenylcyclopropyl)methyl, a Mechanistic Differentiation Tool.....	91
Figure 3-10: ORTEP Structure for Carboxylic Acid <b>61b</b> .....	98
Figure 3-11: Characteristic Chemical Shift in <sup>13</sup> C NMR.....	99
Figure 3-12: HMBC Correlations .....	100
Figure 3-13: nOe Correlations .....	100
Figure 3-14: The Not Observed Hypothetical Tetrahydrooxepines <b>70</b> and <b>71</b> .....	103
Figure 4-1: The Most Common Types of Virion Capsids.....	120

Figure 4-2: The Steps of the Viral Infection.....	120
Figure 4-3: The Primary and Secondary Attachments .....	121
Figure 4-4: Chemical Structure of Heparan Sulfate .....	122
Figure 4-5: The Chemical Structure of Sialic Acid (SA) .....	122
Figure 4-6: Natural Compounds Possessing Broad-Spectrum Antiviral Properties.....	124
Figure 4-7: Broad-Spectrum Antivirals Capable of Blocking the Viral Replication .....	125
Figure 4-8: Broad-Spectrum Antiviral Capable of Blocking the Viral Budding.....	125
Figure 4-9: Green Tea Catechins .....	127
Figure 4-10: Polyphenolic Compounds Possessing Gallate Moiety.....	128
Figure 4-11: Studied Alkyl Gallates .....	128
Figure 4-12: Antiviral Activities of Alkyl Gallates. EGCG. (Dose response curves). Cell monolayers were infected with (a) HCV, (b) HSV-1 or (c) IAV pre-exposed to EGCG or alkyl gallates <b>17a-d</b> for 10 min at 37 °C. Infectivity was evaluated by plaquing or focus forming efficiency and is expressed as percentage relative to DMSO-treated control (n=2). .....	129
Figure 4-13: General Structure of the Target Polyphenolic Compounds .....	130
Figure 4-14: Antiviral Activities of Digallate Possessing Flexible Linkers Against IAV, HSV-1 and HCV. (Dose response curves). Cell monolayers were infected with (a) IAV, (b) HSV-1 or (c) HCV pre-exposed to EGCG or digallates <b>23a-d</b> for 10 min at 37 °C. Infectivity was evaluated by plaquing or focus forming efficiency and is expressed as percentage relative to DMSO-treated control. ....	140
Figure 4-15: Antiviral Activities of Digallates Possessing Rigid/Less Flexible Linkers Against IAV, HSV-1 and HCV. (Dose response curves). Cell monolayers were infected with (a) IAV, (b) HCV, or (c) HSV-1 pre-exposed to EGCG or digallates <b>23e-j'</b> for 10 min at 37 °C. Infectivity was evaluated by plaquing or focus forming efficiency and is expressed as percentage relative to DMSO-treated control.....	141
Figure 4-16: Antiviral Activities of Polygallates Against IAV, HSV-1 and HCV. (Dose response curves). Cell monolayers were infected with (a) IAV, (b) HSV-1 or (c) HCV pre-exposed to EGCG, PGG or polygallates <b>23k-m</b> for 10 min at 37 °C. Infectivity was evaluated by plaquing or focus forming efficiency and is expressed as percentage relative to DMSO-treated control. ....	142

Figure 4-17: Antiviral Activities of Digallates Possessing Amide Linkers gainst IAV, HSV-1 and HCV. (Dose response curves). Cell monolayers were infected with (a) IAV, (b) HSV-1 or (c) HCV pre-exposed to EGCG or compounds <b>26a-c</b> for 10 min at 37 °C. Infectivity was evaluated by plaquing or focus forming efficiency and is expressed as percentage relative to DMSO-treated control. ....	146
Figure 4-18: Target Molecule Possessing <i>trans</i> -1,4-Disubstituted Cyclohexane and Ketone Linkers .....	147
Figure 4-19: Retro-synthesis of Compound <b>33</b> .....	148
Figure 4-20: Antiviral Activities of Compounds <b>32</b> and <b>47</b> vs. OG Against HSV-1 and IAV. (Dose response curves). Cell monolayers were infected with (a) HSV-1 and (b) IAV pre-exposed to EGCG or compounds <b>32</b> and <b>47</b> for 10 min at 37 °C. Infectivity was evaluated by plaquing or focus forming efficiency and is expressed as percentage relative to DMSO-treated control (n=2). ....	152

## List of Schemes

Scheme 1-1: Possible Pathways for the Formation Oxonium Ylides.....	2
Scheme 1-2: The First Reported Method to Ammonium Ylide from Diazo Compounds.....	3
Scheme 1-3: Metal Catalyzed Generation of Oxonium Ylides from Dicarboxyl Compounds	3
Scheme 1-4: Rh(II) Catalyzed Decomposition of Iodonium Ylides .....	4
Scheme 1-5: The Formation of Metalcarbene from 1,2,3-Triazoles .....	4
Scheme 1-6: The Formation of Oxonium Ylides from the Decomposition of Triazoles .....	5
Scheme 1-7: The Formation of Cyclic Oxonium Ylides .....	5
Scheme 1-8: The First Example of the Stevens [1,2]-Rearrangement .....	7
Scheme 1-9: Initial Proposed Mechanism of the Stevens [1,2]-Shift.....	8
Scheme 1-10: Crossover Experiment for the Stevens Rearrangement.....	8
Scheme 1-11: The Retention of Configuration of Chiral Migrating Group in the Stevens Rearrangement.....	9
Scheme 1-12: The Effect of the Solvent Viscosity and Temperature on the Stevens Rearrangement.....	9
Scheme 1-13: The Proposed Mechanism for the Stevens Rearrangement .....	10
Scheme 1-14: Isolation of the Homodimers During the Stevens Rearrangement of Oxonium Ylides.....	11
Scheme 1-15: The Proposed Concerted Mechanism for the Stevens Rearrangement via the Frontal Attack .....	12
Scheme 1-16: Copper Mediated Mechanism of the Stevens Rearrangement.....	12
Scheme 1-17: Rh-mediated Mechanism of the Stevens Rearrangement.....	13
Scheme 1-18: Early Report of the Stevens Rearrangement of the Cyclic Oxonium Ylides ...	14
Scheme 1-19: Generation of Tetrahydrofurans via the Stevens Rearrangement.....	14
Scheme 1-20: Employing Iodonium Ylide to Form Cyclic Oxonium Ylides .....	15
Scheme 1-21: Gold Catalyzed Generation of Cyclic Oxonium Ylide.....	15
Scheme 1-22: The Stevens Rearrangement of the Bicyclic Oxonium Ylide.....	16
Scheme 1-23: The Formation of Cyclooctanones from Bicyclic Oxonium Ylides.....	17
Scheme 1-24: The Formation of Cyclooctanedione Studied by Doyle .....	18
Scheme 1-25: Conformation-Dependent Mechanism for the Formation of <b>116</b> and <b>117</b> .....	19
Scheme 1-26: Formation of Hydrazulene through the Stevens Rearrangement.....	20

Scheme 1-27: Diastereoselective Formation of Cyclootanoloid .....	20
Scheme 1-28: Enantioselective [1,2]-Stevens Rearrangement.....	21
Scheme 1-29: The Stevens Rearrangement of the Oxonium Ylides Possessing Cyclic Acetal .....	22
Scheme 1-30: The Formation of Alkene <b>145</b> .....	22
Scheme 1-31: The Effect of Migrating Group Substituents on the Stevens Rearrangement	23
Scheme 1-32: The effect of the Size of the Cyclic Acetal.....	23
Scheme 1-33: Reactivity of the Cyclic Ketals with Pendant Diazo Ketone Moiety .....	24
Scheme 1-34: Proposed Mechanism to Rationalize Lack of Diastereoselectivity .....	25
Scheme 1-35: Rhodium Catalyzed Decomposition of Diazo Ketone <b>167</b> .....	26
Scheme 1-36: Copper Catalyzed Decomposition of Diazo Ketone <b>167</b> .....	26
Scheme 1-37: The Effect of the Catalyst and Migrating Group on the Stevens Rearrangement.....	27
Scheme 1-38: The Synthesis of the Core Structure of Zaragozaic Acid.....	28
Scheme 1-39: The Synthesis of the Core Structure of Phorbol and Prostratin.....	28
Scheme 1-40: The [2,3]-Rearrangement of Oxonium Ylides.....	29
Scheme 1-41: The [2,3]-Migration of Allyl and Propargylic Groups in Oxonium Ylide .....	30
Scheme 1-42: Copper Catalyzed [2,3]-Rearrangement .....	31
Scheme 1-43: Diastereoselective [2,3]-Rearrangement .....	32
Scheme 1-44: Construction of Polypyran Core Structure via [2,3]-Rearrangement .....	33
Scheme 1-45: Metal- Catalyzed Reactions of <sup>13</sup> C-Labelled Diazo Ketones .....	34
Scheme 1-46: Crossover Studies .....	35
Scheme 1-47: The Total Synthesis of (+)-Griseofulvin .....	36
Scheme 1-48: The [1,4]-Rearrangement of Diazo Ketone <b>197</b> .....	36
Scheme 1-49: The [1,4]-rearrangement of Benzyl Ethers .....	37
Scheme 1-50: The Possible Mechanisms for [1,4]-Benzyl Migration .....	37
Scheme 1-51: Aromatic Substituent Effect on the [1,4]-Shift.....	38
Scheme 2-1: Retro Aldol Reaction to 1,5-diketones .....	45
Scheme 2-2: The Key Step in the Total Synthesis of the Taxol Analogue .....	45
Scheme 2-3: Grob Fragmentation of the Siloxycyclobutane.....	46
Scheme 2-4: Baeyer-Villiger Oxidation of the Cyclobutanones .....	46



Scheme 2-5: Oxy-Cope Ring Expansion of Vinyl Cyclobutanone .....	47
Scheme 2-6: Ring Expansion of Cyclobutanones to Cyclopentanones .....	47
Scheme 2-7: Ring Contraction of Cyclobutanones .....	48
Scheme 2-8: Construction of Cyclobutanone Employing [1,3]-Dithiane .....	48
Scheme 2-9: Intramolecular [2+2]-Cycloaddition.....	49
Scheme 2-10: Cyclopropane Ring Expansions to Cyclobutanones.....	51
Scheme 2-11: Rhodium (II) Catalyzed Formation of Cyclobutanones .....	52
Scheme 2-12: Synthesis of Cyclobutanones From Homopropargylic Ethers .....	52
Scheme 2-13: Carbonylation of Titanacyclobutanes .....	53
Scheme 2-14: Preliminary Results.....	54
Scheme 2-15: Plausible Pathways for Decomposition of Diazo Ketone <b>76</b> .....	55
Scheme 2-16: Retrosynthesis of the Diazo Ketone <b>76</b> .....	56
Scheme 2-17: Synthesis of Ester <b>82a</b> via Michael Addition .....	57
Scheme 2-18: Synthesis of Secondary Alcohols <b>83</b> .....	58
Scheme 2-19: Attempted Alkylation of Alcohols under Basic Condition .....	58
Scheme 2-20: Synthesis of Required Acid Precursors .....	59
Scheme 2-21: Preparation of Diazo Ketones <b>76</b> .....	59
Scheme 2-22: Proposed Mechanism.....	64
Scheme 2-23: Proposed Mechanism for Decomposition of Diazo Ketone <b>76e</b> .....	65
Scheme 3-1: Proposed Mechanism of HppE Catalyzed Formation of Fosfomycin .....	88
Scheme 3-2: Employing (Methylenecyclopropyl)methyl Radical Probe .....	89
Scheme 3-3: Proposed Pathways for the Enzyme Deactivation .....	89
Scheme 3-4: Reaction of Aldehyde <b>30</b> with Allylmagnesium Reagent .....	90
Scheme 3-5: Cyclopropylcarbinyl Moiety as a Migrating Group in Exocyclic [1,2]-shift ....	92
Scheme 3-6: Synthesis of the Acid Precursor.....	93
Scheme 3-7: Unsuccessful Attempted Pathways.....	93
Scheme 3-8: Generation of Diazo Ketone <b>37a</b> .....	94
Scheme 3-9: Proposed Mechanism for the Formation of Alkenes <b>54</b> and <b>55</b> .....	95
Scheme 3-10: Synthesis of Diazo Ketone <b>37b</b> .....	96
Scheme 3-11: Copper Catalyzed Decomposition of Diazo Ketone <b>37b</b> .....	97
Scheme 3-12: Synthesis of Diazo Ketones <b>62</b> .....	98

Scheme 3-13: Treatment of Diazo Ketones <b>62</b> with Cu(hfacac) <sub>2</sub> .....	99
Scheme 3-14: Proposed Mechanism.....	102
Scheme 4-1: Synthesis of Acids <b>20</b> .....	130
Scheme 4-2: Unsuccessful Esterifications.....	131
Scheme 4-3: Formation of Ketone <b>32</b> .....	147
Scheme 4-4: Preparation of Starting Materials <b>34</b> and <b>40</b> .....	148
Scheme 4-5: Unsuccessful Attempts for Preparation of Diol .....	149
Scheme 4-6: Employing Weinreb Amide.....	150
Scheme 4-7: Formation of Compound <b>47</b> .....	151
Scheme 4-8: Unsuccessful Attempts to Synthesis Ether <b>50</b> .....	151

## List of Symbols and Abbreviations

$^1\text{H-NMR}$	proton nuclear magnetic resonance
$^{13}\text{C-NMR}$	carbon 13 nuclear magnetic resonance
$\alpha$	bond angle
Ac	acetyl
$\text{Ac}_2\text{O}$	acetic anhydride
acac	acetylacetonate
Ar	aryl
app	apparent (spectral)
aq	aqueous solution
Bn	benzyl
br	broad (spectral)
BS	broad-spectrum
Bu	butyl
$^{\circ}\text{C}$	degrees Celsius
calcd	calculated
CAN	cerium ammonium nitrate
cat	catalytic
CIDNP	Chemically Induced Dynamic Nuclear Polarization
$\text{cm}^{-1}$	wave numbers
COSY	homonuclear correlation spectroscopy
conc.	concentrated
CoV	coronavirus
$\delta$	chemical shift in parts per million downfield from tetramethylsilane
d	doublet (spectral)
dd	doublet-of-doublets
DAA	directly acting antivirals
DBU	1,8-diazabicyclo[5.4.0.]undec-7-ene
DCC	N,N'-dicyclohexylcarbodiimide
DCE	1,2-dichloroethane
DCM	dichloromethane

DMAP	4-dimethylaminopyridine
DMF	N,N-dimethylformamide
DMSO	dimethyl sulfoxide
DNA	deoxyribonucleic acid
dq	doublet of quartets (spectral)
dr	diastereomeric ratio
dt	doublet of triplets (spectral)
EDCI	1-ethyl-3-(3-dimethylaminopropyl)carbodiimide
EC	epicatechin
EC <sub>50</sub>	half maximal effective concentration
ECG	epicatechin gallate
EDG	electron-donating group
ee	enantiomeric excess
EGC	epigallocatechin
EGCG	epigallocatechin gallate
EBV	ebola virus
EI	electron impact (mass spectrometry)
ESI	electrospray ionization (mass spectrometry)
Et	ethyl
EtOAc	ethyl acetate
eq.	equation
equiv.	equivalents
EWG	electron-withdrawing group
g	gram(s)
GAG	glycosaminoglycans
h	hour(s)
hfacac	hexafluoroacetylacetonate
HAA	host-coating antivirals
HBV	hepatitis B virus
HCV	hepatitis C virus
HIV	human immunodeficiency virus

HMBC	heteronuclear multiple bond coherence
HMQC	heteronuclear multiple quantum coherence
HOMO	highest occupied molecular orbital
( <i>S</i> )-HPP	hydroxypropylphosphonic acid
HppE	hydroxypropylphosphonic acid epoxidase
HRMS	high resolution mass spectrum
HSQC	heteronuclear single quantum coherence (spectral)
HSV-1	herpes simplex virus 1
HSV-2	herpes simplex virus 2
hν	electromagnetic irradiation
Hz	hertz
HWE	Horner-Wadsworth-Emmons reaction
IAV	influenza A
IBV	influenza B
ICV	influenza C
IR	infrared spectroscopy
ISAV	isavirus
<i>J</i>	coupling constant (in NMR)
kcal	kilocalorie
<i>k<sub>r</sub></i>	rate constant
L	litre(s)
LAH	lithium aluminum hydride
LDA	lithium diisopropylamide
<i>L<sub>n</sub></i>	ligand
LUMO	lowest unoccupied molecular orbital
M	moles per litre
m	multiplet (spectral)
mg	milligram(s)
μ	micro
M	metal atom
M <sup>+</sup>	parent molecular ion

mCPBA	meta-chloroperoxybenzoic acid
Me	methyl
MHz	megahertz
min	minute(s)
ML <sub>n</sub>	unspecified metal-ligand complex
mmol	millimole(s)
mol	mole(s)
m.p.	melting point
MS	mass spectrometry
MOM	methoxymethyl
4S-MPPIM	methyl 1-(3-phenylpropanoyl)-2-oxaimidazolidine-4(S)-carboxylate
NMR	nuclear magnetic resonance
nOe	nuclear Overhauser enhancement
Nu	nucleophile
OAc	acetate
OEt	ethoxy
OMe	methoxy
OMOM	methoxymethyl ether
ORTEP	Oak Ridge Thermal-Ellipsoid Plot
OTf	triflate
PG	protecting group
Ph	phenyl
PIV	parainfluenza virus
pfb	tetrakis(perfluorobutyrate)
ppm	parts per million (spectral)
<i>n</i> -Pr	propyl
<i>i</i> -Pr	isopropyl
PVP	polyvinylpyrrolidone
q	quartet (spectral)
quant.	quantitative yield
R	generalized alkyl group of substituent

SARA-CoV	respiratory syndrome coronavirus
$R_f$	retention factor (chromatography)
RNA	ribonucleic acid
rt	room temperature
s	singlet (spectral); second (s)
SA	sialic acid
sept	septet (spectral)
SET	single electron transfer
SG	sialoglycans
SM	starting material
t	triplet (spectral)
temp	temperature
TFA	trifluoroacetic acid
tfacac	trifluoroacetylacetonate
THF	tetrahydrofuran
TLC	thin layer chromatography
Tol	toluene
TMS	trimethylsilyl
TMV	tobacco mosaic virus
TROESY	Transverse Rotating-frame Overhauser Enhancement Spectroscopy
Ts	<i>p</i> -toluenesulfonyl
wt.	weight
X	generalized heteroatom

## Chapter 1 The Stevens [1,2]-Rearrangement of the Cyclic Oxonium Ylides

### 1.1 The Chemistry of Onium Ylides

An *ylide* is a dipolar chemical substance containing a negatively charged carbon atom directly attached to a heteroatom with a positive charge. The most common ylides are oxonium (**1a**, **1a'**), sulfonium (**2**), ammonium (**3**), phosphonium (**4**) and iodonium (**5**) ylides (Figure 1-1) Among the reported ylide species, some ammonium, phosphonium and most sulfonium ylides are isolable and can be detected during the reaction mechanism, whereas most of the oxonium ylides are very versatile and reactive intermediates and cannot be isolated;<sup>1,2</sup> although isomünchnones (**1a'**) are known to be stable and isolable carbonyl ylides.<sup>3</sup> Isolation of the iodonium ylides has been reported to be difficult due to their fast decomposition even at low temperatures;<sup>4</sup> however, recently a few isolable iodonium ylides have been synthesized and characterized.<sup>5</sup>

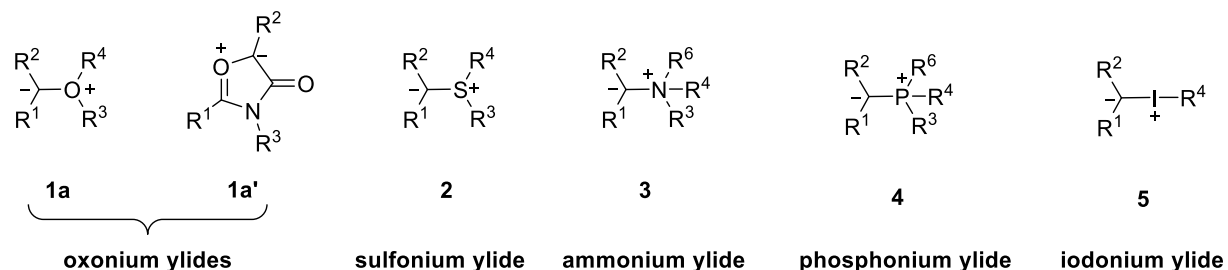
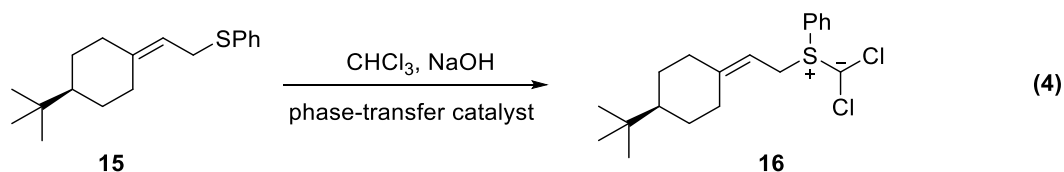
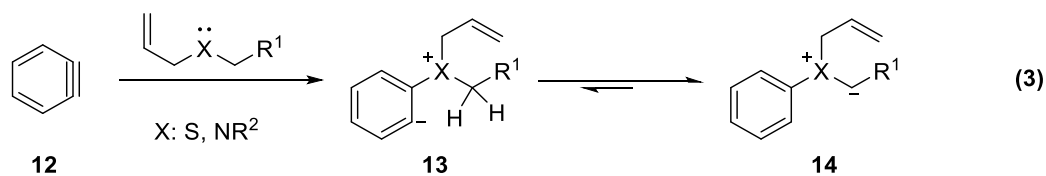
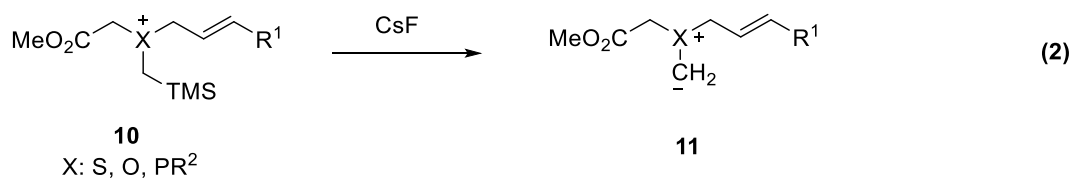
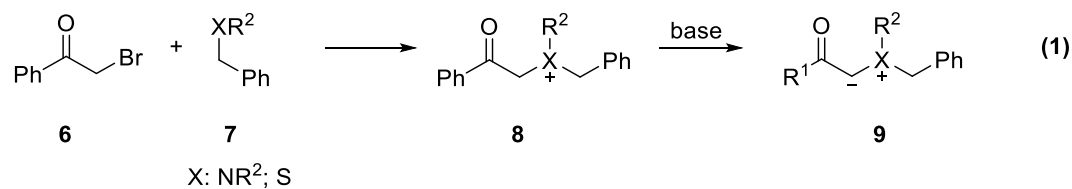


Figure 1-1: Common Onium Ylides

Various methods have been reported for the formation of onium ylides.<sup>6,7</sup> One of the oldest methods to generate onium ylides is by deprotonation of the corresponding salt (Scheme 1-1, eq. 1). It is known that ammonium and sulfonium ylides **9** can be generated from the corresponding salts **8** which are obtained from the reaction of phenacyl bromide **6** and a tertiary amine or dialkylsulfide **7**.<sup>8,9</sup> In 1979, Vedejs reported the desilylation of the salt **10** as an alternative to obtain oxonium, sulfonium and phosphonium ylides **11** (Scheme 1-1, eq. 2).<sup>10</sup> Ollis and coworkers reported the application of benzyne **12** for generation of the sulfonium and ammonium ylides **14**. 1,3-Dipole **13** is formed first from benzyne **12** followed by the deprotonation of the more acidic ylide proton to afford the desired onium ylides (Scheme 1-1,

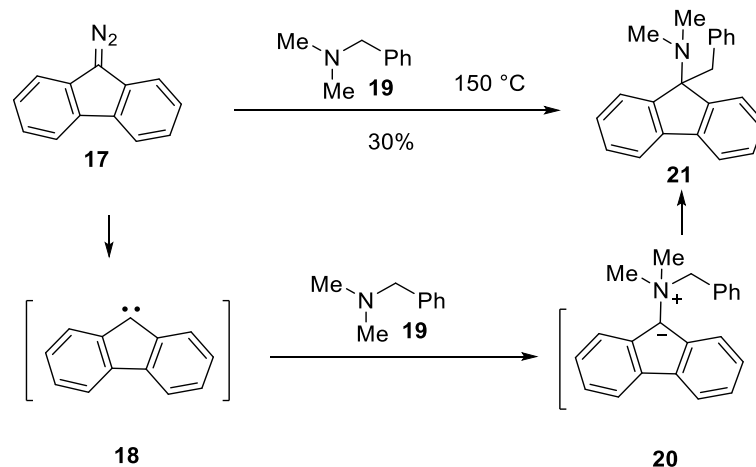


eq. 3).<sup>11</sup> The most common method for the formation of the onium ylide is the reaction of the heteroatom with carbenes. In 1972, Evans reported *in situ* generation of dichlorocarbene from the reaction of chloroform with sodium hydroxide followed by the nucleophilic attack of the sulfur atom in compound **15** to generate sulfonium ylide **16** (Scheme 1-1, eq. 4).<sup>12</sup>



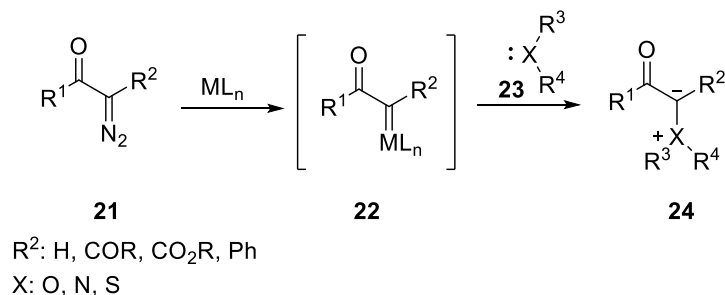
### Scheme 1-1: Possible Pathways for the Formation Onium Ylides

Diazo compounds are an important class of molecules which are used as precursors to carbenes and carbenoids via thermal, photochemical and catalytic decompositions.<sup>13</sup> The first example of ylide formation from a diazo compound was reported by Bamford and Stevens in 1952.<sup>14</sup> Diazo compound **17** generated free carbene **18** after loss of nitrogen, which was trapped by a tertiary amine **19** to form ammonium ylide **20**. The *in situ* generated ylide rearranged further to form a new C-C bond in compound **21** (Scheme 1-2).



### Scheme 1-2: The First Reported Method to Ammonium Ylide from Diazo Compounds

However, during the last decades, catalytic decomposition of diazocarbonyls in the presence of transition metals has been employed to effectively generate onium ylides.<sup>6,13</sup> Generally, a metallocarbene such as **22** is obtained from the transition metal catalyzed decomposition of diazocarbonyl **21**. The metallocarbene can then be trapped by a heteroatom to generate the desired onium ylide **24**. (Scheme 1-3).

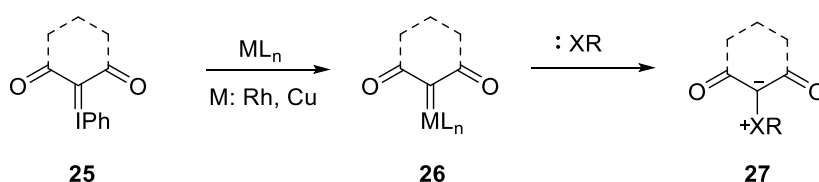


### Scheme 1-3: Metal Catalyzed Generation of Onium Ylides from Diazocarbonyl Compounds

Among the effective catalysts, copper complexes have been extensively employed in the formation of metallocarbenes.<sup>15</sup> The detailed mechanism of copper catalyzed decomposition of diazo compounds including electronic and steric effects were described by W. R. Moser in 1968.<sup>16,17</sup> The most common copper catalysts reported in the literature are: copper powder, copper bronze, Cu (I) complexes such as copper triflate (CuOTf) and copper chloride (CuCl), copper (II) salts and complexes such as copper (II) sulfate, Cu(acac)<sub>2</sub>, Cu(hfacac)<sub>2</sub> or Cu(tfacac)<sub>2</sub>.<sup>6</sup>

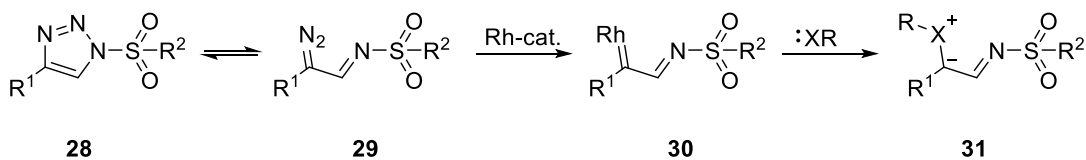
In 1973, Teyssié and coworkers, introduced dirhodium (II) tetraacetate  $\text{Rh}_2(\text{OAc})_4$  as an effective catalyst for the decomposition of diazo compounds<sup>18</sup> and later on, Doyle and coworkers reported the application of  $\text{Rh}_2(\text{OAc})_4$  in onium ylide generation.<sup>19</sup>

Other metalcarbene-mediated reactions have also been investigated as a convenient route to the formation of onium ylides. Over the last decade, phenyliodonium ylides have attracted organic chemists' attention.<sup>4</sup> Transition metal catalyzed decomposition of iodonium ylide **25** provides the required metalcarbene **26** that can be trapped by a heteroatom to generate the desired onium ylide **27** (Scheme 1-4).



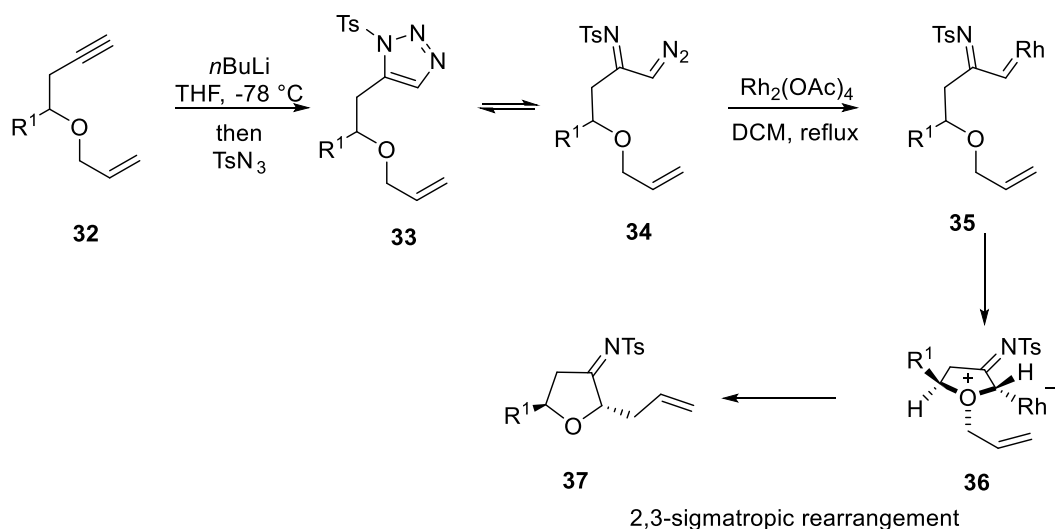
**Scheme 1-4: Rh(II) Catalyzed Decomposition of Iodonium Ylides**

*N*-Sulfonyl-1,2,3-triazoles have recently been employed as powerful precursors to generate metalcarbenes.<sup>20</sup> Gevorgyan and Fokin performed a significant study in the field of rhodium catalyzed formation of imino carbenes from *N*-sulfonyl-1,2,3-triazoles.<sup>21</sup> They reported that *N*-sulfonyl-1,2,3-triazoles **28**, which are under Dimroth type<sup>22</sup> equilibrium with the ring opened isomer **29**, formed metalcarbenes **30**. The Rh carbenoid can then be trapped by a heteroatom to generate the corresponding onium ylide **31** (Scheme 1-5).



**Scheme 1-5: The Formation of Metalcarbene from 1,2,3-Triazoles**

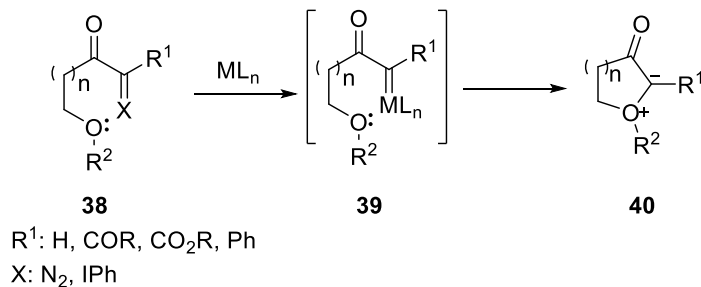
Recently, Boyer showed that  $\text{Rh}_2(\text{OAc})_4$  catalyzed decomposition of *N*-sulfonyl-1,2,3-triazoles **33** can generate allylic oxonium ylide **36** which undergoes a sigmatropic rearrangement to afford tetrahydrofuran **37**.<sup>23</sup> Alkyne **32** was used as a precursor to form the required triazole in the presence of  $\text{TsN}_3$  and *n*BuLi (Scheme 1-6).



**Scheme 1-6: The Formation of Oxonium Ylides from the Decomposition of Triazoles**

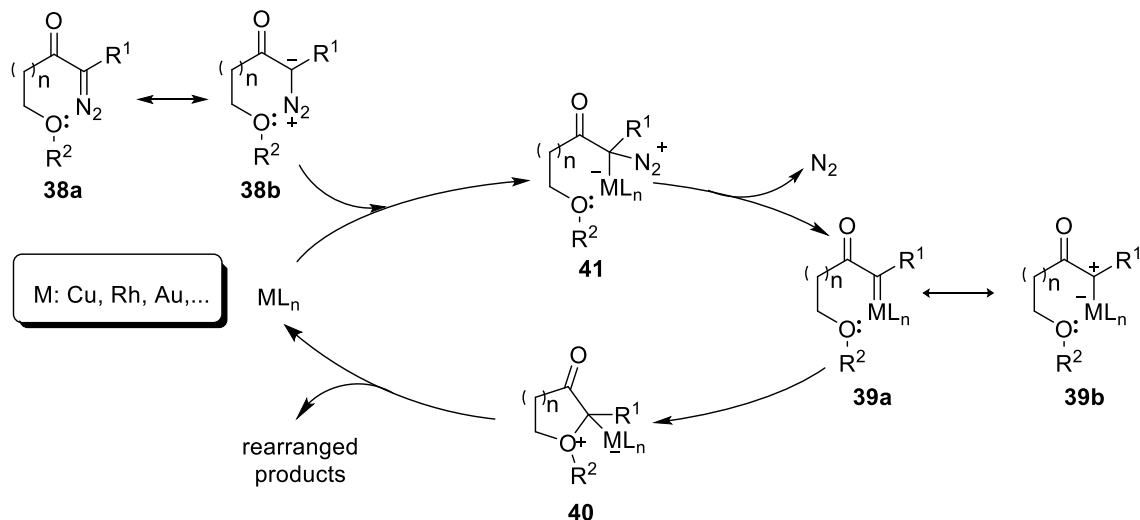
## 1.2 Cyclic Oxonium Ylides

Cyclic oxonium ylides can be generated via an intramolecular nucleophilic attack of the ethereal oxygen to the carbon center of the metallocarbene (Scheme 1-7).



**Scheme 1-7: The Formation of Cyclic Oxonium Ylides**

It has been proposed that electrophilic addition of diazocarbonyl resonance form **38b** to the Lewis acidic transition metal complex ( $ML_n$ ) generates metallocarbene **39** with the loss of the nitrogen. The positively charged carbon in metallocarbene **39** can be trapped by the intramolecular nucleophilic attack of the ethereal oxygen to generate the cyclic oxonium ylide **40** and release the catalyst (Figure 1-2).<sup>6</sup>



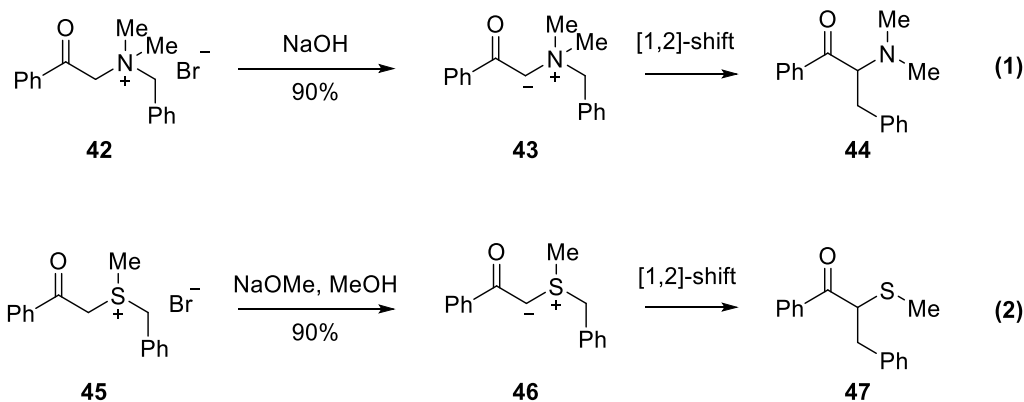
**Figure 1-2: Proposed Mechanism for the Formation of Cyclic Oxonium Ylides**

Reactive cyclic oxonium ylides undergo various reactions after generation,<sup>7,24,25</sup> for example fragmentation,<sup>26–28</sup> nucleophilic trapping<sup>29,30</sup> and sigmatropic rearrangements.<sup>24</sup> Among the reported pathways, [1,2], [2,3] and [1,4]-rearrangements of cyclic oxonium ylides and their synthetic application have been extensively studied.<sup>6,7,24,31,32</sup> In this chapter we will focus on the sigmatropic rearrangements, and in particular, the synthetic applications and mechanism of the Stevens [1,2]-rearrangement will be discussed in detail.

## 1.2.1 The Stevens [1,2]-Rearrangement

### 1.2.1.1 Discovery of the Stevens [1,2]-Rearrangement

The [1,2]-Stevens rearrangement is a valuable carbon-carbon bond forming process that was discovered by Thomas Stevens and coworkers, in 1928.<sup>9</sup> They revealed that the ammonium salt **42** could be deprotonated to generate an ammonium ylide **43** which underwent [1,2]-migration of the benzyl group to form the tertiary amine **44** under basic conditions (Scheme 1-8, eq. 1). They also discovered that the similar sulfonium ylide **46** can rearrange under basic conditions from the corresponding salt **45** (Scheme 1-8, eq. 2).<sup>33</sup>

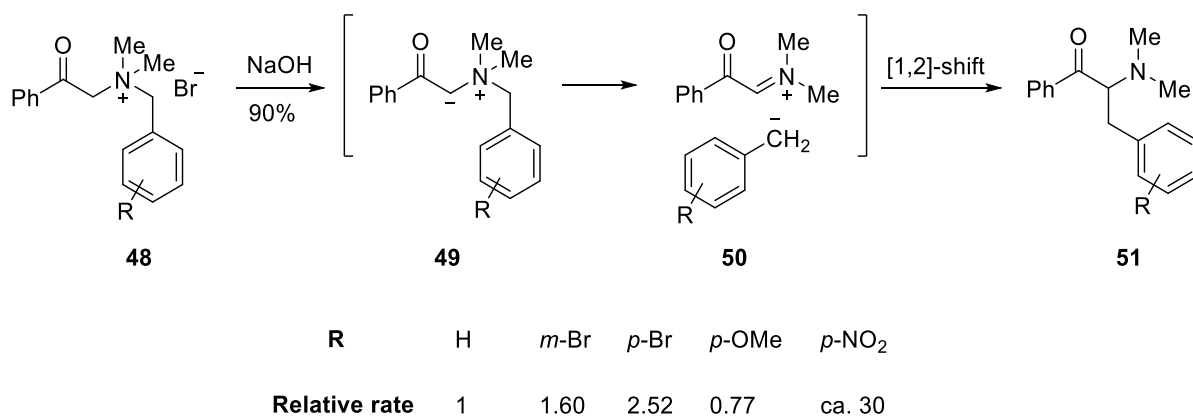


**Scheme 1-8: The First Example of the Stevens [1,2]-Rearrangement**

### 1.2.1.2 Mechanism of the Stevens [1,2]-Rearrangement

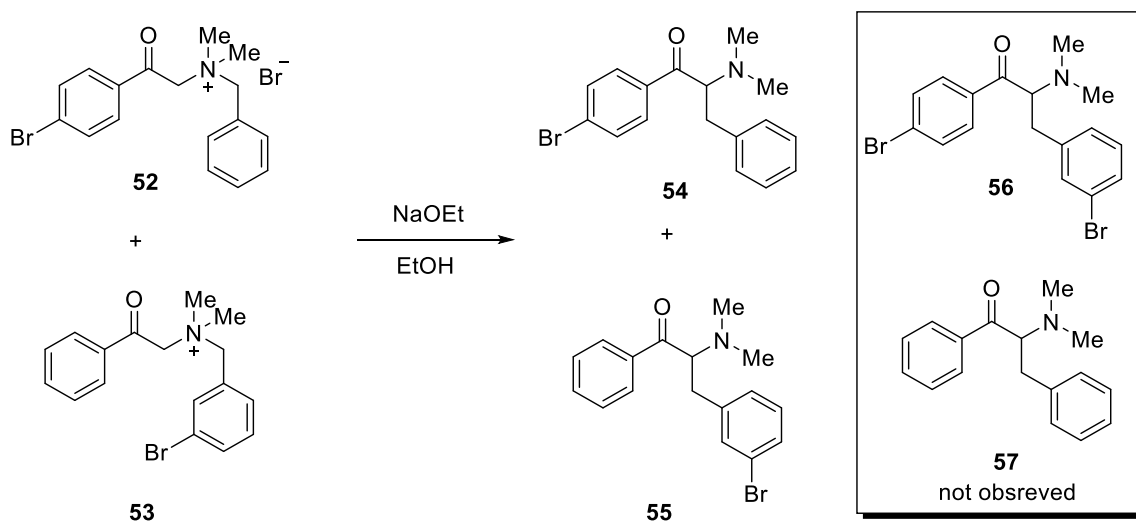
Although the Stevens rearrangement and its synthetic applications have been widely studied over the decades, its mechanism has remained controversial. In general, three possible pathways have been proposed for the [1,2]-shift: 1) the formation of radical pair intermediates, 2) the formation of zwitterionic intermediates and 3) concerted [1,2]-migration.<sup>25</sup> Also, the [1,2]-rearrangement of the cyclic oxonium ylides have been proposed to be through metal assisted pathways.<sup>24</sup> Oxonium ylides cannot usually be isolated due to their high reactivity. As a result, the mechanism of the [1,2]-shift is proposed based on the product distribution.

**Preliminary studies:** After the discovery of the [1,2]-migration of the benzyl group in ammonium ylide **43**, further mechanistic studies by Stevens determined the effect of the phenyl ring substitution on the rate of the Stevens rearrangement. It was shown that electron-withdrawing substituents increase the relative rate of the benzyl group migration. These observation led Stevens to propose a stepwise mechanism involving the formation of the benzyl anion **50** during the [1,2]-shift (Scheme 1-9).<sup>8</sup>



### Scheme 1-9: Initial Proposed Mechanism of the Stevens [1,2]-Shift

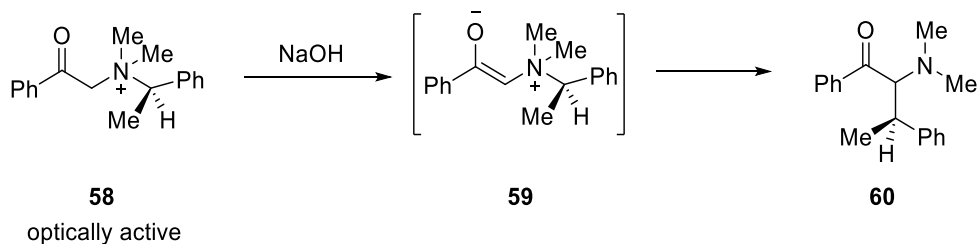
Subsequent studies by Stevens showed the benzyl migration occurs through an intramolecular process. When the mixture of salts **52** and **53** was treated with sodium ethoxide, no crossover products (**56** and **57**) were isolated, suggesting an intramolecular process during the [1,2]-rearrangement (Scheme 1-10).<sup>9</sup>



### Scheme 1-10: Crossover Experiment for the Stevens Rearrangement

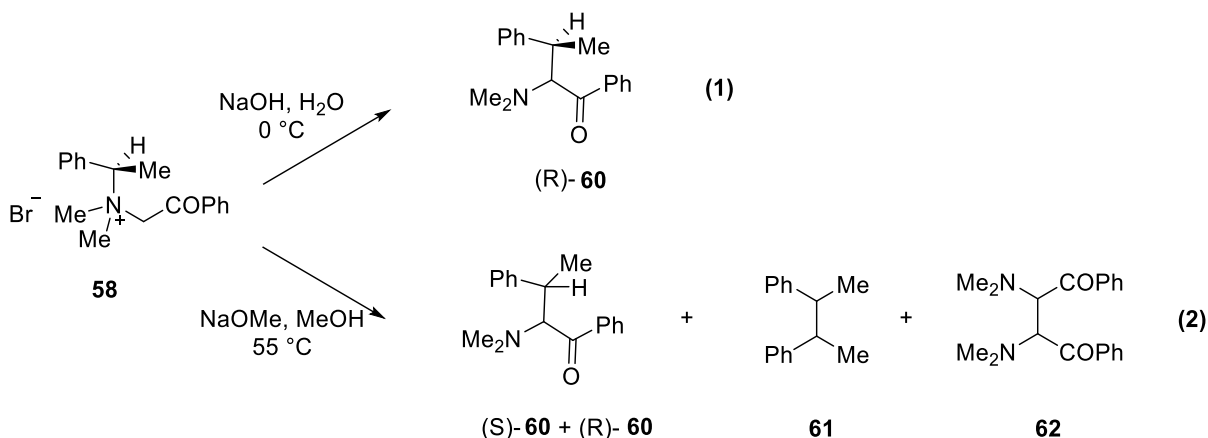
Later on, Kenyon and coworkers revealed that the Stevens rearrangement occurs via the retention of configuration of the migrating group. They treated an enantiomerically enriched ammonium salt **58** under basic conditions and subsequently, isolated the optically active

product **60** resulting from the Stevens rearrangement of the chiral migrating group in intermediate **59** with almost complete retention of configuration (Scheme 1-11).<sup>34</sup>



**Scheme 1-11: The Retention of Configuration of Chiral Migrating Group in the Stevens Rearrangement**

**Mechanism of the Stevens Rearrangement Involving Radical Intermediates:** In 1975, Ollis, *et al.* reported significant results including the effect of the solvent viscosity and reaction temperature on the Stevens rearrangement.<sup>35</sup> They found that ammonium ylide **58** possessing chiral migrating group underwent the Stevens rearrangement to generate amine (R)-**60** with 99% retention of configuration in NaOH-H<sub>2</sub>O at 0 °C (Scheme 1-12, eq. 1) whereas the same substrate rearranged with 56% retention and 44% racemization ((R)-**60** + (S)-**60**) at 55 °C in MeOH-NaOMe (Scheme 1-12, eq. 2) along with the formation of homodimers **61** and **62**.



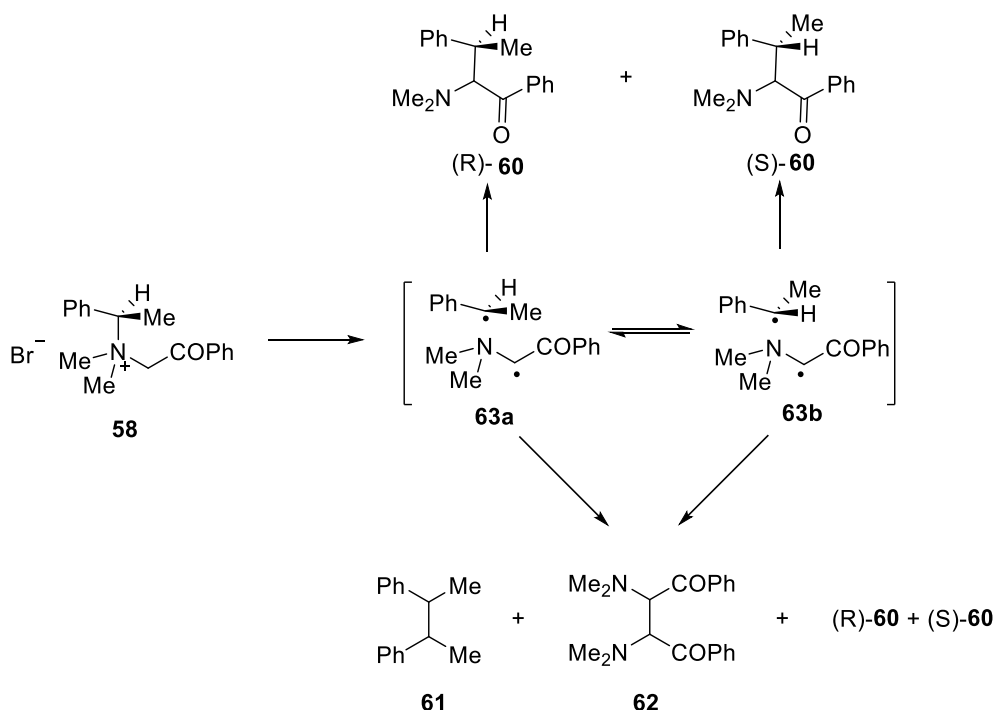
**Scheme 1-12: The Effect of the Solvent Viscosity and Temperature on the Stevens Rearrangement**

They noticed that decreasing the solvent viscosity and increasing the reaction temperature diminished the stereoselectivity and increased the possibility of the intermolecular reactions.



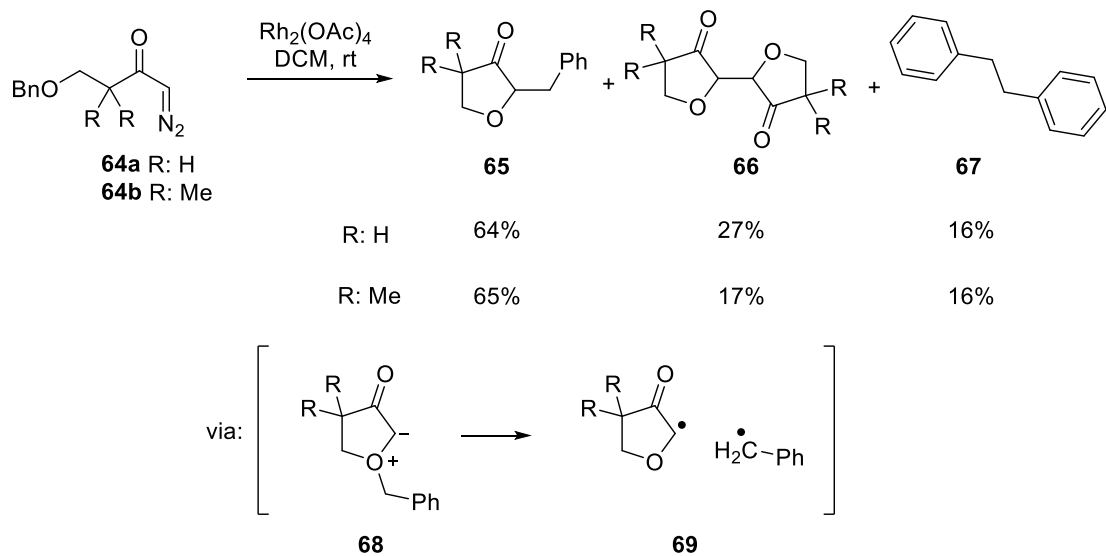
With these results in hand, they deduced the reaction occurred through the formation of radical pairs **63a** and **63b** in a solvent cage facilitating very fast recombination. Having a higher temperature and lower solvent viscosity provided conditions for the radicals to escape from the solvent cage to form homodimers and decrease the stereoselectivity (Scheme 1-13).<sup>35,36</sup>

This mechanistic proposal was in accordance with the previous studies using CIDNP (chemically induced dynamic nuclear polarization) spectroscopy by Iwamura<sup>37,38</sup> and Closs<sup>39</sup> reporting radical pair intermediates in the mechanism of the Stevens rearrangement.



**Scheme 1-13: The Proposed Mechanism for the Stevens Rearrangement**

The formation of homodimers was also observed by West and coworkers during the Stevens rearrangement of the benzyl group in the cyclic oxonium ylide **68**.<sup>40</sup> Along with the formation of the Stevens product, tetrahydrofuran **65**, they reported the formation of the homodimers **66** and **67** in a considerable yield suggesting the presence of radical pairs **69** in the reaction mechanism (Scheme 1-14). The similar homodimer **67** was also isolated during the Stevens rearrangement of cyclic ammonium ylides.<sup>41</sup>



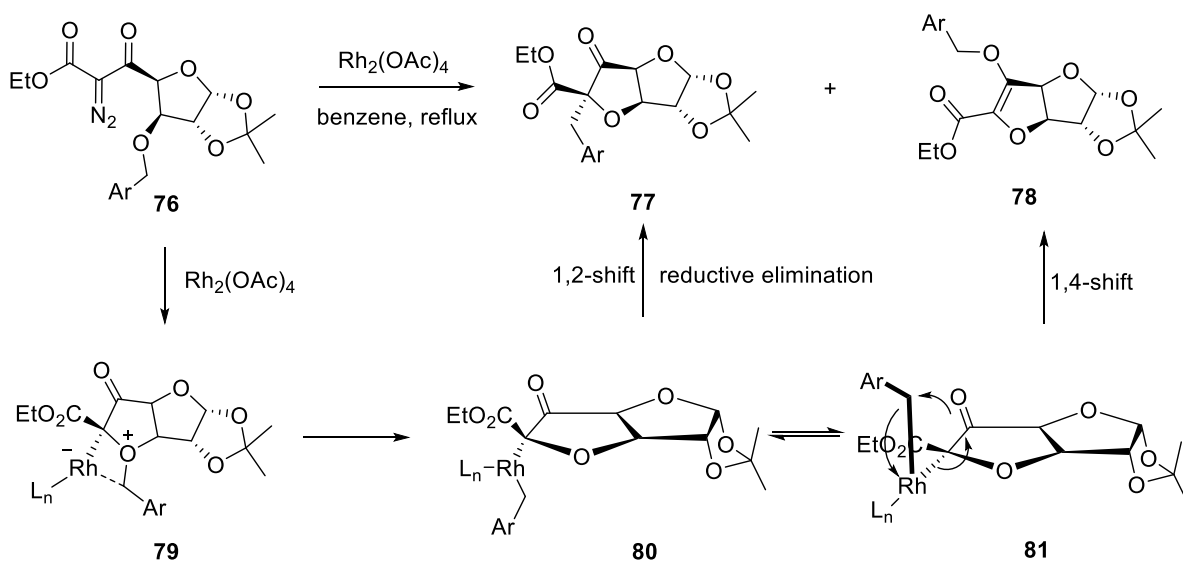
**Scheme 1-14: Isolation of the Homodimers During the Stevens Rearrangement of Oxonium Ylides**

**Mechanism of the Stevens Rearrangement Involving Concerted Pathway:** Hauser and Kantor, in 1951, proposed a concerted mechanism for the [1,2]-Stevens rearrangement.<sup>42</sup> They believed that the mechanism proposed by Stevens involving a benzyl anion (Scheme 1-9) seemed unlikely due to the fast protonation of the benzyl anion in aqueous or alcoholic media. They also rejected the involvement of the benzyl cation in the reaction mechanism proposed by Wittig,<sup>43</sup> since the Stevens rearrangement occurs with retention of configuration whereas the benzyl cation can be inverted to provide a racemic mixture. Having these results in hand they proposed a concerted mechanism in which the carbanion attacks the carbon center of the migrating group at the front or side and not from the back side (Scheme 1-15).

A year later, Brewster and Kline also proposed a nucleophilic displacement via frontal attack at carbon center of the chiral migrating group.<sup>44</sup> They found that the Stevens rearrangement of a chiral migrating group provided an optically active product. They deduced this process might happen intramolecularly and without complete C-C dissociation.



Dhavale and coworkers also proposed a similar mechanism for the [1,2]-migration of the benzyl group in oxonium ylide **79**.<sup>47</sup> They proposed that a four-centered transition state **79** containing Rh metal is responsible for the formation of the C-Rh bond in **80** which underwent a reductive elimination to form **77** (Scheme 1-17).

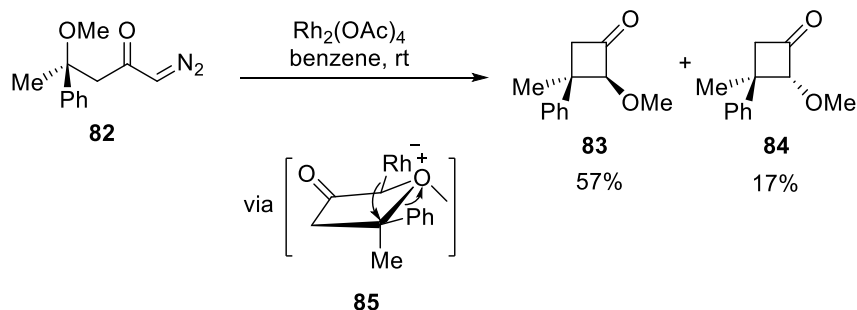


**Scheme 1-17: Rh-mediated Mechanism of the Stevens Rearrangement**

### 1.2.1.3 Synthetic Applications of the Stevens [1,2]-Shift in Cyclic Oxonium Ylides

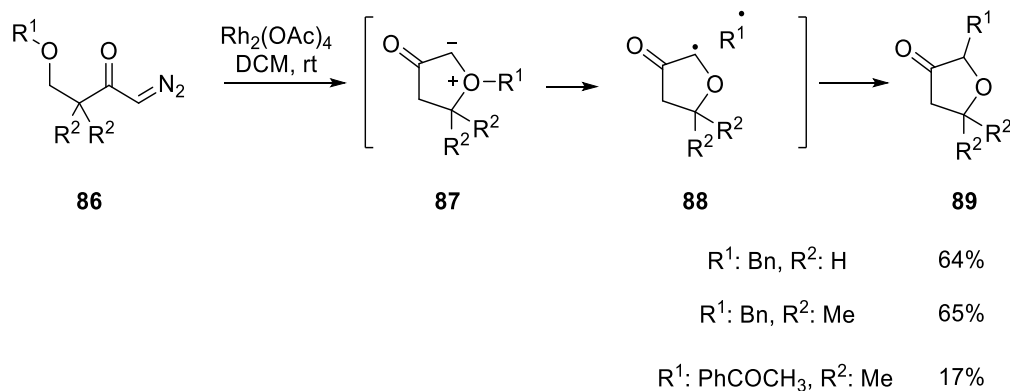
The Stevens rearrangement of cyclic oxonium ylides has been widely used to construct important cyclic and acyclic core structures. The [1,2]-shift has also been employed as a key step in the total synthesis of several natural products.<sup>24,25</sup>

One of the early examples of the Stevens rearrangement of a cyclic oxonium ylide was reported by Johnson and Roskamp in 1986.<sup>48</sup> They showed that diazo ketone **82**, in the presence of the catalytic Rh(II) generated cyclobutanones **83** and **84** via an endocyclic [1,2]-rearrangement (**85**) as the dominant reaction route (Scheme 1-18). The presence of the adjacent radical stabilizing moiety on the migrating carbon, in this case phenyl, was essential to promote the Stevens rearrangement.



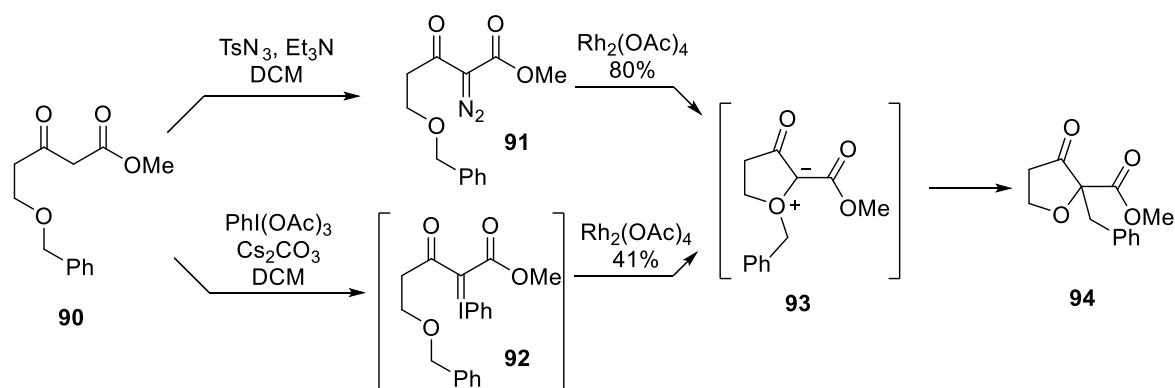
### Scheme 1-18: Early Report of the Stevens Rearrangement of the Cyclic Oxonium Ylides

[1,2]-Stevens rearrangement can also be employed to generate tetrahydrofuranone structures. The formation of tetrahydrofuranones **89** was demonstrated by the West group in 1992.<sup>40</sup> Diazo ketone **86** generated the cyclic oxonium ylide **87** in the presence of the Rh(II) catalyst. The exocyclic Stevens rearrangement occurred in the presence of both benzyl and acyl migrating groups which are able to stabilize the radical center of the migrating group  $\text{R}^1$  (**88**) in moderate yields (Scheme 1-19).



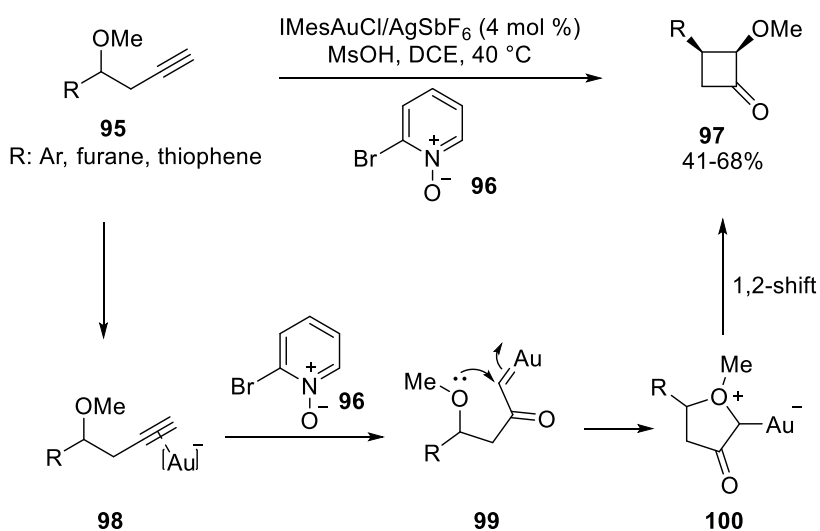
### Scheme 1-19: Generation of Tetrahydrofuranons via the Stevens Rearrangement

As mentioned previously, iodonium ylides are also considered as potential precursors to oxonium ylides. West and Murphy showed that, similar to diazo ketone **91**, iodonium ylide **92** was capable of generating monocyclic oxonium ylide **93**, which underwent [1,2]-rearrangement of the benzyl group to form disubstituted hydrofuranone **94** (Scheme 1-20).<sup>49</sup>



**Scheme 1-20: Employing Iodonium Ylide to Form Cyclic Oxonium Ylides**

The gold catalyzed generation of cyclic oxonium ylides from homopropargylic ethers was reported in 2012 by Li and coworkers as a convenient route to generate cyclobutanone derivatives **97**.<sup>50</sup> They investigated the substrate scope of this reaction in 2013 and found that homopropargylic ethers **95** having electron donating ethereal substituent can generate *cis*-cyclobutanones **97** via the Stevens rearrangement of oxonium ylides **100** in the presence of an 2-bromopyridine N-oxide **96** as an oxidant (Scheme 1-21).<sup>51</sup>

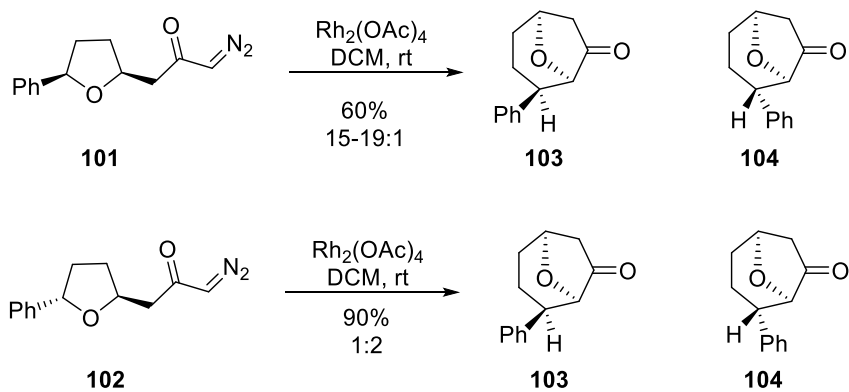


**Scheme 1-21: Gold Catalyzed Generation of Cyclic Oxonium Ylide**

Apart from the monocyclic oxonium ylides, the [1,2]-rearrangements and synthetic applications of the bicyclic oxonium ylide from cyclic ethers have been extensively investigated.

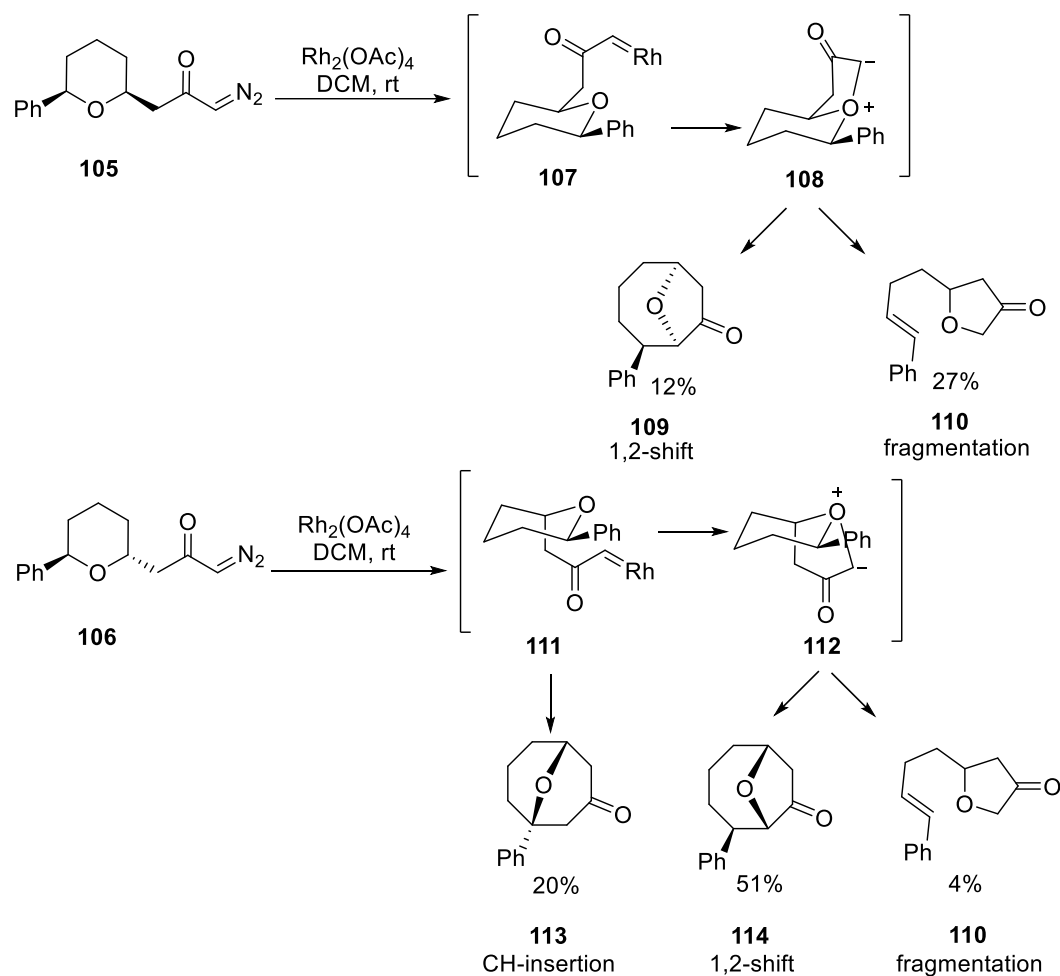
The formation of the *O*-bridged medium sized rings via the [1,2]-Stevens rearrangement was reported by the West group in 1993.<sup>52</sup> They observed that diastereomers **101** and **102**

containing cyclic ethers are capable of generating *O*-bridged cycloheptanones **103** and **104** via the Stevens rearrangement with the retention of configuration of the migrating center (Scheme 1-22).



**Scheme 1-22: The Stevens Rearrangement of the Bicyclic Oxonium Ylide**

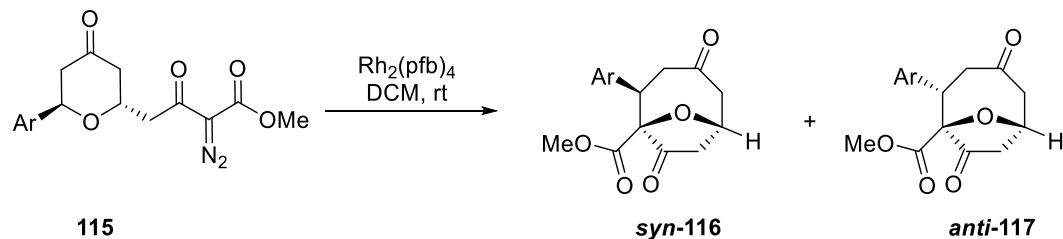
They also showed tetrahydropyrans **105** and **106** can undergo exocyclic-[1,2]-shift to form cyclooctanones **109** and **114** respectively, with low yield but complete stereoretention. The competitive C-H insertion **113** and fragmentation products **110** were also isolated (Scheme 1-23).<sup>52</sup>



### Scheme 1-23: The Formation of Cyclooctanones from Bicyclic Oxonium Ylides

On the other hand, Doyle and coworkers showed that the Rh(II) catalyzed decomposition of diazo ketone **115** could generate *O*-bridged cyclooctanedione in both *syn*-**116** and *anti*-**117** diastereomers. They showed that by increasing the size of the migrating group (**115d-f**), the [1,2]-shift occurred diastereoselectively in favor of *syn*-**116** (Scheme 1-24).<sup>53,54</sup>

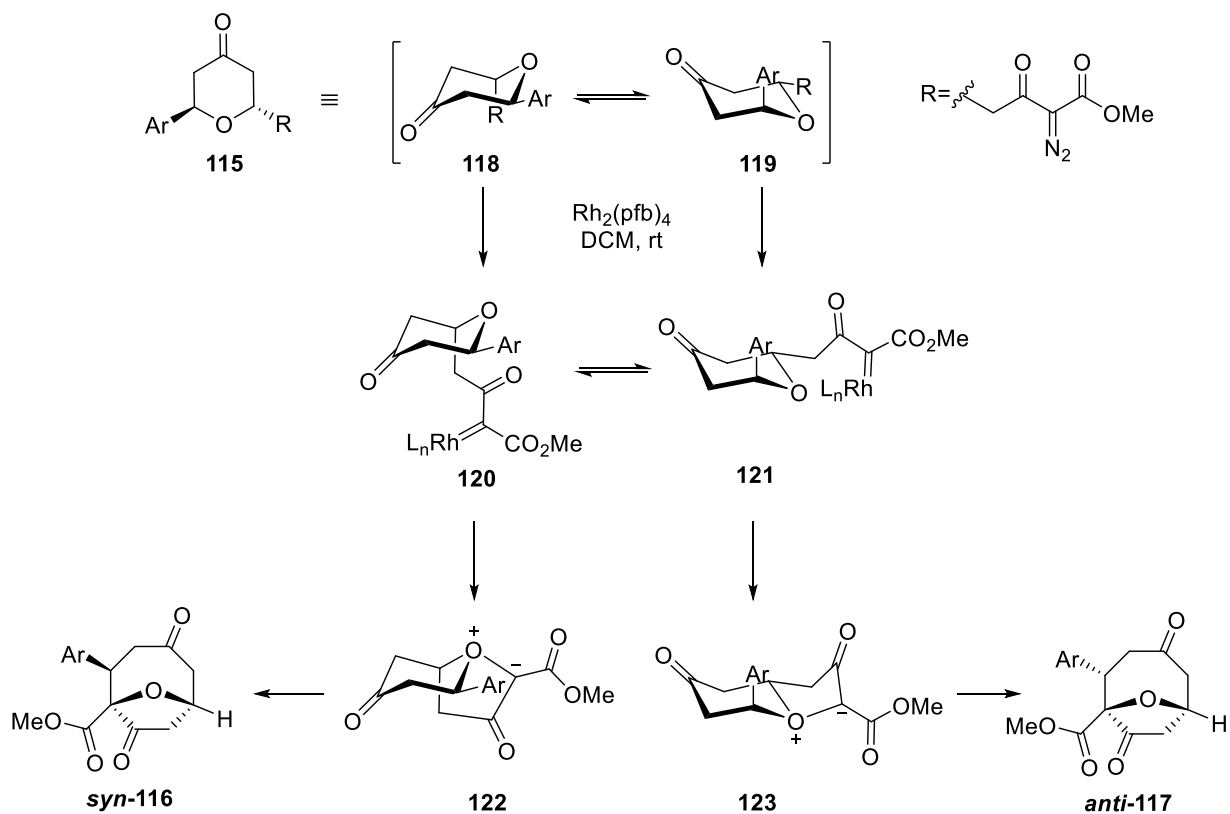




<b>122</b>	Ar	yield%	<b>116:117</b>
<b>115a</b>	Ph	77	71:29
<b>115b</b>	<i>p</i> -NO <sub>2</sub> Ph	94	74:26
<b>115c</b>	<i>p</i> -CF <sub>3</sub>	92	74:26
<b>115d</b>	mesityl	42	100:0
<b>115e</b>	9-anthranyl	45	100:0
<b>115f</b>	2,6-dimethyl-4-nitrophenyl	77	100:0

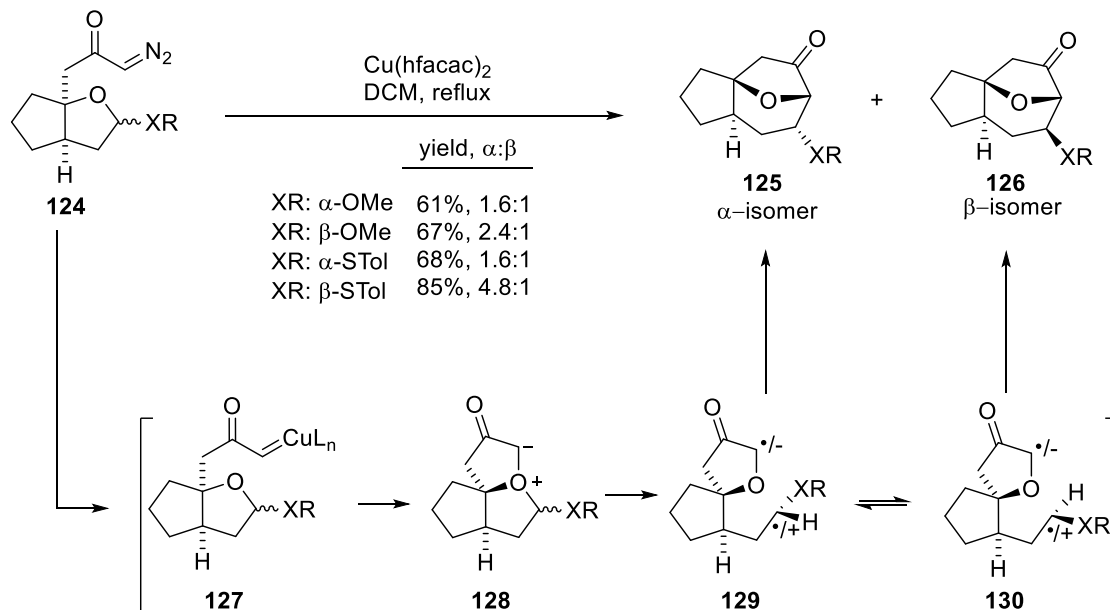
### Scheme 1-24: The Formation of Cyclooctanedione Studied by Doyle

The authors proposed that the formation of both *syn* and *anti* diastereomers could be rationalized by proposing two noninterconvertible ylides **122** and **123** resulted from the conformers **118** and **119**. In the case of diazo substrates with larger aromatic substituent (**115d-f**), *syn* diastereomer **116** was exclusively isolated showing the large contribution of conformational isomers in the product ratio (Scheme 1-25).<sup>54</sup>



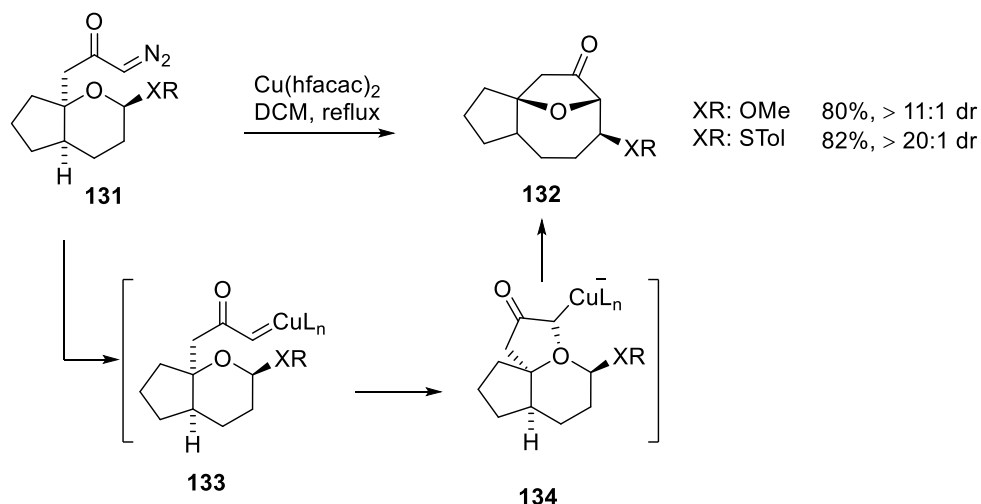
### Scheme 1-25: Conformation-Dependent Mechanism for the Formation of 116 and 117

The [1,2]-Stevens rearrangement was further explored by West and Murphy to construct hydrazulene ring systems.<sup>55,56</sup> Oxonium ylide **128** underwent [1,2]-shift through either homolytic or heterolytic cleavage. They proposed that the stereochemical erosion observed in this transformation could be the result of a fast bond rotation (**129** and **130**) compared to the rate of the radical or zwitterion recombination (Scheme 1-26).



**Scheme 1-26: Formation of Hydrazulene through the Stevens Rearrangement**

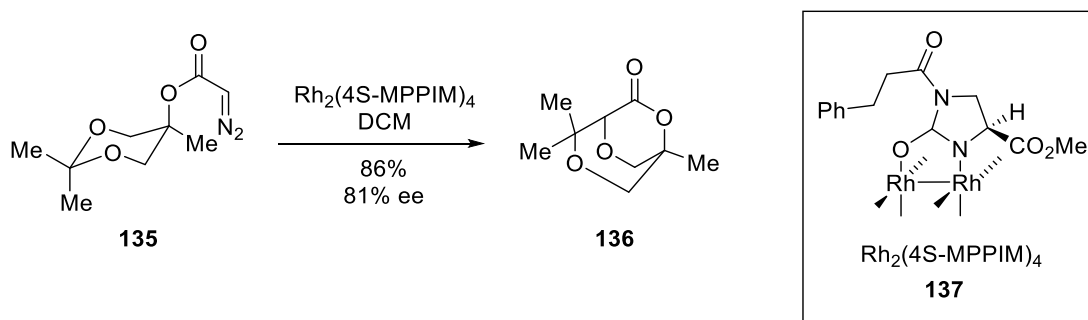
Despite of the lack of diastereoselectivity in the Stevens rearrangement of the oxonium ylide **128**, West and coworkers showed that bicyclic diazo ketone **131** possessing a tetrahydropyran ring generated cyclootanoid ring **132** with high diastereoselectivity in the presence of the Cu(II) catalyst (Scheme 1-27).<sup>57</sup>



**Scheme 1-27: Diastereoselective Formation of Cyclootanoid**

An enantioselective [1,2]-shift of an oxonium ylide can be achieved by employing a catalyst possessing chiral ligands in the diazo ketone decomposition. Doyle et al., reported an enantioselective formation of **136** resulting from the diazo decomposition of dioxolane **135**

with chiral catalyst  $\text{Rh}_2(4S\text{-MPPIM})_4$  followed by the [1,2]-shift in high yield and moderate enantioselectivity (Scheme 1-28).<sup>58</sup>

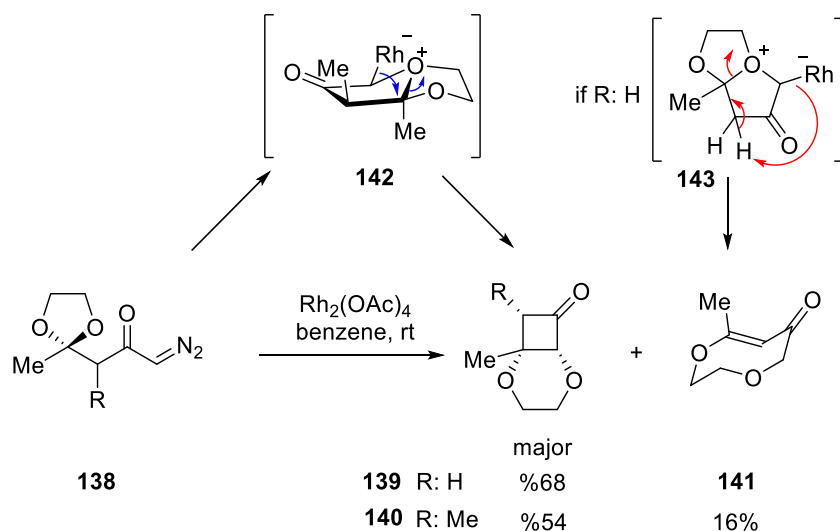


**Scheme 1-28: Enantioselective [1,2]-Stevens Rearrangement**

#### 1.2.1.4 Important Factors in the [1,2]-Stevens Rearrangement of the Cyclic Oxonium Ylides

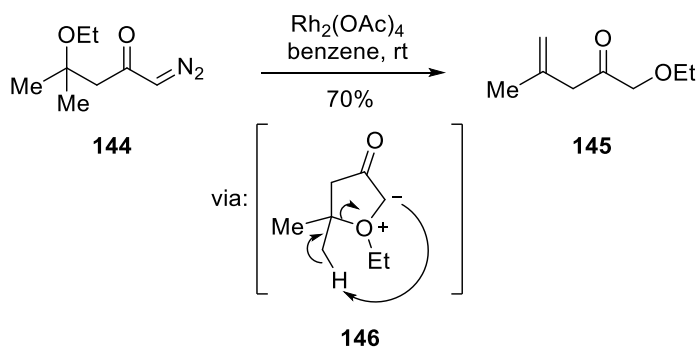
Several factors can affect the Stevens [1,2]-rearrangement of oxonium ylides. One important factor is the nature of the migrating group. The presence of a suitable migrating group capable of stabilizing the radical or ionic intermediate during the Stevens rearrangement plays a crucial role.

Johnson and Roskamp demonstrated that the phenyl stabilizing effect on the electron deficient migrating group promoted the endocyclic [1,2]-shift (Scheme 1-18).<sup>48</sup> They also showed that diazo ketones possessing cyclic acetals (**138**) underwent [1,2]-rearrangement in the presence of catalytic Rh(II) to generate bicyclic cyclobutanones **139** and **140**. They also isolated alkene **141** resulting from the deprotonation of the acidic  $\alpha$ -proton in oxonium ylide **143** in the absence of a substituent R. This result showed that the existence of the adjacent oxygen atom on the migrating group may facilitate the [1,2]-migration by stabilizing the electron deficient migrating carbon (Scheme 1-29).



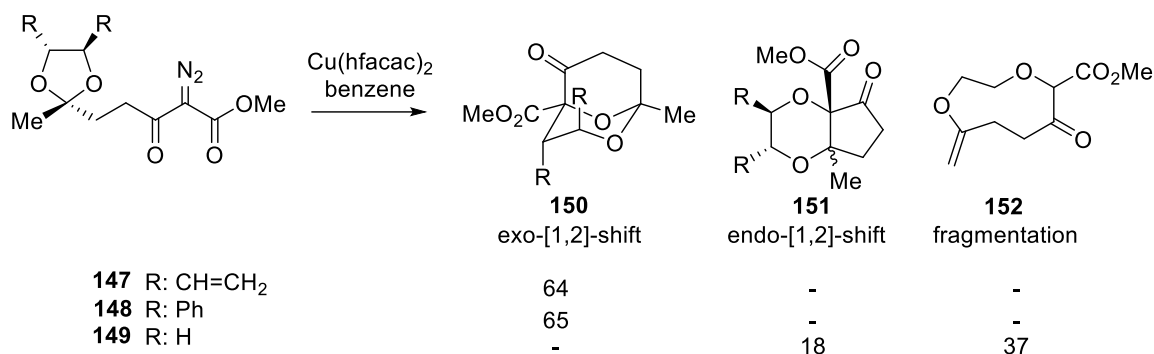
**Scheme 1-29: The Stevens Rearrangement of the Oxonium Ylides Possessing Cyclic Acetal**

The importance of the stabilizing group on the migrating center can be confirmed by the reaction of diazo ketone **144** under the same conditions. In the absence of the stabilizing group, alkene **145** was the only isolated compound resulting from the fragmentation process, and no [1,2]-rearrangement was observed (Scheme 1-30).



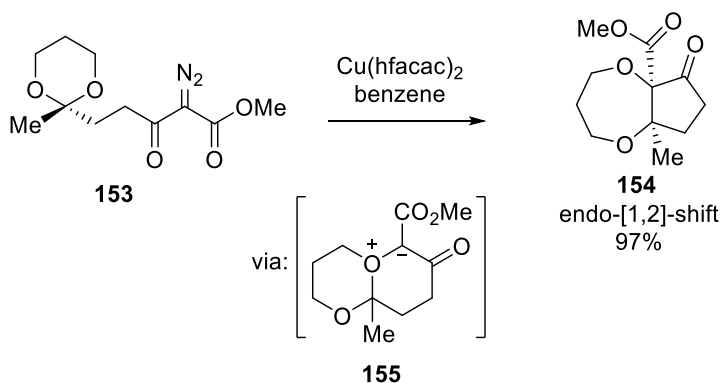
**Scheme 1-30: The Formation of Alkene 145**

The effect of the migrating group on the Stevens rearrangement was further studied by Zercher and Brogan.<sup>59</sup> They found that diazo ketones **147** and **148** having vinyl and phenyl substituents on the acetal moiety generated *O*-bridged bicyclic compounds **150** resulting from the exocyclic [1,2]-shift whereas the unsubstituted acetal **149** underwent an endocyclic [1,2]-shift to generate fused bicyclic product **151** as well as oxonium ylide fragmentation forming ring-expanded compound **152** (Scheme 1-31).



### Scheme 1-31: The Effect of Migrating Group Substituents on the Stevens Rearrangement

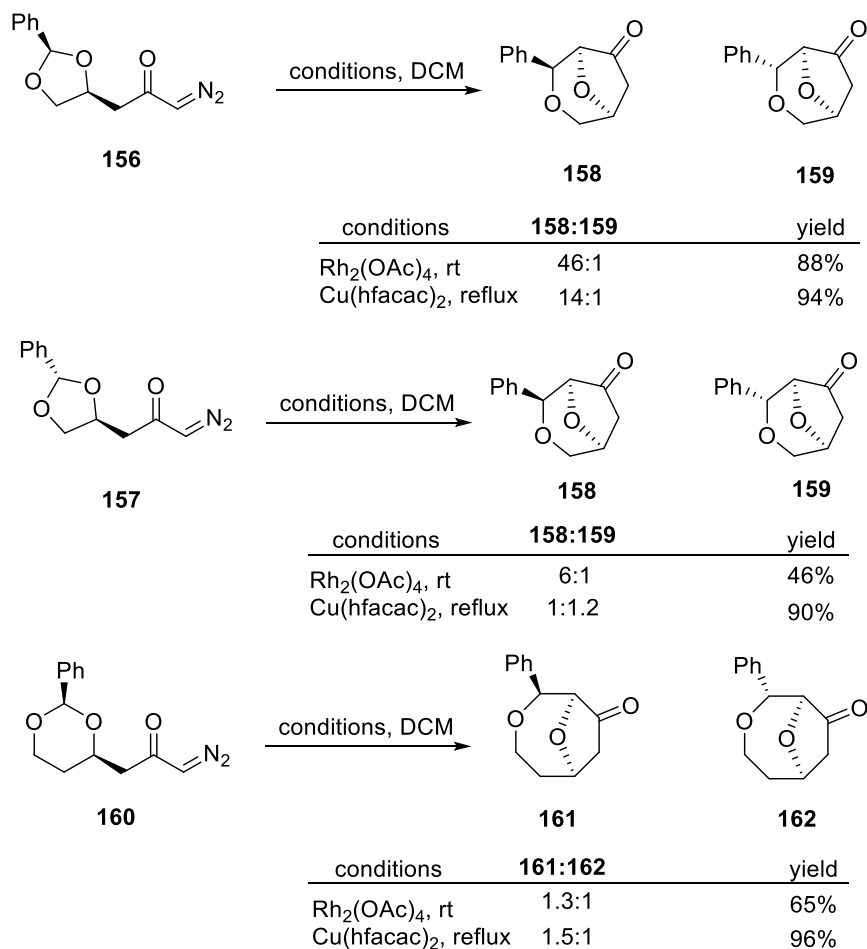
On the other hand, increasing the size of the cyclic acetal facilitated the endo-[1,2]-rearrangement and no fragmentation products were isolated. The endocyclic-[1,2]-shift of the oxygen bridged oxonium ylide **155** resulting from diazo ketone **153** showed that in the presence of the larger acetals, the fragmentation pathway is eliminated and the endocyclic [1,2]-Stevens shift can be more facile to generate **154** (Scheme 1-32). These results showed that [1,2]- migration of stabilizing migrating groups such as phenyl and vinyl, is more favored than the migration of groups having an oxygen substituent although in the presence of the proper ring size, an oxygen neighboring group can also promote the Stevens rearrangement.<sup>59</sup>



### Scheme 1-32: The effect of the Size of the Cyclic Acetal

Furthermore, the West group showed the reactivity of cyclic ketals with pendant diazo ketones.<sup>60</sup> They observed that in the presence of catalytic Rh<sub>2</sub>(OAc)<sub>4</sub>, both benzylidene acetals **156** and **157** formed *O*-bridged medium ring ethers **158** and **159** in favor of the formation of **158** regardless of the stereochemistry of the migrating group in the parent diazo ketone. The reaction in the presence of Cu(hfacac)<sub>2</sub> occurred with retention of configuration although the

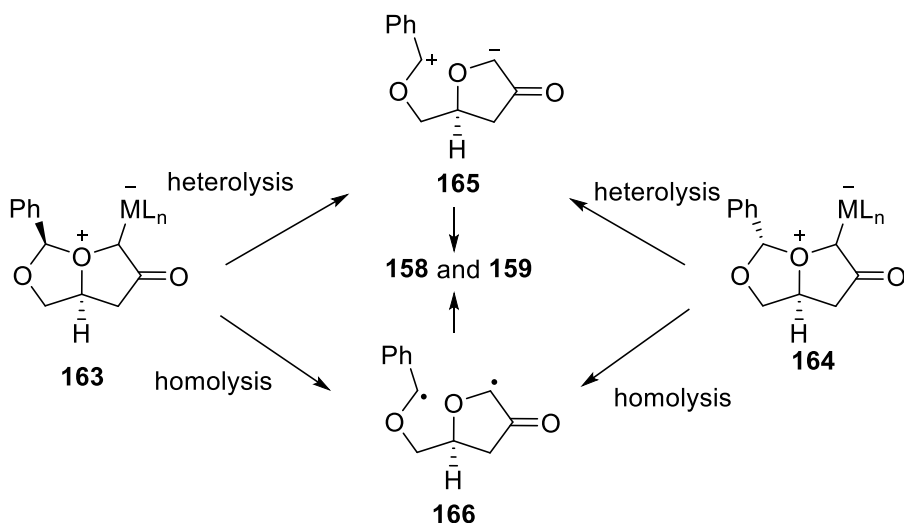
magnitude of the stereoselectivity in the case of diazo ketone **157** was not very significant. A lack of stereospecificity was also observed for **160** in the presence of the both Rh(II) and Cu(II) catalysts (Scheme 1-33).



### Scheme 1-33: Reactivity of the Cyclic Ketals with Pendant Diazo Ketone Moiety

It was noted previously that, in most cases, [1,2]-rearrangement occurs with substantial or complete retention. A fair explanation for the lack of stereospecificity, during the catalytic decomposition of these diazo ketones, could be related to the stabilizing effect of the oxygen on the carbocation **165** or radical **166** obtained from bicyclic oxonium ylides **163** and **164** through either heterolytic or homolytic C-O bond cleavage. It seemed that longer lifetime of the intermediates provided by the extra stabilization effect of the oxygen permits greater likelihood of bond rotation, resulting in erosion of stereospecificity (Scheme 1-34). The large difference in stereospecificity seen with diastereomeric substrates **156** and **157** is striking, but difficult to explain. One notable difference is the likelihood one predominant low-energy

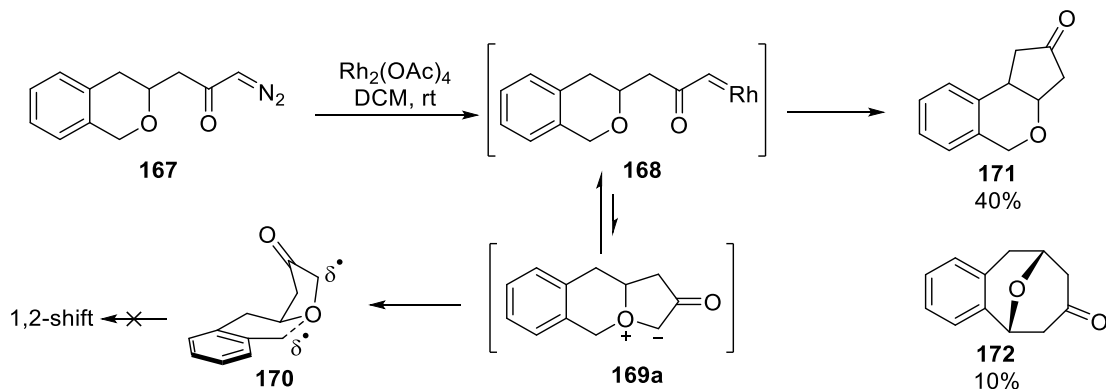
conformation for *cis*- isomer **156**, which could affect the stereoselectivity of ylide formation and the degree of retention during migration. In comparison, **157** is expected to exist in several conformers of comparable stability, which could lead to a mixture of ylide intermediates and/or greater randomization during [1,2]-shift.



#### Scheme 1-34: Proposed Mechanism to Rationalize Lack of Diastereoselectivity

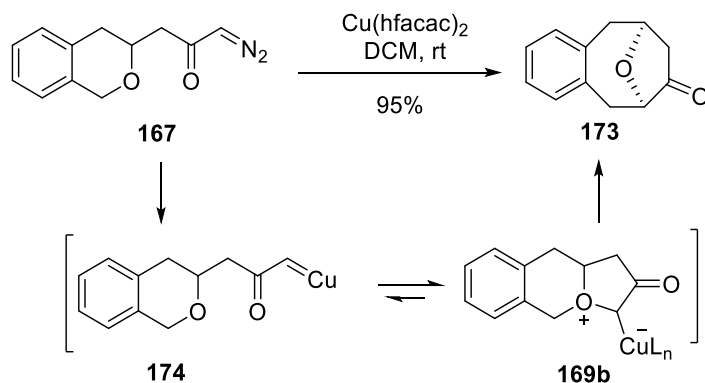
It is noteworthy to mention that although in most cases the benzyl moiety has been known as a proper migrating group in the [1,2]-rearrangement, it cannot always facilitate this process. West and coworkers showed that the Rh(II) catalyzed decomposition of the diazo ketone **167** generated the metalcarbene C-H insertion products **171** and **172** and no product resulting from [1,2]-rearrangement was isolated.<sup>52</sup> They proposed that the equilibrium between metalcarbene **168** and oxonium ylide **169a** favors the metalcarbene which can generate C-H insertion products (Scheme 1-35). The expected [1,2]-shift in the oxonium ylide was not observed since the developing benzyl radical cannot be stabilized by the phenyl ring due to less orbital overlap between the orthogonal p-orbital and phenyl  $\pi$ -system (**170**).





**Scheme 1-35: Rhodium Catalyzed Decomposition of Diazo Ketone 167**

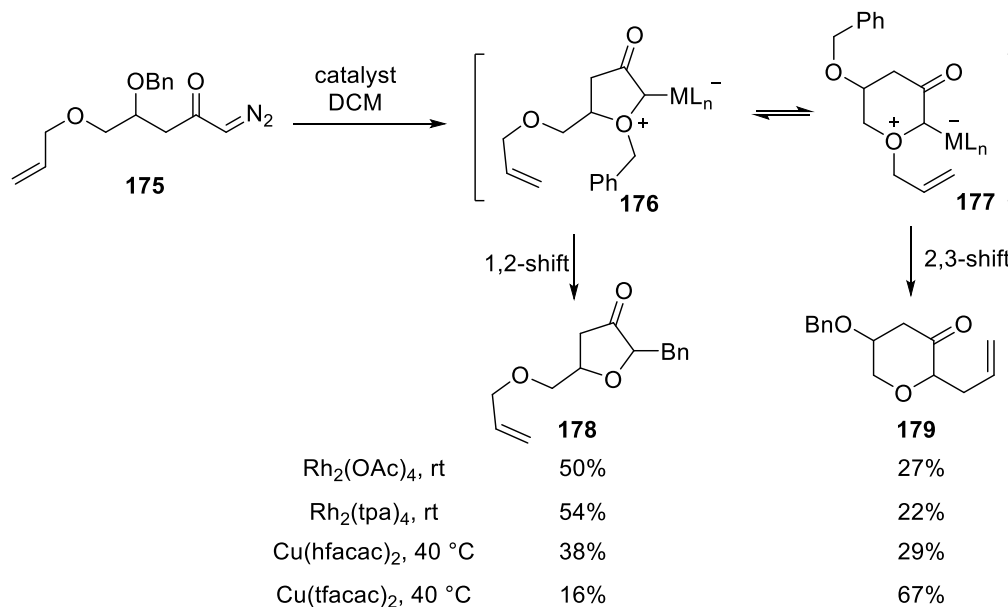
The catalyst involved in the reaction also has a significant impact on the reactivity of cyclic oxonium ylides. West and coworkers reported that diazo ketone **167** shows different reactivity in the presence of Rh and Cu catalysts. In contrast to Rh catalyzed decomposition of **167** which generated C-H insertion products (Scheme 1-35), treatment of **167** with  $\text{Cu}(\text{hfacac})_2$  afforded product **173** resulting from [1,2]-rearrangement in high yield.<sup>61</sup> It is known that copper carbenoid **174** is more electrophilic, therefore the generation of oxonium ylide **169b** in the presence of the Cu catalyst is more favored furnishing the [1,2]-shift product (Scheme 1-36).<sup>19,62</sup> Authors proposed a possible copper-assisted mechanism (Scheme 1-50) which may facilitate the [1,2]-Stevens rearrangement of ylide **169b** to the product **173**.



**Scheme 1-36: Copper Catalyzed Decomposition of Diazo Ketone 167**

The effect of the catalyst and migrating group on the Stevens rearrangement was also reported by the West group in 2004.<sup>19,62,63</sup> Diazo ketone **175** possessing both benzyl group capable of undergoing a [1,2]-shift and an allyl group set up for a [2,3]-rearrangement was

treated with Rh and Cu catalysts. Cu(tfacac)<sub>2</sub> showed a greater tendency to generate six-membered oxonium ylide **177** to facilitate [2,3]-rearrangement whereas Rh<sub>2</sub>(OAc)<sub>4</sub>, Rh<sub>2</sub>(tpa)<sub>4</sub> and Cu(hfacac)<sub>2</sub> preferentially formed the five membered oxonium ylide **176** to afford [1,2]-benzyl migration (Scheme 1-37).



**Scheme 1-37: The Effect of the Catalyst and Migrating Group on the Stevens Rearrangement**

### 1.2.1.5 The Application of the Stevens Rearrangement in Total Synthesis

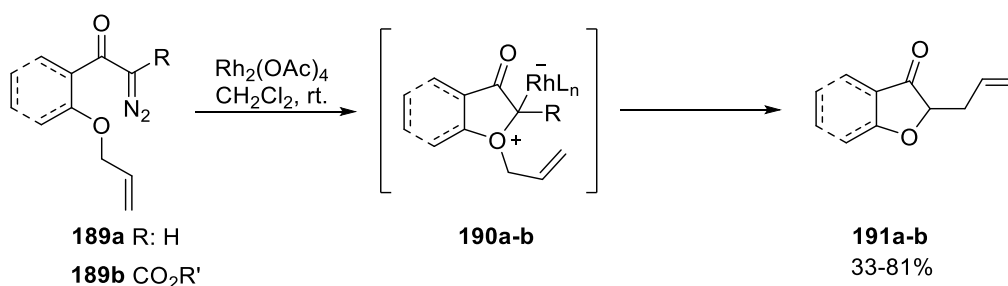
The [1,2]-Stevens rearrangement of cyclic oxonium ylides has been employed as an effective tool to construct the core structures for total synthesis of numerous natural products. Brogan and Zercher, in 1998, showed that [1,2]-rearrangement of oxonium ylides can be used to synthesize the bicyclic core structure of zaragozic acid (**180**), a biologically active compound known to control cholesterol levels.<sup>64</sup> Treatment of dioxolane **147** with Rh<sub>2</sub>(OAc)<sub>4</sub> provided the *O*-bridged bicyclic core structure **182** of the zaragozic acid through the stereoselective Stevens rearrangement of oxonium ylide **181** (Scheme 1-38).



## 1.2.2 [2,3]-Sigmatropic Rearrangement of Cyclic Oxonium Ylides

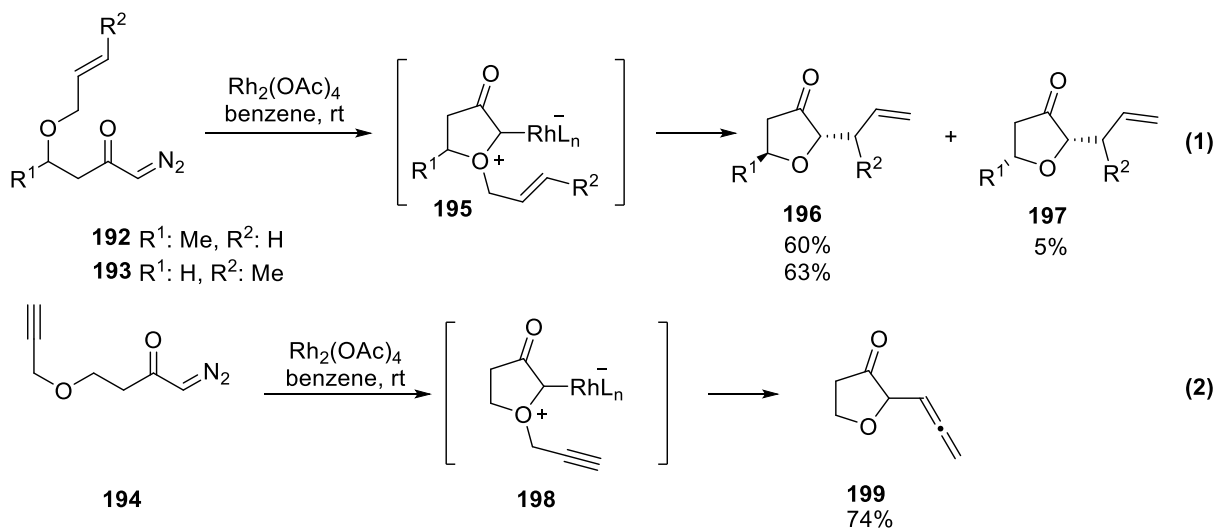
The favorable concerted [2,3]-sigmatropic rearrangement is a symmetry-allowed process according to the Woodward-Hoffmann rules and occurs rapidly in the presence of allylic or propargylic type migrating groups.<sup>45</sup>

The first [2,3]-sigmatropic rearrangements of the oxonium ylides generated from catalytic decomposition of diazocarbonyl compounds were reported in two different publications by Pirrung and Johnson in 1986. Pirrung and coworkers demonstrated that cyclopentanone **191** could be obtained via the Rh(II) catalyzed formation of oxonium ylides from diazocarbonyls **189** followed by [2,3]-rearrangement of allyl group in ylide **190** (Scheme 1-40).<sup>65</sup>



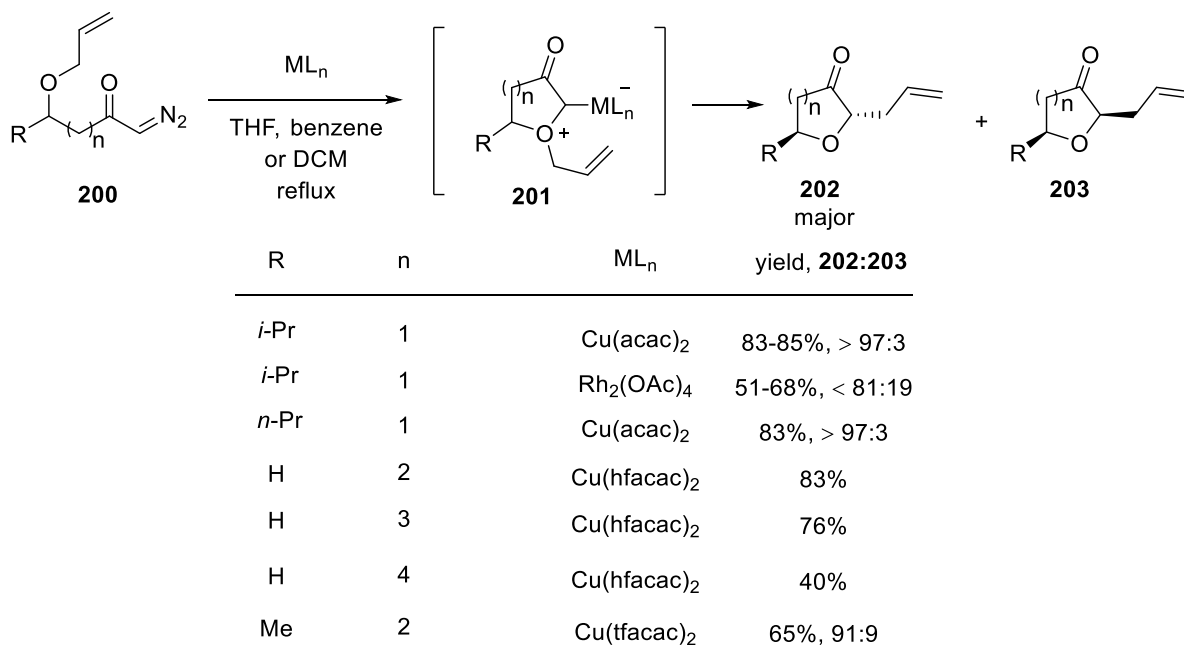
**Scheme 1-40: The [2,3]-Rearrangement of Oxonium Ylides**

In a parallel investigation, Roskamp and Johnson showed exocyclic [2,3]-rearrangement of allylic (Scheme 1-41, eq. 1) and propargylic (Scheme 1-41, eq. 2) migrating groups.<sup>48</sup> Similar to Pirrung's finding, they employed catalytic Rh<sub>2</sub>(OAc)<sub>4</sub> for the *in situ* generation of oxonium ylides **195** and **198** capable of undergoing [2,3]-rearrangement.



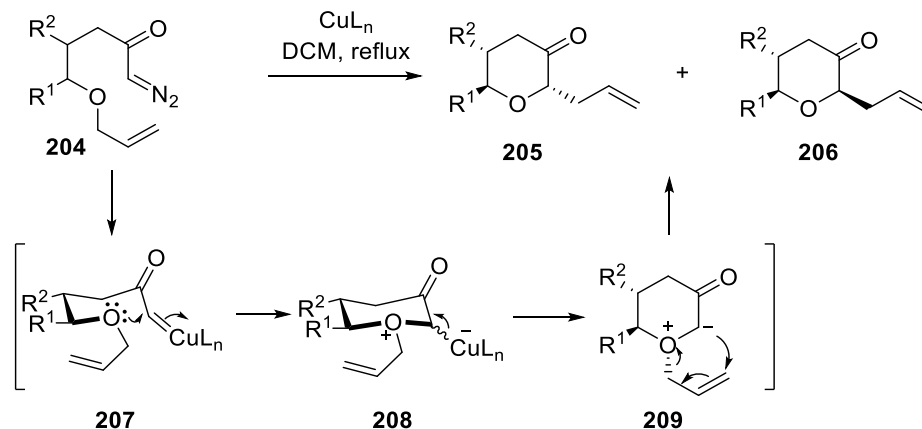
### Scheme 1-41: The [2,3]-Migration of Allyl and Propargylic Groups in Oxonium Ylide

Later, Clark reported the [2,3]-rearrangement of oxonium ylides for the generation of the substituted tetrahydrofuranones in the presence of both copper and rhodium catalysts.<sup>66</sup> He also reported the formation of the larger cyclic ethers via the same protocol.<sup>62</sup> He showed that Cu(hfacac)<sub>2</sub> is the most effective catalyst for the generation of oxonium ylides and medium sized cyclic ethers (Scheme 1-42).



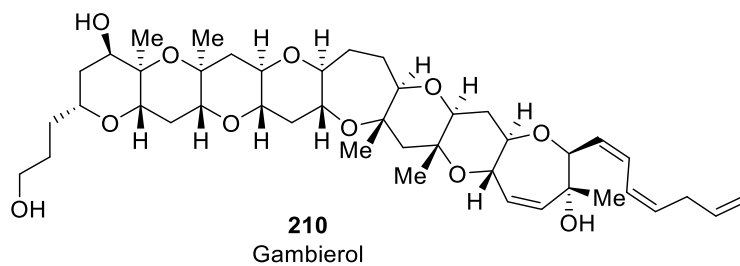
### Scheme 1-42: Copper Catalyzed [2,3]-Rearrangement

Additionally, it has been found the [2,3]-rearrangements of cyclic ylides usually occur with high diastereoselectivity. The Clark group reported a stereoselective synthesis of tetrahydropyrans **205** and **206** through the [2,3]-shift of the allyl group in the oxonium ylide **209** favoring formation of the *trans*- isomer.<sup>67</sup> They explained the observed stereoselectivity using a chair-like transition state **208** with all substituent in the equatorial position. Since the inversion barrier for the oxonium center is higher compared to the migration of the allyl group, the [2,3]-shift occurs faster to generate the *trans*-tetrahydropyranone **205** as the major diastereomer (Scheme 1-43).

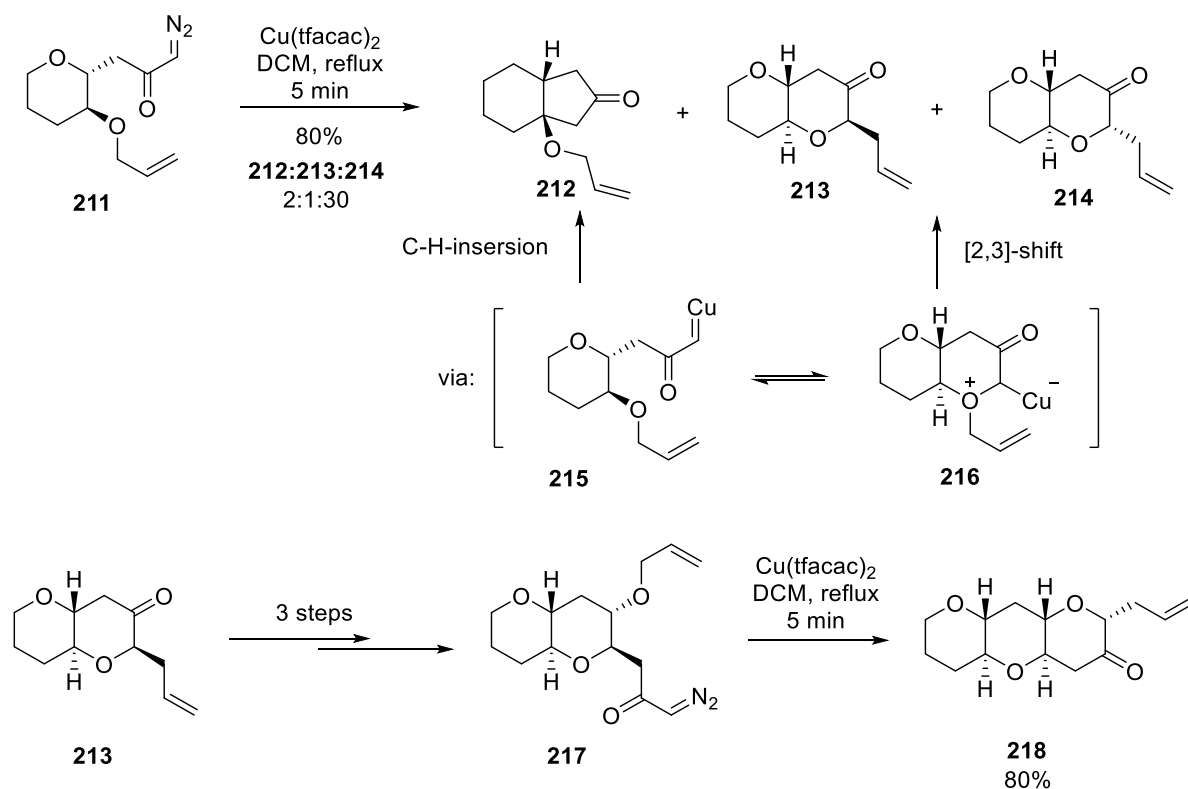


**Scheme 1-43: Diastereoselective [2,3]-Rearrangement**

West and Marmsäter reported the application of the [2,3]-rearrangement to construct the repetitive core structure of gambierol (**210**) (Figure 1-3).<sup>68</sup> They showed that pyrans **213** and **214** could be obtained from the  $\text{Cu}(\text{tfacac})_2$  catalyzed decomposition of diazocarbonyl **211** containing pyran ring. Fused cyclopentanone (**212**) was also isolated resulting from competing C-H insertion of the metalcarbene **215**. Oxonium ylide **216** underwent allylic [2,3]-shift to generate the second pyran in two diastereomers **213** and **214**. The desired bicyclic diastereomer **213** was further used to construct another pyran ring through multistep synthesis (Scheme 1-44).



**Figure 1-3: The Structure of Gambierol**

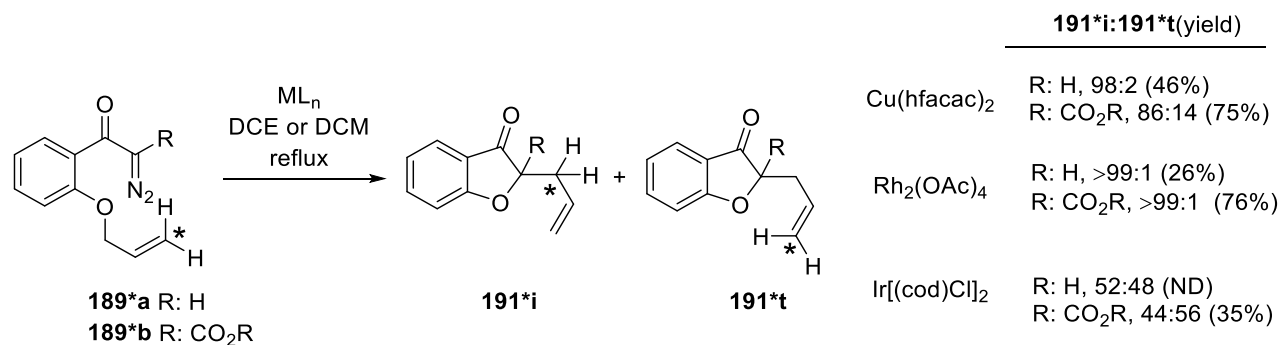


### Scheme 1-44: Construction of Polypyran Core Structure via [2,3]-Rearrangement

Both Clark and West identified that copper complexes are more effective catalysts in [2,3]-rearrangements than Rh(II) regarding the possible rhodium carbenoid C-H insertion which can compete with ylide formation.<sup>46,62,68</sup> In 2014, the Clark group reported an interesting mechanistic study to demonstrate the presence of the free oxonium or metal bound ylides in the [2,3]-sigmatropic rearrangement.<sup>69</sup> They employed diazo ketones **189\*** labeled with  $^{13}\text{C}$  at the terminal position of allyl moiety and they observed that the decomposition of diazo ketone **189\*a** in the presence of both copper and rhodium catalysts afforded cyclic ethers **191\*i** and **191\*t** via [2,3] and [1,2]-migrations, respectively, favoring the [2,3]-shift. The observed ratio of the products is consistent with the presence of the free oxonium ylide, although the possibility of the metal bound ylide cannot be ignored. Copper catalyzed decomposition of **189\*b** gave higher proportion of the **191\*t** compared to Rh(II) catalyzed reaction. On the other hand, both **189\*a** and **189\*b** provided cyclic ethers **191\*i** and **191\*t** with almost the same ratio employing an iridium catalyst. This result shows that the ratio of the products

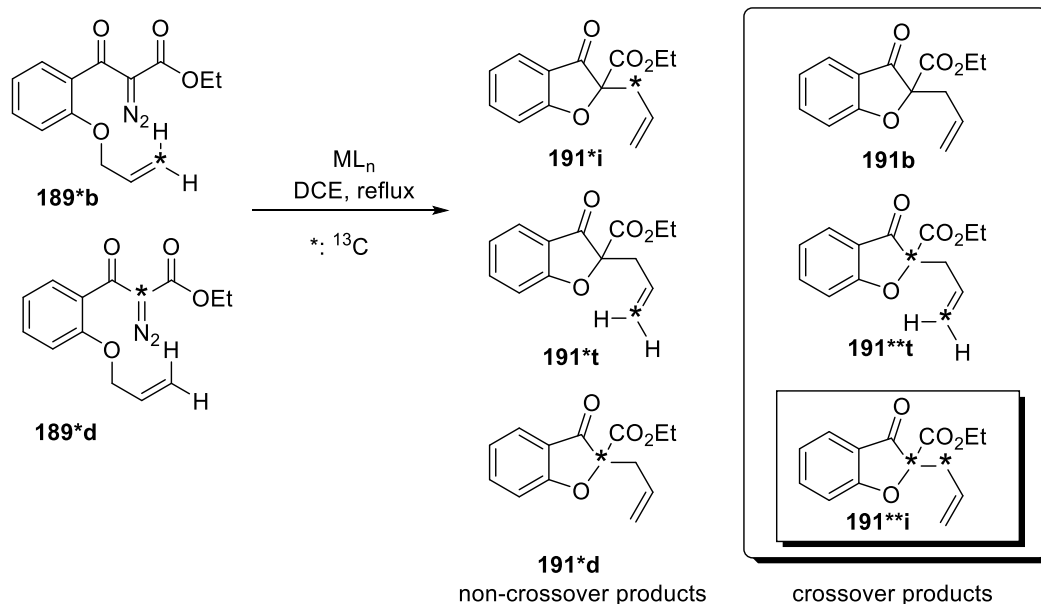


depends on the nature of the catalyst which can be an evidence for the absence of the free ylides in the reaction mechanism (Scheme 1-45).



### Scheme 1-45: Metal-Catalyzed Reactions of <sup>13</sup>C-Labelled Diazo Ketones

Crossover studies employing a mixture of diazo ketones **189\*b** and **189\*d** showed a significant amount of the crossover product **191\*\*i** in the presence of iridium catalyst. By having these results in hand, they proposed a non-ylide pathway involving the dissociation of iridium metal to form an iridium enolate and allylic cation followed by C-C bond formation (Scheme 1-46). A trace amount of the crossover product **191\*\*i** was observed when using Cu(hfacac)<sub>2</sub>. This results demonstrate a little dissociation of the copper-bound ylide during the intramolecular transferring of the allyl group.

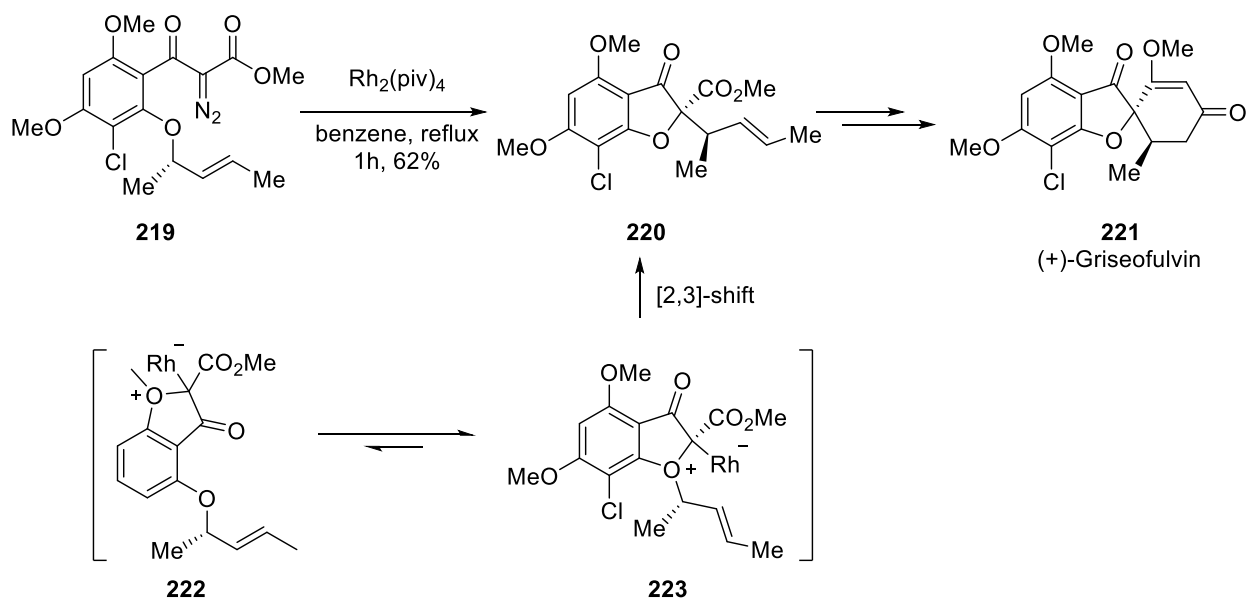


**Scheme 1-46: Crossover Studies**

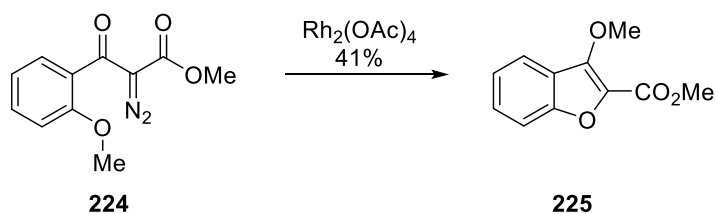
### 1.2.3 The [1,4]-Rearrangement of Cyclic Oxonium Ylides

Among the sigmatropic rearrangements of onium ylides, the [1,4]-rearrangement is observed rarely compared to [2,3] and [1,2]-shifts. Although there are limited reports of [1,4]-shifts in cyclic oxonium ylides, they provide valuable information about the nature of the active intermediates during ylide rearrangements.

The Pirrung group showed the [1,4]-migration of a methyl group during the total synthesis of (+)-griseofulvin (Scheme 1-47).<sup>70</sup> They employed a Rh(II) catalyzed decomposition of diazo ketone **219** possessing two O-alkoxy moieties to generate two possible oxonium ylides **222** and **223**. They showed that [2,3]-rearrangement of allyl oxonium ylide has lower activation energy compared to the [1,2]-methyl migration. According to the Curtin-Hammett principle the process possessing lower activation energy will provide the major product.<sup>71</sup> This hypothesis was supported by treatment of diazo ketone **224** with  $\text{Rh}_2(\text{OAc})_4$ . They isolated benzofuran **225** obtained from the [1,4]-rearrangement and no [1,2]-methyl shift was isolated (Scheme 1-48).

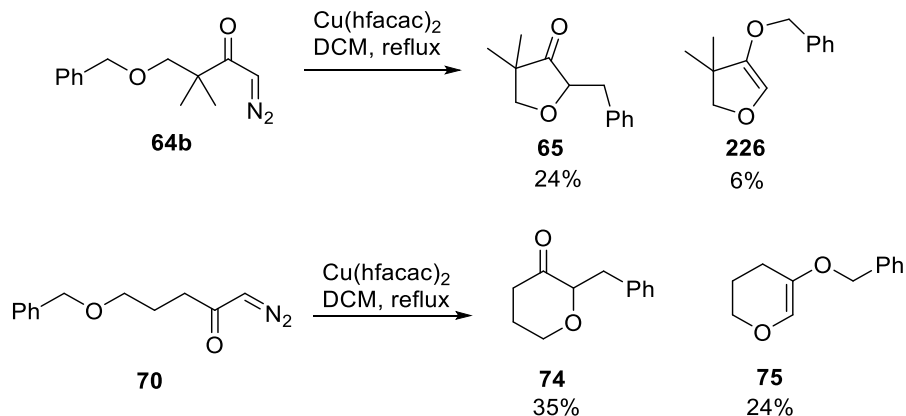


**Scheme 1-47: The Total Synthesis of (+)-Griseofulvin**



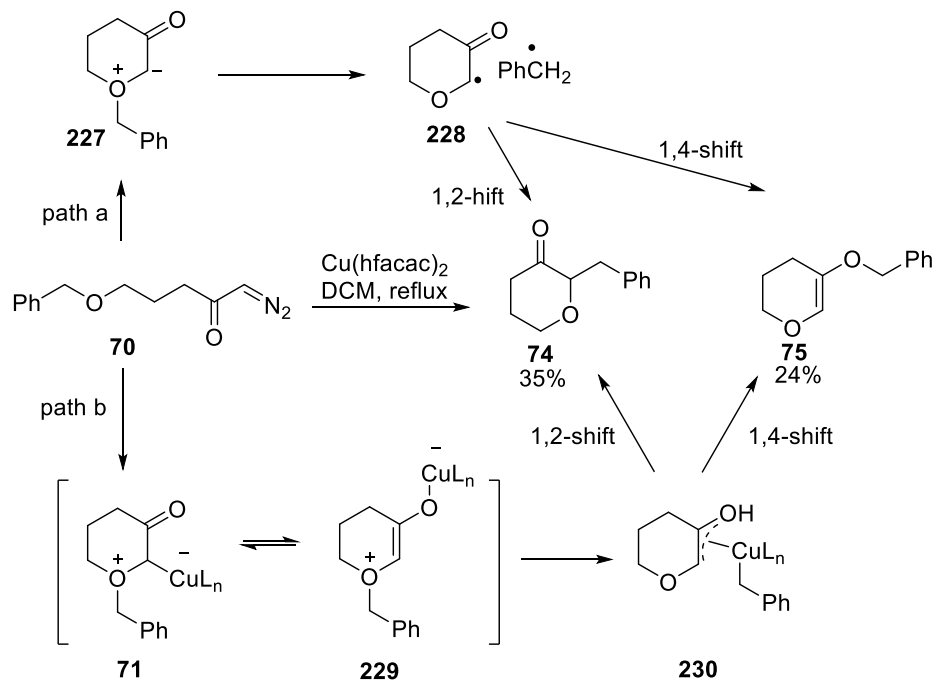
**Scheme 1-48: The [1,4]-Rearrangement of Diazo Ketone 197**

West and coworkers also observed a [1,4]-rearrangement when a benzyl moiety was the migrating group in an oxonium ylide resulting from benzyl ethers **64b** and **70**.<sup>46</sup> The copper catalyzed reaction of diazo ketone **64b** and **70** with  $\text{Cu}(\text{hfacac})_2$  provided both [1,2] and [1,4]-shift of the benzyl group (Scheme 1-49).



### Scheme 1-49: The [1,4]-rearrangement of Benzyl Ethers

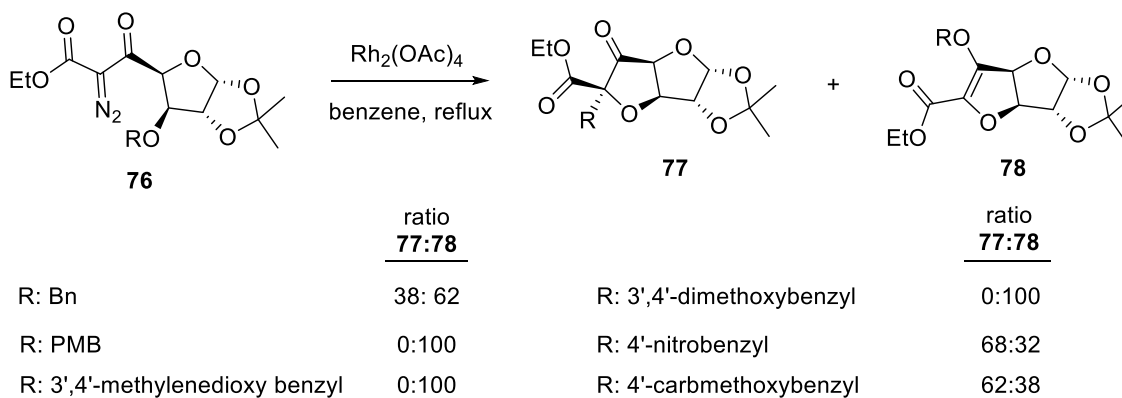
They proposed that the [1,4]-rearrangement to form C-O bond occurs through the formation of the same radical pairs **228** for the Stevens [1,2]-shift (Scheme 1-50, path a). Since no homodimer products were isolated, the copper assisted mechanism to facilitate both [1,2] and [1,4]-rearrangement cannot be ignored (Scheme 1-50, path b).<sup>46,63</sup>



### Scheme 1-50: The Possible Mechanisms for [1,4]-Benzyl Migration

The [1,4]-rearrangement was also reported by the Dhavale group.<sup>47,72</sup> They studied the effect of the aryl substituent on the rearrangement pathway of the benzyl migrating group

during the decomposition of diazo ketone **76** in the presence of a Rh(II) catalyst. It was observed that in the presence of an electron donating substituent, [1,4]-rearrangement was the only reaction pathway whereas [1,2]-shift was the dominant pathway in the presence of the electron withdrawing aryl substituents (Scheme 1-51). They also correlated the effect of the resonance contribution ( $\sigma_R$ ) of the aromatic substituents on the product selectivity. They showed that substituent having positive  $\sigma_R$  favored [1,2]-shift whereas negative  $\sigma_R$  provided [1,4]-migration.



**Scheme 1-51: Aromatic Substituent Effect on the [1,4]-Shift**

### 1.3 Conclusion

Since the discovery of the Stevens [1,2]-rearrangement in 1928, its synthetic value has been extensively demonstrated by new synthesis methodologies and total synthesis of complex natural products. A significant part of the studies related to ylide chemistry encompass the application of the Stevens rearrangement. Oxonium ylides, which are the most reactive intermediates, are capable of undergoing the Stevens [1,2]-shift to generate complex structures and advanced core structures found in natural products. Their rearrangement is highly dependent on the migrating group. Despite the considerable studies toward the application of the Stevens rearrangement, the mechanism and actual intermediates involved in the reaction pathway are still ambiguous. There are several pieces of evidence confirming the presence of radical pair intermediates although the existence of the zwitterionic species cannot be ruled out. As a result, we decided to study the mechanism of the Stevens [1,2]-shift as well as its application in an endocyclic [1,2]-shift to generate cyclobutanones. For this purpose we employed a cyclopropylmethyl moiety as the possible migrating group to study its migration ability in a [1,2]-rearrangement. The results related to the formation of

cylobutanones from the Stevens rearrangement of the oxonium ylides will be discussed in Chapter 2. Furthermore, in Chapter 3, we will show that the cyclopropylmethyl group plays a crucial role in the mechanistic studies regarding its potential in radical clock chemistry which is a valuable method to understand the nature of the involved intermediates in a reaction mechanism.

## Chapter 2 Construction of Substituted Cyclobutanones via [1,2]-Stevens Rearrangement of Oxonium Ylides




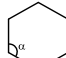
### 2.1 Introduction

#### 2.1.1 Ring Strain

Cycloalkanes are a vast category of saturated carbon ring systems with the general formula of  $C_nH_{2n}$ . In general, all carbons are assumed to possess  $sp^3$  hybridization. The ideal bond angle for  $sp^3$  hybridized carbon is  $109.5^\circ$  and it is conventional to observe greater ring strain and decreased stability for the three and four membered carbocycles with smaller bond angles.<sup>73</sup>

The concept of the “strain theory” was developed by Adolf von Baeyer in 1885.<sup>74,75</sup> He proposed small rings such as cyclopropane **1** and cyclobutane **2** suffer from ring strain due to bond angle deviation from the ideal value.

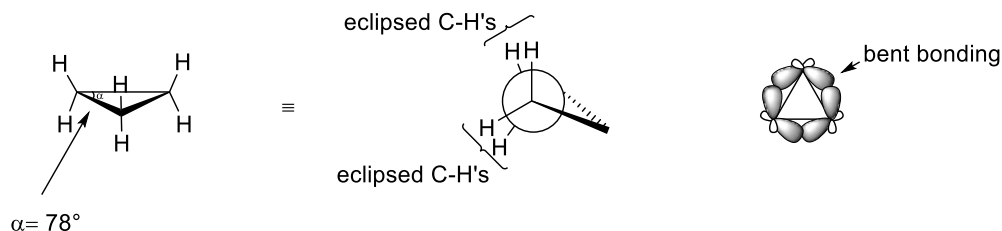
Later, in 1949 and 1950 the heats of combustion for three and four membered rings were calculated which helped in determining the strain energy (Figure 2-1).<sup>74,76</sup> These calculations correctly showed the more strain energy and subsequently higher reactivity for the smaller rings compared to five and six membered rings.

				
	<b>1</b>	<b>2</b>	<b>3</b>	<b>4</b>
	<b>cyclopropane</b>	<b>cyclobutane</b>	<b>cyclopentane</b>	<b>cyclohexane</b>
<b>bond angle (<math>\alpha^\circ</math>)</b>	experimentally: 78 theoretically: 60	experimentally: 88 theoretically: 90	108	120
<b>strain energy (kcal mol<sup>-1</sup>)</b>	27.5	26.2	6.3	0

**Figure 2-1: The Strain Energy of Cycloalkanes**

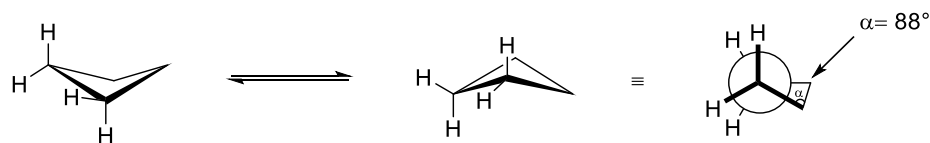
Although the majority of the ring strain arises from the bond angle deviation, the effect of the torsional strain (twisting strain) observed in the smaller rings cannot be ignored. In the case of planar cyclopropane, eclipsing C-H bonds provides torsional effects (Figure 2-2).<sup>73</sup> To relieve the torsional strain, bonds in cyclopropane are bent by involving greater p-orbital contribution in the sigma C-C bond. As a result, the actual bond angle becomes slightly larger than theoretical value ( $60^\circ$ ) and has been reported to be  $78^\circ$ .<sup>74</sup> Consequently, contribution of

the p-orbitals results in weaker C-C bonds. The dissociation energy of C-C bond in ordinary aliphatic hydrocarbons molecules is  $84 \text{ kcal. mol}^{-1}$  whereas this value has been measured at  $65 \text{ kcal mol}^{-1}$  for cyclopropane.<sup>74</sup>



**Figure 2-2: Eclipsed C-H Bonds in Cyclopropane Resulting Torsional Strain**

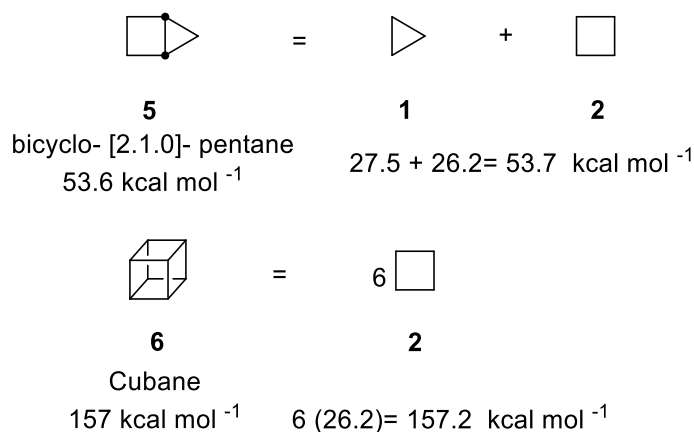
Similarly, C-H bond eclipsing can be observed for planar cyclobutane. Therefore cyclobutane is twisted into a puckered wing conformation to avoid eclipsing C-H bond interactions and relieve torsional strain. This behavior results in smaller bond angles ( $88^\circ$ ), but less torsional strain in the four membered rings (Figure 2-3).<sup>73</sup>



**Figure 2-3: Torsional Strain in Cyclobutanes**

In most cases the ring strain energies are additive. For instance the strain energies for bicyclo- [2.1.0]- pentane **5** and cubane **6** have been reported to be  $53.6 \text{ kcal mol}^{-1}$  and  $157 \text{ kcal mol}^{-1}$  respectively which is comparable to the total strain energy of all involved cycloalkanes in their structure (Figure 2-4).<sup>77</sup> Consequently, having more than one small ring in the structure increases the strain energy leading to unusual reactivity and molecular conformations.

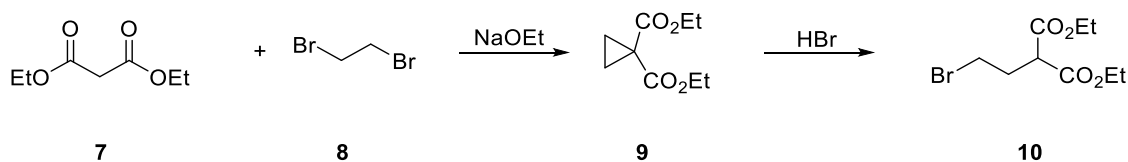




**Figure 2-4: The Strain Energy of the Bicycloalkanes**

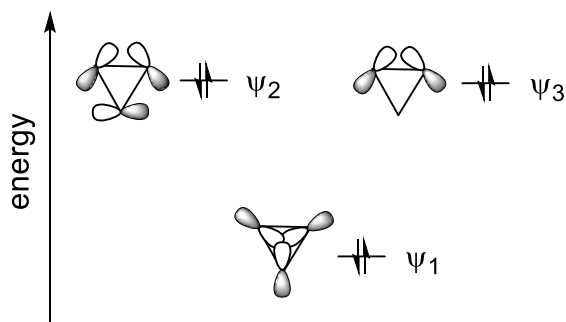
### 2.1.2 The Chemistry of Cyclopropanes

W. H. Perkin, in 1884, reported the first synthesis of the cyclopropane ring.<sup>78</sup> He showed diethyl malonate **7** in reaction with dibromoethane **8** under basic conditions generated disubstituted cyclopropane **9** which underwent rapid ring opening with HBr to generate acyclic diester **10** (Figure 2-5).



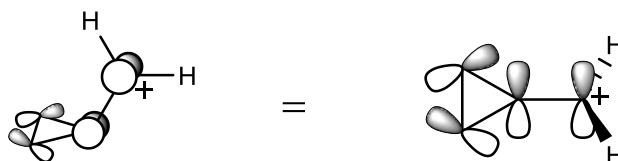
**Figure 2-5: The First Synthesis of a Cyclopropane by Perkin**

Due to the aforementioned strain energy of cyclopropanes, they are considered to be a very reactive class of cycloalkanes. Their reactivity is comparable to an alkene C=C bond because of the similarities in their molecular orbital properties. Both cyclopropanes and olefins can react with acids and halogens, form metal complexes and participate in pericyclic transformations.<sup>79</sup> The particular behavior of the cyclopropane is dictated by the nature of the sigma ( $\sigma$ ) C-C bonds in cyclopropane structure. This concept can be well explained by the Walsh molecular orbital model (Figure 2-6).<sup>80</sup>



**Figure 2-6: Walsh Cyclopropane Molecular Orbitals**

Based on the Walsh description, the nature of the C-C bond is more similar to a  $\pi$ -bond than  $\sigma$ -bond resulting from overlap of the orbitals with pure p-character. This depiction explains the similar reactivity observed for cyclopropanes and alkenes. This also explains the strong stabilization of the cyclopropylmethyl cation by the hyperconjugation of C-C bonds to the empty p-orbital (Figure 2-7).<sup>71</sup>

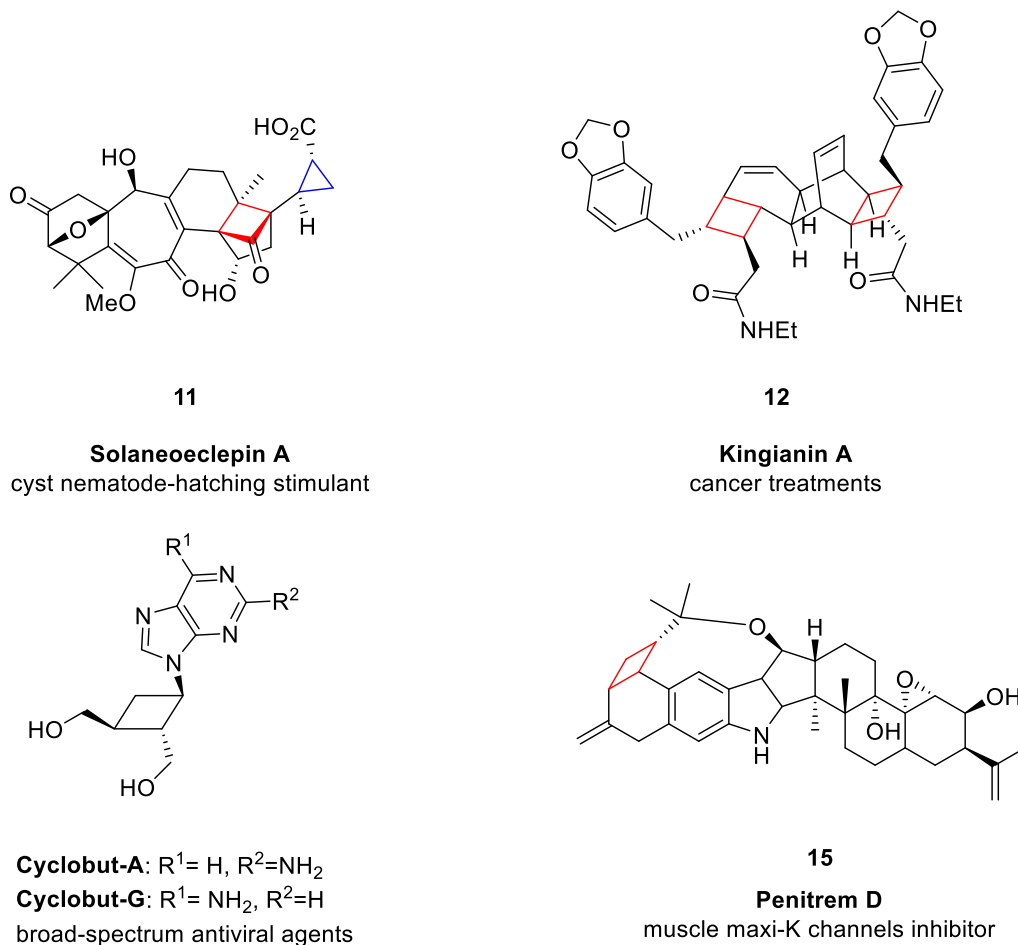


**Figure 2-7: Stabilization of Cyclopropylmethyl Cation by Hyperconjugation**

### 2.1.3 The Chemistry of Cyclobutanes

Among the small carbocycles, four-membered rings have always attracted organic chemists' attentions. Despite of their high strain structure, their presence in organic natural products has been extensively explored.<sup>81</sup> There is a large group of natural compounds possessing biological activity containing cyclobutane and cyclobutanone structures.<sup>82</sup> For instance, solanoecelepin A (**11**), a cyst nematode-hatching stimulant contains cyclopropyl substituted cyclobutanones,<sup>82,83</sup> kingianin A (**12**), used in cancer treatments has two cyclobutane moieties,<sup>84</sup> cyclobut A (**13**) and G (**14**), are broad-spectrum antiviral agents,<sup>85-87</sup>

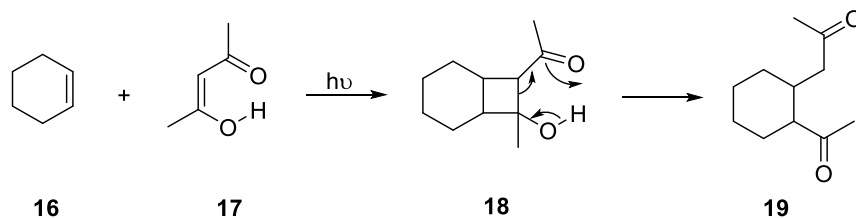
and penitrem D (**15**), which is an architecturally complex alkaloid, acts as a muscle maxi-K channel inhibitor (Figure 2-8).<sup>88–90</sup>



**Figure 2-8: Complex Natural Compounds Containing Cyclobutanes and Cyclobutanones**

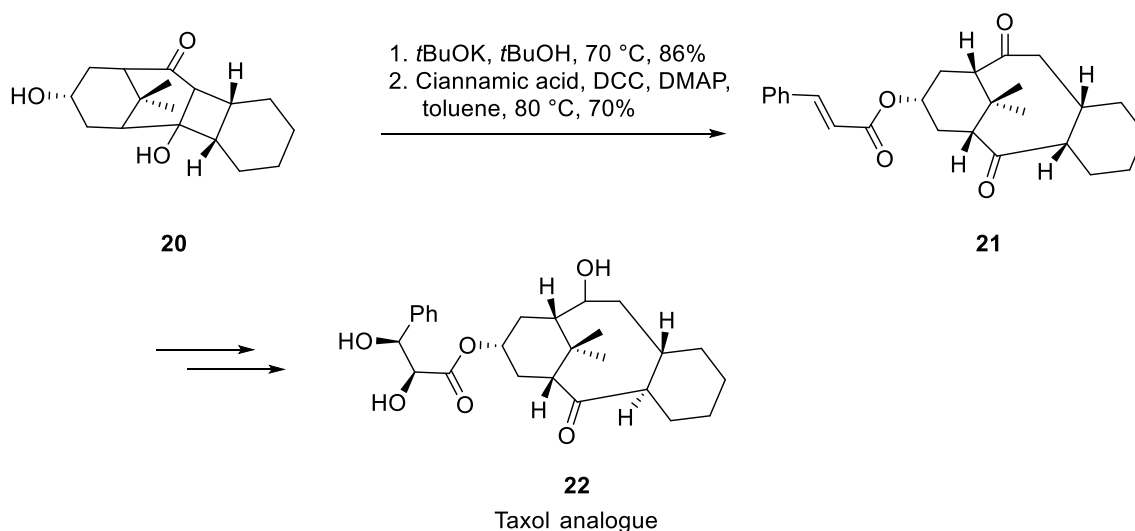
Despite the higher stability of cyclobutanes relative to cyclopropanes, they have noticeable reactivity under proper reaction conditions.<sup>91</sup> Cyclobutanes can undergo ring opening, oxidative ring expansion, fragmentation and ring contraction which are all synthetically applicable processes.<sup>92</sup>

In 1963, De Mayo and Takeshita showed the ring opening of the cyclobutane to generate 1,5-diketones **19** in a retro aldol reaction under photochemical conditions (Scheme 2-1).<sup>93</sup>



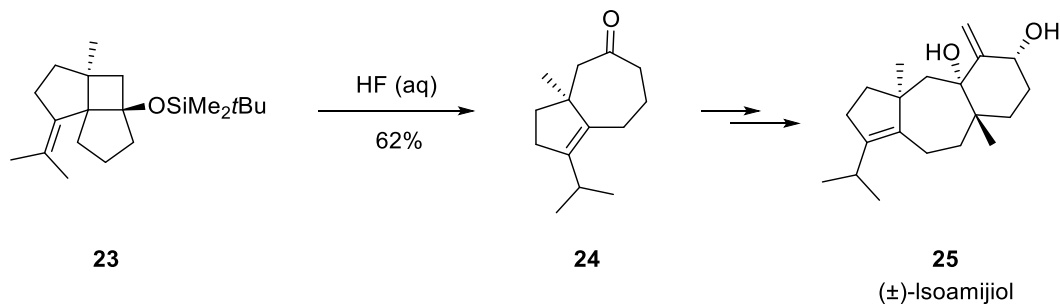
**Scheme 2-1: Retro Aldol Reaction to 1,5-diketones**

Later on, this method was applied as a key step in the total synthesis of taxol analogue **22** by Blechert, *et al.*<sup>94</sup> They were able to construct the medium sized ring core structure via cyclobutane ring opening of compound **20** under basic conditions (Scheme 2-2).



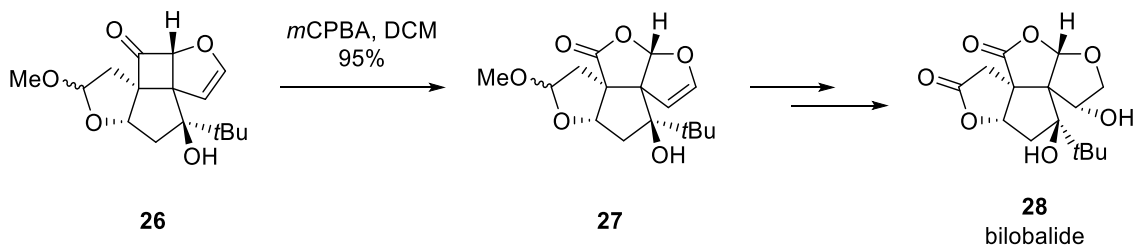
**Scheme 2-2: The Key Step in the Total Synthesis of the Taxol Analogue**

Cyclobutane fragmentation processes have been extensively used in a variety of total syntheses. For example, Pattenden in 1998 reported a Grob fragmentation of the siloxycyclobutane **23** to construct the hydroazulene ring **24** in the presence of aqueous HF. This method was applied in the total synthesis of (±)-isoamijiol **25** (Scheme 2-3).<sup>95</sup>



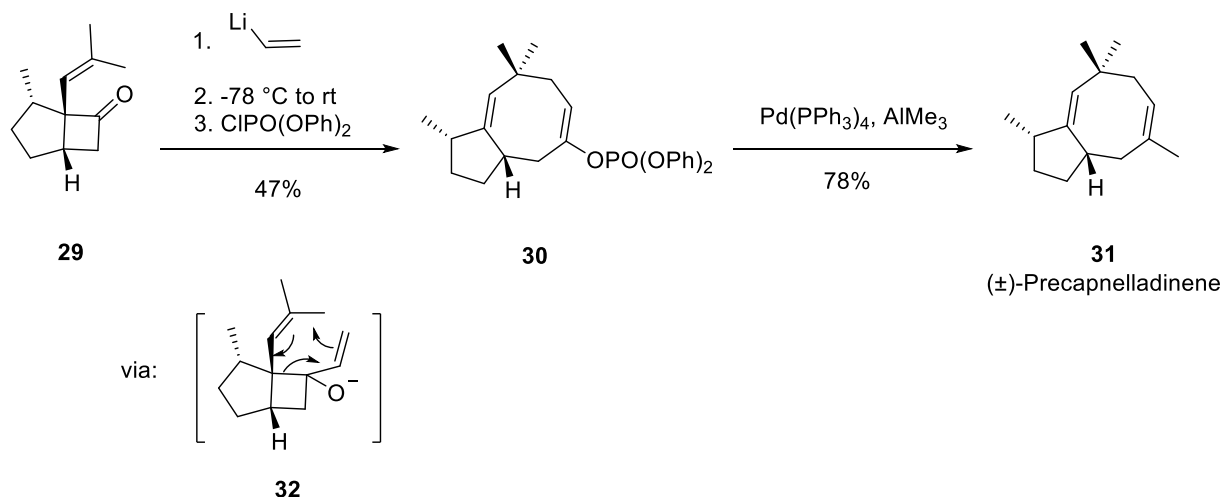
### Scheme 2-3: Grob Fragmentation of the Siloxycyclobutane

Not only cyclobutanes, but also cyclobutanones have been used effectively in synthetic pathways, which readily undergo ring expansion under oxidative conditions. The Baeyer-Villiger oxidation of cyclobutanones can be applied to introduce  $\gamma$ -lactone rings. An interesting example of this process was shown in the total synthesis of the tetracyclic trilactone bilobalide **28** by the Crimmins group.<sup>96</sup> They performed a regioselective Baeyer-Villiger oxidation of the cyclobutanone **26** to install the second  $\gamma$ -lactone ring in late stage intermediate **27** (Scheme 2-4).



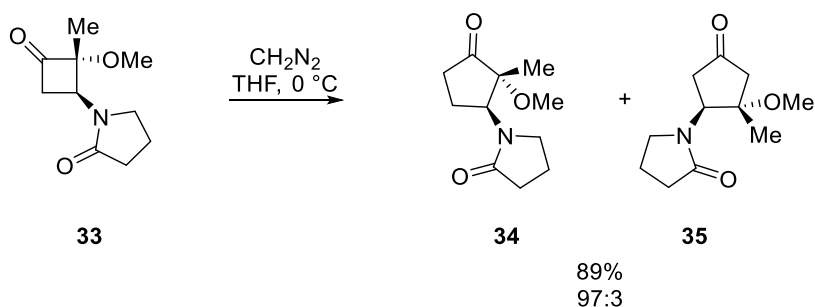
### Scheme 2-4: Baeyer-Villiger Oxidation of the Cyclobutanones

Vinyl substituted cyclobutanones have been considered as a potential precursor for the formation of eight membered rings. In 1998, Moore *et. al*, reported the ring expansion of  $\alpha$ -vinyl cyclobutanone **29** in the presence of vinyl lithium. Oxy-Cope rearrangement via intermediate **32** introduces the eight membered ring (**30**) required for the synthesis of (±)-precapnelladiene **31** (Scheme 2-5).<sup>97</sup>



### Scheme 2-5: Oxy-Cope Ring Expansion of Vinyl Cyclobutanone

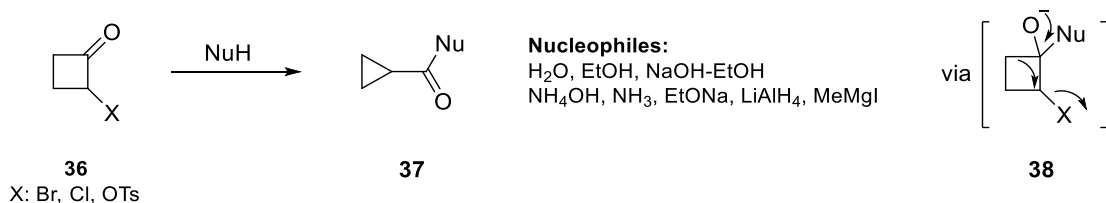
Further studies on the ring expansion of cyclobutanones were reported by Hegedus, *et al.*<sup>98</sup> They reported a regioselective homologation of the cyclobutanone **33** to generate cyclopentanones **34** and **35** in the presence of diazomethane. The ring expansion occurs via the migration of the less substituted carbon to generate cyclopentanones with high regioselectivity (Scheme 2-6).



### Scheme 2-6: Ring Expansion of Cyclobutanones to Cyclopentanones

In addition, cyclobutanones can also undergo ring contraction to three membered rings.<sup>99,100</sup> Interconversion of  $\alpha$ -halogenated (or tosylated) cyclobutanones **36** to the corresponding cyclopropanecarboxylic acid **37** occurs under basic condition with high yield and stereospecificity. Conia and Salaun found this ring contraction does not happen through

a Favorskii rearrangement; in fact it occurs under a pinacol type interconversion (Scheme 2-7).<sup>99</sup>

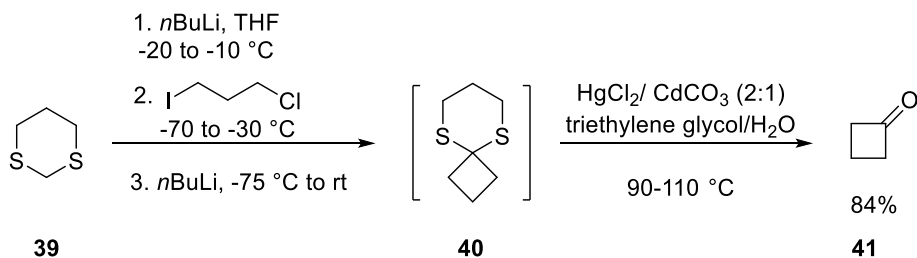


**Scheme 2-7: Ring Contraction of Cyclobutanones**

### 2.1.4 Synthesis of Cyclobutanones

In light of the synthetic utility of four-membered rings, along with the importance of this unit in the structure of natural products, a variety of methods to develop strained cyclobutane and cyclobutanones have been reported.

One of the earliest examples for the synthesis of cyclobutanones was reported by Seebach and Corey in 1967.<sup>101</sup> They studied a one-pot reaction of 1,3-dithiane derivatives (**39**) with 1,3-dihalopropanes in the presence of a strong base. Deprotection of spiro dithiane **40** provided cyclobutanone **41** in 84% yield (Scheme 2-8).



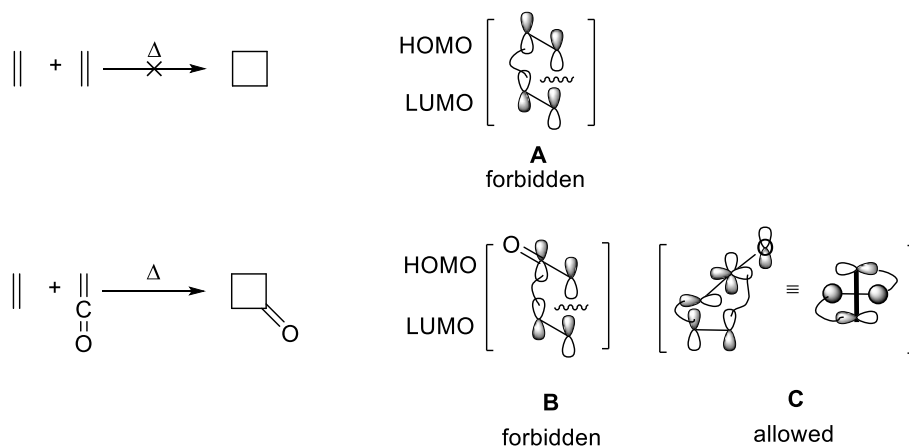
**Scheme 2-8: Construction of Cyclobutanone Employing [1,3]-Dithiane**

Despite extensive applications of this method to afford more highly substituted rings in various sizes, this method suffered from a limited reaction scope. The presence of sensitive functional groups such as ketones and hydroxyl moieties can prevent cyclization to desired products. Therefore, exploring more efficient pathways to construct cyclobutanone rings was inescapable.

#### 2.1.4.1 [2+2]-Cycloaddition of Ketenes and Alkenes

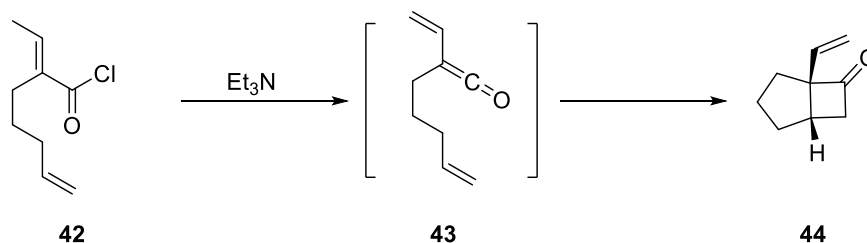
One of the most common methods to establish a cyclobutanone ring is the concerted [2+2]-cycloaddition of ketenes and alkenes. Generally, thermal [2+2]-cycloaddition is a symmetry

forbidden process according to the Woodward-Hoffmann rules (Figure 2-9, model A),<sup>45</sup> however, the [2+2]-cycloaddition of ketenes with alkenes is considered as an allowed process (model B). The ketene possesses two sets of  $\pi$ -orbitals at right angles. This orbital alignment allows the molecule to adopt the orthogonal orientation to develop the desired orbital overlapping required for concerted thermal cycloaddition (model C).<sup>45</sup>



**Figure 2-9: Orbital Symmetry For the [2+2]-Cycloadditions**

There are a large number of reported reactions involving concerted [2+2]-cycloadditions to cyclobutanones.<sup>102–105</sup> For example, the Snider group reported an intramolecular [2+2]-cycloaddition of an alkene with unsaturated ketene. *In situ* generation of ketene **43** was achieved by the treatment of acid chloride **42** with  $\text{Et}_3\text{N}$  followed by intramolecular cycloaddition to cyclobutanone **44** (Scheme 2-9).<sup>105</sup>



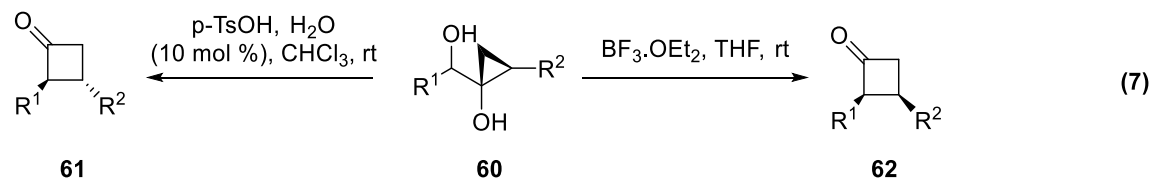
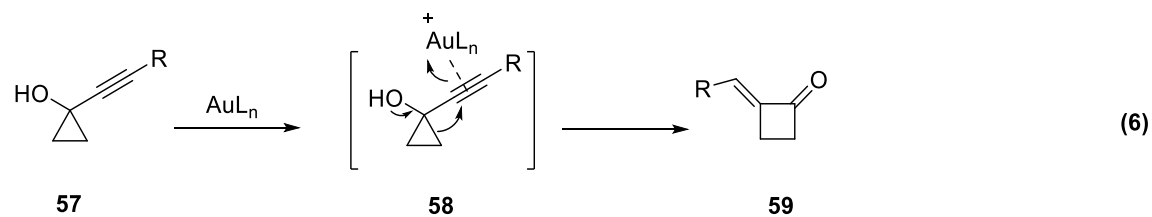
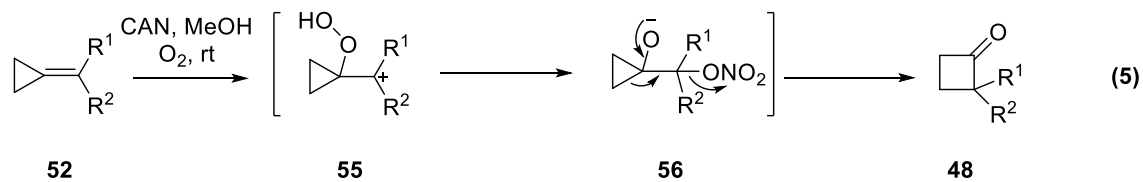
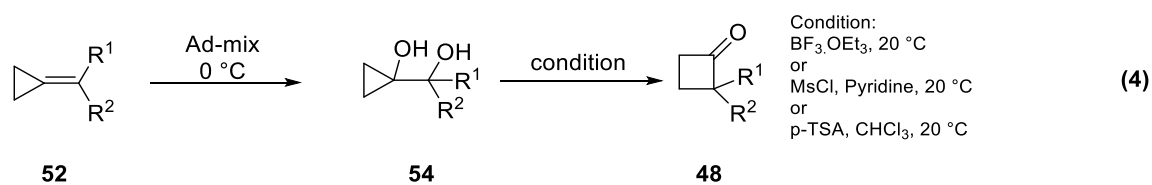
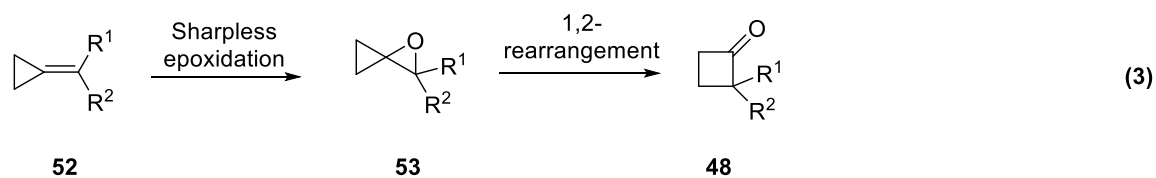
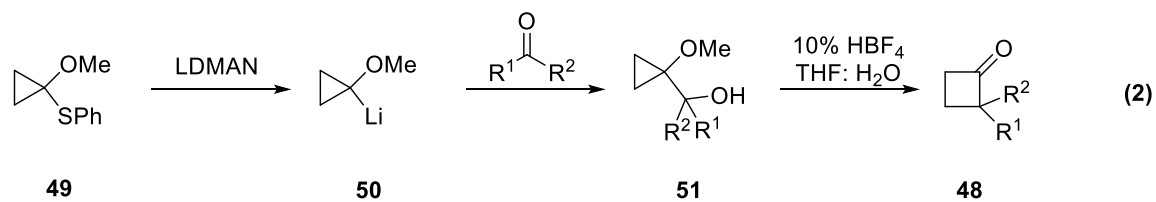
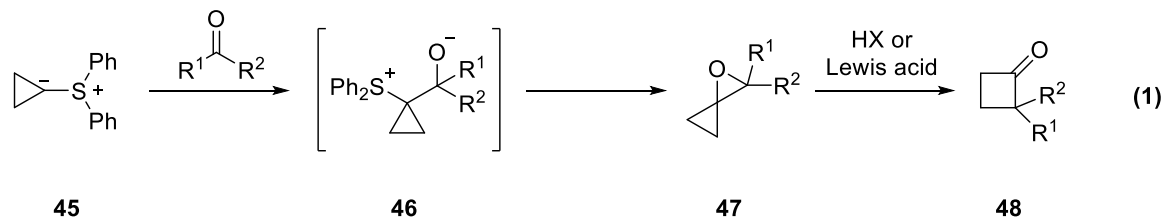
**Scheme 2-9: Intramolecular [2+2]-Cycloaddition**

#### 2.1.4.2 Cyclopropyl Ring Expansion to Cyclobutanones

Cyclopropyl ring expansion processes have been widely used in the synthesis of the cyclobutanones. A large number of reactions have been reported employing different types of the reagents and intermediates possessing cyclopropane rings capable of ring expansion to cyclobutanones (Scheme 2-10). Trost and coworkers employed sulfur ylide **45** to construct



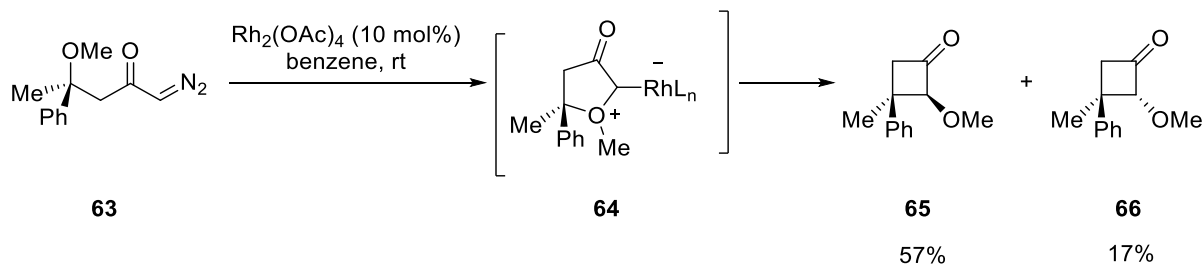
oxaspiropentanes **47** as efficient precursors to cyclobutanones **48** under Brønsted or Lewis acidic conditions (eq. 1).<sup>106-111</sup> In 1981, Cohen and Matz explored the lithiation of 1-thiophenyl-1-methoxy cyclopropane **49** to construct substituted cyclobutanones **48** (eq. 2).<sup>112</sup> Also, epoxidation (eq. 3)<sup>113</sup>, dihydroxylation (eq. 4)<sup>114,115</sup> and CAN mediated oxidation<sup>116</sup> (eq. 5) of methylenecyclopropanes **52** (MCPs) have been widely used as potential pathways to construct cyclobutanone rings. Gold-catalyzed ring expansion of alkynylcyclopropanols<sup>117</sup> **57** (eq. 6) and acid promoted ring expansion cyclopropylmethanols<sup>118</sup> **60** (eq. 7) were also employed as facile methods to construct cyclobutanones.



**Scheme 2-10: Cyclopropane Ring Expansions to Cyclobutanones**

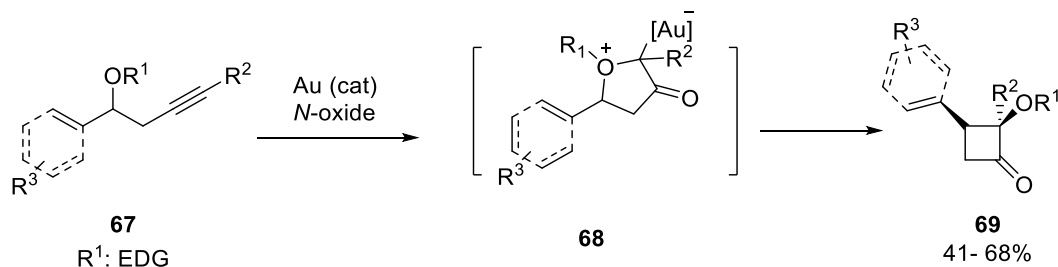
### 2.1.4.3 Transition Metal Catalyzed Synthesis of Cyclobutanones

In 1986, Roskamp and Johnson reported the rhodium (II) catalyzed formation of oxonium ylide **64** generated from diazo ketone **63**. The [1,2]-Stevens rearrangement of oxonium ylide **64** afforded cyclobutanone derivatives in moderate yield provided the substituents on the migrating carbon were aromatic groups, vinyl, or ether moieties (Scheme 2-11).<sup>48</sup>



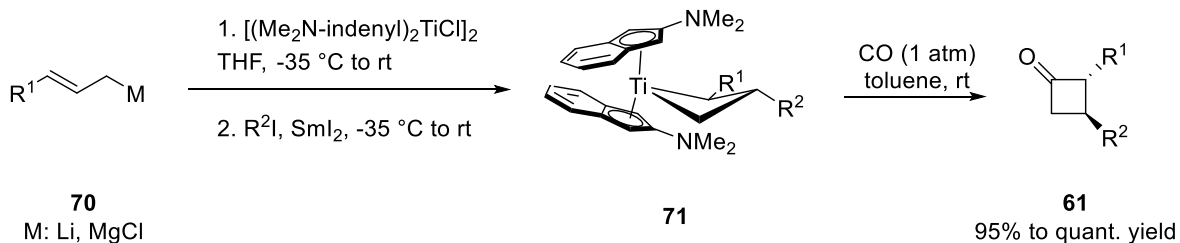
**Scheme 2-11: Rhodium (II) Catalyzed Formation of Cyclobutanones**

Also, in 2013, Li and coworkers reported the gold catalyzed formation of oxonium ylide **68** from homopropargylic ethers **67**. They showed the Stevens rearrangement of the ylide **68** provided cyclobutanones **69** provided an aromatic or allyl substituent was present on the migrating carbon (Scheme 2-12).<sup>50,51</sup> The *cis*-cyclobutanone was the only isolated diastereomer.



**Scheme 2-12: Synthesis of Cyclobutanones From Homopropargylic Ethers**

Stryker and coworkers also reported that cyclobutanones **61** can be obtained in high yield through the carbonylation of titanacyclobutane complexes **71**, which are prepared from allylic Grignard or lithium reagents **70**.<sup>119</sup> This transformation can be carried out in a one-pot process in moderate yield (Scheme 2-13).



### Scheme 2-13: Carbonylation of Titanacyclobutanes

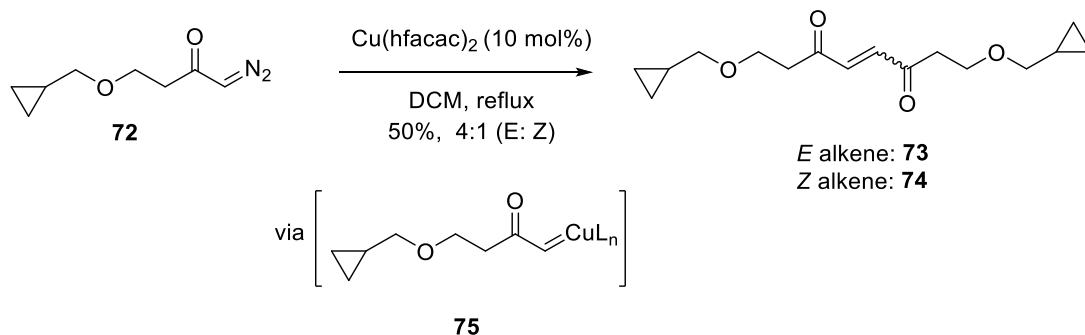
Enantioselective Rh(I) catalyzed synthesis of cyclobutanones,<sup>119</sup> photolytic reaction of chromium carbene complexes with alkenes,<sup>120</sup> are also other valuable pathways to construct cyclobutanones.

## 2.2 Results and Discussions

### 2.2.1 Background

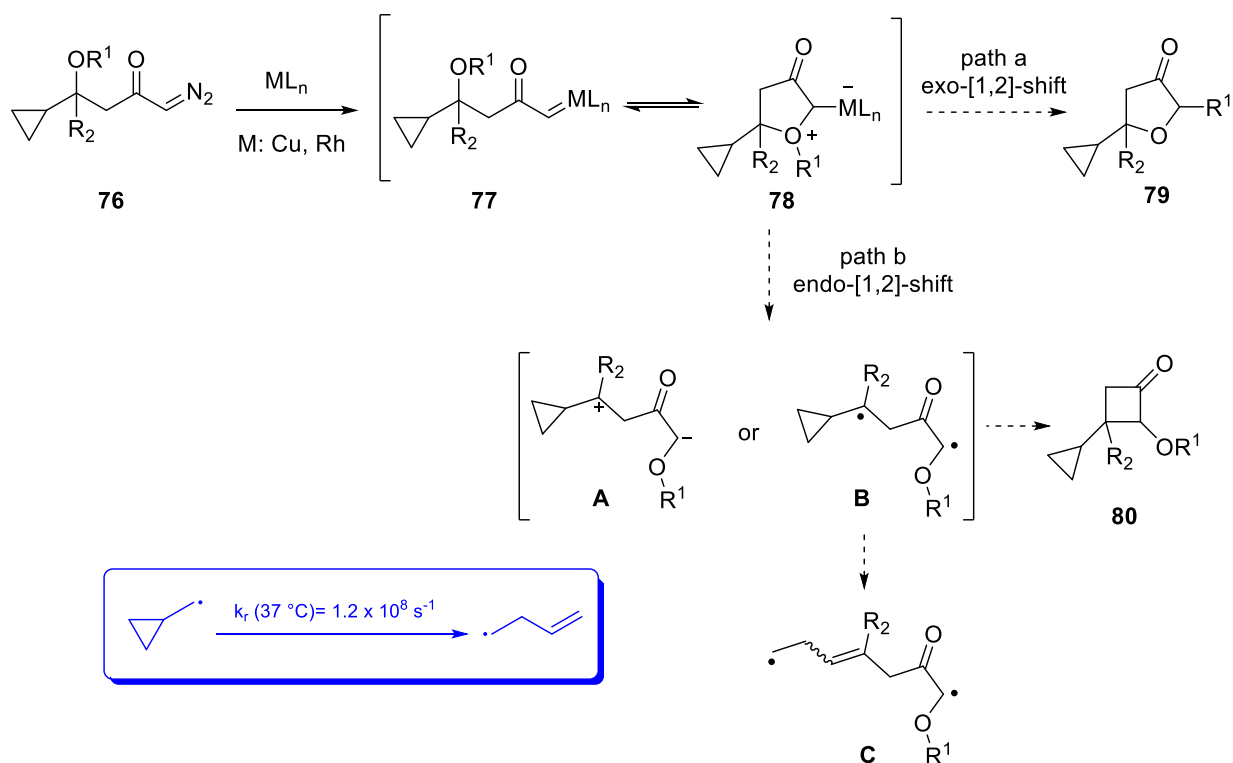
The chemistry of oxonium and ammonium ylides has been studied extensively by the West group.<sup>24,46,52,56,57,68,121–125</sup> The Stevens [1,2]-shift of oxonium ylides has been employed by West and coworkers to prepare a variety of natural products and heterocycles.<sup>40,46,52,68</sup> Aside from a very unique application of the Stevens rearrangement, we were also interested in investigating its mechanism. It has been proposed that the Stevens rearrangement occurs through the formation of radical pairs. Except CIDNP spectroscopy for the ammonium ylides<sup>36</sup> and the formation of homodimers during the Stevens rearrangement<sup>40</sup> no strong evidence demonstrating the presence of radical pairs has been reported. For this purpose we considered employing a cyclopropylcarbinyl moiety as a radical clock to study whether the reaction mechanism involves radical intermediates.

The preliminary studies on the mechanism of the Stevens rearrangement by our previous group member, Dr. Jeffrey Johnston, showed that treatment of unbranched diazo ketone **72** with Cu(hfacac)<sub>2</sub> did not provide the *exo*-[1,2]-shift of cyclopropylmethyl group and *trans*- and *cis*- alkenes **73** and **74** were the only isolated products (Scheme 2-14).



### Scheme 2-14: Preliminary Results

On the other hand, he investigated the formation of oxonium ylide **78** possessing the cyclopropylcarbiny moiety as a tentative migrating group from the diazo ketone **76**. In the case of an endocyclic [1,2]-shift (Scheme 2-15, path b) both ionic **A** and biradical **B** intermediates may be envisioned. According to the fast ring opening of the cyclopropylcarbiny, observing the hypothetical products from acyclic biradical **C** will demonstrate the intermediacy of radical pair intermediates in the reaction mixture. During our studies we encountered the formation of cyclobutanones **80** possessing cyclopropane substituents resulting from an endocyclic Stevens rearrangement. Observing no cyclopropane ring opening during the Stevens rearrangement prompted us to study the generality of this methodology as well as further mechanistic investigation of the Stevens rearrangement.



### Scheme 2-15: Plausible Pathways for Decomposition of Diazo Ketone 76

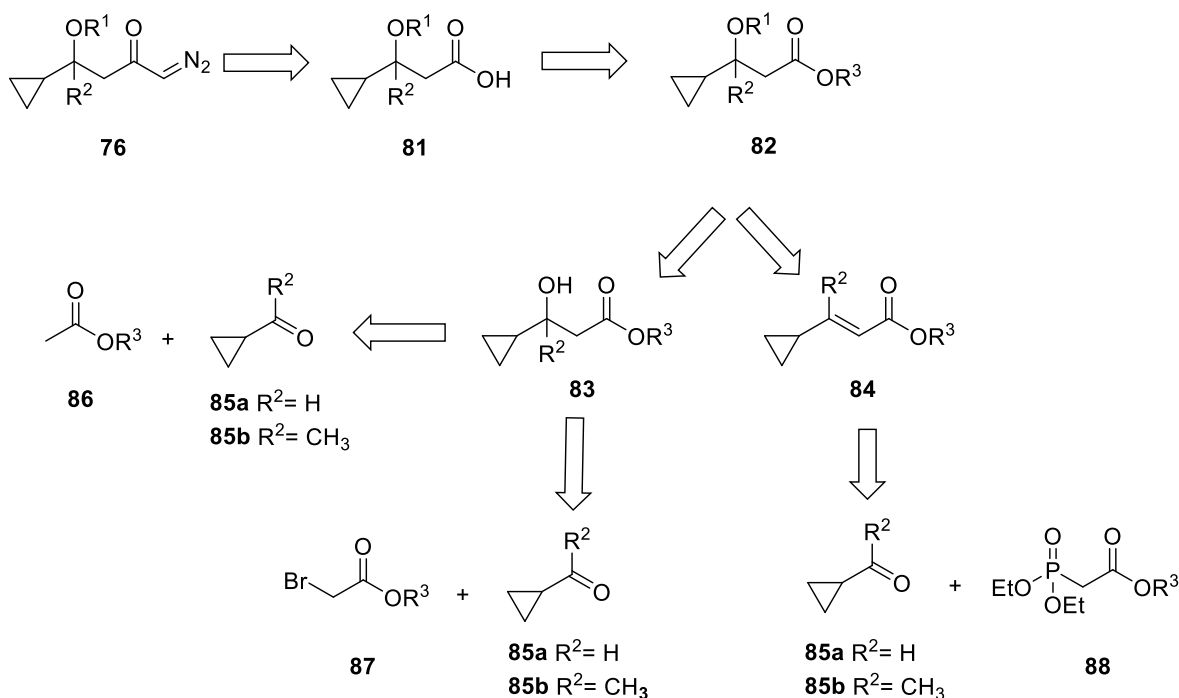
In this chapter the generality of the formation of cyclobutanones via the endocyclic Stevens rearrangement of the cyclopropylcarbinyll moiety will be described and more results regarding the reactivity of unbranched diazo ketone **72** as well as the detailed mechanistic studies will be discussed in Chapter 3.

Regarding the importance of the cyclobutanones in natural products and synthetic chemistry, along with the attractiveness of constructing strained structures we were inspired to further expand substrate scope studies. To the best of our knowledge, cyclopropylcarbinyll has never been employed as a migrating group in the Stevens rearrangement. Considering the stabilizing effect of the cyclopropyl ring by hyperconjugation in cyclopropylmethyl cation (Figure 2-7) and radical, we wanted to determine if the cyclopropylcarbinyll could be a competent migrating group in the [1,2]-Stevens rearrangement of cyclic oxonium ylides. This fundamental question led us to propose diazo ketone substrate **76** capable of forming a cyclic oxonium ylide **78** in the presence of transition metal catalyst. The migratory aptitude of the cyclopropyl can be studied in the presence of competing migrating group  $R^1$  in ylide **78**. The

exocyclic Stevens rearrangement may take place to generate tetrahydrofuran **79** by the [1,2]-shift of the R<sup>1</sup> group (Scheme 2-15, path a), or an endocyclic process would occur to construct a highly strained and synthetically interesting structure possessing both cyclobutanone core structure and cyclopropyl substituent **80** (Scheme 2-15, path b).

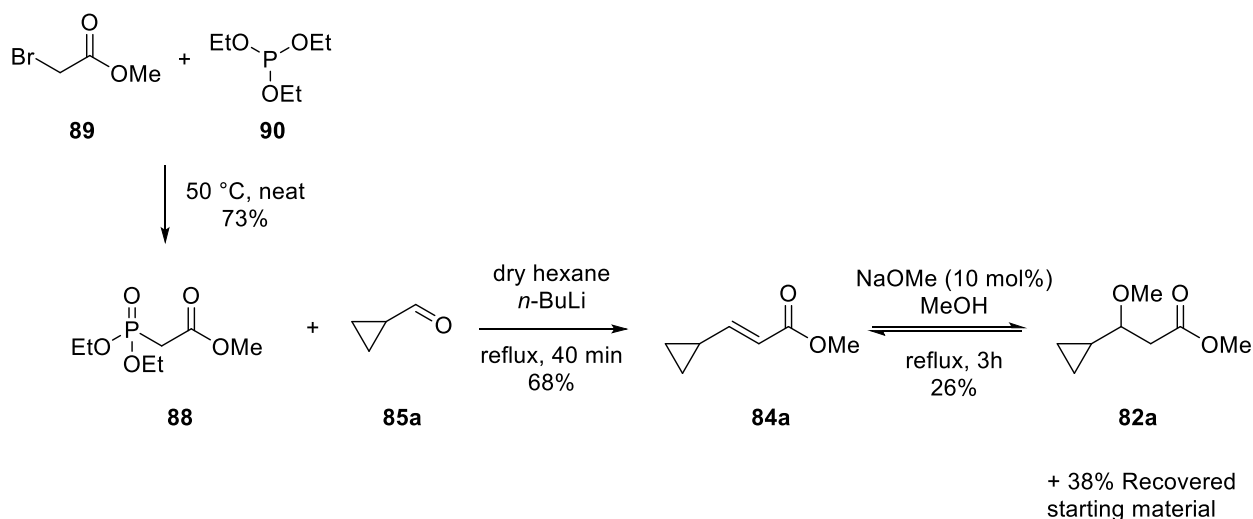
### 2.2.2 Substrate Synthesis

Several pathways were considered to construct the requisite diazo ketones **76**. The precursor acid **81** can be synthesized from the hydrolysis of the corresponding ester **82** which is derived from either alkylation of the secondary alcohol **83** or Michael addition of alkoxide to unsaturated ester **84**. The required alcohol **83** may be generated via aldol addition or Reformatsky reaction between aldehyde **85a** and ketone **85b** with alkyl acetate **86** or bromoacetic ester **87** respectively. On the other hand, we proposed a Horner-Wadsworth-Emmons reaction between **85** and phosphonate **88** to generate unsaturated ester **84** (Scheme 2-16).



**Scheme 2-16: Retrosynthesis of the Diazo Ketone 76**

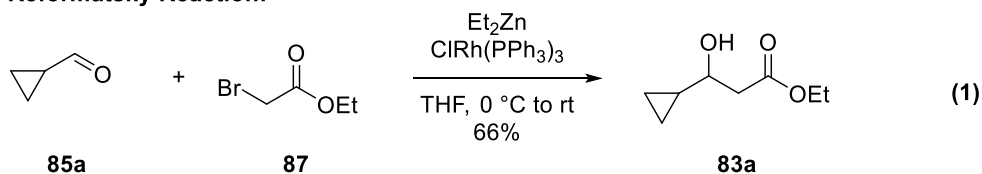
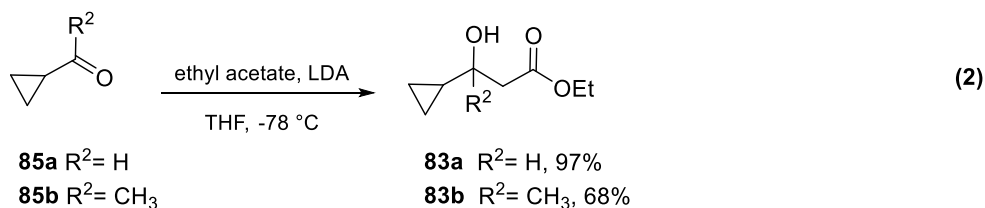
The first effort for the preparation of  $\alpha,\beta$ -unsaturated ester **84a** was successful via Horner-Wadsworth-Emmons (HWE) reaction in a moderate yield (Scheme 2-17). The required phosphonate **88** was prepared using methyl bromoacetate **89** and triethylphosphite **90**<sup>126</sup> followed by the reaction with cyclopropylcarboxaldehyde **85a** under basic condition. Michael addition of the methoxide ion to the  $\alpha,\beta$ -unsaturated methyl ester **84a** provided the branched cyclopropane **82a** in a low yield, along with unreacted starting material (Scheme 2-17). We proposed an equilibrium between the product and  $\alpha,\beta$ -unsaturated ester under basic conditions is responsible for the low yield.



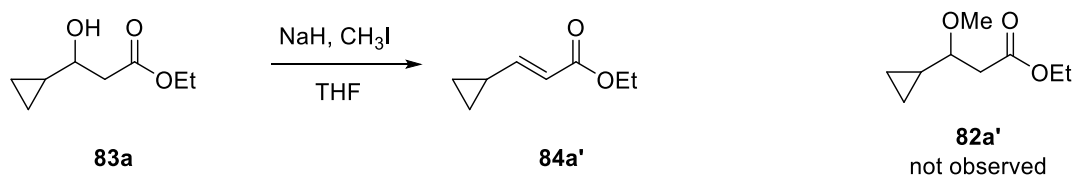
### Scheme 2-17: Synthesis of Ester **82a** via Michael Addition

The poor yield for the formation of **82a** led us to a different approach, alkylation of alcohol **83**. Alcohol **83a** was prepared via rhodium-catalyzed Reformatsky reaction of cyclopropanecarboxaldehyde **85a** and bromoester **87** (Scheme 2-18, eq. 1)<sup>127</sup> as well as the aldol reaction between cyclopropylcarboxaldehyde **85a** and ethyl acetate (Scheme 2-18, eq. 2). Both methods provided the required alcohols in acceptable yield.

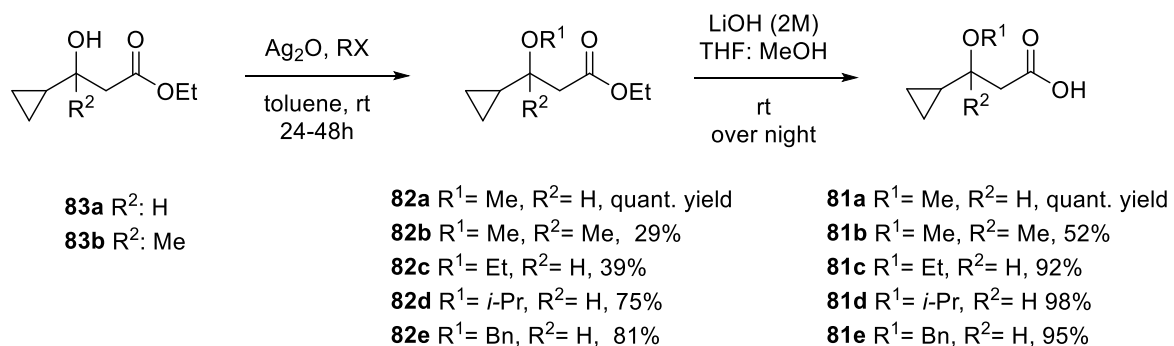


**Reformatsky Reaction:****Aldol Reaction****Scheme 2-18: Synthesis of Secondary Alcohols 83**

With secondary alcohols **83a** in hand, we opted to alkylate the alcohol to prepare the desired ester **82**. Treating the alcohol **83a** with methyl iodide under basic condition generated cyclopropyl acrylate **84a'** and no alkylated alcohol (**82a'**) was observed (Scheme 2-19).

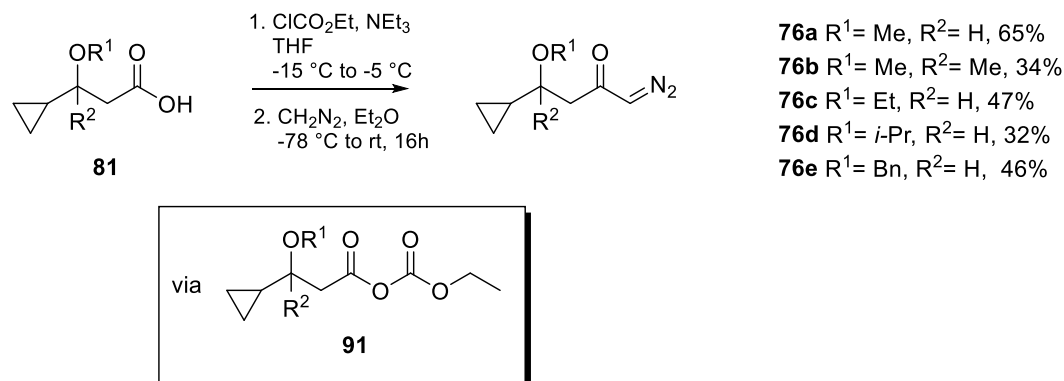
**Scheme 2-19: Attempted Alkylation of Alcohols under Basic Condition**

It seemed the presence of acidic  $\alpha$ -protons in alcohol **83a** competes with the elimination of MeOH from the **82a'** under basic conditions to generate  $\alpha,\beta$ -unsaturated ethyl ester **84a'**. Fortunately we found that freshly prepared silver oxide and appropriate alkyl halide could be used to generate ethers **82** from alcohols **83** in acceptable yield.<sup>128</sup> We continued our synthesis by hydrolyzing the esters **82** to the corresponding acids **81** in the presence LiOH. The required carboxylic acids could be isolated as precursors for the preparation of diazo ketones **76** (Scheme 2-20).



**Scheme 2-20: Synthesis of Required Acid Precursors**

Our first attempt to complete the synthesis of the desired diazo ketones **76** necessary for the oxonium ylide formation was unsuccessful. Treatment of the carboxylic acid **81** with oxalyl chloride to generate the corresponding acyl chloride. Unfortunately these conditions led to the decomposition of the starting material without producing the desired product. We shifted to an alternative method to construct the mixed anhydrides **91**, which reacted with diazomethane to afford the desired diazo ketones **76** with reasonable yields (Scheme 2-21).

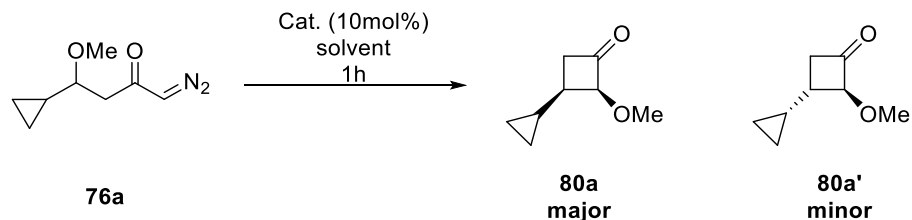


**Scheme 2-21: Preparation of Diazo Ketones 76**

### 2.2.3 Formation of the Cyclobutanone Derivatives

The initial effort to study the migratory aptitude of cyclopropylcarbonyl in an endocyclic [1,2]-Stevens rearrangement provided the isolable and stable cyclobutanones **80** with the intact cyclopropane substituent (Table 2-1). We treated the diazo ketone **76a** with catalytic Cu(hfacac)<sub>2</sub> in DCM at room temperature and the cyclobutanones **80a** and **80a'** were isolated in 60% yield and 6:1 diastereomeric ratio (Table 2-1, entry 1). Reducing the reaction temperature to -10 °C resulted in incomplete consumption of starting material (entry 2). On the other hand, refluxing DCM (entry 3) provided an improved yield without affecting the

diastereoselectivity. We were also interested in studying the effect of the catalyst on this reaction. We treated the diazo ketone **76a** with less electron-poor Cu catalysts  $\text{Cu}(\text{tfacac})_2$  (entry 4) and  $\text{Cu}(\text{acac})_2$  (entry 5). In both cases, cyclobutanones **80** were isolated in lower yield and diastereoselectivity. Treatment of diazo ketone **76a** with Cu powder showed no reaction and starting material was recovered. This observation demonstrates no catalytic activity of copper powder to form the metallocarbene in this reaction (entry 6). Using stoichiometric copper powder while increasing reaction time and temperature provided trace cyclobutanones observed in crude  $^1\text{H}$  NMR (entry 7).  $\text{Rh}_2(\text{OAc})_4$  was also a competent catalyst to generate cyclobutanones, although the yield and diastereoselectivity were lower compared to  $\text{Cu}(\text{hfacac})_2$  (entry 8). To study the effect of the solvent, both toluene (entry 9) and benzene (entry 10) were examined, and both provided comparable yields, although the diastereoselectivities showed a significant decrease in both cases.

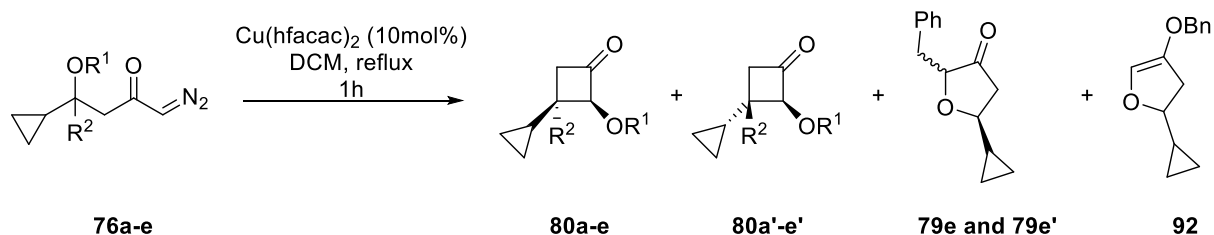
**Table 2-1: Optimization of Cyclobutanones Formation**

Entry	Catalyst	Solvent	Temp (°C)	Yield (%) <sup>a</sup>	dr <sup>b</sup>
1	Cu(hfacac) <sub>2</sub>	DCM	rt	60	6:1
2	Cu(hfacac) <sub>2</sub>	DCM	-10	50 <sup>c</sup>	6:1
<b>3</b>	<b>Cu(hfacac)<sub>2</sub></b>	<b>DCM</b>	<b>reflux</b>	<b>80</b>	<b>6:1</b>
4	Cu(tfacac) <sub>2</sub>	DCM	reflux	72	2:1
5	Cu(acac) <sub>2</sub>	DCM	reflux	65	1:1
6	Cu powder	DCM	reflux	No reaction	-
7	Cu powder (1 eq)	DCM	reflux	ND <sup>d</sup>	1:1
8	Rh <sub>2</sub> (OAc) <sub>4</sub>	DCM	reflux	73	2.2:1
9	Cu(hfacac) <sub>2</sub>	toluene	reflux	75 <sup>e</sup>	2.5:1
10	Cu(hfacac) <sub>2</sub>	benzene	reflux	80	4:1

<sup>a</sup>Combined yield of both diastereomers. <sup>b</sup>Ratio was determined by <sup>1</sup>H NMR analysis of products via the integration of the OMe peaks. <sup>c</sup>45% starting diazocarbonyl was recovered. <sup>d</sup>Reaction mixture was heated at reflux for 16h and a very messy crude mixture was obtained and the presence of cyclobutanones and starting material was confirmed by crude <sup>1</sup>H-NMR spectrum. <sup>e</sup>The cyclobutanones **80a** and **80a'** were not isolated as a pure mixture due to very complicated reaction mixture.

With optimized conditions in hand (Table 2-1, entry 3), we investigated the substrate scope for the formation of cyclopropane substituted cyclobutanones. Diazo ketones **76** were synthesized via the aforementioned procedure and were subjected to the optimized condition.

**Table 2-2: Substrate Scope**

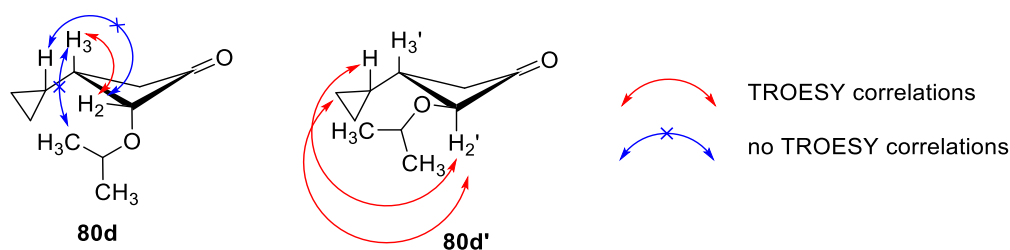


Entry	Diazo ketone	R <sup>1</sup>	R <sup>2</sup>	Product (s) [dr] <sup>a</sup>	Yield (%) <sup>b</sup>
1	<b>76a</b>	Me	H	<b>80a+80a'</b> [6:1]	80
2	<b>76b</b>	Me	Me	<b>80b+80b'</b> [1.4:1]	50
3	<b>76c</b>	Et	H	<b>80c+80c'</b> [6:1]	70
4	<b>76d</b>	<i>i</i> -Pr	H	<b>80d+80d'</b> [4.8:1]	78
5	<b>76e</b>	Bn	H	<b>80e+80e'</b> [2.5:1]/ <b>79e+79e'</b> [1.5:1]	40 <sup>c,d</sup>

<sup>a</sup>Ratio was determined by <sup>1</sup>H NMR analysis of products via the integration of the OMe peaks.

<sup>b</sup>Combined yield of both diastereomers. <sup>c</sup>Combined yield of four inseparable products. <sup>d</sup>A trace amount of **92** was also isolated

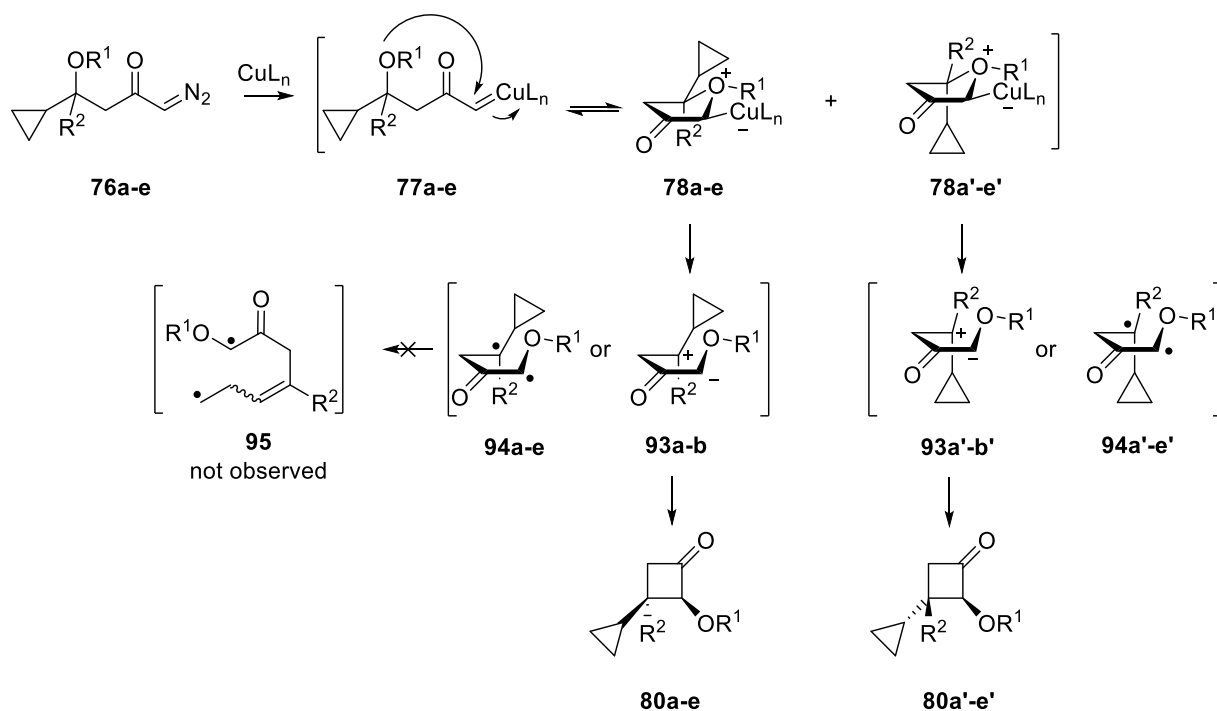
Diazo carbonyl **76b** having a quaternary migrating carbon provided the desired *cis*- and *trans*- cyclobutanones **80b** and **80b'** with 50% yield and 1.4:1 diastereoselectivity (entry 2). Also, diazo ketones **76c** and **76d** containing O-ethyl and O-*i*Pr substituents provided the corresponding cyclobutanones in acceptable yield (entry 3 and 4). Interestingly, having a benzyl substituent on the oxygen furnished two [1,2]-rearrangement pathways, giving cyclobutanones **80e** and **80e'**, as well as inseparable tetrahydrofurans **79e** and **79e'**. A trace amount of enol ether **92** was also isolated resulted from Cu assisted [1,4]-benzyl migration.<sup>63</sup> The relative configuration of the two cyclobutanone diastereomers was determined by a careful analysis of the TROESY spectra of **80d** and **80d'**, which is in agreement with the previously reported cyclobutanone formation from oxonium ylides.<sup>48,129</sup> TROESY analysis of the major diastereomer **80d** indicated a *cis*- relationship between H-2/H-3 as well as the absence of the correlations between methyl protons/H-3 and cyclopropyl protons/H-2. In the case of the minor diastereomer **80d'**, correlations between cyclopropyl protons and H-2' provided evidence for *trans* geometry (Figure 2-10). These assignment could be applied to the other cyclobutanone derivatives due to very close similarity of their <sup>1</sup>H NMR spectra.



**Figure 2-10: TROESY Correlations of Cyclobutanones 80d and 80d'**

### 2.2.4 Mechanistic Proposal

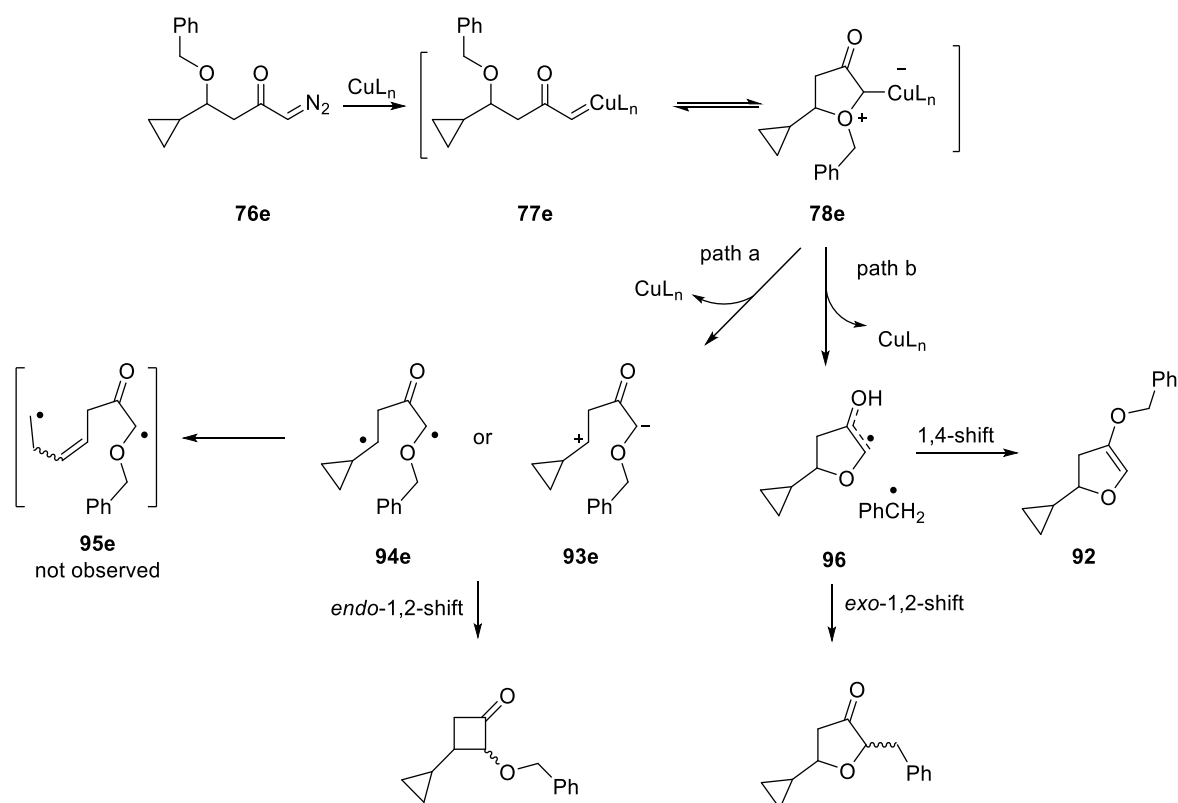
The formation of metallocarbenes from diazo compounds in the presence of transition metal catalysts is a known process. With this fact in mind, we assumed that metallocarbene **77**, resulting from the treatment of diazo ketone **76** with copper catalyst undergoes a very fast intramolecular cyclization using the ethereal oxygen to form the cyclic oxonium ylide **78** (Scheme 2-22). Since a concerted [1,2]-shift with the retention of configuration is symmetry-forbidden,<sup>45</sup> the presumed stepwise pathway could proceed via either heterolytic or homolytic cleavage while reactive intermediates do not drift apart in a solvent cage. The [1,2]-rearrangement could take place by either the migration of the R group from oxygen to generate tetrahydrofuran derivatives (Scheme 2-15, path a) or by ring contraction to cyclobutanones by the [1,2]-shift of the cyclopropylcarbinyl moiety (Scheme 2-15, path b). In case of a sluggish migrating group (Me, Et, *i*-Pr), ring contraction is the only reactive pathway showing the strong ability of cyclopropylcarbinyl as a migrating group. The reason for the observed diastereoselectivity is not clear. It might be explained by a very fast recombination of the short-lived zwitterionic species **93** or biradicals **94** dictated by the conformation of the oxonium ylide **78**. The reactive oxonium ylides are considered as two possible intermediates **78a-e** and **78a'-e'** with the predominant **78a-e** having Cu catalyst and cyclopropane ring in pseudo-equatorial positions (**78a-e**), which leads to the *cis*-relationship for the major cyclobutanone products. The dependence of the diastereomeric ratio to the catalyst may support the presence of metal bound intermediates in the reaction mechanism (Scheme 2-22).



### Scheme 2-22: Proposed Mechanism

On the other hand, when a competent exocyclic migrating group such as O-benzyl (**76e**) is used (Scheme 2-23), [1,2]-rearrangements of both cyclopropylcarbinyl and benzyl moiety can take place to afford cyclobutanones (Scheme 2-23, path a) and tetrahydrofurans (Scheme 2-23, path b) respectively. Also radical pairs **96** obtained from oxonium ylide **78e** can rearrange to form a trace amount of **92** resulting from [1,4]-migration of the benzyl group. [1,4]-benzyl migration to the oxygen has been shown by the West *et. al* to occur in the presence of Cu catalysts in which rearrangement is believed to take place via radical-pair intermediates.<sup>63</sup>

Observing the intact cyclopropyl ring in the products resulting from the migration of cyclopropylcarbinyl derivatives in an *endo*-[1,2]-shift can be rationalized either by very fast biradical **94e** recombination relative to the ring opening of cyclopropylcarbinyl radical, or the absence of radical pairs and instead existing zwitterionic intermediates **93e** in the reaction mechanism. To attain more mechanistic evidence for distinguishing between radical pair and ionic intermediates we opted to consider hypersensitive radical clocks which will be discussed extensively in Chapter 3.



**Scheme 2-23: Proposed Mechanism for Decomposition of Diazo Ketone 76e**

### 2.3 Conclusion

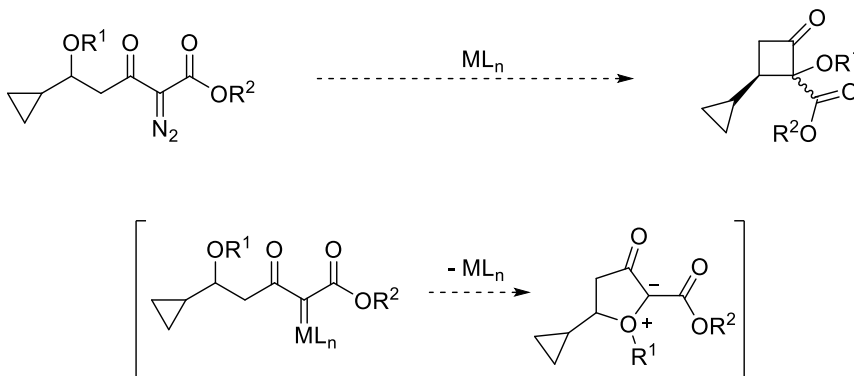
In summary, we have described an efficient synthetic method to construct strained cyclobutanone core structures via the [1,2]-Stevens rearrangement of diazo ketones. The presence of a cyclopropyl substituent in the synthesized cyclobutanones provides more strained but stable structure which is synthetically notable. We also showed the competitive ability of the cyclopropylcarbinyl moiety in endocyclic [1,2]-Stevens rearrangement. To the best of our knowledge, this is the first reported observations for cyclopropylcarbinyl migration in the [1,2]-Stevens rearrangement.

These results provide a framework for deeper mechanistic studies into the [1,2]-Stevens rearrangement. Observing the intact cyclopropane ring conceived us to study if radical pairs are the actual intermediates in this rearrangement or if a new mechanistic pathway involving zwitterion intermediates is being observed.



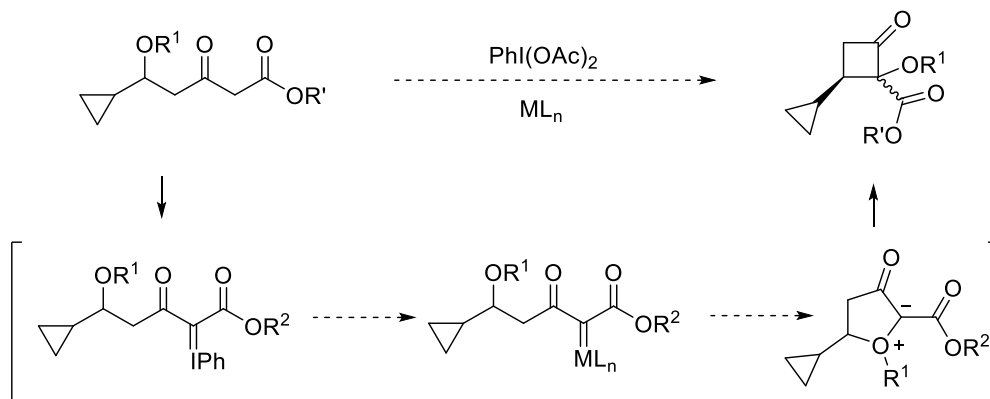
## 2.4 Future Directions

Doyle *et. al.* have reported diastereocontrolled rhodium(II) catalyzed ring closure to construct cyclobutanones utilizing *O*-silylated diazoacetates and benzyl migrating group in [1,2]-Stevens rearrangement.<sup>129</sup> On the other hand, we have observed the cyclopropylcarbinyl moiety to be a competent migrating group in the endocyclic Stevens rearrangement. This competence might be employed to construct highly substituted cyclobutanones with cyclopropyl ring as a strained substituent using diazoacetates instead of diazo ketones.



Also, the West group has studied the application of iodonium ylides as a diazo ketone alternatives in development of oxonium ylides.<sup>49</sup> Iodonium ylides can be generated *in situ* from bis(acetoxy)iodobenzene and can form metallocarbenes in the presence of Rh(II) catalysts.

The migratory aptitude of the cyclopropylcarbinyl moiety might be considered in the formation of strained cyclobutanones by employing iodonium ylides instead of diazo ketone substrates under Cu or Rh catalysis.



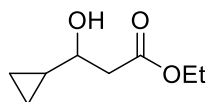
## 2.5 Experimental

### 2.5.1 General Information

Reactions were carried out in flame or oven dried glassware under a positive argon atmosphere unless otherwise stated. Transfer of anhydrous solvents and reagents was accomplished with oven-dried syringes or cannulae. Solvents and some reagents were distilled before use: methylene chloride, diisopropylamine from calcium hydride, tetrahydrofuran and diethylether from sodium/benzophenone ketyl and toluene from sodium. Diazomethane was generated based on the Sigma-Aldrich protocol from Diazald<sup>®</sup>.<sup>130</sup> All other solvents and commercially available reagents were used without further purification. Thin layer chromatography was performed on glass plates precoated with 0.25 mm silica gel; the stains for TLC analysis were conducted with 2.5 % *p*-anisaldehyde in AcOH-H<sub>2</sub>SO<sub>4</sub>-EtOH (1:3:86) and further heating until development of color. Flash chromatography was performed on 230-400 mesh silica gel with the indicated eluents. Nuclear magnetic resonance (NMR) spectra were recorded in indicated deuterated solvents and are reported in ppm in the presence of TMS as internal standard and coupling constants (*J*) are reported in hertz (Hz). The spectra are referenced to residual solvent peaks: CDCl<sub>3</sub> (7.26 ppm, <sup>1</sup>H; 77.26 ppm, <sup>13</sup>C). Proton nuclear magnetic spectra (<sup>1</sup>H NMR) and carbon nuclear magnetic resonance spectra (<sup>13</sup>C NMR) were recorded at 500 and 125 MHz respectively. Infrared (IR) spectra were recorded neat and reported in cm<sup>-1</sup>. Mass spectra were recorded by using electron impact ionization (EI) or electrospray ionization (ESI) as specified in each case.

### 2.5.2 General Procedure for Construction of Diazo Ketones 76a-e:

#### Ethyl 3-cyclopropyl-3-hydroxypropanoate (83a)



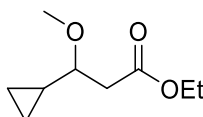
83a

A flame dried round bottom flask was charged with diisopropylamine (3.30 mL, 23.5 mmol) in THF (80 mL) and was cooled to -78 °C. A solution of *n*-BuLi in hexane (2.50 M, 9.40 mL, 23.5 mmol) was added dropwise and the reaction was stirred for 15 min at -78 °C. Ethyl acetate (1.95 mL, 21.4 mmol) was added dropwise with an additional 45 min stirring at -78 °C. Then a solution of cyclopropanecarboxaldehyde (1.60 mL, 21.4 mmol) in THF (10 mL)

was added to the reaction mixture. The reaction temperature was maintained at  $-78\text{ }^{\circ}\text{C}$  over 2 h and the reaction completion was monitored with TLC. Then the reaction was warmed to room temperature followed by the addition of saturated ammonium chloride and the organic layer was separated. The aqueous layer was extracted with  $\text{Et}_2\text{O}$  ( $3\times 10\text{ mL}$ ). The combined organic layers were dried over  $\text{MgSO}_4$  and filtered. The crude product was purified by flash chromatography (30:70 EtOAc: hexane) after concentration under reduced pressure and alcohol **83a** was isolated as a yellow oil.

**83a**: (3.30 g, 97%);  $R_f$  0.27 (30:70 EtOAc: hexane); IR (cast film) 3447, 3003, 2983, 1735, 1412, 1372, 1343, 1280, 1249, 1186, 1139, 1025  $\text{cm}^{-1}$ ;  $^1\text{H}$  NMR (500 MHz,  $\text{CDCl}_3$ )  $\delta$  4.16 (q,  $J = 7.2\text{ Hz}$ , 2H), 3.32 (ddd,  $J = 8.4, 8.4, 3.1\text{ Hz}$ , 1H), 2.63 (dd,  $J = 16.0, 3.8\text{ Hz}$ , 1H), 2.57 (dd,  $J = 16.0, 8.4\text{ Hz}$ , 1H), 1.26 (t,  $J = 7.2\text{ Hz}$ , 3H), 0.94 (dddd,  $J = 8.1, 8.1, 8.1, 4.9, 4.9, \text{ Hz}$ , 1H), 0.57-0.47 (m, 2H), 0.40 (dddd,  $J = 4.5, 4.5, 4.5, 4.5\text{ Hz}$ , 1H), 0.22 (dddd,  $J = 4.5, 4.5, 4.5, 4.5\text{ Hz}$ , 1H);  $^{13}\text{C}$  NMR (125 MHz,  $\text{CDCl}_3$ )  $\delta$  172.7, 72.7, 60.7, 41.4, 16.8, 14.2, 3.2, 2.2; HRMS (ESI) calcd for  $\text{C}_8\text{H}_{14}\text{NaO}_3$   $[\text{M} + \text{Na}]^+$  181.0835; found 181.0836.

### Ethyl 3-cyclopropyl-3-methoxypropionate (**82a**)

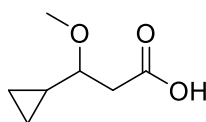


**82a**

To a stirred solution of alcohol **83a** (1.50 g, 9.48 mmol) in dry toluene (20 mL) was added anhydrous  $\text{CaSO}_4$  (2.60 g, 18.9 mmol) and freshly prepared  $\text{Ag}_2\text{O}$ <sup>128</sup> (4.40 g, 18.9 mmol). The reaction mixture was cooled down to  $0\text{ }^{\circ}\text{C}$  and iodomethane (1.20 mL, 18.9 mmol) was added dropwise. The ice bath was removed and the flask was covered in aluminum foil. The reaction mixture was stirred for 3 h at room temperature. An additional aliquots of  $\text{Ag}_2\text{O}$ ,  $\text{CaSO}_4$  and MeI (the same amount as before) were added and the reaction progress was monitored by TLC. (Addition of excess  $\text{Ag}_2\text{O}$ ,  $\text{CaSO}_4$  and MeI may be required if the starting alcohol has not been consumed completely.) The reaction mixture was stirred overnight and was filtered through a Celite plug. The Celite was washed with ethyl acetate and the reaction mixture was concentrated under reduced pressure. The crude mixture was used in the next step without further purifications.

**82a**: yellow oil (1.63 g, quant.);  $R_f$  0.29 (20:80 EtOAc: hexane); IR (cast film) 3082, 2982, 2937, 2824, 1738, 1394, 1279, 1250, 1138, 1111, 1027  $\text{cm}^{-1}$ ;  $^1\text{H}$  NMR (500 MHz,  $\text{CDCl}_3$ )  $\delta$  4.18-4.08 (m, 2H), 3.39 (s, 3H), 2.98 (ddd,  $J = 8.2, 8.2, 4.9$  Hz, 1H), 2.61 (dd,  $J = 14.9, 8.1$  Hz, 1H), 2.52 (dd,  $J = 14.9, 4.9$  Hz, 1H), 1.24 (t,  $J = 7.1$  Hz, 3H), 0.88-0.81 (m, 1H), 0.66-0.59 (m, 1H), 0.47-0.40 (m, 2H), 0.12-0.06 (m, 1H);  $^{13}\text{C}$  NMR (125 MHz,  $\text{CDCl}_3$ )  $\delta$  171.5, 81.9, 60.3, 57.0, 40.9, 14.4, 14.2, 4.7, 0.6; HRMS (ESI) calcd for  $\text{C}_9\text{H}_{17}\text{O}_3$   $[\text{M} + \text{H}]^+$  173.1172; found 173.1173.

### 3-Cyclopropyl-3-methoxypropanoic acid (**81a**)

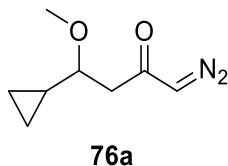


**81a**

Crude **82a** (1.63 g, 9.50 mmol) from the previous step was dissolved in MeOH:THF (1:1, 72 mL) and the aqueous solution of LiOH (2.00 M, 9.50 mL, 19.0 mmol) was added dropwise. The reaction mixture was stirred overnight at room temperature until complete consumption of starting materials. An equal volume of water was added to the reaction and the organic layer was separated. The aqueous layer was acidified with 1.0 M HCl to pH = 1 followed by extraction with  $\text{Et}_2\text{O}$  ( $3 \times 10$  mL). Combined organic layers were dried over  $\text{MgSO}_4$ , filtered and concentrated under reduced pressure. Acid **81a** was obtained as a pure mixture and was used for the next step without further purification.

**81a**: yellow oil (1.36 g, quant.); IR (cast film) 3083, 3006, 2983, 2828, 1711, 1408, 1286, 1218, 1190, 1107, 1069  $\text{cm}^{-1}$ ;  $^1\text{H}$  NMR (500 MHz,  $\text{CDCl}_3$ )  $\delta$  3.48 (s, 3H), 3.00 (ddd,  $J = 8.8, 7.9, 5.0$  Hz, 1H), 2.69 (dd,  $J = 15.2, 7.7$  Hz, 1H), 2.66 (dd,  $J = 15.2, 4.7$  Hz, 1H), 0.93-0.87 (m, 1H), 0.74-0.69 (m, 1H), 0.55-0.47 (m, 2H), 0.17-0.14 (m, 1H), (the peak corresponding to the carboxylic acid proton was not observed);  $^{13}\text{C}$  NMR (125 MHz,  $\text{CDCl}_3$ )  $\delta$  176.4, 81.8, 57.0, 40.5, 14.2, 5.2, 0.6; HRMS (ESI) calcd for  $\text{C}_7\text{H}_{11}\text{O}_3$   $[\text{M} - \text{H}]^-$  143.0714; found 143.0714.

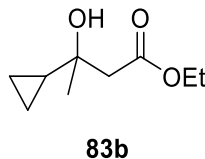
#### 4-Cyclopropyl-1-diazo-4-methoxybutan-2-one (76a)



To a solution of carboxylic acid **81a** (700 mg, 4.86 mmol) in dry THF (25 mL) was added Et<sub>3</sub>N (0.74 mL, 5.34 mmol) followed by the addition of a solution of ethylchloroformate (0.51 mL, 5.34 mmol) in THF (4 mL) at -15 °C. The reaction was stirred for 1 h at -15 °C and an additional 3h at -5 °C. After the formation of the white salt the reaction mixture was filtered and the filtrate was concentrated under reduced pressure. The residue was immediately dissolved in Et<sub>2</sub>O and transferred to an ethereal solution of CH<sub>2</sub>N<sub>2</sub> (~5 equivalents, prepared from Diazald<sup>®</sup>) at -78 °C. The reaction mixture was stirred overnight by gradual warming to the room temperature. The excess CH<sub>2</sub>N<sub>2</sub> was quenched with glacial acetic acid (1 mL) and the reaction mixture was washed with water. The organic layer was separated, combined and dried over MgSO<sub>4</sub> followed by filtration. The crude mixture was obtained after solvent removal and was purified by column chromatography (40:60 EtOAc: hexane) to isolate diazo ketone **76a**.

**76a**: yellow oil (530 mg, 65%); R<sub>f</sub> 0.27 (50:50 EtOAc: hexane); IR (cast film) 3082, 3004, 2981, 2932, 2824, 2104, 1637, 1367, 1105, 1023 cm<sup>-1</sup>; <sup>1</sup>H NMR (500 MHz, CDCl<sub>3</sub>) δ 5.35 (br s, 1H), 3.41 (s, 3H), 2.99 (ddd, *J* = 8.5, 8.5, 4.5 Hz, 1H), 2.55 (m, 2H), 0.89 (dddd, *J* = 13.5, 10.0, 7.9, 5.5 Hz, 1H), 0.70-0.64 (m, 1H), 0.49-0.43 (m, 2H), 0.14-0.10 (m, 1H); <sup>13</sup>C NMR (125 MHz, CDCl<sub>3</sub>) δ 193.1, 82.2, 57.1, 55.4, 46.9, 14.6, 5.2, 0.6; HRMS (EI) calcd for C<sub>7</sub>H<sub>9</sub>ON<sub>2</sub> [M-OCH<sub>3</sub>]<sup>+</sup> 137.0714; found 137.0715.

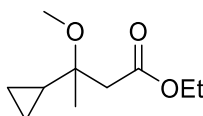
#### Ethyl 3-cyclopropyl-3-hydroxybutanoate (83b)



Alcohol **83b** was synthesized according to the procedure provided for **83a** using cyclopropylmethylketone instead of aldehyde.

**83b**: yellow oil, (1.14 g, 68%);  $R_f$  0.35 (20:80 EtOAc: hexane); IR (cast film) 3512, 3087, 3004, 2980, 2935, 2907, 1713, 1464, 1395, 1372, 1330, 1218, 1200, 1140, 1096  $\text{cm}^{-1}$ ;  $^1\text{H}$  NMR (500 MHz,  $\text{CDCl}_3$ )  $\delta$  4.21 (q,  $J = 7.1$  Hz, 1H), 4.20 (q,  $J = 7.1$  Hz, 1H), 3.34 (br s, 1H), 2.59 (d,  $J = 14.9$  Hz, 1H), 2.53 (d,  $J = 14.9$  Hz, 1H), 1.31 (t,  $J = 7.1$  Hz, 3H), 1.21 (s, 3H), 0.94-0.88 (m, 1H), 0.47-0.35 (m, 4H);  $^{13}\text{C}$  NMR (125 MHz,  $\text{CDCl}_3$ )  $\delta$  172.9, 69.1, 60.6, 46.1, 27.0, 20.8, 14.2, 0.7, 0.0; HRMS (ESI) calcd for  $\text{C}_9\text{H}_{16}\text{NaO}_3$   $[\text{M}^+ \text{Na}]^+$  195.0992; found 195.0990.

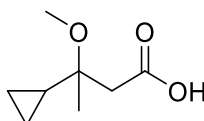
### Ethyl 3-cyclopropyl-3-methoxybutanoate (**82b**)



**82b**

Compound **82b** was synthesized according to the procedure provided for **82a** as a yellow oil in 30% yield;  $R_f$  0.50 (20:80 EtOAc: hexane); IR (cast film) 3086, 2981, 2942, 2829, 1735, 1465, 1368, 1313, 1238, 1199, 1144, 1096  $\text{cm}^{-1}$ ;  $^1\text{H}$  NMR (500 MHz,  $\text{CDCl}_3$ )  $\delta$  4.13 (q,  $J = 7.2$  Hz, 2H), 3.28 (s, 3H), 2.55 (d,  $J = 13.2$  Hz, 1H), 2.49 (d,  $J = 13.2$  Hz, 1H), 1.26 (t,  $J = 7.2$  Hz, 3H), 1.09 (s, 3H), 1.07-1.03 (m, 1H), 0.48-0.39 (m, 3H);  $^{13}\text{C}$  NMR (125 MHz,  $\text{CDCl}_3$ )  $\delta$  170.9, 75.2, 60.2, 46.7, 44.4, 16.5, 18.5, 14.2, 1.3, 1.2; HRMS (ESI) calcd for  $\text{C}_{10}\text{H}_{18}\text{NaO}_3$   $[\text{M}^+ \text{Na}]^+$  208.1148; found 209.1147.

### 3-Cyclopropyl-3-methoxybutanoic acid (**81b**)

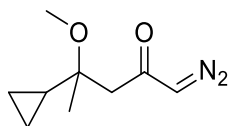


**81b**

Acid **81b** was prepared according to the procedure provided for **81a** as a colorless oil in 52% yield; IR (cast film) 3086, 3010, 2984, 2944, 2831, 1732, 1709, 1465, 1436, 1409, 1386, 1314, 1239, 1201, 1150, 1095  $\text{cm}^{-1}$ ;  $^1\text{H}$  NMR (500 MHz,  $\text{CDCl}_3$ )  $\delta$  3.41 (s, 3H), 2.61 (d,  $J = 15.2$  Hz, 1H), 2.52 (d,  $J = 15.2$  Hz, 1H), 1.04 (s, 3H), 1.02-0.97 (m, 1H), 0.65-0.47 (m, 3H), 0.20-

0.13 (m, 1H), (the peak corresponding to the carboxylic acid proton was not observed);  $^{13}\text{C}$  NMR (125 MHz,  $\text{CDCl}_3$ )  $\delta$  172.5, 76.7, 50.0, 45.5, 17.7, 17.4, 2.4, 0.7; HRMS (ESI) calcd for  $\text{C}_8\text{H}_{13}\text{O}_3$   $[\text{M}-\text{H}]^-$  157.0943; found 157.0870.

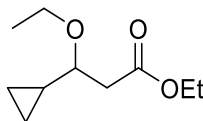
#### 4-Cyclopropyl-1-diazo-4-methoxypropan-2-one (76b)



**76b**

Diazo ketone **76b** was prepared according to the procedure provided for **76a** as a yellow oil, 34% yield;  $R_f$  0.49 (30:70 EtOAc: hexane); IR (cast film) 3271, 3086, 2979, 2944, 2829, 2102, 1634, 1465, 1429, 1356, 1163, 1093  $\text{cm}^{-1}$ ;  $^1\text{H}$  NMR (500 MHz,  $\text{CDCl}_3$ )  $\delta$  5.49 (br s, 1H), 3.30 (s, 3H), 2.55-2.44 (br m, 2H), 1.03 (s, 3H), 1.00-0.95 (m, 1H), 0.55-0.42 (m, 3H), 0.22-0.14 (m, 1H);  $^{13}\text{C}$  NMR (125 MHz,  $\text{CDCl}_3$ )  $\delta$  193.2, 76.0, 55.9, 51.4, 49.7, 18.5, 1.9 (2C), 0.9; HRMS (ESI) calcd for  $\text{C}_9\text{H}_{15}\text{N}_2\text{O}_2$   $[\text{M}+\text{H}]^+$  183.1128; found 183.1130.

#### Ethyl 3-cyclopropyl-3-ethoxypropanoate (82c)

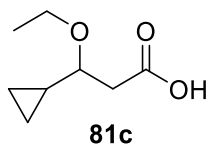


**82c**

Compound **82c** was synthesized with the same procedure as compound **82a** using iodoethane as an alkyl halide. The reaction was stirred for 40 h and 60% starting alcohol was recovered. **82c**: yellow oil (230 mg, 39%);  $R_f$  0.47 (20:80 EtOAc: hexane); IR (cast film) 3082, 2978, 2932, 2873, 1738, 1463, 1445, 1430, 1390, 1372, 1317, 1279, 1189, 1139, 1096, 1028  $\text{cm}^{-1}$ ;  $^1\text{H}$  NMR (500 MHz,  $\text{CDCl}_3$ )  $\delta$  4.18 (q,  $J = 7.1$  Hz, 2H), 3.75 (dq,  $J = 9.2, 7.0$  Hz, 1H), 3.50 (dq,  $J = 9.2, 7.0$  Hz, 1H), 3.12 (ddd,  $J = 8.2, 8.2, 5.0$  Hz, 1H), 2.66 (dd,  $J = 14.7, 8.1$  Hz, 1H), 2.57 (dd,  $J = 14.7, 5.0$  Hz, 1H), 1.29 (t,  $J = 7.0$  Hz, 3H), 1.19 (t,  $J = 7.0$  Hz, 3H), 0.95-0.88 (m, 1H), 0.66-0.61 (m, 1H), 0.51-0.43 (m, 2H), 0.18-0.14 (m, 1H);  $^{13}\text{C}$  NMR (125 MHz,

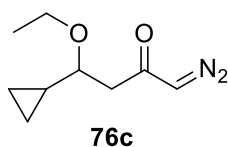
CDCl<sub>3</sub>)  $\delta$  171.7, 80.3, 64.7, 60.3, 41.3, 15.5, 15.1, 14.2, 4.5, 1.0; HRMS (ESI) calcd for C<sub>10</sub>H<sub>19</sub>O<sub>3</sub> [M+H]<sup>+</sup> 187.1329; found 187.1328.

### 3-Cyclopropyl-3-[(propan-2-yl)oxy]propanoic acid (**81c**)



Compound **81c** was prepared with the same procedure as compound **81a** as a yellow oil (180 mg, 92%); IR (cast film) 3082, 3006, 2977, 2931, 2897, 1712, 1429, 1406, 1293, 1206, 1140, 1122, 1096 cm<sup>-1</sup>; <sup>1</sup>H NMR (500 MHz, CDCl<sub>3</sub>)  $\delta$  3.85 (dq,  $J$  = 9.2, 7.0 Hz, 1H), 3.54 (dq,  $J$  = 9.2, 7.0 Hz, 1H), 3.10 (ddd,  $J$  = 8.4, 8.4, 4.9 Hz, 1H), 2.71 (dd,  $J$  = 15.4, 7.0 Hz, 1H), 2.67 (dd,  $J$  = 15.2, 4.8 Hz, 1H), 1.24 (t,  $J$  = 7.0 Hz, 3H), 0.92 (dddd,  $J$  = 8.4, 8.4, 8.4, 5.2, 5.2 Hz, 1H), 0.70 (dddd,  $J$  = 8.9, 7.9, 5.7, 4.5, 1H), 0.56-0.51 (m, 1H), 0.50-0.45 (m, 1H), 0.17 (dddd,  $J$  = 9.5, 5.9, 4.8, 4.8, 1H), (the peak corresponding to the carboxylic acid proton was not observed); <sup>13</sup>C NMR (125 MHz, CDCl<sub>3</sub>)  $\delta$  175.8, 80.1, 64.8, 40.7, 15.4, 14.7, 5.0, 0.9; HRMS (ESI) calcd for C<sub>8</sub>H<sub>13</sub>O<sub>3</sub> [M-H]<sup>-</sup> 157.0870; found 157.0871.

### 4-Cyclopropyl-1-diazo-4-ethoxypentan-2-one (**76c**)

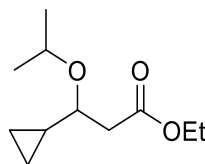


Compound **76c** was prepared synthesized with the same procedure as compound **76a**.

**76c**: yellow oil (99 mg, 47%);  $R_f$  0.42 (40:60 EtOAc: hexane); IR (cast film) 3081, 3005, 2975, 2929, 2894, 2871, 21.03, 1638, 1361, 1092, 1053 cm<sup>-1</sup>; <sup>1</sup>H NMR (500 MHz, CDCl<sub>3</sub>)  $\delta$  5.40 (br s, 1H), 3.77 (dq,  $J$  = 6.9, 9.1 Hz, 1H), 3.45 (dq,  $J$  = 6.9, 9.1 Hz, 1H), 3.12 (ddd,  $J$  = 8.5, 8.5, 4.2 Hz, 1H), 2.69-2.55 (br s, 2H), 1.21 (t,  $J$  = 6.8 Hz, 3H), 0.87 (dddd,  $J$  = 8.2, 8.2, 8.2, 5.0, 5.0 Hz, 1H), 0.67-0.62 (m, 1H), 0.52-0.43 (m, 2H), 0.18-0.14 (m, 1H); <sup>13</sup>C NMR (125 MHz, CDCl<sub>3</sub>)  $\delta$  193.4, 80.5, 64.8, 55.3, 47.4, 15.6, 15.4, 4.9, 1.0; HRMS (EI) calcd for C<sub>9</sub>H<sub>15</sub>N<sub>2</sub>O<sub>2</sub> [M+H]<sup>+</sup> 183.1128; found 183.1129.



### Ethyl 3-cyclopropyl-3-[(propan-2-yl)oxy]propanoate (**82d**)

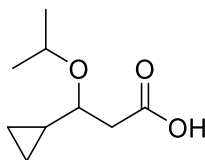


**82d**

Ester **82d** was synthesized with the same procedure as compound **82a** using isopropyl bromide as an alkyl halide.

**82d**: yellow oil (1.90 g, 75%);  $R_f$  0.63 (30:70 EtOAc: hexane); IR (cast film) 2974, 2934, 2902, 1738, 1466, 1369, 1340, 1311, 1278, 1188, 1140, 1063  $\text{cm}^{-1}$ ;  $^1\text{H}$  NMR (500 MHz,  $\text{CDCl}_3$ )  $\delta$  4.16 (q,  $J = 7.1$  Hz, 2H), 3.79 (sep,  $J = 6.0$  Hz, 1H), 3.79 (ddd,  $J = 5.3, 7.9, 7.9$  Hz, 1H), 2.61 (dd,  $J = 14.5, 7.8$  Hz, 1H), 2.54 (dd,  $J = 14.5, 5.5$  Hz, 1H), 1.28 (t,  $J = 7.1$  Hz, 3H), 1.17 (d,  $J = 6.3$  Hz, 3H), 1.11 (d,  $J = 6.3$  Hz, 3H), 0.94-0.81 (m, 1H), 0.63-0.57 (m, 1H), 0.51-0.45 (m, 1H), 0.43-0.38 (m, 1H), 0.20-0.16 (m, 1H);  $^{13}\text{C}$  NMR (125 MHz,  $\text{CDCl}_3$ )  $\delta$  171.7, 77.8, 69.7, 60.3, 41.7, 23.1, 22.3, 15.8, 14.2, 4.3, 1.5; HRMS (ESI) calcd for  $\text{C}_{11}\text{H}_{20}\text{NaO}_3$  [ $\text{M} + \text{Na}$ ] $^+$  223.1305; found 223.1304.

### 3-Cyclopropyl-3-[(propan-2-yl)oxy]propanoic acid (**81d**)

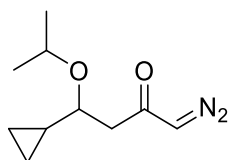


**81d**

Compound **81d** was prepared with the same procedure as compound **81a** as a light yellow oil (1.60 g, 98%); IR (cast film) 3083, 3006, 2974, 2934, 1711, 1466, 1408, 1311, 1208, 1122, 1061, 1048  $\text{cm}^{-1}$ ;  $^1\text{H}$  NMR (500 MHz,  $\text{CDCl}_3$ )  $\delta$  3.89 (sep,  $J = 6.3$  Hz, 1H), 3.21 (ddd,  $J = 7.1, 7.1, 5.5$  Hz, 1H), 2.67 (dd,  $J = 15.1, 7.0$  Hz, 1H), 2.64 (dd,  $J = 15.1, 5.2$  Hz, 1H), 1.21 (d,  $J = 6.3$  Hz, 3H), 1.15 (d,  $J = 6.3$  Hz, 3H), 0.94 (dddd,  $J = 4.9, 4.9, 8.2, 8.2, 8.2$  Hz, 1H), 0.65 (dddd,  $J = 9.0, 8.9, 5.8, 4.5$  Hz, 1H), 0.52 (dddd,  $J = 8.6, 8.6, 5.7, 4.6$  Hz, 1H), 0.44 (ddd,  $J = 9.6, 9.6, 5.1$  Hz, 1H), 0.19 (dddd,  $J = 9.7, 4.9, 4.9, 4.9$  Hz,

1H), (the peak corresponding to the carboxylic acid proton was not observed);  $^{13}\text{C}$  NMR (125 MHz,  $\text{CDCl}_3$ )  $\delta$  176.6, 77.5, 69.9, 41.2, 23.2, 22.0, 15.5, 4.6, 1.4; HRMS (ESI) calcd for  $\text{C}_9\text{H}_{15}\text{O}_3$   $[\text{M}-\text{H}]^-$  171.1027; found 171.1029.

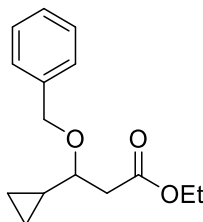
#### 4-Cyclopropyl-1-diazo-4-[(propan-2-yl)oxy]butan-2-one (76d)



**76d**

Compound **76d** was prepared synthesized with the same procedure as compound **76a** as a yellow oil (220 mg, 32%);  $R_f$  0.24 (30:70 EtOAc: hexane); IR (cast film) 3081, 3005, 2972, 2913, 2102, 1637, 1366, 1328, 1170, 1122, 1065  $\text{cm}^{-1}$ ;  $^1\text{H}$  NMR (500 MHz,  $\text{CDCl}_3$ )  $\delta$   $^1\text{H}$  NMR (500 MHz,  $\text{CDCl}_3$ )  $\delta$  5.39 (br s, 1H), 3.80 (sep,  $J = 6.1$  Hz, 1H), 3.24 (ddd,  $J = 8.1, 8.1, 4.8$  Hz, 1H), 2.67-2.52 (m, 2H), 1.17 (d,  $J = 6.1$  Hz, 3H), 1.11 (d,  $J = 6.1$  Hz, 3H), 0.88 (dddd,  $J = 5.1, 5.1, 8.2, 8.2, 8.2$  Hz, 1H), 0.61 (dddd,  $J = 9.0, 8.1, 5.6, 4.4$  Hz, 1H), 0.48 (dddd,  $J = 8.6, 8.6, 5.5, 4.6$  Hz, 1H), 0.41 (ddd,  $J = 9.5, 9.5, 5.1$  Hz, 1H), 0.19 (dddd,  $J = 9.7, 5.0, 5.0, 5.0$  Hz, 1H);  $^{13}\text{C}$  NMR (125 MHz,  $\text{CDCl}_3$ )  $\delta$  193, 77.9, 69.8, 55.4, 47.8, 23.2, 22.2, 16.0, 4.5, 1.5; HRMS (ESI) calcd for  $\text{C}_{10}\text{H}_{16}\text{N}_2\text{NaO}_2$   $[\text{M} + \text{Na}]^+$  219.1104; found 219.1098.

#### Ethyl 3-(benzyloxy)-3-cyclopropylpropanoate (82e)

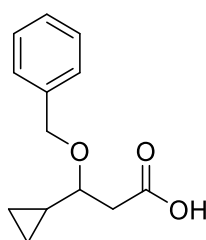


**82e**

Ester **82e** was prepared by the procedure provided for **82a** using BnBr (2.4 eq) as an alkylhalide in 64% yield as a yellow oil;  $R_f$  0.50 (20:80 EtOAc: hexane); IR (cast film) 3082, 3030, 3003, 2981, 2931, 2872, 1735, 1496, 1454, 1386, 1369, 1279, 1189, 110, 1095  $\text{cm}^{-1}$ ;

$^1\text{H}$  NMR (500 MHz,  $\text{CDCl}_3$ )  $\delta$  7.31-7.25 (m, 5H), 4.75 (d,  $J = 11.8$ , 1H), 4.58 (d,  $J = 11.8$ , 1H), 4.15 (q,  $J = 7.5$ , 2H), 3.25 (ddd,  $J = 8.3, 8.3, 4.9$  Hz, 1H), 2.73 (dd,  $J = 14.5, 7.9$  Hz, 1H), 2.62 (dd,  $J = 14.5, 4.9$  Hz, 1H), 1.27 (t,  $J = 7.5$  Hz, 3H), 1.01-0.92 (m, 1H), 0.70-0.64 (m, 1H), 0.53-0.41 (m, 2H), 0.18-0.12 (m, 1H);  $^{13}\text{C}$  NMR (125 MHz,  $\text{CDCl}_3$ )  $\delta$  171.6, 138.7, 128.3, 127.5, 127.4, 80.2, 71.1, 60.4, 41.3, 14.9, 14.2, 4.9, 0.9; HRMS (ESI) calcd for  $\text{C}_{15}\text{H}_{20}\text{NaO}_3$   $[\text{M} + \text{Na}]^+$  271.1305; found 271.1299.

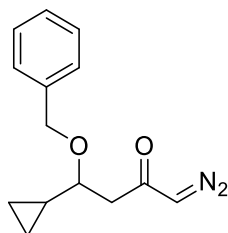
### 3-(Benzyloxy)-3-cyclopropylpropanoic acid (**81e**)



**81e**

Acid **81e** was prepared via the procedure provided for **81a** and was isolated as a yellow oil in 95%; IR (cast film) 3066, 3086, 3031, 3006, 2931, 2877, 1710, 1496, 1454, 1428, 1293, 1206, 1146, 1098, 1070, 1027  $\text{cm}^{-1}$ ;  $^1\text{H}$  NMR (500 MHz,  $\text{CDCl}_3$ )  $\delta$  7.36-7.29 (m, 5H), 4.81 (d,  $J = 11.7$  Hz, 1H), 4.62 (d,  $J = 11.7$  Hz, 1H), 3.27 (ddd,  $J = 8.5, 8.5, 4.8$  Hz, 1H), 2.81 (dd,  $J = 15.3, 8.2$  Hz, 1H), 2.72 (dd,  $J = 15.3, 4.5$  Hz, 1H), 1.01 (dddd,  $J = 8.5, 8.5, 8.5, 5.2, 5.2$  Hz, 1H), 0.72 (dddd,  $J = 8.8, 8.0, 5.7, 4.5$  Hz, 1H), 0.74-0.69 (m, 1H), 0.58-0.53 (m, 1H), 0.51-0.46 (m, 1H), 0.21-0.16 (m, 1H), (the peak corresponding to the carboxylic acid proton was not observed);  $^{13}\text{C}$  NMR (125 MHz,  $\text{CDCl}_3$ )  $\delta$  177.0, 138.3, 128.3, 127.7, 127.6, 79.8, 71.1, 40.9, 14.7, 5.2, 0.9; HRMS (ESI) calcd for  $\text{C}_{13}\text{H}_{15}\text{O}_3$   $[\text{M} - \text{H}]^-$  219.1027; found 219.1026.

#### 4-(Benzyloxy)-4-cyclopropyl-1-diazobutan-2-one (76e)



76e

Diazo ketone **76e** was prepared according to the procedure provided for **76a** and was isolated as a yellow oil in 46% yield;  $R_f$  0.17 (20:80 EtOAc: hexane); IR (cast film) 3083, 3031, 3004, 2869, 2103, 1638, 1496, 1454, 1366, 1094  $\text{cm}^{-1}$ ;  $^1\text{H}$  NMR (500 MHz,  $\text{CDCl}_3$ )  $\delta$  7.38-7.28 (m, 5H), 5.36 (br s, 1H), 4.77 (d,  $J = 11.3$  Hz, 1H), 4.54 (d,  $J = 11.2$  Hz, 1H), 3.26 (ddd,  $J = 8.6, 8.6, 4.2$  Hz, 1H), 2.70-2.68 (bm, 2H), 1.00-0.92 (m, 1H), 0.72-0.66 (m, 1H), 0.53-0.44 (m, 2H), 0.19-0.14 (m, 1H);  $^{13}\text{C}$  NMR (125 MHz,  $\text{CDCl}_3$ )  $\delta$  193.2, 138.6, 128.3, 127.6, 127.5, 80.6, 79.9, 71.3, 40.6, 15.1, 5.3, 1.0; HRMS (ESI) calcd for  $\text{C}_{14}\text{H}_{17}\text{N}_2\text{O}_2$   $[\text{M}+\text{H}]^+$  245.1285; found 245.1288.

#### 2.5.3 General procedure for Decomposition of Diazo Ketone 72a-e with Cu catalysts:

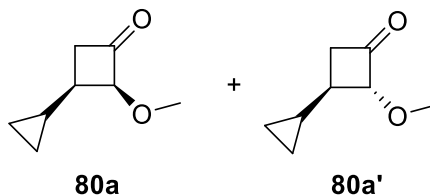
To a refluxing solution of Cu catalyst (10 mol%) in  $\text{CH}_2\text{Cl}_2$  (0.01M) was added the solution of diazo ketone **76** (1 equiv.) in  $\text{CH}_2\text{Cl}_2$  (0.1M) via syringe pump over 1 h. Consumption of starting diazo ketone was monitored by TLC and the reaction mixture was quenched by 10% solution of  $\text{K}_2\text{CO}_3$ . The organic layer was separated and the aqueous layer was washed with DCM (3 $\times$ ). The combined organic layers were dried over  $\text{MgSO}_4$ , filtered and concentrated under reduced pressure and purified by flash chromatography.

#### 2.5.4 General procedure for Decomposition of Diazo ketone 76a with $\text{Rh}_2(\text{OAc})_4$ :

To a refluxing solution of  $\text{Rh}_2(\text{OAc})_4$  (10 mol%) in  $\text{CH}_2\text{Cl}_2$  (0.01M) was added the solution of diazo ketone **76a** (1 equiv.) in  $\text{CH}_2\text{Cl}_2$  (0.1M) via syringe pump over 1h. Consumption of starting diazo ketone was monitored by TLC and the reaction mixture was passed through a short silica plug and was washed with DCM. The filtrate was concentrated under reduced pressure and purified by flash chromatography.

**(2*S*,3*R*)-3-Cyclopropyl-2-methoxycyclobutan-1-one (80a)**

**(2*R*,3*R*)-3-Cyclopropyl-2-methoxycyclobutan-1-one (80a')**



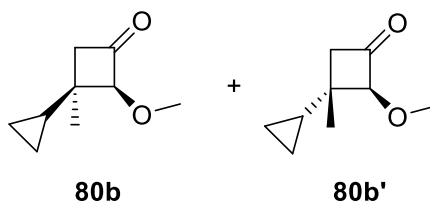
**80a** and **80a'** were isolated by flash chromatography (40:60 EtOAc: hexane) in 6:1 ratio (20 mg, 80%).

**80a**: yellow oil;  $R_f$  0.60 (40:60 EtOAc: hexane); IR (cast film) 3081, 3003, 2952, 2834, 1787, 1436, 1268, 1214, 1344, 1214, 1165, 1145, 1020  $\text{cm}^{-1}$ ;  $^1\text{H}$  NMR (500 MHz,  $\text{CDCl}_3$ )  $\delta$  4.46 (ddd,  $J = 8.8, 2.9, 2.9$  Hz, 1H), 3.41 (s, 3H), 2.82 (ddd,  $J = 17.0, 2.9, 9.5$  Hz, 1H), 2.31 (ddd,  $J = 17.0, 3.5, 2.7$  Hz, 1H), 2.01 (dddd,  $J = 9.5, 9.5, 3.5$  Hz, 1H), 0.73 (dddd,  $J = 8.3, 8.3, 8.3, 5.0, 5.0$  Hz, 1H), 0.58-0.53 (m, 1H), 0.42-0.36 (m, 1H), 0.13 (ddd,  $J = 9.5, 5.0, 5.0$  Hz, 1H), 0.08 (ddd,  $J = 9.5, 5.0, 5.0$  Hz, 1H);  $^{13}\text{C}$  NMR (125 MHz,  $\text{CDCl}_3$ )  $\delta$  206.0, 89.6, 58.8, 44.6, 35.2, 9.7, 4.8, 2.1; HRMS (EI) calcd for  $\text{C}_8\text{H}_{12}\text{O}_2$   $[\text{M}]^+$  140.0837; found 140.0835.

**80a'**: yellow oil;  $R_f$  0.65 (40:60 EtOAc: hexane); IR (cast film) 3082, 3004, 2953, 1786, 1437, 1267, 1267, 1192, 1166, 1087  $\text{cm}^{-1}$ ;  $^1\text{H}$  NMR (500 MHz,  $\text{CDCl}_3$ )  $\delta$  4.23 (ddd,  $J = 7.5, 2.6, 2.6$  Hz, 1H), 3.46 (s, 3H), 2.69 (ddd,  $J = 16.8, 9.5, 2.6$  Hz, 1H), 2.42 (ddd,  $J = 16.8, 9.5, 2.6$  Hz, 1H), 2.01 (dddd,  $J = 9.5, 9.5, 7.5, 7.5$  Hz, 1H), 1.03 (dddd,  $J = 7.8, 7.8, 7.8, 5.0, 5.0, 5.0$  Hz, 1H), 0.60-0.54 (m, 2H), 0.28-0.21 (m, 2H);  $^{13}\text{C}$  NMR (125 MHz,  $\text{CDCl}_3$ )  $\delta$  204.9, 92.8, 58.0, 42.9, 36.6, 14.1, 3.6, 3.2; HRMS (EI) calcd for  $\text{C}_8\text{H}_{12}\text{O}_2$   $[\text{M}]^+$  140.0837; found 140.0835.

**(2*S*,3*R*)-3-Cyclopropyl-2-methoxy-3-methylcyclobutan-1-one (80b)**

**(2*S*,3*S*)-3-Cyclopropyl-2-methoxy-3-methylcyclobutan-1-one (80b')**



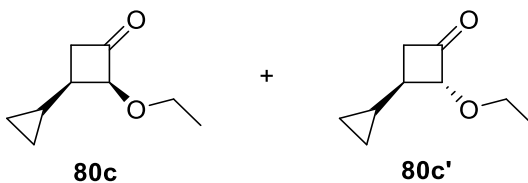
Cyclobutanones **80b** and **80b'** were isolated by flash chromatography (20:80 EtOAc: hexane) in 1.4:1 ratio (8 mg, 50%).

**80b**: colorless oil;  $R_f$  0.47 (20:80 EtOAc: hexane); IR (cast film) 3083, 3002, 2931, 1788, 1461, 1412, 1347, 1194, 1144, 1112, 1020  $\text{cm}^{-1}$ ;  $^1\text{H}$  NMR (500 MHz,  $\text{CDCl}_3$ )  $\delta$  4.22 (dd,  $J = 2.6, 2.6$  Hz, 1H), 3.55 (s, 3H), 2.45 (dd,  $J = 16.8, 2.9$  Hz, 1H), 2.31 (dd,  $J = 16.8, 2.4$  Hz, 1H), 1.43 (s, 3H), 0.97 (dddd,  $J = 8.4, 8.4, 5.5, 5.5$  Hz, 1H), 0.50-0.43 (m, 1H), 0.49-0.43 (m, 1H), 0.29-0.21 (m, 2H);  $^{13}\text{C}$  NMR (125 MHz,  $\text{CDCl}_3$ )  $\delta$  204.9, 95.0, 59.2, 48.1, 35.9, 26.0, 13.6, 0.7, 0.6; HRMS (EI) calcd for  $\text{C}_9\text{H}_{13}\text{O}_2$   $[\text{M}-\text{H}]^+$  14.0915; found 151.0916.

**80b'**: colorless oil;  $R_f$  0.33 (20:80 EtOAc: hexane); IR (cast film) 3088, 3006, 2952, 2849, 1788, 1463, 1434, 1293, 1196  $\text{cm}^{-1}$ ;  $^1\text{H}$  NMR (500 MHz,  $\text{CDCl}_3$ )  $\delta$  4.12 (dd,  $J = 2.6, 2.6$  Hz, 1H), 3.52 (s, 3H), 2.42 (dd,  $J = 16.3, 2.6$  Hz, 1H), 2.14 (dd,  $J = 16.3, 2.6$  Hz, 1H), 1.20 (dddd,  $J = 8.4, 8.4, 5.4, 5.4$  Hz, 1H), 1.15 (s, 3H), 0.59-0.55 (m, 2H), 0.38-0.33 (m, 1H), 0.25-0.21 (m, 1H);  $^{13}\text{C}$  NMR (125 MHz,  $\text{CDCl}_3$ )  $\delta$  205.0, 92.9, 59.0, 48.2, 36.1, 16.5, 19.0, 2.3, 1.7; HRMS (EI) calcd for  $\text{C}_9\text{H}_{13}\text{O}_2$   $[\text{M}-\text{H}]^+$  14.0915; found 151.0916.

**(2*S*,3*R*)-3-Cyclopropyl-2-ethoxycyclobutan-1-one (80c)**

**(2*R*,3*R*)-3-Cyclopropyl-2-ethoxycyclobutan-1-one (80c')**



**80c** and **80c'** were isolated by flash chromatography (20:80 EtOAc: hexane) in 6:1 ratio (56 mg, 70%).

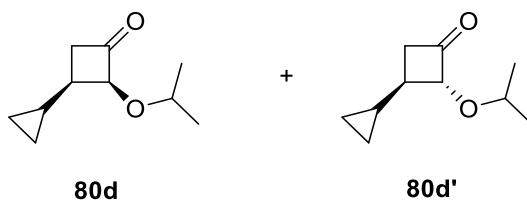
**80c**: yellow oil;  $R_f$  0.41 (20:80 EtOAc: hexane); IR (cast film) 3080, 3001, 2979, 2933, 2875, 1788, 1431, 1337, 1182, 1064  $\text{cm}^{-1}$ ;  $^1\text{H}$  NMR (500 MHz,  $\text{CDCl}_3$ )  $\delta$  4.64 (ddd,  $J = 8.8, 2.7, 2.7$  Hz, 1H), 3.69 (q,  $J = 7.0$  Hz, 1H), 3.68 (q,  $J = 7.0$  Hz, 1H), 2.90 (ddd,  $J = 17.1, 2.8, 9.7$  Hz, 1H), 2.42 (ddd,  $J = 17.1, 3.1, 3.1$ , 1H), 2.10 (dddd,  $J = 9.2, 9.2, 9.2, 3.6$  Hz, 1H), 1.26 (t,  $J = 7.1, 3\text{H}$ ), 0.86 (dddd,  $J = 8.2, 8.2, 8.2, 5.2, 5.2$  Hz, 1H), 0.69-0.54 (m, 1H), 0.53-0.47

(m, 1H), 0.25-0.16 (m, 2H);  $^{13}\text{C}$  NMR (125 MHz,  $\text{CDCl}_3$ )  $\delta$  206.3, 88.3, 66.8, 44.5, 35.5, 15.1, 10.0, 4.9, 2.2; HRMS (EI) calcd for  $\text{C}_9\text{H}_{14}\text{O}_2$   $[\text{M}]^+$  154.0994; found 154.0989.

**80c'**: yellow oil;  $R_f$  0.50 (20:80 EtOAc: hexane); IR (cast film) 3080, 2979, 2929, 2874, 1786, 1444, 1398, 1334, 1212, 1177, 1122, 1052, 1019  $\text{cm}^{-1}$ ;  $^1\text{H}$  NMR (500 MHz,  $\text{CDCl}_3$ )  $\delta$  4.33 (ddd,  $J = 7.7, 2.9, 2.9$  Hz, 1H), 3.77 (dq,  $J = 9.3, 7.1$  Hz, 1H), 3.69 (dq,  $J = 9.3, 6.8$  Hz, 1H), 2.73 (ddd,  $J = 17.0, 9.6, 2.7$  Hz, 1H), 2.42 (ddd,  $J = 17.0, 9.5, 2.9$  Hz, 1H), 2.08 (dddd,  $J = 9.7, 9.7, 7.2, 7.2$  Hz, 1H), 1.27 (t,  $J = 7.1$  Hz, 3H), 1.10 (dddd,  $J = 8.2, 8.2, 7.3, 5.0, 5.0$  Hz, 1H), 0.63-0.58 (m, 2H), 0.34-0.27 (m, 2H);  $^{13}\text{C}$  NMR (125 MHz,  $\text{CDCl}_3$ )  $\delta$  205.4, 91.7, 66.2, 42.7, 36.9, 15.3, 14.1, 3.6, 3.1; HRMS (EI) calcd for  $\text{C}_9\text{H}_{14}\text{O}_2$   $[\text{M}]^+$  154.0994; found 154.1002.

**(2*S*,3*R*)-3-Cyclopropyl-2-[(propan-2-yl)oxy]cyclobutan-1-one (80d)**

**(2*R*,3*R*)-3-Cyclopropyl-2-[(propan-2-yl)oxy]cyclobutan-1-one (80d')**



**80d** and **80d'** were isolated by flash chromatography (20:80 EtOAc: hexane) in 4.8:1 ration (120 mg, 78%)

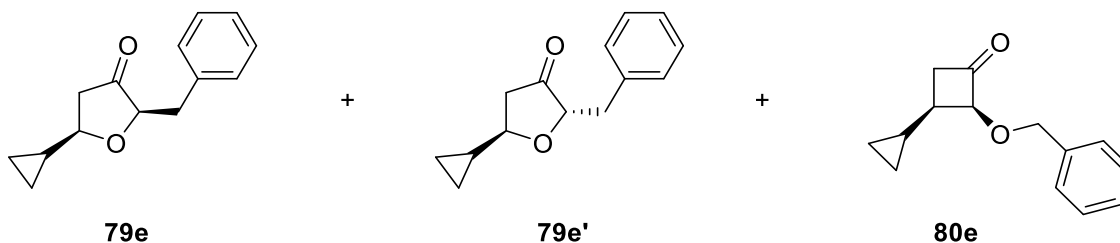
**80d**: colorless oil;  $R_f$  0.42 (20:80  $\text{E}_2\text{O}$ : Pentane); IR (cast film) 3080, 2974, 2933, 2875, 1788, 1731, 1382, 1182, 1139, 1119  $\text{cm}^{-1}$ ;  $^1\text{H}$  NMR (500 MHz,  $\text{CDCl}_3$ )  $\delta$  4.71 (ddd,  $J = 8.9, 2.7, 2.7$  Hz, 1H), 3.77 (sep,  $J = 6.2$  Hz, 1H), 2.90 (ddd,  $J = 17.1, 9.7, 2.9$  Hz, 1H), 2.41 (ddd,  $J = 17.1, 3.5, 2.4$  Hz, 1H), 2.10 (dddd,  $J = 8.9, 8.9, 8.9, 3.4$  Hz, 1H), 1.26 (d,  $J = 6.2$  Hz, 6H), 0.92-0.84 (m, 1H), 0.70-0.65 (m, 1H), 0.52-0.48 (m, 1H), 0.26-0.18 (m, 2H);  $^{13}\text{C}$  NMR (125 MHz,  $\text{CDCl}_3$ )  $\delta$  206.9, 86.6, 72.6, 44.2, 35.8, 22.6, 21.8, 10.2, 5.0, 2.2; HRMS (EI) calcd for  $\text{C}_{10}\text{H}_{16}\text{NaO}_2$   $[\text{M}+\text{Na}]^+$  191.1043; found 191.1038.

**80d'**: colorless oil;  $R_f$  0.31 (20:80  $\text{E}_2\text{O}$ : Pentane); IR (cast film) 3347, 3080, 2973, 2926, 2850, 1787, 1465, 1431, 1382, 1323, 1142, 1120, 1083  $\text{cm}^{-1}$ ;  $^1\text{H}$  NMR (500 MHz,  $\text{CDCl}_3$ )  $\delta$  4.35 (ddd,  $J = 7.7, 2.6, 2.6$  Hz, 1H), 3.84 (sep,  $J = 6.2$  Hz, 1H), 2.90 (ddd,  $J = 17.0, 9.5, 2.5$  Hz,

1H), 2.43 (ddd,  $J = 17.0, 9.7, 2.6$  Hz, 1H), 2.05 (dddd,  $J = 9.8, 9.8, 9.8, 7.3, 7.3$  Hz, 1H), 1.26 (d,  $J = 6.2$  Hz, 3H), 1.24 (d,  $J = 6.2$  Hz, 3H), 1.13-1.07 (m, 1H), 0.62-0.57 (m, 2H), 0.35-0.26 (m, 2H);  $^{13}\text{C}$  NMR (125 MHz,  $\text{CDCl}_3$ )  $\delta$  206, 90.1, 72.7, 42.4, 37.3, 22.5, 22.4, 13.9, 3.4, 2.9; HRMS (EI) calcd for  $\text{C}_{10}\text{H}_{16}\text{NaO}_2$   $[\text{M}+\text{Na}]^+$  191.1043; found 191.1038.

## 2-Benzyl-5-cyclopropyloxolan-3-one (79e and 79e')

### (2*S*,3*R*)-2-(Benzyloxy)-3-cyclopropylcyclobutan-1-one (80e)



Inseparable compounds **79e** and **79e'** and **80e** were isolated by gradient flash chromatography (10:90, 20:80, 30:70, 10:10 EtOAc: Hexane).

IR (cast film) 3081, 3064, 3004, 2926, 2867, 1787, 1755, 1496, 1454, 1397, 1280, 1208, 1164, 1068, 1055, 1021  $\text{cm}^{-1}$ .

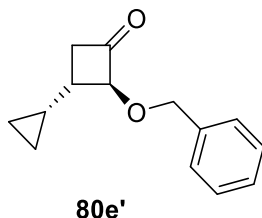
**80e**: colorless oil;  $R_f$  0.33 (50:50 EtOAc: hexane);  $^1\text{H}$  NMR (500 MHz,  $\text{CDCl}_3$ )  $\delta$  7.41-7.22 (m, 5H), 4.75 (d,  $J = 12.5$  Hz, 1H), 4.71 (d,  $J = 12.5$  Hz, 1H), 4.70 (ddd,  $J = 5.6, 2.8, 2.8$  Hz, 1H), 2.92 (m, 1H), 2.45 (ddd,  $J = 17.1, 3.5, 2.5$  Hz, 1H), 2.10 (ddd,  $J = 9.1, 9.1, 3.6$  Hz, 1H), 0.96-0.89 (m, 1H), 0.72-0.64 (m, 1H), 0.55-0.50 (m, 1H), 0.36-0.17 (m, 2H);  $^{13}\text{C}$  NMR (125 MHz,  $\text{CDCl}_3$ )  $\delta$  206.3, 137.3, 129.8, 128.5, 127.9, 87.1, 72.6, 44.7, 35.4, 15.5, 5.0, 2.2.

**79e**: yellow oil;  $R_f$  0.33 (50:50 EtOAc: hexane);  $^1\text{H}$  NMR (500 MHz,  $\text{CDCl}_3$ )  $\delta$  7.39-7.32 (m, 5H), 4.31 (dd,  $J = 6.5, 4.6$  Hz, 1H), 3.51-3.47 (m, 1H), 3.00 (dd,  $J = 14.2, 4.5$  Hz, 1H), 2.96-2.92 (m, 1H), 2.35 (d,  $J = 7.0$  Hz, 1H), 2.34 (d,  $J = 7.0$  Hz, 1H), 1.03-0.98 (m, 1H), 0.71-0.61 (m, 1H), 0.55-0.51 (m, 2H), 0.26-0.18 (m, 1H);  $^{13}\text{C}$  NMR (125 MHz,  $\text{CDCl}_3$ )  $\delta$  216.3, 136.9, 128.4, 128.2, 127.9, 80.3, 79.9, 42.3, 37.2, 10.0, 3.2, 1.6.

**79e'** (observed peaks):  $^1\text{H}$  NMR (500 MHz,  $\text{CDCl}_3$ )  $\delta$  7.39-7.32 (m, 5H), 4.02 (dd,  $J = 6.4, 4.0$  Hz, 1H), 3.59 (ddd,  $J = 10.4, 7.2, 5.5$  Hz, 1H), 3.12 (dd,  $J = 14.5, 4.1$  Hz, 1H), 1.03-0.98 (m, 1H), 0.63-0.57 (m, 1H), 0.43-0.38 (m, 2H), 0.26-0.18 (m, 1H);  $^{13}\text{C}$  NMR (125 MHz,  $\text{CDCl}_3$ )  $\delta$  215.8, 129.7, 126.6, 97.7, 81.9, 69.7, 43.0, 40.3, 15.0, 2.9, 1.4.

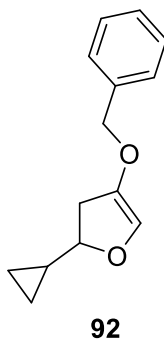


**(2*R*,3*R*)-2-(Benzyloxy)-3-cyclopropylcyclobutan-1-one (80e')**



**80e**: colorless oil;  $R_f$  0.40 (50:50 EtOAc: hexane); IR (cast film) 3078, 3030, 3002, 2924, 2867, 1785, 1496, 1454, 1431, 1393, 1163, 1116, 1019  $\text{cm}^{-1}$ .  $^1\text{H}$  NMR (500 MHz,  $\text{CDCl}_3$ )  $\delta$  7.40-7.31 (m, 5H), 4.79 (d,  $J = 12.2$  Hz, 1H), 4.69 (d,  $J = 12.2$  Hz, 1H), 4.40 (ddd,  $J = 5.4, 2.6, 2.6$  Hz, 1H), 2.73 (ddd,  $J = 12.2, 9.7, 2.8$  Hz, 1H), 2.45 (ddd,  $J = 12.2, 9.6, 2.8$  Hz, 1H), 2.11 (dddd,  $J = 9.7, 9.7, 7.5, 7.5$  Hz, 1H), 1.04-0.97 (m, 1H), 0.61-0.53 (m, 2H), 0.55-0.50 (m, 1H), 0.29-0.24 (m, 1H);  $^{13}\text{C}$  NMR (125 MHz,  $\text{CDCl}_3$ )  $\delta$  205.3, 137.3, 128.4, 128.0, 127.9, 90.6, 72.3, 42.9, 37.1, 14.0, 3.6, 3.2; HRMS (ESI) calcd for  $\text{C}_{14}\text{H}_{16}\text{NaO}_2$   $[\text{M}+\text{Na}]^+$  239.1043; found 239.1043.

**(2*R*)-4-(Benzyloxy)-2-cyclopropyl-2,3-dihydrofuran (92)**



**92**: colorless oil;  $R_f$  0.60 (50:50 EtOAc: hexane); IR (cast film) 3111, 3082, 3032, 3006, 2918, 2855, 1666, 1497, 1454, 1336, 1302, 1233, 1086  $\text{cm}^{-1}$ .  $^1\text{H}$  NMR (500 MHz,  $\text{CDCl}_3$ )  $\delta$  7.40-7.29 (m, 5H), 5.99 (dd,  $J = 2.0, 2.0$  Hz, 1H), 4.73 (s, 2H), 3.92 (ddd,  $J = 10.0, 8.5, 8.5$  Hz, 1H), 2.90 (ddd,  $J = 14.8, 9.9, 2.0$  Hz, 1H), 2.72 (ddd,  $J = 14.8, 8.2, 2.1$  Hz, 1H), 1.19 (dddd,  $J = 8.2, 8.2, 8.2, 5.2, 5.2$  Hz, 1H), 0.65-0.54 (m, 2H), 0.46-0.41 (m, 1H), 0.33-0.28 (m, 1H);  $^{13}\text{C}$  NMR (125 MHz,  $\text{CDCl}_3$ )  $\delta$  141.4, 136.8, 128.5, 128.1, 127.6, 83.7, 72.1, 37.7, 36.2, 16.0, 3.0, 1.6; HRMS (EI) calcd for  $\text{C}_{14}\text{H}_{16}\text{O}_2$   $[\text{M}]^+$  216.1150; found 216.1148.

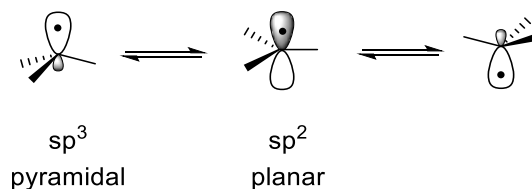
## Chapter 3 Mechanistic Studies of the Stevens [1,2]-Rearrangement of the Cyclic Oxonium Ylides Employing Hypersensitive Radical Clock

### 3.1 Introduction: Free Radicals

Reactive intermediates are defined as short lived intermediates which are generated in a chemical process and are consumed further in the next step to generate the reaction product. These intermediates are usually not isolable but can be detected and inferred by chemical traps, spectroscopy methods or product distributions. Among the most common reactive intermediates are free radicals, carbenes, allenes, carbonium ions, carbanions, ketenes and benzyne.

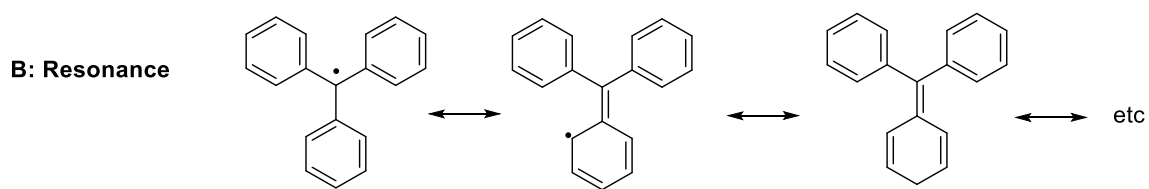
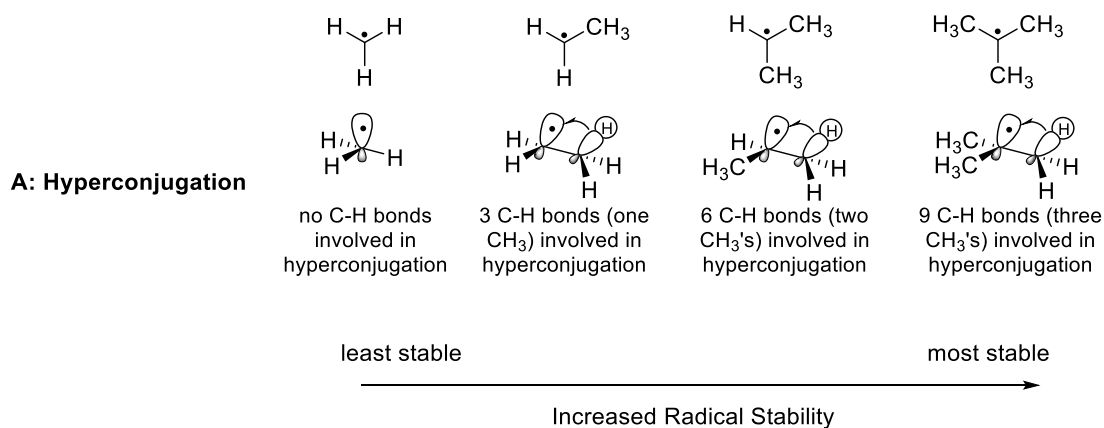
Free radicals have been known as reactive intermediates in reaction pathways. “*Radical*” is a term used to describe reactive chemical species possessing an unpaired electron.<sup>131</sup> The first identified free radical was the stable triphenylmethyl radical reported by Moses Gomberg in 1900.<sup>132</sup> Later, Friedrich Paneth and Wilhelm Hofeditz generated the methyl free radical which, in contrast to triphenylmethyl, is not isolable.<sup>132</sup> Discovery of radicals opened new windows to the chemistry world. Their reactivity including dimerization, rearrangements and polymerization has been further employed in industry and organic synthesis.<sup>133</sup>

The geometry of free radicals is assumed to be somewhere between the  $sp^2$  and  $sp^3$  hybridization. The energy barrier for the inversion of the pyramidal  $sp^3$  free radicals is very low, allowing easy inversion through a planar  $sp^2$  geometry. As a result, the geometry of free radicals is considered between pyramidal and planar geometry (Figure 3-1).



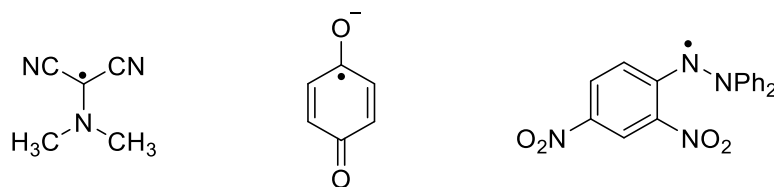
**Figure 3-1: Rapid Radical Inversion Bearing both Pyramidal and Planar Geometry**

A radical species is normally generated by the homolysis of a covalent bond through photochemical and thermal processes or single electron transfer. This bond cleavage requires energy which is called “homolytic bond dissociation energy” ( $\Delta H^\circ$ ) and depends on the strength of the bond. Formation of the more stable radicals typically requires less energy. Free radicals can be stabilized by hyperconjugation (Figure 3-2, A) and resonance (Figure 3-2, B).<sup>134</sup>



**Figure 3-2: Stability of Free Radical**

Radicals can also be stabilized by adjacent electron donating (EDG) and electron withdrawing (EWG) substituents. Radical centers that are directly attached to both EWG and EDG are considered to be long-lived radicals. This effect is called “captodative stabilization” (Figure 3-3).<sup>71</sup>

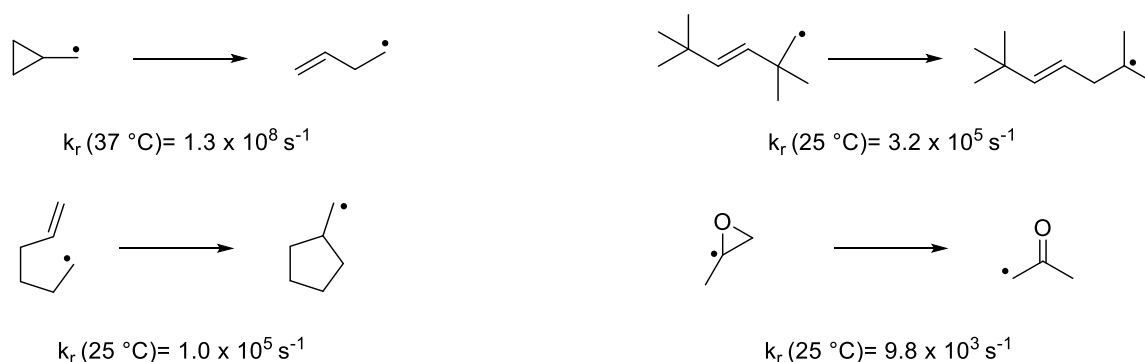


**Figure 3-3: Captodative Long-Lived Free Radicals**

### 3.2 Radical Clocks

Characterization of the reactive intermediate can provide evidence to support the actual reaction mechanism and explain product formation, regio, chemo and diastereoselectivity. Free radicals have been proposed to be reactive intermediates involved in the reaction mechanism. Therefore, strong evidences to prove their presence in the reaction mechanism can help chemists to gain insight into the chemical reaction pathways.

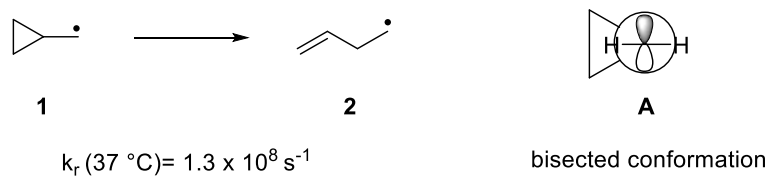
One of the early methods to distinguish radical intermediates in reaction pathways was suggested by Keith U. Ingold in 1980.<sup>135</sup> He proposed a wide range of alkyl radical clocks as a tool to demonstrate the existence of free radicals as well as to provide kinetic studies of the radical-molecule reactions (Figure 3-4). They employed radical moieties that undergo very fast and irreversible rearrangement and can be installed easily at the proper molecular position at which radicals are formed. In the case of radical intermediates, the isolation and characterization of rearranged products can be powerful evidence to confirm the presence of free radicals.



**Figure 3-4: Examples of Radical Clocks Proposed by Ingold**

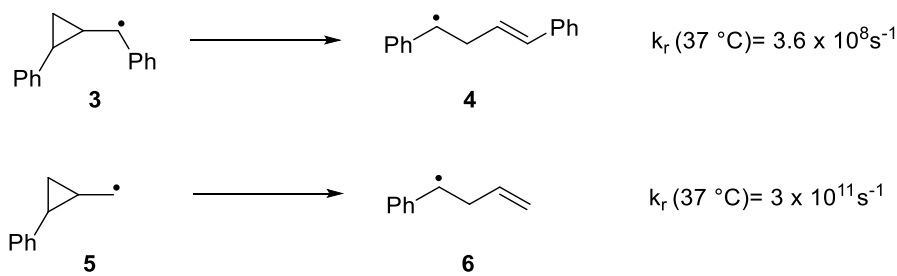
### 3.2.1 Cyclopropylcarbinyl Radical Clock

As was mentioned in Chapter 2, small cyclopropane rings have high ring strain. It is also known that the parent cyclopropylcarbinyl radical (**1**) possesses  $115\text{ kJ mol}^{-1}$  ring strain.<sup>136</sup> Although the C-C bonds of the cyclopropane ring apply significant radical stabilization via the bisected conformation (Figure 3-5, conformation A), very fast cyclopropane ring opening ( $k_r$ ) occurs to the but-3-enyl radical (**2**) to relieve the ring strain (Figure 3-5).<sup>136</sup> This behavior provides the opportunity to employ cyclopropylmethyl radical as a facile and simple probe for the mechanistic studies of the reactions potentially involving radical intermediates.



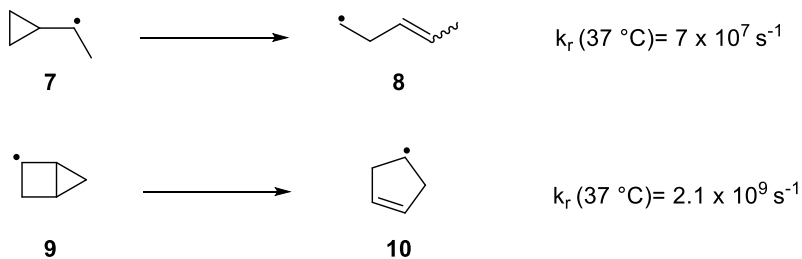
**Figure 3-5: Cyclopropylcarbinyl Radical**

Several factors can affect the rate of ring opening in cyclopropylmethyl radicals. The stabilities of the resulting radicals are important factors (Figure 3-6). For instance, phenyl substituted phenylcyclopropylmethyl radical **3** ring opens more slowly than radical **5** due to the stability of benzylic radical in the parent radical **3**, and both radicals **3** and **5** undergo faster ring opening compared to the unsubstituted cyclopropylcarbinyl radical **1**.<sup>136,137</sup>



**Figure 3-6: The Rate of the Ring Opening of the Phenyl Substituted Cyclopropylcarbinyl Radicals**

On the other hand, it is expected to observe faster ring opening for more strained cyclopropylcarbinyl radicals. Bicyclo-[2.1.0]-pent-2-yl radical **9** ring opens faster compared to monocyclic radical **7** to relieve the ring strain (Figure 3-7).<sup>138</sup>

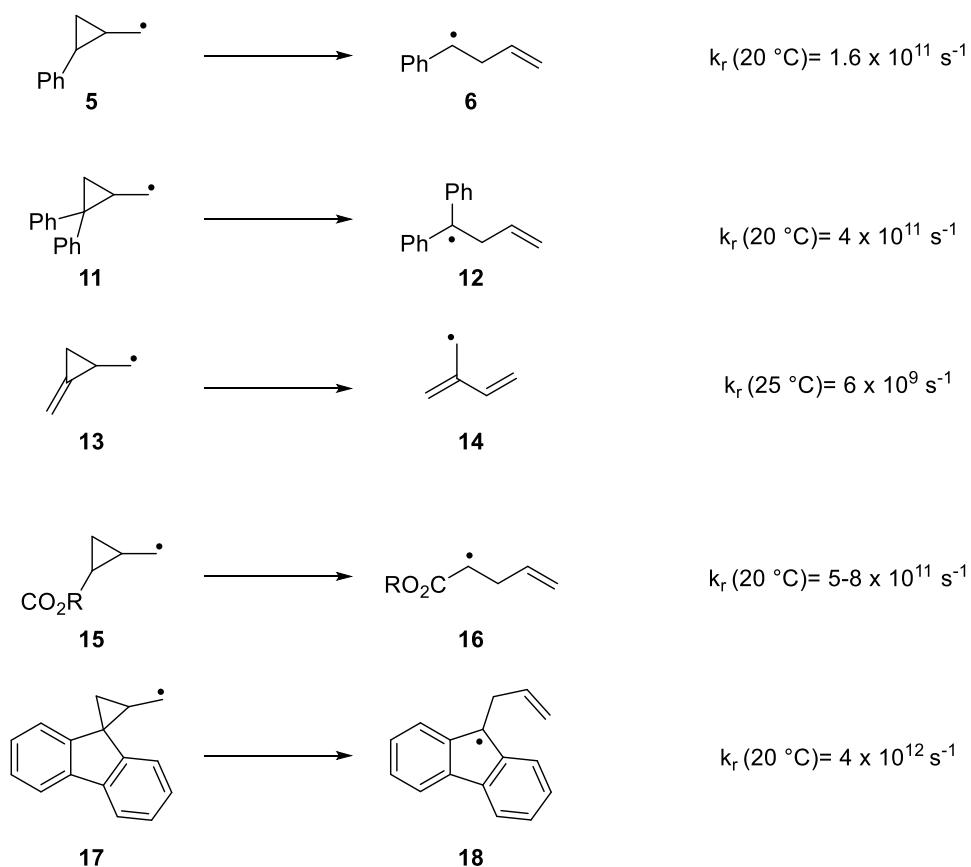


**Figure 3-7: Increasing Ring Opening Rate of the Strained Radicals**

### 3.2.2 Ultrafast Cyclopropylmethyl Radical Probes

Employing a suitable radical probe to study the existence of radical species in a reaction mechanism depends on the lifetime of the radical intermediates. It is noteworthy to mention that the absence of the rearranged products in the reaction mixture does not eliminate the possibility of a radical pathway. It is always required to consider a faster radical recombination than radical rearrangement. As a result, employing ultrafast radical clocks having a more rapid rearrangement rate is valuable.

Newcomb and coworkers have studied and calibrated the rate of the ring opening of a variety of the cyclopropylcarbiny derivatives possessing extremely short lifetimes.<sup>139–146</sup> They have reported aryl substituted cyclopropylmethyl radicals undergo ultrafast ring opening and can be used in the mechanistic and kinetic studies of the reactions with very short lived radical intermediates (Figure 3-8).<sup>145,147</sup>

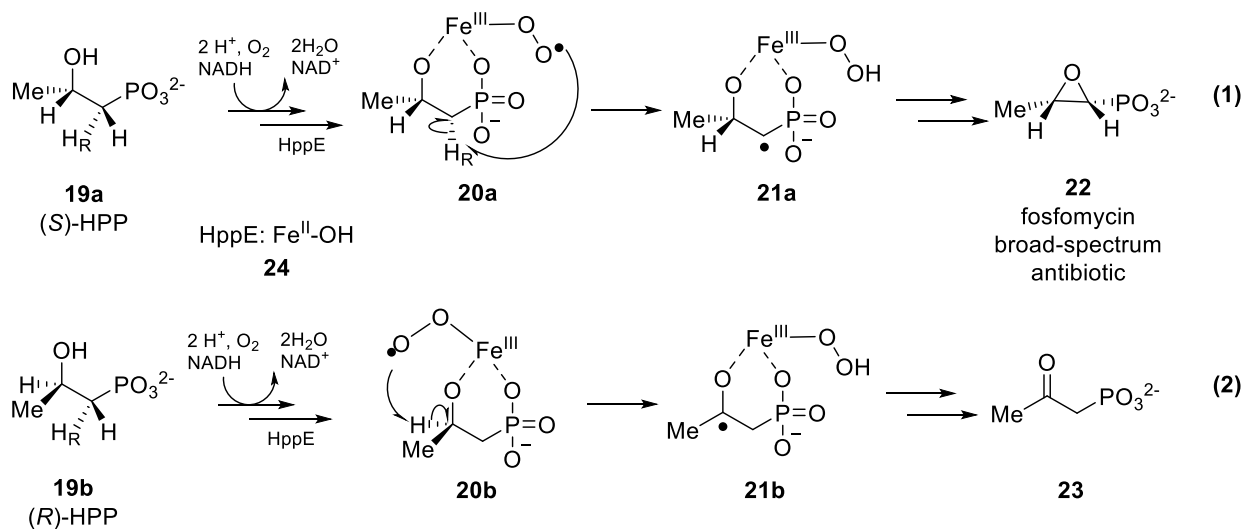


**Figure 3-8: Ultrafast Radical Probes**

### 3.2.3 Application of Cyclopropylmethyl Radicals in Mechanistic Studies

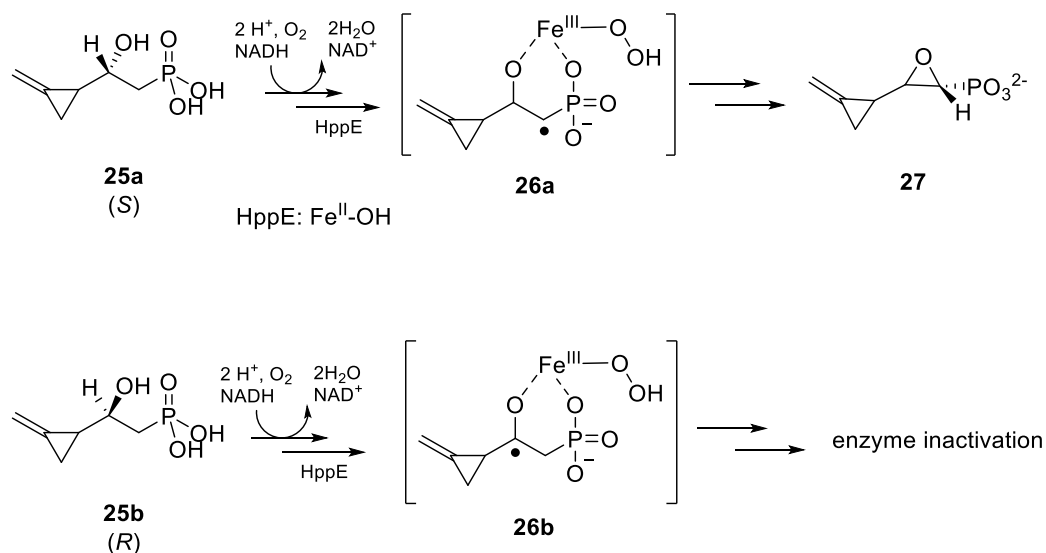
Over the past decades, cyclopropylmethyl radicals have been extensively employed in mechanistic studies of chemical and biochemical reactions to study the existence of radical intermediates.<sup>148–151</sup> In 2013, the mechanism of the oxidative epoxidation of (*S*)-2-hydroxypropylphosphonic acid ((*S*)-HPP) **19a** to fosfomicin **22**, a broad spectrum antibiotic against bacterial infections, in the presence of (*S*)-2-hydroxypropylphosphonic acid epoxidase (HppE) **24** was studied (Scheme 3-1).<sup>148</sup> It is known that (*R*)-HPP **19b** is not an active

enantiomer to form the epoxide and instead 2-oxopropylphosphonic acid **23** is generated. It has been proposed that the process occurs through the formation of the radical intermediates **20a** and **20b** for *S* and *R* enantiomers respectively but further evidence to prove the presence of radicals was still required.



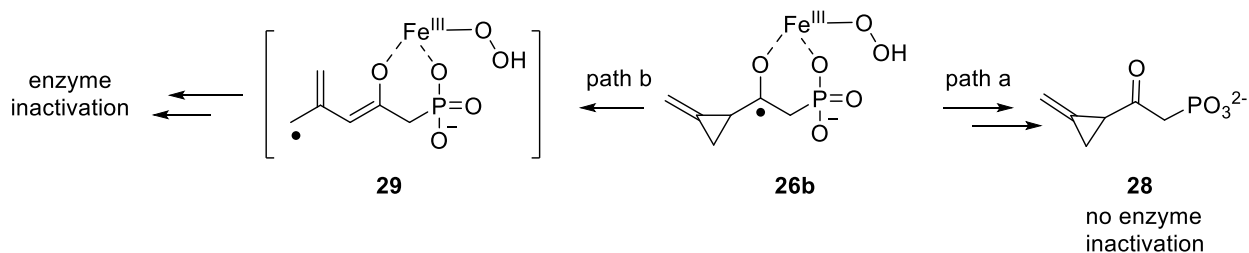
### Scheme 3-1: Proposed Mechanism of HppE Catalyzed Formation of Fosfomicin

For this purpose, Pai and Liu employed (methylene)cyclopropyl carbonyl radical **13** as an ultrafast radical clock to detect radical formation. Treatment of (*S*)-**25a** provided the expected epoxide **27** whereas treatment of the (*R*)-**25b** induced enzyme deactivation (Scheme 3-2).



### Scheme 3-2: Employing (Methylenecyclopropyl)methyl Radical Probe

They proposed two reasons for the enzyme deactivation (Scheme 3-3): (1) the formation of corresponding 2-oxophosphonate **28** (path a) or (2) the generation of the rearranged cyclopropane to corresponding alkene **29**. When they added chemically synthesized **28** to the original biochemical process (Scheme 3-1, eq. 1) no enzyme deactivation was observed, implicating the presence of the rearranged radical **29** as a species for the enzyme inactivation. These observations successfully showed the presence of the radical intermediate in the mechanism of the HppE catalyzed epoxidation.

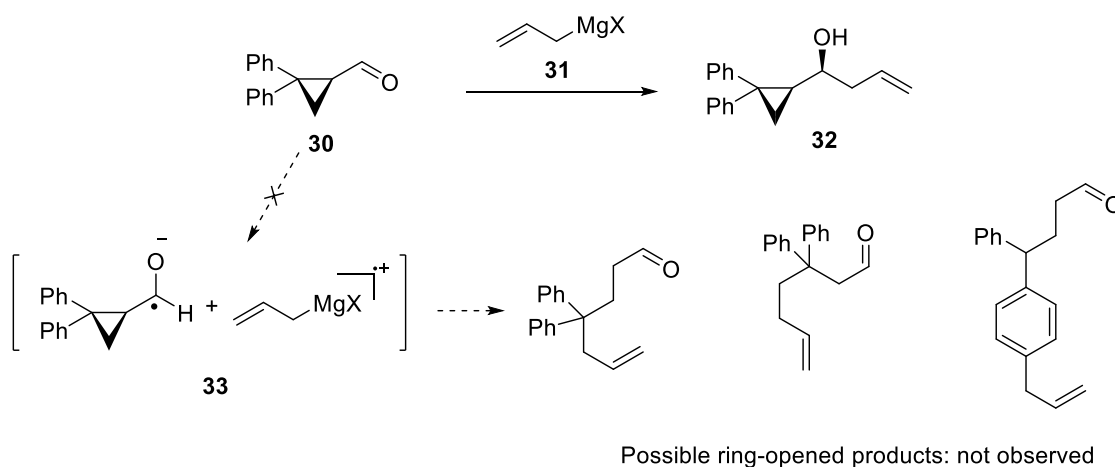


### Scheme 3-3: Proposed Pathways for the Enzyme Deactivation

More recently, Otte and Woerpel chose very fast radical clock, 2,2-diphenylcyclopropylcarbonyl radical, to study the mechanism of the addition of allylic



Grignard reagent to aliphatic aldehydes to investigate whether the reaction occurs through a single electron transfer (SET) mechanism.<sup>149</sup> They treated aldehyde **30** with allylmagnesium Grignard reagent **31** and no products resulted from the ring opened radical intermediates were observed and 1,2-addition product **32** was the only isolated compound (Scheme 3-4). Therefore they deduced the addition of allylmagnesium to the aliphatic aldehydes doesn't occur through the formation of radical intermediates **33** resulting from SET mechanism.

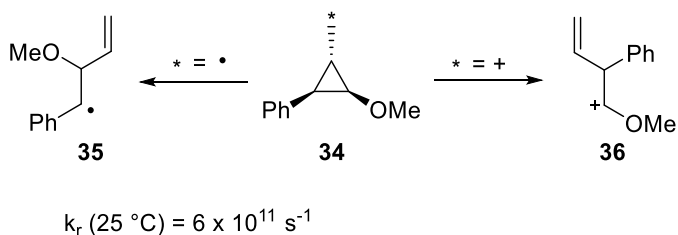


**Scheme 3-4: Reaction of Aldehyde 30 with Allylmagnesium Reagent**

### 3.2.4 Hypersensitive Radical Probes to Distinguish between Radical and Carbocation Intermediates

Despite of the usefulness of the aforementioned radical clocks to study the presence of radical intermediates in reaction mechanisms, it is possible to observe the same product distributions in the case of the carbocation species. This problem is mostly observed for hypersensitive radical clocks. As a result, to obtain more mechanistic evidence to be able to distinguish between radical pair and ionic intermediates, Newcomb and coworkers in 1994 reported hypersensitive probe (*trans-trans*)-2-methoxy-3-phenylcyclopropylmethyl **34**, as a mechanistic differentiation tool.<sup>152,153</sup> The phenyl substituent on the cyclopropylcarbinyl stabilizes a radical more efficient than the methoxy group, while carbocations are more stabilized by the alkoxy group. Therefore, cyclopropylcarbinyl radical undergoes ring opening toward phenyl group to form benzyl radical **35** whereas the cyclopropylcarbinyl cation will generate oxocarbenium ion **36**. It is noteworthy to mention that formation of benzylic radical occurs with high regioselectivity, 170:1 whereas oxocarbenium ion is formed with >1000:1

ratio under cyclopropylcarbinyl cation ring opening. Hence, high regioselectivity during the cyclopropane ring opening under distinct reaction pathways will furnish different products showing the nature of the active intermediates in the reaction mechanism. On the other hand, cyclopropylcarbinyl has been known as a very fast radical clock ( $k_r$  (25 °C) =  $6 \times 10^{11} \text{ s}^{-1}$ ); so it may be employed in the kinetic and mechanistic studies of the reactions containing very short lived intermediates.

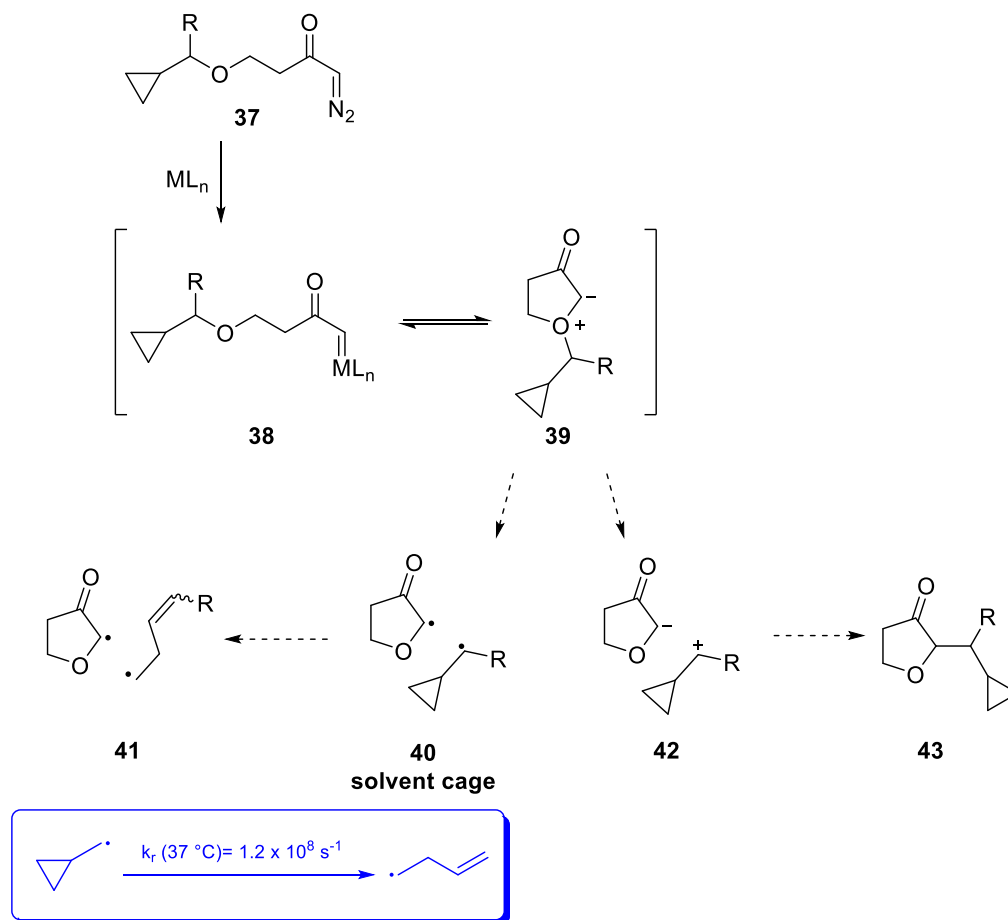


**Figure 3-9: (*trans, trans*)-2-Methoxy-3-phenylcyclopropyl)methyl, a Mechanistic Differentiation Tool**

### 3.3 Background

In Chapter 2, we discussed the endocyclic Stevens [1,2]-rearrangement of cyclopropylmethyl moiety in oxonium ylides. We showed endo-[1,2]-shift of the cyclopropylcarbinyl moiety generated cyclobutanones with the intact cyclopropane ring. It was expected to observe cyclopropane ring opening if the Stevens [1,2]-rearrangement occurs through the intermediacy of biradicals. We assumed the absence of the ring opened products could be the result of the either very fast biradical recombination or an alternative mechanism involving ionic intermediates (Scheme 2-22). Thus, we opted to study the detailed migratory aptitude of cyclopropylmethyl moiety to understand the nature of the intermediates in the Stevens rearrangement (Scheme 3-5). We also discussed the reactivity of the unbranched diazo ketone possessing cyclopropylcarbinyl migrating group. We mentioned that no exocyclic migration occurs in the case of unsubstituted cyclopropylmethyl group. For further studies due to generality of this observation as well as the mechanistic studies we opted to study the reactivity of diazo ketones **37** as the substrate to generate oxonium ylides **39** possessing cyclopropylmethyl moiety as a migrating group. In the case of *exo*-[1,2]-rearrangement we expect two possible pathways including the formation of radical pairs **40**

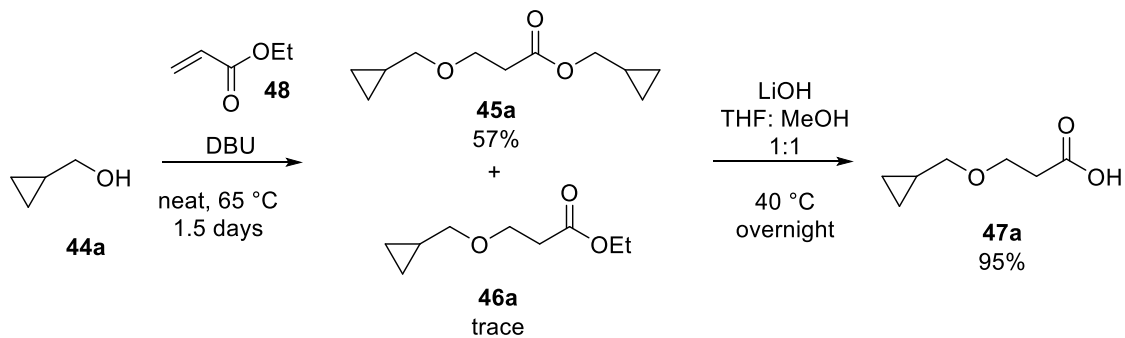
(path a) or zwitterions **42** (path b). Isolation of the products resulting from cyclopropane ring opened intermediates **41** will be a strong evidence for the presence of radical intermediates.



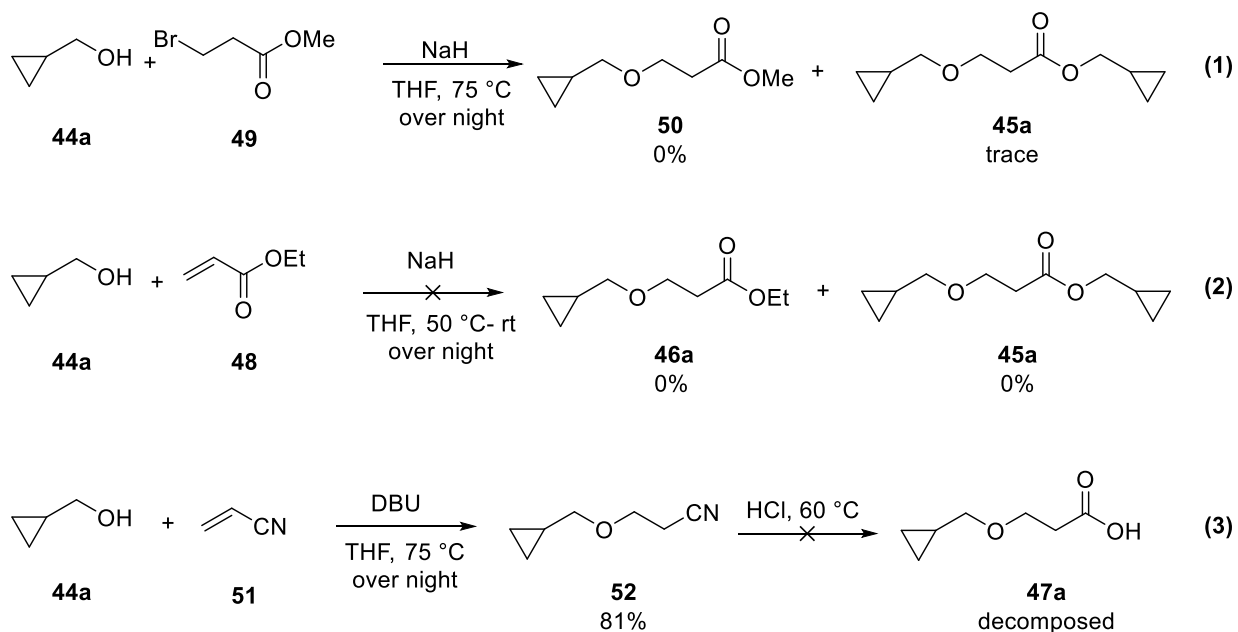
**Scheme 3-5: Cyclopropylcarbinyl Moiety as a Migrating Group in Exocyclic [1,2]-shift**

### 3.3.1 The Migratory Aptitude of Cyclopropylmethyl Moiety in Exocyclic [1,2]-Shift

To synthesize the required diazo ketone **37a** (R: H), we prepared the corresponding carboxylic acid precursor **47** in two steps from the cyclopropanemethanol **44a** and ethyl acrylate **48** to afford esters **45a** and **46a**, followed by the hydrolysis of the esters to the carboxylic acid **47a** (Scheme 3-6). All other attempts to prepare ester **45a**, including nucleophilic substitution of the alcohol **44a** (Scheme 3-7, eq. 1 and eq. 2) and the preparation of the acid **47a** from the hydrolysis of cyanide **52** (Scheme 3-7, eq. 3),<sup>154,155</sup> were unsuccessful or occurred with very low yields.

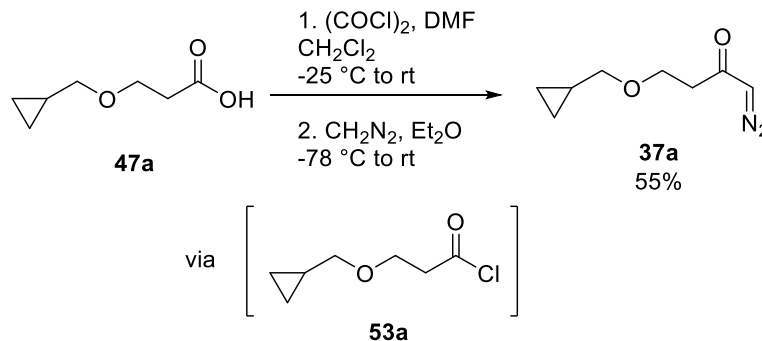


**Scheme 3-6: Synthesis of the Acid Precursor**



**Scheme 3-7: Unsuccessful Attempted Pathways**

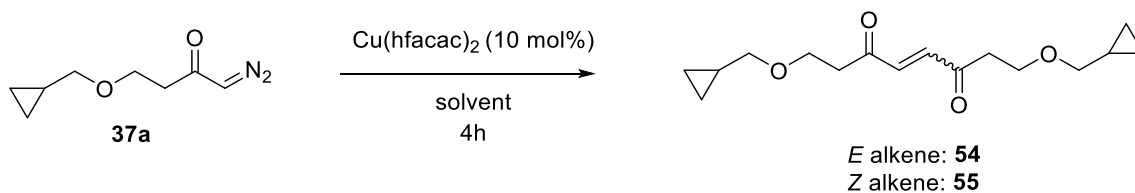
*In situ* generation of acid chloride **53a** by the treatment of the acid **47a** with oxalyl chloride followed by the addition of freshly prepared diazomethane generated required diazo ketone **37a** having cyclopropylmethyl moiety at the suitable position for the exocyclic Stevens rearrangement (Scheme 3-8)



### Scheme 3-8: Generation of Diazo Ketone **37a**

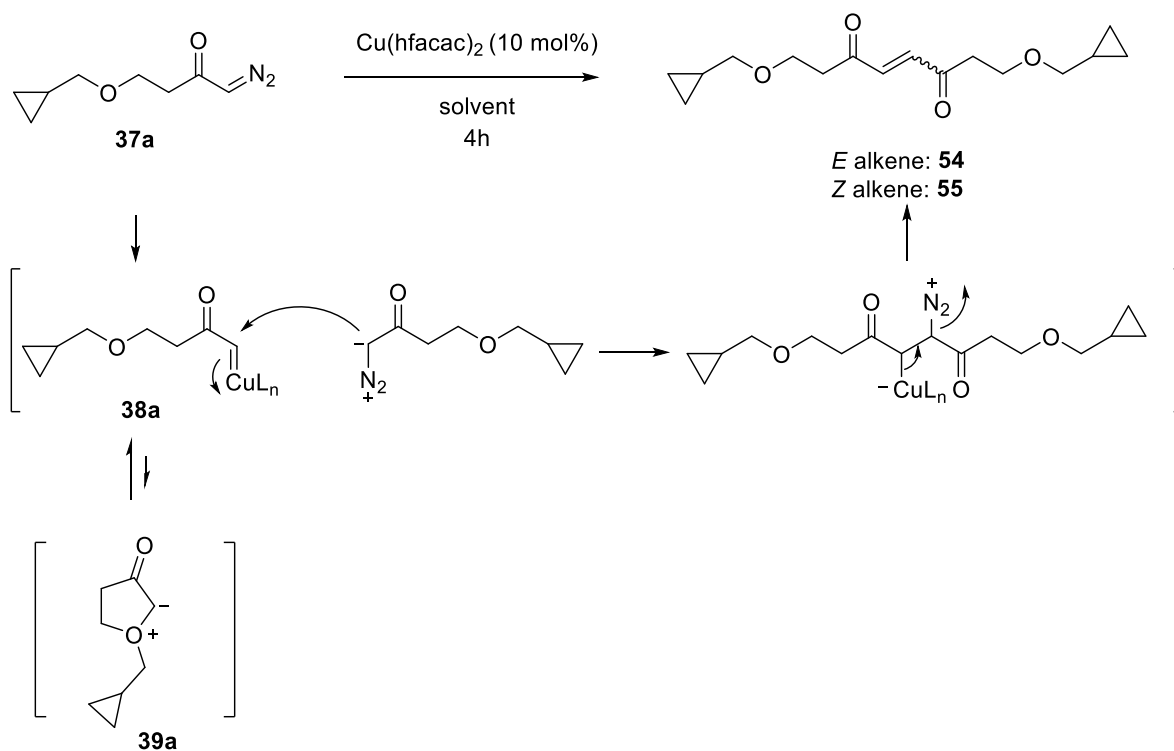
Similar to the conditions that were applied for endocyclic [1,2]-rearrangement (Chapter 2), we started our studies by the treatment of diazo ketone **37a** with  $\text{Cu}(\text{hfacac})_2$  in dichloromethane at reflux. Surprisingly no [1,2]-shift was observed and symmetrical *E* and *Z* enediones **54** and **55** were isolated (Table 3-1, entry 1). The *E*:*Z* ratio of enediones was determined by the integration of the olefin singlet peak in  $^1\text{H}$  NMR which appears at a higher chemical shift for the *E* isomer.<sup>156</sup> Slower addition and lower concentration of the diazo ketone solution during the reaction did not prevent dimerization. We assumed the higher activation energy for the [1,2]-Stevens rearrangement of oxonium ylide **39a** leads the equilibrium mostly in favor of the formation of acyclic metallocarbene **38a**, which can be trapped with diazo ketone **37a** to afford dimeric product (Scheme 3-9). However, reflux in dichloroethane, providing higher temperature to afford the required energy for the Stevens rearrangement, did not change the reaction pathway and dimeric products **54** and **55** were isolated in 53% yield and with 3:1 ratio (Table 3-1, entry 2). A very complex reaction mixture was obtained after refluxing in toluene and only 23% of the dimeric product was isolated with a diastereomeric ratio of 3:1 (Table 3-1, entry 3). These results indicated a poor ability of cyclopropylcarbinyloxy substituent as a migrating group in exocyclic [1,2]-Stevens rearrangement.

**Table 3-1: Copper Catalyzed Decomposition of Diazo Ketone 37a**



Entry	Solvent	Yield % <sup>a</sup>	Ratio (E:Z) <sup>b</sup>
1	DCM	50	4:1
2	DCE	53	3:1
3	toluene	23 <sup>c</sup>	3:1

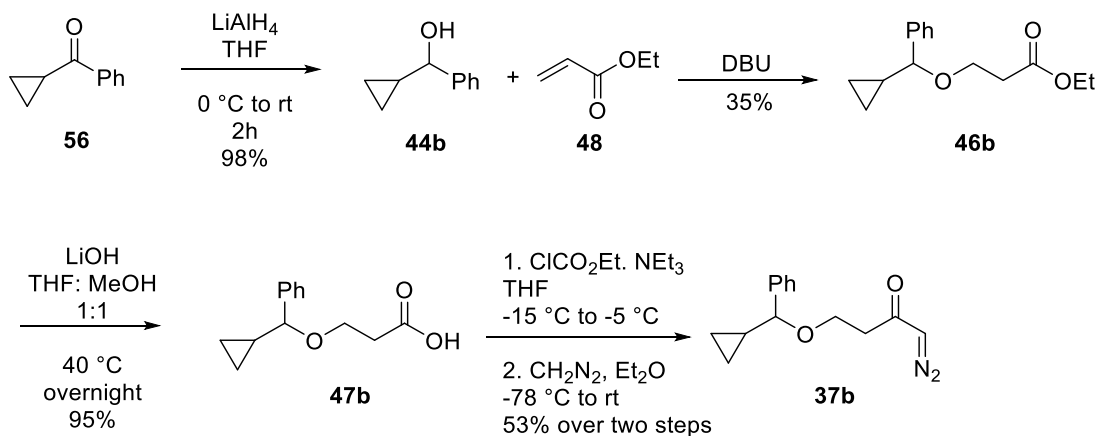
<sup>a</sup>Combined isolated yield. <sup>b</sup>Ratio was determined by <sup>1</sup>H-NMR analysis of the crude via the integration of the olefin peaks. <sup>c</sup>Small isolated yield due to complex reaction mixture.



**Scheme 3-9: Proposed Mechanism for the Formation of Alkenes 54 and 55**

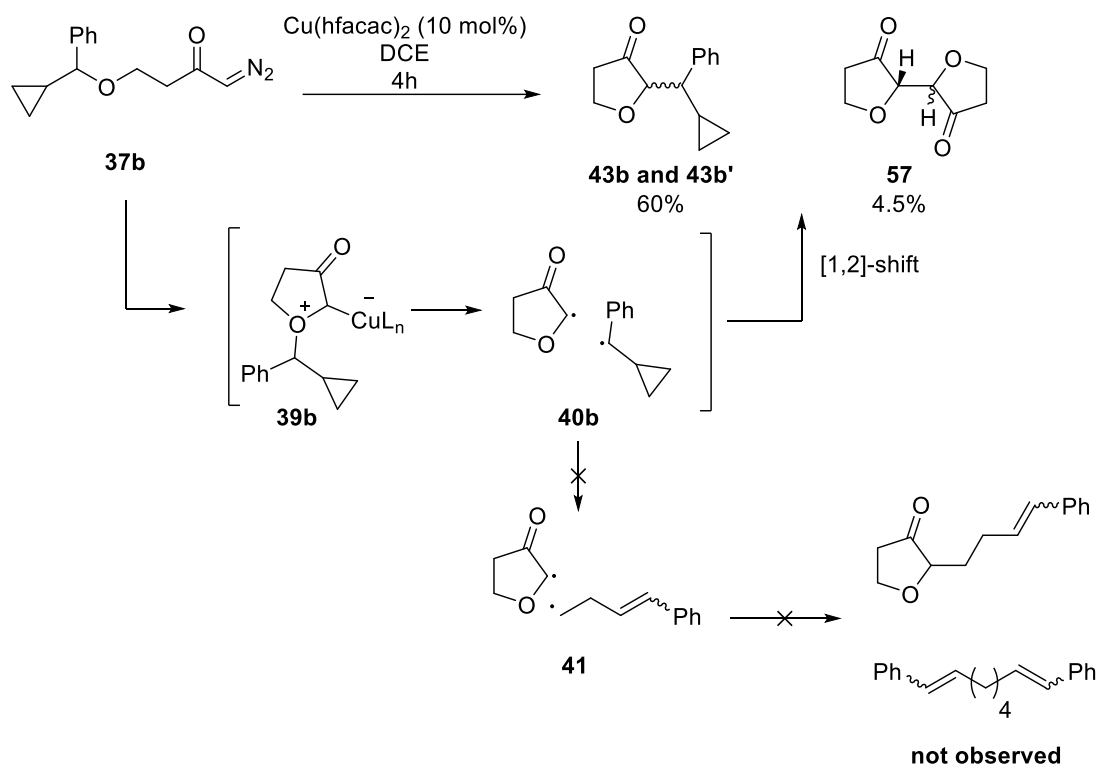
Thus we opted to install cyclopropylphenylcarbinyl group possessing an additional phenyl ring as a stabilizing group to be able to promote the exocyclic [1,2]-Stevens rearrangement. For this purpose, diazo ketone **37b** was synthesized by the treatment of carboxylic acid **47b**

with ethylchloroformate and through the formation of mixed anhydride. The carboxylic acid **47b** was also obtained from the hydrolysis of ethyl ester **46b** which was synthesized through the same process as **46a** starting from secondary alcohol **44b** (Scheme 3-10). The diazo ketone **37b** was then treated with  $\text{Cu}(\text{hfacac})_2$  in dichloroethane.



**Scheme 3-10: Synthesis of Diazo Ketone 37b**

Interestingly, tetrahydrofuranones **43b** and **43b'** resulting from the exocyclic [1,2]-Stevens rearrangement were isolated in 60% yield as two inseparable diastereomers with 50:50 diastereomeric ratio, accompanied by the formation of homodimer **57** in 4.5% yield (Scheme 3-11). Other products showing the presence of radical pairs **41** were not isolated. Observing the tetrahydrofurans **43** showed that increasing radical or carbocation stabilization effect of phenyl substituent on the migrating group. Although the formation of the homodimer **57** was a strong evidence for the presence of the radical intermediates **40b** in the reaction mechanism, observing no ring opening of strained cyclopropyl ring after formation of radical pairs **40b** to rearranged radical pairs **41b** was not consistent with the formation of radical pair intermediates. It is noteworthy to mention that the rate of the ring opening of phenylcyclopropylcarbinyl ( $k_r$  (22 °C) =  $2.7 \times 10^5 \text{ s}^{-1}$ )<sup>157</sup> compared to cyclopropylcarbinyl radical is known to be slower due to the stabilizing effect of phenyl ring. This fact could explain the observed [1,2]-shift without cyclopropyl ring opening which might be slower than the rate of the recombination of radical pairs **40b** in a solvent cage to form tetrahydrofurans **43** and homodimers **57**.



**Scheme 3-11: Copper Catalyzed Decomposition of Diazo Ketone 37b**

### 3.3.2 Employing 2-Methoxy-3-phenyl-cyclopropylcarbinyl

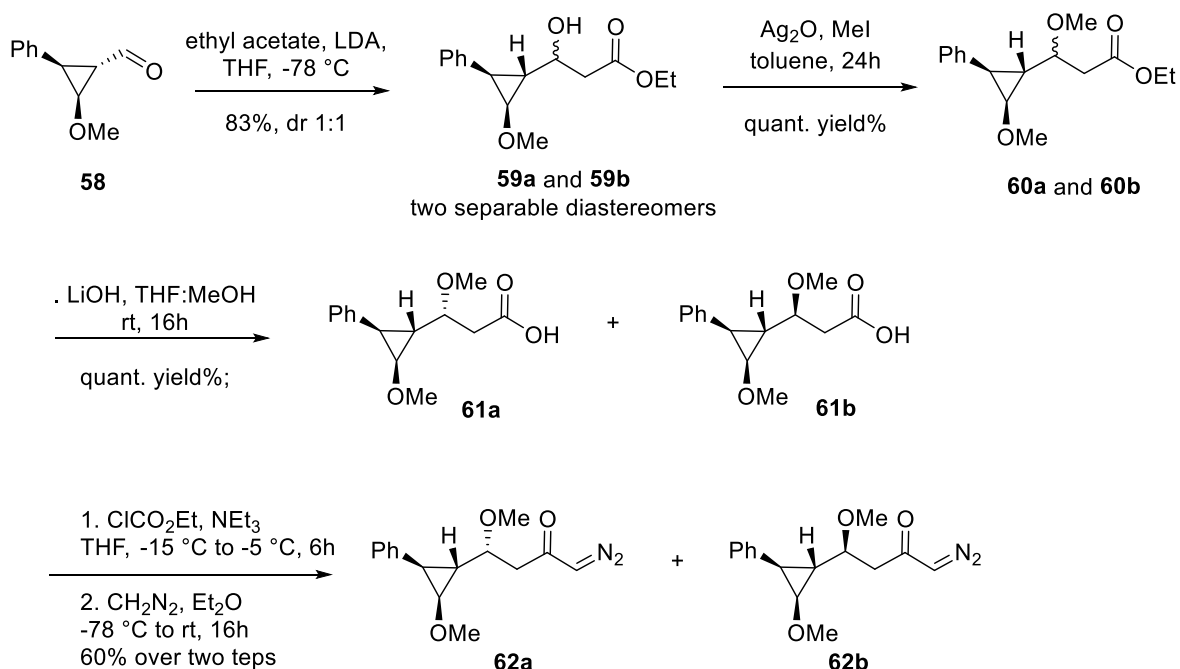
Observing no cyclopropane ring opening in both exo and endocyclic-[1,2]-shift (Chapter 2, section 0) can be rationalized by either very fast biradical recombination or an alternative reaction manifold involving zwitterionic intermediates. As a result, to be able to distinguish between radical pairs and ionic intermediates, we employed the hypersensitive probe, (*trans-trans*)-2-methoxy-3-phenyl-cyclopropylcarbinyl **34** (section 0) reported by Newcomb and *et. al* (Figure 3-9). The regioselective cyclopropane rearrangement of substructure **34** in the presence of radical or cation may provide valuable information to understand the nature of the active intermediates during the Stevens rearrangement. Also very fast cyclopropane ring opening of methoxy-3-phenyl-cyclopropylcarbinyl radical ( $k_r$  (25 °C) =  $6 \times 10^{11} \text{ s}^{-1}$ ) may overcome the possibility of the fast radical recombination in the Stevens rearrangement.

The requisite diazo ketones **62** were prepared efficiently starting from the aldol reaction between ethyl acetate and aldehyde **58**, which could be synthesized according to the literature procedure reported by Newcomb *et. al.*<sup>142</sup> to form alcohols **59a** and **59b** in a 1:1 diastereomeric

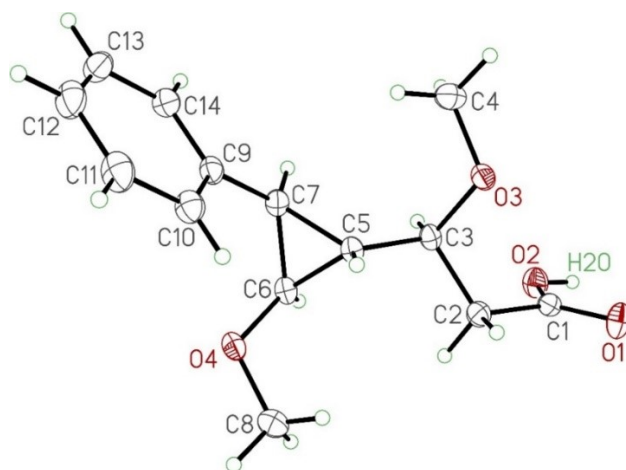


ratio. Two separable alcohols could be methylated using  $\text{Ag}_2\text{O}$  and iodomethane to generate ester **60a** and **60b** which can then be then hydrolyzed to the corresponding acids **61**.

The relative configuration of the stereogenic centres of acid **61b** was confirmed by X-ray crystallography (Figure 3-10). The desired diazo ketones **62a** and **62b** were synthesized by treating the corresponding mixed anhydrides with freshly prepared diazomethane (Scheme 3-12).

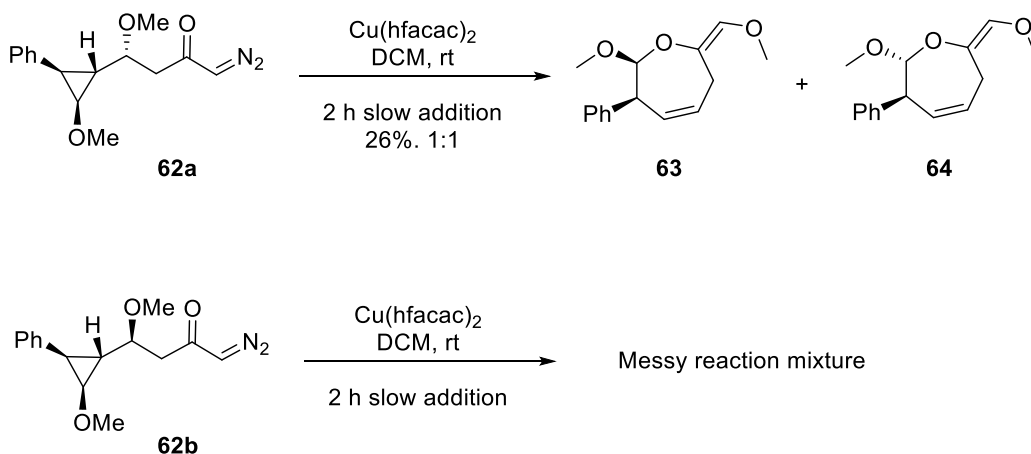


**Scheme 3-12: Synthesis of Diazo Ketones 62**



**Figure 3-10: ORTEP Structure for Carboxylic Acid 61b**

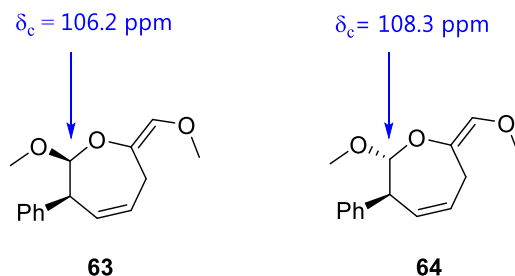
Treatment of diazo ketone **62a** with  $\text{Cu}(\text{hfacac})_2$  in  $\text{CH}_2\text{Cl}_2$  at reflux furnished tetrahydrooxepine diastereomers **63** and **64** in 1:1 diastereomeric ratio and 26% isolated yield. It is noteworthy to mention that diazo ketone **62b** gave a complicated reaction mixture under the similar reaction condition and all efforts to purify products were unsuccessful (Scheme 3-13).



**Scheme 3-13: Treatment of Diazo Ketones 62 with  $\text{Cu}(\text{hfacac})_2$**

### 3.3.3 Characterization of Products

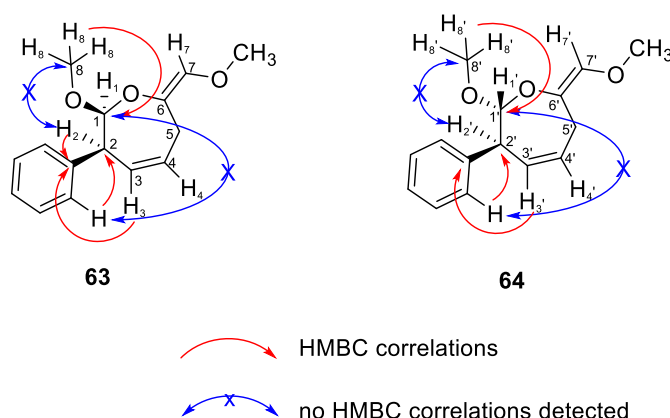
The structures of acetals **63** and **64** were confirmed by 1D and 2D-NMR analysis. Observing the  $^{13}\text{C}$  NMR peak which corresponds to the acetal carbon of **63** and **64** at 106.2 and 108.3 ppm respectively supports the formation of the acetals (Figure 3-11).



**Figure 3-11: Characteristic Chemical Shift in  $^{13}\text{C}$  NMR**

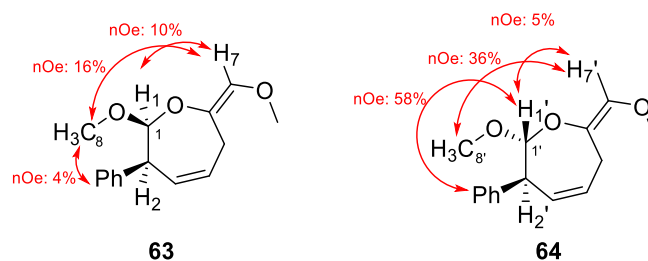
On the other hand, in the HMBC spectrum for **63**, very strong correlations were observed between protons H2/H3 and the ipso carbon of the phenyl ring as well as the correlation

between the methoxy protons (H8's) and C1. Also an obvious correlations between aromatic protons and C2 may confirm the proposed structure. The absence of correlations between H2 and C8 likewise aromatic protons and C1 are other evidences confirming the proposed structures. In case of isomer **64**, the same correlations were distinguished confirming the proposed structure for **64** although no distinct correlation was observed between H2' and phenyl carbons (Figure 3-12).



**Figure 3-12: HMBC Correlations**

Moreover, *cis*- and *trans*- geometry of the methoxy and phenyl substituents could be assigned on the basis of the larger coupling constant value of the adjacent H1' and H2' for the *trans*- isomer **64** ( $J_{H1'-H2'} = 8.2$  Hz) compared to the *cis*- isomer **63** ( $J_{H1'-H2'} = 1.9$  Hz). nOe studies also showed helpful correlations between H1' and the aromatic protons. The (*E*)-geometry of the external alkene moiety was distinguished by nOe correlations between H7/H7' and H1/H1' as well as H8/H8' of the methoxy groups in **63** and **64** respectively (Figure 3-13).

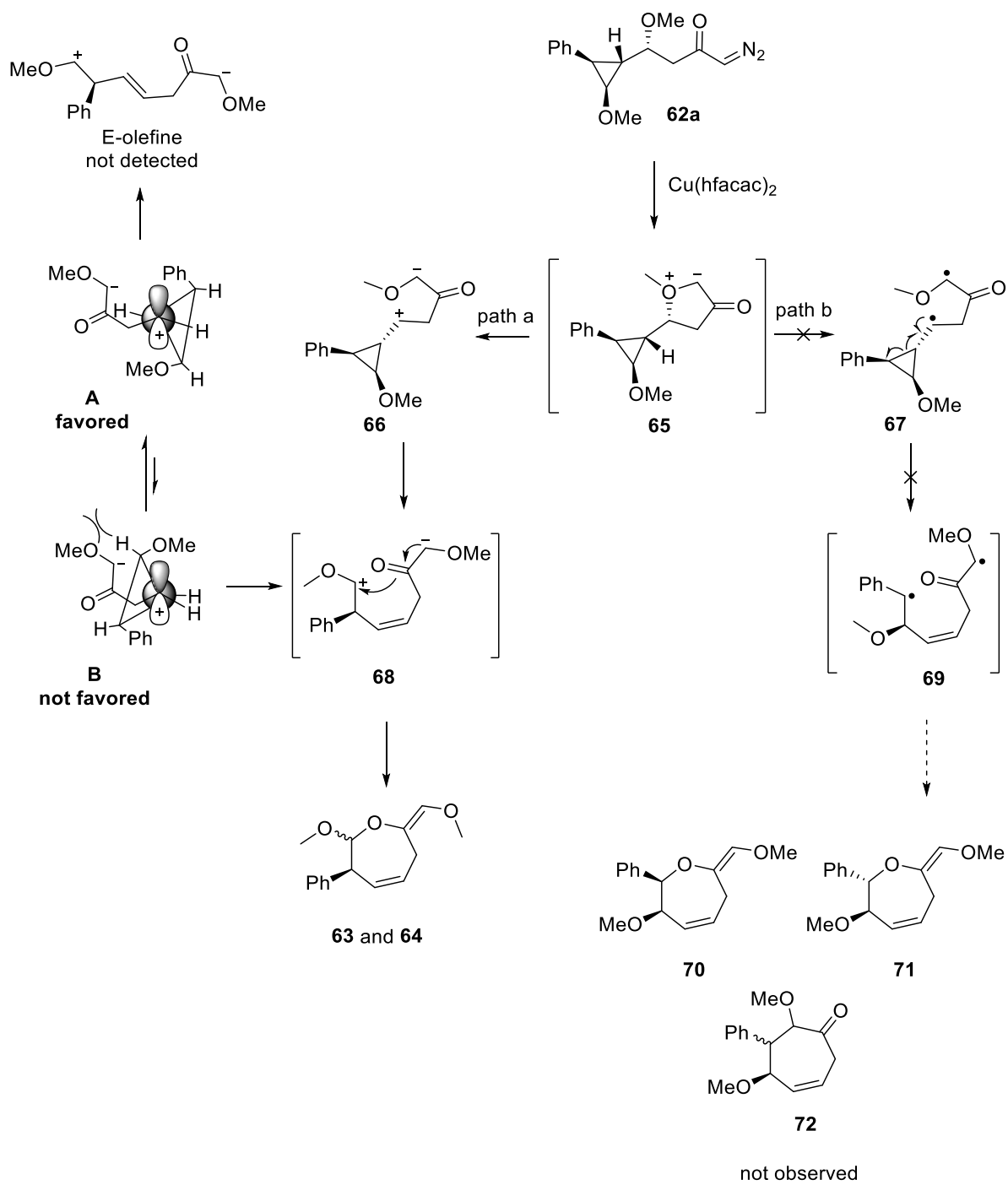


**Figure 3-13: nOe Correlations**

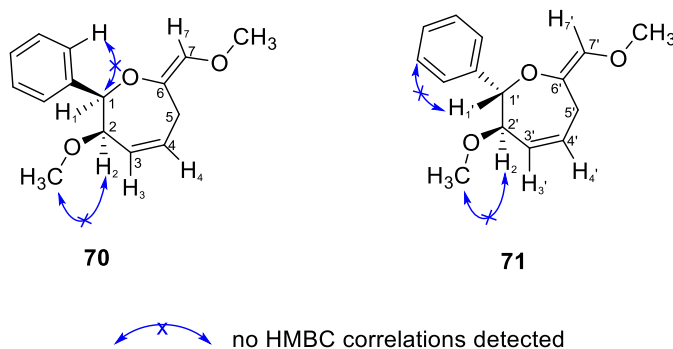
### 3.3.4 Proposed Mechanism

As discussed previously, two possible mechanistic pathways can be envisioned for this reaction. These results strongly support the presence of the ionic intermediates leading to the formation of the most stable carbocation next to the MeO after cyclopropane ring opening to afford tetrahydrooxepines **63** and **64** (Scheme 3-14, path a). Relatively low yields of the tetrahydrooxepines **63** and **64** can be explained by the formation of the two possible conformers **A** and **B** in different double bond geometries. Only the (*Z*)-olefin resulting from conformer **B** can undergo cyclization to the isolable seven membered ring products. The (*E*)-olefin resulting from what is likely to be the major conformer (**A**) is prevented from cyclization to cancel the charges, and is presumed to undergo a variety of unselective reactions furnishing a complex mixture. Based on these observations we can conclude the [1,2]-Stevens rearrangement of oxonium ylide **65** may occur mainly through a stepwise ionic mechanism. The C-O bond breaking in **65** occurs first to generate cyclopropylmethyl carbocation **66** which undergoes very fast ring opening to afford required *cis*-geometry for ring closure. The low mass balance observed for the isolated tetrahydrooxepines **63** and **64** may also be rationalized by the partial decomposition of **63** and **64** during the work up and purification. It was found that these structures underwent decomposition in the presence of air resulting in a very complex reaction mixture. The NMR characterization of these molecules were performed quickly while the samples were dissolved in less acidic CD<sub>2</sub>Cl<sub>2</sub> purged with inert argon gas.

Other products showing the presence of biradical intermediate **67** weren't detected (Scheme 3-14, path b). It was expected to observe strong HMBC correlations between aromatic ring and C1/C1' or H1/H1' as well as C2/C2' or H2/H2' and methoxy group in the hypothetical tetrahydrooxepines **70** and **71** provided if biradical **67** was involved in the reaction pathway. The absence of these correlations strongly supports the formation of **63** and **64** instead of seven membered structures **70** and **71** (Figure 3-14). The formation of tetrahydrocyclohexanone **72** resulting from the cyclization of biradical **67**, can also be ruled out based on the absence of the peak representing carbonyl group in the carbon NMR spectrum of the isolated products.



**Scheme 3-14: Proposed Mechanism**



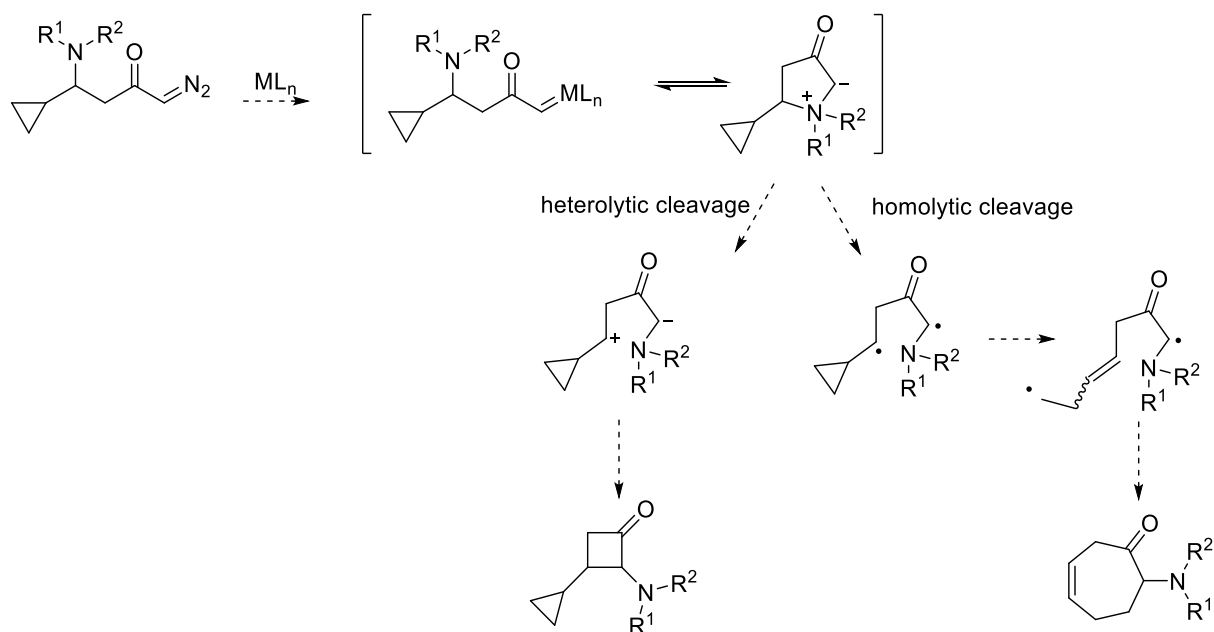
**Figure 3-14: The Not Observed Hypothetical Tetrahydrooxepines 70 and 71**

### 3.4 Conclusion

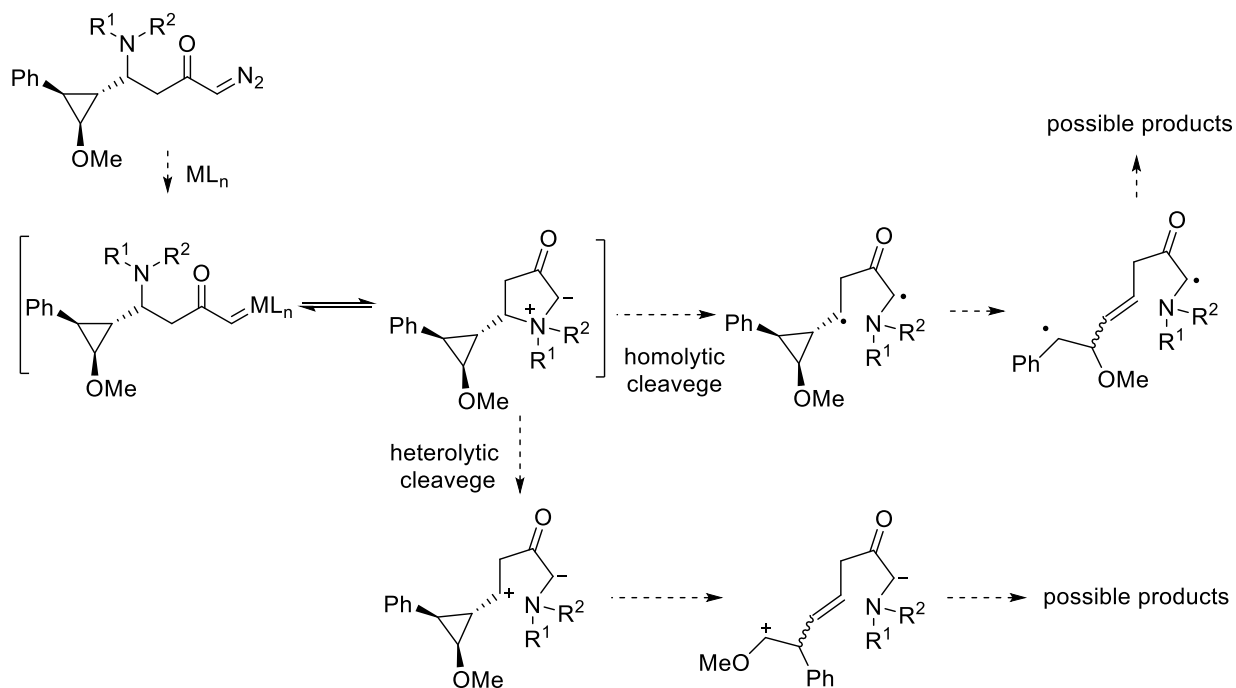
In summary, we have concluded that the mechanism pathway of the [1,2]-Stevens rearrangement is strongly dependent on the nature of migrating group. The [1,2]-Stevens rearrangement may proceed through competing radical and ionic pathways. A [1,2]-radical shift may occur when the migrating moiety contains a group capable of stabilizing a radical (i.e., aryl ring). Alternatively, carbocation stabilization of the migrating group by neighboring substituents such as cyclopropyl, may contribute to a zwitterionic pathway. To the best of our knowledge, these results are the first definitive evidence for of a zwitterionic mechanism of the [1,2]-Stevens rearrangement of oxonium ylides.

### 3.5 Future Directions

In this chapter we described the application of the ultrafast radical clocks in understanding the mechanism of the [1,2]-Stevens rearrangement of the oxonium ylides. We are now interested to study the mechanism of the Stevens rearrangement in ammonium ylides. In order to probe this mechanistic studies, the migration aptitude of the cyclopropylcarbinyl group in the Stevens rearrangement of ammonium ylide will be investigated. The observation of the products resulting from the cyclopropane rearrangement will provide valuable information regarding the active intermediates in the [1,2]-rearrangement mechanism.



Similar to the mechanistic studies discussed in this chapter, an ultrafast radical clock, (*trans-trans*)-2-methoxy-3-phenyl-cyclopropylcarbinyl may be further employed. The regioselective C-C bond cleavage of the cyclopropane in the presence of the radical or carbocation intermediate will help us to determine the mechanism of the Stevens rearrangement of the ammonium ylides.



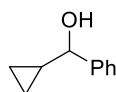
## 3.6 Experimental

### 3.6.1 General Information

Reactions were carried out in flame or oven dried glassware under a positive argon atmosphere unless otherwise stated. Transfer of anhydrous solvents and reagents was accomplished with oven-dried syringes or cannulae. Solvents and some reagents were distilled before use: methylene chloride, diisopropylamine from calcium hydride, tetrahydrofuran and diethylether from sodium/benzophenone ketyl and toluene from sodium. Diazomethane was generated based on the Sigma-Aldrich protocol from Diazald<sup>®</sup>.<sup>130</sup> All other solvents and commercially available reagents were used without further purification. Thin layer chromatography was performed on glass plates precoated with 0.25 mm silica gel; the stains for TLC analysis were conducted with 2.5 % *p*-anisaldehyde in AcOH-H<sub>2</sub>SO<sub>4</sub>-EtOH (1:3:86) and further heating until development of color. Flash chromatography was performed on 230-400 mesh silica gel with the indicated eluents. Nuclear magnetic resonance (NMR) spectra were recorded in indicated deuterated solvents and are reported in ppm in the presence of TMS as internal standard and coupling constants (*J*) are reported in hertz (Hz). The spectra are referenced to residual solvent peaks: CDCl<sub>3</sub> (7.26 ppm, <sup>1</sup>H; 77.26 ppm, <sup>13</sup>C), CD<sub>2</sub>Cl<sub>2</sub> (5.32 ppm, <sup>1</sup>H, 54.00 ppm, <sup>13</sup>C) as internal standard. Proton nuclear magnetic spectra (<sup>1</sup>H NMR) and carbon nuclear magnetic resonance spectra (<sup>13</sup>C NMR) were recorded at 500 and 125 MHz respectively. Infrared (IR) spectra were recorded neat and reported in cm<sup>-1</sup>. Mass spectra were recorded by using electron impact ionization (EI) or electrospray ionization (ESI) as specified in each case.

### 3.6.2 Procedures and Characterizations

#### Cyclopropyl(phenyl)methanol (**44b**)



**44b**

Solid LiAlH<sub>4</sub> (0.31 g, 8.2 mmol) was added to dry THF (25 mL) and the suspension was cooled down to 0 °C. A solution of cyclopropyl phenyl ketone **56** (0.95 mL, 6.8 mmol) in dry THF (5 mL) was added dropwise. The reaction was allowed to stir at 0 °C, with gradual



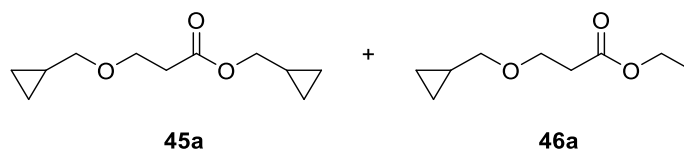
warming to room temperature over 2h. The reaction mixture was cooled down again to 0 °C after completion and was quenched with a very slow addition of the saturated NH<sub>4</sub>Cl to avoid severe gas evolution. The reaction mixture was filtered over Celite to separate the insoluble white precipitate and the filtrate was retained. The aqueous layer was extracted with Et<sub>2</sub>O (3×5 mL). The organic layers were combined and dried over MgSO<sub>4</sub>, filtered and concentrated under reduced pressure. No further purification was required and alcohol **44b** was obtained as a pale yellow oil (1.00 g, 98%); R<sub>f</sub> 0.40 (30:70 EtOAc: hexane); IR (cast film) 3366, 3082, 3005, 1493, 1452, 1025 cm<sup>-1</sup>; <sup>1</sup>H NMR (500 MHz, CDCl<sub>3</sub>) δ 7.44-7.41 (m, 2H), 7.38-7.34 (m, 2H), 7.29 (ddd, *J* = 6.5, 1.4, 1.4 Hz, 1H), 4.01 (d, *J* = 8.3 Hz, 1H), 2.06 (br s, 1H), 1.22 (dddd, *J* = 8.2, 8.2, 8.2, 5.0, 5.0 Hz, 1H), 0.64 (dddd, *J* = 8.8, 8.0, 5.6, 4.2 Hz, 1H), 0.56 (dddd, *J* = 10.0, 8.3, 5.6, 4.4 Hz, 1H), 0.50-0.45 (m, 1H), 0.40-0.35 (m, 1H); <sup>13</sup>C NMR (125 MHz, CDCl<sub>3</sub>) δ 143.8, 128.3, 127.5, 126.0, 78.5, 19.2, 3.59, 2.83; HRMS (EI) calcd for C<sub>10</sub>H<sub>12</sub>O [M]<sup>+</sup> 148.0888; found 148.0884.

### 3.6.3 General Procedure for the Synthesis of Esters **45** and **46**

Ethyl acrylate (1.0 equiv.) was added to a flask containing corresponding alcohols **44** (3.5 equiv.) followed by the slow addition of DBU (1.0 equiv.) to the reaction mixture. The reaction was heated up to 65 °C overnight. The crude mixture was cooled to room temperature and was then directly loaded on a silica gel column and chromatographed eluting with mixture of EtOAc: hexane (30:70) to isolate the desired product.

#### Cyclopropylmethyl 3-(cyclopropylmethoxy)propanoate (**45a**)

#### Ethyl 3-(cyclopropylmethoxy)propanoate (**46a**)

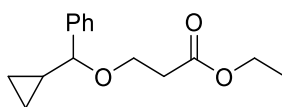


**45a**: column chromatography (30:70 EtOAc: hexane) was used to isolate inseparable esters **45** and **46** in a 7:1 ratio. Pale yellow (565 mg, 57%), R<sub>f</sub> 0.50 (30:70 EtOAc: hexane); IR (cast film) 3083, 3006, 2869, 1737, 1384, 1187, 1109 cm<sup>-1</sup>; <sup>1</sup>H NMR (500 MHz, CDCl<sub>3</sub>) δ 3.86 (d, *J* = 7.5 Hz, 2H), 3.66 (t, *J* = 6.5 Hz, 2H), 3.22 (d, *J* = 6.9 Hz, 2H), 2.54 (t, *J* = 6.5 Hz, 2H),

1.24-1.15 (m, 2H), 0.50-0.43 (m, 4H), 0.22-0.19 (m, 2H), 0.14-0.11 (m, 2H);  $^{13}\text{C}$  NMR (125 MHz,  $\text{CDCl}_3$ )  $\delta$  171.6, 75.6, 69.1, 65.8, 35.1, 10.4, 9.7, 3.1, 2.9; HRMS (ESI) calcd for  $\text{C}_{11}\text{H}_{19}\text{O}_3$   $[\text{M}+\text{H}]^+$  198.1256; found 198.1254.

**46a**: observed peaks:  $^1\text{H}$  NMR (500 MHz,  $\text{CDCl}_3$ )  $\delta$  4.17 (q,  $J = 7.3$  Hz, 2H), 3.73-3.70 (m, 2H), 3.22 (d,  $J = 7.0$  Hz, 2H), 2.61-2.58 (m, 2H), 1.29 (t,  $J = 7.2$  Hz, 3H), 1.08-0.94 (m, 2H);  $^{13}\text{C}$  NMR (125 MHz,  $\text{CDCl}_3$ )  $\delta$  171.5, 66.2, 65.7, 60.3, 15.0, 14.1.

### Ethyl 3-[cyclopropyl(phenyl)methoxy]propanoate (**46b**)



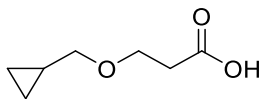
**46b**

**46b**: column chromatography (30:70 EtOAc: hexane) was used to isolate esters **46b** as a pale yellow oil (853 mg, 35%);  $R_f$  0.60 (30:70 EtOAc: hexane); IR (cast film) 3083, 3004, 2981, 2906, 2873, 1736, 1603, 1492, 1453, 1372, 1346, 1262, 1185, 1137, 1095, 1068  $\text{cm}^{-1}$ ;  $^1\text{H}$  NMR (500 MHz,  $\text{CDCl}_3$ )  $\delta$  7.38-7.30 (m, 5H), 4.18 (q,  $J = 7.2$  Hz, 2H), 3.73 (d,  $J = 8.0$  Hz, 1H), 3.66-3.62 (m, 2H), 2.63-2.59 (m, 2H), 1.29 (t,  $J = 7.2$  Hz, 3H), 1.24-1.15 (m, 1H), 0.68-0.54 (m, 1H), 0.53-0.42 (m, 2H), 0.33-0.26 (m, 1H);  $^{13}\text{C}$  NMR (125 MHz,  $\text{CDCl}_3$ )  $\delta$  171.6, 142.0, 128.3, 127.5, 126.6, 86.1, 64.2, 60.4, 35.4, 17.7, 14.2, 4.1, 2.1; HRMS (EI) calcd for  $\text{C}_{15}\text{H}_{20}\text{NaO}_3$   $[\text{M}+\text{Na}]^+$  271.1305; found 271.1302.

### 3.6.4 General Procedure for the Synthesis of Carboxylic Acids **47**

The mixture of esters **45** and **46** was dissolved in MeOH: THF (1:1, 0.25 M) and an aqueous solution of LiOH (2M, 2.0 equiv.) was added dropwise. The reaction mixture was stirred overnight at 40  $^\circ\text{C}$  until the consumption of starting materials. An equal volume of water was added to the reaction and the organic layer was separated. The aqueous layer was acidified with 1M HCl to pH = 1 followed by extraction with  $\text{Et}_2\text{O}$  (3 x 5 mL). Combined organic layers were dried over  $\text{MgSO}_4$ , filtered and concentrated under reduced pressure. Acids **47** were obtained pure and were used for the next step without further purification.

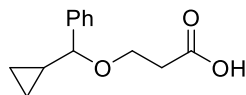
### 3-(Cyclopropylmethoxy)propanoic acid (47a)



47a

**47a:** light yellow oil (95%); IR (cast film) 3082, 3006, 2873, 1712, 1399, 1239, 1189, 1098, 1069  $\text{cm}^{-1}$ ;  $^1\text{H}$  NMR (500 MHz,  $\text{CDCl}_3$ )  $\delta$  3.72 (t,  $J = 6.2$  Hz, 2H), 3.30 (d,  $J = 7.0$  Hz, 2H), 2.64 (t,  $J = 6.2$  Hz, 2H), 1.11-1.02 (m, 1H), 0.55-0.47 (m, 2H), 0.23-0.17 (m, 2H), (the peak corresponding to the carboxylic acid proton did not observed);  $^{13}\text{C}$  NMR (125 MHz,  $\text{CDCl}_3$ )  $\delta$  177.1, 75.7, 65.3, 34.8, 10.3, 2.9; HRMS (ESI) calcd for  $\text{C}_7\text{H}_{11}\text{O}_3$   $[\text{M}-\text{H}]^-$  143.0714; found 143.0713.

### 3-[Cyclopropyl(phenyl)methoxy]propanoic acid (47b)

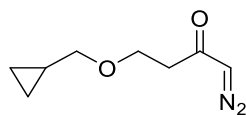


47b

**47b:** yellow oil (82%); IR (cast film) 3083, 3028, 3007, 2918, 2876, 1713, 1453, 1137  $\text{cm}^{-1}$ ;  $^1\text{H}$  NMR (500 MHz,  $\text{CDCl}_3$ )  $\delta$  7.43-7.29 (m, 5H), 3.73 (d,  $J = 7.9$  Hz, 1H), 3.67 (dt,  $J_{\text{AB}} = 16.2$  Hz,  $J_{\text{AX}} = 6.5$  Hz, 1H), 3.65 (dt,  $J_{\text{AB}} = 16.2$  Hz,  $J_{\text{AX}} = 6.5$  Hz, 1H), 2.68 (dt,  $J_{\text{AB}} = 16.7$  Hz,  $J_{\text{AX}} = 6.4$  Hz, 1H), 2.68 (dt,  $J_{\text{AB}} = 16.7$  Hz,  $J_{\text{AX}} = 6.4$  Hz, 1H), 1.20 (dddd,  $J = 8.0, 8.0, 8.0, 5.2, 5.2$ , 1H), 0.69-0.63 (m, 1H), 0.53-0.46 (m, 2H), 0.34-0.29 (m, 1H), (the peak corresponding to the carboxylic acid proton did not observed);  $^{13}\text{C}$  NMR (125 MHz,  $\text{CDCl}_3$ )  $\delta$  177.2, 141.6, 128.4, 127.7, 126.7, 86.5, 63.8, 35.0, 17.6, 4.2, 2.2; HRMS (EI) calcd for  $\text{C}_{13}\text{H}_{16}\text{O}_3$   $[\text{M}]^+$  220.1099; found 220.1097.

### 3.6.5 Procedure for the Synthesis of Diazo Ketone 37a and 37b

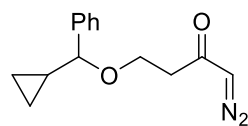
#### 4-(Cyclopropylmethoxy)-2-oxobutane-1-diazonium (37a)



37a

Oxalyl chloride (0.16 mL, 1.9 mmol) and catalytic amount of DMF (2 drops) was added to a solution of carboxylic acid **47a** (0.25 g, 1.6 mmol) in dichloromethane (11 mL) at -25 °C and the reaction was stirred for 1 h then warmed to room temperature and stirred overnight. CH<sub>2</sub>Cl<sub>2</sub> was removed under reduced pressure and the residue was immediately dissolved in Et<sub>2</sub>O (10 mL). The acid chloride solution was added to a fresh solution of CH<sub>2</sub>N<sub>2</sub> (~5 equivalents, prepared from Diazald®) in Et<sub>2</sub>O via cannulae at -78 °C. The reaction was warmed gradually to room temperature overnight. Excess amount of diazomethane was quenched by dropwise addition of glacial acetic acid (1 mL) and the reaction mixture was washed with water. Combined organic layers were dried over MgSO<sub>4</sub>, filtered and concentrated under reduced pressure. Purification by flash chromatography, using a 50:50 mixture of hexane: EtOAc, gave diazo ketone **37a** in 55 % yield as a yellow oil (145 mg, 55%); R<sub>f</sub> 0.40 (50:50 EtOAc: hexane); IR (cast film) 3082, 3005, 2866, 2104, 1639, 1359, 1096 cm<sup>-1</sup>; <sup>1</sup>H NMR (500 MHz, CDCl<sub>3</sub>) δ 5.38 (br s, 1H), 3.71 (t, *J* = 6.5 Hz, 2H), 3.26 (d, *J* = 6.8 Hz, 2H), 2.58 (br s, 2H), 1.03 (dddd, *J* = 6.8, 6.8, 6.8, 5.0, 5.0, 1H), 0.54-0.50 (m, 2H), 0.20-0.17 (m, 2H); <sup>13</sup>C NMR (125 MHz, CDCl<sub>3</sub>) δ 193.1, 75.9, 66.0, 55.0, 41.4, 10.5, 3.0; HRMS (ESI) calcd for C<sub>8</sub>H<sub>13</sub>N<sub>2</sub>O<sub>2</sub> [M+H]<sup>+</sup> 169.0972; found 169.0969.

#### 4-[Cyclopropyl(phenyl)methoxy]-2-oxobutane-1-diazonium (**37b**)



**37b**

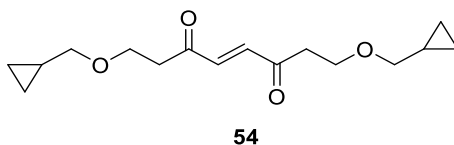
To a solution of carboxylic acid **47b** (0.52 mg, 2.4 mmol) in dry THF (12 mL) was added Et<sub>3</sub>N (0.36 mL, 2.6 mmol) followed by the addition of ethylchloroformate solution (0.25 mL, 2.6 mmol) in THF (2 mL) at -15 °C. The reaction was stirred for 1 h at -15 °C and an additional 3 h of stirring at -5 °C. After the formation of white solid the reaction mixture was filtered and the filtrate was concentrated under reduced pressure. The residue was immediately dissolved in Et<sub>2</sub>O and transferred to an ethereal solution of CH<sub>2</sub>N<sub>2</sub> (~5 equivalents, prepared from Diazald®) at -78 °C. The reaction mixture was stirred overnight with gradual warming to room temperature. The excess CH<sub>2</sub>N<sub>2</sub> was quenched with glacial acetic acid (2 mL) and the reaction mixture was washed with water. The organic layer was separated and the aqueous phase was washed with Et<sub>2</sub>O (2×5 mL). The organic layers were combined and dried over

MgSO<sub>4</sub>. The crude mixture was obtained after filtration and solvent removal by reduced pressure and was purified by column chromatography (30:70 EtOAc: hexane) to isolate diazo ketone **37b** as a yellow solid (310 mg, 53%); mp 38-40 °C *R<sub>f</sub>* 0.20 (30:70 EtOAc: hexane); IR (cast film) 3085, 3005, 2869, 2103, 1639, 1453, 1360, 1088 cm<sup>-1</sup>; <sup>1</sup>H NMR (500 MHz, CDCl<sub>3</sub>) δ 7.40-7.30 (m, 5H), 5.39 (br s, 1H), 3.72 (d, *J* = 7.7 Hz, 1H), 3.68-3.60 (m, 2H), 2.59 (br s, 2H), 1.18 (dddd, *J* = 8.0, 8.0, 8.0, 5.2, 5.2, 1H), 0.68-0.63 (m, 1H), 0.52-0.45 (m, 2H), 0.33-0.28 (m, 1H); <sup>13</sup>C NMR (125 MHz, CDCl<sub>3</sub>) δ 193.1, 141.8, 128.4, 127.6, 126.7, 68.4, 64.5, 54.9, 41.6, 17.6, 4.2, 2.1; HRMS (ESI) calcd for C<sub>14</sub>H<sub>16</sub>N<sub>2</sub>NaO<sub>2</sub> [M+ Na]<sup>+</sup> 267.1104; found 267.1096.

### 3.6.6 General Procedure for the Reaction of Diazo Ketones **37a** and **37b** with Cu(hfacac)<sub>2</sub>:

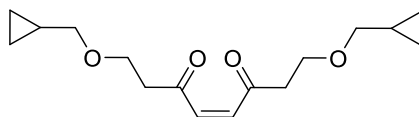
To a refluxing solution of Cu(hfacac)<sub>2</sub> (10 mol%) in the solvents mentioned in Table 1 (0.01M) was added a solution of diazo ketone **37** (1.0 equiv.) in the same solvent (0.1 M) via syringe pump over 4h. Consumption of diazo ketone **37** was monitored by TLC and the reaction mixture was quenched by 10% aqueous solution of K<sub>2</sub>CO<sub>3</sub>. The organic layer was separated and the aqueous layer was washed with DCM (3x). The combined organic layers were dried over MgSO<sub>4</sub>, filtered and concentrated under reduced pressure and the products were purified by flash chromatography.

#### (4*E*)-1,8-bis(cyclopropylmethoxy)oct-4-ene-3,6-dione (**54**)



**54**: column chromatography (30:70 EtOAc: hexane) was used to isolate alkene **54** as a white solid; mp 50-52 °C; *R<sub>f</sub>* 0.37 (30:70 EtOAc: hexane); IR (cast film) 3081, 3004, 2899, 2820, 1675, 1407, 1388, 1351, 1110, 1059 cm<sup>-1</sup>; <sup>1</sup>H NMR (500 MHz, CDCl<sub>3</sub>) δ 6.94 (s, 2H), 3.79 (t, *J* = 6.5 Hz, 4H), 3.30 (d, *J* = 7.0 Hz, 4H), 2.95 (t, *J* = 6.5 Hz, 4H), 1.07-1.02 (m, 2H), 0.56-0.52 (m, 4H), 0.22-0.19 (m, 4H); <sup>13</sup>C NMR (125 MHz, CDCl<sub>3</sub>) δ 198.8, 136.7, 75.9, 65.1, 41.8, 10.5, 3.0; HRMS (ESI) calcd for C<sub>16</sub>H<sub>24</sub>NaO<sub>4</sub> [M+ Na]<sup>+</sup> 303.1567; found 303.1561.

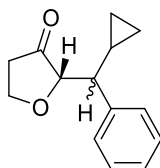
**(4Z)-1,8-bis(cyclopropylmethoxy)oct-4-ene-3,6-dione (55)**



**55**

**55**: column chromatography (30:70 EtOAc: hexane) was used to isolate alkene **55** as a colorless oil;  $R_f$  0.26 (40:60 EtOAc: hexane); IR (cast film) 3005, 2867, 1696, 1608, 1393, 1255, 1143, 1097  $\text{cm}^{-1}$ ;  $^1\text{H}$  NMR (500 MHz,  $\text{CDCl}_3$ )  $\delta$  6.38 (s, 2H), 3.76 (t,  $J = 6.4$  Hz, 4H), 3.28 (d,  $J = 6.8$  Hz, 4H), 2.85 (t,  $J = 6.5$  Hz, 4H), 1.06 -1.03 (m, 2H), 0.56 - 0.52 (m, 4H), 0.22-0.19 (m, 4H);  $^{13}\text{C}$  NMR (125 MHz,  $\text{CDCl}_3$ )  $\delta$  201.5, 135.7, 76.8, 65.3, 42.8, 10.5, 3.0; HRMS (ESI) calcd for  $\text{C}_{16}\text{H}_{24}\text{NaO}_4$  [ $\text{M} + \text{Na}$ ] $^+$  303.1567; found 303.1566.

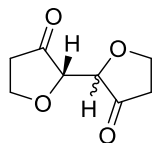
**2-[Cyclopropyl(phenyl)methyl]oxolan-3-one (43b 43b')**



**43b and 43b'**

**43a** and **43b**: column chromatography (30:70 EtOAc: hexane) was used to isolate an inseparable mixture of diastereomers **43b** and **43b'** as a colorless oil (53.5 mg, 60%);  $R_f$  0.51 (30:70 EtOAc: hexane); IR (cast film) 3079, 3063, 3028, 3001, 2925, 2888, 1755, 1602, 1495, 1453, 1430, 1402, 1360, 1155, 1142, 1093, 1042, 1019  $\text{cm}^{-1}$ ;  $^1\text{H}$  NMR (500 MHz,  $\text{CDCl}_3$ )  $\delta$  7.35 (m, 2H), 7.32-7.29 (m, 2H), 7.29-7.18 (m, 6H), 4.37-4.31 (m, 1H), 4.13 (d,  $J = 2.7$  Hz, 1H), 4.05 (dd,  $J = 9.2, 7.4$  Hz, 1H), 4.01-3.98 (m, 3H), 2.52-2.40 (m, 2H), 2.32 (dd,  $J = 10.6, 2.4$  Hz, 1H), 2.26 (dddd,  $J = 18.0, 6.1, 6.1, 0.7$  Hz, 1H), 2.17 (dd,  $J = 10.6, 2.6$  Hz, 1H), 1.82 (dddd,  $J = 18.0, 9.3, 9.3, 0.4$  Hz, 1H), 1.53-1.40 (m, 2H), 0.66 (dddd,  $J = 9.1, 8.0, 5.7, 4.6$  Hz, 1H), 0.59-0.45 (m, 3H), 0.33 (dddd,  $J = 9.4, 5.6, 4.6, 4.6$  Hz, 1H), 0.28-0.24 (m, 1H), 0.15-0.08 (m, 2H);  $^{13}\text{C}$  NMR (125 MHz,  $\text{CDCl}_3$ )  $\delta$  216.2, 215.9, 142.6, 140.0, 129.3, 128.3, 128.1, 128.0, 126.8, 126.6, 83.7, 83.2, 65.1, 64.9, 52.8, 52.4, 37.7, 37.1, 14.2, 11.4, 6.1, 5.4, 5.2, 4.2; HRMS (EI) calcd for  $\text{C}_{14}\text{H}_{16}\text{O}_2$  [ $\text{M}$ ] $^+$  216.1150; found 216.1149.

### [2,2'-Bioxolane]-3,3'-dione (**57**)



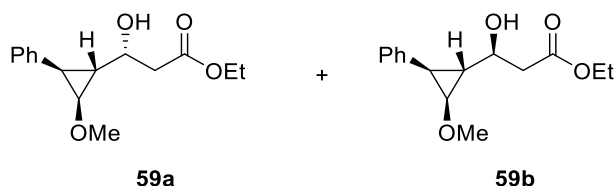
**57**

**57**: was isolated as two inseparable diastereomers; colorless oil (1.5 mg, 4.3%);  $R_f$  0.20 (30:70 EtOAc: hexane); IR (cast film) 3200, 2967, 2918, 1743, 1402, 1365, 1178, 1070, 1026  $\text{cm}^{-1}$ ;  $^1\text{H}$  NMR (500 MHz,  $\text{CDCl}_3$ ) 4.39-4.32 (m, 4H), 4.20-4.12 (m, 8H), 2.62-2.54 (m, 8H);  $^{13}\text{C}$  NMR (125 MHz,  $\text{CDCl}_3$ )  $\delta$  213.2, 212.5, 80.3, 79.3, 66.0, 65.7, 37.0, 36.8; HRMS (EI) calcd for  $\text{C}_8\text{H}_{10}\text{O}_4$   $[\text{M}]^+$  170.0579; found 170.0580.

### 3.6.7 Procedure for the Formation of Alcohols **59a** and **59b**

**Ethyl (3*R*)-3-[(1*R*,2*S*,3*S*)-2-benzyl-3-methoxycyclopropyl]-3-hydroxypropanoate (**59a**)**

**Ethyl (3*S*)-3-[(1*R*,2*S*,3*S*)-2-benzyl-3-methoxycyclopropyl]-3-hydroxypropanoate (**59b**)**



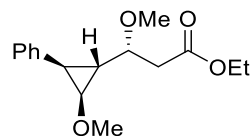
A flame dried flask was charged with diisopropylamine (1.90 mL, 13.7 mmol) in THF (50 mL) and was cooled down to  $-78\text{ }^\circ\text{C}$ . A solution of *n*-BuLi in hexane (2.50 M, 5.50 mL, 13.7 mmol) was added dropwise and the reaction was stirred for 15 min at  $-78\text{ }^\circ\text{C}$ . Ethyl acetate (1.20 mL, 12.5 mmol) was added dropwise with an additional 45 min stirring at  $-78\text{ }^\circ\text{C}$ . Then a solution of 2-methoxy-3-phenyl carlopropanecarboxaldehyde (2.20 g, 12.5 mmol) in THF (2.5 mL) was added to the reaction mixture. The reaction temperature was kept at  $-78\text{ }^\circ\text{C}$  over 2 h and the reaction completion was monitored with TLC. Then the reaction was warmed to room temperature followed by the addition of saturated ammonium chloride (30 mL) and the organic layer was separated. The aqueous layer was extracted with  $\text{Et}_2\text{O}$  ( $3 \times 10$  mL). The combined organic layers was dried over  $\text{MgSO}_4$ , filtered and concentrated under reduced pressure. The alcohols **59a** and **59b** were separated by flash chromatography (40:60 EtOAc: hexane) as two diastereomers in a 1:1 ratio (2.42 g, 74%).

**59a**: colorless oil;  $R_f$  0.29 (40:60 EtOAc: hexane); IR (cast film) 3447, 3086, 3060, 3026, 2983, 2936, 2904, 2826, 1731, 1603, 1498, 1462, 1399, 1372, 1294, 1251, 1178, 1116, 1087  $\text{cm}^{-1}$ ;  $^1\text{H}$  NMR (500 MHz,  $\text{CDCl}_3$ )  $\delta$  7.32-7.20 (m, 5H), 4.19 (dq,  $J_{\text{AB}} = 11.0$  Hz,  $J_{\text{AX}} = 7.3$  Hz, 1H), 4.15 (dq,  $J_{\text{AB}} = 11.0$  Hz,  $J_{\text{AX}} = 7.3$  Hz, 1H), 3.76 (dddd,  $J = 7.4, 7.4, 3.6, 3.6$  Hz, 1H), 3.54 (dd,  $J = 6.8, 3.3$  Hz, 1H), 3.21 (s, 3H), 3.14 (b, 1H), 2.68 (dd,  $J = 16.0, 3.9$  Hz, 1H), 2.64 (dd,  $J = 16.0, 8.2$  Hz, 1H), 2.06 (dd,  $J = 6.7, 6.7$  Hz, 1H), 1.64 (ddd,  $J = 7.1, 7.1, 3.3$  Hz, 1H), 1.27 (t,  $J = 7.3$  Hz, 3H);  $^{13}\text{C}$  NMR (125 MHz,  $\text{CDCl}_3$ )  $\delta$  172.6, 136.7, 128.0 (2C), 125.9, 68.7, 63.6, 60.8, 58.2, 40.9, 31.4, 27.3, 14.1; HRMS (ESI) calcd for  $\text{C}_{15}\text{H}_{20}\text{NaO}_4$  [ $\text{M} + \text{Na}$ ] $^+$  287.1254; found 287.1255.

**59b**: light yellow oil;  $R_f$  0.38 (40:60 EtOAc: hexane); IR (cast film) 3457, 3060, 2983, 2936, 2904, 2825, 1732, 1603, 1498, 1462, 1447, 1424, 1400, 1372, 1348, 1296, 1250, 1219, 1177, 1086  $\text{cm}^{-1}$ ;  $^1\text{H}$  NMR (500 MHz,  $\text{CDCl}_3$ )  $\delta$  7.32-7.26 (m, 4H), 7.23-7.20 (m, 1H), 4.23-4.13 (m, 2H), 3.93 (ddd,  $J = 10.3, 7.8, 3.9$  Hz, 1H), 3.46 (dd,  $J = 6.8, 3.3$  Hz, 1H), 3.16 (s, 3H), 2.97 (d,  $J = 4.1$  Hz, 1H), 2.72 (dd,  $J = 16.3, 3.9$  Hz, 1H), 2.64 (dd,  $J = 16.3, 8.6$  Hz, 1H), 2.20 (dd,  $J = 7.1, 7.1$  Hz, 1H), 1.64 (ddd,  $J = 6.5, 6.5, 3.2$  Hz, 1H), 1.28 (t,  $J = 7.2$  Hz, 3H);  $^{13}\text{C}$  NMR (125 MHz,  $\text{CDCl}_3$ )  $\delta$  172.6, 137.0, 128.0, 127.9, 125.8, 68.1, 63.1, 60.9, 58.1, 41.0, 31.4, 27.1, 14.1; HRMS (ESI) calcd for  $\text{C}_{15}\text{H}_{20}\text{NaO}_4$  [ $\text{M} + \text{Na}$ ] $^+$  287.1254; found 287.1255.

### 3.6.8 Procedure for the Formation of Esters 60a and 60b

#### Ethyl (3*R*)-3-[(1*R*,2*S*,3*S*)-2-benzyl-3-methoxycyclopropyl]-3-methoxypropanoate (60a)



**60a**

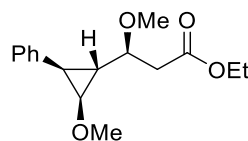
To a stirred solution of the corresponding alcohol **59a** (0.72 g, 2.7 mmol) in dry toluene (0.5 M, 5.5 mL) was added anhydrous  $\text{CaSO}_4$  (0.74 g, 5.5 mmol) and freshly prepared  $\text{Ag}_2\text{O}$ <sup>127</sup> (1.3 g, 5.5 mmol). The reaction mixture was cooled down to 0 °C and iodomethane (0.51 mL, 8.2 mmol) was added dropwise. The ice bath was removed and the flask was covered in aluminum foil. The reaction mixture was stirred for 3 h at room temperature. Additional aliquots of  $\text{Ag}_2\text{O}$ ,  $\text{CaSO}_4$  and  $\text{MeI}$  (the same amount as before) were added and the reaction



progress was monitored by TLC (Addition of excess Ag<sub>2</sub>O, CaSO<sub>4</sub> and MeI may be required if the starting alcohol has not been consumed completely). The reaction mixture was stirred overnight and was filtered through Celite. The Celite was washed with ethyl acetate (2×5 mL) and the filtrate was concentrated under reduced pressure. The crude mixture was used in the next step without further purifications.

**60a**: Colorless oil (0.70 mg, 92%); R<sub>f</sub> 0.45 (50:50 EtOAc: hexane); IR (cast film) 3059, 2983, 2937, 2902, 2825, 1734, 1603, 1498, 1461, 1447, 1372, 1302, 1273, 1244, 1209, 1112, 1030 cm<sup>-1</sup>; <sup>1</sup>H NMR (500 MHz, CDCl<sub>3</sub>) δ 7.32-7.22 (m, 5H), 4.13 (dq, J<sub>AB</sub> = 10.5 Hz, J<sub>AX</sub> = 7.1 Hz, 1H), 4.06 (dq, J<sub>AB</sub> = 10.5 Hz, J<sub>AX</sub> = 7.1 Hz, 1H), 3.52 (dd, J = 6.7, 3.2 Hz, 1H), 3.51 (s, 3H), 3.39 (ddd, J = 7.9, 7.9, 5.3 Hz, 1H), 3.20 (s, 3H), 2.68 (dd, J = 14.9, 7.8 Hz, 1H), 2.56 (dd, J = 14.9, 5.4 Hz, 1H), 1.93 (dd, J = 6.6, 6.6 Hz, 1H), 1.63 (ddd, J = 6.7, 6.7, 3.4 Hz, 1H), 1.21 (t, J = 7.1 Hz, 3H); <sup>13</sup>C NMR (125 MHz, CDCl<sub>3</sub>) δ 171.3, 136.6, 128.0, 127.9, 125.9, 78.4, 64.7, 60.6, 58.1, 57.4, 39.9, 29.8, 26.5, 14.1; HRMS (ESI) calcd for C<sub>16</sub>H<sub>22</sub>NaO<sub>4</sub> [M+ Na]<sup>+</sup> 301.1410; found 301.1407.

#### Ethyl (3*S*)-3-[(1*R*,2*S*,3*S*)-2-benzyl-3-methoxycyclopropyl]-3-methoxypropanoate (**60a**)



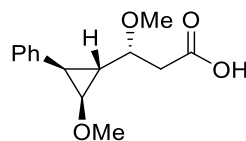
**60b**

Ester **60b** was prepared according to the procedure provided for **60a**.

**60b**: Yellow oil (1.10 g, quant.); R<sub>f</sub> 0.55 (40:60 EtOAc: hexane); IR (cast film) 3060, 2989, 2936, 2906, 2825, 1734, 1603, 1498, 1461, 1447, 1374, 1350, 1222, 1208, 1192, 1173, 1115, 1093 cm<sup>-1</sup>; <sup>1</sup>H NMR (500 MHz, CDCl<sub>3</sub>) δ 7.32-7.27 (m, 4H), 7.25-7.20 (m, 1H), 4.21 (dq, J<sub>AB</sub> = 10.8 Hz, J<sub>AX</sub> = 7.2 Hz, 1H), 4.17 (dq, J<sub>AB</sub> = 10.8 Hz, J<sub>AX</sub> = 7.3 Hz, 1H), 3.51 (ddd, J = 7.7, 7.7, 5.0 Hz, 1H), 3.40 (s, 3H), 3.38 (dd, J = 6.7, 3.4 Hz, 1H), 3.17 (s, 3H), 2.73 (dd, J = 15.2, 7.7 Hz, 1H), 2.64 (dd, J = 15.2, 5.3 Hz, 1H), 2.17 (dd, J = 6.9, 6.9 Hz, 1H), 1.62 (ddd, J = 7.7, 6.8, 3.3 Hz, 1H), 1.29 (t, J = 7.1 Hz, 3H); <sup>13</sup>C NMR (125 MHz, CDCl<sub>3</sub>) δ 171.3, 136.7, 128.0, 127.9, 125.9, 78.1, 62.5, 60.6, 58.2, 57.3, 40.2, 29.8, 29.3, 14.2; HRMS (ESI) calcd for C<sub>16</sub>H<sub>22</sub>NaO<sub>4</sub> [M+ Na]<sup>+</sup> 301.1410; found 301.1412.

### 3.6.9 Procedure for the Formation of Carboxylic Acids **61a** and **61b**

#### (3*R*)-3-[(1*R*,2*S*,3*S*)-2-Benzyl-3-methoxycyclopropyl]-3-methoxypropanoic acid (**61a**)

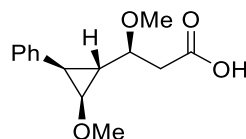


**61a**

Corresponding ester **60a** (70 mg, 0.25 mmol) was dissolved in MeOH: THF (1:1, 0.26 M, 2 mL) and an aqueous solution of LiOH (2 M, 0.25 mL, 0.50 mmol) was added dropwise. The reaction mixture was stirred overnight at room temperature until the consumption of starting materials. An equal volume of water was added to the reaction and the organic layer was separated. The aqueous layer was acidified with 1M HCl to pH = 1 followed by extraction with Et<sub>2</sub>O (3×10 mL). The combined organic layers were dried over MgSO<sub>4</sub> and concentrated under reduced pressure. The pure acid **61a** was obtained and used in the next step without further purification

**61a**: yellow solid (625 mg, quant.); mp: 68 - 70 °C; IR (cast film) 3087, 3060, 3026, 2987, 2937, 2826, 1730, 1710, 1603, 1498, 1447, 1424, 1348, 1224, 1178, 1111, 1091 cm<sup>-1</sup>; <sup>1</sup>H NMR (500 MHz, CDCl<sub>3</sub>) δ 7.34-7.21 (m, 5H), 3.54 (s, 3H), 3.41-3.37 (m, 1H), 3.40 (ddd, *J* = 4.9, 8.0, 8.0 Hz, 1H), 3.21 (s, 3H), 2.70 (dd, *J* = 15.5, 8.6 Hz, 1H), 2.63 (dd, *J* = 15.5, 4.3 Hz, 1H), 1.93 (dd, *J* = 6.6, 6.6 Hz, 1H), 1.64 (ddd, *J* = 8.0, 8.0, 3.3 Hz, 1H), (the peak corresponding to the carboxylic acid proton did not observed); <sup>13</sup>C NMR (125 MHz, CDCl<sub>3</sub>) δ 176.1, 136.3, 128.1, 128.0, 126.0, 78.1, 68.8, 58.2, 57.4, 39.5, 29.5, 26.4; HRMS (ESI) calcd for C<sub>14</sub>H<sub>17</sub>O<sub>4</sub> [M- H]<sup>-</sup> 249.1132; found 249.1137.

#### (3*S*)-3-[(1*R*,2*S*,3*S*)-2-Benzyl-3-methoxycyclopropyl]-3-methoxypropanoic acid (**61b**)



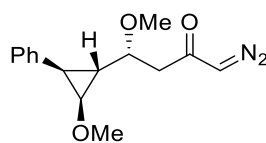
**61b**

Ester **61b** was prepared according to the procedure provided for **61a**.

**61b**: green oil (500 mg, 54%); IR (cast film) 3086, 3061, 3027, 2987, 2936, 2826, 1734, 1710, 1603, 1498, 1447, 1424, 1351, 1300, 1225, 1196, 1178, 1113, 1090  $\text{cm}^{-1}$ ;  $^1\text{H}$  NMR (500 MHz,  $\text{CDCl}_3$ )  $\delta$  7.34-7.28 (m, 4H), 7.25-7.22 (m, 1H), 3.49-3.45 (m, 1H), 3.39 (s, 3H), 3.39 (dd,  $J = 6.7, 3.0$  Hz, 1H), 3.19 (s, 3H), 2.81-2.72 (m, 2H), 2.19 (dd,  $J = 7.4, 7.4$  Hz, 1H), 1.64 (ddd,  $J = 7.5, 3.1$  Hz, 1H), (the peak corresponding to the carboxylic acid proton did not observed);  $^{13}\text{C}$  NMR (125 MHz,  $\text{CDCl}_3$ )  $\delta$  176.3, 136.4, 128.1, 128.0, 126.0, 78.0, 62.4, 58.2, 57.3, 39.9, 29.7, 29.6; HRMS (ESI) calcd for  $\text{C}_{14}\text{H}_{17}\text{O}_4$   $[\text{M} - \text{H}]^-$  249.1132; found 249.1129.

### 3.6.10 Procedure for the Formation of Diazo Ketones **62a** and **62b**

#### (4*R*)-4-[(1*R*,2*S*,3*S*)-2-Benzyl-3-methoxycyclopropyl]-1-diazo-4-methoxybutan-2-one (**62a**)



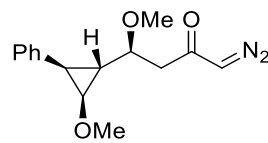
**62a**

To a solution of carboxylic acid **61a** (0.30 g, 1.2 mmol) in dry THF (6 mL, 0.20 M) was added  $\text{Et}_3\text{N}$  (0.18 mL, 1.3 mmol) followed by the addition of ethyl chloroformate solution (0.13 mL, 1.3 mmol) in THF (1 mL, 1.2 M) at  $-15$   $^\circ\text{C}$ . The reaction was stirred for 1 h at  $-15$   $^\circ\text{C}$  and an additional 3 h stirring at  $-5$   $^\circ\text{C}$ . After the formation of a white salt the reaction mixture, it was filtered and the filtrate was concentrated under reduced pressure. The residue was immediately dissolved in  $\text{Et}_2\text{O}$  and transferred to an ethereal solution of  $\text{CH}_2\text{N}_2$  (~5 equivalents, prepared from Diazald<sup>®</sup>) at  $-78$   $^\circ\text{C}$ . The reaction mixture was stirred overnight with gradual warming to the room temperature. The  $\text{CH}_2\text{N}_2$  was quenched with excess glacial acetic acid and the reaction mixture was washed with water. The organic layer was separated and dried over  $\text{MgSO}_4$  and filtered. The crude mixture was obtained after solvent removal and was purified by column chromatography to isolate diazo ketones **62a** as a yellow oil

**62a**: yellow oil (190, 58%);  $R_f$  0.17 (30:70 EtOAc: hexane); IR (cast film) 3088, 3026, 2984, 2936, 2825, 2102, 1635, 1603, 1498, 1424, 1447, 1353, 1228, 1179, 1151, 1105, 1032, 1008  $\text{cm}^{-1}$ ;  $^1\text{H}$  NMR (500 MHz,  $\text{CDCl}_3$ )  $\delta$  7.32-7.11 (m, 5H), 5.28 (br s, 1H), 3.53 (ddd,  $J = 6.8, 6.8, 3.3$  Hz, 1H), 3.51 (s, 3H), 3.41 (ddd,  $J = 8.2, 8.2, 4.9$  Hz, 1H), 3.19 (s, 3H), 2.67-2.49 (br m, 2H), 1.89 (dd,  $J = 7.2, 7.2$  Hz, 1H), 1.57 (ddd,  $J = 6.7, 6.7, 3.3$  Hz, 1H);  $^{13}\text{C}$  NMR (125

MHz, CDCl<sub>3</sub>)  $\delta$  192.5, 136.7, 128.0, 127.8, 125.9, 78.7, 65.2, 58.2, 57.5, 55.8, 45.9, 30.4, 26.5; HRMS (ESI) calcd for C<sub>15</sub>H<sub>19</sub>N<sub>2</sub>O<sub>3</sub> [M+ H]<sup>+</sup> 275.1390; found 275.1385.

**(4R)-4-[(1R,2S,3S)-2-Benzyl-3-methoxycyclopropyl]-1-diazo-4-methoxybutan-2-one  
(62b)**



**62b**

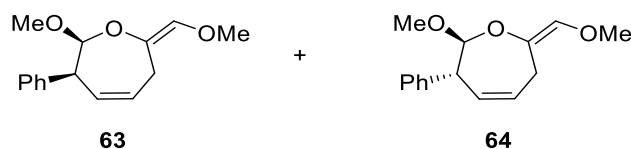
Ester **62b** was prepared according to the procedure provided for **62a**.

**62b**: yellow oil (80 mg, 73%); R<sub>f</sub> 0.28 (40:60 EtOAc:hexane); IR (cast film) 3088, 2984, 2935, 2825, 2104, 1637, 1603, 1498, 1447, 1422, 1371, 1338, 1150, 1110, 1089 cm<sup>-1</sup>; <sup>1</sup>H NMR (500 MHz, CDCl<sub>3</sub>)  $\delta$  7.32-7.26 (m, 4H), 7.24-7.21 (m, 1H), 5.36 (br s, 1H), 3.50 (ddd, *J* = 7.6, 7.6, 4.4 Hz, 1H), 3.38 (s, 3H), 3.36 (ddd, *J* = 6.8, 6.8, 3.3 Hz, 1H), 3.16 (s, 3H), 2.70- 2.60 (br m, 2H), 2.16 (dd, *J* = 7.0, 7.0 Hz, 1H), 1.57 (ddd, *J* = 7.4, 7.4, 3.3 Hz, 1H); <sup>13</sup>C NMR (125 MHz, CDCl<sub>3</sub>)  $\delta$  192.5, 136.7, 128.1, 127.9, 126.0, 78.4, 62.5, 58.2, 57.4, 55.7, 46.2, 30.1, 29.7; HRMS (ESI) calcd for C<sub>15</sub>H<sub>18</sub>N<sub>2</sub>NaO<sub>3</sub> [M+Na]<sup>+</sup> 297.1210; found 297.1204.

**3.6.11 Procedure for the Treatment of Diazo Ketone 62a with Cu(hfacac)<sub>2</sub>**

**(2S,3S,7E)-2-Methoxy-7-(methoxymethylidene)-3-phenyl-2,3,6,7-tetrahydrooxepine  
(63)**

**(2S,3R,7E)-2-methoxy-7-(methoxymethylidene)-3-phenyl-2,3,6,7-tetrahydrooxepine  
(64)**



To a solution of Cu(hfacac)<sub>2</sub> (18 mg, 0.03 mmol) in CH<sub>2</sub>Cl<sub>2</sub> (3.6 mL, 0.01 M) at reflux was added a solution of diazo ketone **62a** (0.10 g, 0.36 mmol) in CH<sub>2</sub>Cl<sub>2</sub> (3.6 mL, 0.1 M) via syringe pump over 2 h. Consumption of diazo ketone **62a** was monitored by TLC and the reaction mixture was quenched by 10% solution of aqueous K<sub>2</sub>CO<sub>3</sub>. The organic layer was separated and the aqueous layer was washed with DCM (3×5 mL). The combined organic layers were dried over MgSO<sub>4</sub>, filtered and concentrated under reduced pressure and purified

by flash chromatography. The obtained oxepines **63** and **64** were isolated in 1:1 ratio. (13 mg, 26%)

**63**: colorless oil;  $R_f$  0.59 (20:80 EtOAc: hexane); IR (cast film) 3060, 3026, 2993, 2931, 2898, 2833, 1689, 1655, 1602, 1492, 1543, 1417, 1361, 1349, 1246, 1221, 1154, 3311, 1110, 1072, 1036, 1003  $\text{cm}^{-1}$ ;  $^1\text{H}$  NMR (500 MHz,  $\text{CD}_2\text{Cl}_2$ )  $\delta$  7.31-7.28 (m, 4H), 7.25-7.22 (m, 1H), 6.06 (dd,  $J = 0.7, 0.7$  Hz, 1H), 5.80 (dddd,  $J = 11.0, 5.4, 4.8, 2.4$  Hz, 1H), 5.54 (dddd,  $J = 11.0, 4.0, 1.7, 0.6, 0.6$  Hz, 1H), 4.84 (dd,  $J = 1.9, 0.6$  Hz, 1H), 3.93 (dddd,  $J = 4.1, 4.1, 1.9, 1.9$  Hz, 1H), 3.53 (s, 3H), 3.39 (s, 3H), 3.28 (dddd,  $J = 17.5, 5.4, 1.8, 1.8, 0.7$  Hz, 1H), 3.12 (dddd,  $J = 17.5, 4.7, 2.2, 1.9, 1.0$  Hz, 1H);  $^{13}\text{C}$  NMR (125 MHz,  $\text{CD}_2\text{Cl}_2$ )  $\delta$  140.8, 138.3, 135.4, 129.7, 129.3, 128.0, 126.8, 126.7, 106.2, 59.8, 55.9, 50.7, 27.3; HRMS (ESI) calcd for  $\text{C}_{15}\text{H}_{18}\text{NaO}_3$   $[\text{M} + \text{Na}]^+$  269.1148; found 269.1145.

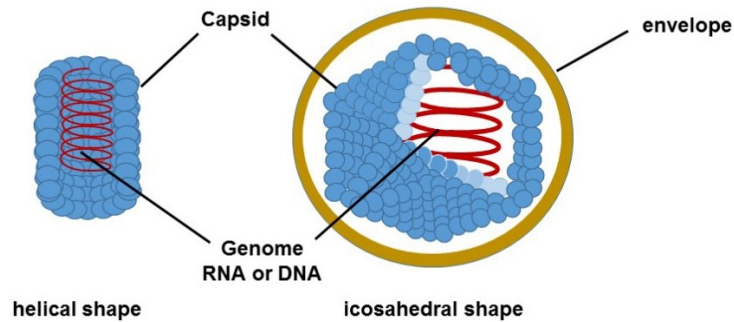
**64**: colorless oil;  $R_f$  0.55 (20:80 EtOAc: hexane); IR (cast film) 3085, 3061, 3028, 3001, 2931, 2834, 1696, 1654, 1599, 1494, 1453, 1357, 1251, 1211, 1170, 1130, 1035, 1009  $\text{cm}^{-1}$ ;  $^1\text{H}$  NMR (500 MHz,  $\text{CD}_2\text{Cl}_2$ )  $\delta$  7.32-7.29 (m, 2H), 7.25-7.22 (m, 3H), 6.05 (ddd,  $J = 2.1, 1.0, 0.5$  Hz, 1H), 5.67 (dddd,  $J = 11.1, 5.6, 3.7, 2.3, 0.5$  Hz, 1H), 5.51 (dddd,  $J = 11.1, 4.5, 2.4, 1.6$  Hz, 1H), 4.81 (d,  $J = 8.2$  Hz, 1H), 3.92-3.88 (m, 1H), 3.57, (s, 3H), 3.34-3.29 (m, 1H), 3.31 (s, 3H), 3.07- 3.01 (m, 1H);  $^{13}\text{C}$  NMR (125 MHz,  $\text{CD}_2\text{Cl}_2$ )  $\delta$  141.5, 137.6, 136.2, 129.9, 128.5, 128.3, 126.6, 126.5, 108.3, 59.8, 55.5, 50.1, 27.9; HRMS (ESI) calcd for  $\text{C}_{15}\text{H}_{18}\text{NaO}_3$   $[\text{M} + \text{Na}]^+$  269.1148; found 269.1145.

## Chapter 4 Design and Synthesis of Broad-Spectrum Antivirals

### 4.1 Introduction: Virus Structure and Infectivity

Viruses are infectious species threatening the global health of humans, animals and plants. Approximately 0.6 million, 0.5 million and 2 million human deaths per year have been reported for hepatitis B, hepatitis C and HIV respectively.<sup>158</sup> During the last decade, several viruses have threatened the global health such as respiratory syndrome coronavirus (SARS-CoV) in 2003, Middle East respiratory coronavirus (MERS-CoV) in 2012 and Ebola virus (EBOV) in 2014.<sup>158</sup> Viruses are required to live inside the host organism to be able to reproduce. Although the infectious property of viruses was known at the end of the 19<sup>th</sup> century, their structure and detailed properties were not clear until 1935 when Wendell M. Stanley isolated tobacco mosaic virus (TMV) from tobacco leaves.<sup>159</sup> Further studies by Bernal and Fankuchen revealed the first detailed information regarding the size and the shape of TMV.<sup>160</sup> The main part of a virus contains a virus genome which consists of one or more molecules of nucleic acid, DNA or RNA. Based on the type of the virus genomes, viruses can be categorized in four types: 1) single-stranded RNA (ssRNA), 2) double-stranded RNA (dsRNA), 3) single-stranded DNA (ssDNA) and 4) double-stranded DNA (dsDNA). Nucleic acids can also exist as either linear or circular mode.<sup>161</sup>

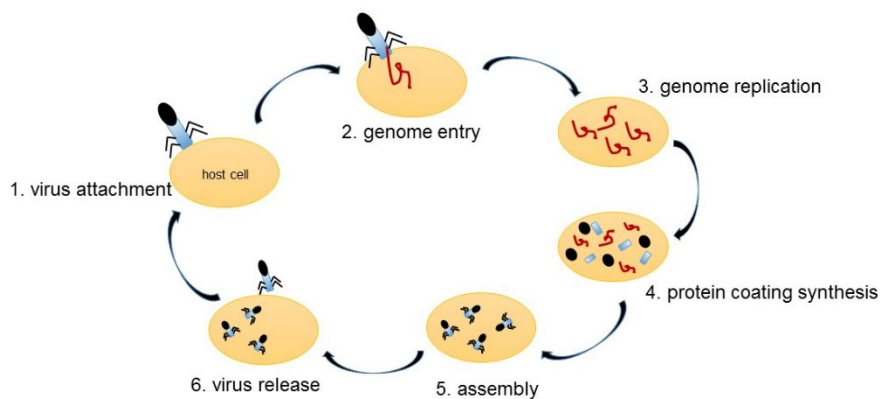
Genomes are located inside symmetric protein coating which is commonly called the “*capsid*”. The capsid, not only is responsible for the activation and protection of virion genome, but is required for the virus attachment to the host cell membrane. Capsids are classified based on their structural symmetry. The most common types of capsids have been defined as helical and icosahedral capsids (Figure 4-1).<sup>162</sup> Apart from the capsids, in many viruses, there is a lipid component containing protein molecules that surround the capsid. The lipid- protein coating which is called the “*envelope*” is playing a crucial role in the viral entry step into the host cell. Therefore, viruses can be divided in two categories, enveloped and non-enveloped, according to the presence or the absence of the lipid coating.<sup>161</sup>



**Figure 4-1: The Most Common Types of Virion Capsids**

Another important category of the viruses can be introduced by the type of the host cells they can infect. Viruses can infect eukaryotic cells such as human, animal and plants cells. They are also known to be infectious to the prokaryotic cells, as in the case of bacteriophages which infect bacteria.<sup>162</sup>

Viral infection occurs through viral replication and via several steps: 1) attachment to the host cell membrane, 2) genome entry into the cell, 3) genome transcription and replication, 4) protein coat synthesis, 5) protein and genome assembly and 6) virion release from the cell (Figure 4-2).



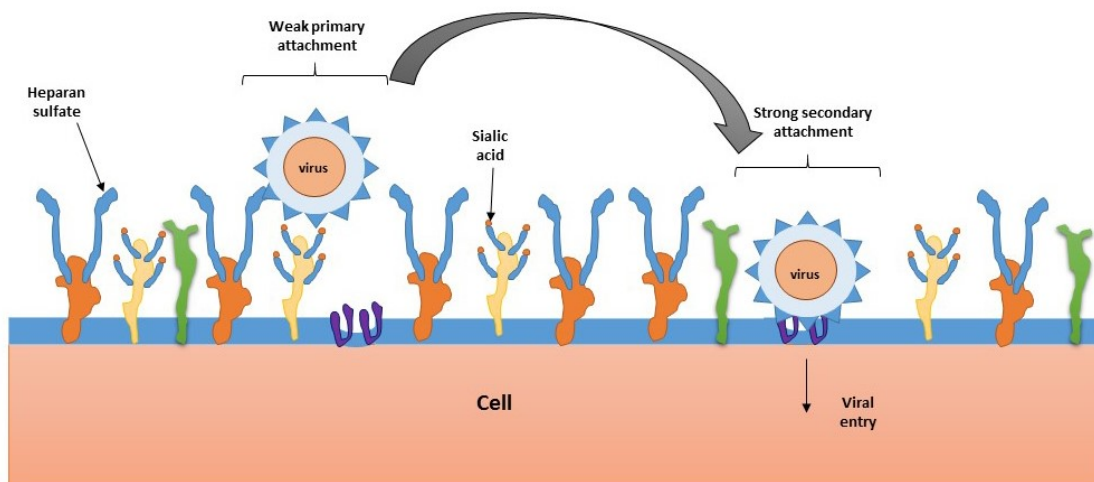
**Figure 4-2: The Steps of the Viral Infection**

Most antiviral drugs target the genome replication, therefore they are specifically active against one particular virus or a group of similar viruses. On the other hand, the virion attachment commonly occurs through a similar mechanism for most viruses. As a result, design

and synthesis of the antivirals that target virus attachment may provide the opportunity to design and develop broad spectrum antivirals which are active against a large group of viruses (section 4.3).

## 4.2 Viral Attachment

Virion attachment occurs through two major steps and via chemical interactions such as hydrogen bonding, ionic interactions and van der Waals forces. The first binding is a reversible primary attachment with a low affinity and weak interactions which increases the concentration of the virus close to the cell surface, while the secondary binding comprises a strong molecular interactions between virion proteins and host cell receptors promoting virion entry (Figure 4-3). Depending on the type of the viruses, the secondary attachment can be facilitated by glycoprotein conformational changes.<sup>163</sup>



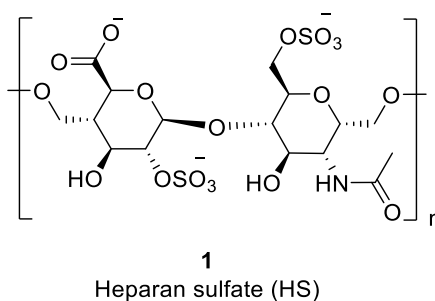
**Figure 4-3: The Primary and Secondary Attachments**

Host cell receptors are commonly cell surface glycans. According to the type of the involved receptors, viruses can be classified into three major classes.<sup>163–166</sup> Virus attachment may occur through the binding between glycosaminoglycans (GAGs) and virion receptors. The virion attachment can also engage sialoglycans (SGs) on the host cell surface.<sup>167</sup> There are also a small group of viruses that are bounded to neither GAGs nor SGs.

GAGs consist of polysaccharide chains and are attached to proteins via O- or N-linked glycosylations. Based on the type of the structurally involved polysaccharide, there are four

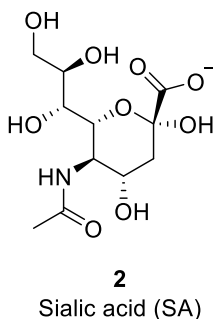


classes of GAGs: heparin/heparan sulfate (HS), chondroitin (CS)/dermatan sulfate (DS), keratan and hyaluronic acid.<sup>168</sup> Among the known GAG receptors, heparan sulfates (HS) **1** are the most common type of receptors that are involved in the process of virus attachment (Figure 4-4).<sup>169-171</sup> It is known that the positively charged sites of viral glycoproteins interact with the negatively charged moieties of the HS to promote the attachment.<sup>172,173</sup> A large group of viruses are known that are able to bind to the HS moiety, for example, human immunodeficiency virus (HIV),<sup>174</sup> hepatitis C virus (HCV),<sup>175</sup> hepatitis B virus (HBV),<sup>176</sup> herpes simplex virus 1 (HSV-1),<sup>177</sup> herpes simplex virus 2 (HSV-2).<sup>177</sup>



**Figure 4-4: Chemical Structure of Heparan Sulfate**

On the other hand, sialic acid (SA) **2** is an active receptor in the case of SGs mediated binding (Figure 4-5). The carboxylate group at C1, N-acetyl moiety at C5, glycerol at C6 and hydroxyl group at C2 are responsible for the hydrogen bonding between virion proteins and sialic acid receptors.<sup>167</sup> Several viruses are known to be attached to SA such as, influenza A,B and C viruses (IAV, IBV and ICV),<sup>178-180</sup> coronavirus (CoV)<sup>181</sup> and isavirus (ISAV)<sup>182</sup>.



**Figure 4-5: The Chemical Structure of Sialic Acid (SA)**

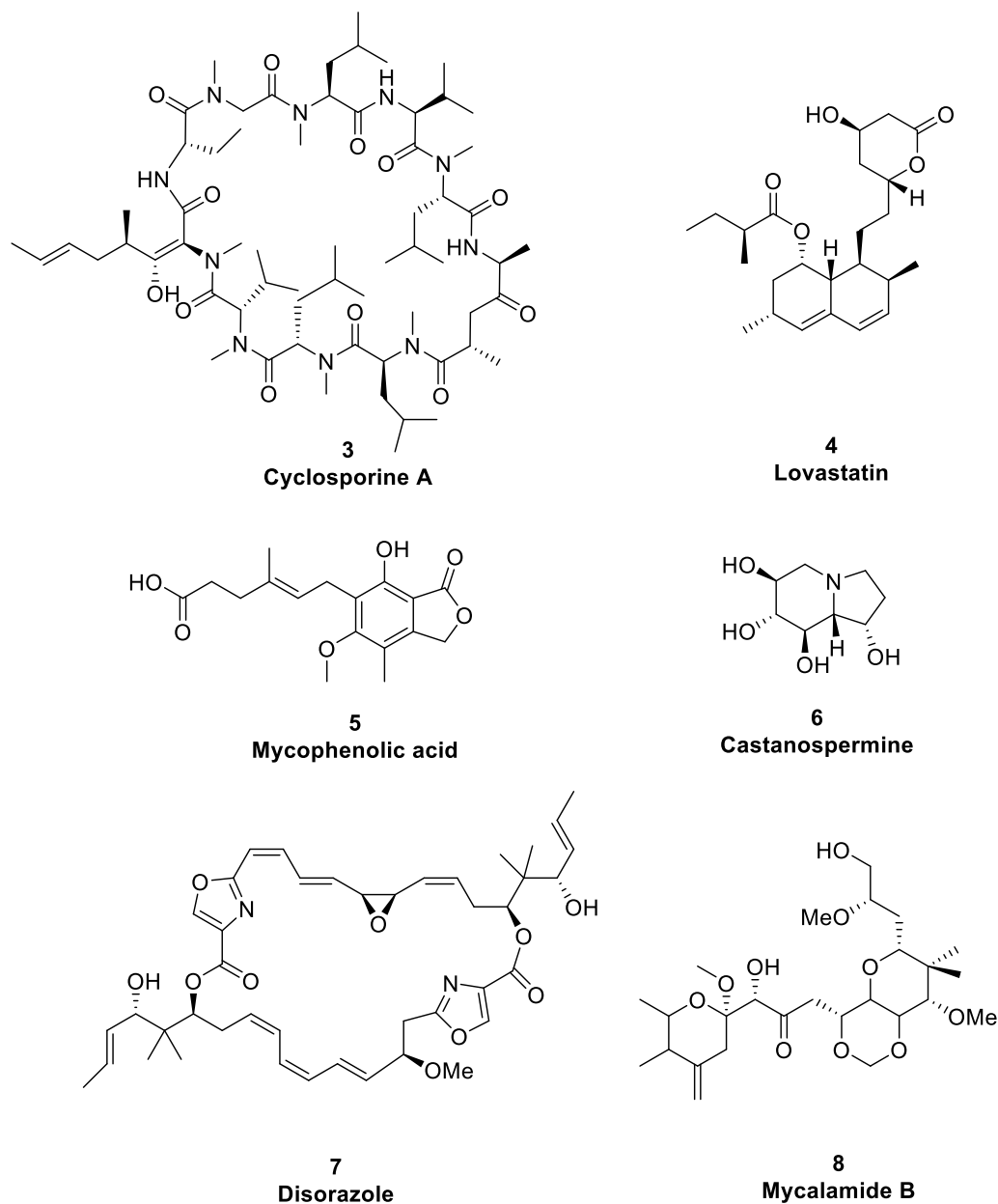
### 4.3 Broad-Spectrum Antivirals

With growth of the number of viruses in the world and their threats against the human and animal global health, concerns about developing antivirals and virus treatments have been increased. There are a large group of viruses from different families that are responsible for the major cause of the human death over the recent decade such as, hepatitis C virus (HCV), human immunodeficiency virus (HIV) and more recently Ebola virus (EBOV) and respiratory syndrome coronavirus (SARA-CoV).<sup>158</sup> On the other hand, it is predicted that close to half a million mammalian viruses are not known yet and are expected to be discovered in future.<sup>183</sup>

Design and development of antiviral agents against various viruses have been a big challenge over the years. Antivirals can be designed as directly acting antivirals (DAA) or host-acting antivirals (HAA). DAA's are a group of antivirals that can directly affect viruses and their components such as proteins or genomes. HAA's are responsible to modify the effective component of host cell to prevent virus infection, such as vaccines and antibodies.<sup>158,184,185</sup> Each virus has specific genomes and they can infect a particular host cell. As a result, the design of antivirals typically focuses on one drug for one virus. This "one bug-one drug" strategy has been successfully developed and is widely used against different viruses.<sup>183</sup> However, with increasing diversity of viruses, there will be a large number of antivirals required to treat each single virus which may not be an effective strategy and is not economically affordable.

Therefore, the design and development of broad-spectrum antivirals seems essential in the field of drug discovery. Broad-spectrum antivirals (BS antivirals) are a group of drugs that can inhibit the viral infection of two or more viruses from different families through a similar mechanism of action.<sup>158,183</sup> Several drugs in the category of broad-spectrum antivirals have been recently developed and their mechanism of action has been widely studied.<sup>86,158,183,186</sup> BS antivirals target the critical viral infection steps such as viral attachment, membrane fusion, viral replication/assembly and budding.<sup>186</sup> Several natural compounds extracted from fungi, bacteria, plants and marine life have been known to act as broad spectrum antivirals.<sup>158</sup> For example, cyclosporine A **3**, which is an active antiviral against HIV, influenza viruses and HSV-1,<sup>187,188</sup> lovastatin **4** which has antiviral activity against hepatitis B and C (HBV and HCV),<sup>189,190</sup> mycophenolic acid **5** that is active against HCV and HIV,<sup>191,192</sup> castanospermine **6** which is an antiviral to inhibit HIV and HSV-2,<sup>193,194</sup> disorazole **7** which acts a broad-

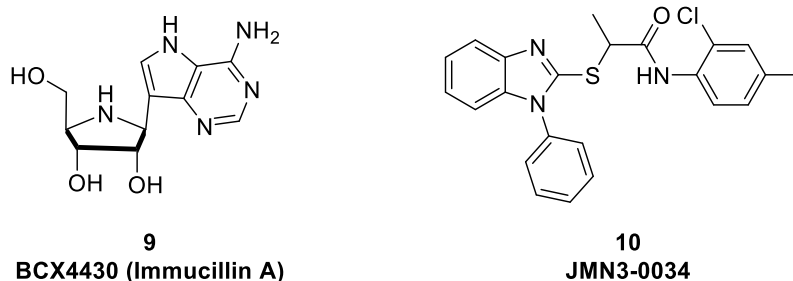
spectrum antiviral against HCV and HIV<sup>195,196</sup> and mycalamide B **8** which is active against HSV-1 and influenza (Figure 4-6).<sup>197,198</sup> The mechanism of action of these antivirals are known to be via the inhibition of viral replication, tubulin polymerization or viral protein synthesis.<sup>158</sup>



**Figure 4-6: Natural Compounds Possessing Broad-Spectrum Antiviral Properties**

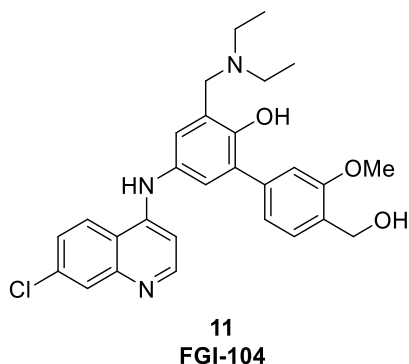
Apart from the isolated natural compounds, there are a few molecules capable of blocking the viral replication step. BCX4430 (Immucillin A) **9** is an adenosine analog which is known

to inhibit the viral replication of hepatitis C virus (HCV) and flavivirus.<sup>199</sup> Similarly, JMN3-003<sup>200</sup> **10** and dihydroorotate dehydrogenase (DHODH)<sup>201</sup> are also active against several viruses through the inhibition of viral genome replication (Figure 4-7).



**Figure 4-7: Broad-Spectrum Antivirals Capable of Blocking the Viral Replication**

Viral assembly and budding are late stages of the viral infection and are important targets in the development of the broad-spectrum antivirals. There are a few compounds which inhibit the viral assembly. A phenolic compound, FGI-104 **11**, is known to be active against EBOV as well as HCV, HIV, IFV-A and HSV-1 by inhibiting the viral budding (Figure 4-8).<sup>202</sup>



**Figure 4-8: Broad-Spectrum Antiviral Capable of Blocking the Viral Budding**

However, the earliest step of the viral infection is the viral attachment to the host cell membrane that can occur through a weak primary binding followed by a strong secondary attachment to provide the condition for viral genome entry. It was previously mentioned that the primary attachment occurs via the interaction between the virus proteins and host membrane receptors. These receptors are mainly glycosaminoglycans (GAG's) and sialoglycans (SG's). Usually, the molecules that competitively bind to these receptors or virus proteins possess antiviral activities. DAS181 is a sialidase which hydrolyzes sialic acid on the cell membrane and prevents the sialic acid attachment of influenza A virus (IAV) and

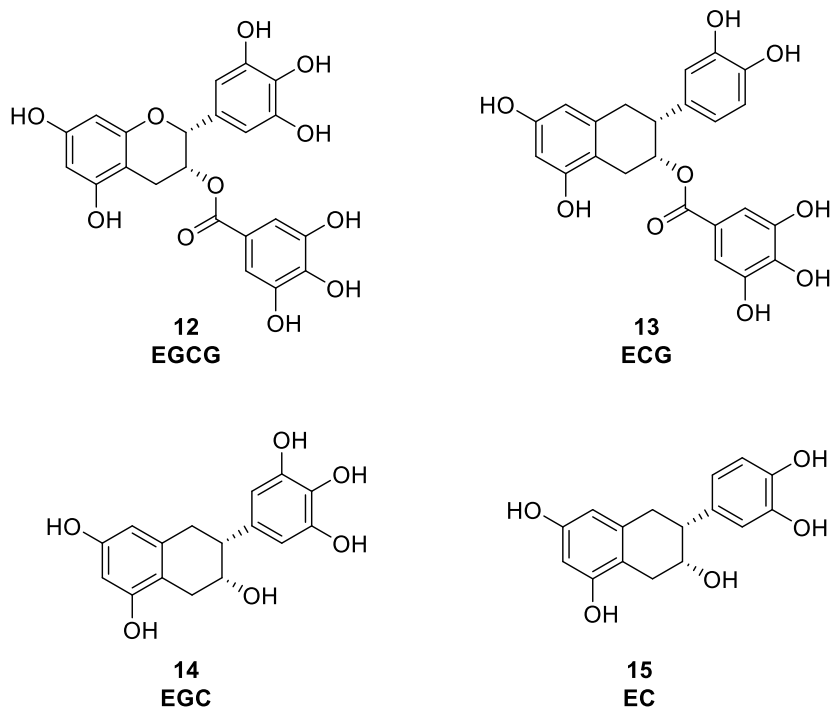
parainfluenza virus (PIV).<sup>186</sup> On the other hand, gp120, an enveloped glycoprotein on the virion membrane which is responsible for the viral attachment, can competitively bind to the polyvinylpyrrolidone (PVP) silver coated nanoparticle instead of CD4 receptors on the host cell. As a result, PVP silver coated compounds are considered as a broad-spectrum antivirals against the viruses attachment involving virion gp120.<sup>203</sup>

Despite the significant studies on the design and development of the broad-spectrum antivirals to inhibit the viral attachment, they are targeting either GAG or SG attachments and no antivirals have been found to be able to inhibit both type of attachments. Therefore, it is very desirable to develop potent antivirals inhibiting both GAG's and SG's binding. In this chapter, we will focus on design and synthesis of small molecules capable of inhibiting the attachment of viruses from different families.

## **4.4 Results and Discussions**

### **4.4.1 Background**

Polyphenolic natural products, known as tannins, are ubiquitously present in the plants. It is demonstrated that hydrolysable tannins (HS) are active broad-spectrum antivirals against viruses such as HSV, HCV, HBV and HIV.<sup>204–206</sup> Among the known phenolic compounds, the green tea catechins are polyphenolic molecules that are known to have pharmaceutical activities such as, antimutagenic, anticancer, antidiabetic, antiinflammatory, antibacterial and antiviral. They are also popular as antioxidants and active molecules to prevent obesity.<sup>207</sup> The most important extracted polyphenols from green tea are epigallocatechin gallate (EGCG) **12**, epicatechin gallate (ECG) **13**, epigallocatechin (EGC) **14** and epicatechin (EC) **15** (Figure 4-9).<sup>207</sup>

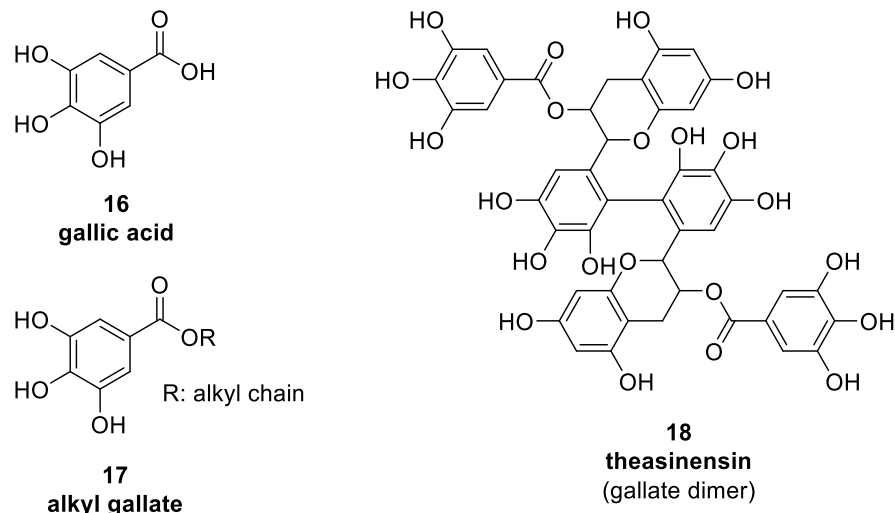


**Figure 4-9: Green Tea Catechins**

Several studies have demonstrated the potential pharmaceutical properties of the EGCG **12**. It has been known that EGCG is an active molecule against cancer cell growth and metastasis<sup>208–210</sup> as well as maintaining cardiovascular and metabolic health.<sup>211</sup> It has also been shown that EGCG possesses antidiabetic activity by modifying glucose and lipid metabolism.<sup>212</sup> Besides all of these significant properties, the broad-spectrum antiviral activity of EGCG has been demonstrated against the variety of enveloped and non-enveloped viruses such as HCV, HBV, HIV, IAV, HSV-1 and 2, HBV and adenovirus.<sup>213</sup>

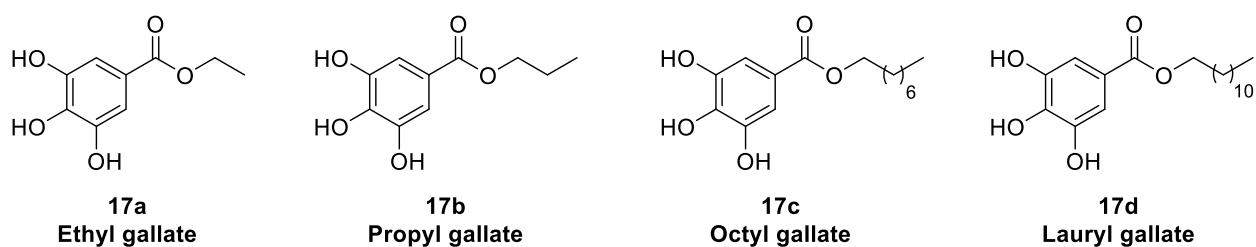
Recently, Schang and Colpitts investigated the mechanism of antiviral activity of EGCG.<sup>214</sup> They showed that EGCG is active against a series of unrelated enveloped and non-enveloped viruses that bind to either heparan sulfate or sialic acid. They demonstrated that EGCG inhibits the viral entry via direct interaction with the virion surface proteins. It seems that EGCG competes with heparan sulfate or sialic acid on the cell surface to bind to the virion proteins.

On the other hand, the potent antiviral activities of the gallic acid **16**, alkyl gallates **17** and EGCG dimers such as theasinensin **18** have been demonstrated, showing the important role of the gallate moiety in the inhibition of viral infections (Figure 4-10).<sup>215–218</sup>

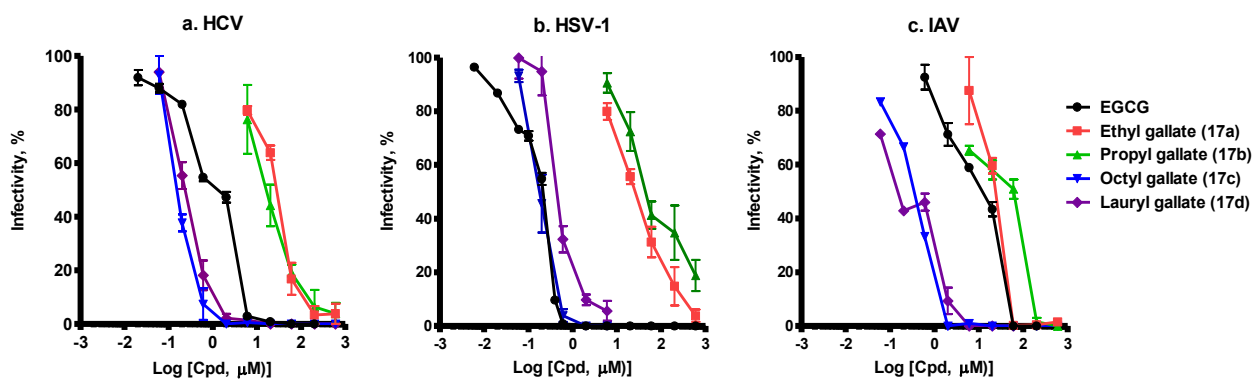


**Figure 4-10: Polyphenolic Compounds Possessing Gallate Moiety**

Therefore, in collaboration with the Schang group, we opted to design and develop small molecules possessing gallate moieties. Preliminary results by the Schang group showed that epicatechin (EC) **15** which is structurally similar to EGCG did not inhibit the viral entry. It seems that the presence of the gallate moiety in EGCG is essential for the antiviral activities.<sup>214</sup> The infectivity assays performed by the Schang group also showed that antiviral activities against three chosen viruses HCV, HSV-1 (GAG's binding) and IAV (SG binding) was enhanced by increasing the length of the alkyl chain from ethyl to lauryl **17a-d** in the monogallates, although octyl gallate **17c** showed better antiviral activity compared to lauryl gallate **17d** (Figure 4-11 and Figure 4-12).



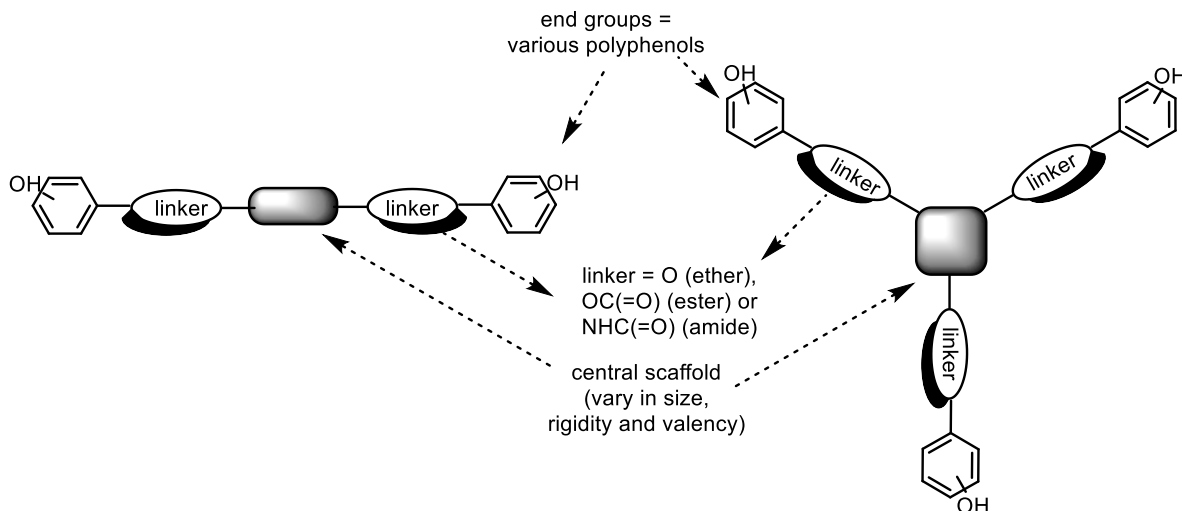
**Figure 4-11: Studied Alkyl Gallates**



**Figure 4-12: Antiviral Activities of Alkyl Gallates. EGCG.** (Dose response curves). Cell monolayers were infected with (a) HCV, (b) HSV-1 or (c) IAV pre-exposed to EGCG or alkyl gallates **17a-d** for 10 min at 37 °C. Infectivity was evaluated by plaquing or focus forming efficiency and is expressed as percentage relative to DMSO-treated control (n=2).

Although EGCG and monogallates with long alkyl chains showed significant antiviral activities via the inhibition of viral entry, design and development of the modified gallate derivatives seems necessary due to the drawbacks in employing EGCG or alkyl gallates. EGCG is unstable in aqueous medium and can undergo chemical transformations such as oxidation.<sup>219</sup> It is also known that EGCG similar to other green tea catechins are toxic against normal cells at concentration of 50μM.<sup>220</sup> Regarding alkyl gallates, longer hydrocarbon chains not only decrease the water solubility but also causes the formation of the multimeric complexes in aqueous solution as well as insertion into the cell membrane and increasing the local concentration. As the result, to overcome these limitations, we decided to design and synthesize a family of small and simple polyphenolic molecules and their broad spectrum antiviral activities against unrelated viruses were studied by Dr. Che Colpitts and Furkat Mukhtarov in the Schang group. Polyphenolic derivatives were designed to possess flexible or rigid central scaffolds and various functional groups as the linkers (Figure 4-13).

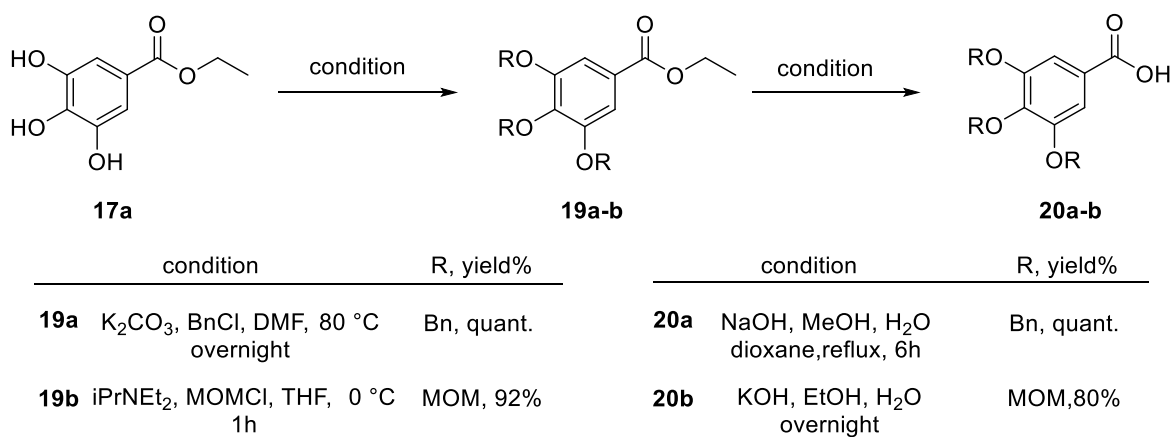




**Figure 4-13: General Structure of the Target Polyphenolic Compounds**

#### 4.4.2 Synthesis of Polyphenolic Derivatives Possessing Ester Linkers

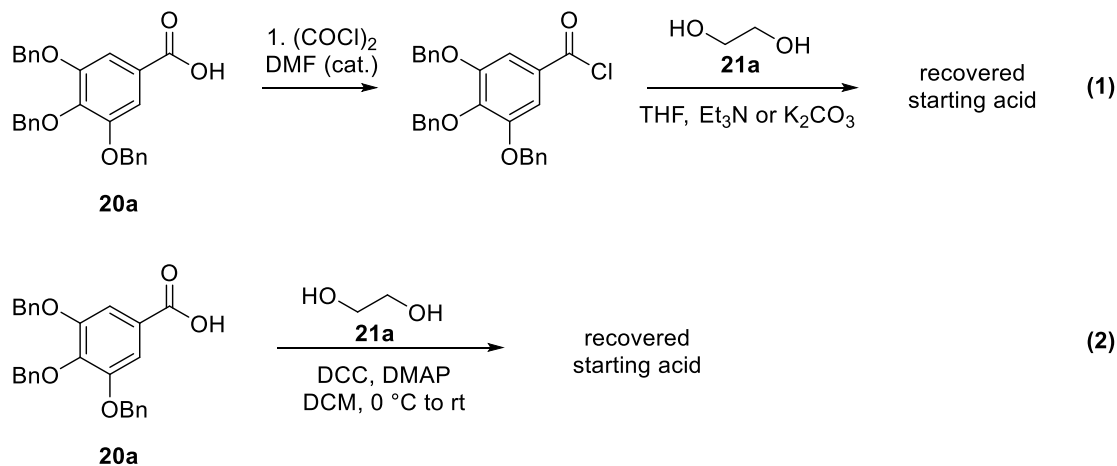
We started our synthesis by protection of the phenolic hydroxyls in ethyl gallate **17a** to avoid the possible side reactions resulting from the acidic phenolic protons. Deprotonation of hydroxyls with potassium carbonate or *i*-PrNEt<sub>2</sub> followed by the addition of required reagents (BnCl or MOMCl) provided fully protected phenolic compounds **19a-b** in excellent yield.<sup>221</sup> Ethyl esters **19a-b** then were saponified under aqueous basic condition to afford the corresponding carboxylic acids **20a-b** (Scheme 4-1).<sup>221</sup>



**Scheme 4-1: Synthesis of Acids 20**

The first attempts for the formation of ester linker from the carboxylic acid **20a** and ethylene glycol **21a**, employing oxalyl chloride for the *in situ* generation of the corresponding acid chloride, were unsuccessful (Scheme 4-2, eq. 1). Also the Steglich esterification using

dicyclohexylcarbodiimide (DCC) and 4-dimethylaminopyridine (DMAP) did not provide the desired digallate (Scheme 4-2, eq. 2).



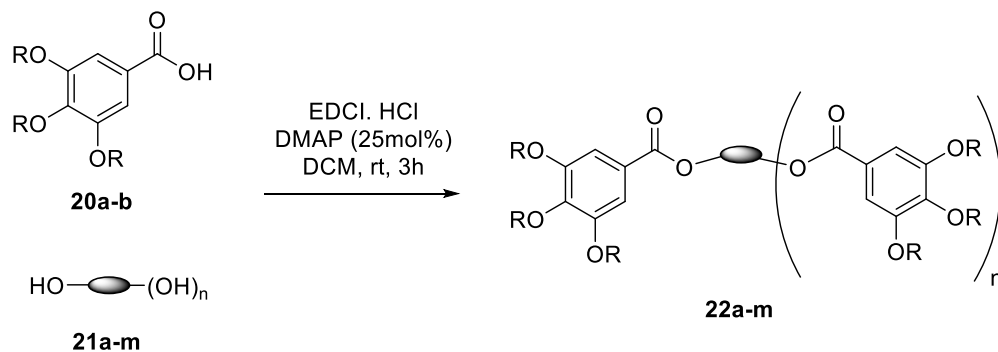
#### Scheme 4-2: Unsuccessful Esterifications

We found that replacement of DCC by EDCI. HCl in Steglich esterification provided the desired digallates **22a-m** (Table 4-1). The Bn or MOM protected carboxylic acid **20a** and **20b** reacted with diols **21a-m** in the presence of EDCI. HCl and DMAP to provide the protected digallates **22a-m** including various types of the acyclic flexible linkers (entries 1-4) and less flexible or rigid linkers (entries 5-10). The similar strategy was employed to synthesize tri and poly-gallates. Glycerol was chosen as a flexible linker to provide a trigallate derivative (entry 11). 1,3,5-benzenetrimethanol **21i** and 2,5-anhydromannitol **21m** were selected as a rigid tri- and tetravalent linkers respectively (entry 12 and 13). Unfortunately, some of the synthesized molecules (Table 4-1) were isolated in very low yields and our attempts to recover the starting acids or by products were unsuccessful.

Characterization of the *cis*- and *trans*- 1,4-digallates **22j** and **22j'** was a bit challenging since the starting 1,4-cyclohexandiol **21j** was commercially available only in a mixture of *cis*- and *trans*- isomers. Fortunately, the two diastereomers **22j** and **22j'** were separable in case of using OBn protecting group whereas OMOM protected phenols provided a mixture of inseparable diastereomers. Although two diastereomers were isolated easily, still determining their relative stereochemistry was challenging regarding the rapid cyclohexane ring conversion. NOE and TROESY experiments did not provide useful information even at lower temperatures. As a result, we decided to hydrolyze the isolated diastereomers to recover the parent *cis*- or *trans*-1,4-cyclohexanediol **21j**. Fortunately, comparing the distinct and well

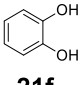
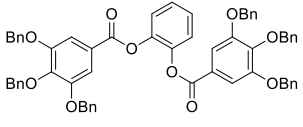
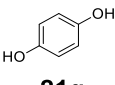
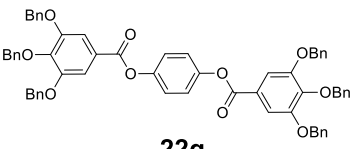
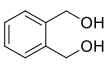
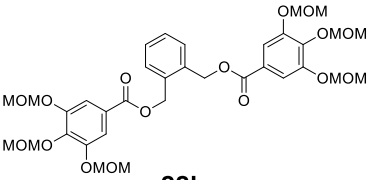
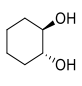
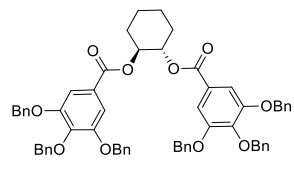
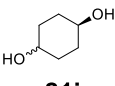
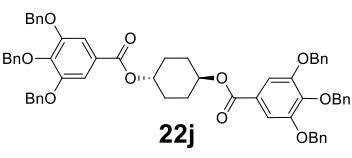
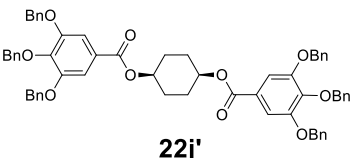
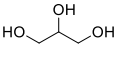
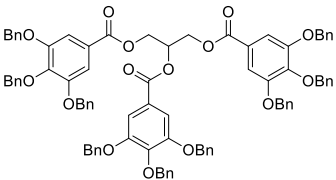
resolved peaks in the  $^1\text{H-NMR}$  of the obtained diols with the literature data afforded enough information to determine the relative stereochemistry of the obtained digallates.<sup>222,223</sup>

**Table 4-1: Formation of Protected Gallate Derivatives Possessing Ester Linkers**

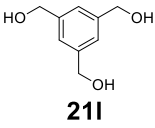
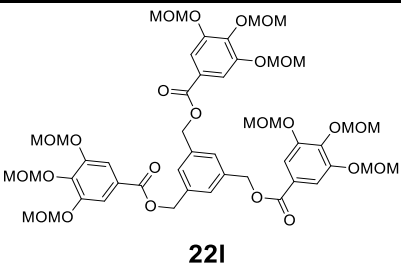
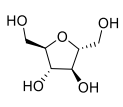
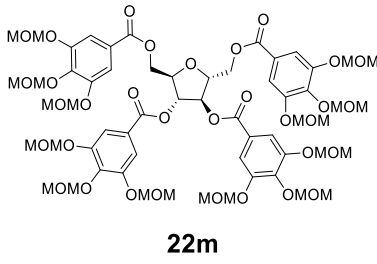


Entry	Acid 20	Central Scaffold	Product	Yield (%) <sup>a</sup>
1	20a	21a	22a	13%
2	20a	21b	22b	28%
3	20a	21c	22c	17%
4	20a	21d	22d	15%
5	20a	21e	22e	11% <sup>b,d</sup>

Table 4-1: Formation of Protected Gallate Derivatives Possessing Ester Linkers (Continued)

Entry	Acid 20	Central scaffold	Product 22	Yield% <sup>a</sup>
6	20a	 <b>21f</b>	 <b>22f</b>	49% <sup>d</sup>
7	20a	 <b>21g</b>	 <b>22g</b>	96% <sup>d</sup>
8	20b	 <b>21h</b>	 <b>22h</b>	85% <sup>d</sup>
9	20a	 <b>21i</b>	 <b>22i</b>	64%
10 <sup>c</sup>	20a	 <b>21j</b>	 <b>22j</b>	22%
			 <b>22j'</b>	17%
11	20a	 <b>21k</b>	 <b>22k</b>	31% <sup>d</sup>

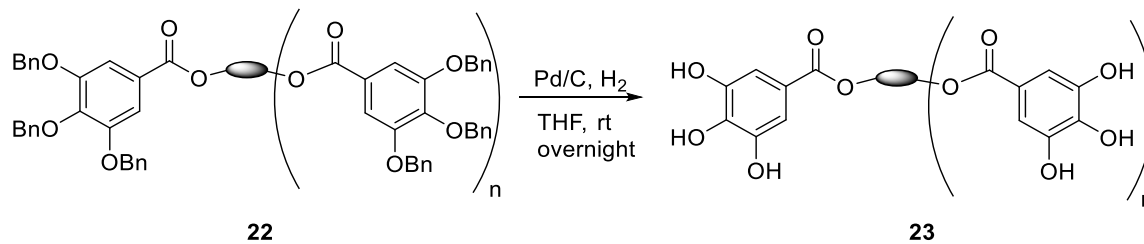
**Table 4-1: Formation of Protected Gallate Derivatives Possessing Ester Linkers (Continued)**

Entry	Acid 20	Central scaffold	Product 22	Yield% <sup>a</sup>
12	20b	 <p><b>21l</b></p>	 <p><b>22l</b></p>	98% <sup>d</sup>
13	20b	 <p><b>21m</b></p>	 <p><b>22m</b></p>	12%

<sup>a</sup>Isolated yields after chromatographic purification. <sup>b</sup>25% mono-gallate was also isolated which was submitted to the same reaction condition to provide the desired digallate in 71% yield. <sup>c</sup>Mixture of *cis*- and *trans*- (1:1) diols was used. <sup>d</sup>Denoted compounds were synthesized by D. J. Schatz during his undergraduate research experience

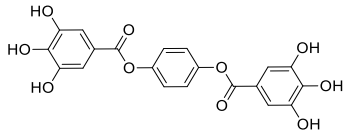
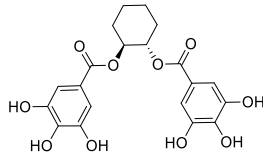
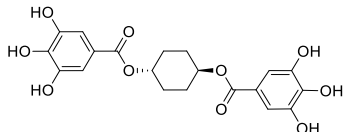
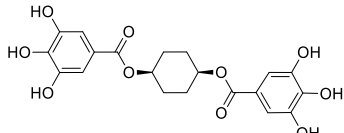
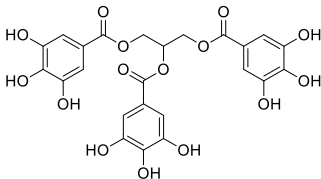
Deprotection of the benzyl protecting group in compounds **22a-g** and **22i-m** was achieved under the standard conditions of hydrogenolysis employing Pd/C. The desired polyphenolic compounds **23**, were obtained in moderate to quantitative yields (Table 4-2).

**Table 4-2: Deprotection of Benzyl Group**



Entry	Substrate	Product	Yield (%) <sup>a</sup>
1	22a	<p style="text-align: center;"><b>23a</b></p>	90%
2	22b	<p style="text-align: center;"><b>23b</b></p>	84%
3	22c	<p style="text-align: center;"><b>23c</b></p>	90%
4	22d	<p style="text-align: center;"><b>23d</b></p>	quant.
5	22e	<p style="text-align: center;"><b>23e</b></p>	55% <sup>b</sup>
6	22f	<p style="text-align: center;"><b>23f</b></p>	54% <sup>b</sup>

Table 4-2: Deprotection of Benzyl Group (Continued)

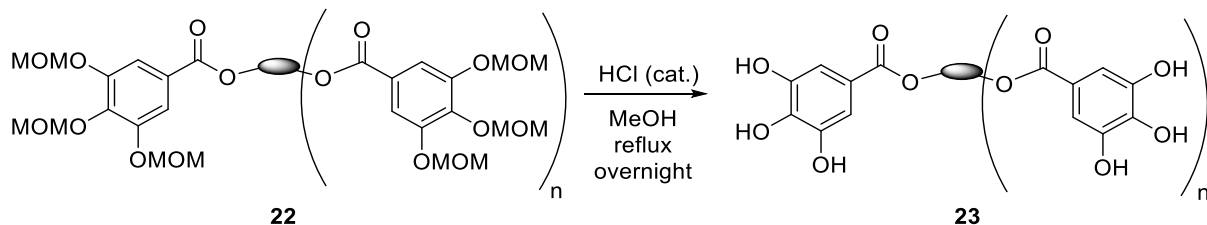
Entry	Substrate	Product	Yield (%) <sup>a</sup>
7	22g	 <p><b>23g</b></p>	78% <sup>b</sup>
8	22i	 <p><b>23i</b></p>	85%
9	22j	 <p><b>23j</b></p>	Quant.
10	22j'	 <p><b>23j'</b></p>	quant
11	22k	 <p><b>23k</b></p>	24% <sup>b</sup>

<sup>a</sup>Isolated yields after purification. <sup>b</sup>These polyphenols were synthesized by D. j. Schatz during his undergraduate research experience

MOM deprotection also was performed under acidic condition using catalytic amount of hydrochloric acid and reflux in methanol. The desired polyphenolic molecules **23h** and **23i** were obtained in low yields and our attempts to isolate the starting material or partially deprotected products were unsuccessful. However, tetragallate **23m** which was deprotected in pretty high yield.



**Table 4-3: Deprotection of MOM Group**



Entry	Substrate	Product	Yield (%) <sup>a</sup>
1	<b>22h</b>	<p style="text-align: center;"><b>23h</b></p>	11% <sup>b</sup>
2	<b>22i</b>	<p style="text-align: center;"><b>23i</b></p>	13% <sup>b</sup>
3	<b>22m</b>	<p style="text-align: center;"><b>23m</b></p>	quant.

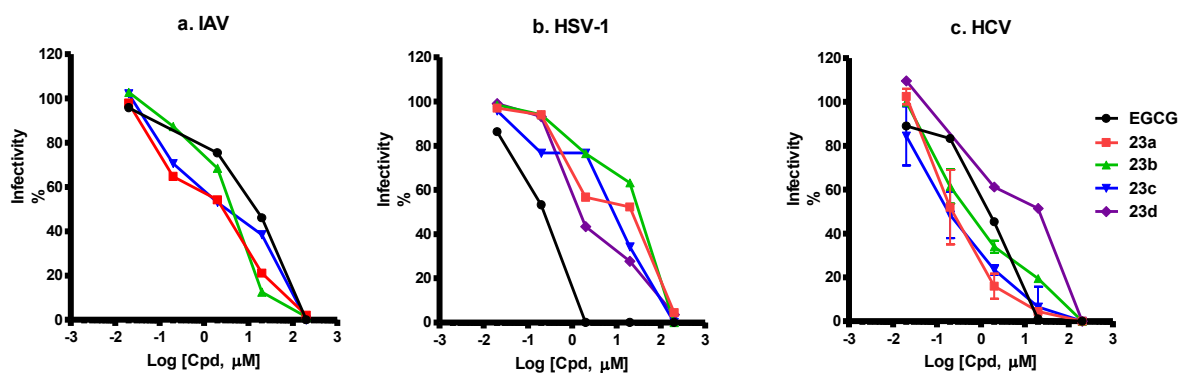
<sup>a</sup>Isolated yields after purification. <sup>b</sup>These polyphenol compounds were synthesized by D. J. Schatz during his undergraduate research experience

By having a library of the polyphenolic compounds **23a-m** in hand, we turned to test their antiviral activities against unrelated viruses. Similar to preliminary studies (part 4-4-1), the viral inhibition activities of the synthesized polyphenolic molecules **23a-m** were examined against the HS binding viruses HCV, HSV-1 and SA binding virus IAV.

### 4.4.3 Antiviral Activities of the Synthesized Polyphenolic Compounds

#### 4.4.3.1 Digallates with Flexible Linkers

Digallates **23a-d** with linear flexible central scaffold and ester linkers were the first group of synthesized molecules that were tested against HS binding viruses HCV, HSV-1 and SA binding virus IAV, we found that digallates **23a-d**, similar to EGCG, inhibited the viral infection against all three viruses in a similar manner. Improved IAV inhibitions were observed for digallates **23a-c** with flexible linkers compared to EGCG ( $EC_{50}$ = 9.5, 2.0, 3.7 and 2.9  $\mu$ M for EGCG, **23a**, **23b** and **23c** respectively) (Figure 4-14, a). Digallates **23a-d** also showed viral inhibition against HSV-1 with  $EC_{50}$ s of 0.14, 11.3, 23.8, 8.0 and 2.0  $\mu$ M for EGCG, **23a**, **23b** and **23c** and **23d** respectively (Figure 4-14, b). Inhibition of HCV by EGCG, **23a**, **23b** and **23c** and **23d** was also observed in low micromolar concentration ( $EC_{50}$ , 1.50, 0.26, 0.60, 0.20, 12.1  $\mu$ M respectively) (Figure 4-14, c). Comparing  $EC_{50}$  of EGCG with digallates **23a-d** having flexible linkers showed an improved inhibition by digallates against HCV except digallate **23d** possessing longer 6 carbon linker which exhibited a decreased viral inhibition. Although EGCG showed a better antiviral activity against HSV-1 compared to the other synthesized digallates, in the case of IAV and HCV, digallates **23a-c** showed more potent antiviral activities than EGCG. As a result, digallate molecules might be considered as a potential broad spectrum antivirals against unrelated viruses although modification of central scaffold is still required in order to have lower  $EC_{50}$  values for all three unrelated viruses.



**Figure 4-14: Antiviral Activities of Digallate Possessing Flexible Linkers Against IAV, HSV-1 and HCV.** (Dose response curves). Cell monolayers were infected with (a) IAV, (b) HSV-1 or (c) HCV pre-exposed to EGCG or digallates **23a-d** for 10 min at 37 °C. Infectivity was evaluated by plaquing or focus forming efficiency and is expressed as percentage relative to DMSO-treated control. For the most compounds infectivity test was performed once.

#### 4.4.3.2 Digallates with Rigid or Less Flexible Linkers

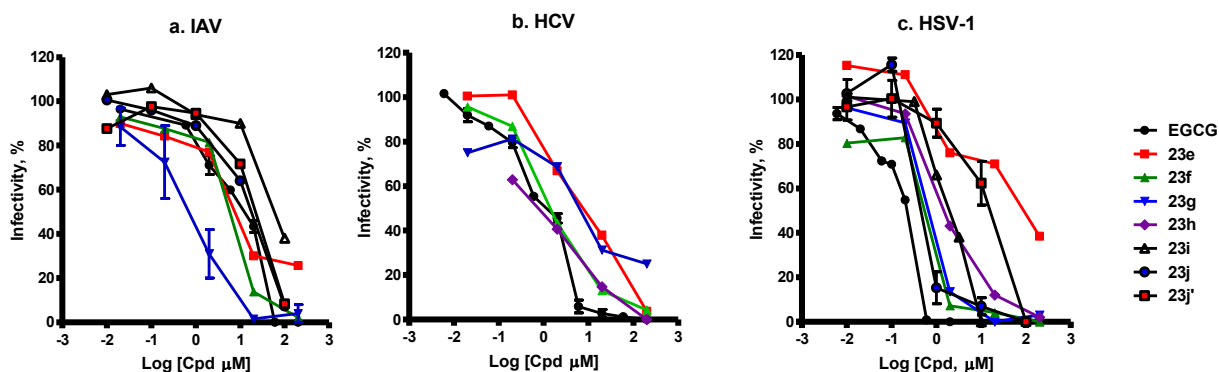
In order to study the effect of the central scaffold of the digallates on the antiviral activities of these compounds, another group of synthesized molecules were designed to have rigid linkers such as aromatic rings **23f-h**, or less flexible scaffolds such as diethyleneglycol **23e** and cyclohexane rings **23i**, **23j** and **23j'**.

In case of IAV, **23g** containing 1,4-disubstituted aromatic ring was observed to have the best antiviral activities ( $EC_{50} = 0.25 \mu\text{M}$ ). Digallates **23j**, **23j'** and **23i** containing cyclohexane scaffold did not exhibit potent activities against IAV ( $EC_{50} = 22.0, 48.0, 59.0 \mu\text{M}$  respectively). Also molecule **23e** was demonstrated not to be a comparable antiviral agent against IAV ( $EC_{50} = 8.5 \mu\text{M}$ ) compared to **23g** (Figure 4-15, a).

Studying the antiviral activities of these compounds against HCV demonstrated that **23h** possessing 1,2-benzenedimethylene as the central linker exhibited more potent antiviral activities against HCV compared to the other synthesized digallates and EGCG ( $EC_{50} = 1.50, 7.90, 1.60, 6.50, 0.83 \mu\text{M}$  for EGCG, **23e**, **23f**, **23g** and **23h** respectively). Again, **23e** did not exhibit satisfying antiviral activity (Figure 4-15, b). Further studies are required to investigate the HCV inhibition of **23i**, **23j** and **23j'**.

In contrast to IAV, the best HSV-1 inhibition was observed for compound **23j** possessing *trans*-1,4-disubstitution cyclohexane ( $EC_{50}$ = 0.40  $\mu$ M). *Cis*- diastereomer **23j'** did not show comparable antiviral activity against HSV-1 ( $EC_{50}$ = 23.8  $\mu$ M). On the other hand, compound **23i**, containing *trans*-1,2-disubstituted cyclohexane inhibited HSV-1 potently with  $EC_{50}$  of 0.66  $\mu$ M. Digallates **23f-h** with rigid aromatic linkers also showed proper HSV-1 inhibition ( $EC_{50}$ = 0.50, 0.67 and 1.70  $\mu$ M respectively). Similar to IAV and HCV, molecule **23e** containing diethyleneglycol scaffold did not show significant HSV-1 inhibition ( $EC_{50}$ = 81.6  $\mu$ M) (Figure 4-15, c).

By considering these results, we concluded that digallate **23g**, containing 1,4-disubstituted benzene ring, showed potent antiviral activities against the chosen viruses particularly, HSV-1 and IAV. This finding may lead us to employ the 1,4-disubstituted benzene ring as a potential central scaffold for the design and synthesis of the broad-spectrum antivirals in future studies. Although further investigation is required to test the antiviral activity of **23h** having 1,2-cyclohexanedimethylene central scaffold against IAV, it can be considered as a broad spectrum antiviral according to the potent results obtained for its viral inhibition against HSV-1 and HCV ( $EC_{50}$ = 1.70, 0.83  $\mu$ M respectively).

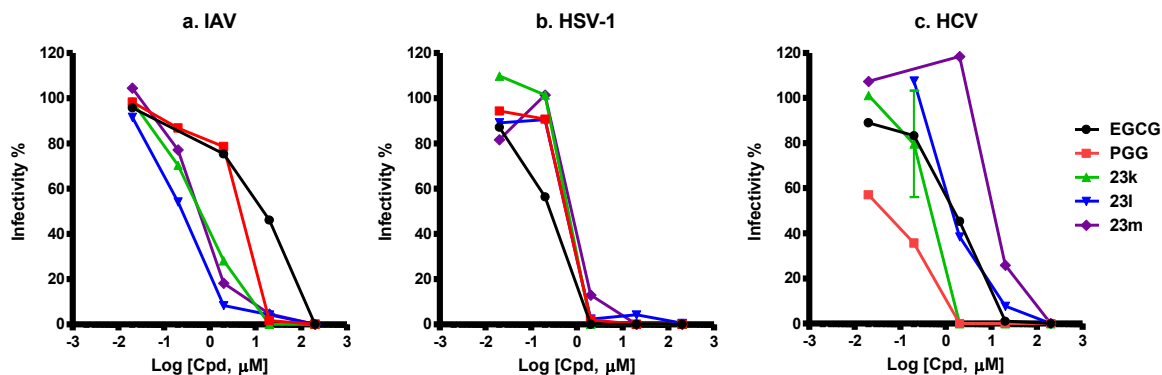


**Figure 4-15: Antiviral Activities of Digallates Possessing Rigid/Less Flexible Linkers Against IAV, HSV-1 and HCV.** (Dose response curves). Cell monolayers were infected with (a) IAV, (b) HCV, or (c) HSV-1 pre-exposed to EGCG or digallates **23e-j'** for 10 min at 37  $^{\circ}$ C. Infectivity was evaluated by plaquing or focus forming efficiency and is expressed as percentage relative to DMSO-treated control. For a few compounds infectivity test was performed once.

#### 4.4.3.3 The Effect of the Number of Gallate Moieties

We were also interested in studying whether increasing the number of gallate moieties can affect the antiviral activities of the polyphenolic compounds. For this purpose, in addition to commercially available pentagalloyl glucose (PGG) a group of tri- and tetragallate compounds **23k-m** were synthesized and their antiviral activities were compared to EGCG.

IAV inhibition by the tri- and tetra-gallates **23k-m** was significantly improved compared to EGCG and PGG ( $EC_{50}$  for EGCG, PGG, **23k**, **23l**, **23m** were 9.50, 4.10, 0.60, 0.23 and 0.59  $\mu$ M respectively) (Figure 4-16, a). Although, EGCG was more potent against HSV-1 infection, synthesized molecules **23k-m** exhibited valuable antiviral activities ( $EC_{50}$  for EGCG, PGG, **23k**, **23l**, **23m** were 0.14, 5.50, 0.66, 0.55 and 0.78  $\mu$ M respectively) (Figure 4-16, b). Significant HCV inhibitions were also observed for the polygallates. PGG inhibited HCV potently with an  $EC_{50}$  of 0.05  $\mu$ M. Trigallates **23k** and **23l** were also active against HCV with  $EC_{50}$ s of 0.43 and 1.70  $\mu$ M respectively. However, a higher concentration of tetragallate **23m** was needed to inhibit HCV ( $EC_{50}$  13.2  $\mu$ M) (Figure 4-16, c).



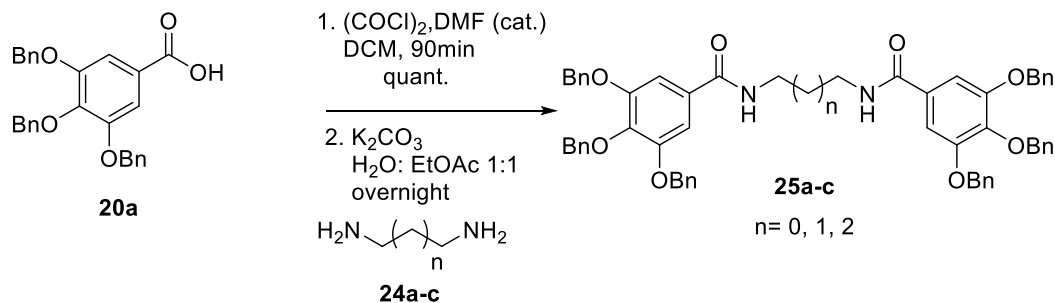
**Figure 4-16: Antiviral Activities of Polygallates Against IAV, HSV-1 and HCV.** (Dose response curves). Cell monolayers were infected with (a) IAV, (b) HSV-1 or (c) HCV pre-exposed to EGCG, PGG or polygallates **23k-m** for 10 min at 37 °C. Infectivity was evaluated by plaquing or focus forming efficiency and is expressed as percentage relative to DMSO-treated control. For the most compounds infectivity test was performed once.

## 4.5 Polyphenolic Compounds Possessing Other Functional Groups

Commonly, ester functional group is not widely used in drug synthesis. Esters can undergo rapid in vivo cleavage due to the presence of esterase enzymes that are ubiquitously present in the blood stream and cell medium. Although the aforementioned polyphenolic compounds containing ester functional group exhibited potent antiviral activities, we decided to find robust moieties to overcome the limitations related to ester functional group. Therefore, we turned our attention to design a series of compounds possessing amide, ketone and linear carbon chain moieties. Our attempts to construct the molecules containing ether functional group were unsuccessful due to fast decomposition of the target molecules.

### 4.5.1 Polyphenolic Molecules Possessing Amide Linkers

In order to study the effect of the functional groups in the structure of the polyphenolic compounds, we decided to synthesize simple digallamides. Based on our previous observations, diesters **23a-c** possessing linear flexible hydrocarbons exhibited acceptable broad spectrum antiviral activities. As a result, we planned to synthesize their analogues to study the role of the amide functional group in the viral inhibition. Compounds **25a-c** were prepared by the coupling of the corresponding acid chloride with linear diamines **24a-c** in very good yield (Table 4-1). The use of DCC or EDCI . HCl to construct amide linker between carboxylic acids **20** and diamines **24** provided the desired product in a very low yield.

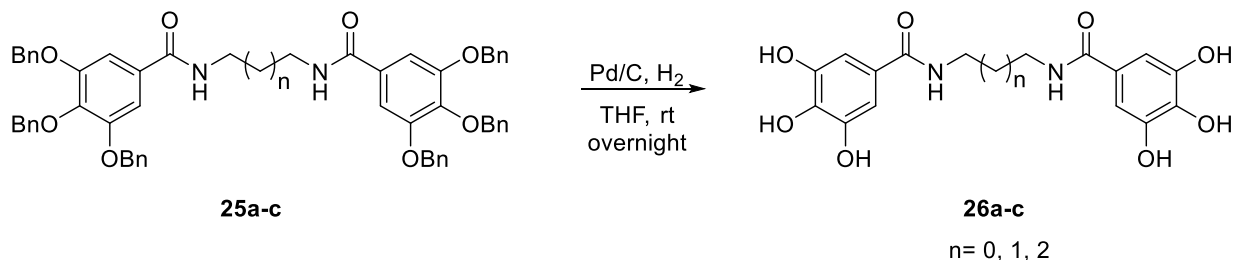
**Table 4-4: Formation of Polyphenolic Compounds Possessing Amide Linker**

Entry	Central Scaffold	Product <sup>b</sup>	Yield (%) <sup>a</sup>
1	 <b>24a</b>	 <b>25a</b>	76%
2	 <b>24b</b>	 <b>25b</b>	89%
3	 <b>24c</b>	 <b>25c</b>	80%

<sup>a</sup>Isolated yields after purification. <sup>b</sup>Digallamides **25a-c** were synthesized by D. J. Schatz during his undergraduate research experience

The benzyl protecting group removal in compounds **25a-c** was achieved under the standard conditions of hydrogenolysis employing Pd/C to form the desired polyphenolic compounds **26a-c** containing amide linkers (Table 4-5).

**Table 4-5: Deprotection of Benzyl Group in Compounds 25a-c**



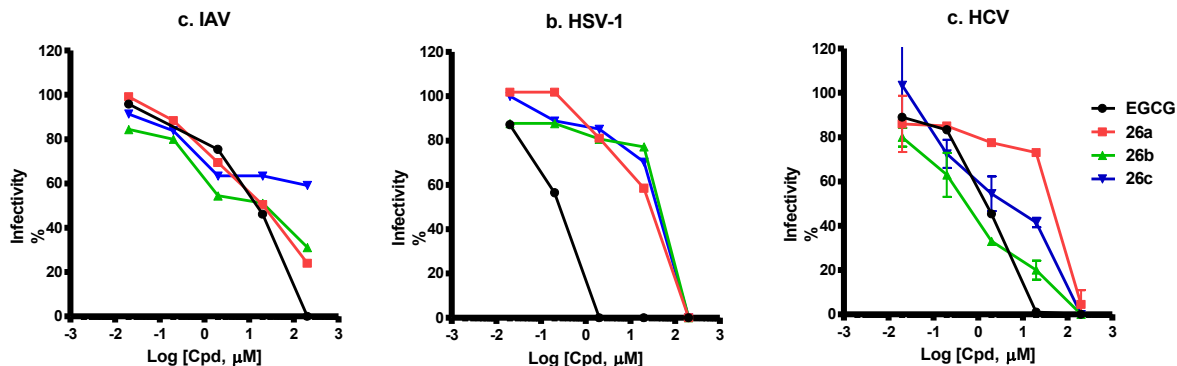
Entry	Substrate	Product <sup>b</sup>	Yield (%) <sup>a</sup>
1	<b>25a</b>	<p style="text-align: center;"><b>26a</b></p>	19%
2	<b>25b</b>	<p style="text-align: center;"><b>26b</b></p>	88%
3	<b>25c</b>	<p style="text-align: center;"><b>26c</b></p>	84%

<sup>a</sup>Isolated yields after purification. <sup>b</sup>Digallamides **26a-c** were synthesized by D. J. Schatz during his undergraduate research experience.

Compounds **26a-c** containing flexible scaffold and amide linkers were then tested against HCV, HSV-1 and IAV. We found out that EGCG was more potent antiviral compared to the synthesized diamide compounds. Diamides **26a-c** showed very poor viral inhibition against IAV ( $EC_{50}$ , 9.5, 17.9, 14.1 and 186  $\mu\text{M}$  for EGCG, **26a**, **26b** and **26c** respectively) (Figure 4-17, a). Similar results were found in case of HSV-1. It was also observed that EGCG is a better antiviral against HSV-1 with the  $EC_{50}$  0.14  $\mu\text{M}$  compared to the diamides **26a-c** ( $EC_{50}$ , 21.6, 36.9, 31.6  $\mu\text{M}$  for EGCG, **26a**, **26b** and **26c** respectively) (Figure 4-17, b). However, compound **26b** possessing three carbon linker showed more potent antiviral activity than EGCG against HCV ( $EC_{50}$ , 1.5, 34.4, 0.4 and 3.6  $\mu\text{M}$  for EGCG, **26a**, **26b** and **26c**



respectively) (Figure 4-17, c). By comparing the obtained results from the compounds **23a-c** containing ester linkers and molecules **26a-c** with amide linkers, we concluded that amide linker is not a suitable moiety for designing antiviral agents against unrelated viruses.

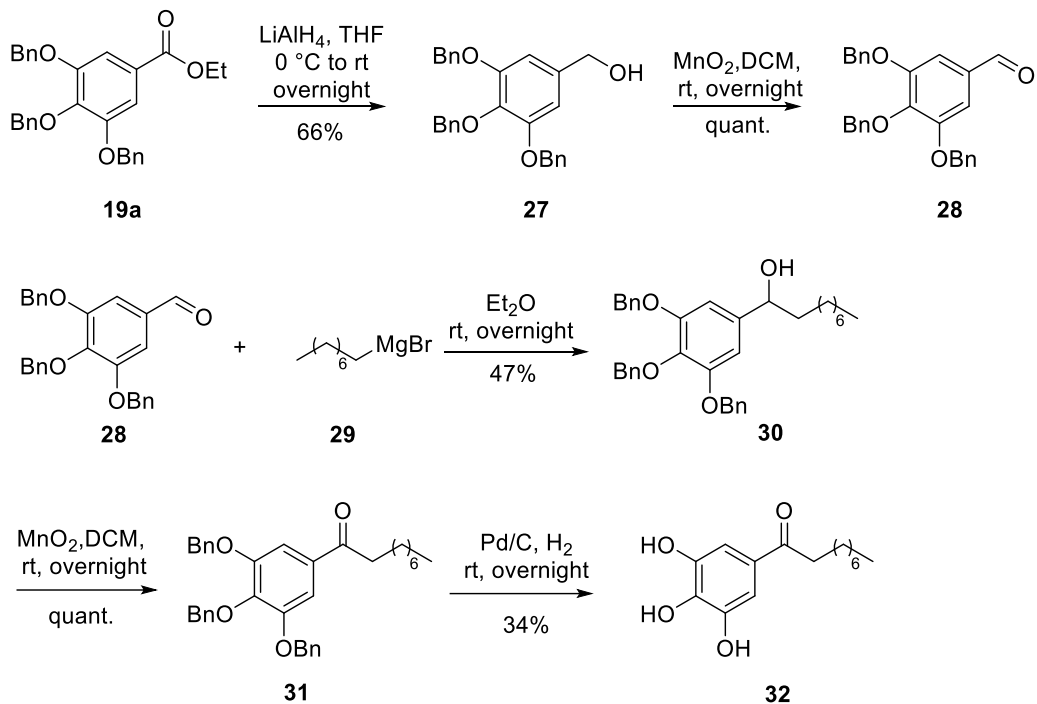


**Figure 4-17: Antiviral Activities of Digallates Possessing Amide Linkers against IAV, HSV-1 and HCV.** (Dose response curves). Cell monolayers were infected with (a) IAV, (b) HSV-1 or (c) HCV pre-exposed to EGCG or compounds **26a-c** for 10 min at 37 °C. Infectivity was evaluated by plaquing or focus forming efficiency and is expressed as percentage relative to DMSO-treated control. For the most compounds infectivity test was performed once.

#### 4.5.2 Polyphenolic Molecules Possessing Ketone Linkers

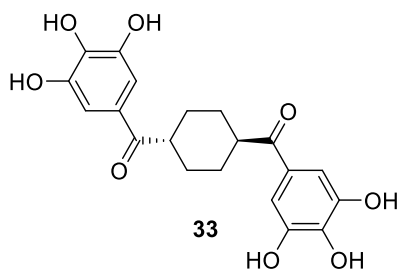
As previously mentioned, octyl gallate (OG) exhibited potent broad-spectrum antiviral activity against HS binding viruses HCV, HSV-1 and SA binding virus IAV. However, octyl gallate contains an ester functional group which limits its potential in vivo antiviral application due to the presence of esterase enzyme in the blood stream. As a result, we decided to synthesize and study the viral inhibition of polyphenolic compounds possessing ketone functional group as an alternative linker.

The required polyphenolic compound **32** containing ketone linker was synthesized readily by the oxidation of alcohol **30** followed by the deprotection of benzyl protecting groups in compound **31** under standard condition. Alcohol **30** was obtained by the reaction of protected aldehyde **28** with the Grignard reagent **29**. Benzyl protected aldehyde **28** was also prepared from the hydrolysis of ester **19a** to the benzylic alcohol **27** followed by the oxidation with  $\text{MnO}_2$  in high yield (Scheme 4-3).



**Scheme 4-3: Formation of Ketone 32**

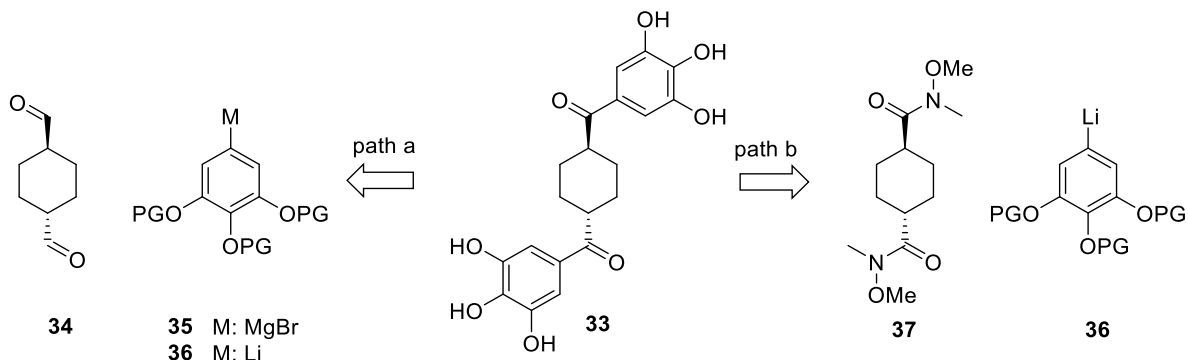
As previously shown, rigid and less flexible central scaffolds demonstrated potent antiviral activities. Therefore, in our first attempts to employ these type of linkers along with ketone functional group, we decided to synthesize molecule **33** containing *trans*-1,4-disubstituted cyclohexane (Figure 4-18).



**Figure 4-18: Target Molecule Possessing *trans*-1,4-Disubstituted Cyclohexane and Ketone Linkers**

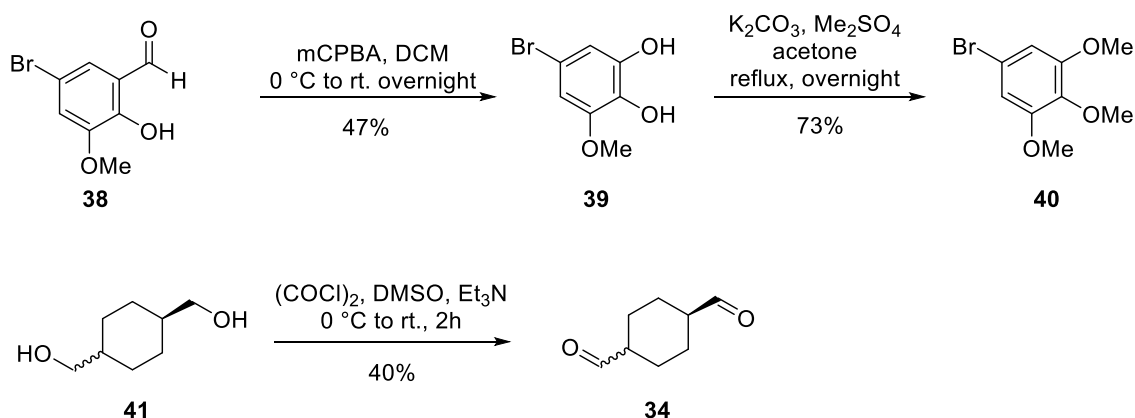
We proposed three possible synthetic pathways to prepare compound **33**. This compound can be prepared by the 1,2-addition of Grignard reagent **35** or aryl lithium **36** to 1,4-cyclohexanedialdehyde **34** (Figure 4-19, path a). We also envisioned that compound **33** can

be synthesized by the treatment of Weinreb amide **37** with aryl lithium **36** (Figure 4-19, path b).



**Figure 4-19: Retro-synthesis of Compound 33**

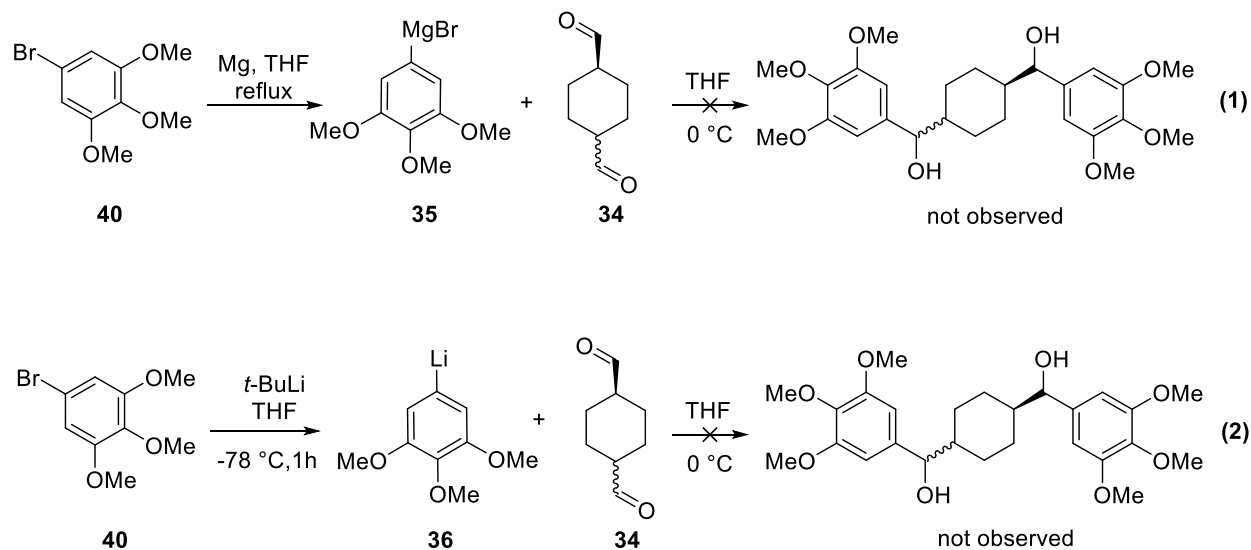
The required bromobenzene **39** was prepared via the Baeyer-Villiger oxidation of 5-bromo-*o*-vanillin **38** in the presence of mCPBA<sup>224</sup> followed by methylation of the phenolic hydroxyl group in **39** with the methyl sulfate under basic condition. Bromobenzene **40** can be further used as a precursor to generate Grignard reagent **35** or aryl lithium **36** by its treatment with Mg or *t*-BuLi respectively. The required dialdehyde **34** was readily prepared as a mixture of *cis*- and *trans*- isomers from the Swern oxidation of 1,4-cyclohexanedimethanol **41** in moderate yield (Scheme 4-4).



**Scheme 4-4: Preparation of Starting Materials 34 and 40**

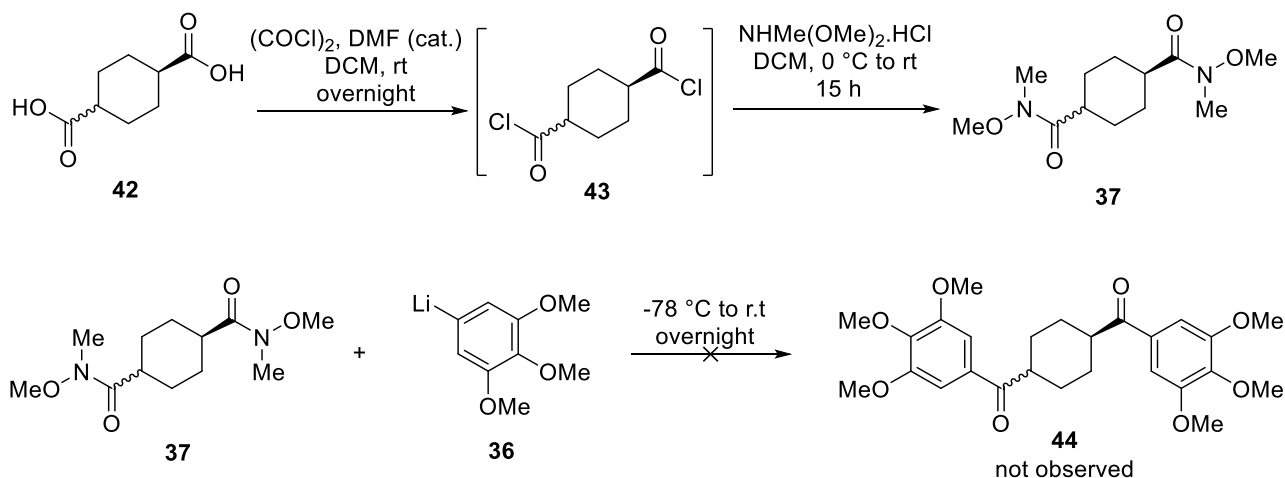
Grignard reagent **35** was prepared by treatment of the protected bromobenzene **40** with magnesium turnings in refluxing THF. Unfortunately, the reaction of dialdehyde **34** with Grignard reagent **35** did not yield the desired diol which can act as the precursor to generate

diketone **33** (Scheme 4-5, eq. 1). Similarly, the reaction of 1,4-cyclohexanedialdehyde **34** with aryl lithium **36**, obtained by the treatment of aryl bromide **40** with *t*-BuLi, provided a complex reaction mixture and no desired diol was isolated (Scheme 4-5, eq. 2).



#### Scheme 4-5: Unsuccessful Attempts for Preparation of Diol

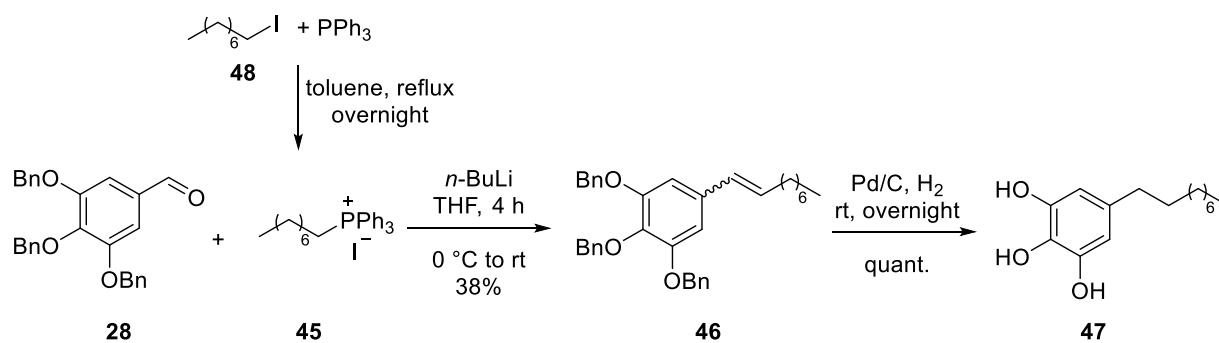
After these unsuccessful attempts, we decided to directly synthesize diketone **44** using Weinreb amide **37** which was obtained in two steps starting from 1,4-cyclohexanedicarboxylic acid **42**. Weinreb amide **37** was treated with aryl lithium **36** at  $-78\text{ }^{\circ}\text{C}$  and unfortunately a complex mixture was isolated instead of the desired diketone **44** (Scheme 4-6).



**Scheme 4-6: Employing Weinreb Amide**

#### 4.5.3 Studying the Impact of the Functional Group

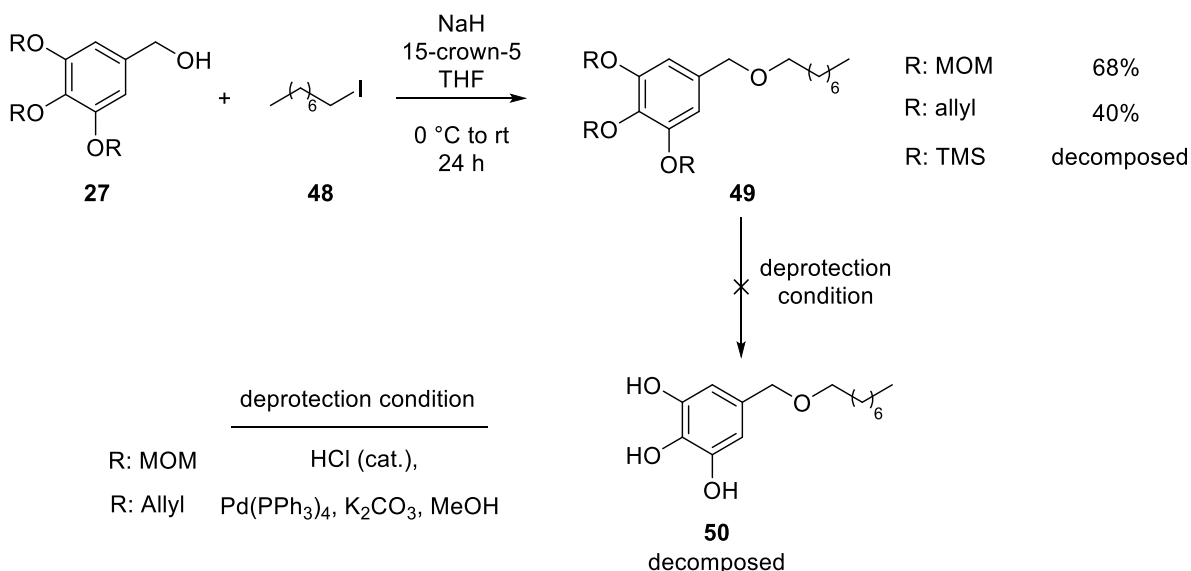
As previously mentioned, we were studying the impact of the different functional groups in the antiviral activities of the polyphenolic compounds against unrelated viruses. In order to investigate whether the presence of the functional groups are essential for potent antiviral activities, we decided to synthesize octyl gallate analogue **47** with linear carbon chain. Compound **47** was prepared via the Wittig reaction between the aldehyde **28** and the corresponding phosphonium salt **45** that was simply obtained by the treatment of triphenylphosphine with *n*-octyl iodide **48**. Reduction of alkene double bond and deprotection of benzyl protecting groups in molecule **46** were achieved in one step and under the standard hydrogenolysis condition employing Pd/C to afford the target molecule **47** (Scheme 4-7).



**Scheme 4-7: Formation of Compound 47**

#### 4.5.4 Construction of Ether Functional Group

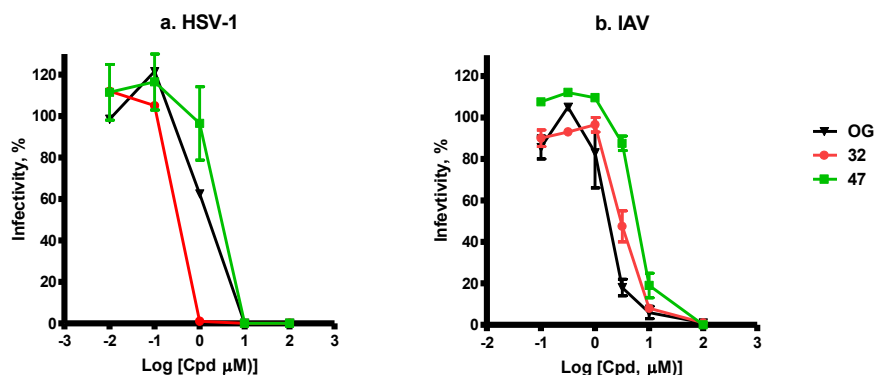
Regarding our investigation on the role of the functional group we opted to install an ether moiety as a possible functional group. Our attempts to synthesize compound **50** having an ether functional group were unsuccessful (Scheme 4-8). The formation of ethereal C-O bond through the reaction of primary benzylic alcohol **27** and octyl iodide **48** was successfully achieved whereas the deprotection of phenolic hydroxyls led us to a complex reaction mixture. Trying various protection groups such as MOM, allyl and TMS did not provide the desired product.



**Scheme 4-8: Unsuccessful Attempts to Synthesis Ether 50**

#### 4.5.5 Antiviral Activities of Compounds 32 and 47

Having the compounds **32** and **47** in hand, their antiviral activities were examined against HS binding HSV-1 and SA binding IAV (Figure 4-20). Interestingly, ketone **32** inhibited HSV-1 potently with the  $EC_{50}= 0.30 \mu\text{M}$  (Figure 4-20, a). This compound also exhibited efficient viral inhibition against IAV ( $EC_{50}= 3.90$ ) (Figure 4-20, b). On the other hand, compound **47** possessing carbon chain did not show competent viral inhibition against HSV-1 and IAV compared to OG and ketone **32** ( $EC_{50}$ , 2.80 and 6.60  $\mu\text{M}$  for HSV-1 and IAV respectively) (Figure 4-20). As a result, the ketone functional group can be considered as an effective and robust moiety in the design and synthesis of the broad-spectrum antiviral agents. Further studies on inhibition of HCV are still required.



**Figure 4-20: Antiviral Activities of Compounds 32 and 47 vs. OG Against HSV-1 and IAV.** (Dose response curves). Cell monolayers were infected with (a) HSV-1 and (b) IAV pre-exposed to EGCG or compounds **32** and **47** for 10 min at 37 °C. Infectivity was evaluated by plaquing or focus forming efficiency and is expressed as percentage relative to DMSO-treated control (n=2).

#### 4.6 Conclusion

We have found that natural compound EGCG, a catechin extracted from green tea, possesses broad-spectrum antiviral activity against HS binding viruses HCV, HSV-1 and SA binding virus IAV. Further studies on the EGCG mechanism of action showed that polyphenol moiety plays a crucial role in viral inhibition through the blocking of the primary virion attachment to the host cell receptors which is one of the key steps during the viral infection. Preliminary results showed the octyl gallate (OG) also inhibited all three unrelated viruses via the same mechanism of action. Due to the limitations in employing EGCG and OG as an

antiviral we opted to synthesize a series of molecules containing polyphenol substructure and their antiviral activities were compared to EGCG (Table 4-6). We found that molecules possessing two polyphenol moieties (digallates) showed satisfying antiviral activities. Digallate **23g** containing 1,4-disubstituted benzene central scaffold is very promising and exhibited potent antiviral activities against unrelated HSV-1 and IAV. We also found that increasing the number of polyphenol moieties improved the antiviral activity in case of trigallates **23k** and **23l**. Although larger molecules such as **23k** and **23l** showed significant broad-spectrum antiviral activities but they are not preferred rather than digallates. This preference originates from our primary goal which was design and synthesis of small molecules as BS antivirals since the study of the larger molecules is pharmacologically harder due to their higher polarity. It is also more difficult in the case of larger molecules to determine the active sites involved in viral inhibition.

Apart from the effect of the central scaffolds and number of polyphenolic moieties, the impact of the different functional groups was also studied. We found that ketone **32** showed competent antiviral activity compared to its ester analogue (OG) whereas amide linker (**26a-c**) and compound **47** possessing long hydrocarbon chain did not provide satisfying antiviral activities. As a result, ester linker can be replaced by ketone functional group to cope with the pharmaceutical challenges regarding employing ester linkers.



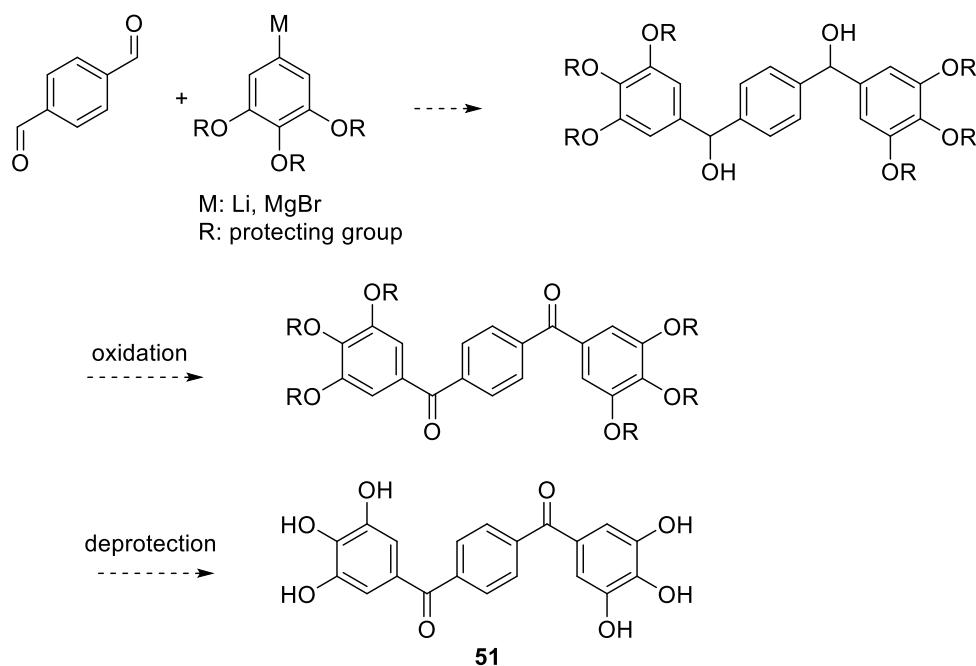
**Table 4-6: EC<sub>50</sub> against HSV-1, IAV and HCV**

Polyphenol Compound	EC <sub>50</sub> (μM)			
	HSV-1	IAV	HCV	
Green tea catechins	EGCG	0.14	9.50	1.50
	EG	26.3	18.8	22.8
	PG	61.0	28.6	16.4
	OG	0.17	0.53	0.11
	LG	0.52	0.20	0.44
Digallates with flexible linker	23a	11.3	2.00	n.t <sup>a</sup>
	23b	23.8	3.70	0.60
	23c	8.00	2.90	0.20
	23d	2.00	n.t	12.1
Digallates with rigid/less flexible linkers	23e	81.6	8.50	7.90
	23f	0.50	5.50	1.60
	<b>23g</b>	<b>0.67</b>	<b>0.25</b>	<b>6.50</b>
	23h	1.70	n.t	0.83
	23i	0.66	59.0	n.t
	23j	0.40	22.0	n.t
Poly-gallates	23j'	23.8	48.0	n.t
	<b>23k</b>	<b>0.66</b>	<b>0.60</b>	<b>0.43</b>
	<b>23l</b>	<b>0.55</b>	<b>0.23</b>	<b>1.70</b>
	23m	0.78	0.59	13.2
Digallates with amide linkers	PGG	5.50	4.10	0.05
	26a	21.6	17.9	34.4
	26b	36.9	14.1	0.40
Mono-gallate with ketone linker	26c	31.6	186	3.60
	<b>32</b>	<b>0.30</b>	<b>3.90</b>	<b>n.t</b>
Mono-gallate with carbon chain	47	2.80	6.60	n.t

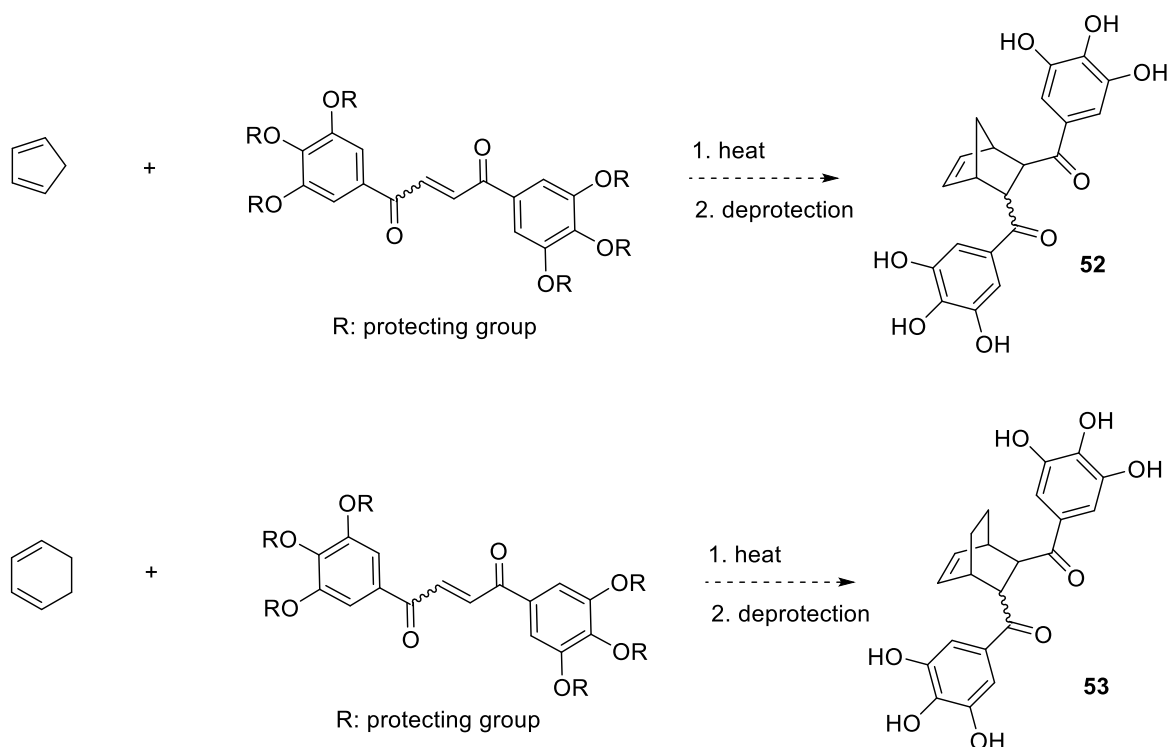
<sup>a</sup>Not tested

## 4.7 Future Directions

The research discussed in this chapter was an expanded investigation of the effect of the various factors in design and synthesis of the broad-spectrum antivirals inspired from green tea catechins. Important information was obtained during this study; however, more scope of improvements can be envisioned in the synthesis of new molecules. One of the interesting directions, can be the synthesis of the molecules possessing more rigid central scaffolds and ketone linkers. According to the data obtained from **23g**, a 1,4-disubstituted benzene ring can be considered to be a suitable scaffold. Molecule **51**, containing a 1,4-disubstituted benzene and ketone linker might be a simple candidate as an active broad-spectrum antiviral.



We can also screen more rigid scaffolds such as molecules **52** and **53** in further investigations. **52** and **53** may be synthesized through a Diels-Alder reaction followed by the deprotection of phenolic hydroxyls.



## 4.8 Experimental

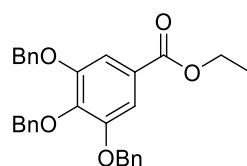
### 4.8.1 General Information

Reactions were carried out in flame or oven dried glassware under a positive argon atmosphere unless otherwise stated. Transfer of anhydrous solvents and reagents was accomplished with oven-dried syringes or cannulae. Solvents and some reagents were distilled before use: methylene chloride from calcium hydride, tetrahydrofuran and diethylether from sodium/benzophenone ketyl and toluene from sodium. All other solvents and commercially available reagents were used without further purification. Thin layer chromatography was performed on glass plates precoated with 0.25 mm silica gel; the stains for TLC analysis were conducted with 2.5 % *p*-anisaldehyde in AcOH-H<sub>2</sub>SO<sub>4</sub>-EtOH (1:3:86) and further heating until development of color. Flash chromatography was performed on 230-400 mesh silica gel with the indicated eluents. Nuclear magnetic resonance (NMR) spectra were recorded in indicated deuterated solvents and are reported in ppm in the presence of TMS as internal standard and coupling constants (*J*) are reported in hertz (Hz). The spectra are referenced to residual solvent peaks: CDCl<sub>3</sub> (7.26 ppm, <sup>1</sup>H; 77.26 ppm, <sup>13</sup>C), DMSO-d<sub>6</sub> (2.50 ppm, <sup>1</sup>H; 39.51 ppm, <sup>13</sup>C), acetone-d<sub>6</sub> (2.05 ppm, <sup>1</sup>H; 206.68 and 29.92 ppm, <sup>13</sup>C) and CD<sub>3</sub>OD (3.31

ppm,  $^1\text{H}$ ; 49.00 ppm,  $^{13}\text{C}$ ). Proton nuclear magnetic spectra ( $^1\text{H}$  NMR) and carbon nuclear magnetic resonance spectra ( $^{13}\text{C}$  NMR) were recorded at 500/400 and 125/100 MHz respectively. Infrared (IR) spectra were recorded neat and reported in  $\text{cm}^{-1}$ . Mass spectra were recorded by using electrospray ionization (ESI). Carboxylic acids **20a**<sup>221</sup>, **20b**<sup>225</sup>, 2,5-anhydro-*D*-mannitol which is the starting material to synthesize compound **22m**<sup>226</sup> and phosphonium salt **45**<sup>227</sup> were prepared according to the literature procedure.

#### 4.8.2 Procedure for the Construction of the esters 19a-b

##### Ethyl 3,4,5-tribenzyloxybenzoate (**19a**)

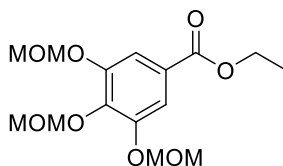


**19a**

To a stirred solution of ethyl gallate **17a** (2.00 g, 10.1 mmol) in DMF (14 mL, 0.7 M) was added  $\text{K}_2\text{CO}_3$  (4.90 g, 35.3 mmol) followed by the slow addition of  $\text{BnCl}$  (4.10 mL, 35.3 mmol) at room temperature. The reaction mixture was stirred for 15 h at 80 °C. After the reaction completion, it was quenched by adding  $\text{H}_2\text{O}$  (30 mL) and was extracted by DCM (10 mL). The organic layer was separated and the aqueous layer was washed with DCM (2×10 mL). Combined organic layers were dried over  $\text{MgSO}_4$ , filtered and concentrated under reduced pressure. Ester **19a** was purified by column chromatography (30:70 EtOAc: hexanes) as a white solid (4.70 g, quant.).

**19a**:  $R_f$  0.30 (10:90 EtOAc: hexanes); mp 95-98 °C; IR (cast film) 3089, 3067, 3031, 2954, 1705, 1596, 1498, 1454, 1429, 1381, 1367, 1229, 1126  $\text{cm}^{-1}$ ;  $^1\text{H}$  NMR (500 MHz,  $\text{CDCl}_3$ )  $\delta$  7.47-7.27 (m, 17H), 5.17 (s, 4H), 5.14 (s, 2H), 4.37 (q,  $J = 7.1$  Hz, 2H), 1.41 (t,  $J = 7.1$  Hz, 3H);  $^{13}\text{C}$  NMR (125 MHz,  $\text{CDCl}_3$ )  $\delta$  166.1, 152.5, 142.4, 137.5, 136.7, 128.6, 128.5, 128.2, 128.0, 127.9, 127.6, 125.6, 109.1, 75.1, 71.3, 61.1, 14.4; HRMS (ESI) calcd for  $\text{C}_{30}\text{H}_{28}\text{NaO}_5$   $[\text{M}+\text{Na}]^+$  491.1829; found 491.1834.

### Ethyl 3,4,5-tris(methoxymethoxy)benzoate (**19b**)



**19b**

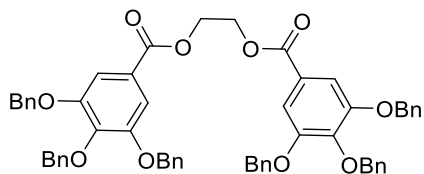
To a stirred solution of ethyl gallate **17a** (1.00g, 5.10 mmol) in THF (3.60 mL, 1.40 M) was added *i*Pr<sub>2</sub>NEt (3.12 mL, 17.8 mmol) followed by the slow addition of MOMCl (1.40 mL, 17.8 mmol) at 0 °C. The reaction mixture was stirred for 15 h at 80 °C. After the reaction completion, it was quenched by adding cold saturated solution of NaHCO<sub>3</sub> (5 mL) and was extracted by Et<sub>2</sub>O (5 mL). The organic layer was separated and the aqueous layer was washed with Et<sub>2</sub>O (2×5 mL). Combined organic layers were dried over MgSO<sub>4</sub>, filtered and concentrated under reduced pressure. Ester **19b** was purified by column chromatography (40:60 EtOAc: hexanes) as a yellow thick oil (1.67 g, 92%).

**19a:** *R*<sub>f</sub> 0.60 (40:60 EtOAc: hexanes); IR (cast film) 2959, 2914, 2828, 1716, 1594, 1499, 1465, 1434, 1393, 1327, 1303, 1249, 1225, 1156 cm<sup>-1</sup>; <sup>1</sup>H NMR (500 MHz, CDCl<sub>3</sub>) δ 7.55 (s, 2H), 5.27 (s, 4H), 5.23 (s, 2H), 4.38 (q, *J* = 7.3 Hz, 2H), 3.63 (s, 3H), 3.56 (s, 6H), 1.39 (t, *J* = 7.3 Hz, 3H); <sup>13</sup>C NMR (125 MHz, CDCl<sub>3</sub>) δ 165.9, 150.6, 140.7, 126.3, 111.6, 98.5, 95.3, 61.1, 57.2, 56.4, 14.4; HRMS (ESI) calcd for C<sub>15</sub>H<sub>22</sub>NaO<sub>8</sub> [M+Na]<sup>+</sup> 353.1207; found 353.1207.

#### 4.8.3 General Procedure for Construction of Compounds **22a-m** Possessing Ester Linkers:

In a flame dried round bottom flask carboxylic acid **20**<sup>221,225</sup> (1.50 equiv.) was suspended in DCM (0.07 M) at room temperature followed by the sequential addition of EDCI . HCl (2.25 equiv.) and DMAP (0.25 equiv.). After the formation of a clear solution, corresponding alcohol **21** (1.00 equiv.) was added and the reaction mixture was stirred at room temperature for 3 h. It was then concentrated under reduced pressure and the product was purified by flash chromatography.

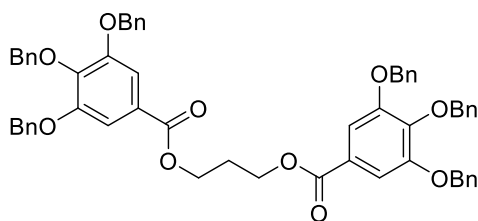
### Ethane-1,2-diyl bis(3,4,5-tribenzyloxybenzoate) (**22a**)



**22a**

Flash chromatography (1:99 acetone: DCM) gave compound **22a** as a white solid (85 mg, 13%);  $R_f$  0.55 (1:99 acetone: DCM); mp 138-140 °C; IR (cast film) 3089, 3064, 3031, 2923, 2870, 1726, 1596, 1502, 1454, 1430, 1399, 1386, 1369, 1342, 1258, 1222, 1202, 1133  $\text{cm}^{-1}$ ;  $^1\text{H}$  NMR (500 MHz,  $\text{CDCl}_3$ )  $\delta$  7.42-7.34 (m, 34H), 5.10 (s, 4H), 5.08 (s, 8H), 4.64 (s, 4H);  $^{13}\text{C}$  NMR (125 MHz,  $\text{CDCl}_3$ )  $\delta$  165.9, 152.6, 142.7, 137.4, 136.5, 128.5, 128.4, 128.2, 128.0, 127.9, 127.5, 124.8, 109.3, 75.1, 71.3, 62.7; HRMS (ESI) calcd for  $\text{C}_{58}\text{H}_{50}\text{NaO}_{10}$   $[\text{M}+\text{Na}]^+$  929.3296; found 929.3291.

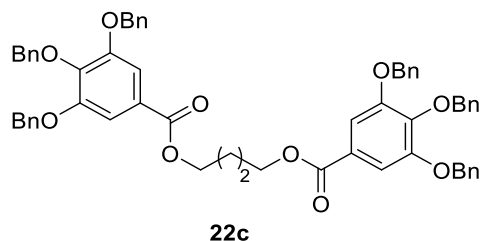
### Propane-1,3-diyl bis(3,4,5-tribenzyloxybenzoate) (**22b**)



**22b**

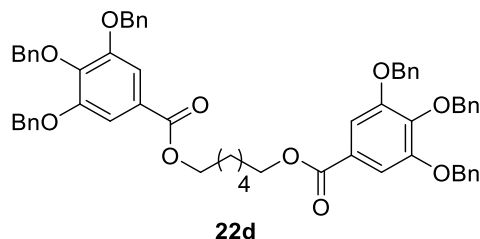
Flash chromatography (1:99 acetone: DCM) gave compound **22b** as a white solid (145 mg, 28%);  $R_f$  0.44 (1:99 acetone: DCM); mp 93-96 °C; IR (cast film) 3088, 3031, 2949, 1713, 1590, 1500, 1454, 1428, 1376, 1335, 1211, 1115  $\text{cm}^{-1}$ ;  $^1\text{H}$  NMR (500 MHz,  $\text{CDCl}_3$ )  $\delta$  7.45-7.26 (m, 34H), 5.13 (s, 4H), 5.12 (s, 8H), 4.46 (t,  $J = 6.2$  Hz, 4H), 2.23 (pent,  $J = 6.2$  Hz, 2H);  $^{13}\text{C}$  NMR (125 MHz,  $\text{CDCl}_3$ )  $\delta$  166.0, 152.5, 142.6, 137.4, 136.6, 128.5, 128.4, 128.2, 128.0, 127.9, 127.5, 128.1, 109.2, 75.1, 71.3, 61.8, 28.2; HRMS (ESI) calcd for  $\text{C}_{59}\text{H}_{52}\text{NaO}_{10}$   $[\text{M}+\text{Na}]^+$  943.3444; found 943.3453.

### Butane-1,4-diyl bis(3,4,5-tribenzyloxybenzoate) (**22c**)



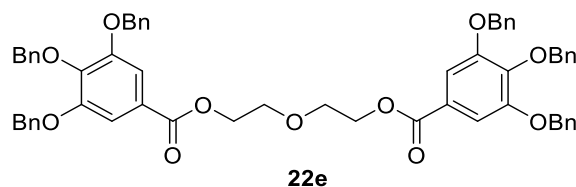
Flash chromatography (1:99 acetone: DCM) gave compound **22c** as a white solid (95 mg, 17%);  $R_f$  0.46 (1:99 acetone: DCM); mp 137-140 °C; IR (cast film) 3063, 3032, 2952, 1712, 1589, 1499, 1454, 1428, 1373, 1334, 1214, 1115  $\text{cm}^{-1}$ ;  $^1\text{H}$  NMR (500 MHz,  $\text{CDCl}_3$ )  $\delta$  7.45-7.44 (m, 34H), 5.14 (s, 12H), 4.39 (t,  $J = 5.6$  Hz, 4H), 1.92 (t,  $J = 5.6$  Hz, 4H);  $^{13}\text{C}$  NMR (125 MHz,  $\text{CDCl}_3$ )  $\delta$  166.1, 152.5, 137.4, 136.7, 128.5, 128.2, 128.0, 127.9, 127.5, 125.3, 108.1, 75.1, 71.3, 64.6, 25.6; HRMS (ESI) calcd for  $\text{C}_{60}\text{H}_{54}\text{NaO}_{10}$   $[\text{M}+\text{Na}]^+$  957.3609; found 957.3590.

### Hexane-1,6-diyl bis(3,4,5-tribenzyloxybenzoate) (**22d**)



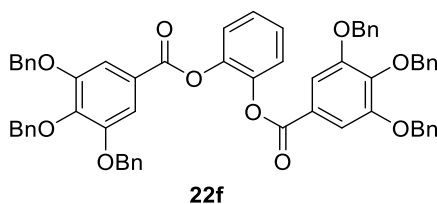
Flash chromatography (1:99 acetone: DCM) gave compound **22d** as a white solid (130 mg, 15%);  $R_f$  0.50 (1:99 acetone: DCM); mp 106-108 °C; IR (cast film) 3064, 3032, 2932, 2860, 1712, 1589, 1499, 1454, 1428, 1373, 1333, 1213, 1115  $\text{cm}^{-1}$ ;  $^1\text{H}$  NMR (500 MHz,  $\text{CDCl}_3$ )  $\delta$  7.46-7.27 (m, 34H), 5.15 (s, 8H), 5.13 (s, 4H), 4.33 (t,  $J = 6.6$  Hz, 4H), 1.82 (m, 4H), 1.52 (m, 4H);  $^{13}\text{C}$  NMR (125 MHz,  $\text{CDCl}_3$ )  $\delta$  166.1, 152.5, 142.5, 137.4, 136.7, 128.5, 128.2, 128.0, 127.9, 127.5, 125.4, 109.2, 75.1, 71.3, 64.9, 28.7, 25.7; HRMS (ESI) calcd for  $\text{C}_{62}\text{H}_{58}\text{NaO}_{10}$   $[\text{M}+\text{Na}]^+$  985.3918; found 985.3922.

**{2-[(3,4,5-Trihydroxybenzoyl)oxy]ethoxy}methyl (3,4,5-tribenzyloxybenzoate) (22e)**



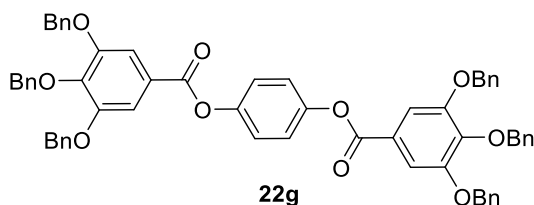
Flash chromatography (5:95 MeOH: DCM) gave compound **22e** as a white solid (442 mg, 11%);  $R_f$  0.16 (5:95 MeOH: DCM); mp 103-105 °C; IR (cast film) 3063, 3032, 2946, 2867, 1714, 1590, 1500, 1454, 1428, 1374, 1333, 1213, 1115  $\text{cm}^{-1}$ ;  $^1\text{H}$  NMR (400 MHz,  $\text{CDCl}_3$ )  $\delta$  7.42-7.23 (m, 34H), 5.08 (s, 4H), 5.07 (s, 8H), 4.47 (t,  $J = 5.0$  Hz, 4H), 3.86 (t,  $J = 5.0$  Hz, 4H);  $^{13}\text{C}$  NMR (125 MHz,  $\text{CDCl}_3$ )  $\delta$  166.2, 152.7, 142.7, 137.6, 136.8, 128.7, 128.6, 128.3, 128.1, 128.0, 127.6, 125.1, 109.3, 75.2, 71.3, 69.3, 64.3; HRMS (ESI) calcd for  $\text{C}_{60}\text{H}_{54}\text{NaO}_{11}$   $[\text{M}+\text{Na}]^+$  973.3550; found 973.3558.

**1,2-Phenylene bis(3,4,5-tribenzyloxybenzoate) (22f)**



Flash chromatography (5:95 MeOH: DCM) gave compound **22f** as a white solid (257 mg, 49%);  $R_f$  0.5 (1:99 acetone: DCM); mp 124-126 °C; IR (cast film) 3064, 3032, 2870, 1739, 1589, 1498, 1454, 1428, 1379, 1337, 1243, 1195  $\text{cm}^{-1}$ ;  $^1\text{H}$  NMR (500 MHz,  $\text{CDCl}_3$ )  $\delta$  7.45-7.21 (m, 38H), 5.01 (s, 4H), 4.94 (s, 8H);  $^{13}\text{C}$  NMR (125 MHz,  $\text{CDCl}_3$ )  $\delta$  164.0, 152.8, 143.4, 142.7, 137.5, 136.4, 128.6, 128.4, 128.3, 128.2, 128.0, 127.7, 126.8, 123.8, 123.7, 109.6, 75.2, 71.3; HRMS (ESI) calcd for  $\text{C}_{62}\text{H}_{50}\text{NaO}_{10}$   $[\text{M}+\text{Na}]^+$  977.3296; found 977.3288.

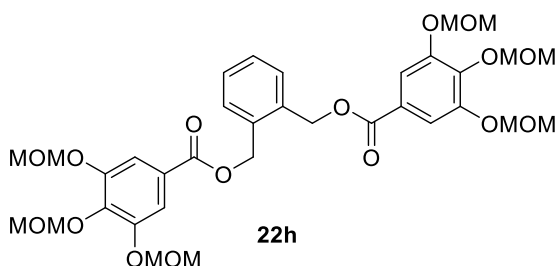
**1,4-Phenylene bis(3,4,5-tribenzyloxybenzoate) (22g)**





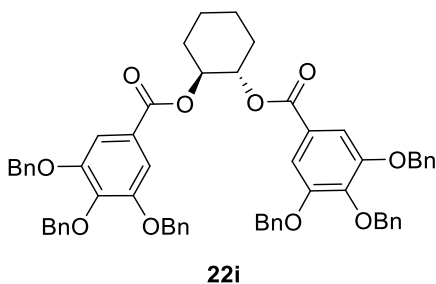
Flash chromatography (5:95 MeOH: DCM) gave compound **22g** as a white solid (418 mg, 96%);  $R_f$  0.71 (1:99 acetone: DCM); mp 194-197 °C; IR (cast film) 3063, 3030, 2989, 1733, 1590, 1506, 1454, 1430, 1337, 1202, 1180  $\text{cm}^{-1}$ ;  $^1\text{H}$  NMR (500 MHz,  $\text{CDCl}_3$ )  $\delta$  7.55 (s, 4H), 7.47-7.37 (m, 24H), 7.29-7.26 (m, 10H), 5.19 (s, 8H), 5.18 (s, 4H);  $^{13}\text{C}$  NMR (125 MHz,  $\text{CDCl}_3$ )  $\delta$  164.7, 152.7, 148.5, 143.2, 137.4, 136.6, 128.7, 128.6, 128.2, 128.1, 128.0, 127.6, 124.3, 122.7, 109.7, 75.2, 71.4; HRMS (ESI) calcd for  $\text{C}_{62}\text{H}_{50}\text{NaO}_{10}$   $[\text{M}+\text{Na}]^+$  977.3296; found 977.3303.

**(1,2-Phenylene)bis(methylene) bis[3,4,5-tris(methoxymethoxybenzoate)] (22h)**



Flash chromatography (2:98 acetone: DCM) gave compound **22h** as a white solid (373 mg, 85%);  $R_f$  0.48 (2:98 acetone: DCM); mp 75-77 °C; IR (cast film) 2907, 2828, 1718, 1593, 1498, 1433, 1393, 1327, 1303, 1222, 1188  $\text{cm}^{-1}$ ;  $^1\text{H}$  NMR (500 MHz,  $\text{CDCl}_3$ )  $\delta$  7.55 (s, 4H), 7.49-7.47 (m, 2H), 7.36-7.34 (m, 2H), 5.22 (s, 4H), 5.23 (s, 8H), 5.21 (s, 4H), 3.60 (s, 6H), 3.49 (s, 12H);  $^{13}\text{C}$  NMR (125 MHz,  $\text{CDCl}_3$ )  $\delta$  164.7, 152.7, 148.5, 143.2, 137.4, 136.6, 128.7, 128.6, 128.2, 128.1, 128.0, 127.6, 124.3, 122.7, 109.7, 75.2, 71.4; HRMS (ESI) calcd for  $\text{C}_{34}\text{H}_{42}\text{NaO}_{16}$   $[\text{M}+\text{Na}]^+$  729.2365; found 729.2359.

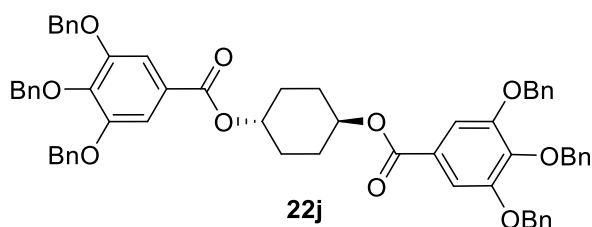
**Cyclohexane-1,2-diyl bis(3,4,5-tribenzyloxybenzoate) (22i)**



Flash chromatography (1:99 acetone: DCM) gave compound **22i** as a colorless sticky oil (190 mg, 64%);  $R_f$  0.57 (1:99 acetone: DCM); IR (cast film) 3064, 3031, 2914, 2866, 1712, 1589,

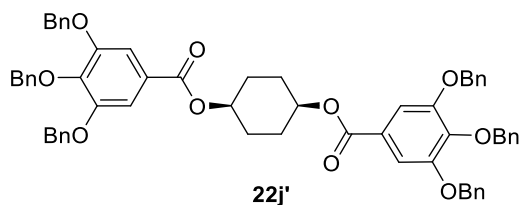
1499, 1454, 1428, 1371, 1335, 1213, 1115  $\text{cm}^{-1}$ ;  $^1\text{H}$  NMR (500 MHz,  $\text{CDCl}_3$ )  $\delta$  7.55-7.22 (m, 34H), 5.22-5.19 (m, 2H), 5.08 (s, 4H), 5.04 (s, 8H), 2.33-2.26 (m, 2H), 1.91-1.82 (m, 2H), 1.65-1.60 (m, 2H), 1.59-1.48 (m, 2H);  $^{13}\text{C}$  NMR (125 MHz,  $\text{CDCl}_3$ )  $\delta$  165.7, 152.5, 142.5, 137.5, 136.6, 128.5, 128.4, 128.1, 128.0, 127.9, 127.6, 125.3, 109.1, 75.1, 74.8, 71.2, 30.3, 23.6; HRMS (ESI) calcd for  $\text{C}_{62}\text{H}_{56}\text{NaO}_{10}$   $[\text{M}+\text{Na}]^+$  983.3766; found 983.3752.

**(1S,2S)-Cyclohexane-1,4-diyl bis(3,4,5-tribenzyloxybenzoate) (22j)**



Flash chromatography (0.5:95.5 acetone: DCM) gave compound **22j** as a white solid (175 mg, 22%);  $R_f$  0.33 (1:99 acetone: DCM); mp 158-160  $^\circ\text{C}$ ; IR (cast film) 3089, 3063, 3031, 2947, 2866, 1709, 1589, 1499, 1454, 1428, 1372, 1335, 1201, 1113  $\text{cm}^{-1}$ ;  $^1\text{H}$  NMR (500 MHz,  $\text{CDCl}_3$ )  $\delta$  7.47-7.31 (m, 28H), 7.30-7.28 (m, 6H), 5.18 (s, 8H), 5.17 (s, 4H), 5.12 (br s, 2H), 2.05-2.02 (m, 4H), 1.77-1.75 (m, 4H);  $^{13}\text{C}$  NMR (125 MHz,  $\text{CDCl}_3$ )  $\delta$  165.4, 152.5, 142.5, 137.4, 136.7, 128.6 (2C), 128.2, 128.0, 127.9, 127.4, 125.6, 109.3, 75.2, 71.3, 71.1, 27.4; HRMS (ESI) calcd for  $\text{C}_{62}\text{H}_{56}\text{NaO}_{10}$   $[\text{M}+\text{Na}]^+$  983.3768; found 983.3766.

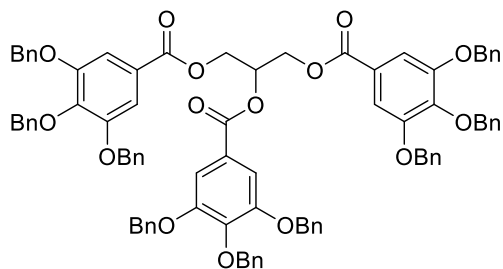
**(1R,2S)-Cyclohexane-1,2-diyl bis(3,4,5-tribenzyloxybenzoate) (22j')**



Flash chromatography (0.5:95.5 acetone: DCM) gave compound **22j'** as a colorless oil (140 mg, 17%);  $R_f$  0.22 (1:99 acetone: DCM); IR (cast film) 3089, 3064, 3031, 2946, 2870, 1709, 1589, 1499, 1453, 1428, 1370, 1331, 1213, 1112  $\text{cm}^{-1}$ ;  $^1\text{H}$  NMR (400 MHz,  $\text{DMSO-d}_6$ )  $\delta$  7.45-7.28 (m, 34H), 5.18-5.12 (m, 2H), 5.16 (s, 12H), 2.03 (m, 4H), 1.92 (m, 4H);  $^{13}\text{C}$  NMR (125 MHz,  $\text{DMSO-d}_6$ )  $\delta$  165.0, 152.4, 142.6, 137.4, 136.7, 128.6, 128.5, 128.2, 128.1, 128.0,

127.5, 126.7, 109.4, 75.2, 71.4, 71.0, 27.7; HRMS (ESI) calcd for C<sub>62</sub>H<sub>56</sub>NaO<sub>10</sub> [M+Na]<sup>+</sup> 983.3766; found 983.3766.

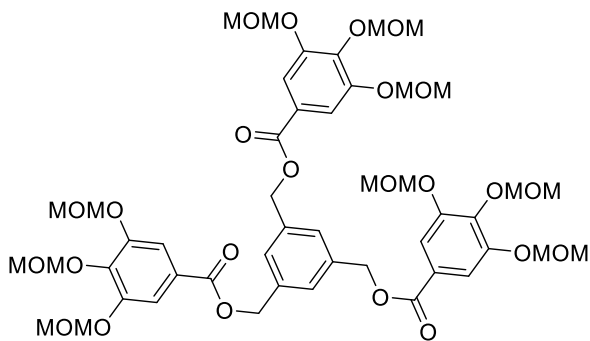
**Propane-1,2,3-triyl (3,4,5- tribenzyloxybenzoate) (22k)**



**22k**

Flash chromatography (1:99 acetone: DCM) gave compound **22k** as a white solid (159 mg, 31%); R<sub>f</sub> 0.67 (1:99 acetone: DCM); mp 128-130 °C; IR (cast film) 3089, 3064, 3032, 2944, 1719, 1589, 1500, 1454, 1429, 1373, 1336, 1200, 1116 cm<sup>-1</sup>; <sup>1</sup>H NMR (400 MHz, CDCl<sub>3</sub>) δ 7.38-7.24 (m, 51H), 5.74 (p, *J* = 5.6 Hz, 1H), 5.08 (s, 4H), 5.05 (s, 8H), 5.02 (s, 2H), 5.00 (s, 4H), 4.72 (dd, *J* = 12.0, 4.5 Hz, 2H), 4.52 (dd, *J* = 12.0, 6.0 Hz, 2H); <sup>13</sup>C NMR (125 MHz, CDCl<sub>3</sub>) δ 164.8, 164.7, 152.0 (2C), 141.7, 141.5, 137.2, 137.1, 136.4 (2C), 136.3, 128.4 (2C), 128.3, 128.1, 128.0, 128.0, 127.9, 127.8, 127.8, 127.7, 127.6 (2C), 124.3, 108.3, 108.2, 74.2, 74.1, 70.2, 70.1, 62.9, 54.9; HRMS (ESI) calcd for C<sub>87</sub>H<sub>74</sub>NaO<sub>15</sub> [M+Na]<sup>+</sup> 1381.4909; found 1381.4920.

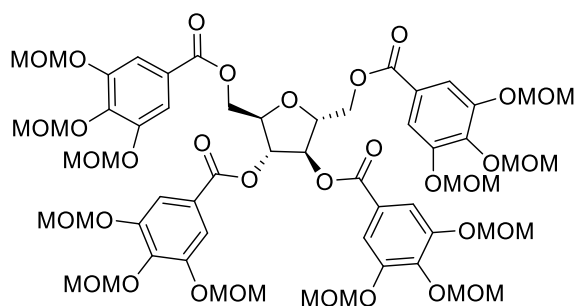
**Benzene-1,2,3-triyl (3,4,5- methoxymethoxybenzoate) (22l)**



**22l**

Flash chromatography (10:90 acetone: DCM) gave compound **22i** as a colorless oil (433 mg, 98%);  $R_f$  0.80 (10:90 acetone: DCM); IR (cast film) 2957, 2922, 2850, 2828, 1718, 1593, 1498, 1433, 1412, 1393, 1372, 1327, 1303, 1245, 1222, 1188  $\text{cm}^{-1}$ ;  $^1\text{H}$  NMR (500 MHz,  $\text{CDCl}_3$ )  $\delta$  7.56 (s, 6H), 7.46 (s, 3H), 5.36 (s, 6H), 5.21 (s, 12H), 5.20 (s, 6H), 3.60 (s, 9H), 3.48 (s, 18H);  $^{13}\text{C}$  NMR (125 MHz,  $\text{CDCl}_3$ )  $\delta$  165.7, 150.8, 141.0, 137.1, 127.4, 125.7, 111.9, 98.5, 98.4, 66.3, 57.3, 56.4; HRMS (ESI) calcd for  $\text{C}_{48}\text{H}_{60}\text{NaO}_{24}$   $[\text{M}+\text{Na}]^+$  1043.3367; found 1043.3364.

**[(2*R*,3*R*,4*R*,5*R*)-3,4-bis(3,4,5- methoxymethoxybenzoate)oxolane-2,5-diyl]bis(3,4,5-methoxymethoxybenzoate) (**22m**)**



**22m**

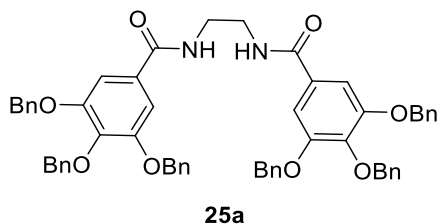
Flash chromatography (10:90 acetone: DCM) gave compound **22m** as a thick colorless oil (110 mg, 12%);  $R_f$  0.62 (10:90 acetone: DCM); IR (cast film) 2958, 2907, 2828, 1721, 1593, 1498, 1467, 1434, 1394, 1329, 1302, 1221, 1187  $\text{cm}^{-1}$ ;  $^1\text{H}$  NMR (500 MHz,  $\text{CDCl}_3$ )  $\delta$  7.62 (s, 4H), 7.58 (s, 4H), 5.79 (s, 2H), 5.28-5.22 (m, 16H), 5.25 (s, 4H), 5.23 (s, 4H), 4.66-4.58 (m, 6H), 3.63 (s, 6H), 3.62 (s, 6H), 3.51 (s, 12H), 3.52 (s, 12H);  $^{13}\text{C}$  NMR (125 MHz,  $\text{CDCl}_3$ )  $\delta$  165.4, 164.6, 150.8, 150.7, 141.4, 141.0, 125.4, 124.5, 111.9, 111.8, 98.5 (2C), 95.4, 95.2, 82.2, 78.9, 63.6, 57.3, 57.2, 56.5, 56.4; HRMS (ESI) calcd for  $\text{C}_{58}\text{H}_{76}\text{NaO}_{33}$   $[\text{M}+\text{Na}]^+$  1323.4161; found 1323.4152.

**4.8.4 General Procedure for Construction of Compounds 25a-c possessing Amide Linkers:**

In a flame dried round bottom flask carboxylic acid **20a** (1.50 equiv.) was suspended in DCM (0.10 M) at room temperature followed by the sequential addition of EDCI . HCl (2.25 equiv.) and DMAP (0.25 equiv.). After the formation of a clear solution, corresponding diamine **24**

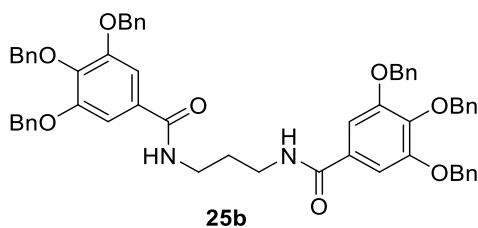
(1.00 equiv.) was added and the reaction mixture was stirred at room temperature for 4h. After the formation of the white solid, it was filtered off and was washed by ethyl acetate. The solid was used in the next step without further purifications.

***N,N'*-(Ethane-1,2-diyl)bis(3,4,5-tribenzyloxybenzoate) (25a)**



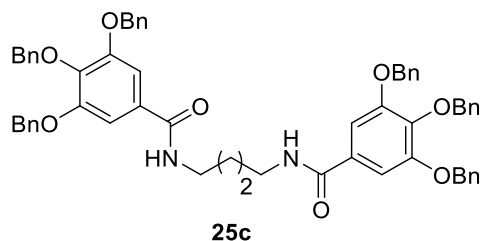
The product **25a** was obtained as a white solid (520 mg, 76%);  $R_f$  0.47 (5:95 MeOH: DCM); mp 206-208 °C; IR (cast film) 3260, 3089, 3062, 3030, 2943, 2867, 1630, 1580, 1542, 1499, 1454, 1441, 1423, 1377, 1350, 1314, 1236, 1127  $\text{cm}^{-1}$ ;  $^1\text{H}$  NMR (500 MHz,  $\text{CDCl}_3$ )  $\delta$  7.40-7.24 (m, 34H), 7.18 (br s, 2H), 5.08 (s, 8H), 5.07 (s, 4H), 3.67 (br s, 4H);  $^{13}\text{C}$  NMR (125 MHz,  $\text{CDCl}_3$ )  $\delta$  168.4, 152.9, 141.4, 137.5, 136.6, 129.3, 128.5 (2C), 128.2, 128.1, 127.9, 127.6, 106.8, 75.2, 71.3, 41.2; HRMS (ESI) calcd for  $\text{C}_{58}\text{H}_{52}\text{N}_2\text{NaO}_8$   $[\text{M}+\text{Na}]^+$  927.3616; found 927.3614.

***N,N'*-(Propane-1,3-diyl)bis(3,4,5-tribenzyloxybenzoate) (25b)**



The compound **25b** was obtained as a white solid (616 mg, 89%);  $R_f$  0.47 (5:95 MeOH: DCM); mp 202-204 °C; IR (cast film) 3287, 3087, 3063, 3032, 2975, 2934, 2887, 1625, 1579, 1537, 1498, 1453, 1424, 1387, 1369, 1330, 1311, 1279, 1253, 1240, 1221, 1131, 1110  $\text{cm}^{-1}$ ;  $^1\text{H}$  NMR (500 MHz,  $\text{DMSO-d}_6$ )  $\delta$  8.47 (br m, 2H), 7.46-7.24 (m, 34H), 5.14 (s, 8H), 4.97 (s, 4H), 3.34-3.30 (br m, 4H), 1.80 (br m, 2H);  $^{13}\text{C}$  NMR (125 MHz,  $\text{DMSO-d}_6$ )  $\delta$  165.4, 151.9, 139.4, 137.4, 136.8, 129.7, 128.4, 128.1, 128.0, 127.9, 127.8, 127.6, 106.3, 74.2, 70.3, 37.2, 29.3; HRMS (ESI) calcd for  $\text{C}_{59}\text{H}_{54}\text{N}_2\text{NaO}_8$   $[\text{M}+\text{Na}]^+$  941.3772; found 941.3772.

### *N,N'*-(Butane-1,4-diyl)bis(3,4,5-tribenzyloxybenzoate) (**25c**)

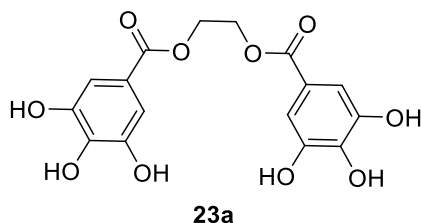


The compound **25c** was obtained as a gray solid (52 mg, 80%);  $R_f$  0.40 (5:95 MeOH: DCM); mp 233-235 °C; IR (cast film) 3242, 3091, 3064, 3037, 2930, 2892, 2858, 1630, 1582, 2556, 1501, 1454, 1434, 1423, 1381, 1337, 1248, 1195, 1176  $\text{cm}^{-1}$ ;  $^1\text{H}$  NMR (500 MHz, DMSO- $d_6$ )  $\delta$  8.42 (br m, 2H), 7.46-7.24 (m, 34H), 5.14 (s, 8H), 4.97 (s, 4H), 3.30 (br m, 4H), 1.57 (br m, 4H);  $^{13}\text{C}$  NMR (125 MHz, DMSO- $d_6$ )  $\delta$  165.3, 151.9, 139.4, 137.4, 136.8, 129.8, 128.4, 128.1, 128.0, 127.8, 127.7, 127.6, 106.3, 74.2, 70.3, 39.0, 26.8; HRMS (ESI) calcd for  $\text{C}_{60}\text{H}_{56}\text{N}_2\text{NaO}_8$   $[\text{M}+\text{Na}]^+$  955.3929; found 955.3928.

#### 4.8.5 General Procedure for Deprotection of Benzyl Group

To a stirred solution of benzyl protected polyphenolic compounds **22a-g**, **22i-k** or **25a-c** (1.00 equiv.) in THF (0.04 M) was added Pd/C (10 wt%, 3.00 equiv.). The reaction mixture was stirred under atmospheric pressure of  $\text{H}_2$  gas overnight. After reaction completion, the mixture was filtered over Celite and the Celite was washed with DCM. The filtrate was concentrated and the product **23** was purified according to the procedures that will be mentioned in each case.

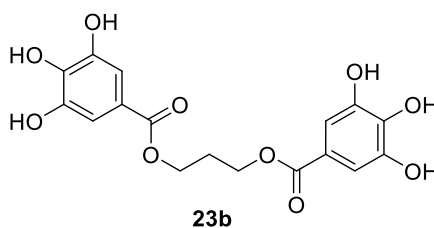
### Ethane-1,2-diyl bis(3,4,5-trihydroxybenzoate) (**23a**)



The compound **23a** was recrystallized from EtOH/water as a white solid (55 mg, 90%); mp 285-287 °C; IR (cast film) 3458, 3380, 3351, 3247, 2970, 1689, 1679, 1617, 1601, 1533, 1439, 1388, 1335, 1293, 1259, 1214, 1194, 1172, 1105, 1092, 1046, 1024  $\text{cm}^{-1}$ ;  $^1\text{H}$  NMR (500 MHz,

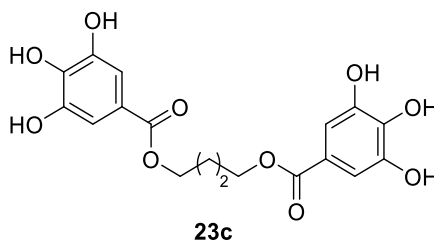
DMSO-d<sub>6</sub>)  $\delta$  6.98 (s, 4H), 4.41 (s, 4H), (peaks corresponding to OH's were not observed); <sup>13</sup>C NMR (125 MHz, DMSO-d<sub>6</sub>)  $\delta$  165.7, 145.5, 138.8, 118.8, 108.5, 62.4; HRMS (ESI) calcd for C<sub>16</sub>H<sub>14</sub>NaO<sub>10</sub> [M+Na]<sup>+</sup> 389.0479; found 389.0476.

### Propane-1,3-diyl bis(3,4,5-trihydroxybenzoate) (**23b**)



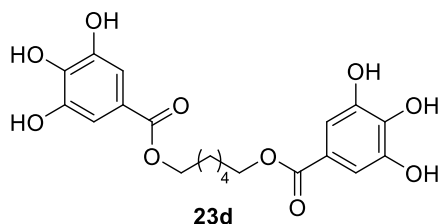
The compound **23b** was recrystallized from water as a white solid (50 mg, 84%); mp 270-274 °C; IR (cast film) 3461, 3311, 3104, 2960, 2924, 2869, 1688, 1608, 1538, 1521, 1461, 1447, 1401, 1356, 1312, 1230, 1194 cm<sup>-1</sup>; <sup>1</sup>H NMR (500 MHz, DMSO-d<sub>6</sub>)  $\delta$  8.80-9.32 (br, 6H) 6.95 (s, 4H), 4.28 (t, *J* = 6.2 Hz, 4H), 2.08 (p, *J* = 6.2 Hz, 2H); <sup>13</sup>C NMR (125 MHz, DMSO-d<sub>6</sub>)  $\delta$  166.2, 146.0, 139.0, 119.7, 108.9, 61.2, 28.3; HRMS (ESI) calcd for C<sub>17</sub>H<sub>16</sub>NaO<sub>10</sub> [M+Na]<sup>+</sup> 403.0636; found 403.0633.

### Butane-1,4-diyl bis(3,4,5-trihydroxybenzoate) (**23c**)



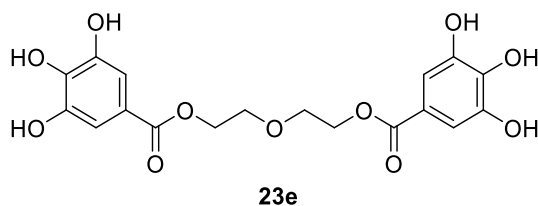
The compound **23c** was recrystallized from water as a white solid (44 mg, 90%); mp 247-249 °C; IR (cast film) 3568, 3445, 3317, 3220, 2981, 2937, 1678, 1609, 1539, 1478, 1449, 1392, 1333, 1239, 1210, 1104 cm<sup>-1</sup>; <sup>1</sup>H NMR (500 MHz, DMSO-d<sub>6</sub>)  $\delta$  9.32-8.65 (br s, 6H), 6.94 (s, 4H), 4.20-4.22 (br m, 4H), 1.76-1.78 (br m, 4H), (peaks corresponding to OH's were not observed); <sup>13</sup>C NMR (125 MHz, DMSO-d<sub>6</sub>)  $\delta$  166.3, 146.0, 138.9, 119.9, 108.9, 64.1, 25.6; HRMS (ESI) calcd for C<sub>18</sub>H<sub>18</sub>NaO<sub>10</sub> [M+Na]<sup>+</sup> 417.0792; found 417.0790.

### Hexane-1,6-diyl bis(3,4,5-trihydroxybenzoate) (**23d**)



The compound **23d** was recrystallized from water as a white solid (60 mg, quant.); mp 204-206 °C; IR (cast film) 3394, 3295, 2958, 2937, 2898, 1681, 1612, 1535, 1518, 1401, 1318, 1254, 1201, 1030  $\text{cm}^{-1}$ ;  $^1\text{H}$  NMR (500 MHz, DMSO- $d_6$ )  $\delta$  9.39-8.95 (br, 6H), 6.93 (s, 4H), 4.15 (t,  $J = 6.6$  Hz, 4H), 1.68-1.66 (br m, 4H), 1.43-1.41 (br m, 4H);  $^{13}\text{C}$  NMR (125 MHz, DMSO- $d_6$ )  $\delta$  165.8, 145.5, 138.3, 119.5, 108.4, 63.9, 28.2, 25.2; HRMS (ESI) calcd for  $\text{C}_{20}\text{H}_{22}\text{NaO}_{10}$   $[\text{M}+\text{Na}]^+$  445.1105; found 445.1103.

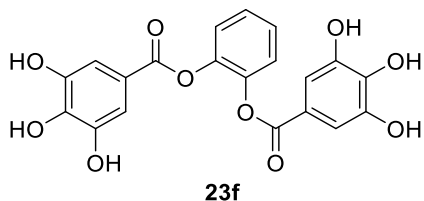
### Oxydi(ethane-2,1-diyl) bis(3,4,5-trihydroxybenzoate) (**23e**)



The compound **23e** was isolated as a grey solid after washing the crude product with hexane (74.4 mg, 55%); mp 82-85 °C; IR (cast film) 3490, 3431, 3375, 3236, 2994, 2973, 2947, 1708, 1683, 1628, 1611, 1551, 1447, 1375, 1317, 1245, 1138  $\text{cm}^{-1}$ ;  $^1\text{H}$  NMR (400 MHz, DMSO- $d_6$ )  $\delta$  9.41-8.95 (br, 6H), 6.95 (s, 4H), 4.29 (t,  $J = 5.0$  Hz, 4H), 3.75 (t,  $J = 5.0$  Hz, 4H);  $^{13}\text{C}$  NMR (125 MHz, DMSO- $d_6$ )  $\delta$  165.7, 145.5, 138.5, 119.2, 108.5, 68.5, 63.4; HRMS (ESI) calcd for  $\text{C}_{18}\text{H}_{18}\text{NaO}_{11}$   $[\text{M}+\text{Na}]^+$  433.0741; found 433.0741.

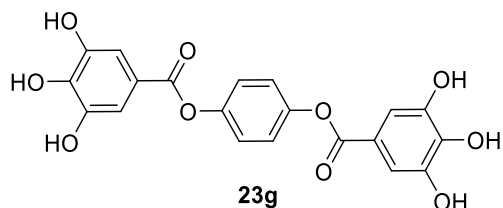


### 1,2-Phenylene bis(3,4,5-trihydroxybenzoate) (**23f**)



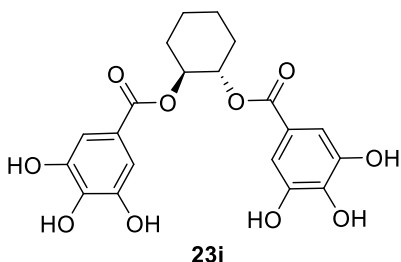
Flash chromatography (3:97 MeOH: DCM) gave compound **23f** as a light gray solid (60 mg, 54%);  $R_f$  0.41 (3:97 MeOH: DCM); mp 258-260 °C; IR (cast film) 3542, 3419, 1720, 1620, 1538, 1498, 1450, 1380, 1328, 1252, 1201, 1172, 1076  $\text{cm}^{-1}$ ;  $^1\text{H}$  NMR (500 MHz, DMSO- $d_6$ )  $\delta$  9.56-8.81 (br, 6H), 7.34, (s, 4H), 6.97 (s, 4H);  $^{13}\text{C}$  NMR (125 MHz, DMSO- $d_6$ )  $\delta$  163.7, 145.6, 142.7, 139.3, 126.5, 123.8, 117.5, 109.0; HRMS (ESI) calcd for  $\text{C}_{20}\text{H}_{14}\text{NaO}_{10}$   $[\text{M}+\text{Na}]^+$  437.0479; found 437.0587.

### 1,4-Phenylene bis(3,4,5-trihydroxybenzoate) (**23g**)



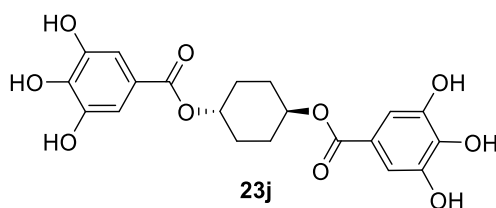
The compound **23g** was isolated as a white solid after washing the crude product with DCM and hexane (139 mg, 78%); mp 270-272 °C; IR (cast film) 3414, 1716, 1615, 1537, 1504, 1419, 1379, 1349, 1214, 1170  $\text{cm}^{-1}$ ;  $^1\text{H}$  NMR (500 MHz, DMSO- $d_6$ )  $\delta$  9.59-9.22 (br, 6H), 7.26 (s, 4H), 7.10 (s, 4H);  $^{13}\text{C}$  NMR (125 MHz, DMSO- $d_6$ )  $\delta$  165.1, 148.6, 146.2, 139.8, 123.4, 118.5, 109.6; HRMS (ESI) calcd for  $\text{C}_{20}\text{H}_{14}\text{NaO}_{10}$   $[\text{M}+\text{Na}]^+$  437.0479; found 437.0483.

### Cyclohexane-1,2-diyl bis(3,4,5-trihydroxybenzoate) (**23i**)



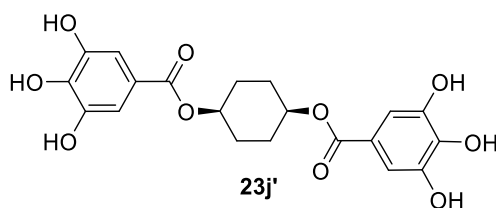
The compound **23i** was isolated as a white solid after washing the crude product with DCM (95 mg, 85%); mp 175-180 °C; IR (cast film) 3359, 2942, 2865, 1685, 1610, 1533, 1447, 1324, 1223, 1096, 1026 cm<sup>-1</sup>; <sup>1</sup>H NMR (500 MHz, acetone-d<sub>6</sub>) δ 8.35-7.99 (br, 6H), 7.16 (s, 4H), 5.18-5.16 (m, 2H), 2.23-2.22 (m, 2H), 1.91-1.83 (m, 2H), 1.69-1.59 (m, 4H); <sup>13</sup>C NMR (125 MHz, acetone-d<sub>6</sub>) δ 166.1, 145.9, 138.7, 121.9, 109.9, 74.2, 30.78, 24.0; HRMS (ESI) calcd for C<sub>20</sub>H<sub>19</sub>O<sub>10</sub> [M-H]<sup>-</sup> 519.0984; found 419.0978.

***trans*-Cyclohexane-1,4-diyl bis(3,4,5-trihydroxybenzoate) (23j)**



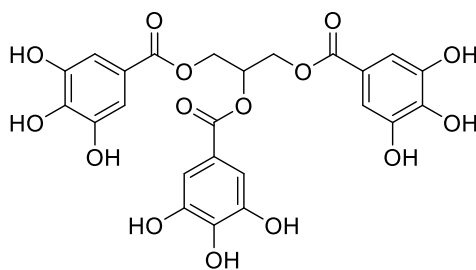
The compound **23j** was isolated as a white solid after washing the crude product with DCM (35 mg, quant.); mp 300 °C (dec.); IR (cast film) 3407, 2956, 2857, 2701, 1674, 1610, 1541, 1440, 1365, 1309, 1252, 1150, 1104 cm<sup>-1</sup>; <sup>1</sup>H NMR (500 MHz, acetone-d<sub>6</sub>) δ 8.39- 7.80 (br, 6H), 7.24 (s, 4H), 5.13 (br s, 2H), 2.37-2.15 (m, 4H), 2.13-1.84 (m, 4H); <sup>13</sup>C NMR (125 MHz, acetone-d<sub>6</sub>) δ 166.1, 146.0, 138.7, 122.4, 109.8, 71.4, 28.4; HRMS (ESI) calcd for C<sub>20</sub>H<sub>19</sub>O<sub>10</sub> [M-H]<sup>-</sup> 419.0984; found 419.0981.

***cis*-Cyclohexane-1,4-diyl bis(3,4,5-trihydroxybenzoate) (23j')**



The compound **23j'** was isolated as a white solid after washing the crude product with hot hexane (55 mg, quant.); mp 148-150 °C; IR (cast film) 3366, 2950, 2872, 2492, 1677, 1609, 1533, 1446, 1315, 1208, 1120 cm<sup>-1</sup>; <sup>1</sup>H NMR (500 MHz, acetone-d<sub>6</sub>) δ 8.23 (br s, 6H), 7.27 (s, 4H), 5.14 (br s, 2H), 2.08-1.98 (m, 8H); <sup>13</sup>C NMR (125 MHz, acetone-d<sub>6</sub>) δ 166.0, 146.1, 138.7, 129.8, 122.4, 109.9, 70.8, 29.4; HRMS (ESI) calcd for C<sub>20</sub>H<sub>19</sub>O<sub>10</sub> [M-H]<sup>-</sup> 419.0984; found 419.0983.

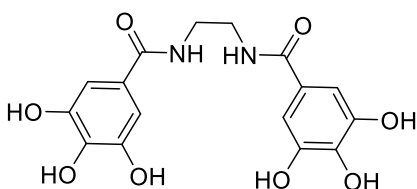
**Propane-1,2,3-triyl (3,4,5-trihydroxybenzoate) (23k)**



**23k**

To the concentrated reaction mixture, DCM was added. The precipitated solid was filtered and washed with DCM. Compound **23k** was dried under the vacuum and collected as a white solid (14.3 mg, 24%); mp 156-160 °C; IR (cast film) 3378, 2837, 1696, 1613, 1536, 1450, 1322, 1212, 1098  $\text{cm}^{-1}$ ;  $^1\text{H}$  NMR (500 MHz, DMSO- $d_6$ )  $\delta$  9.19-8.97 (br s, 9H), 6.93 (s, 6H), 5.53 (tt,  $J = 6.0, 4.0$  Hz, 1H), 4.53 (dd,  $J = 12.0, 4.0$  Hz, 2H), 4.46 (dd,  $J = 12.0, 6.0$  Hz, 2H);  $^{13}\text{C}$  NMR (125 MHz, DMSO- $d_6$ )  $\delta$  165.4, 165.1, 145.6, 125.5, 138.8, 138.7, 118.4, 118.7, 108.7, 108.6, 69.5, 62.5; HRMS (ESI) calcd for  $\text{C}_{24}\text{H}_{20}\text{NaO}_{15}$   $[\text{M}+\text{Na}]^+$  571.0694; found 571.0690.

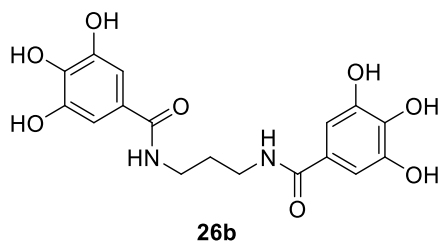
***N,N'*-(Ethane-1,2-diyl)bis(3,4,5-trihydroxybenzamide) (26a)**



**26a**

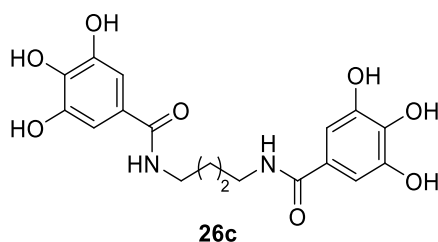
The compound **26a** was recrystallized from water as a gray solid (12 mg, 19%); mp 289-290 °C; IR (cast film) 3524, 3329, 2691, 1584, 1547, 1447, 1361, 1319, 1278, 1229, 1180  $\text{cm}^{-1}$ ;  $^1\text{H}$  NMR (400 MHz,  $\text{CD}_3\text{OD}$ )  $\delta$  6.84 (br s, 4H), 3.51 (s, 4H), (peaks corresponding to OH's and NH's were not observed);  $^{13}\text{C}$  NMR (125 MHz, DMSO- $d_6$ )  $\delta$  166.6, 145.4, 136.2, 124.7, 106.6, 40.1; HRMS (ESI) calcd for  $\text{C}_{16}\text{H}_{16}\text{N}_2\text{NaO}_8$   $[\text{M}+\text{Na}]^+$  389.0799; found 387.0799.

### *N,N'*-(Propane-1,3-diyl)bis(3,4,5-trihydroxybenzamide) (**26b**)



The compound **26b** was recrystallized from water as a white solid (53.3 mg, 88%); mp 119-121 °C; IR (cast film) 3334, 2715, 1700, 1591, 1523, 1442, 1325, 1203, 1123, 1035  $\text{cm}^{-1}$ ;  $^1\text{H}$  NMR (400 MHz, DMSO- $d_6$ )  $\delta$  8.99 (s, 4H), 8.60 (s, 2H), 8.06 (t,  $J = 6.4$  Hz, 2H), 6.81 (s, 4H), 3.21-3.19 (m, 4H), 1.64-1.63 (m, 2H);  $^{13}\text{C}$  NMR (125 MHz, DMSO- $d_6$ )  $\delta$  166.3, 145.3, 136.0, 124.9, 106.6, 36.6, 29.4; HRMS (ESI) calcd for  $\text{C}_{17}\text{H}_{18}\text{N}_2\text{NaO}_8$   $[\text{M}+\text{Na}]^+$  401.0955; found 401.0952.

### *N,N'*-(Butane-1,2-diyl)bis(3,4,5-trihydroxybenzamide) (**26c**)



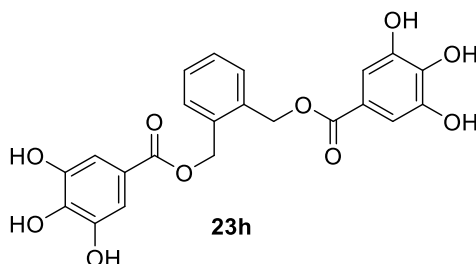
The compound **26c** was recrystallized from water as a gray solid (52.6 mg, 84%); mp 233-235 °C; IR (cast film) 3349, 2947, 2707, 1701, 1588, 1523, 1442, 1329, 1230, 1196  $\text{cm}^{-1}$ ;  $^1\text{H}$  NMR (500 MHz, DMSO- $d_6$ )  $\delta$  8.97 (s, 4H), 8.59 (s, 2H), 8.03 (t,  $J = 6.4$  Hz, 2H), 6.79 (s, 4H), 3.16-3.15 (m, 4H), 1.47-1.45 (m, 4H);  $^{13}\text{C}$  NMR (125 MHz, DMSO- $d_6$ )  $\delta$  166.2, 145.3, 135.9, 125.1, 106.6, 38.8, 26.8; HRMS (ESI) calcd for  $\text{C}_{18}\text{H}_{20}\text{N}_2\text{NaO}_8$   $[\text{M}+\text{Na}]^+$  415.1112; found 415.1104.

#### 4.8.6 General Procedure for Deprotection of MOM Group

To a stirred solution of MOM protected gallates **22h**, **22l**, **22m** (1.00 equiv.) in MeOH (0.06 M), catalytic HCl (1.00 M, 2 drops) was added and the reaction mixture was stirred at reflux overnight. The reaction was quenched by the addition of saturated  $\text{NaHCO}_3$  (0.17 M) and the

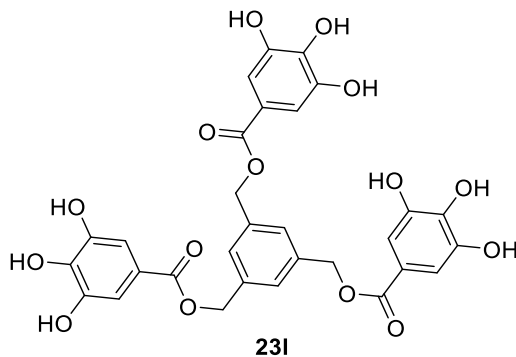
organic layer was extracted by Et<sub>2</sub>O. The aqueous layer was washed with Et<sub>2</sub>O and the combined organic solution was dried over MgSO<sub>4</sub>, filtered and concentrated under reduced pressure. Obtained solid was then purified with specified method in each case.

**(1,2-Phenylene)bis(methylene) bis(3,4,5-trihydroxybenzoate) (23h)**



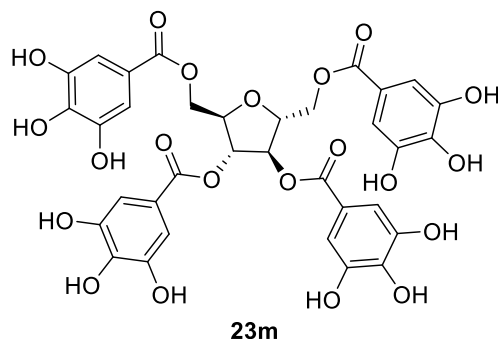
The compound **23h** was recrystallized from acidified water (pH=2) as a white solid (16.5 mg, 11%); mp 229-231 °C; IR (cast film) 3346, 1691, 1612, 1534, 1452, 1383, 1349, 1208, 1040 cm<sup>-1</sup>; <sup>1</sup>H NMR (500 MHz, DMSO-d<sub>6</sub>) δ 7.50-7.48 (m, 2H), 7.40-7.38 (m, 2H), 6.97 (s, 4H), 5.36 (s, 4H), (peaks corresponding to OH's were not observed); <sup>13</sup>C NMR (125 MHz, acetone-d<sub>6</sub>) δ 165.5, 145.6, 138.7, 134.7, 128.8, 128.4, 118.9, 108.6, 63.2; HRMS (ESI) calcd for C<sub>22</sub>H<sub>18</sub>NaO<sub>10</sub> [M+Na]<sup>+</sup> 465.0792; found 465.0792.

**Benzene-1,2,3-triyl (3,4,5-trihydroxybenzoate) (23l)**



The compound **23l** was recrystallized from acidified water (pH=2) as a white solid (32.6 mg, 13%); mp decomp. at 186-190 °C (dec.); IR (cast film) 3363, 1703, 1609, 1533, 1446, 1340, 1214, 1039 cm<sup>-1</sup>; <sup>1</sup>H NMR (400 MHz, acetone-d<sub>6</sub>) δ 7.55 (s, 3H), 7.15 (s, 6H), 5.32 (s, 6H); <sup>13</sup>C NMR (125 MHz, acetone-d<sub>6</sub>) δ 166.5, 146.1, 138.9, 138.5, 128.4, 121.5, 109.9, 66.4; HRMS (ESI) calcd for C<sub>30</sub>H<sub>24</sub>NaO<sub>15</sub> [M+Na]<sup>+</sup> 647.1007; found 647.1006.

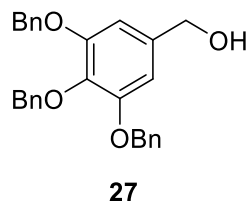
**[(2*R*,3*R*,4*R*,5*R*)-3,4-bis(3,4,5-Trihydroxybenzoate)oxolane-2,5-diyl]bis(3,4,5-trihydroxybenzoate) (23m)**



To the concentrated reaction mixture, DCM was added. The precipitated solid was filtered and washed with DCM. Compound **23m** was dried under vacuum and collected as a light pink solid (60 mg, quant.); mp 75-78 °C; IR (cast film) 3380, 1697, 1613, 1535, 1450, 1317, 1213, 1031  $\text{cm}^{-1}$ ;  $^1\text{H}$  NMR (500 MHz, DMSO- $d_6$ )  $\delta$  8.92 (br s, 12H), 6.98 (s, 8H), 5.46 (s, 2H), 4.49-4.38 (m, 6H);  $^{13}\text{C}$  NMR (125 MHz, DMSO- $d_6$ )  $\delta$  166.6, 164.9, 145.6, 145.5, 139.1, 138.6, 118.8, 118.1, 108.9, 108.7, 80.3, 77.3, 63.3; HRMS (ESI) calcd for  $\text{C}_{34}\text{H}_{28}\text{NaO}_{21}$   $[\text{M}+\text{Na}]^+$  795.1015; found 795.101.

**4.8.7 Procedure for the Formation of Ketone 32**

**(3,4,5-Tribenzyloxyphenyl)methanol (27)**

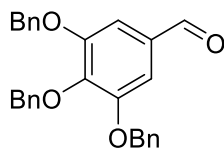


In an oven dried round bottom flask  $\text{LiAlH}_4$  (1.07 g, 28.2 mmol) was suspended in dry THF (19 mL, 1.5 M). The suspension was cooled down to 0 °C followed by the dropwise addition of the solution of benzyl protected ester **19a** (6.00 g, 12.8 mmol) in dry THF (5 mL). The reaction mixture was stirred at 0 °C for 30 min then the ice bath was removed and the reaction mixture was stirred at room temperature overnight. The reaction mixture was cooled down again to 0 °C after completion and was quenched with a very slow addition of saturated  $\text{NH}_4\text{Cl}$  (5 mL) to avoid severe gas evolution. The reaction mixture was filtered over Celite to separate

the insoluble white precipitate and the filtrate was retained. The aqueous layer was extracted with Et<sub>2</sub>O (3×5 mL). The organic layers were combined and dried over MgSO<sub>4</sub>, filtered and concentrated under reduced pressure. No further purification was required and the alcohol **27** was obtained as white solid (3.60 g, 66%).

**27**: R<sub>f</sub> 0.47 (40:60 EtOAc:hexane); mp 95-98 °C; IR (cast film) 3321, 3087, 3031, 3004, 2914, 2863, 1597, 1496, 1455, 1441, 1391, 1373, 1335, 1226, 1151, 1042 cm<sup>-1</sup>; <sup>1</sup>H NMR (500 MHz, CDCl<sub>3</sub>) δ 7.47-7.28 (m, 15H), 6.70 (s, 2H), 5.13 (s, 4H), 5.09 (s, 2H), 4.59 (s, 2H); <sup>13</sup>C NMR (125 MHz, CDCl<sub>3</sub>) δ 153.0, 137.9, 137.8, 137.1, 139.7, 128.6, 128.5, 128.2, 127.9, 127.8, 127.4, 106.4, 75.3, 71.2, 65.4; HRMS (ESI) calcd for C<sub>28</sub>H<sub>26</sub>NaO<sub>4</sub> [M+Na]<sup>+</sup> 449.1723; found 449.1720.

### 3,4,5-Tribenzyloxybenzaldehyde (**28**)

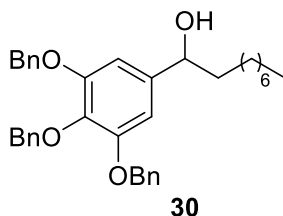


**28**

In an oven dried flask the alcohol **27** (630 mg, 1.48 mmol) was dissolved in dry DCM (6 mL, 0.25 M). MnO<sub>2</sub> powder (4.60 g, 8.86 mmol) was then added to the reaction mixture. The reaction was stirred at room temperature overnight. After reaction completion, it was filtered over Celite and the Celite was washed with DCM (3×5 mL). The filtrate was concentrated under reduced pressure and the aldehyde **28** was obtained as a white solid (625 mg, quant.).

**28**: R<sub>f</sub> 0.20 (10:90 EtOAc:hexane); mp 263-265 °C; IR (cast film) 3089, 3064, 3029, 2856, 1691, 1591, 1500, 1452, 1436, 1386, 1328, 1237, 1143, 1119, 1034 cm<sup>-1</sup>; <sup>1</sup>H NMR (500 MHz, CDCl<sub>3</sub>) δ 9.83 (s, 1H), 7.47-7.22 (m, 15H), 7.22 (s, 2H), 5.19 (s, 6H); <sup>13</sup>C NMR (125 MHz, CDCl<sub>3</sub>) δ 190.9, 153.2, 143.8, 137.3, 136.4, 131.8, 128.6, 128.5, 128.2, 128.1, 128.0, 127.5, 108.9, 75.2, 71.3; HRMS (ESI) calcd for C<sub>28</sub>H<sub>24</sub>NaO<sub>4</sub> [M+Na]<sup>+</sup> 447.1567; found 447.1563.

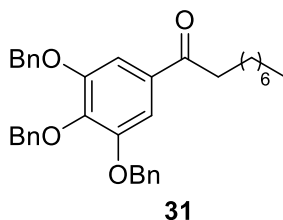
### 1-(3,4,5-Tribenzyloxyphenyl)octane-1-ol (**30**)



A flamed dry round bottom flask was charged with magnesium turnings (500 mg, 20.7 mmol) and dry Et<sub>2</sub>O (12 mL, 1.80 mmol). A solution of 1-bromooctane (500 mg, 2.59 mmol) in dry Et<sub>2</sub>O (5 mL, 0.45 M) was added via syringe pump and over 2 h at room temperature. After the addition was complete, the Grignard solution (4.60 mL, 0.70 mmol) was transferred to the solution of aldehyde **28** (200 mg, 0.47 mmol) in Et<sub>2</sub>O (5 mL, 0.1 M) at room temperature and via the syringe pump over 2 h. The reaction completion was monitored by TLC and the reaction mixture was quenched by saturated aqueous solution of NH<sub>4</sub>Cl (5 mL). The ethereal layer was separated and the aqueous layer was washed with Et<sub>2</sub>O (3×5 mL). The combined organic layers were dried over MgSO<sub>4</sub>, filtered and concentrated under reduced pressure. The alcohol **30** was purified by column chromatography using (30:70 EtOAc: hexane) to provide a white solid (120 mg, 47%).

**30**: R<sub>f</sub> 0.47 (30:70 EtOAc:hexane); mp 57-61 °C; IR (cast film) 3381, 3089, 3064, 3032, 2926, 2855, 1592, 1499, 1454, 1435, 1373, 1326, 1232, 1116 cm<sup>-1</sup>; <sup>1</sup>H NMR (500 MHz, CDCl<sub>3</sub>) δ 7.46-7.28 (m, 15H), 6.67 (s, 2H), 5.14 (s, 4H), 5.07 (s, 2H), 4.56 (t, *J* = 7.9, 1H), 1.77-1.61 (m, 2H), 1.37-1.21 (m, 12H), 0.90 (t, *J* = 7.0, 3H); <sup>13</sup>C NMR (125 MHz, CDCl<sub>3</sub>) δ 152.8, 140.6, 137.9, 137.8, 137.2, 128.5, 128.4, 128.1, 127.8, 127.7, 127.5, 105.7, 75.2, 74.7, 71.3, 39.1, 31.9, 29.6, 29.5, 29.3, 25.8, 22.7, 14.1; HRMS (ESI) calcd for C<sub>36</sub>H<sub>42</sub>NaO<sub>4</sub> [M+Na]<sup>+</sup> 561.2975; found 561.2969.

### 1-(3,4,5-Tribenzyloxyphenyl)octane-1-one (**31**)

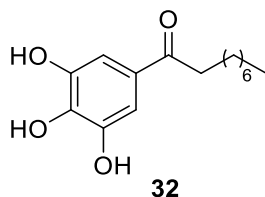




The alcohol **30** (120 mg, 0.22 mmol) was dissolved in dry DCM (5 mL, 0.04 M). MnO<sub>2</sub> powder (390 mg, 4.50 mmol) was then added to the reaction mixture. The reaction stirred at room temperature overnight. After reaction completion, it was filtered over Celite and the Celite was washed with DCM (2×5 mL). The filtrate was concentrated under reduced pressure and the ketone **31** was obtained as a white solid (117 mg, quant.).

**31**: R<sub>f</sub> 0.50 (10:90 EtOAc:hexane); mp 72-75 °C; IR (cast film) 3089, 3063, 2923, 2853, 1678, 1586, 1502, 1454, 1423, 1385, 1365, 1335, 1234, 1162, 1124 cm<sup>-1</sup>; <sup>1</sup>H NMR (500 MHz, CDCl<sub>3</sub>) δ 7.48-7.28 (m, 17H), 5.19 (s, 4H), 5.18 (s, 2H), 2.85 (t, *J* = 7.3 Hz, 2H), 1.71-1.68 (m, 2H), 1.39-1.33 (m, 10H), 0.95-0.92 (m, 3H); <sup>13</sup>C NMR (125 MHz, CDCl<sub>3</sub>) δ 199.3, 152.6, 142.8, 137.4, 136.7, 132.4, 128.6, 128.5, 128.2, 128.1, 128.0, 127.5, 108.2, 75.2, 71.5, 38.4, 31.9, 29.5, 29.4, 29.2, 24.6, 22.7, 14.1; HRMS (ESI) calcd for C<sub>36</sub>H<sub>40</sub>NaO<sub>4</sub> [M+Na]<sup>+</sup> 559.2819; found 559.2821.

### 1-(3,4,5-Trihydroxyphenyl)octane-1-one (**31**)

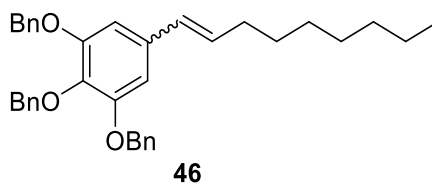


To a stirred solution of ketone **31** (117 mg, 0.22 mmol) in THF (5.50 mL, 0.04 M) was added Pd/C (10 wt%, 70 mg). The reaction mixture was stirred under H<sub>2</sub> gas overnight. After the reaction completion, the mixture was filtered over Celite and the Celite was washed with DCM (2×5 mL). The filtrate was concentrated. The product was purified with column chromatography (1:9 MeOH: DCM) to give a brown solid (15 mg, 34%).

**32**: R<sub>f</sub> 0.25 (10:90 EtOAc:hexane); mp 69-72 °C; IR (cast film) 3343, 2956, 2924, 2853, 1657, 1603, 1535, 1455, 1348, 1198, 1162, 1026 cm<sup>-1</sup>; <sup>1</sup>H NMR (500 MHz, acetone-d<sub>6</sub>) δ 8.25-7.98 (br s, 3H), 7.21 (m, 2H), 2.95 (t, *J* = 7.3 Hz, 2H), 1.74 (t, *J* = 7.3 Hz, 2H), 1.45-1.38 (m, 10H), 0.98 (t, *J* = 7.3 Hz, 3H); <sup>13</sup>C NMR (125 MHz, acetone-d<sub>6</sub>) δ 198.7, 146.1, 138.7, 129.8, 108.6, 38.5, 32.6, 30.3, 30.1, 30.0, 25.5, 23.3, 14.4; HRMS (ESI) calcd for C<sub>15</sub>H<sub>21</sub>O<sub>4</sub> [M-H]<sup>-</sup> 265.1445; found 265.1442.

#### 4.8.8 Procedure for the Formation of Compound 47

##### 5-(Nonane-1-en-1-yl)-1,2,3-trihydroxybenzene (46)



Phosphonium salt **45** was prepared according to the literature procedure.<sup>227</sup>

A round bottom flask was charged with the phosphonium salt **45** (103 mg, 0.27 mmol) and dry THF (3.60 mL, 0.70 M). The reaction was cooled down to 0 °C and a solution of *n*-BuLi in hexane (2.50 M, 0.20 mL, 0.27 mmol) was added dropwise. Then a solution of aldehyde **28** (106 mg, 0.25 mmol) in dry THF (0.10 M, 2.50 mL) was added slowly. The reaction was kept at 0 °C for an additional 15 min then warmed to room temperature and stirred for 4 h. After reaction completion, it was quenched by the slow addition of a solution of saturated aqueous NH<sub>4</sub>Cl (5 mL). The organic layer was separated and aqueous phase was extracted by EtOAc (3×5 mL). Organic layers were combined, dried over MgSO<sub>4</sub>, filtered and concentrated under reduced pressure. The inseparable mixture of *cis*- and *trans*- alkene **46** (2:1) was purified by column chromatography (10:90 EtOAc: hexane) to furnish a colorless oil (50 mg, 38%).

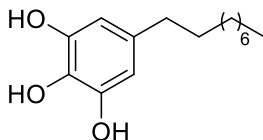
**46** *R<sub>f</sub>* 0.51 (10:90 EtOAc:hexane); IR (cast film) 3064, 3031, 2954, 2925, 2854, 1579, 1502, 1453, 1502, 1427, 1373, 1327, 1115 cm<sup>-1</sup>; HRMS (ESI) calcd for C<sub>36</sub>H<sub>41</sub>O<sub>3</sub> [M+H]<sup>+</sup> 521.3050; found 521.3061.

(*trans*- isomer): <sup>1</sup>H NMR (500 MHz, CDCl<sub>3</sub>) δ 7.47-7.28 (m, 15H), 6.68 (s, 2H), 6.30-6.26 (m, 1H), 6.11 (dt, *J* = 15.8, 6.7 Hz, 1H), 5.13 (s, 4H), 5.01 (s, 2H), 2.25-1.88 (m, 2H), 1.42-1.25 (m, 10H), 0.94-0.88 (m, 3H); <sup>13</sup>C NMR (125 MHz, CDCl<sub>3</sub>) δ 152.9, 137.9, 137.7, 137.3, 133.8, 133.7, 129.4, 128.6, 128.5, 128.1, 127.8, 127.4, 127.3, 108.8, 75.3, 71.3, 32.9, 31.9, 29.4, 29.3, 29.2, 22.7, 14.1;

(*cis*- isomer) observed peaks: <sup>1</sup>H NMR (500 MHz, CDCl<sub>3</sub>) δ 7.47-7.28 (m, 15H), 6.58 (s, 2H), 6.30-6.26 (m, 1H), 2.59 (dt, *J* = 11.5, 7.2 Hz, 1H), 5.13 (s, 4H), 5.10 (s, 2H), 2.25-1.88 (m, 2H), 1.42-1.25 (m, 10H), 0.94-0.88 (m, 3H); <sup>13</sup>C NMR (125 MHz, CDCl<sub>3</sub>) δ 152.4, 133.7,

132.9, 130.8, 128.7, 128.6, 128.5, 128.4, 128.1, 127.8, 127.5, 108.8, 75.3, 71.2, 31.6, 30.9, 30.0, 29.4, 28.6, 22.7, 15.3

**5-Nonyl-1,2,3-trihydroxybenzene (47)**



**47**

Benzyl deprotection was performed according to the procedure provided for ketone **32**. Product **47** was obtained without further purification as a white powder (28.1 mg, quant.).

**47**: mp 69-72 °C; IR (cast film) 3350, 2956, 2923, 2914, 2851, 1616, 1535, 1469, 1384, 1371, 1304, 1224, 1199, 1181, 1055, 1024  $\text{cm}^{-1}$ ;  $^1\text{H}$  NMR (500 MHz,  $\text{CDCl}_3$ )  $\delta$  6.58 (s, 2H), 5.00 (br, 3H), 2.47-2.45 (t,  $J = 7.2$  Hz, 2H), 1.54-1.57 (m, 2H), 1.30-1.27 (m, 12H), 0.91-0.89 (m, 3H);  $^{13}\text{C}$  NMR (125 MHz,  $\text{CDCl}_3$ )  $\delta$  143.6, 135.6, 129.4, 108.1, 35.5, 31.9, 31.4, 29.6, 29.5, 29.3, 29.2, 22.7, 14.1; HRMS (ESI) calcd for  $\text{C}_{15}\text{H}_{23}\text{O}_3$   $[\text{M}-\text{H}]^-$  251.1653; found 251.1653.

## References

- (1) Aitken, R. A. *Angew. Chemie. Ed.* **2003**, *42*, 971–971.
- (2) Maigali, S. S.; Abd-El-Maksoud, M. A.; Soliman, F. M.; Moharam, M. E. *J. Heterocycl. Chem.* **2015**, *52*, 834–840.
- (3) Padwa, A.; Weingarten, M. D. *Chem. Rev.* **1996**, *96*, 223–270.
- (4) Müller, P. *Acc. Chem. Res.* **2004**, *37*, 243–251.
- (5) Geary, G. C.; Hope, E. G.; Singh, K.; Stuart, A. M. *RSC Adv.* **2015**, *5*, 16501–16506.
- (6) Doyle, M. P.; McKervey, M. A.; Ye, T. *Modern Catalytic Methods for Organic Synthesis with Diazo Compounds*; Wiley-Interscience: New York, **1997**.
- (7) Sweeney, J. B. *Chem. Soc. Rev.* **2009**, *38*, 1027–1038.
- (8) Stevens, T. S. *J. Chem. Soc.* **1930**, 2107–2119.
- (9) Stevens, T. S.; Creighton, E. M.; Gordon, A. B.; MacNicol, M. *J. Chem. Soc.* **1928**, 3193–3197.
- (10) Vedejs, E.; Martinez, G. R. *J. Am. Chem. Soc.* **1979**, *101*, 6452–6454.
- (11) Blackburn, G. M.; Ollis, W. D.; Smith, C.; Sutherland, I. O. *J. Chem. Soc. D Chem. Commun.* **1969**, *3*, 99a.
- (12) Andrews, G.; Evans, D. A. *Tetrahedron Lett.* **1972**, *13*, 5121–5124.
- (13) Ye, T.; McKervey, M. A. *Chem. Rev.* **1994**, *94*, 1091–1160.
- (14) Bamford, W. R.; Stevens, T. S. *J. Chem. Soc.* **1952**, 4735–4740.
- (15) Jones, G. *Organic Reactions*; John Wiley & Sons, Inc.: Hoboken, NJ, USA, **2004**.
- (16) Moser, W. R. *J. Am. Chem. Soc.* **1969**, *91*, 1141–1146.
- (17) Moser, W. R. *J. Am. Chem. Soc.* **1969**, *91*, 1135–1140.
- (18) Paulissen, R.; Reimlinger, H.; Hayez, E.; Hubert, A. J.; Teyssié, P. *Tetrahedron Lett.* **1973**, *14*, 2233–2236.

- (19) Doyle, M. P.; Tamblyn, W. H.; Bagheri, V. *J. Org. Chem.* **1981**, *46*, 5094–5102.
- (20) Davies, H. M. L.; Alford, J. S. *Chem. Soc. Rev.* **2014**, *43*, 5151.
- (21) Horneff, T.; Chuprakov, S.; Chernyak, N.; Gevorgyan, V.; Fokin, V. V. *J. Am. Chem. Soc.* **2008**, *130*, 14972–14974.
- (22) Dimroth, O. *Justus Liebig's Ann. Chemie* **1909**, *364*, 183–226.
- (23) Boyer, A. *Org. Lett.* **2014**, *16*, 1660–1663.
- (24) Murphy, G. K.; Stewart, C.; West, F. G. *Tetrahedron* **2013**, *69*, 2667–2686.
- (25) Vanecko, J. A.; Wan, H.; West, F. G. *Tetrahedron* **2006**, *62*, 1043–1062.
- (26) Olah, G. A.; Doggweiler, H.; Felberg, J. D. *J. Org. Chem.* **1984**, *49*, 2116–2120.
- (27) Olah, G. A.; Doggweiler, H.; Felberg, J. D. *J. Org. Chem.* **1984**, *49*, 2112–2116.
- (28) Olah, G. A.; Doggweiler, H.; Felberg, J. D.; Frohlich, S.; Grdina, M. J.; Karpeles, R.; Keumi, T.; Inaba, S.; Ip, W. M.; Lammertsma, K.; Salem, G.; Tabor, D. *J. Am. Chem. Soc.* **1984**, *106*, 2143–2149.
- (29) Kirmse, W.; Van Chiem, P.; Schurig, V. *Tetrahedron Lett.* **1985**, *26*, 197–200.
- (30) Kirmse, W.; Lelgemann, R.; Friedrich, K. *Chem. Ber.* **1991**, *124*, 1853–1863.
- (31) Doyle, M. P. *Chem. Rev.* **1986**, *86*, 919–939.
- (32) Hodgson, D. M.; Pierard, F. Y. T. M.; Stuppel, P. A. *Chem. Soc. Rev.* **2001**, *30*, 50–61.
- (33) Thomson, T.; Stevens, T. S. *J. Chem. Soc.* **1932**, 69-73.
- (34) Campbell, A.; Houston, A. H. J.; Kenyon, J. J. *Chem. Soc.* **1947**, 93-95.
- (35) Ollis, W. D.; Rey, M.; Sutherland, I. O.; Closs, G. L. *J. Chem. Soc. Chem. Commun.* **1975**, *14*, 543-545.
- (36) Ollis, W. D.; Rey, M.; Sutherland, I. O. *J. Chem. Soc. Perkin Trans. I* **1983**, 1009-1027.
- (37) Iwamura, H.; Imahashi, Y.; Kushida, K. *Tetrahedron Lett.* **1975**, *16*, 1401–1404.

- (38) Iwamura, H.; Imahashi, Y.; Kushida, K.; Aoki, K.; Satoh, S. *Bull. Chem. Soc. Jpn.* **1976**, *49*, 1690–1696.
- (39) Dolling, U. H.; Closs, G. L.; Cohen, A. H.; Ollis, W. D. *J. Chem. Soc. Chem. Commun.* **1975**, *14*, 545-547.
- (40) Eberlein, T. H.; West, F. G.; Tester, R. W. *J. Org. Chem.* **1992**, *57*, 3479–3482.
- (41) West, F. G.; Naidu, B. N. *J. Am. Chem. Soc.* **1993**, *115*, 1177–1178.
- (42) Kantor, S. W.; Hauser, C. R. *J. Am. Chem. Soc.* **1951**, *73*, 4122–4131.
- (43) Wittig, G.; Löhmann, L. *Justus Liebig's Ann. Chemie* **1942**, *550*, 260–268.
- (44) Brewster, J. H.; Kline, M. W. *J. Am. Chem. Soc.* **1952**, *74*, 5179–5182.
- (45) Woodward, R. B.; Hoffmann, R. *Angew. Chemie. Ed. English* **1969**, *8*, 781–853.
- (46) West, F. G.; Naidu, B. N.; Tester, R. W. *J. Org. Chem.* **1994**, *59*, 6892–6894.
- (47) Karche, N. P.; Jachak, S. M.; Dhavale, D. D. *J. Org. Chem.* **2001**, *66*, 6323–6332.
- (48) Roskamp, E. J.; Johnson, C. R. *J. Am. Chem. Soc.* **1986**, *108*, 6062–6063.
- (49) Murphy, G. K.; West, F. G. *Org. Lett.* **2006**, *8*, 4359–4361.
- (50) Xu, M.; Ren, T.-T.; Li, C.-Y. *Org. Lett.* **2012**, *14*, 4902–4905.
- (51) Xu, M.; Ren, T.-T.; Wang, K.-B.; Li, C.-Y. *Adv. Synth. Catal.* **2013**, *355*, 2488–2494.
- (52) West, F. G.; Eberlein, T. H.; Tester, R. W. *J. Chem. Soc. Perkin Trans. 1* **1993**, *23*, 2857-2859.
- (53) Jaber, D. M.; Burgin, R. N.; Hepler, M.; Zavalij, P.; Doyle, M. P. *Chem. Commun.* **2011**, *47*, 7623–7625.
- (54) Jaber, D. M.; Burgin, R. N.; Helper, M.; Zavalij, P. Y.; Doyle, M. P. *Org. Lett.* **2012**, *14*, 1676–1679.
- (55) Murphy, G. K.; West, F. G. *Org. Lett.* **2005**, *7*, 1801–1804.
- (56) Murphy, G. K.; Marmsäter, F. P.; West, F. G. *Can. J. Chem.* **2006**, *84*, 1470–1486.
- (57) Marmsäter, F. P.; Murphy, G. K.; West, F. G. *J. Am. Chem. Soc.* **2003**, *125*, 14724–

- 14725.
- (58) Doyle, M. P.; Ene, D. G.; Forbes, D. C.; Tedrow, J. S. *Tetrahedron Lett.* **1997**, *38*, 4367–4370.
- (59) Brogan, J. B.; Zercher, C. K.; Bauer, C. B.; Rogers, R. D. *J. Org. Chem.* **1997**, *62*, 3902–3909.
- (60) Tester, R. W.; West, F. G. *Tetrahedron Lett.* **1998**, *39*, 4631–4634.
- (61) West, F. G.; Naidu, B. N.; Tester, R. W. *J. Org. Chem.* **1994**, *59*, 6892–6894.
- (62) Clark, J. S.; Krowiak, S. A.; Street, L. J. *Tetrahedron Lett.* **1993**, *34*, 4385–4388.
- (63) Marmsäter, F. P.; Vanecko, J. A.; West, F. G. *Org. Lett.* **2004**, *6*, 1657–1660.
- (64) Brogan, J. B.; Zercher, C. K. *Tetrahedron Lett.* **1998**, *39*, 1691–1694.
- (65) Pirrung, M. C.; Werner, J. A. *J. Am. Chem. Soc.* **1986**, *108*, 6060–6062.
- (66) Clark, J. S. *Tetrahedron Lett.* **1992**, *33*, 6193–6196.
- (67) Stephen Clark, J.; Whitlock, G.; Jiang, S.; Onyia, N. *Chem. Commun.* **2003**, *20*, 2578.
- (68) Marmsäter, F. P.; West, F. G. *J. Am. Chem. Soc.* **2001**, *123*, 5144–5145.
- (69) Clark, J. S.; Hansen, K. E. *Chemistry* **2014**, *20*, 5454–5459.
- (70) Pirrung, M. C.; Brown, W. L.; Rege, S.; Laughton, P. *J. Am. Chem. Soc.* **1991**, *113*, 8561–8562.
- (71) Fleming, I. *Molecular Orbitals and Organic Chemical Reactions*, Student Edition; Wiley Online Library; **2009**.
- (72) Desai, V. N.; Saha, N. N.; Dhavale, D. D. *J. Chem. Soc. Perkin Trans. 1* **2000**, *2*, 147–151.
- (73) Anslyn, E. V.; Dougherty, D. A. *Modern Physical Organic Chemistry*; University Science Books, **2006**.
- (74) Wiberg, K. B. *Angew. Chemie. Ed. English* **1986**, *25*, 312–322.
- (75) Fischer, E.; Jourdan, F. *Chem. Ber.* **1883**, *16*, 6–7.

- (76) Bauzá, A.; Quiñonero, D.; Deyà, P. M.; Frontera, A. *Chem. Phys. Lett.* **2012**, *536*, 165–169.
- (77) Ferguson, L. N. *J. Chem. Educ.* **1970**, *47*, 46-53.
- (78) Perkin, W. H. *Berichte der Dtsch. Chem. Gesellschaft* **1884**, *17*, 323–325.
- (79) de Meijere, A. *Angew. Chemie. Ed. English* **1979**, *18*, 809–826.
- (80) WALSH, A. D. *Nature* **1947**, *159*, 165–165.
- (81) Nemoto, H.; Fukumoto, K. *Synlett* **1997**, *1997*, 863–875.
- (82) Dembitsky, V. M. *Phytomedicine* **2014**, *21*, 1559–1581.
- (83) Lin, Y.-T.; Lin, F.-Y.; Isobe, M. *Org. Lett.* **2014**, *16*, 5948–5951.
- (84) Lim, H. N.; Parker, K. A. *Org. Lett.* **2013**, *15*, 398–401.
- (85) Hayashi, S.; Norbeck, D. W.; Rosenbrook, W.; Fine, R. L.; Matsukura, M.; Plattner, J. J.; Broder, S.; Mitsuya, H. *Antimicrob. Agents Chemother.* **1990**, *34*, 287–294.
- (86) Norbeck, D. W.; Kern, E.; Hayashi, S.; Rosenbrook, W.; Sham, H.; Herrin, T.; Plattner, J. J.; Erickson, J.; Clement, J. *J. Med. Chem.* **1990**, *33*, 1281–1285.
- (87) Brown, B.; Hegedus, L. S. *J. Org. Chem.* **1998**, *63*, 8012–8018.
- (88) Smith, A. B.; Kanoh, N.; Ishiyama, H.; Hartz, R. A. *J. Am. Chem. Soc.* **2000**, *122*, 11254–11255.
- (89) Smith, A. B.; Kanoh, N.; Ishiyama, H.; Minakawa, N.; Rainier, J. D.; Hartz, R. A.; Cho, Y. S.; Cui, H.; Moser, W. H. *J. Am. Chem. Soc.* **2003**, *125*, 8228–8237.
- (90) Smith, A. B.; Nolen, E. G.; Shirai, R.; Blase, F. R.; Ohta, M.; Chida, N.; Hartz, R. A.; Fitch, D. M.; Clark, W. M.; Sprengeler, P. A. *J. Org. Chem.* **1995**, *60*, 7837–7848.
- (91) Rappoport, Z.; Liebman J. F. *The Chemistry of Cyclobutanes*; John Wiley & Sons, Ltd; **2005**.
- (92) Namyslo, J. C.; Kaufmann, D. E. *Chem. Rev.* **2003**, *103*, 1485–1537.
- (93) Mayo, P. De; Takeshita, H. *Can. J. Chem.* **1963**, *41*, 440–449.



- (94) Blechert, S.; Kleine-Klausing, A. *Angew. Chemie. Ed. English* **1991**, *30*, 412–414.
- (95) Begley, M. J.; Pattenden, G.; Robertson, G. M. *J. Chem. Soc. Perkin Trans. 1* **1988**, *5*, 1085.
- (96) Crimmins, M. T.; Jung, D. K.; Gray, J. L. *J. Am. Chem. Soc.* **1992**, *114*, 5445–5447.
- (97) MacDougall, J. M.; Santora, V. J.; Verma, S. K.; Turnbull, P.; Hernandez, C. R.; Moore, H. W. *J. Org. Chem.* **1998**, *63*, 6905–6913.
- (98) Wen, X.; Norling, H.; Hegedus, L. S. *J. Org. Chem.* **2000**, *65*, 2096–2103.
- (99) Conia, J. M.; Salaun, J. R. *Acc. Chem. Res.* **1972**, *5*, 33–40.
- (100) Estieu, K.; Ollivier, J.; Salaün, J. *Tetrahedron Lett.* **1996**, *37*, 623–624.
- (101) Seebach, D.; Jones, N. R.; Corey, E. J. *J. Org. Chem.* **1968**, *33*, 300–305.
- (102) Brady, W. T.; Parry, F. H.; Stockton, J. D. *J. Org. Chem.* **1971**, *36*, 1486–1489.
- (103) Hassner, A.; Pinnick, H. W.; Ansell, J. M. *J. Org. Chem.* **1978**, *43*, 1774–1776.
- (104) Jeffs, P. W.; Molina, G.; Cass, M. W.; Cortese, N. A. *J. Org. Chem.* **1982**, *47*, 3871–3875.
- (105) Lee, S. Y.; Kulkarni, Y. S.; Burbaum, B. W.; Johnston, M. I.; Snider, B. B. *J. Org. Chem.* **1988**, *53*, 1848–1855.
- (106) Trost, B. M.; Bogdanowicz, M. J. *J. Am. Chem. Soc.* **1973**, *95*, 5311–5321.
- (107) Trost, B. M.; Bogdanowicz, M. J. *J. Am. Chem. Soc.* **1973**, *95*, 5321–5334.
- (108) Trost, B. M.; Keeley, D. E.; Arndt, H. C.; Bogdanowicz, M. J. *J. Am. Chem. Soc.* **1977**, *99*, 3088–3100.
- (109) Trost, B. M.; Brandi, A. *J. Am. Chem. Soc.* **1984**, *106*, 5041–5043.
- (110) Trost, B. M.; Keeley, D. E.; Arndt, H. C.; Rigby, J. H.; Bogdanowicz, M. J. *J. Am. Chem. Soc.* **1977**, *99*, 3080–3087.
- (111) Trost, B. M.; Keeley, D.; Bogdanowicz, M. J. *J. Am. Chem. Soc.* **1973**, *95*, 3068–3070.

- (112) Cohen, T.; Matz, J. R. *Tetrahedron Lett.* **1981**, *22*, 2455–2458.
- (113) Nemoto, H.; Ishibashi, H.; Nagamochi, M.; Fukumoto, K. *J. Org. Chem.* **1992**, *57*, 1707–1712.
- (114) Krief, A.; Ronvaux, A.; Tuch, A. *Tetrahedron* **1998**, *54*, 6903–6908.
- (115) Cho, S. Y.; Cha, J. K. *Org. Lett.* **2000**, *2*, 1337–1339.
- (116) Nair, V.; Suja, T.; Mohanan, K. *Synthesis* **2006**, *15*, 2531–2534.
- (117) Markham, J. P.; Staben, S. T.; Toste, F. D. *J. Am. Chem. Soc.* **2005**, *127*, 9708–9709.
- (118) Hussain, M. M.; Li, H.; Hussain, N.; Ureña, M.; Carroll, P. J.; Walsh, P. J. *J. Am. Chem. Soc.* **2009**, *131*, 6516–6524.
- (119) Carter, C. A. G.; Greidanus, G.; Chen, J.-X.; Stryker, J. M. *J. Am. Chem. Soc.* **2001**, *123*, 8872–8873.
- (120) Sierra, M. A.; Hegedus, L. S. *J. Am. Chem. Soc.* **1989**, *111*, 2335–2336.
- (121) Bott, T. M.; Vanecko, J. A.; West, F. G. *J. Org. Chem.* **2009**, *74*, 2832–2836.
- (122) Glaeske, K. W.; West, F. G. *Org. Lett.* **1999**, *1*, 31–34.
- (123) Murphy, G. K.; Marmsäter, F. P.; West, F. G. *Can. J. Chem.* **2006**, *84*, 1470–1486.
- (124) Vanecko, J. A.; West, F. G. *Org. Lett.* **2002**, *4*, 2813–2816.
- (125) Vanecko, J. A.; West, F. G. *Org. Lett.* **2005**, *7*, 2949–2952.
- (126) Davies, S. G.; Fletcher, A. M.; Roberts, P. M.; Smith, A. D. *Tetrahedron* **2009**, *65*, 10192–10213.
- (127) Kanai, K.; Wakabayashi, H.; Honda, T. *Org. Lett.* **2000**, *2*, 2549–2551.
- (128) Bouzide, A.; Sauvé, G. *Tetrahedron Lett.* **1997**, *38*, 5945–5948.
- (129) Doyle, M. P.; Kundu, K.; Russell, A. E. *Org. Lett.* **2005**, *7*, 5171–5174.
- (130) A Aldrich® diazomethane-generator with System 45™ compatible connection for the preparation of diazomethane without ether Sigma-Aldrich
- (131) IUPAC Gold Book-radical (free radical) <http://goldbook.iupac.org/R05066.html>

- (accessed Aug 24, 2015).
- (132) Moses Gomberg and Organic Free Radicals - National Historic Chemical Landmark - American Chemical Society  
<http://www.acs.org/content/acs/en/education/whatischemistry/landmarks/freeradicals.html> (accessed Aug 24, 2015).
- (133) Moad, G.; Solomon, D. H. *The Chemistry of Radical Polymerization*; Elsevier, **2006**.
- (134) Bansal. *Organic Reaction Mechanisms*; Tata McGraw-Hill Education, **1998**.
- (135) Griller, D.; Ingold, K. U. *Acc. Chem. Res.* **1980**, *13*, 317–323.
- (136) Nonhebel, D. C. *Chem. Soc. Rev.* **1993**, *22*, 347.
- (137) Hollis, R.; Hughes, L.; Bowry, V. W.; Ingold, K. U. *J. Org. Chem.* **1992**, *57*, 4284–4287.
- (138) Bowry, V. W.; Lusztyk, J.; Ingold, K. U. *J. Am. Chem. Soc.* **1991**, *113*, 5687–5698.
- (139) Newcomb, M.; Johnson, C. C.; Manek, M. B.; Varick, T. R. *J. Am. Chem. Soc.* **1992**, *114*, 10915–10921.
- (140) Liu, K. E.; Johnson, C. C.; Newcomb, M.; Lippard, S. J. *J. Am. Chem. Soc.* **1993**, *115*, 939–947.
- (141) Martin-Esker, A. A.; Johnson, C. C.; Horner, J. H.; Newcomb, M. *J. Am. Chem. Soc.* **1994**, *116*, 9174–9181.
- (142) Le Tadic-Biadatti, M.-H.; Newcomb, M. *J. Chem. Soc. Perkin Trans. 2* **1996**, *7*, 1467-1473.
- (143) Horner, J. H.; Tanaka, N.; Newcomb, M. *J. Am. Chem. Soc.* **1998**, *120*, 10379–10390.
- (144) Halgren, T. A.; Roberts, J. D.; Horner, J. H.; Martinez, F. N.; Tronche, C.; Newcomb, M. *J. Am. Chem. Soc.* **2000**, *122*, 2988–2994.
- (145) Newcomb, M.; Toy, P. H. *Acc. Chem. Res.* **2000**, *33*, 449–455.
- (146) Newcomb, M.; Miranda, N. *J. Am. Chem. Soc.* **2003**, *125*, 4080–4086.
- (147) Choi, S.-Y.; Horner, J. H.; Newcomb, M. *J. Org. Chem.* **2000**, *65*, 4447–4449.

- (148) Huang, H.; Chang, W.; Pai, P.-J.; Romo, A.; Mansoorabadi, S. O.; Russell, D. H.; Liu, H. *J. Am. Chem. Soc.* **2012**, *134*, 16171–16174.
- (149) Otte, D. A. L.; Woerpel, K. A. *Org. Lett.* **2015**, *17*, 3906–3909.
- (150) Paul, B.; Das, D.; Ellington, B.; Marsh, E. N. G. *J. Am. Chem. Soc.* **2013**, *135*, 5234–5237.
- (151) Schmittel, M.; Mahajan, A. A.; Bucher, G.; Bats, J. W. *J. Org. Chem.* **2007**, *72*, 2166–2173.
- (152) Newcomb, M.; Chestney, D. L. *J. Am. Chem. Soc.* **1994**, *116*, 9753–9754.
- (153) Newcomb, M.; Le Tadic-Biadatti, M.-H.; Chestney, D. L.; Roberts, E. S.; Hollenberg, P. F. *J. Am. Chem. Soc.* **1995**, *117*, 12085–12091.
- (154) Katagiri, T.; Irie, M.; Uneyama, K. *Org. Lett.* **2000**, *2*, 2423–2425.
- (155) Murtagh, J. E.; McCooey, S. H.; Connon, S. J. *Chem. Commun.* **2005**, *2*, 227–229.
- (156) Marmsäter, F. P.; Vanecko, J. A.; West, F. . *Tetrahedron* **2002**, *58*, 2027–2040.
- (157) Bowry, V. W.; Luszyk, J.; Ingold, K. U. *J. Chem. Soc. Chem. Commun.* **1990**, *13*, 923–925.
- (158) Martinez, J. P.; Sasse, F.; Brönstrup, M.; Diez, J.; Meyerhans, A. *Nat. Prod. Rep.* **2015**, *32*, 29–48.
- (159) Rossmann, M. G. *Q. Rev. Biophys.* **2013**, *46*, 133–180.
- (160) Bernal, J. D.; Fankuchen, I. *J. Gen. Physiol.* **1941**, *25*, 111–146.
- (161) Carter, J.; Saunders, V. *Virology: Principles and Applications*; Wiley; 2nd Edition, <http://ca.wiley.com/WileyCDA/WileyTitle/productCd-EHEP003007.html> (accessed Oct 17, 2015).
- (162) Mateu, M. G. *Structure and Physics of Viruses*; Subcellular Biochemistry; Springer Netherlands: Dordrecht, **2013**; Vol. 68.
- (163) Grove, J.; Marsh, M. *J. Cell Biol.* **2011**, *195*, 1071–1082.
- (164) Ugolini, S.; Mondor, I.; Sattentau, Q. J. *Trends Microbiol.* **1999**, *7*, 144–149.

- (165) Vlasak, M.; Goesler, I.; Blaas, D. *J. Virol.* **2005**, *79*, 5963–5970.
- (166) Marsh, M.; Helenius, A. *Cell* **2006**, *124*, 729–740.
- (167) Matrosovich, M.; Herrler, G.; Klenk, H. D. *Top. Curr. Chem.* **2015**, *367*, 1–28.
- (168) Raman, R.; Sasisekharan, V.; Sasisekharan, R. *Chem. Biol.* **2005**, *12*, 267–277.
- (169) Bernfield, M.; Kokenyesi, R.; Kato, M.; Hinkes, M. T.; Spring, J.; Gallo, R. L.; Lose, E. J. *Annu. Rev. Cell Biol.* **1992**, *8*, 365–393.
- (170) David, G. *FASEB J.* **1993**, *7*, 1023–1030.
- (171) Dreyfuss, J. L.; Regatieri, C. V.; Jarrouge, T. R.; Cavalheiro, R. P.; Sampaio, L. O.; Nader, H. B. *An. Acad. Bras. Cienc.* **2009**, *81*, 409–429.
- (172) Shukla, D.; Spear, P. G. *J. Clin. Invest.* **2001**, *108*, 503–510.
- (173) Laquerre, S.; Argnani, R.; Anderson, D. B.; Zucchini, S.; Manservigi, R.; Glorioso, J. *C. J. Virol.* **1998**, *72*, 6119–6130.
- (174) Patel, M.; Yanagishita, M.; Roderiquez, G.; Bou-habib, D. C.; Oravec, T.; Hascall, V. C.; Norcross, M. A. *AIDS Res. Hum. Retroviruses* **1993**, *9*, 167–174.
- (175) Barth, H.; Schafer, C.; Adah, M. I.; Zhang, F.; Linhardt, R. J.; Toyoda, H.; Kinoshita-Toyoda, A.; Toida, T.; Van Kuppevelt, T. H.; Depla, E.; Von Weizsacker, F.; Blum, H. E.; Baumert, T. F. *J. Biol. Chem.* **2003**, *278*, 41003–41012.
- (176) Leistner, C. M.; Gruen-Bernhard, S.; Glebe, D. *Cell. Microbiol.* **2008**, *10*, 122–133.
- (177) WuDunn, D.; Spear, P. G. *J. Virol.* **1989**, *63*, 52–58.
- (178) Hirst, G. K. *Science* **1941**, *94*, 22–23.
- (179) Rogers, G. N.; Herrler, G.; Paulson, J. C.; Klenk, H. D. *J. Biol. Chem.* **1986**, *261*, 5947–5951.
- (180) Wang, Q.; Tian, X.; Chen, X.; Ma, J. *Proc. Natl. Acad. Sci.* **2007**, *104*, 16874–16879.
- (181) Vlasak, R.; Luytjes, W.; Spaan, W.; Palese, P. *Proc. Natl. Acad. Sci. U. S. A.* **1988**, *85*, 4526–4529.

- (182) Hellebø, A.; Vilas, U.; Falk, K.; Vlasak, R. *J. Virol.* **2004**, *78*, 3055–3062.
- (183) Vigant, F.; Santos, N. C.; Lee, B. *Nat. Rev. Microbiol.* **2015**, *13*, 426–437.
- (184) Welsch, C.; Jesudian, A.; Zeuzem, S.; Jacobson, I. *Gut* **2012**, *61*, i36–i46.
- (185) Kiser, J. J.; Flexner, C. *Annu. Rev. Pharmacol. Toxicol.* **2013**, *53*, 427–449.
- (186) Zhu, J.-D.; Meng, W.; Wang, X.-J.; Wang, H.-C. *Front. Microbiol.* **2015**, *6*, 517.
- (187) Bienkowska-Haba, M.; Williams, C.; Kim, S. M.; Garcea, R. L.; Sapp, M. *J. Virol.* **2012**, *86*, 9875–9887.
- (188) Gallay, P. A.; Ptak, R. G.; Bobardt, M. D.; Dumont, J.-M.; Vuagniaux, G.; Rosenwirth, B. *Viruses* **2013**, *5*, 981–997.
- (189) Bader, T.; Korba, B. *Antiviral Res.* **2010**, *86*, 241–245.
- (190) Ikeda, M.; Abe, K.; Yamada, M.; Dansako, H.; Naka, K.; Kato, N. *Hepatology* **2006**, *44*, 117–125.
- (191) Diamond, M. S.; Zachariah, M.; Harris, E. *Virology* **2002**, *304*, 211–221.
- (192) Henry, S. D.; Metselaar, H. J.; Lonsdale, R. C. B.; Kok, A.; Haagmans, B. L.; Tilanus, H. W.; van der Laan, L. J. W. *Gastroenterology* **2006**, *131*, 1452–1462.
- (193) Ahmed, S. P.; Nash, R. J.; Bridges, C. G.; Taylor, D. L.; Kang, M. S.; Porter, E. A.; Tyms, A. S. *Biochem. Biophys. Res. Commun.* **1995**, *208*, 267–273.
- (194) Sunkara, P. S.; Bowlin, T. L.; Liu, P. S.; Sjoerdsma, A. *Biochem. Biophys. Res. Commun.* **1987**, *148*, 206–210.
- (195) Gentzsch, J.; Hinkelmann, B.; Kaderali, L.; Irschik, H.; Jansen, R.; Sasse, F.; Frank, R.; Pietschmann, T. *Antiviral Res.* **2011**, *89*, 136–148.
- (196) Martinez, J. P.; Hinkelmann, B.; Fleta-Soriano, E.; Steinmetz, H.; Jansen, R.; Diez, J.; Frank, R.; Sasse, F.; Meyerhans, A. *Microb. Cell Fact.* **2013**, *12*, 85.
- (197) Hagiwara, K.; Kondoh, Y.; Ueda, A.; Yamada, K.; Goto, H.; Watanabe, T.; Nakata, T.; Osada, H.; Aida, Y. *Biochem. Biophys. Res. Commun.* **2010**, *394*, 721–727.
- (198) Perry, N. B.; Blunt, J. W.; Munro, M. H. G.; Pannell, L. K. *J. Am. Chem. Soc.* **1988**,

110, 4850–4851.

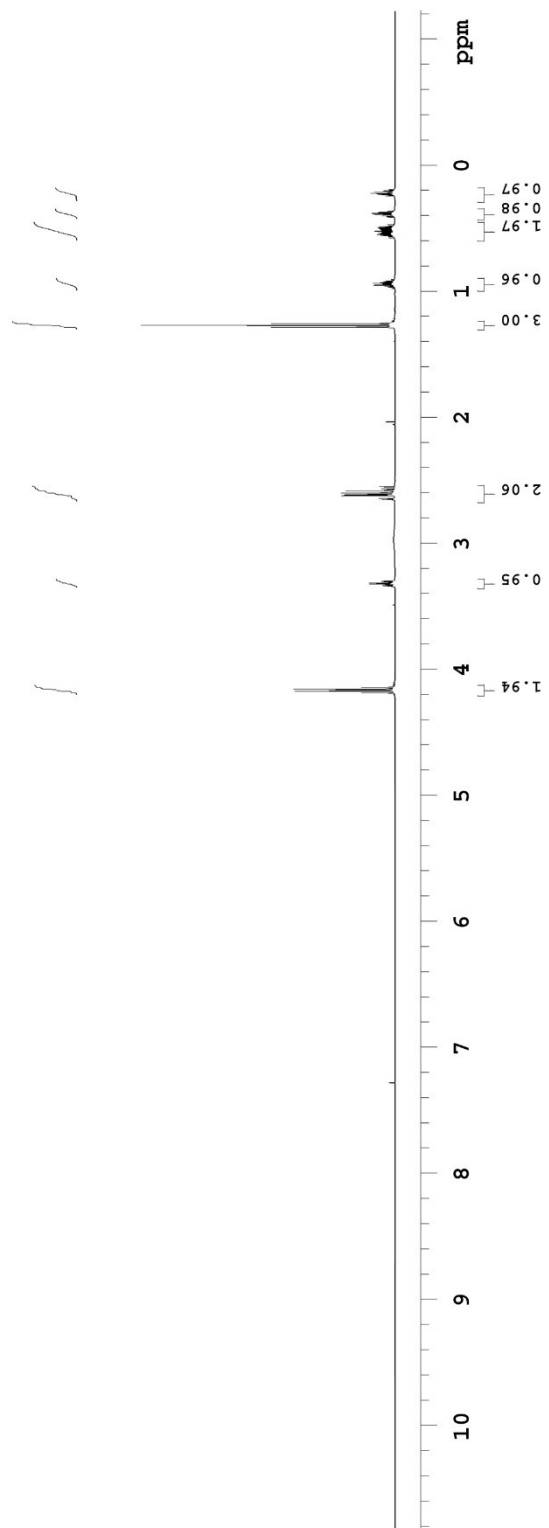
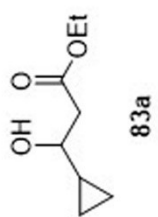
- (199) Warren, T. K.; Wells, J.; Panchal, R. G.; Stuthman, K. S.; Garza, N. L.; Van Tongeren, S. A.; Dong, L.; Retterer, C. J.; Eaton, B. P.; Pegoraro, G.; Honnold, S.; Bantia, S.; Kotian, P.; Chen, X.; Taubenheim, B. R.; Welch, L. S.; Minning, D. M.; Babu, Y. S.; Sheridan, W. P.; Bavari, S. *Nature* **2014**, *508*, 402–405.
- (200) Krumm, S. A.; Ndungu, J. M.; Yoon, J.-J.; Dochow, M.; Sun, A.; Natchus, M.; Snyder, J. P.; Plemper, R. K. *PLoS One* **2011**, *6*, e20069.
- (201) Evans, D. R.; Guy, H. I. *J. Biol. Chem.* **2004**, *279*, 33035–33038.
- (202) Kinch, M. S.; Yunus, A. S.; Lear, C.; Mao, H.; Chen, H.; Fesseha, Z.; Luo, G.; Nelson, E. A.; Li, L.; Huang, Z.; Murray, M.; Ellis, W. Y.; Hensley, L.; Christopher-Hennings, J.; Olinger, G. G.; Goldblatt, M. *Am. J. Transl. Res.* **2009**, *1*, 87–98.
- (203) Lara, H. H.; Ixtepan-Turrent, L.; Garza-Treviño, E. N.; Rodriguez-Padilla, C. *J. Nanobiotechnology* **2010**, *8*, 15.
- (204) Buzzini, P.; Arapitsas, P.; Goretti, M.; Branda, E.; Turchetti, B.; Pinelli, P.; Ieri, F.; Romani, A. *Mini Rev. Med. Chem.* **2008**, *8*, 1179–1187.
- (205) Lin, L.-T.; Chen, T.-Y.; Lin, S.-C.; Chung, C.-Y.; Lin, T.-C.; Wang, G.-H.; Anderson, R.; Lin, C.-C.; Richardson, C. D. *BMC Microbiol.* **2013**, *13*, 187.
- (206) Lin, L.-T.; Chen, T.-Y.; Chung, C.-Y.; Noyce, R. S.; Grindley, T. B.; McCormick, C.; Lin, T.-C.; Wang, G.-H.; Lin, C.-C.; Richardson, C. D. *J. Virol.* **2011**, *85*, 4386–4398.
- (207) Cabrera, C.; Artacho, R.; Giménez, R. *J. Am. Coll. Nutr.* **2006**, *25*, 79–99.
- (208) Chen, Z. P.; Schell, J. B.; Ho, C. T.; Chen, K. Y. *Cancer Lett.* **1998**, *129*, 173–179.
- (209) Sazuka, M.; Murakami, S.; Isemura, M.; Satoh, K.; Nukiwa, T. *Cancer Lett.* **1995**, *98*, 27–31.
- (210) Gupta, S.; Hastak, K.; Afaq, F.; Ahmad, N.; Mukhtar, H. *Oncogene* **2004**, *23*, 2507–2522.
- (211) Wolfram, S. *J. Am. Coll. Nutr.* **2007**, *26*, 373S – 388S.

- (212) Wolfram, S.; Raederstorff, D.; Preller, M.; Wang, Y.; Teixeira, S. R.; Riegger, C.; Weber, P. *J. Nutr.* **2006**, *136*, 2512–2518.
- (213) Steinmann, J.; Buer, J.; Pietschmann, T.; Steinmann, E. *Br. J. Pharmacol.* **2013**, *168*, 1059–1073.
- (214) Colpitts, C. C.; Schang, L. M. *J. Virol.* **2014**, *88*, 7806–7817.
- (215) Kane, C. J.; Menna, J. H.; Sung, C. C.; Yeh, Y. C. *Biosci. Rep.* **1988**, *8*, 95–102.
- (216) Yamasaki, H.; Uozaki, M.; Katsuyama, Y.; Utsunomiya, H.; Arakawa, T.; Higuchi, M.; Higuti, T.; Koyama, A. H. *Int. J. Mol. Med.* **2007**, *19*, 685–688.
- (217) Isaacs, C. E.; Xu, W.; Merz, G.; Hillier, S.; Rohan, L.; Wen, G. Y. *Antimicrob. Agents Chemother.* **2011**, *55*, 5646–5653.
- (218) Kratz, J. M.; Andrighetti-Fröhner, C. R.; Leal, P. C.; Nunes, R. J.; Yunes, R. A.; Trybala, E.; Bergström, T.; Barardi, C. R. M.; Simões, C. M. O. *Biol. Pharm. Bull.* **2008**, *31*, 903–907.
- (219) Smith, T. J. *Expert Opin. Drug Discov.* **2011**, *6*, 589–595.
- (220) MIYAMOTO, Y.; HAYLOR, J. L.; EL NAHAS, A. M. *J. Toxicol. Sci.* **2004**, *29*, 47–52.
- (221) Dodo, K.; Minato, T.; Noguchi-Yachide, T.; Suganuma, M.; Hashimoto, Y. *Bioorg. Med. Chem.* **2008**, *16*, 7975–7982.
- (222) Abraham, R. J.; Byrne, J. J.; Griffiths, L.; Perez, M. *Magn. Reson. Chem.* **2006**, *44*, 491–509.
- (223) Lomas, J. S. *Magn. Reson. Chem.* **2014**, *52*, 745–754.
- (224) Nicolaou, K. C.; Sasmal, P. K.; Xu, H. *J. Am. Chem. Soc.* **2004**, *126*, 5493–5501.
- (225) Gažák, R.; Valentová, K.; Fuksová, K.; Marhol, P.; Kuzma, M.; Medina, M. Á.; Oborná, I.; Ulrichová, J.; Křen, V. *J. Med. Chem.* **2011**, *54*, 7397–7407.
- (226) Horton, D.; Philips, K. D. *Carbohydr. Res.* **1973**, *30*, 367–374.
- (227) Zhu, Y.; Soroka, D. N.; Sang, S. *J. Agric. Food Chem.* **2012**, *60*, 8624–8631.

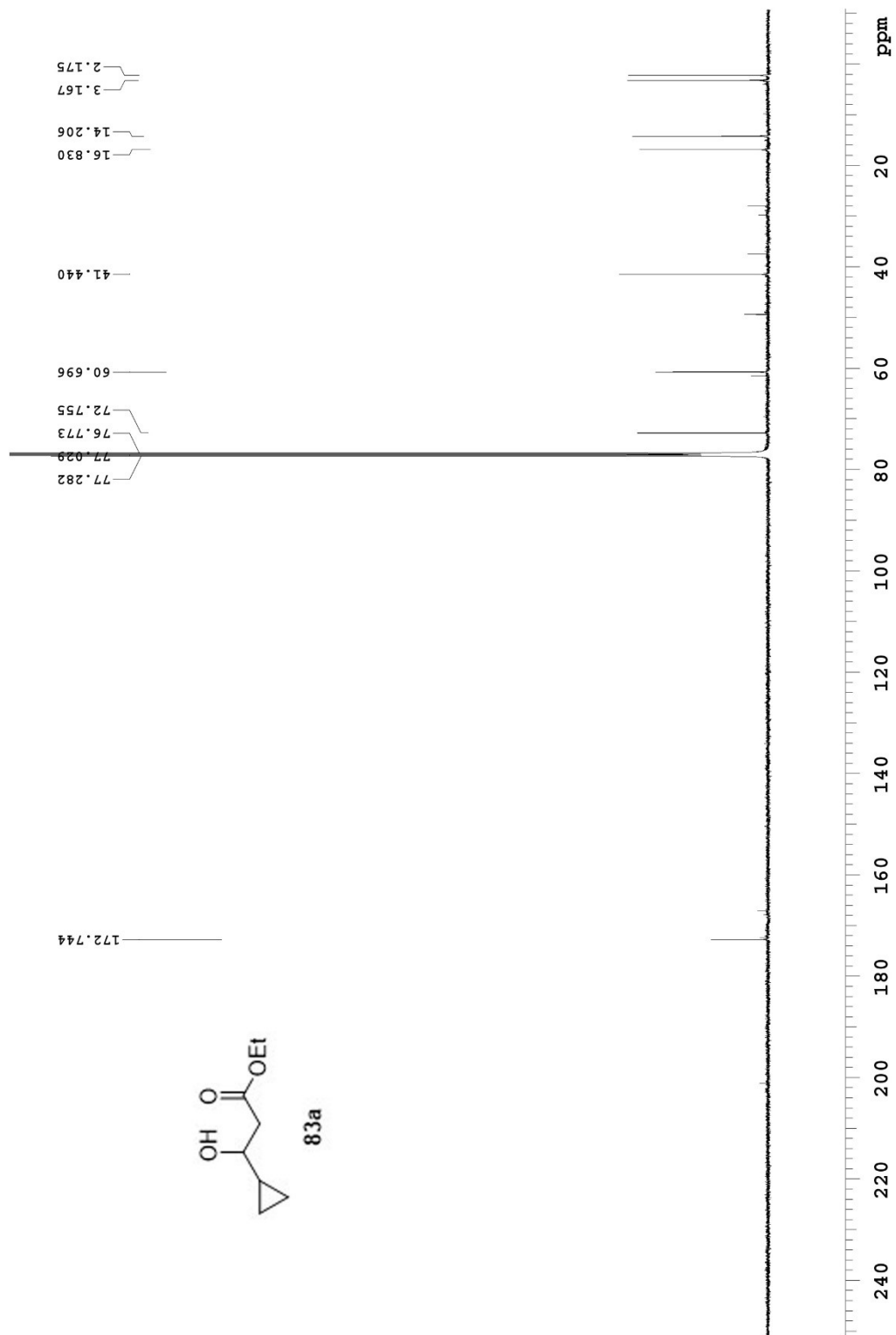


## **Appendix I: Selected NMR Spectra (Chapter 2)**

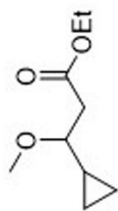
498.118 MHz H1 1D in cdcl3 (ref. to CDC13 @ 7.26 ppm), temp 27.2 C -> actual temp = 27.0 C, autotxdtb probe



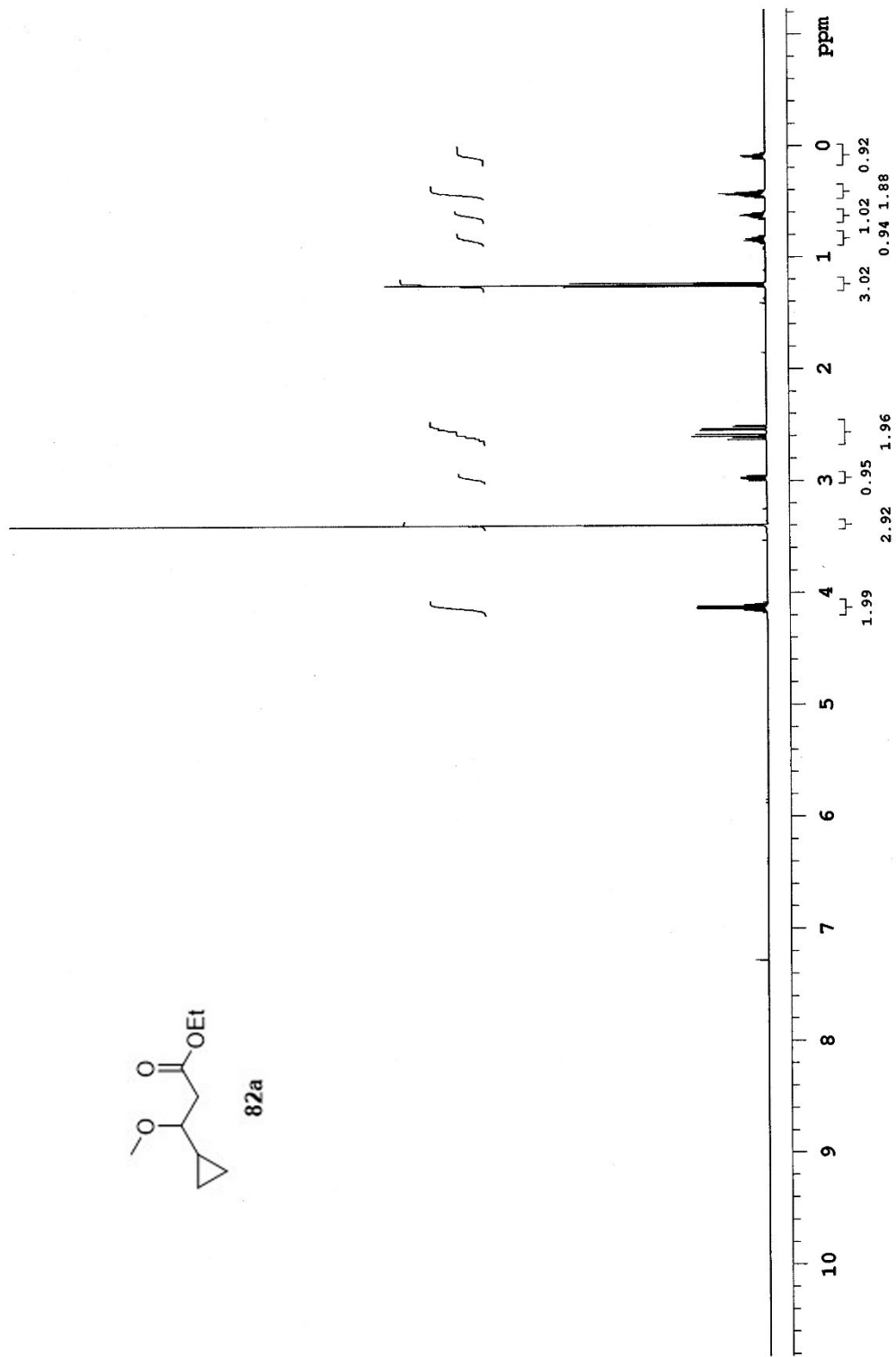
125.693 MHz C13[H1] 1D in cdcl3 (ref. to CDCl3 @ 77.06 ppm), temp 27.7 C -> actual temp = 27.0 C, coldlual probe



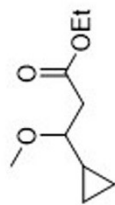
498.118 MHz H1 1D in cdcl3 (ref. to CDCl3 @ 7.26 ppm), temp 26.4 C -> actual temp = 27.0 C, autoxdb probe



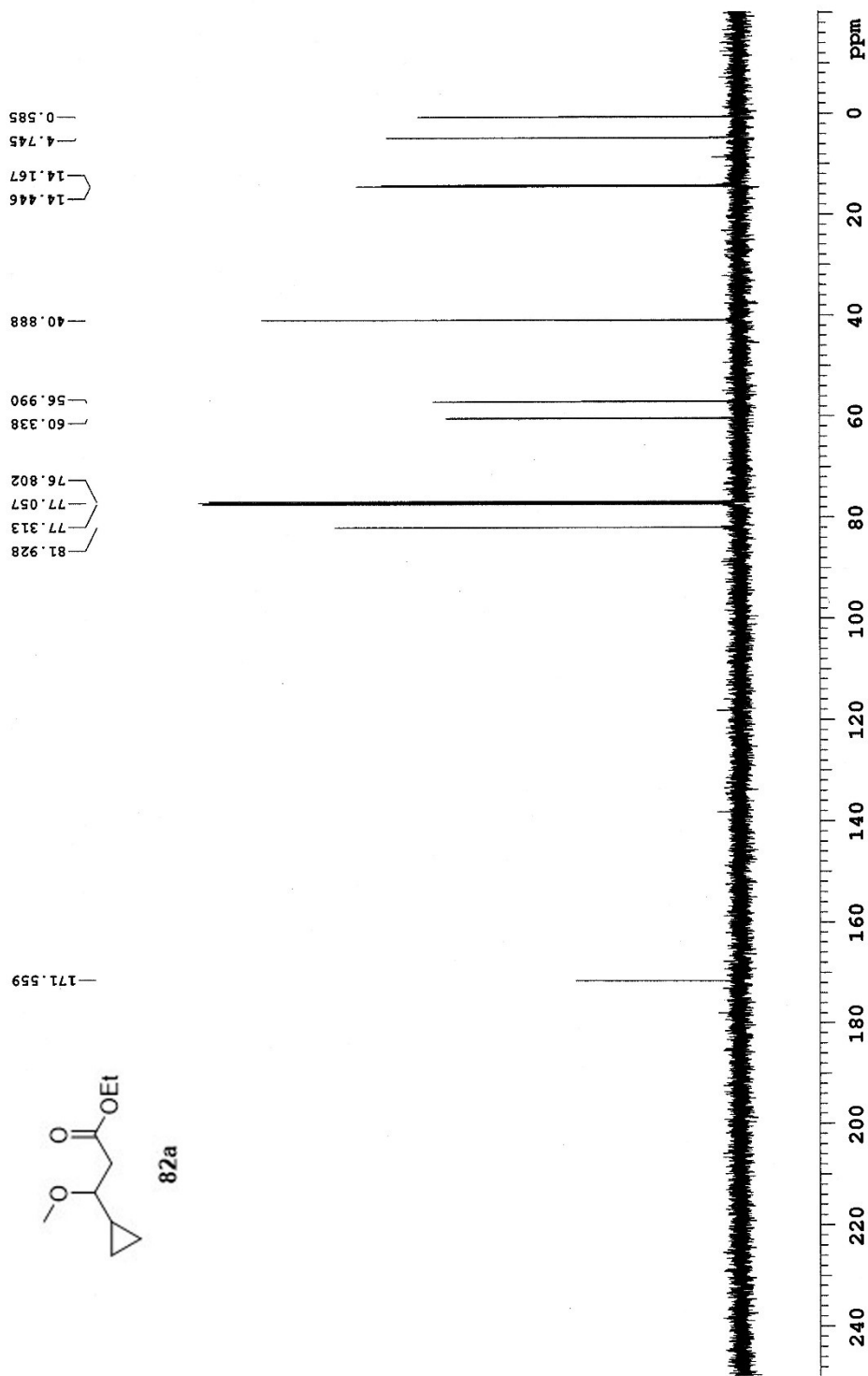
82a



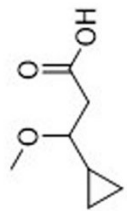
125.266 MHz  $^{13}\text{C}$  NMR (ref. to  $\text{CDCl}_3$  @ 77.06 ppm), temp 26.4 C -> actual temp = 27.0 C; autoexdb probe



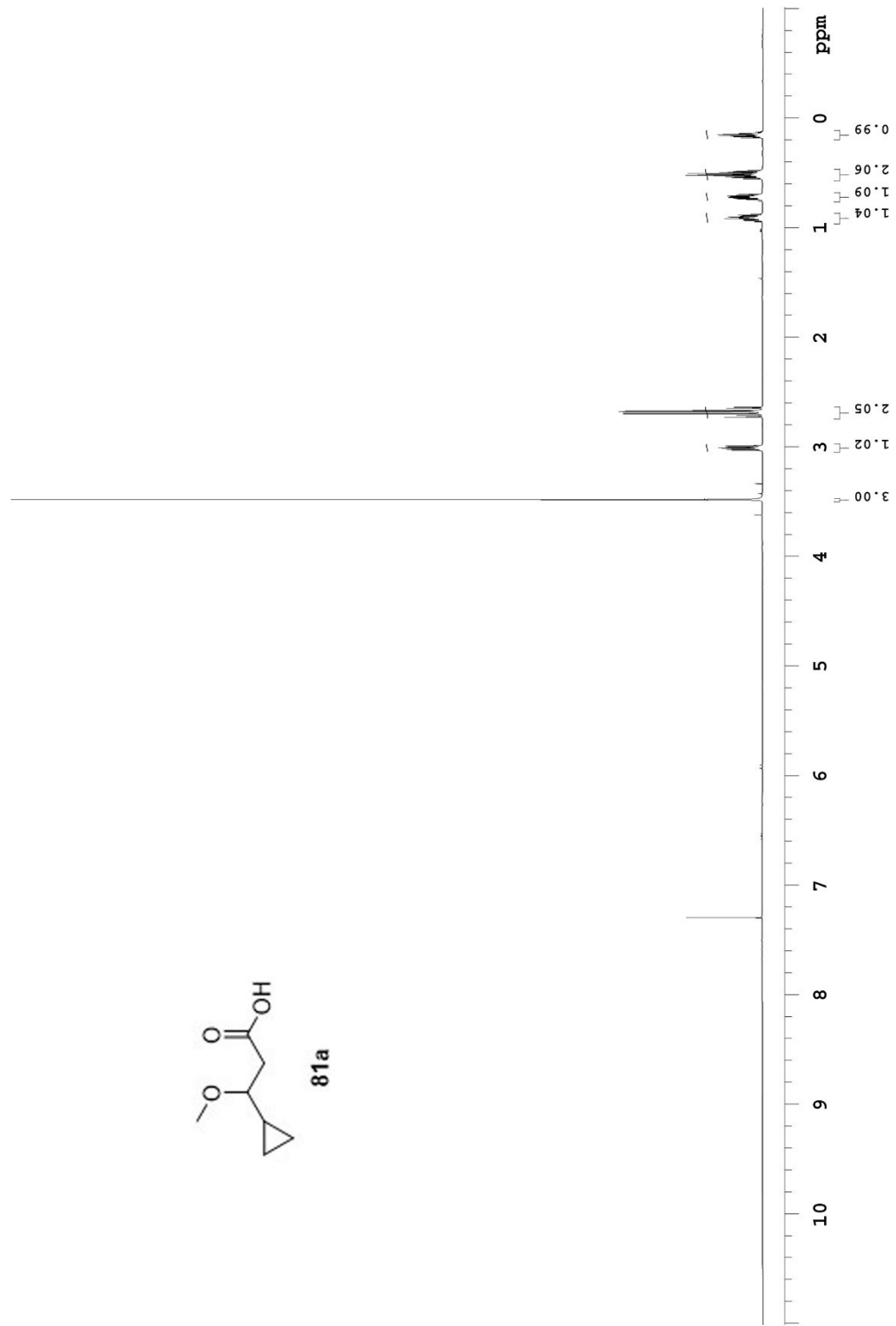
82a



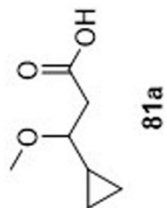
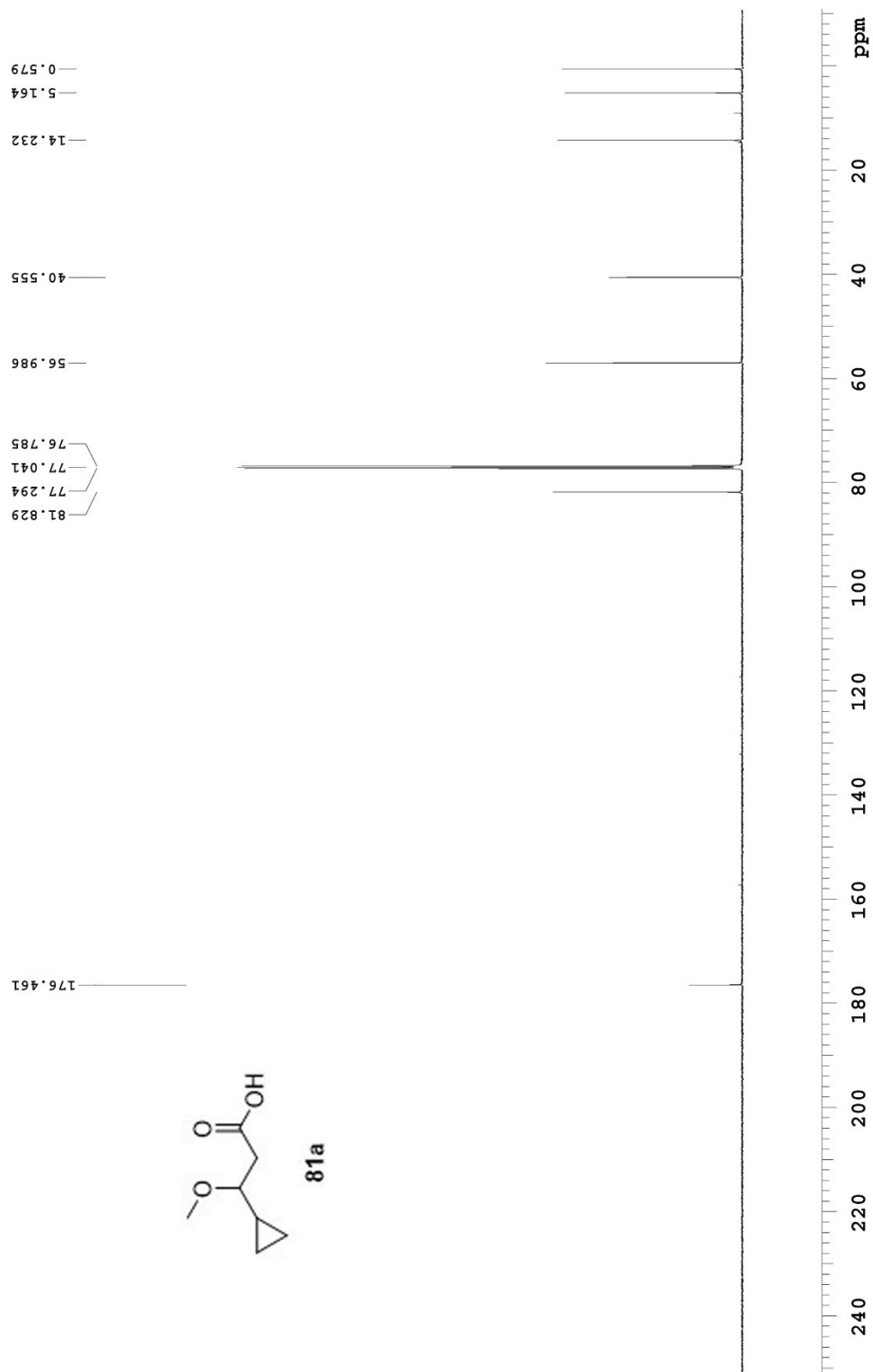
499.815 MHz H1 PRESAT in cdcl3 (ref. to CDCl3 @ 7.26 ppm), temp 27.7 C -> actual temp = 27.0 C, coldludal probe



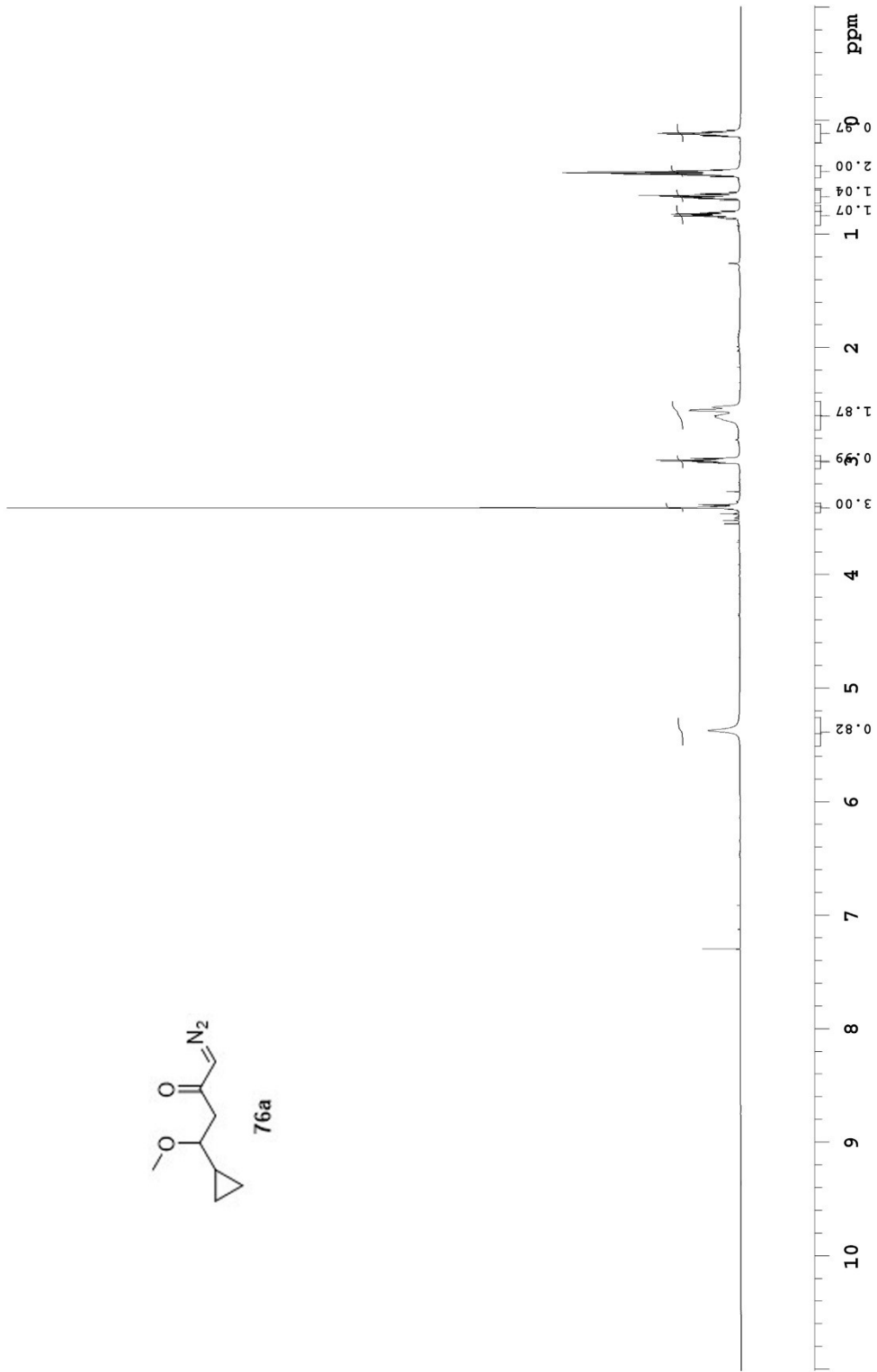
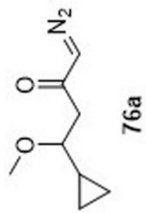
81a



125.693 MHz C13[H1] 1D in cdcl3 (ref. to CDCl3 @ 77.06 ppm), temp 27.7 C -> actual temp = 27.0 C, cold dual probe

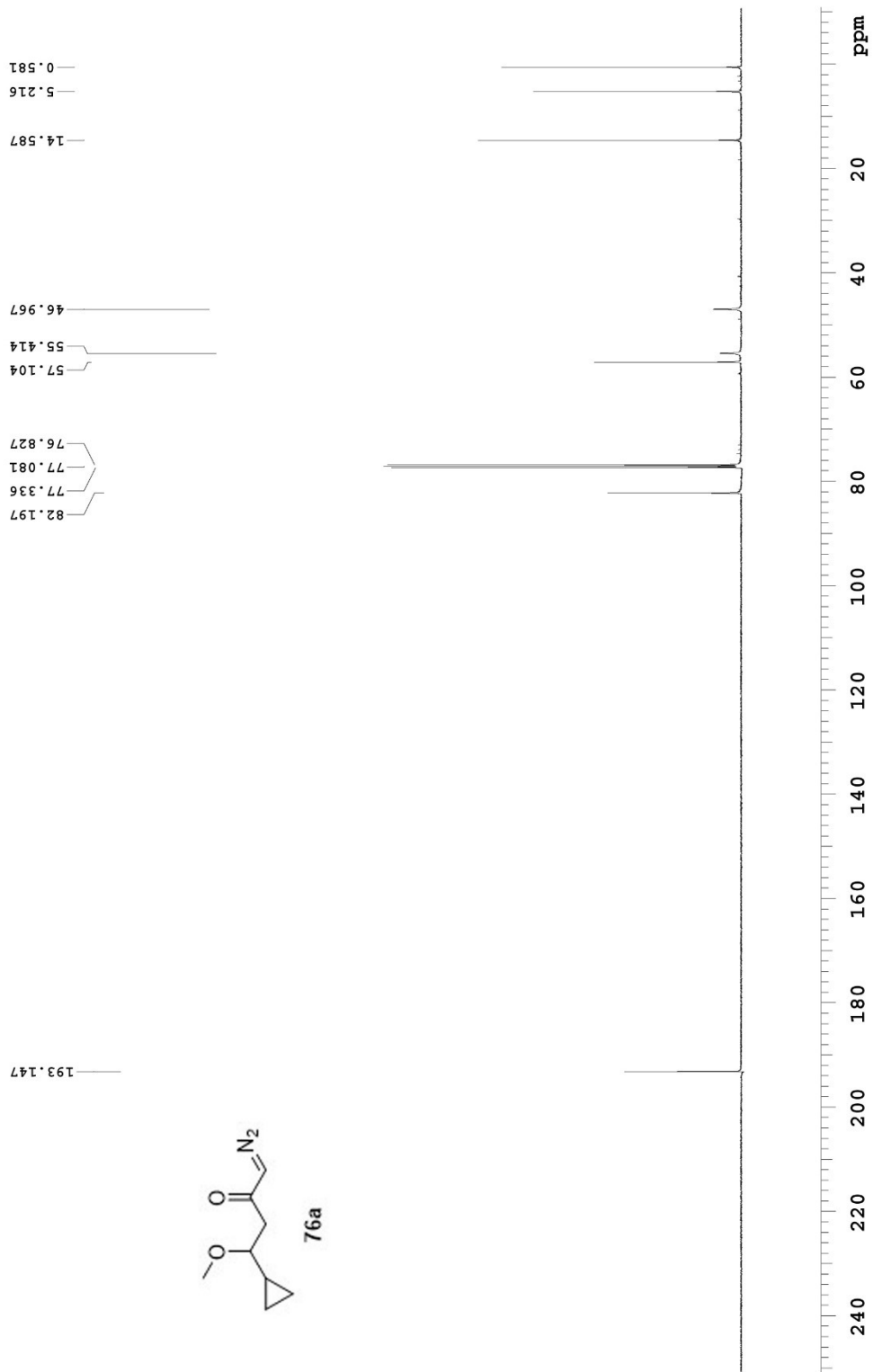
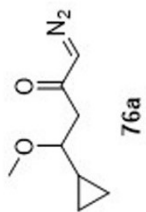


499.815 MHz H1 PRESAT in cdcl3 (ref. to CDC13 @ 7.26 ppm), temp 27.7 C -> actual temp = 27.0 C, coldlual probe

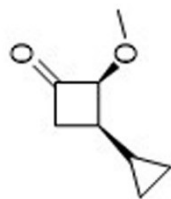




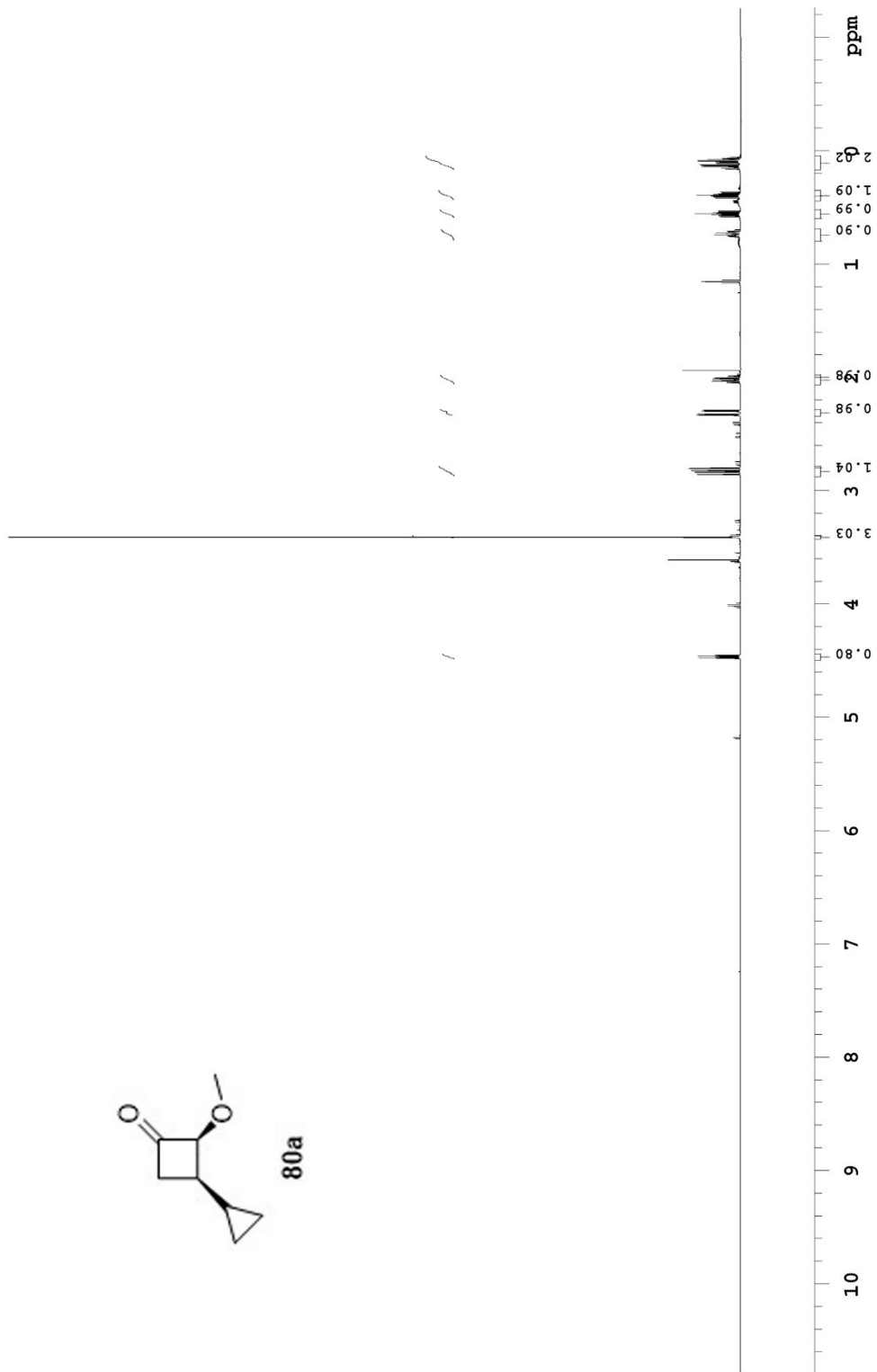
125.683 MHz C13[H1] 1D in cdcl3 (ref. to CDC13 @ 77.06 ppm), temp 27.7 C -> actual temp = 27.0 C, coldludal probe



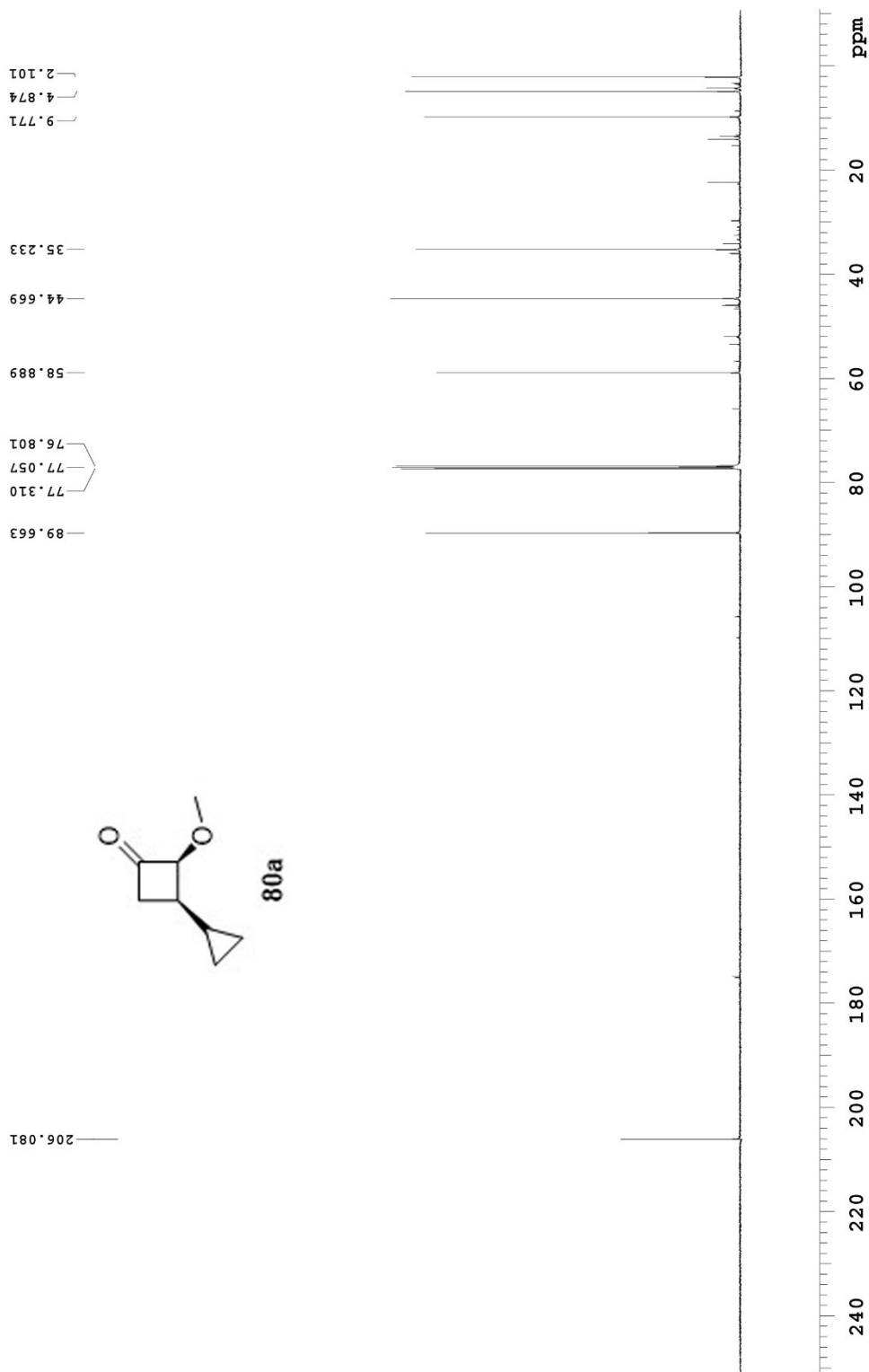
498.118 MHz H1 1D in cdcl3 (ref. to CDCl3 @ 7.26 ppm), temp 27.2 C -> actual temp = 27.0 C, autoudb probe



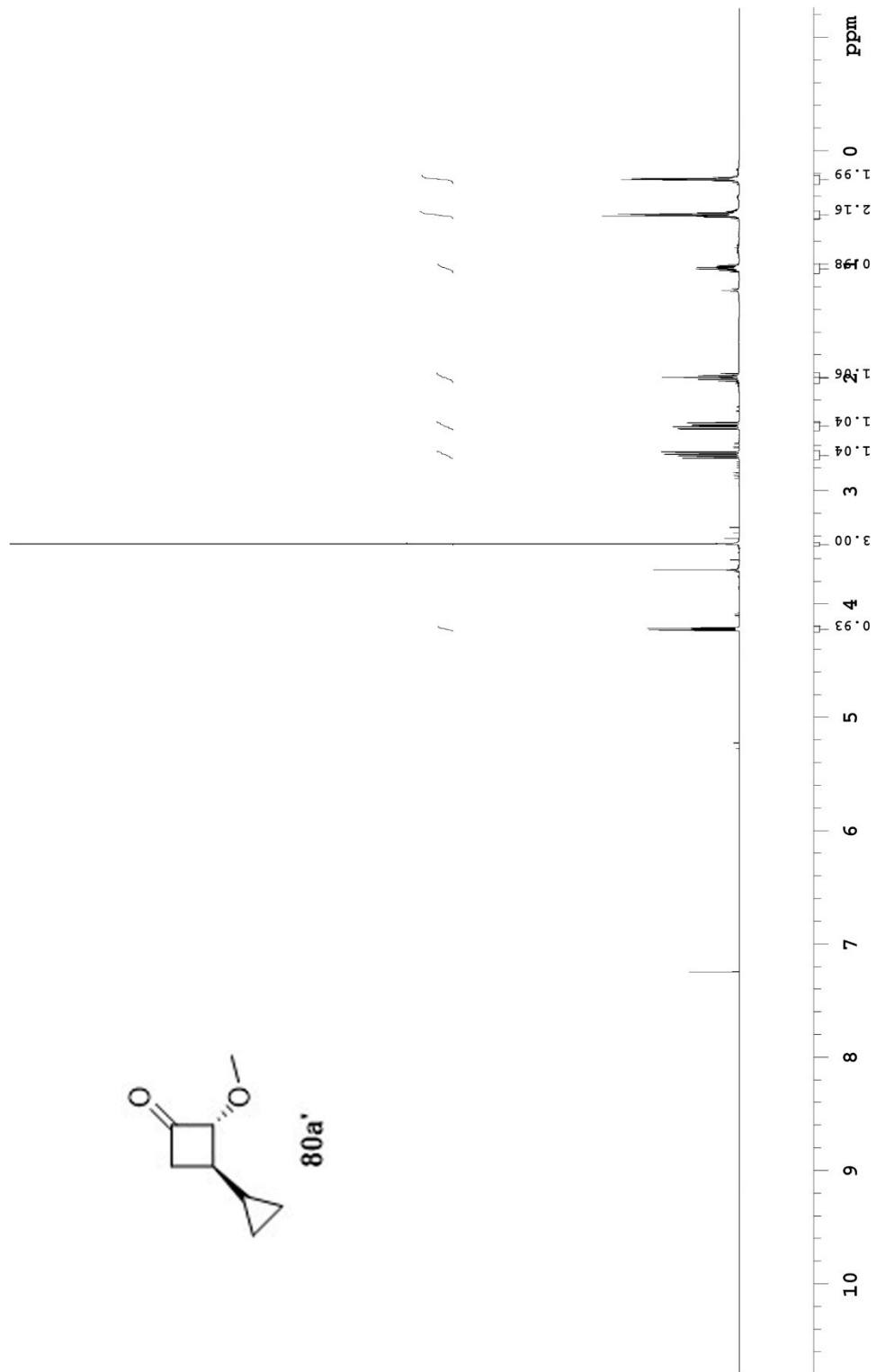
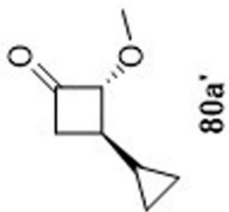
80a



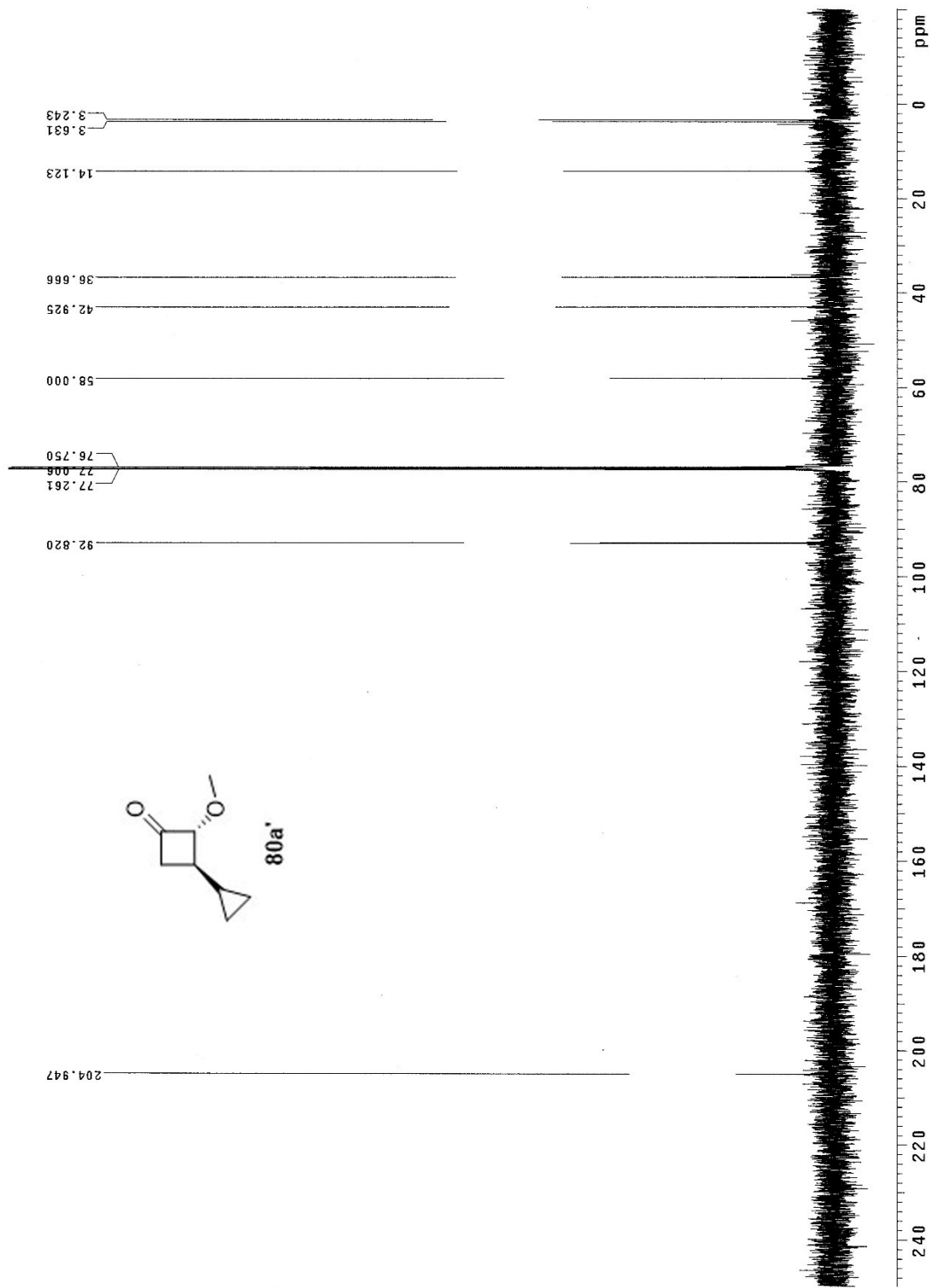
125.683 MHz C13[H1] 1D in cdcl3 (ref. to CDC13 @ 77.06 ppm), temp 27.7 C -> actual temp = 27.0 C, cooldual probe



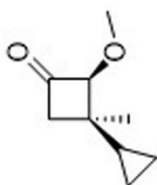
498.118 MHz H1 1D in cdcl3 (ref. to CDCl3 @ 7.26 ppm), temp 27.2 C -> actual temp = 27.0 C, autoxdb probe



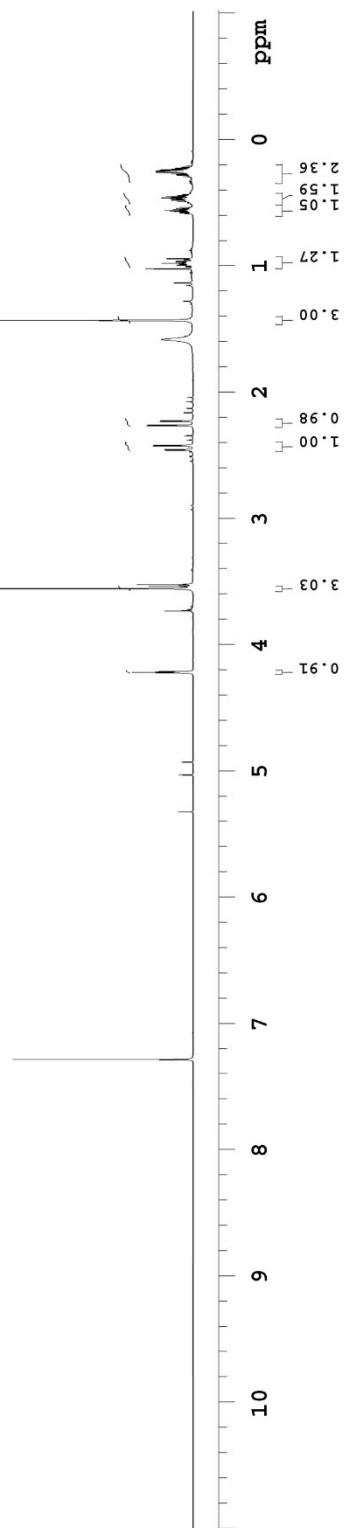
125.266 MHz C13[M1] ID in cdcl3 (ref. to CDC13 @ 77.06 ppm), temp 27.2 C -> actual temp = 27.0 C, autoxdb probe



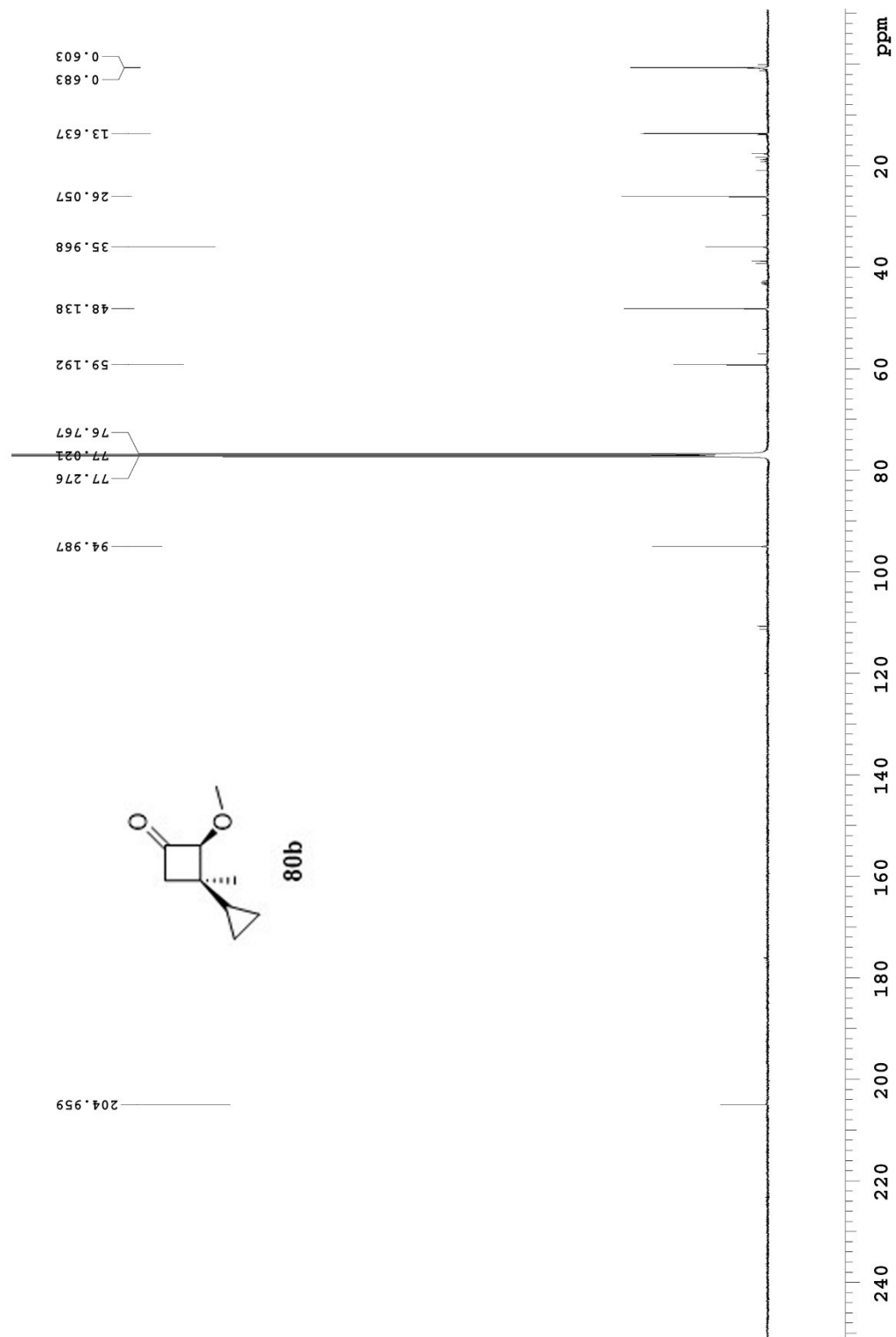
499.806 MHz H1 PRESAT in cdcl3 (ref. to CDC13 @ 7.26 ppm), temp 27.7 C -> actual temp = 27.0 C, coldidial probe



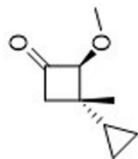
80b



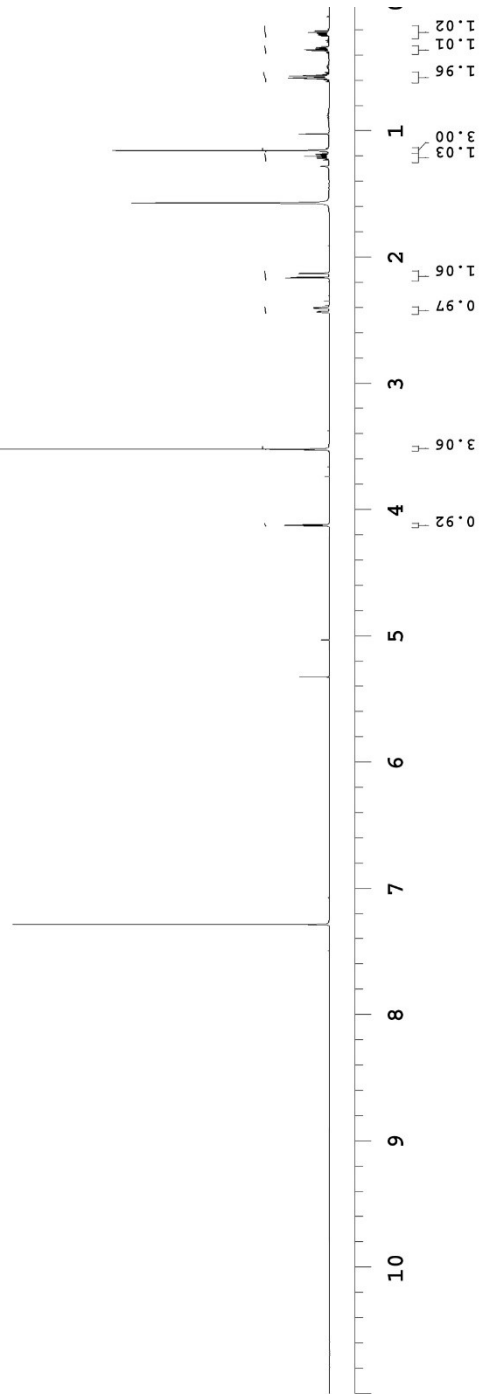
125.691 MHz C13{H1} 1D in cdcl3 (ref. to CDC13 @ 77.06 ppm), temp 27.7 C-> actual temp = 27.0 C, coldltdual probe



499.806 MHz H1 PRESAT in cdcl3 (ref. to CDC13 @ 7.26 ppm), temp 27.7 C -> actual temp = 27.0 C, coldludal probe

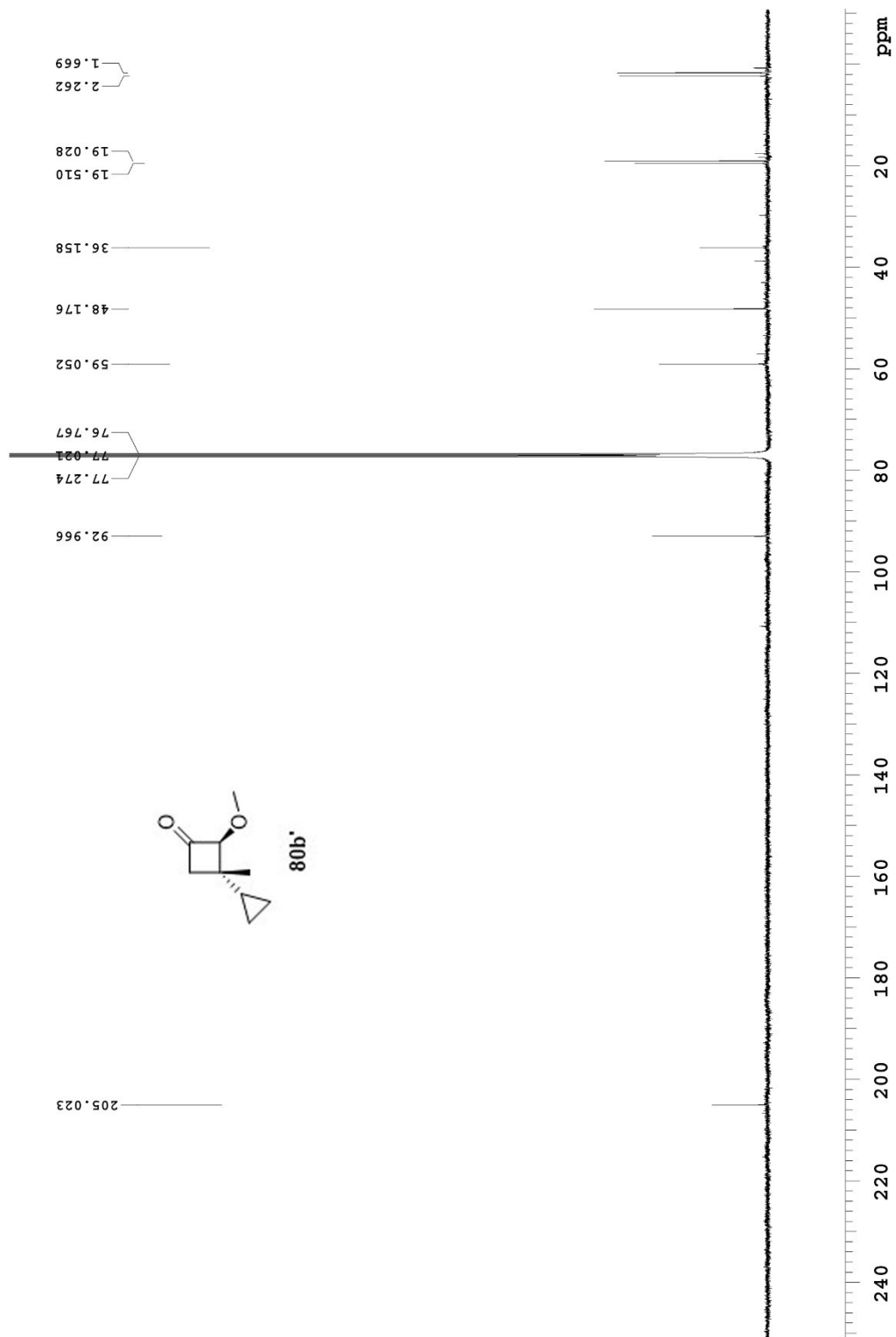


80b'

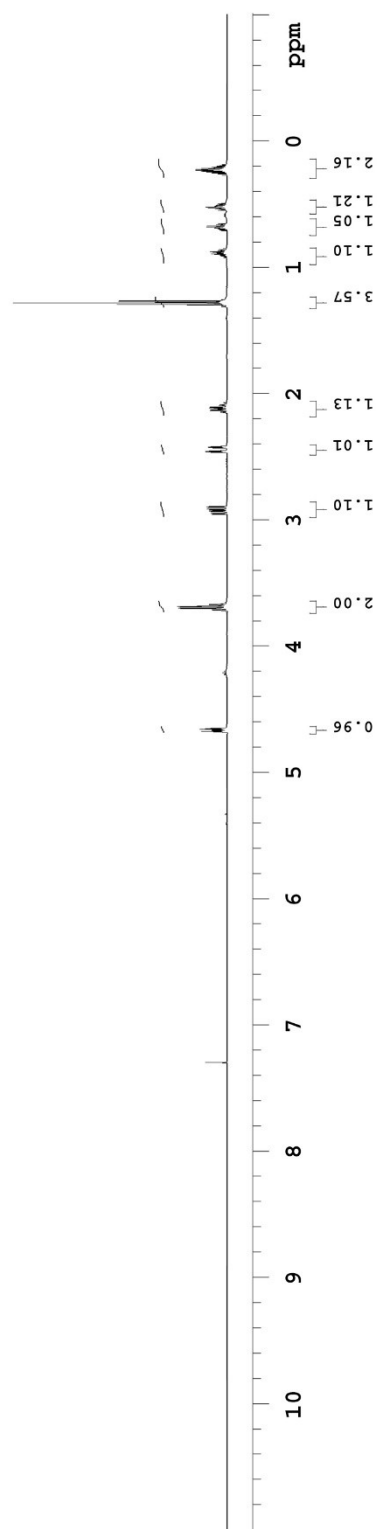
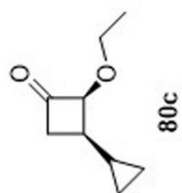




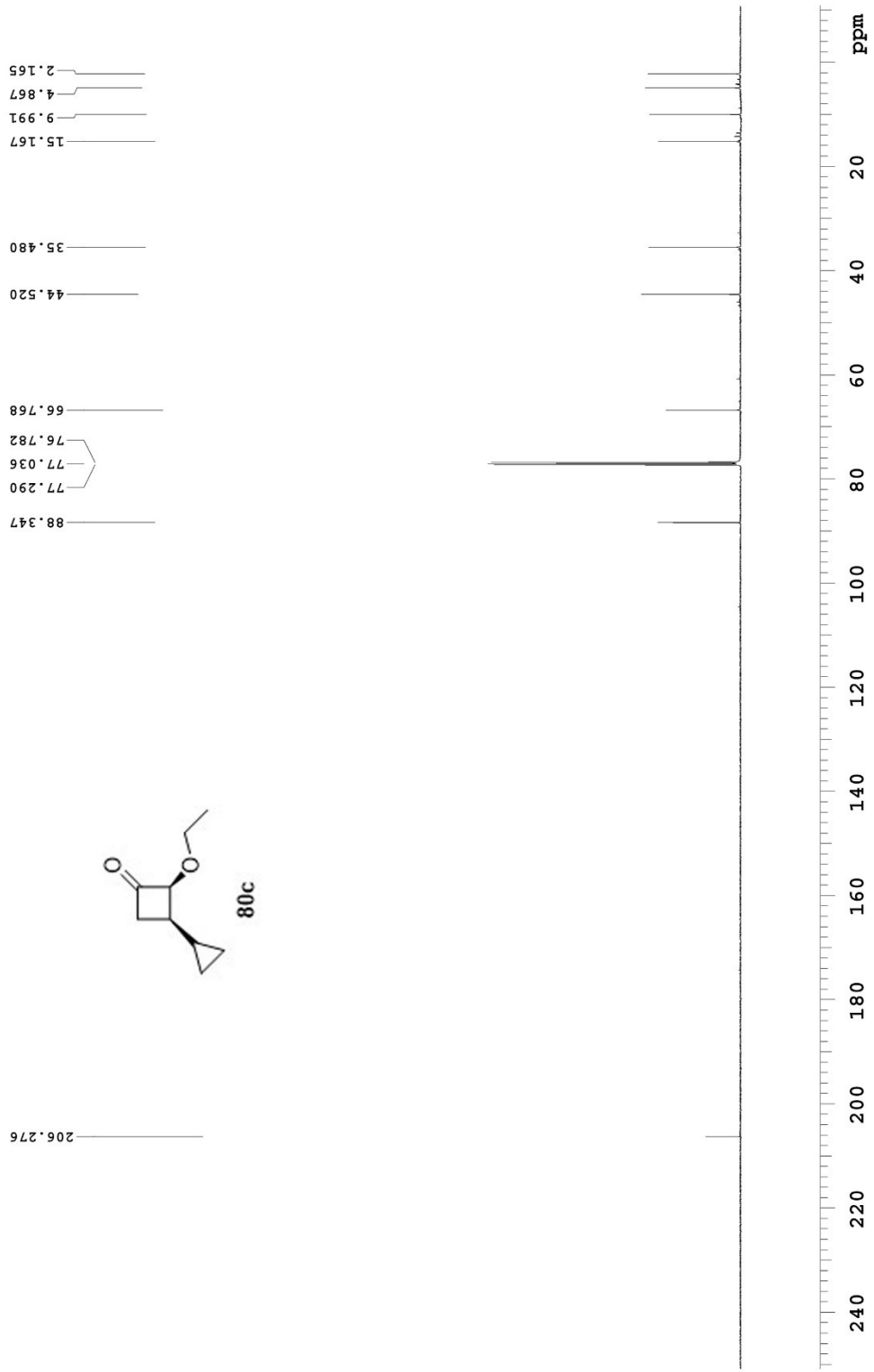
125.691 MHz C13[H1] 1D in cdcl3 (ref. to CDCl3 @ 77.06 ppm), temp 27.7 C -> actual temp = 27.0 C, coldludal probe



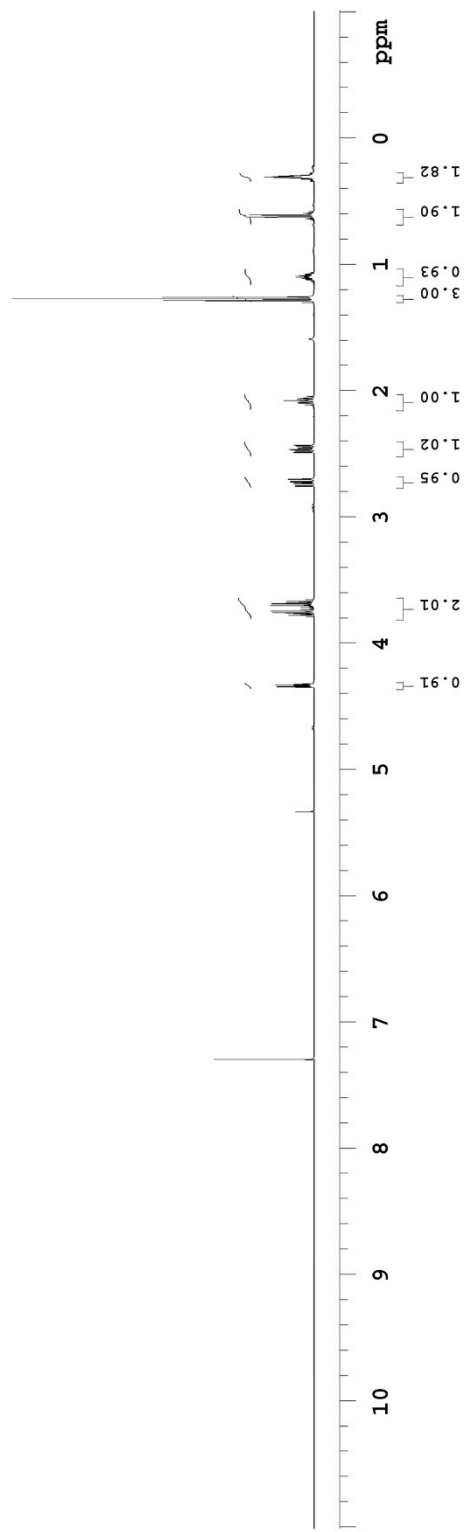
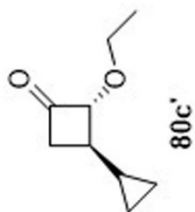
499.806 MHz H1 PRESAT in cdcl3 (ref. to CDC13 @ 7.26 ppm), temp 27.7 C -> actual temp = 27.0 C, coldddual probe



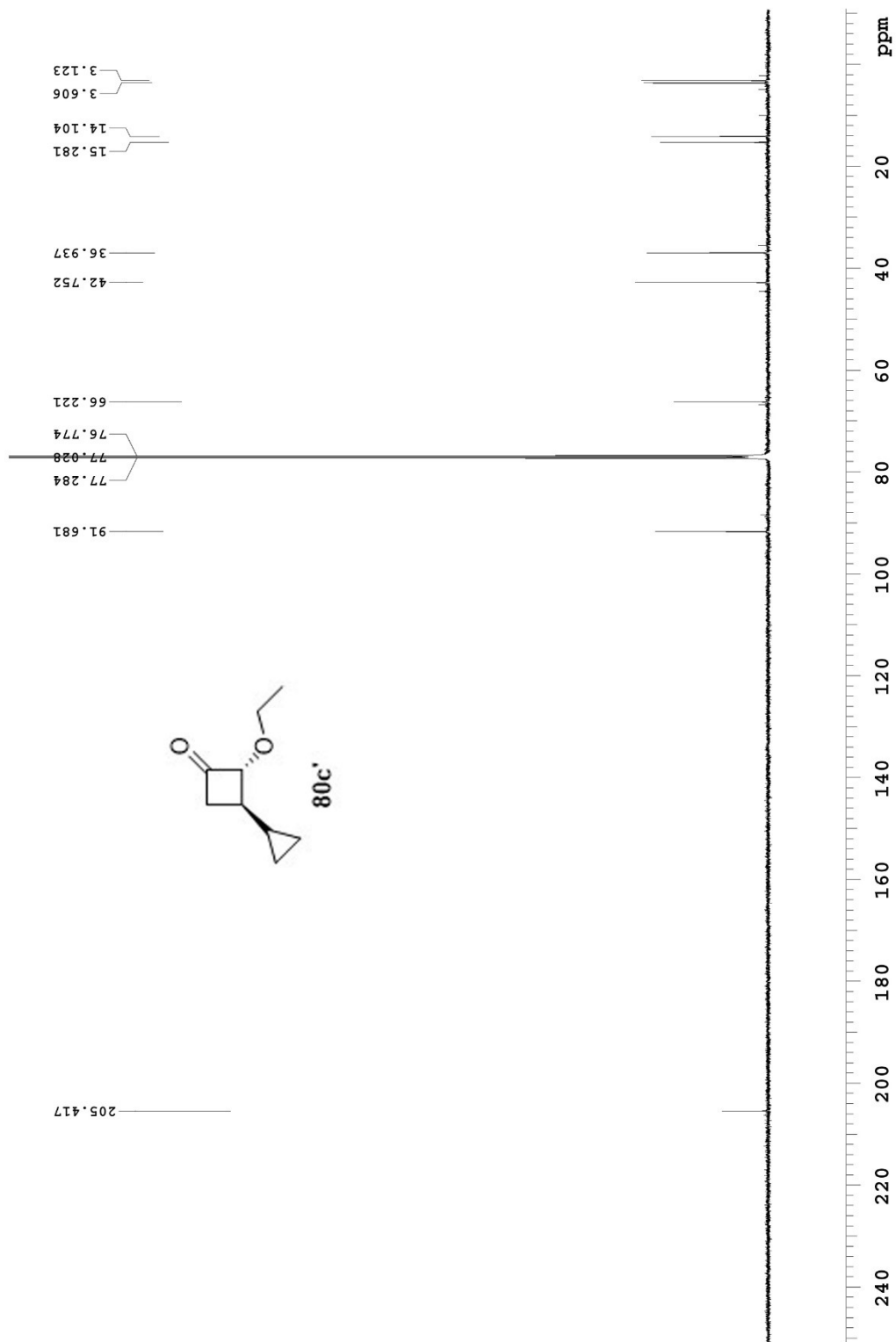
125.691 MHz C13[H1] 1D in cdcl3 (ref. to CDCl3 @ 77.06 ppm), temp 27.7 C -> actual temp = 27.0 C, coldlial probe



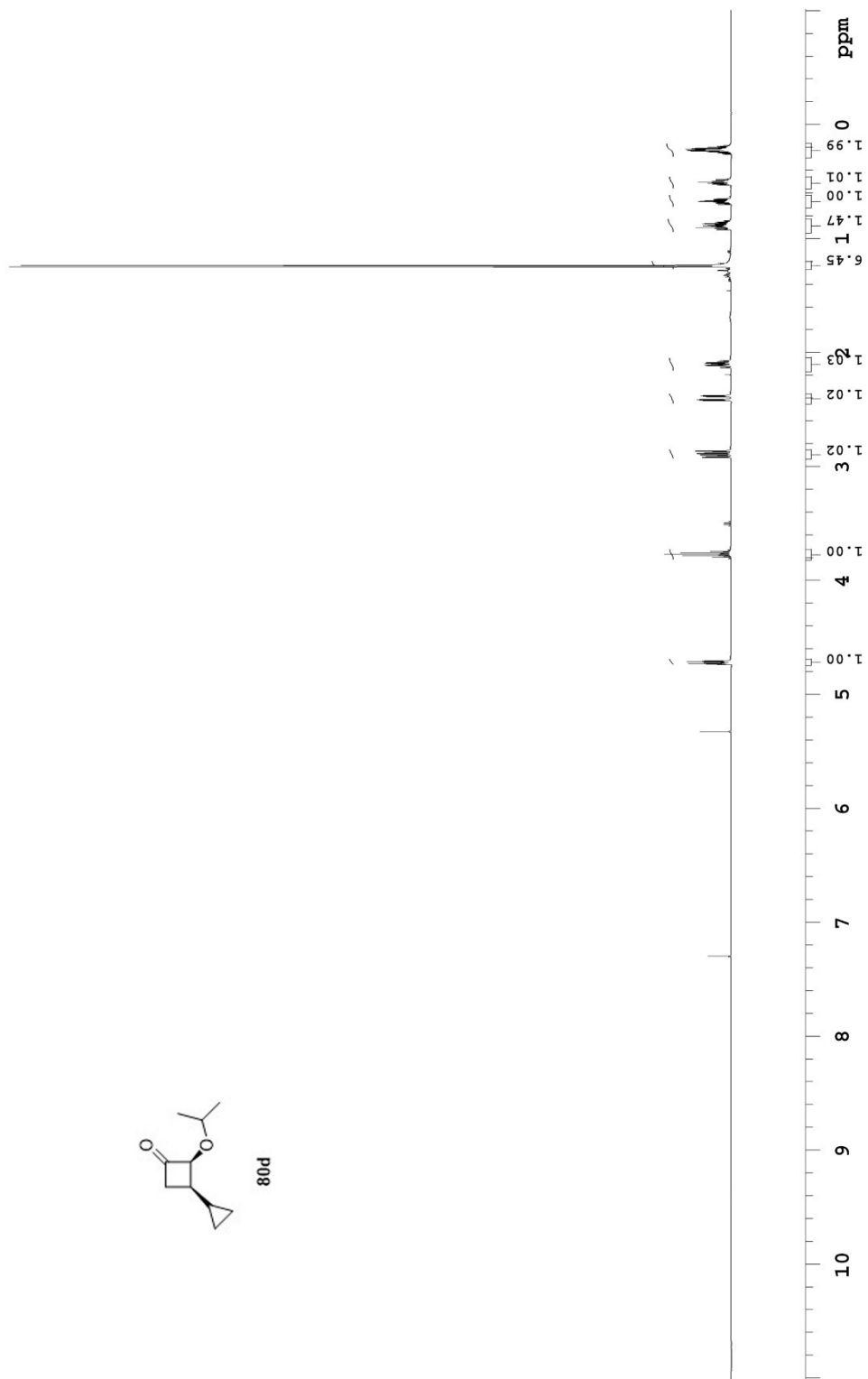
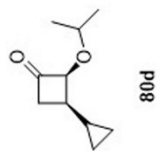
499.806 MHz H1 PRESAT in cdcl3 (ref. to cdcl3 @ 7.26 ppm), temp 27.7 C -> actual temp = 27.0 C, cold dual probe



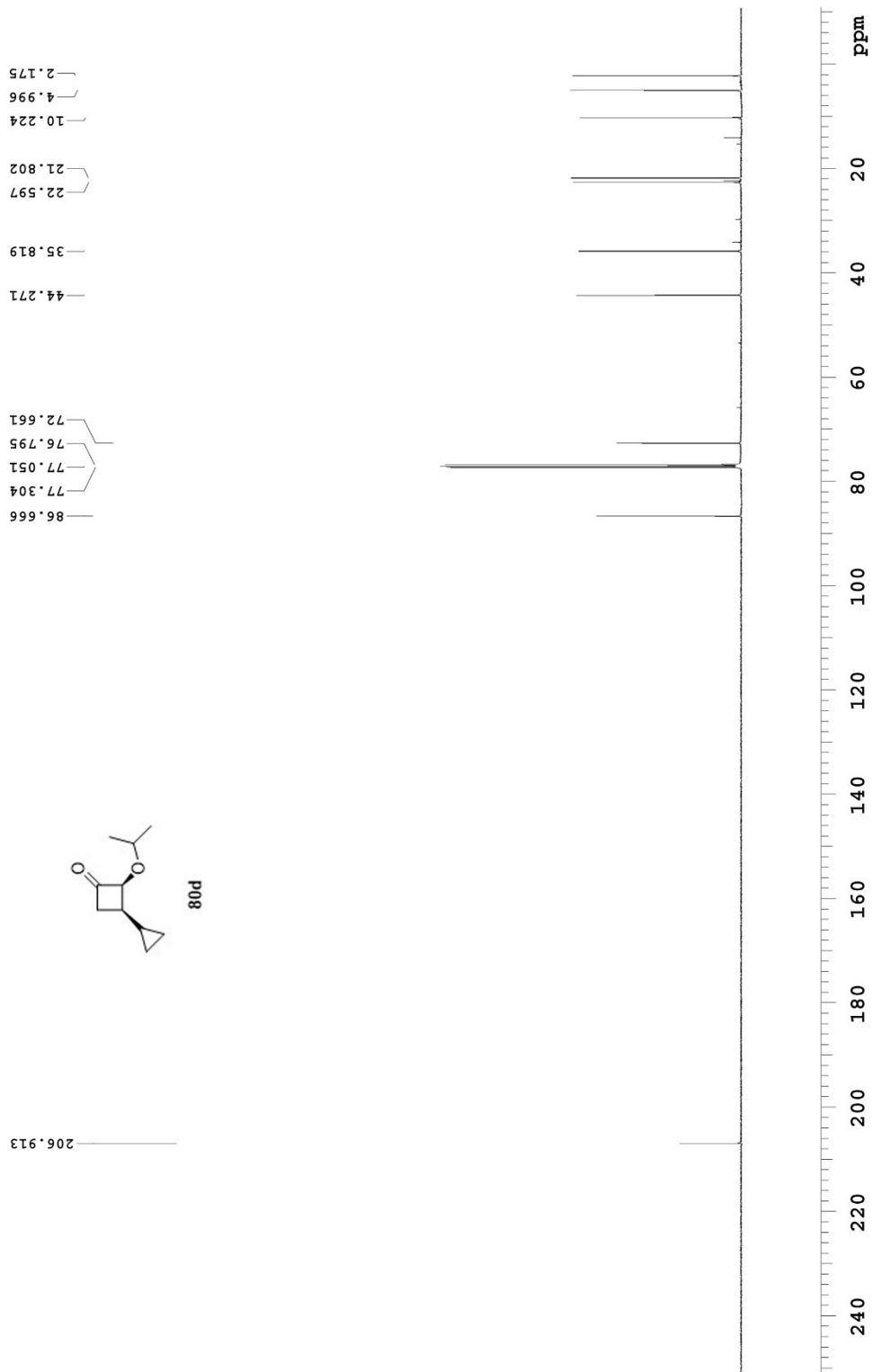
125.681 MHz C13[H1] 1D in cdcl3 (ref. to CDC13 @ 77.06 ppm), temp 27.7 C-> actual temp = 27.0 C, coldtial probe

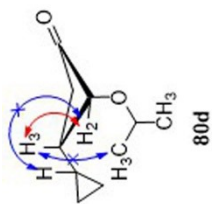


499.815 MHz H1 PRESAT in cdc13 (ref. to CDC13 @ 7.26 ppm), temp 27.7 C -> actual temp = 27.0 C, coldludal probe

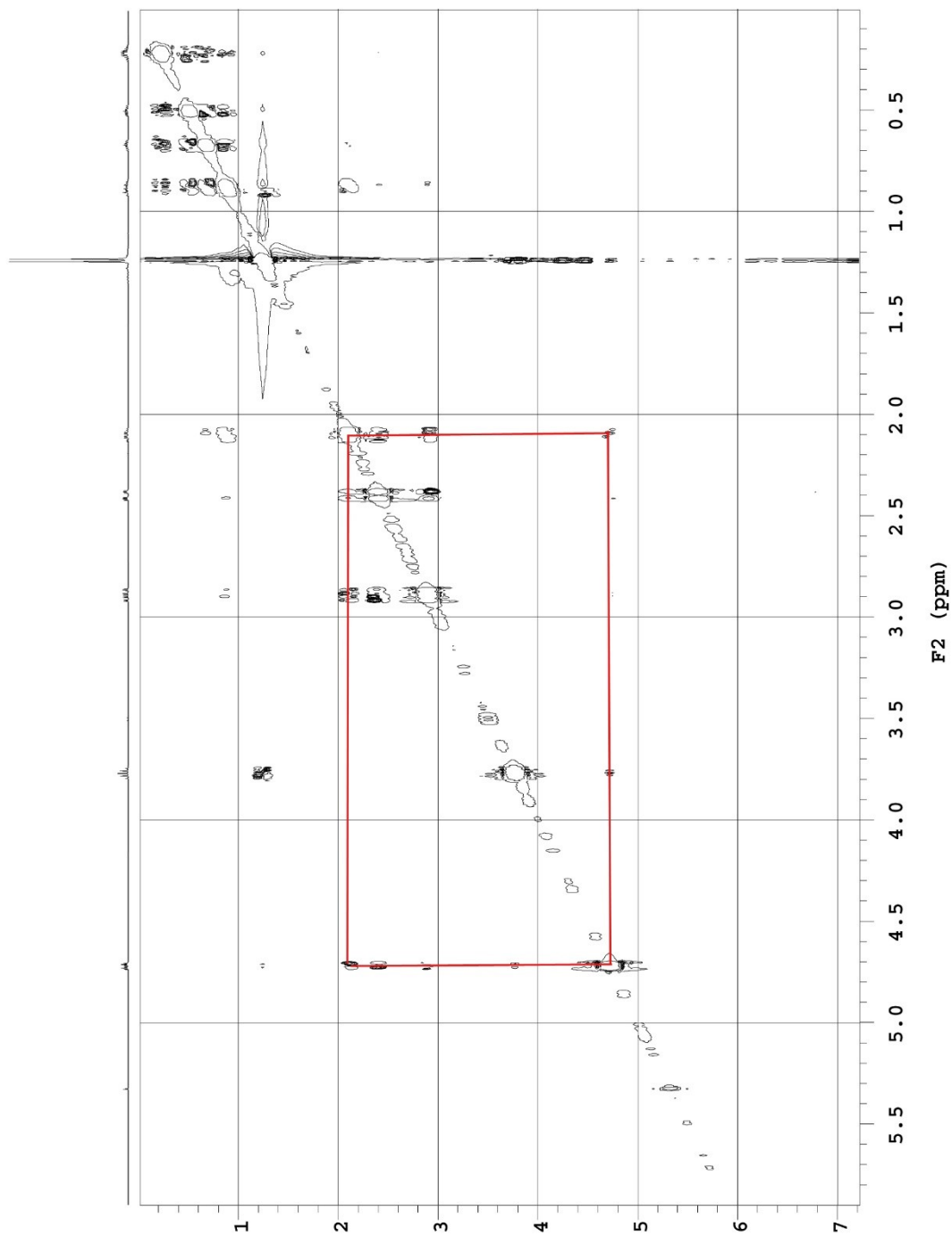


125.693 MHz C13[H1] 1D in cdcl3 (ref. to CDC13 @ 77.06 ppm), temp 27.7 C -> actual temp = 27.0 C, coldlual probe



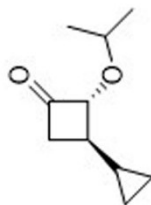


499.815 MHz H1 ROESY in cdcl3 (ref. to CDCl3 @ 7.26 ppm), temp 27.7 C -> actual temp = 27.0 C, coldlual probe

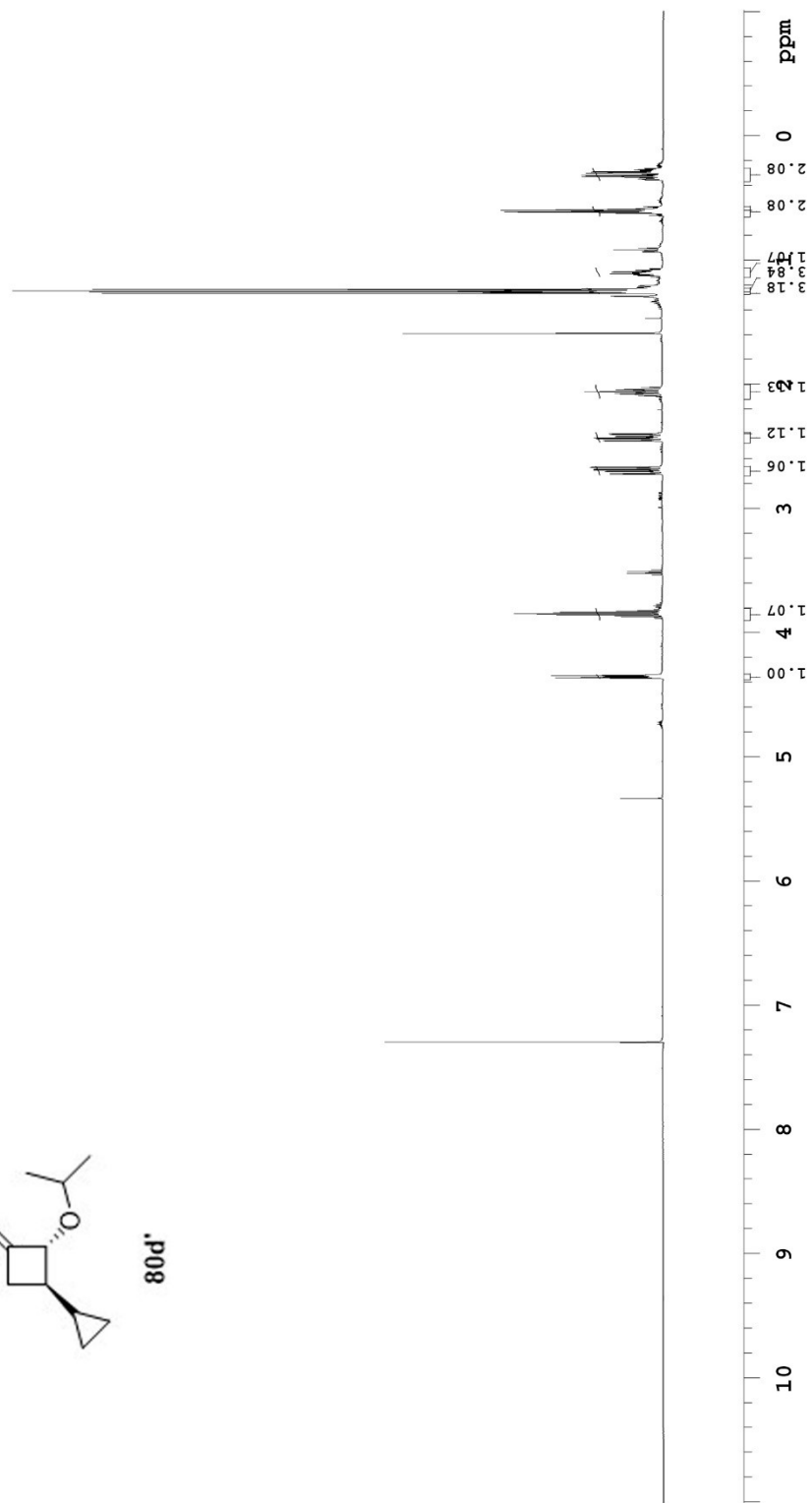




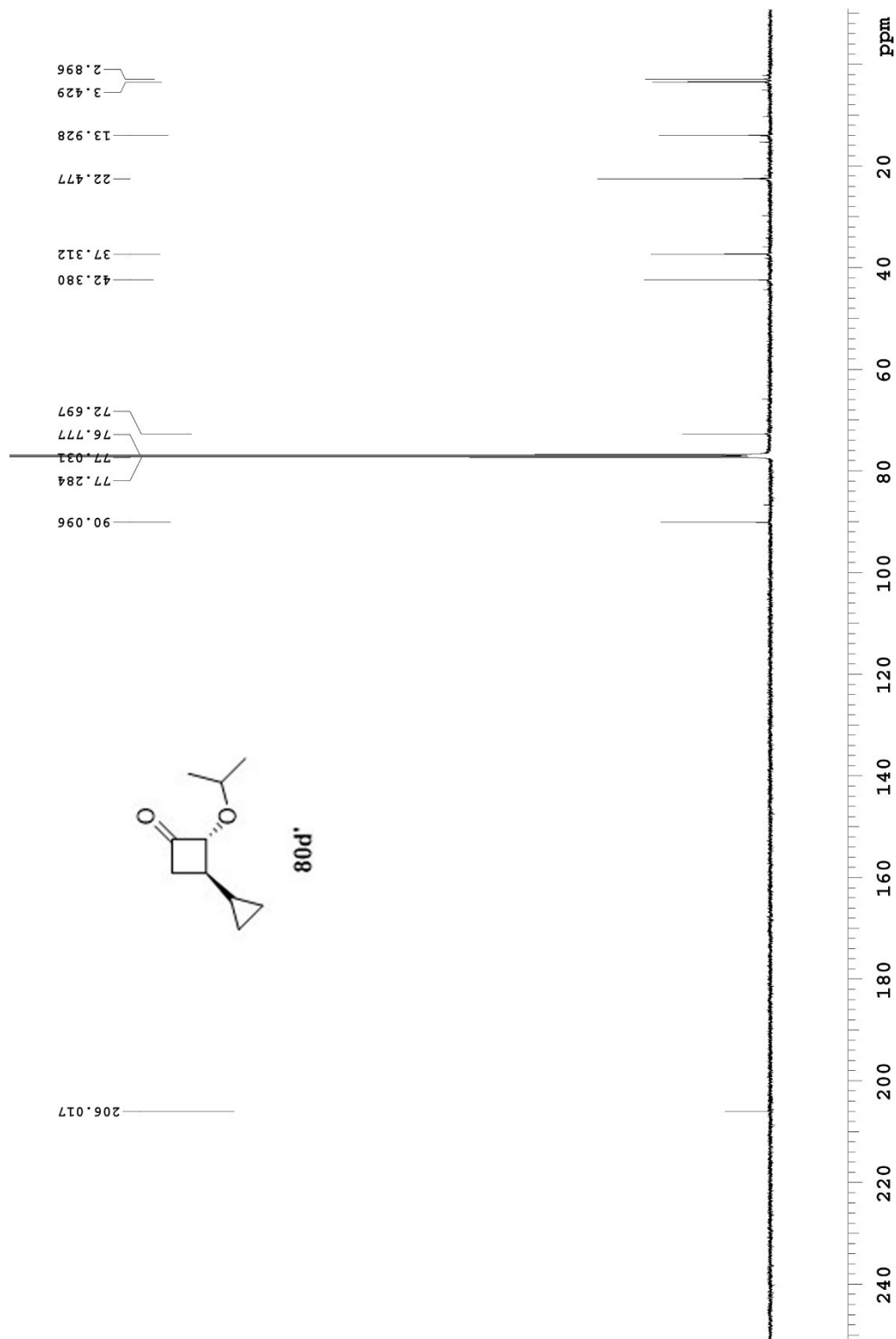
499.815 MHz <sup>1</sup>H PRESAT in cdcl<sub>3</sub> (ref. to cdcl<sub>3</sub> @ 7.26 ppm), temp 27.7 C -> actual temp = 27.0 C, coldlual probe



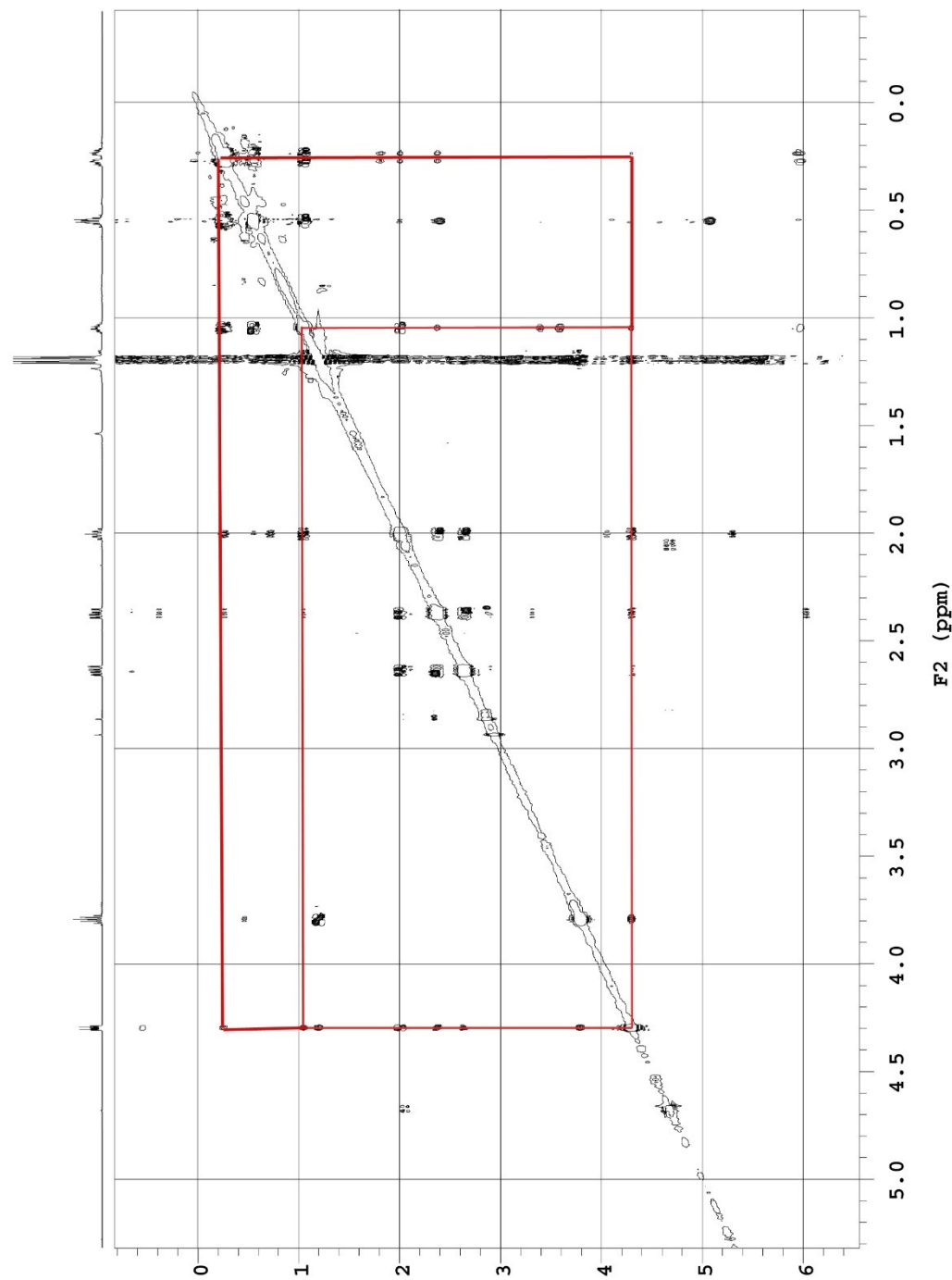
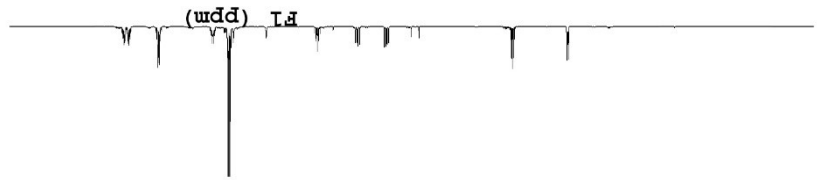
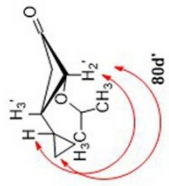
80d'



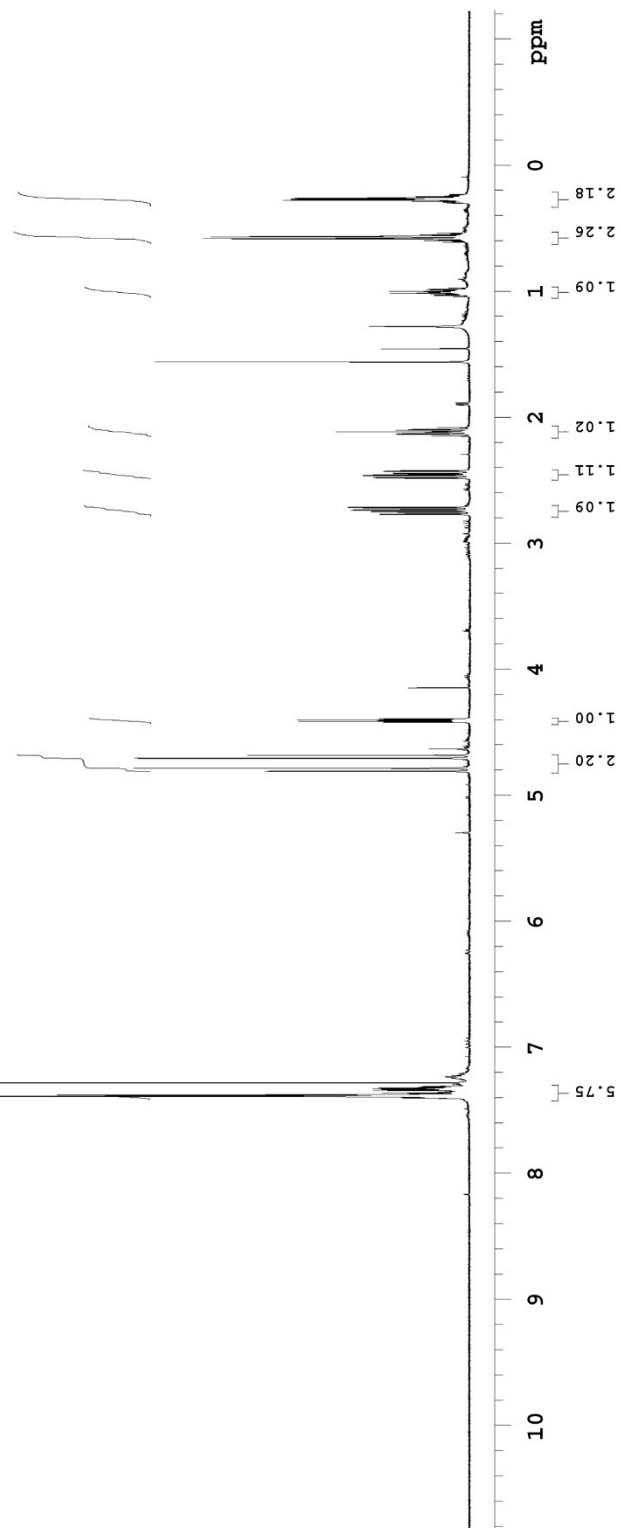
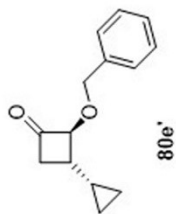
125.683 MHz C13[H1] 1D in cdcl3 (ref. to CDC13 @ 77.06 ppm), temp 27.7 C -> actual temp = 27.0 C, coldlual probe



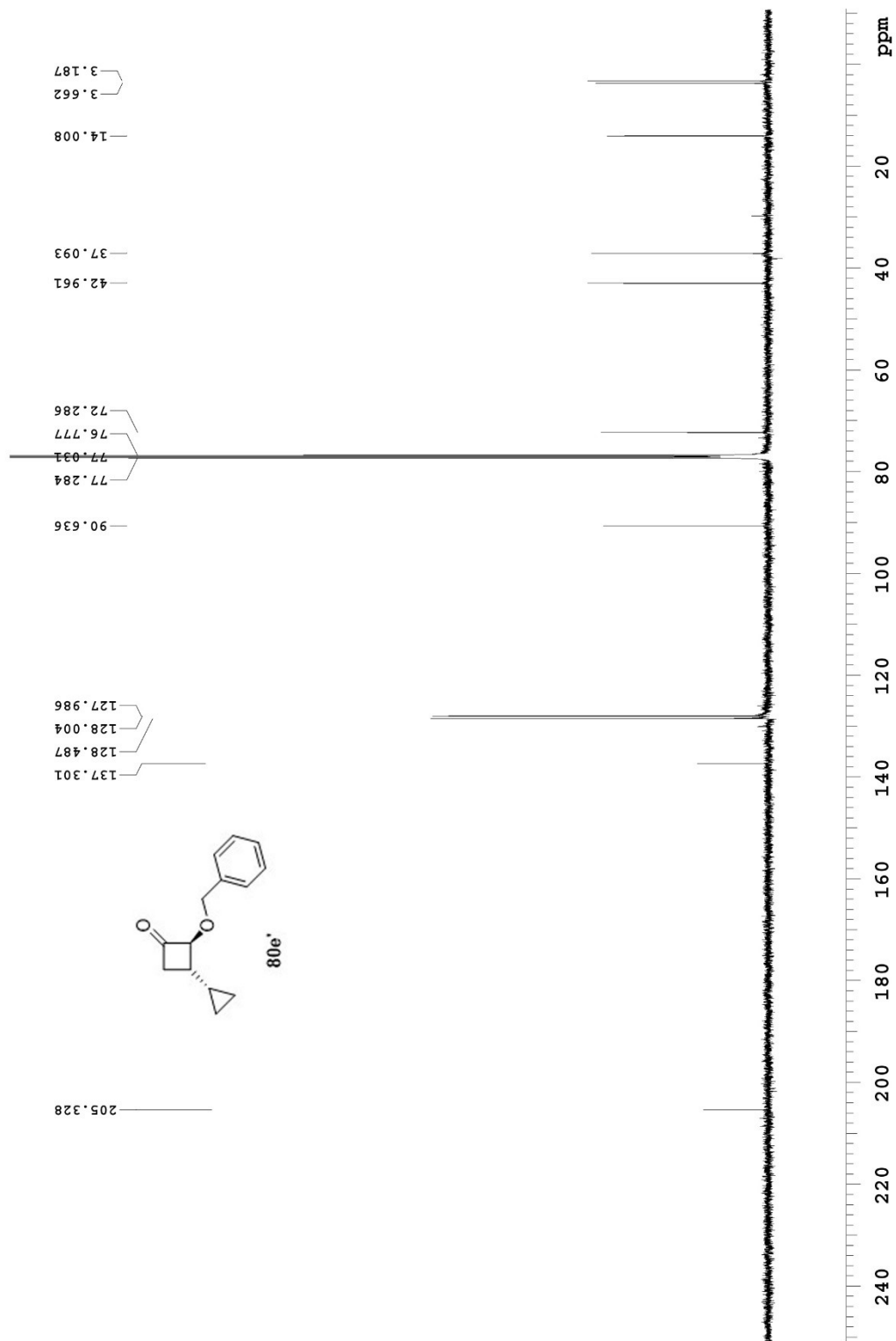
699.769 MHz <sup>1</sup>H1 ROESY in cdcl3 (ref. to CDC13 @ 7.26 ppm), temp 27.5 C -> actual temp = 27.0 C, coldid probe



498.118 MHz H1 1D in cdcl3 (ref. to CDC13 @ 7.26 ppm), temp 27.2 C -> actual temp = 27.0 C, autotxdb probe

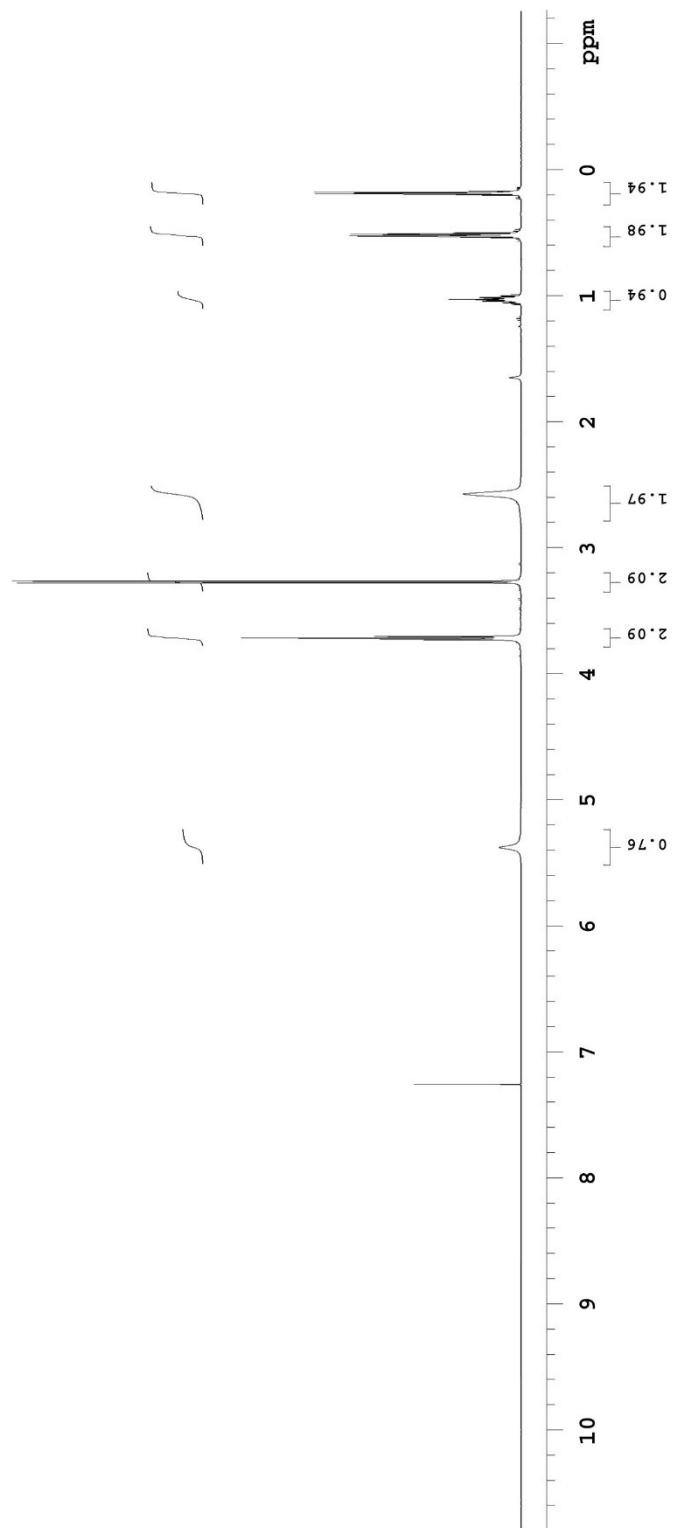
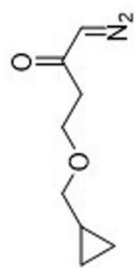


125.693 MHz C13[H1] 1D in cdcl3 (ref. to CDCl3 @ 77.06 ppm), temp 27.7 C -> actual temp = 27.0 C, coldtial probe

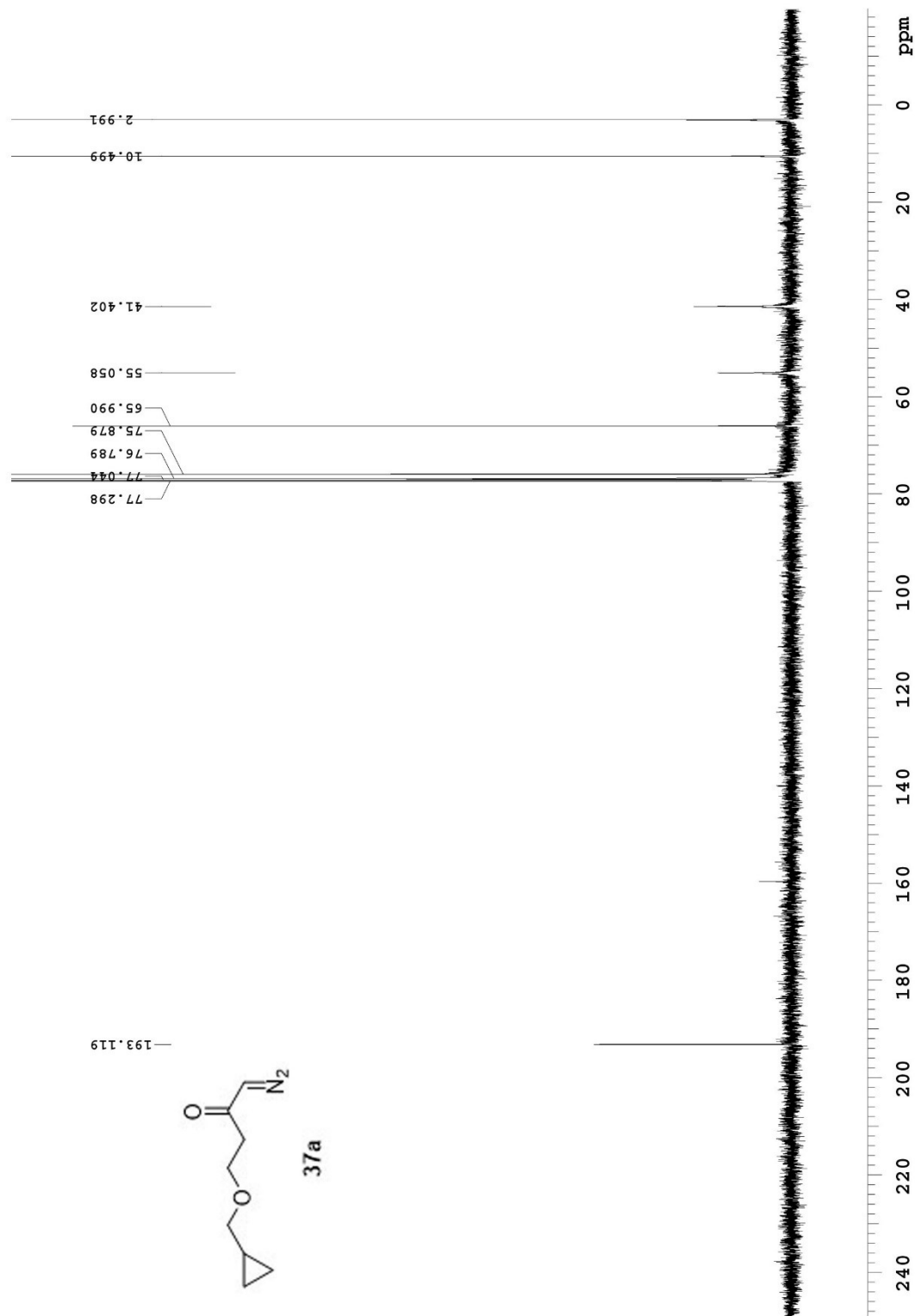


## Appendix II: Selected NMR Spectra (Chapter 3)

498.122 MHz H1 1D in cdcl3 (ref. to cdcl3 @ 7.26 ppm), temp 27.2 C -> actual temp = 27.0 C, autotxdb probe

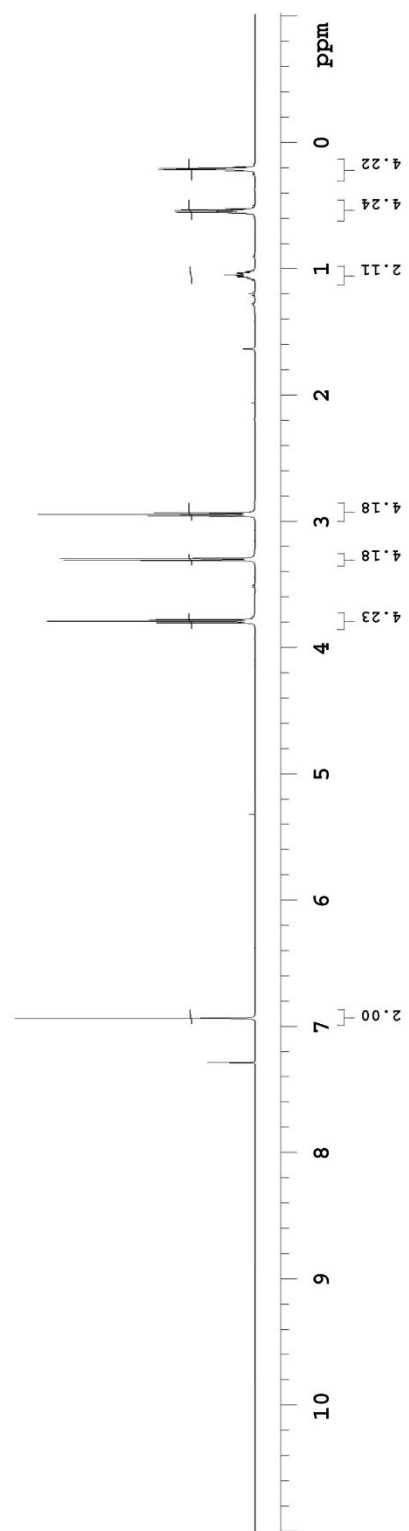
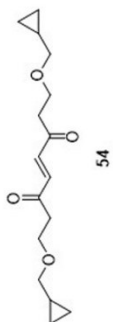


125.690 MHz C13[1H] 1D in cdcl3 (ref. to cdcl3 @ 77.06 ppm), temp 27.7 C -> actual temp = 27.0 C, coldlual probe

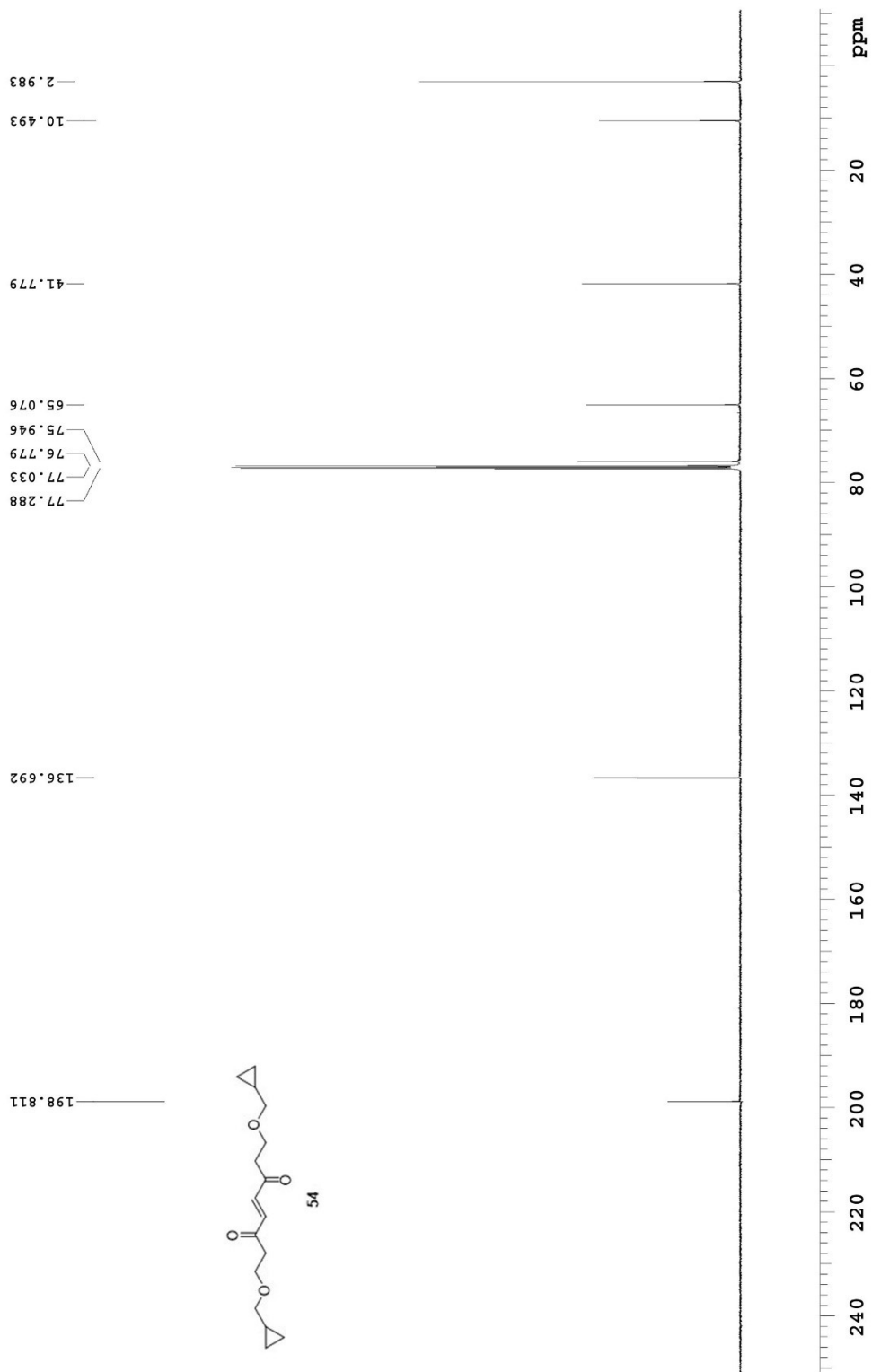




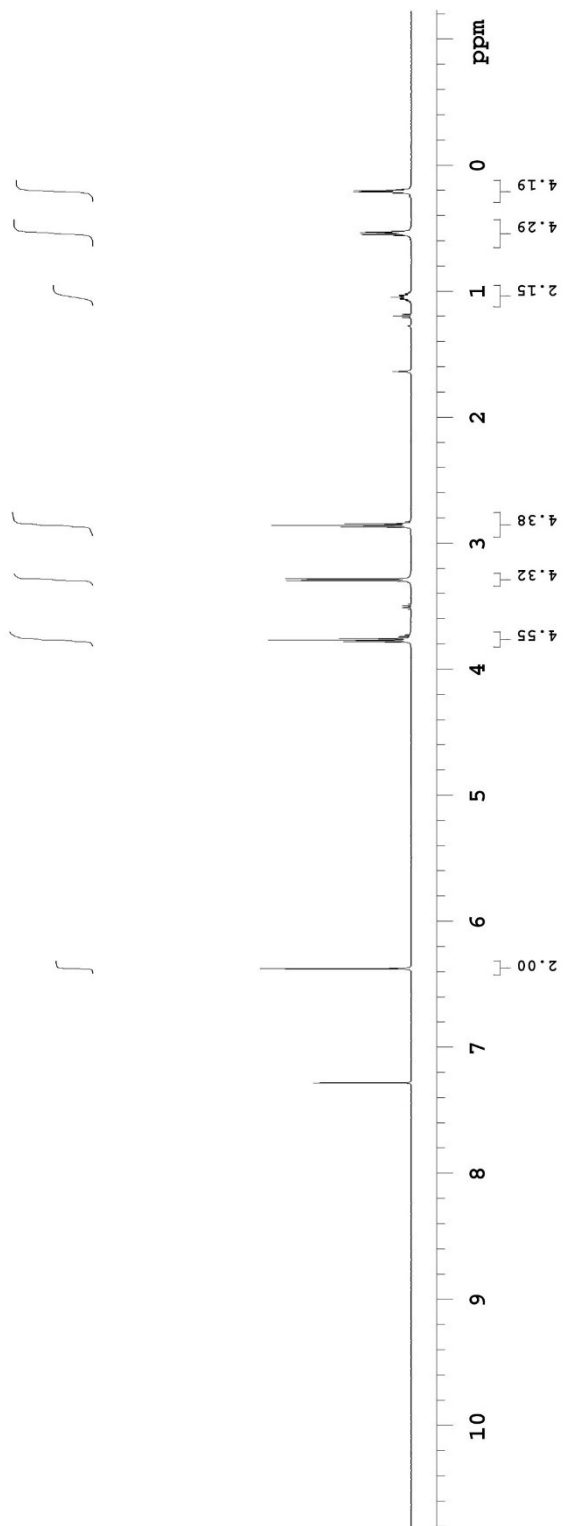
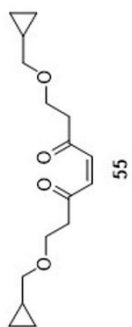
499.806 MHz <sup>1</sup>H PRESAT in cdcl<sub>3</sub> (ref. to cdcl<sub>3</sub> @ 7.26 ppm), temp 27.7 C -> actual temp = 27.0 C, coldludal probe



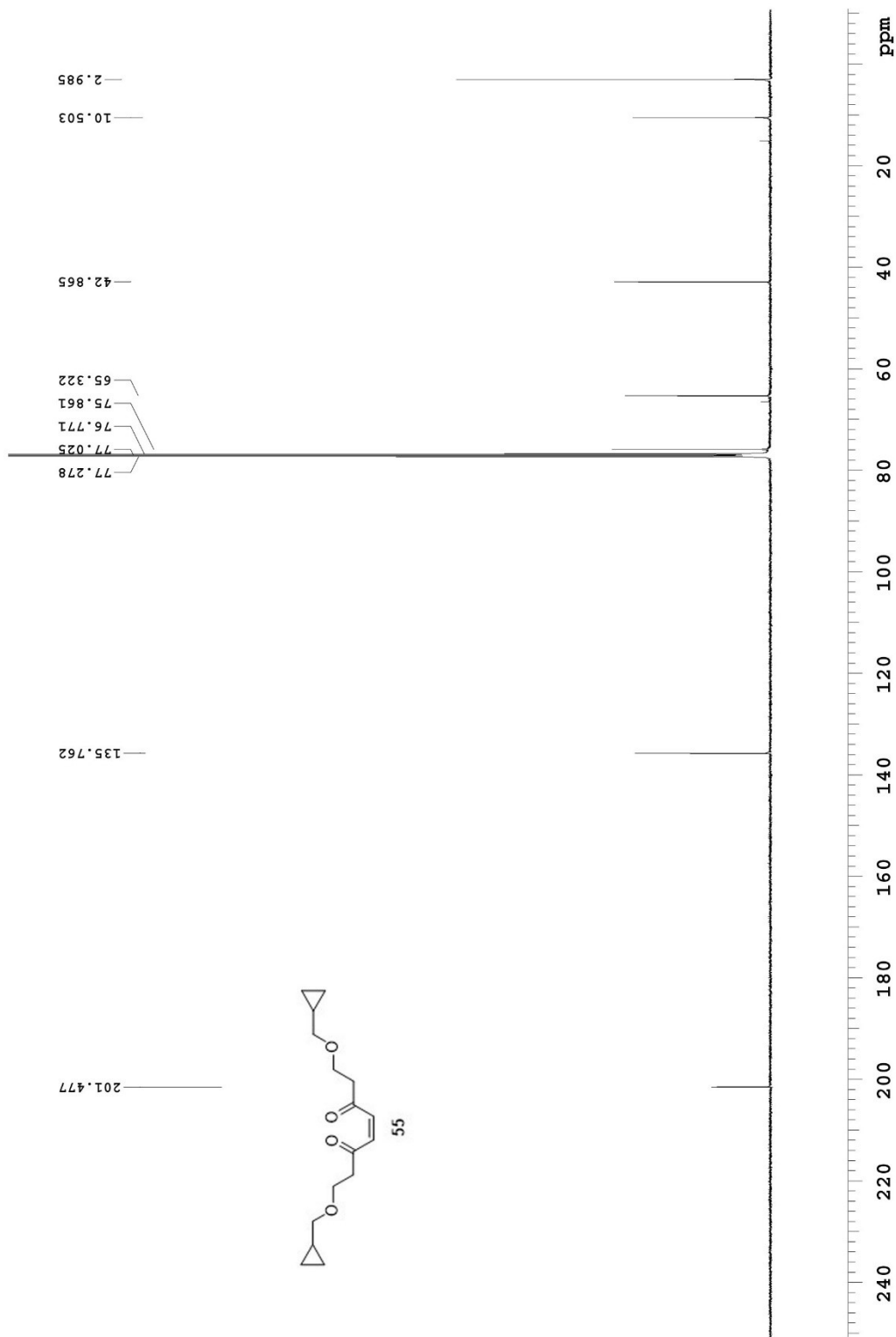
125.691 MHz C13[H1] 1D in cdc13 (ref. to CDC13 @ 77.06 ppm), temp 27.7 C -> actual temp = 27.0 C, coldddual probe



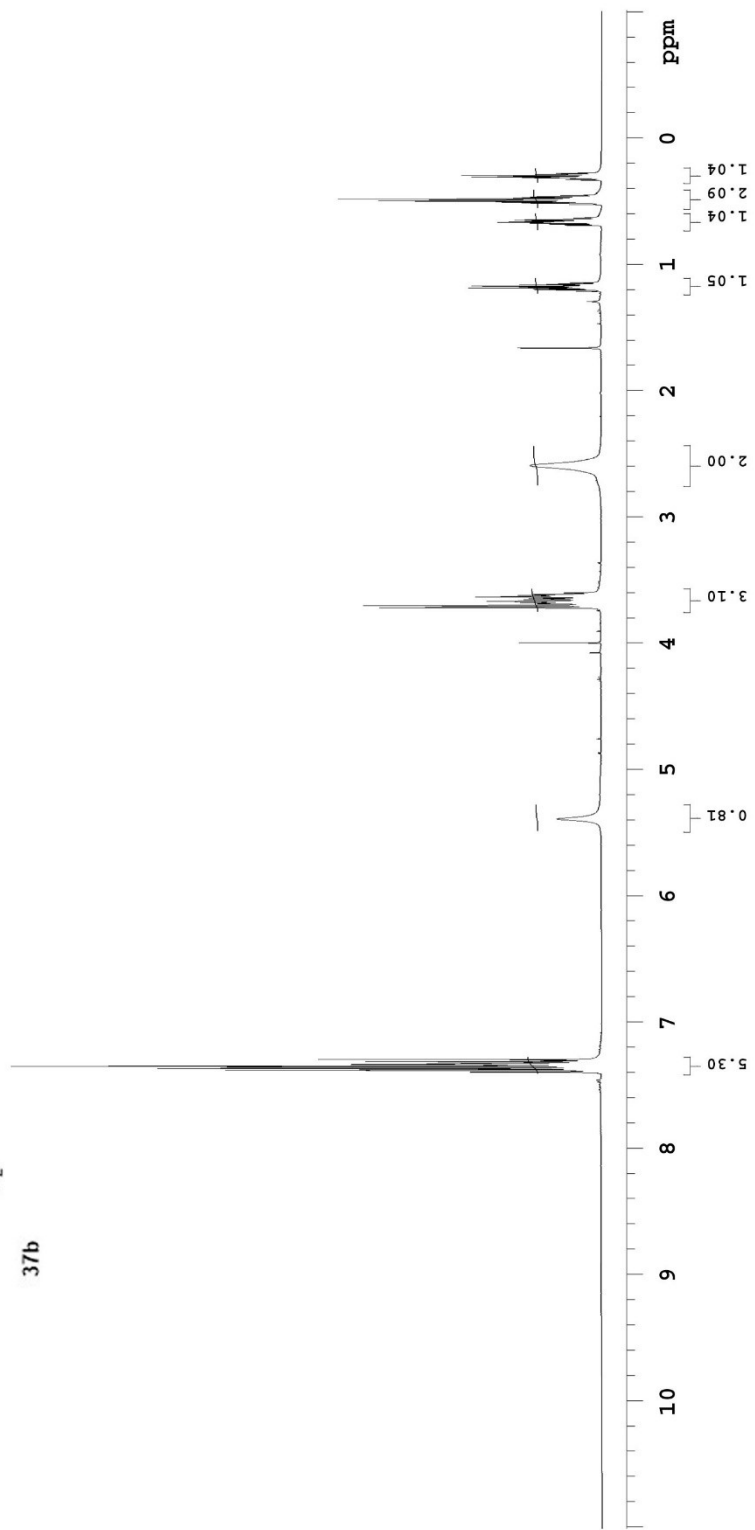
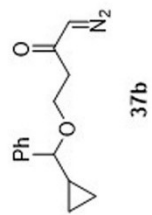
498.118 MHz H1 1D in cdcl3 (ref. to CDC13 @ 7.26 ppm), temp 26.4 C -> actual temp = 27.0 C, autotxdb probe

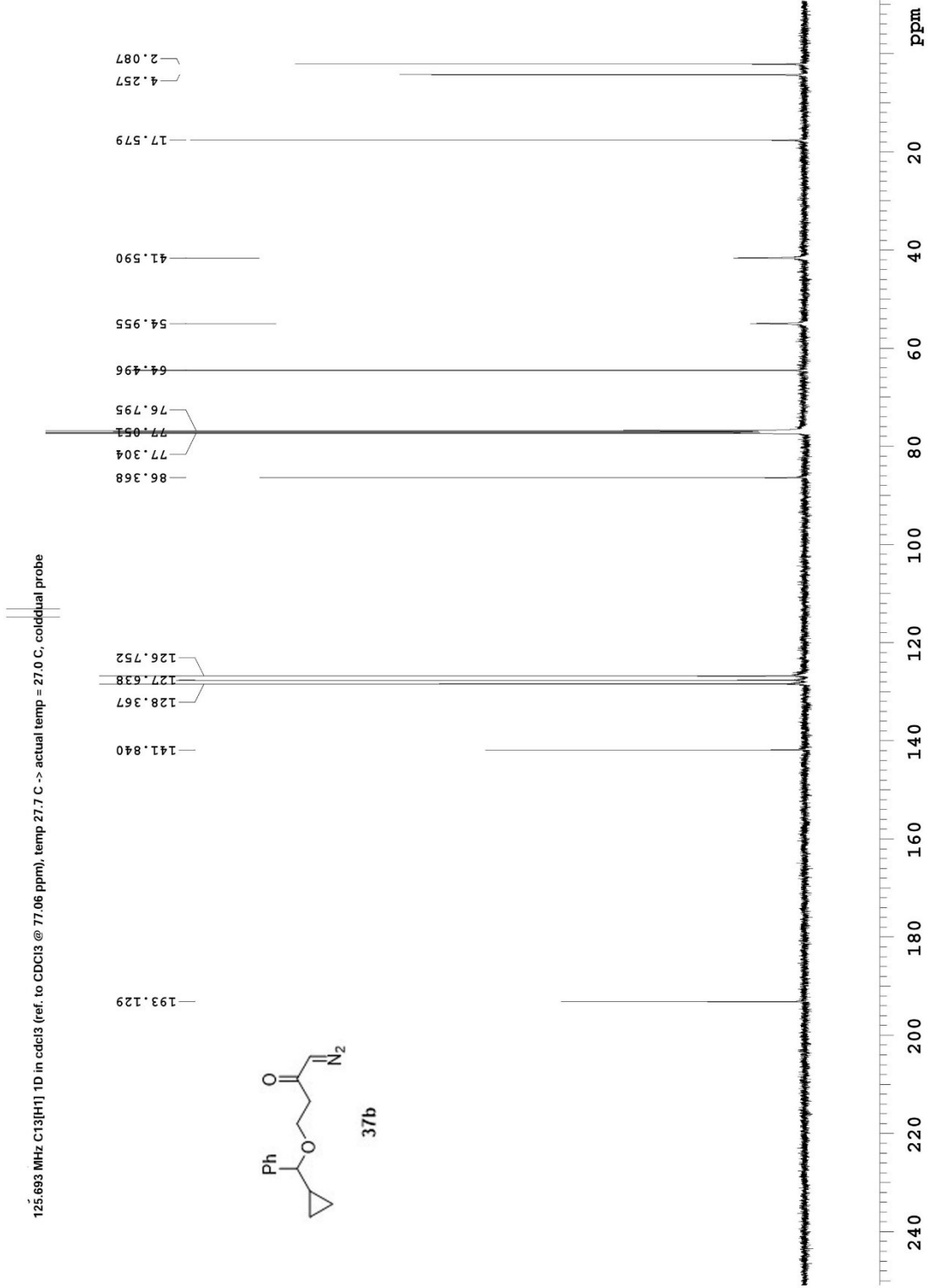


125.691 MHz C13[H1] 1D in cdcl3 (ref. to CDC13 @ 77.06 ppm), temp 27.7 C -> actual temp = 27.0 C, coldltdal probe

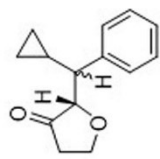


499.815 MHz H1 PRESAT in cdcl3 (ref. to CDC13 @ 7.26 ppm), temp 27.7 C -> actual temp = 27.0 C, coldludal probe

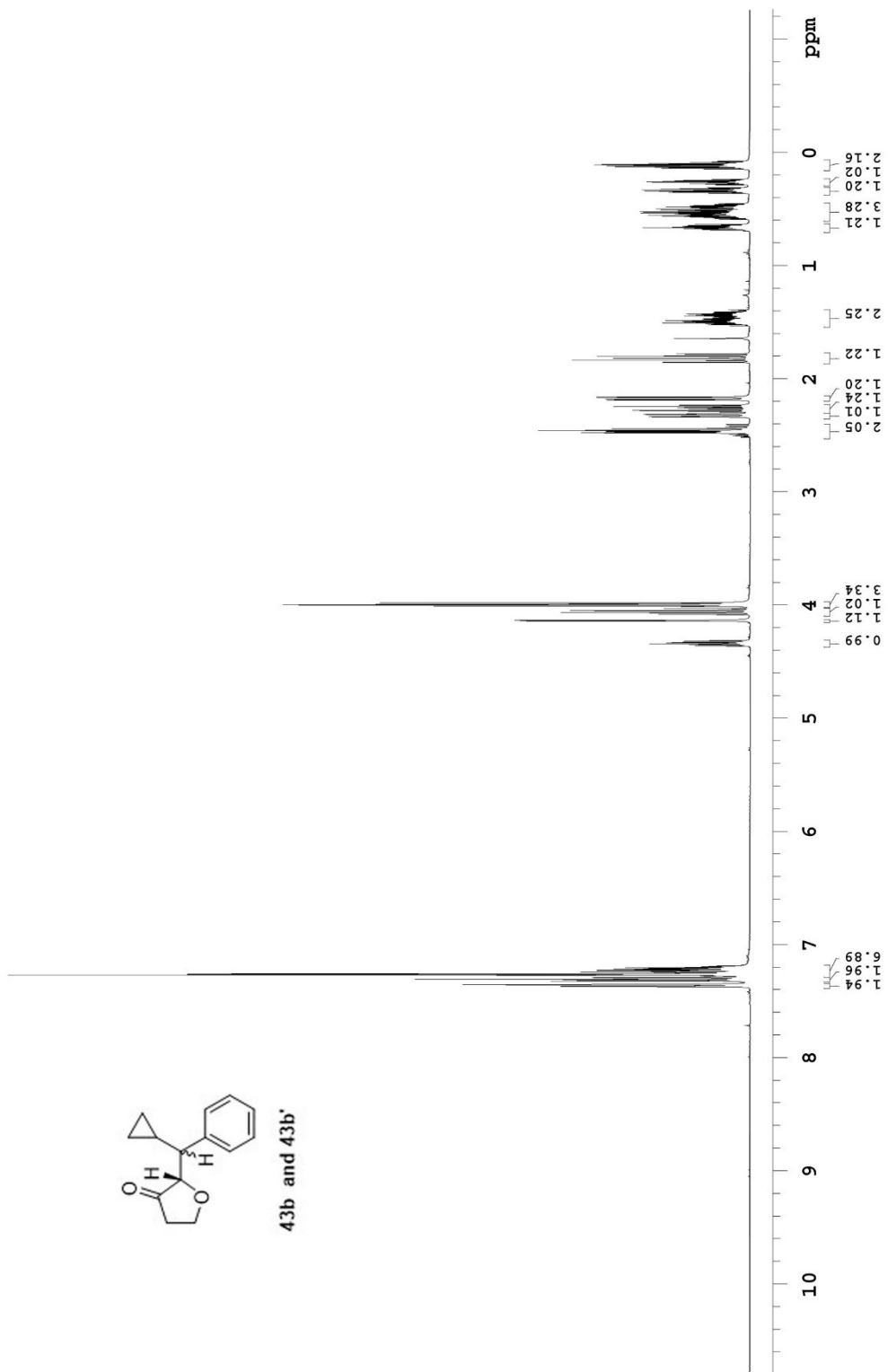




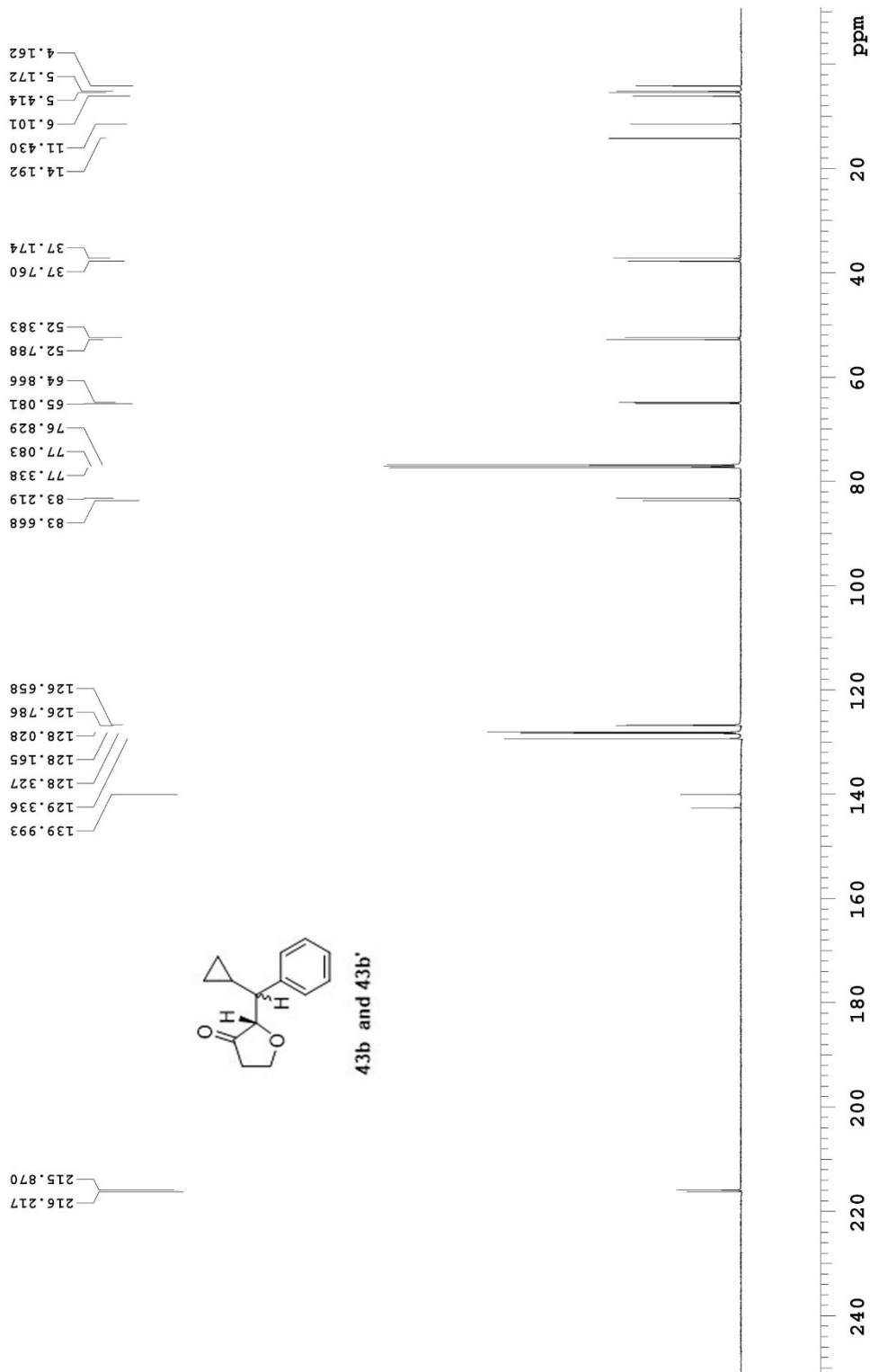
498.122 MHz H1 1D in cdcl3 (ref. to CDC13 @ 7.26 ppm), temp 27.2 C -> actual temp = 27.0 C, autotxdb probe



43b and 43b'

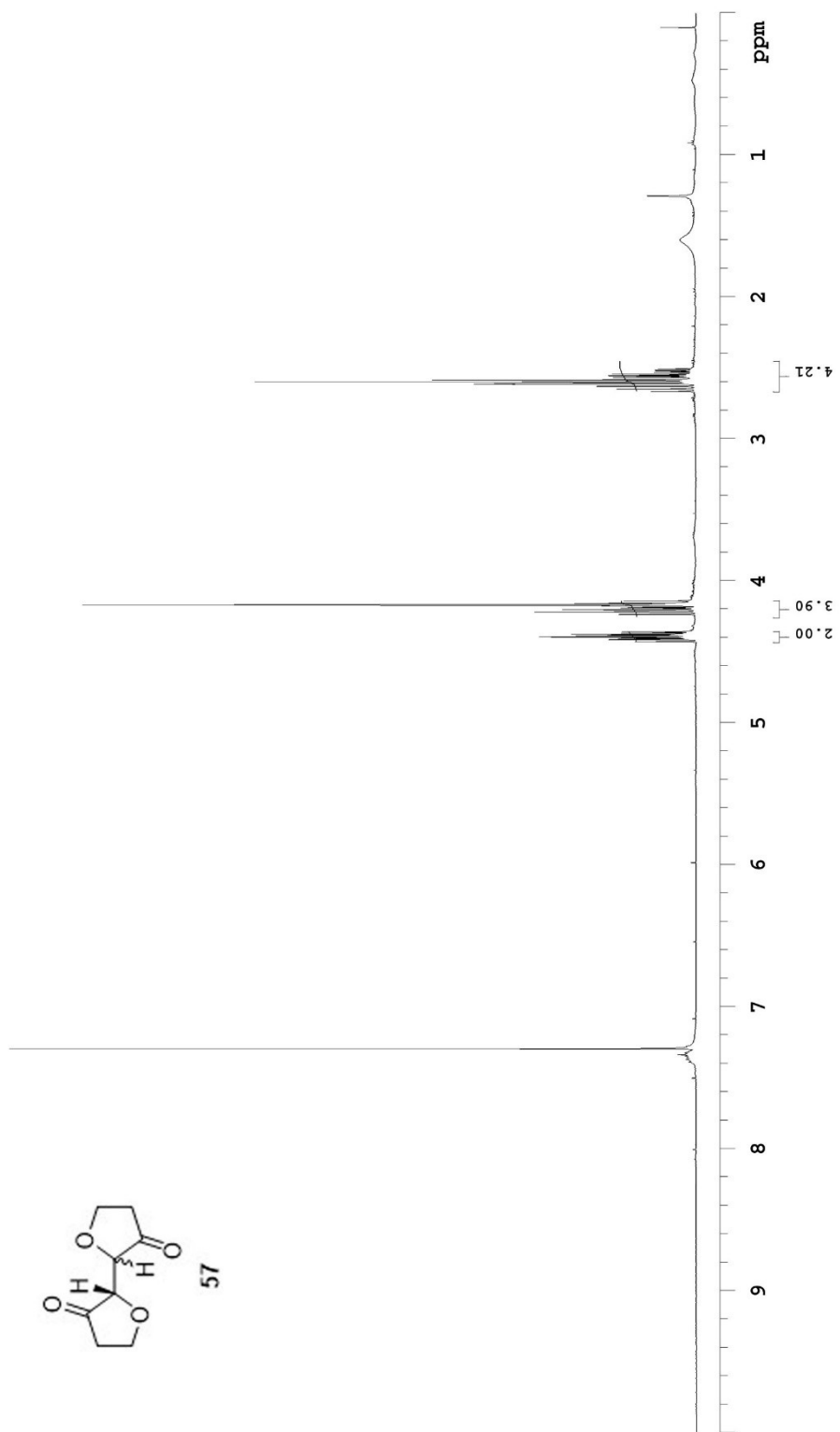


125.693 MHz C13{H1} TD in cdcl3 (ref. to CDCl3 @ 77.06 ppm), temp 27.7 C -> actual temp = 27.0 C, coldludal probe

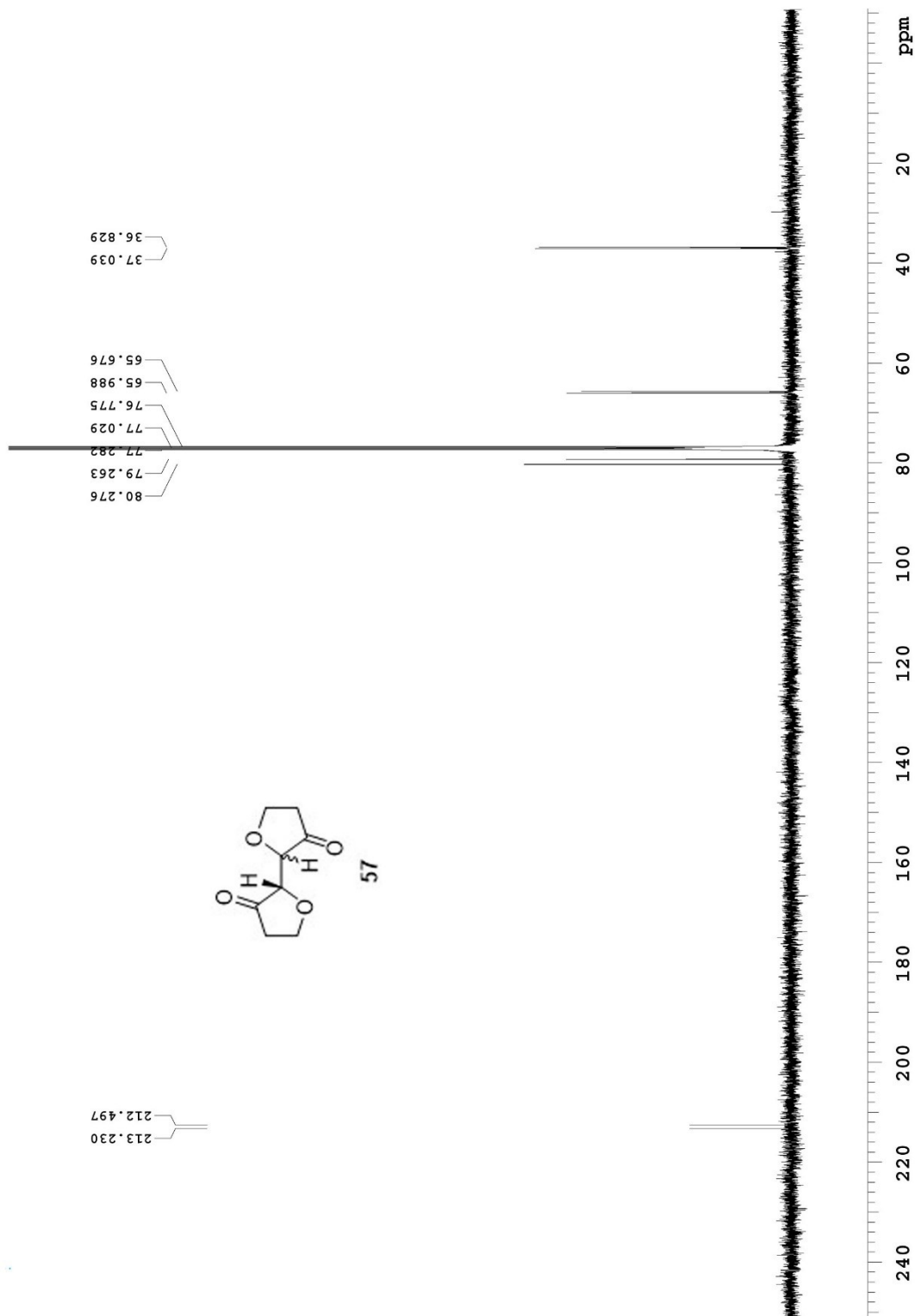




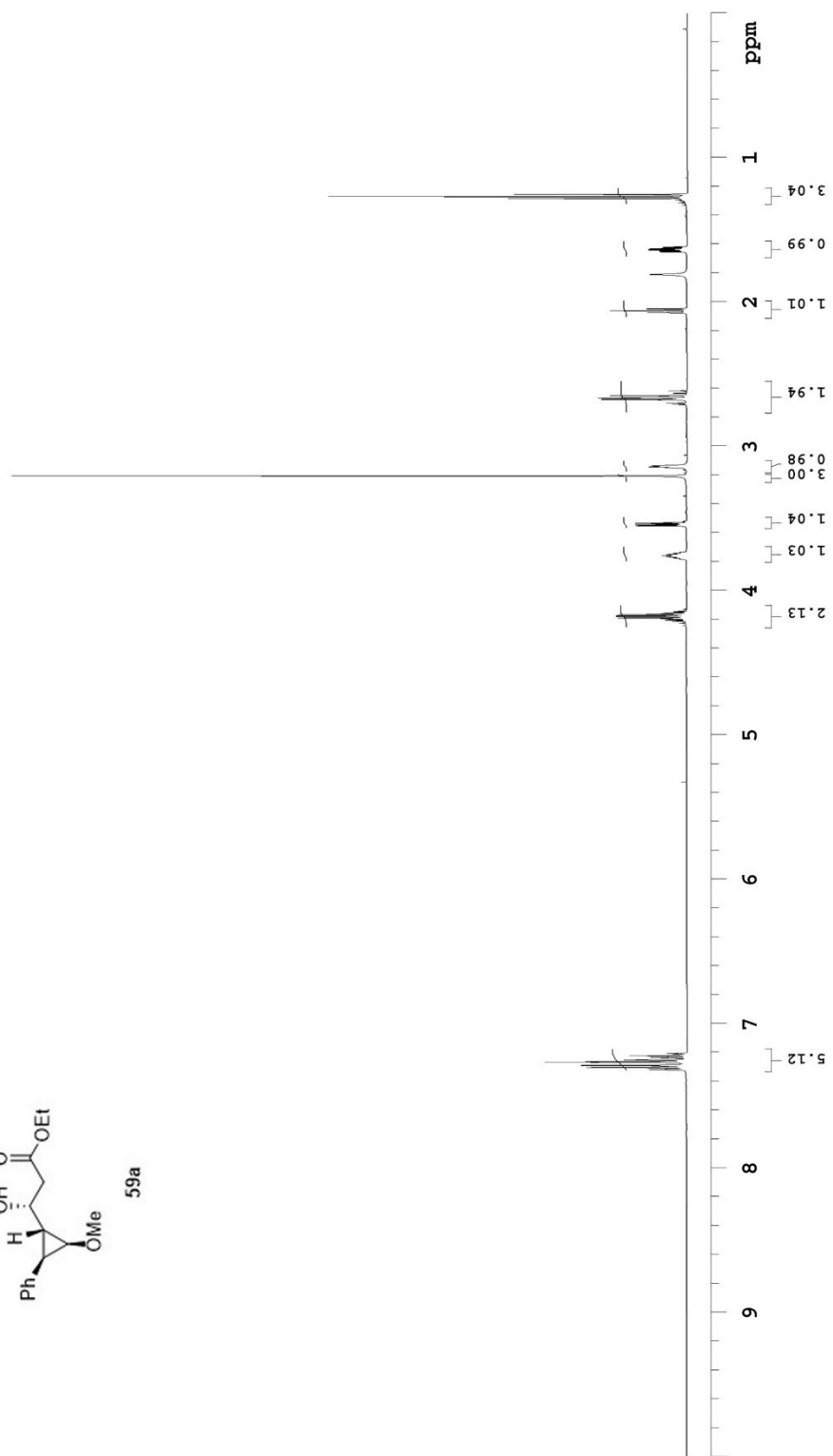
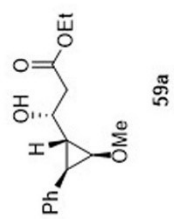
499.815 MHz H1 PRESAT in cdcl3 (ref. to CDC13 @ 7.26 ppm), temp 27.7 C -> actual temp = 27.0 C, cold dual probe



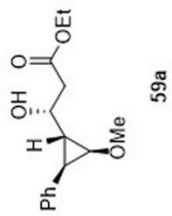
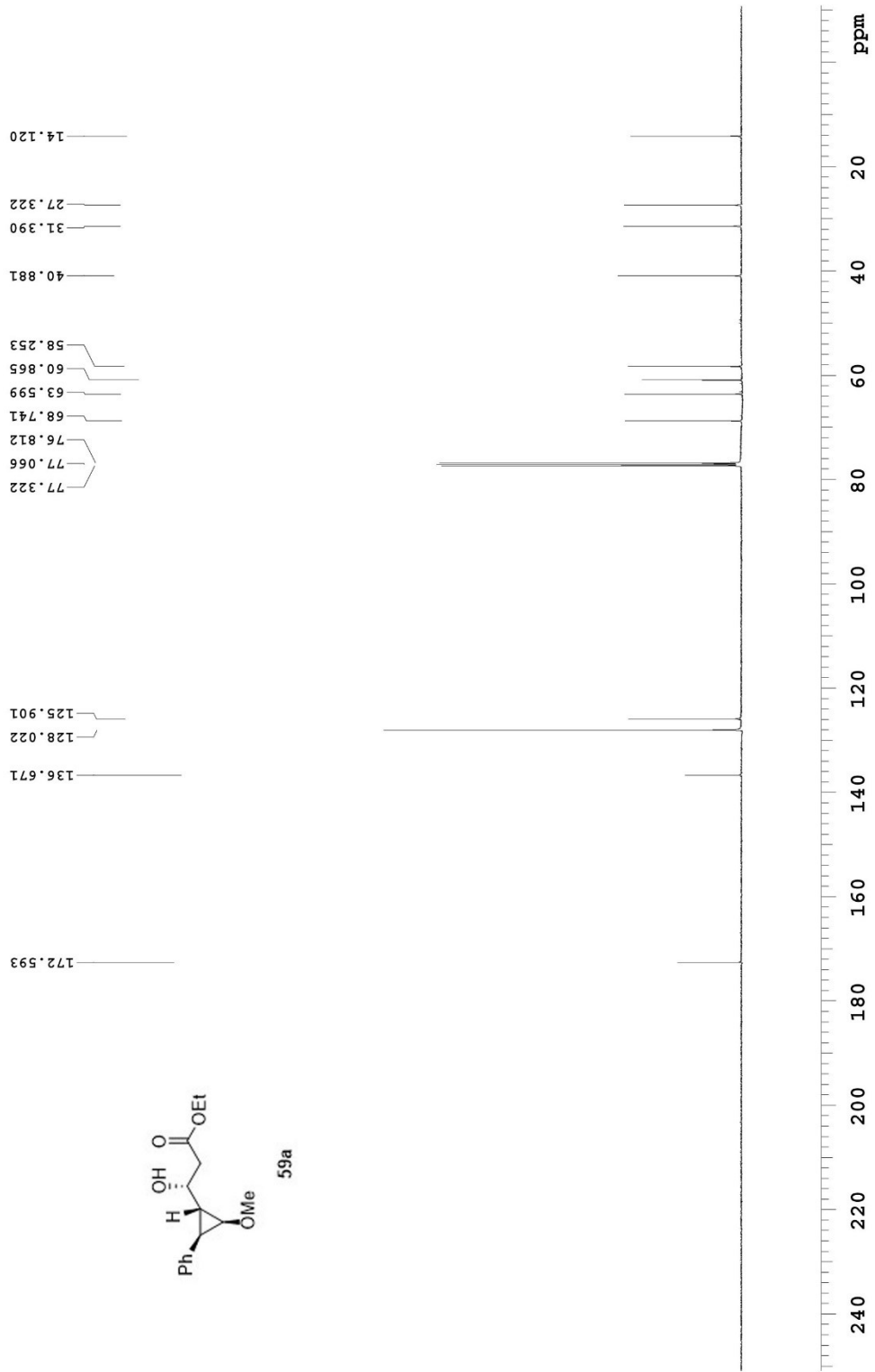
125.693 MHz C13[H1] 1D in cdcl3 (ref. to CDCl3 @ 77.06 ppm), temp 27.7 C -> actual temp = 27.0 C, coldlual probe



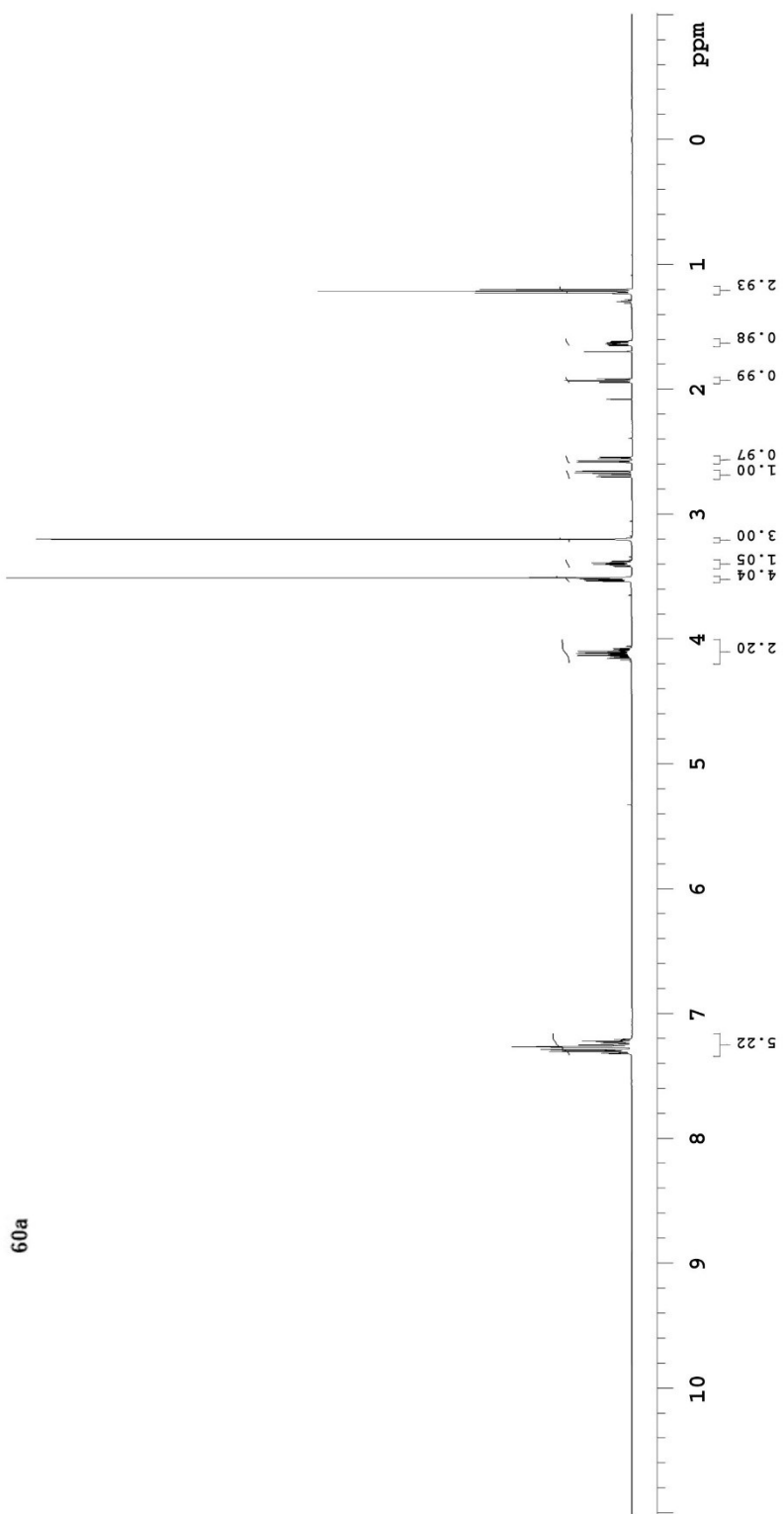
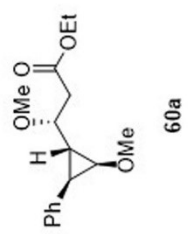
499.806 MHz H1 PRESAT in cdcl3 (ref. to CDC13 @ 7.26 ppm), temp 27.7 C -> actual temp = 27.0 C, coldlual probe



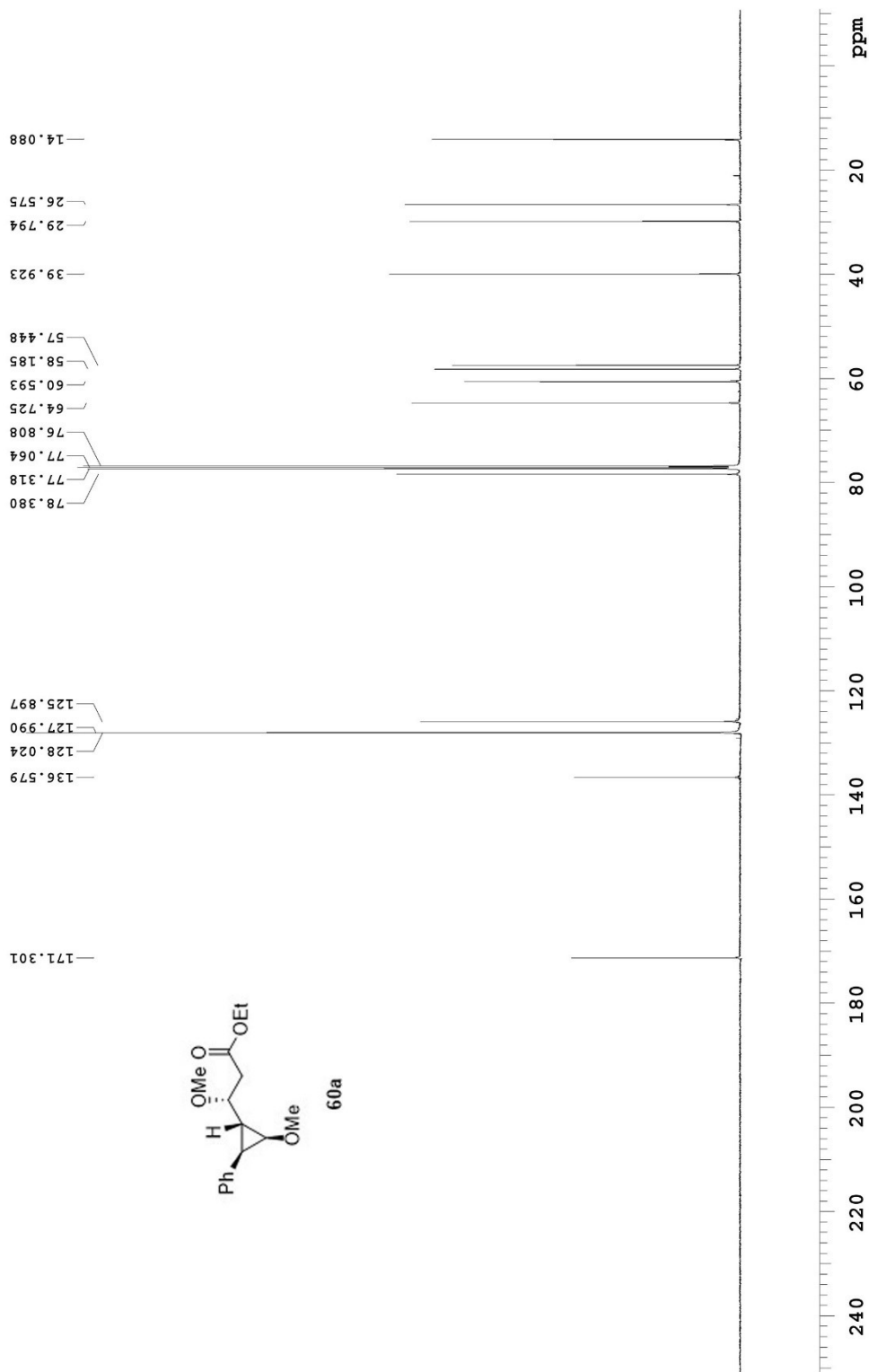
125.691 MHz C13[H1] 1D in cdcl3 (ref. to CDC13 @ 77.06 ppm), temp 27.7 C -> actual temp = 27.0 C, cold dual probe



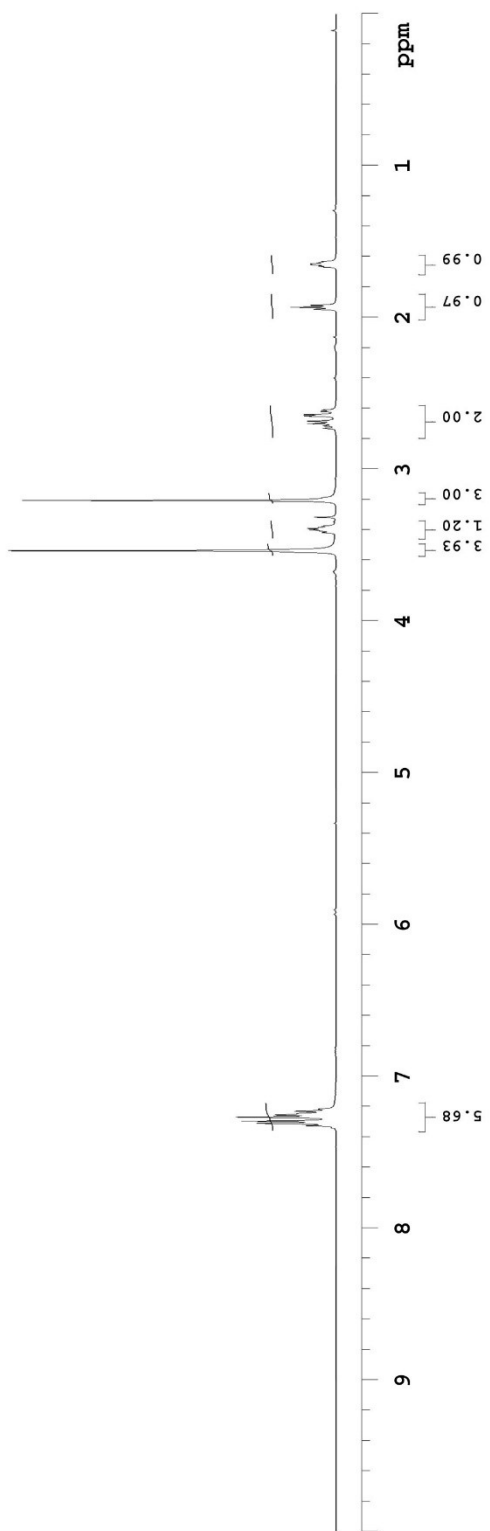
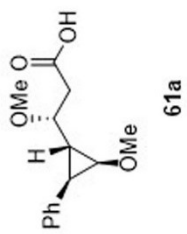
499.806 MHz HT PRESAT in cdcl3 (ref. to CDC13 @ 7.26 ppm), temp 27.7 C -> actual temp = 27.0 C, coldludal probe



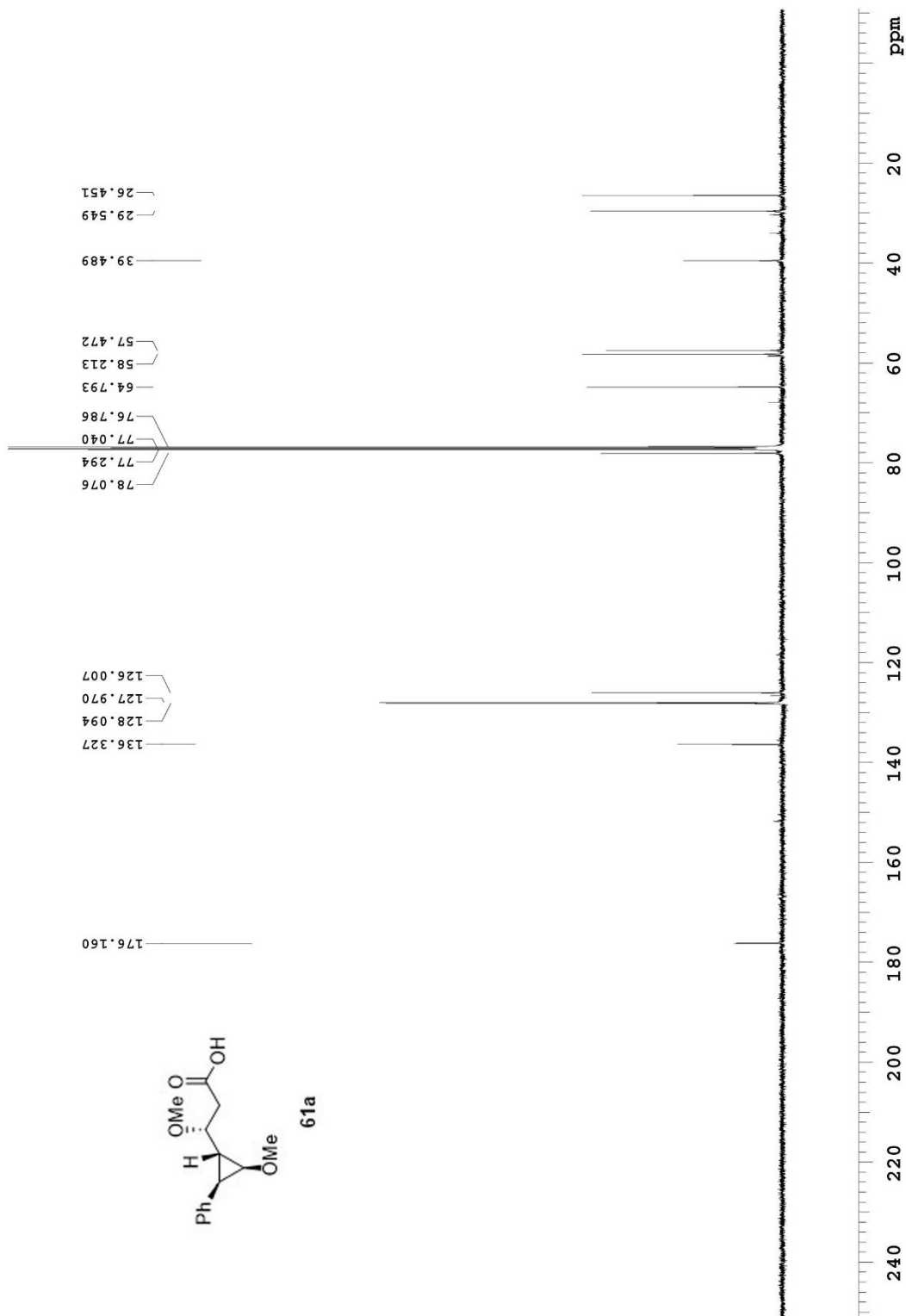
125.691 MHz C13{H1} 1D in cdcl3 (ref. to CDC13 @ 77.06 ppm), temp 27.7 C -> actual temp = 27.0 C, coldludal probe



499.806 MHz <sup>1</sup>H PRESAT in cdcl<sub>3</sub> (ref. to CDC13 @ 7.26 ppm), temp 27.7 C -> actual temp = 27.0 C, coldidul probe

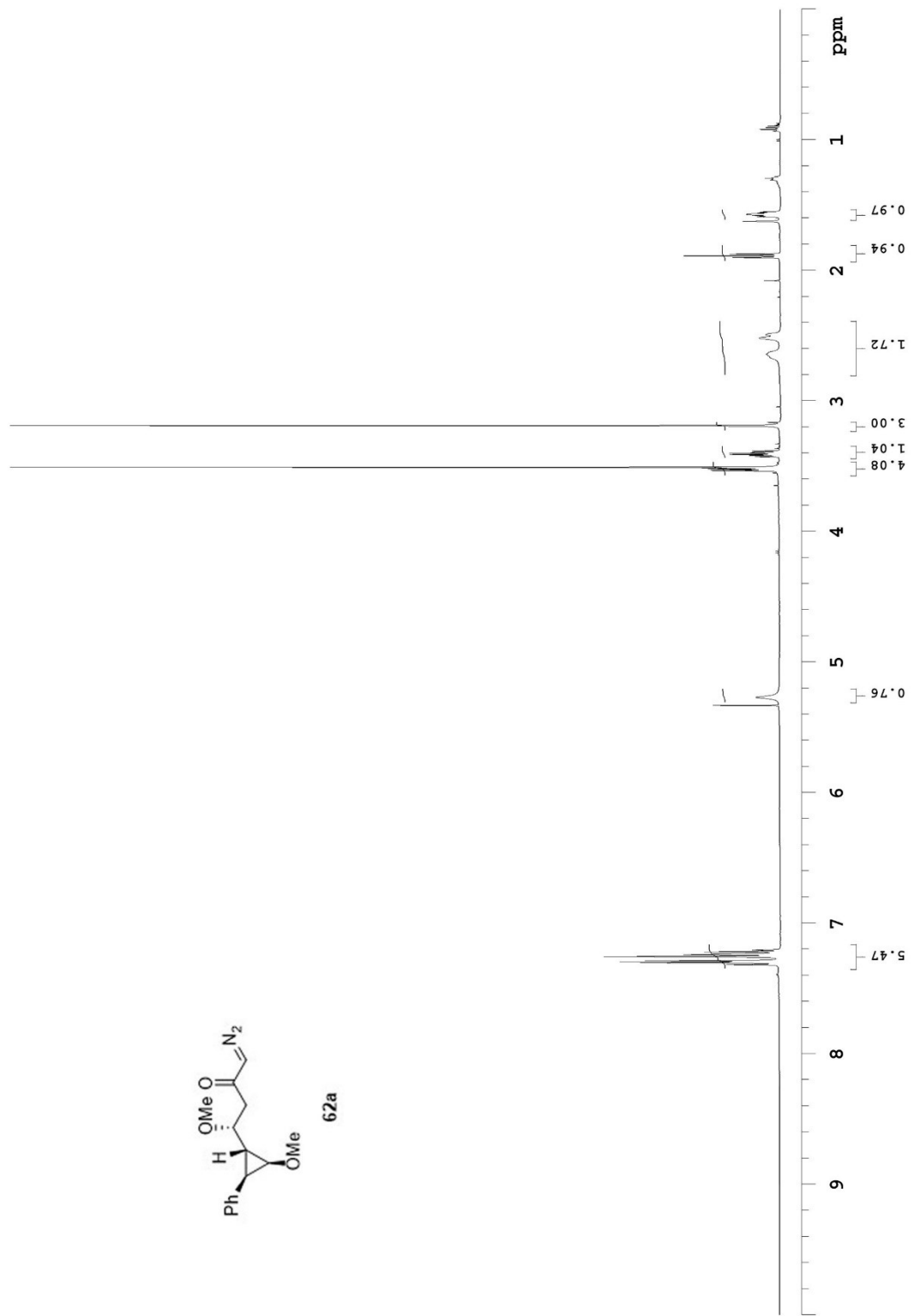
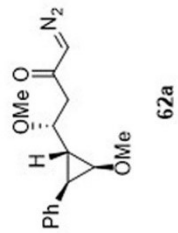


125.691 MHz C13[H1] 1D in cddi3 (ref. to CDCl3 @ 77.06 ppm), temp 27.7 C -> actual temp = 27.0 C, coldludal probe



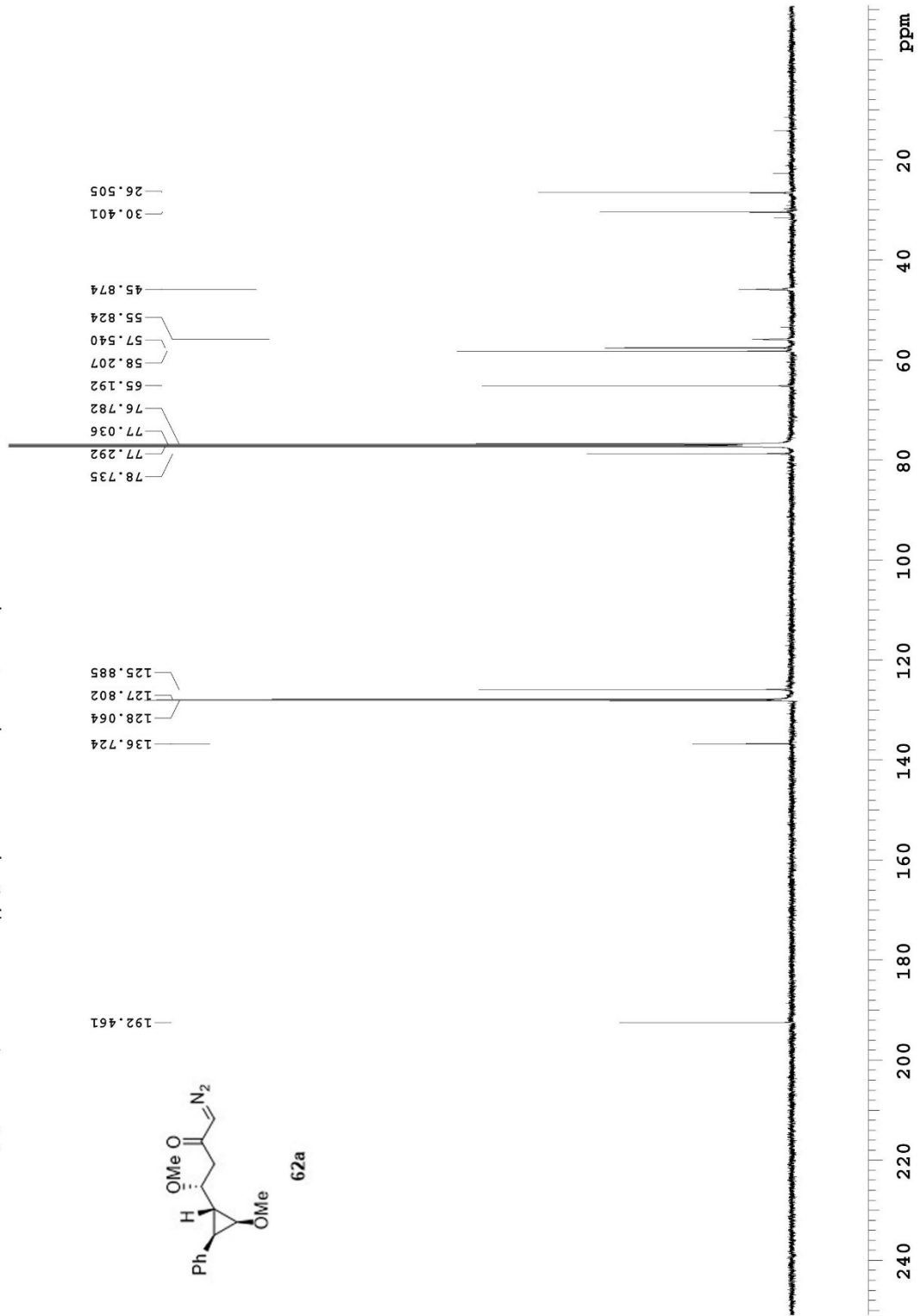
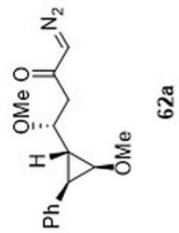


499.806 MHz H1 PRESAT in cdcl3 (ref. to CDCl3 @ 7.26 ppm), temp 27.7 C -> actual temp = 27.0 C, coldttdual probe



File: /mnt/d600/home13/westmtr/nmrdata/DATA\_FROM\_NMRSERVICE/Nargess/2014.02.19.u5\_Diazo\_coming\_from\_f2\_10.37\_H1\_1D

125.691 MHz C13[H1] 1D in cdcl3 (ref. to CDCl3 @ 77.06 ppm), temp 27.7 C -> actual temp = 27.0 C, cold dual probe





# Agilent Technologies

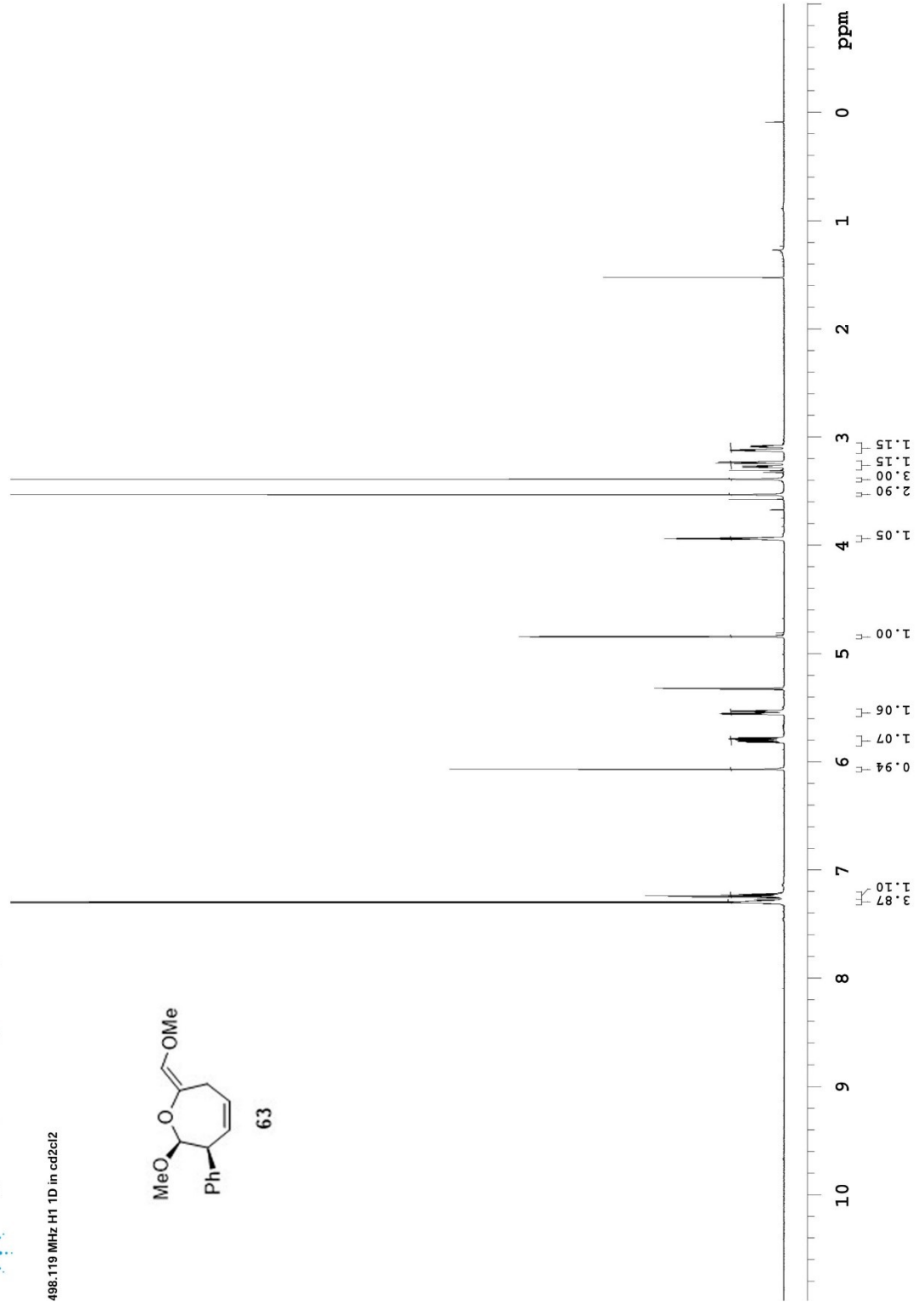
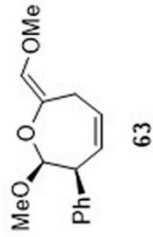
Recorded on: **Mar 6 2014**  
Pulse Sequence: **s2pul**

Sweep Width(Hz): **5971.04**  
Digital Res.(Hz/pp): **0.09**

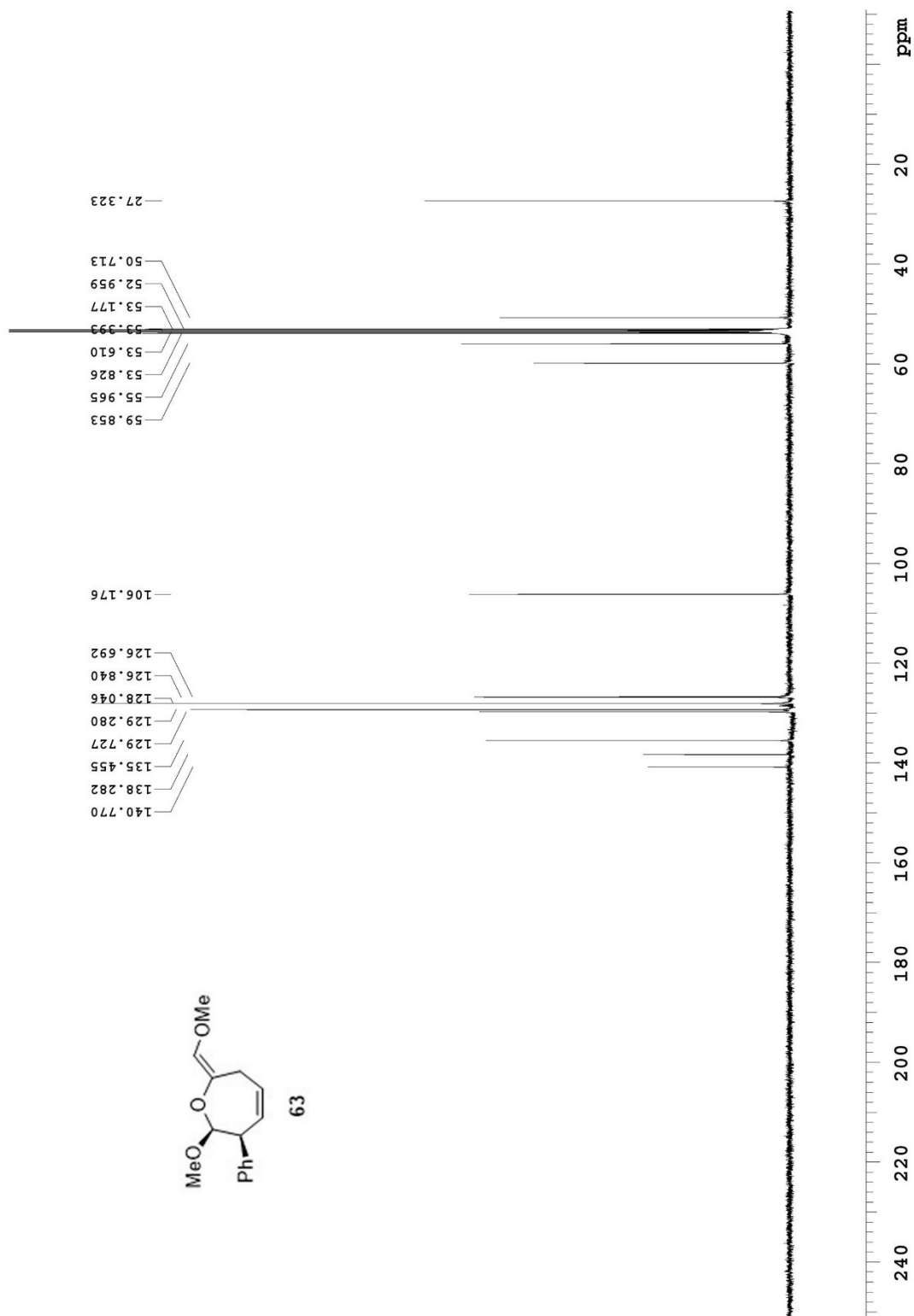
Acquisition Time(s): **5**  
Hz per mm(Hz/mm): **24.88**

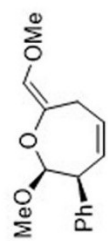
Relaxation Delay(s): **0.1**  
Completed Scans: **16**

498.119 MHz H1 1D in cd2cl2



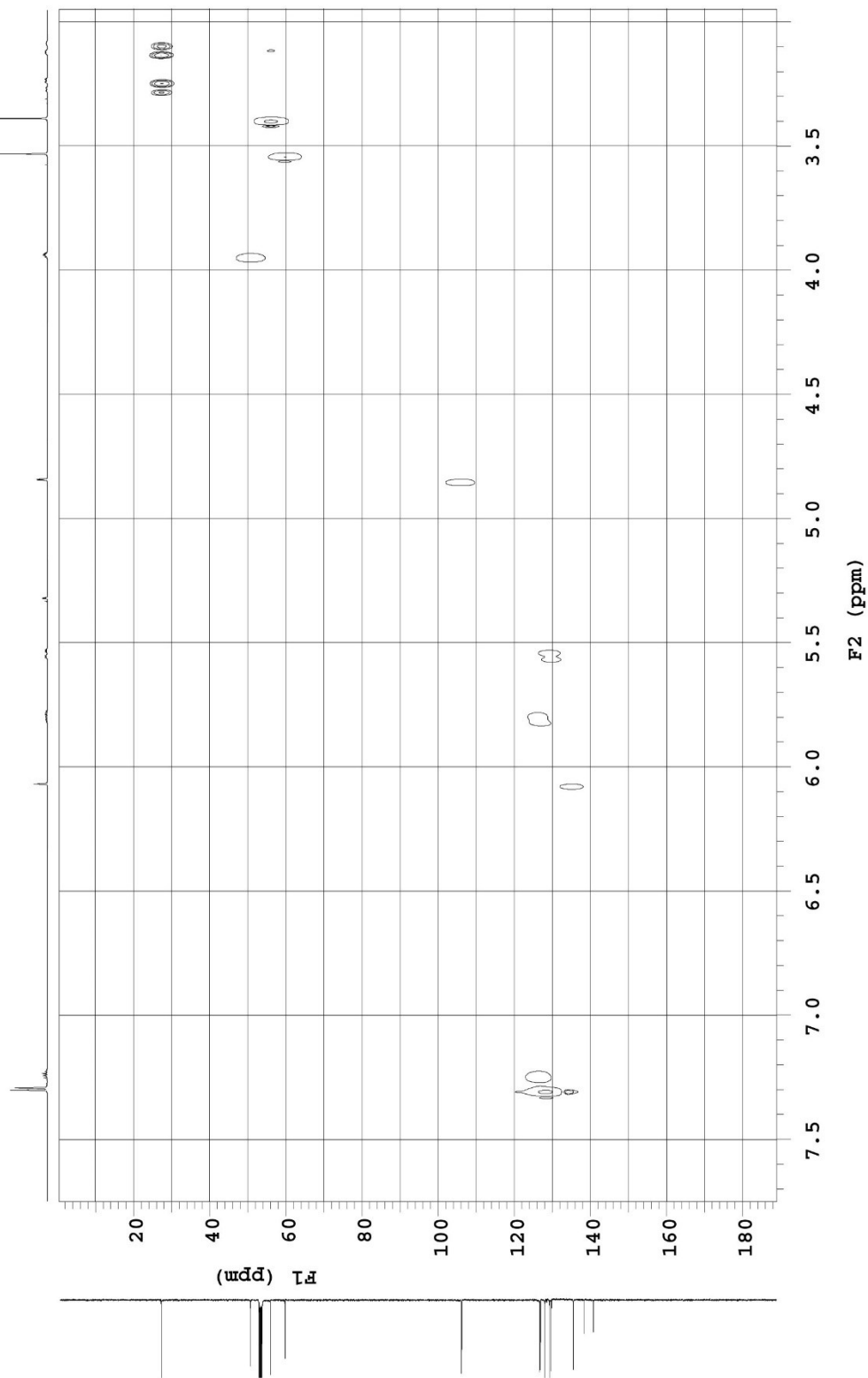
125.691 MHz C13[H1] 1D in cd2cl2 (ref. to cd2cl2 @ 53.8 ppm), temp 27.7 C -> actual temp = 27.0 C, coldludal probe

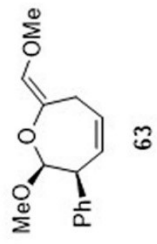




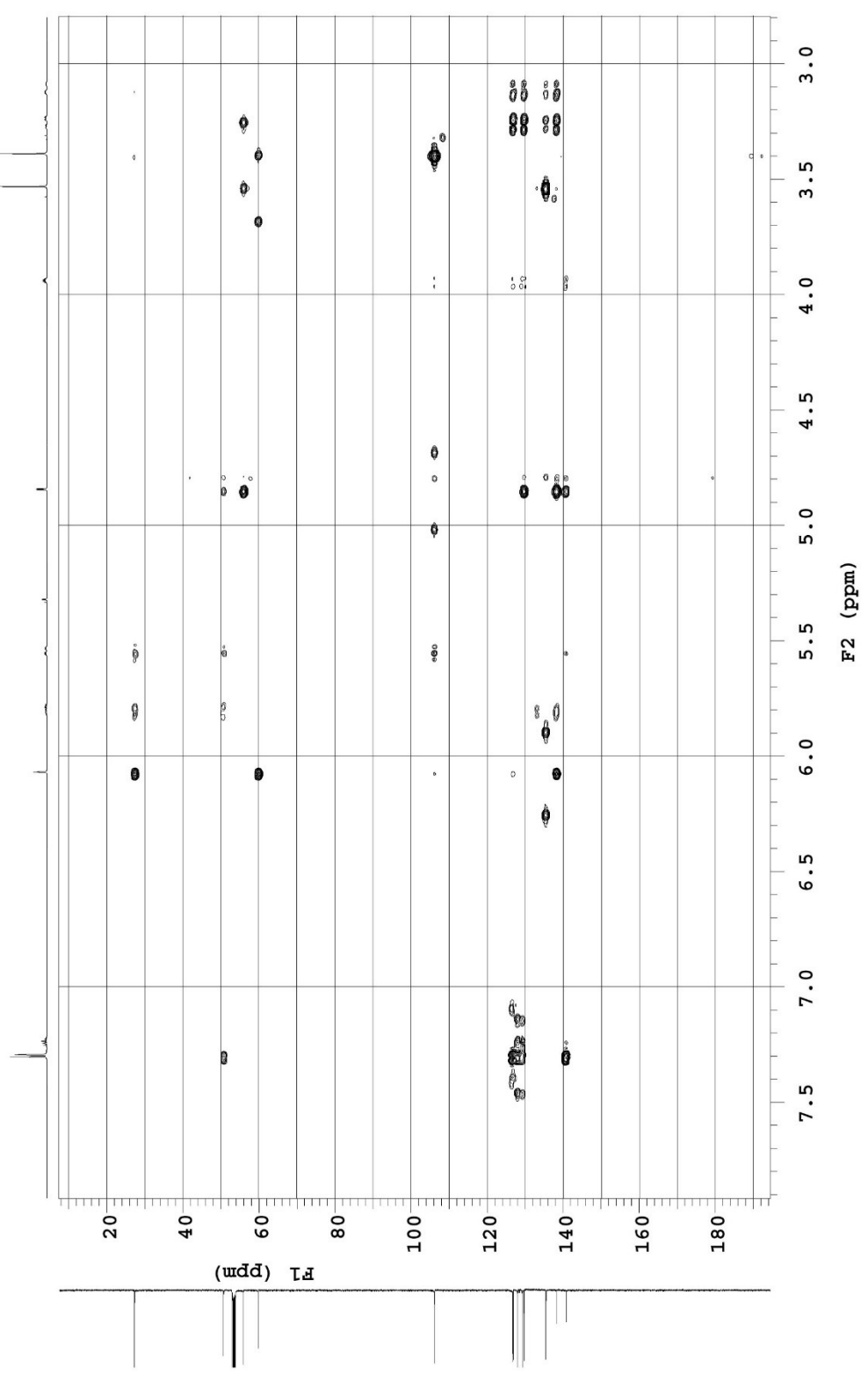
63

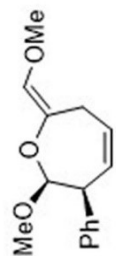
498.119 MHz <sup>1</sup>H gHSQC in cd2cl2 (ref. to CD2Cl2 @ 5.32/53.8 ppm), temp 26.4 C -> actual temp = 27.0 C, autotxdbc probe



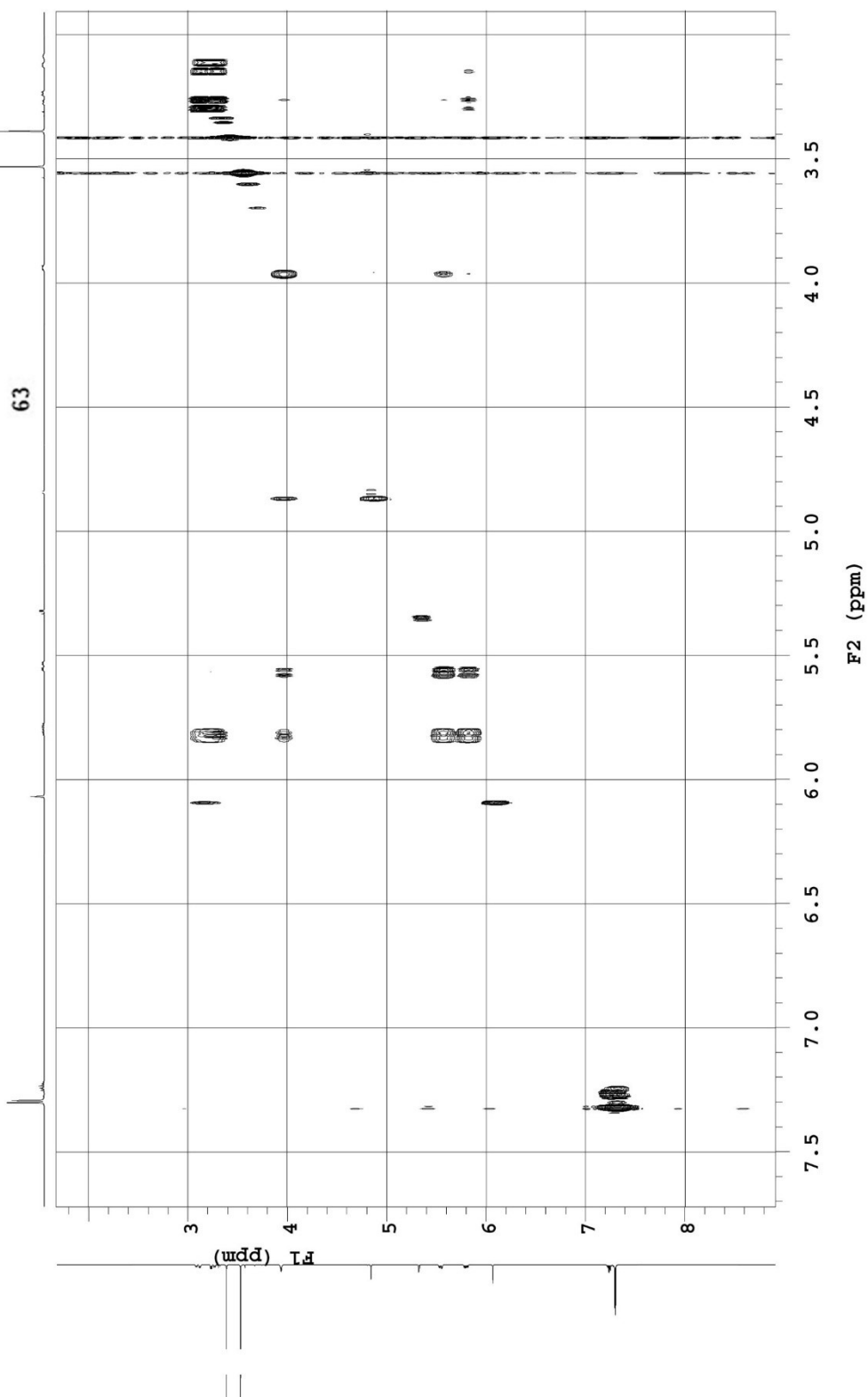


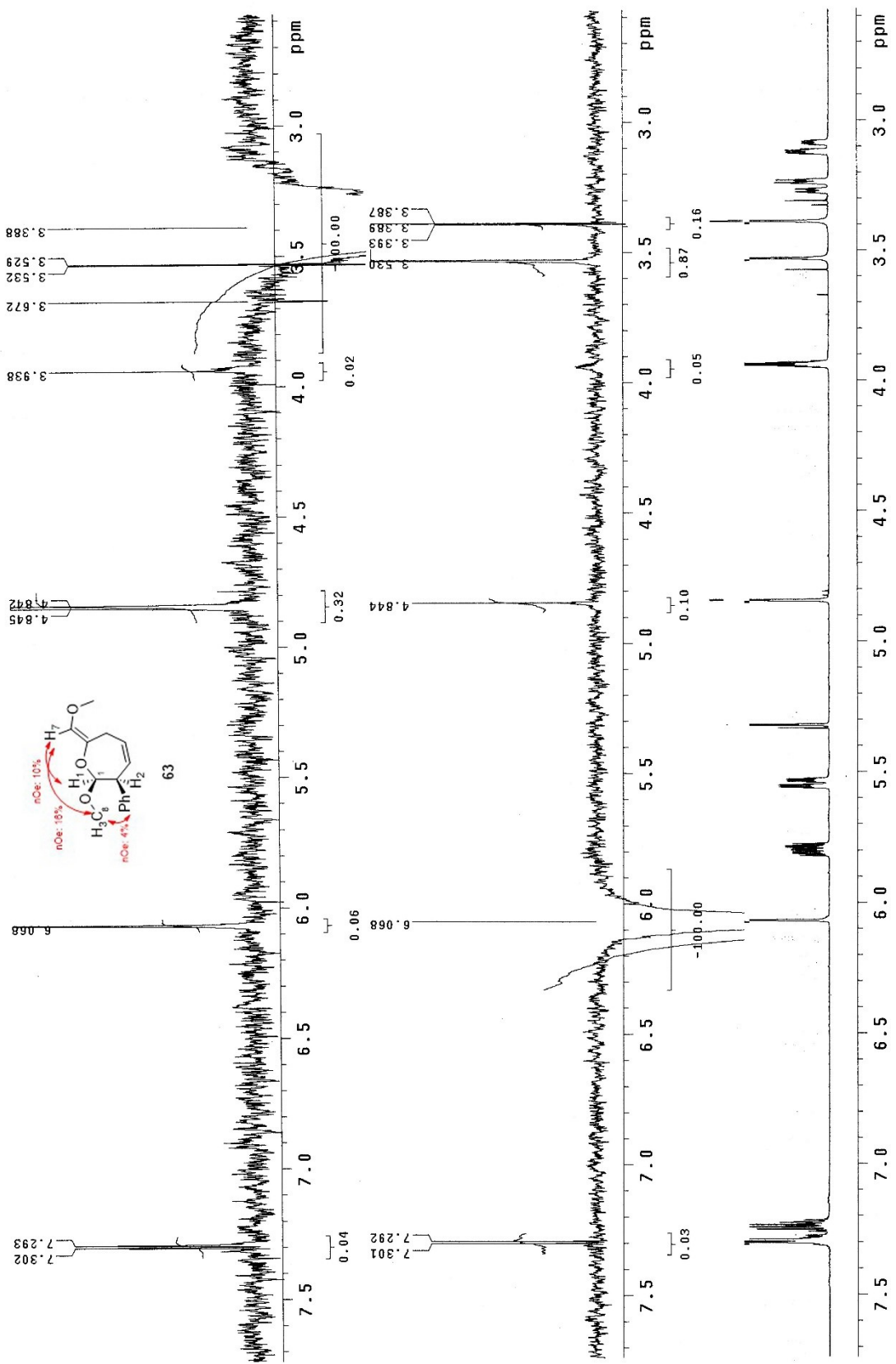
119 MHz <sup>1</sup>H1 gHMBC in cd2cl2 (ref. to CD2Cl2 @ 5.32/53.8 ppm), temp 26.4 C -> actual temp = 27.0 C; autotxdtb probe





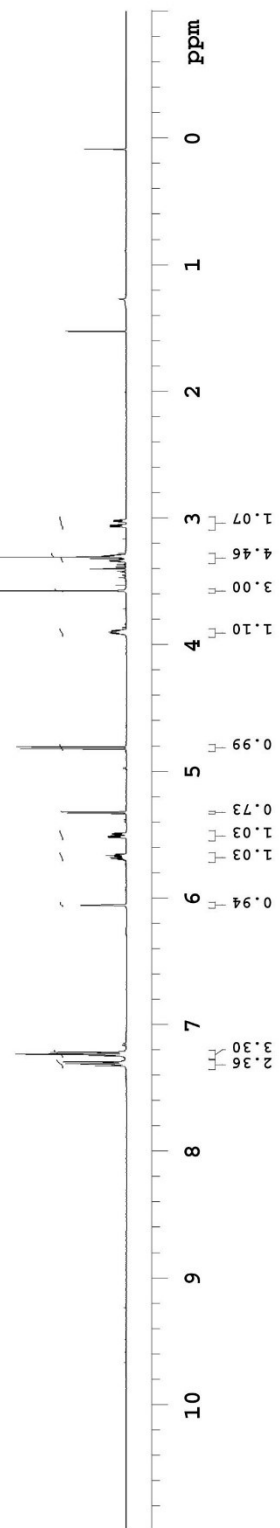
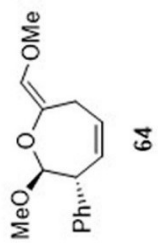
499.807 MHz H1 aogcosy in cd2cl2 (ref. to CD2Cl2 @ 5.32 ppm), temp 27.7 C -> actual temp = 27.0 C, coldidial probe

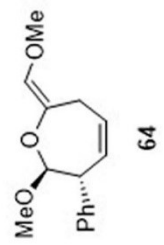
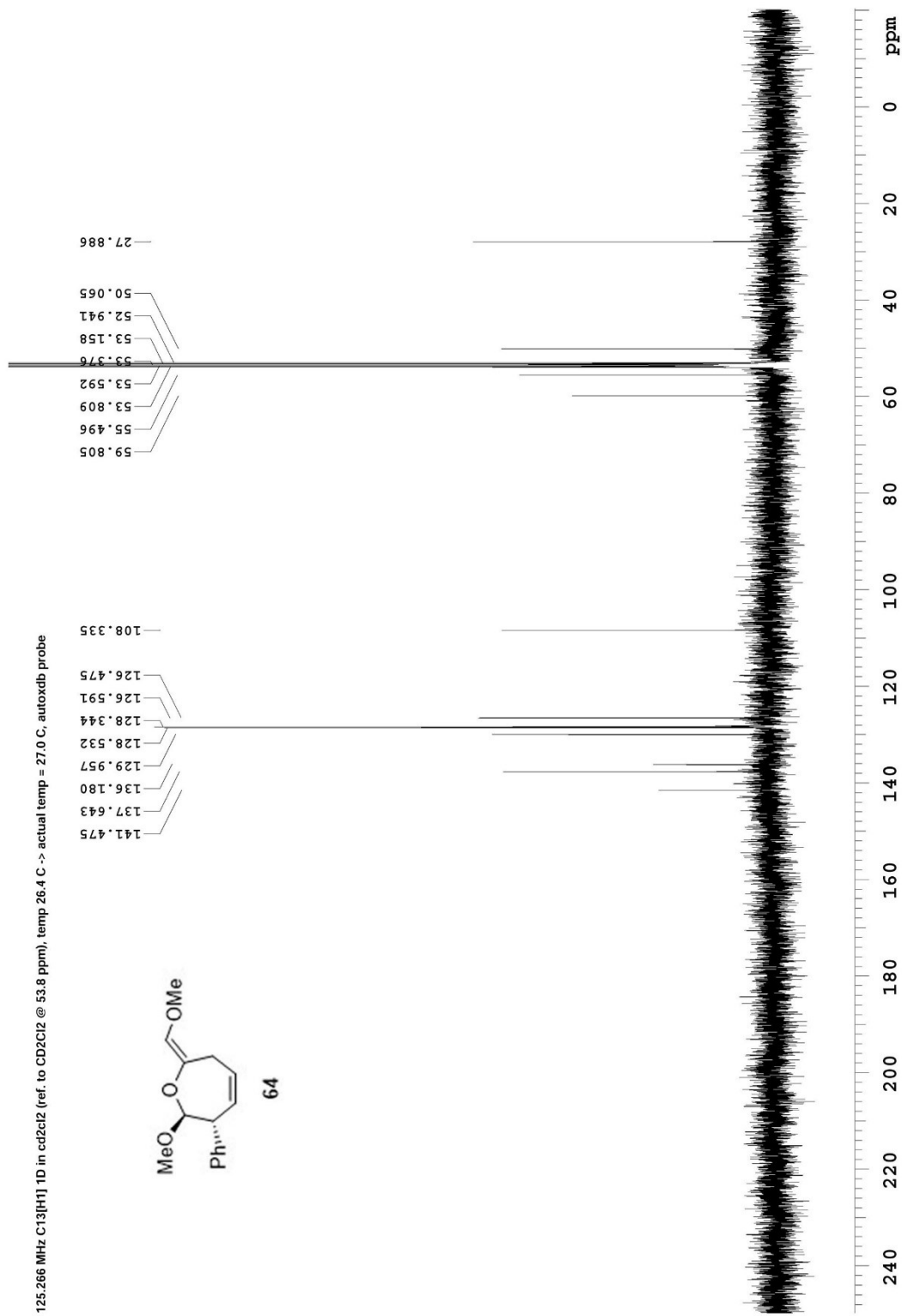


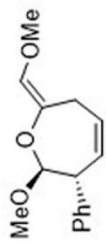




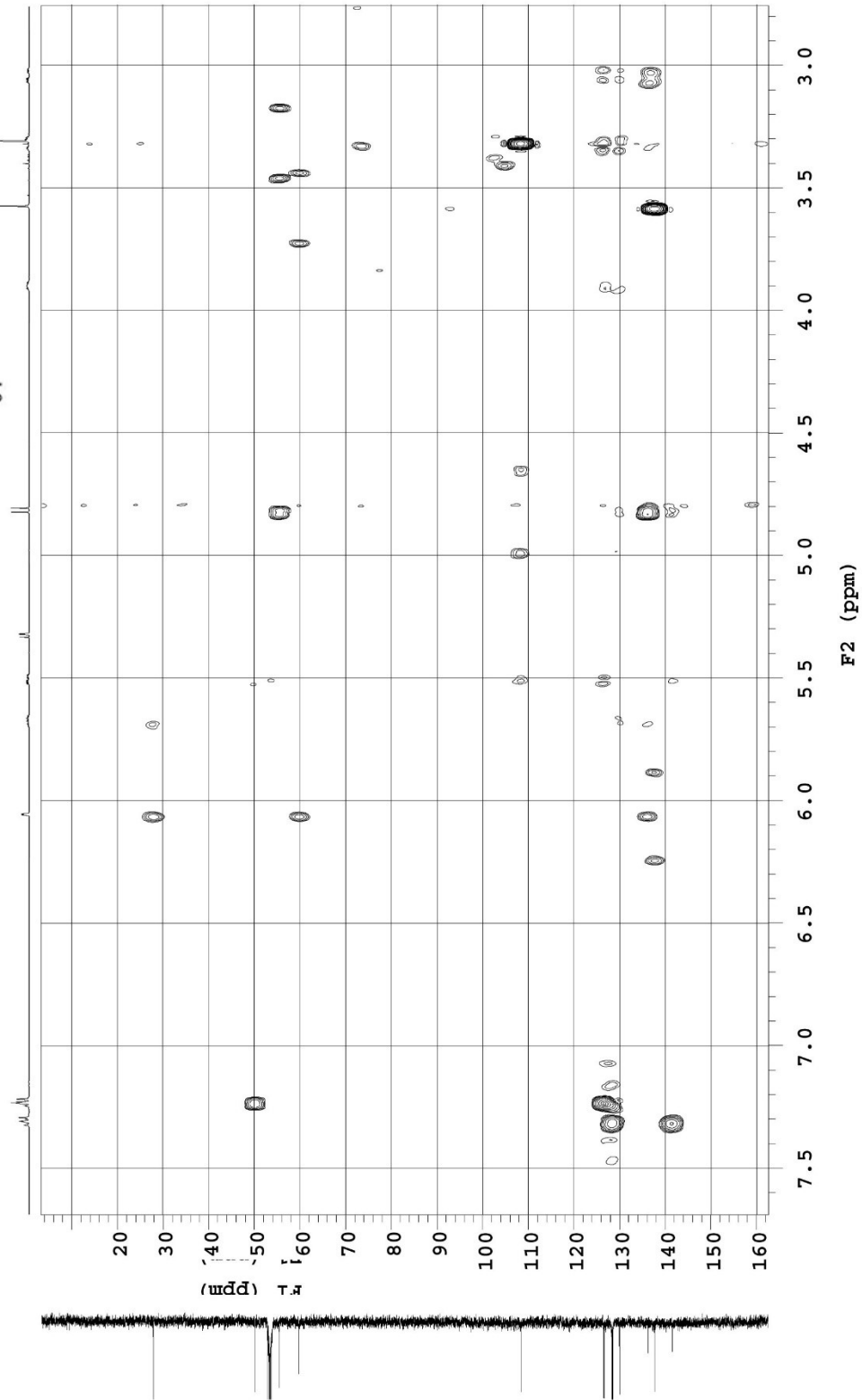
498.119 MHz H1 1D in cd2cl2

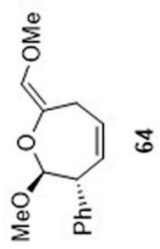




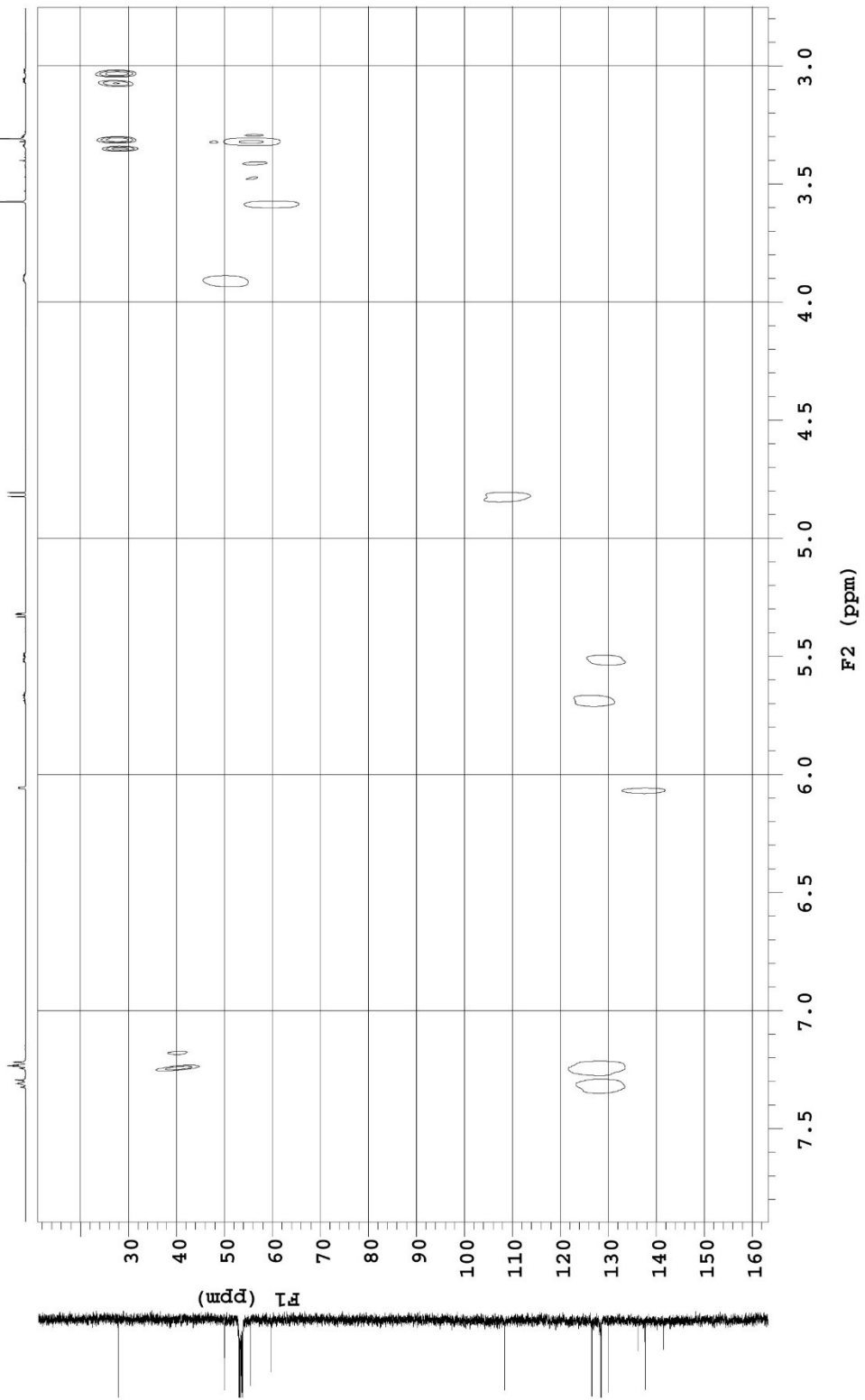


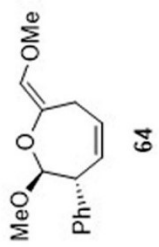
498.119 MHz <sup>1</sup>H1 gHMBC in cd2cl2



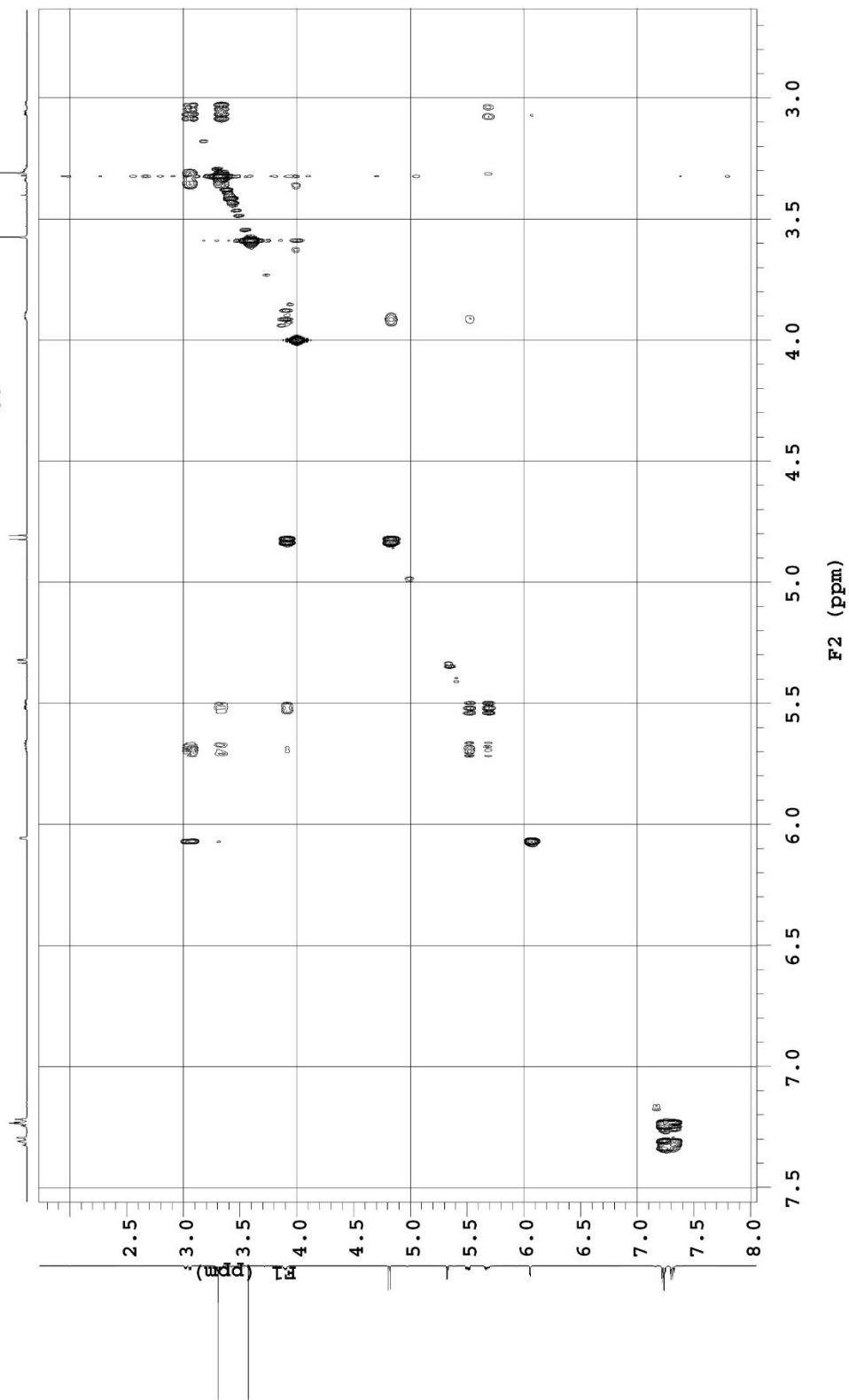


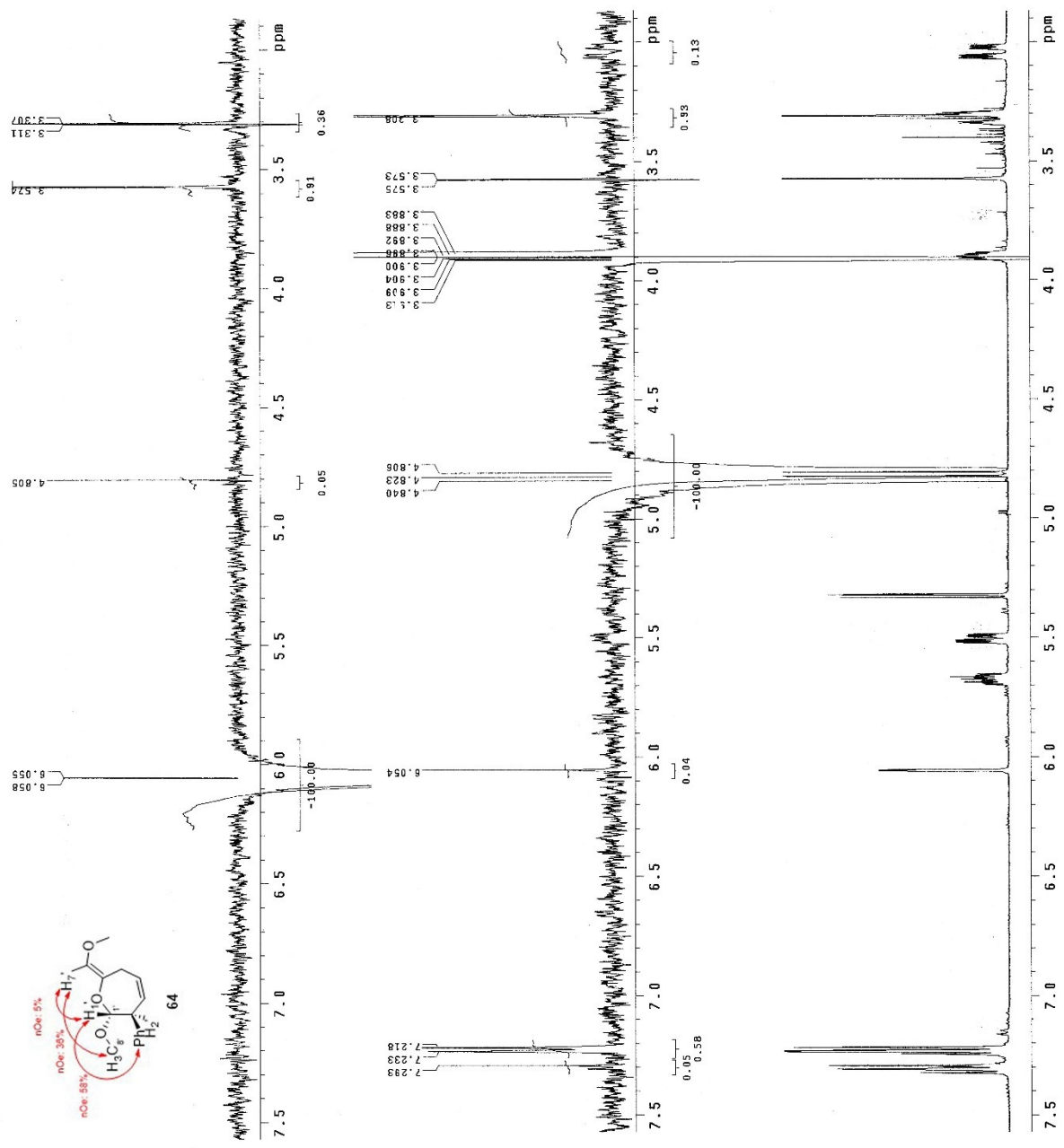
498.119 MHz <sup>1</sup>H gHSQC in cd2cl2





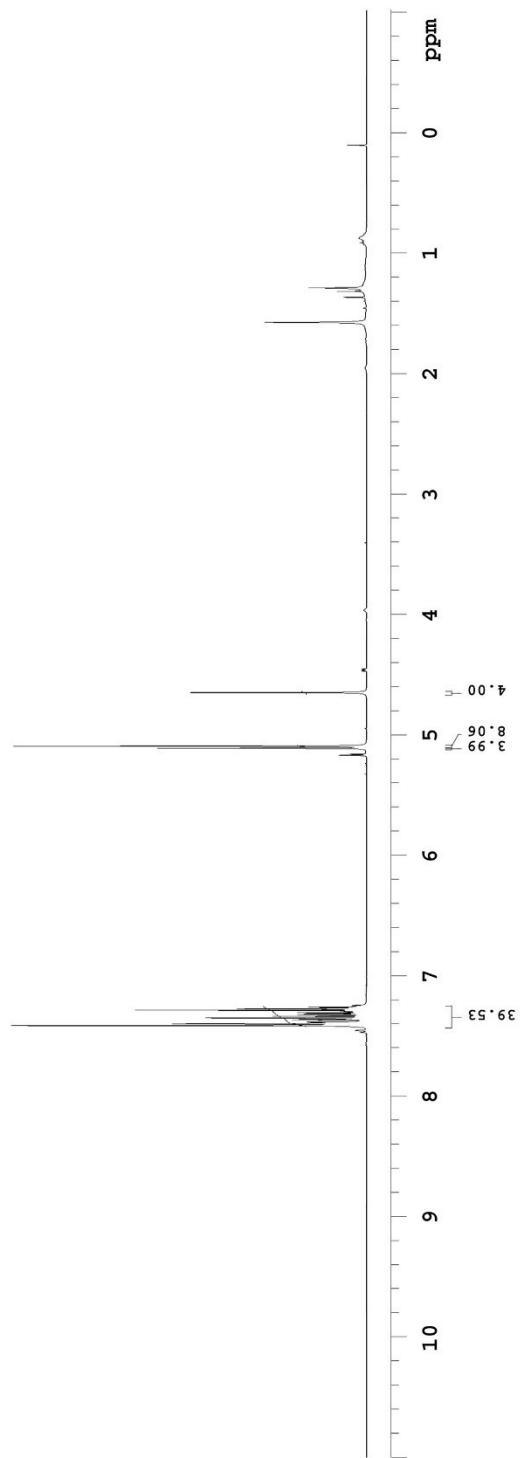
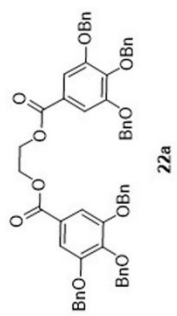
498.118 MHz H1 aogcoxy in cd2cl2





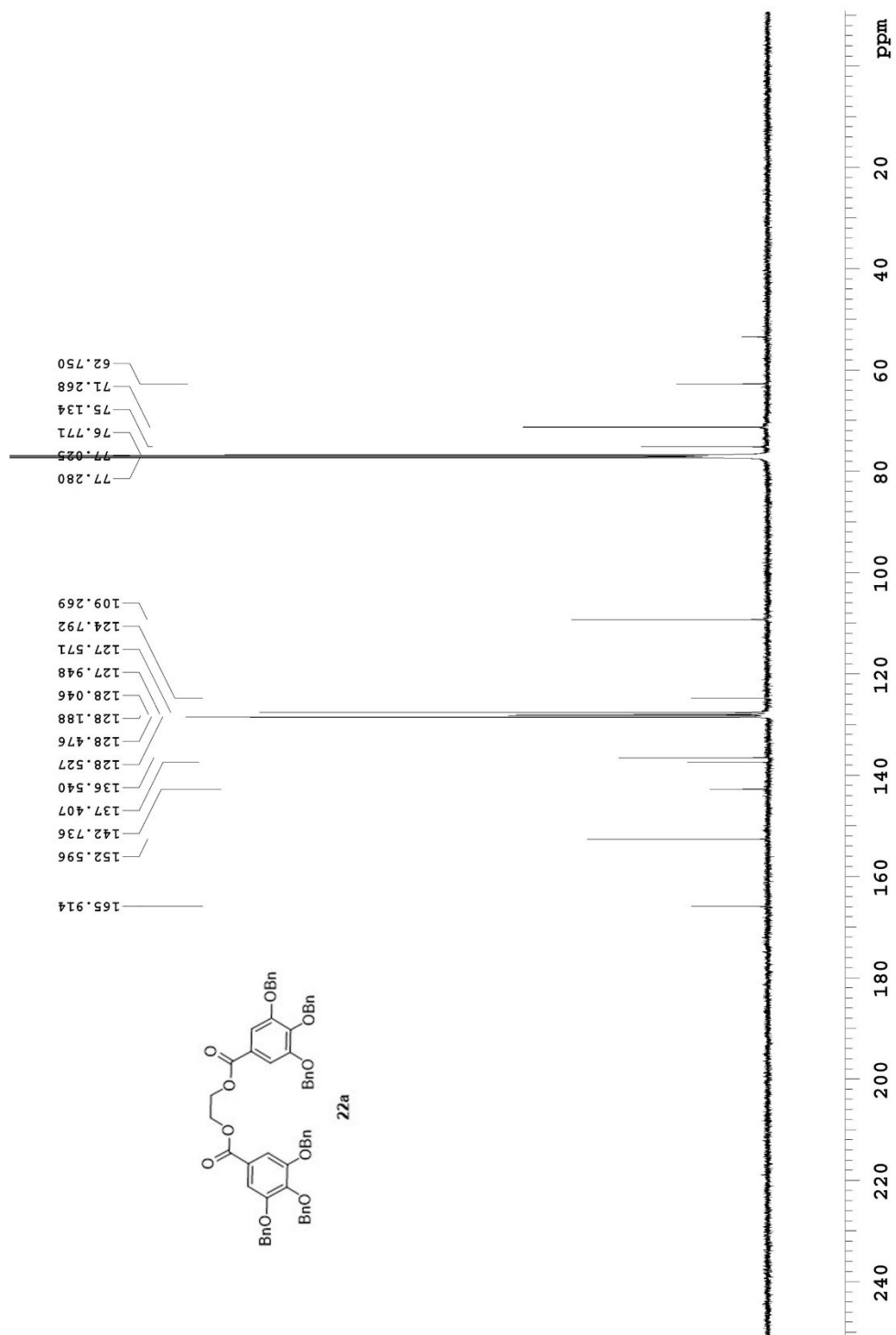
## Appendix III: Selected NMR Spectra (Chapter 4)

499.806 MHz H1 PRESAT in cdcl3 (ref. to CDCl3 @ 7.26 ppm), temp 27.7 C -> actual temp = 27.0 C, coldludal probe

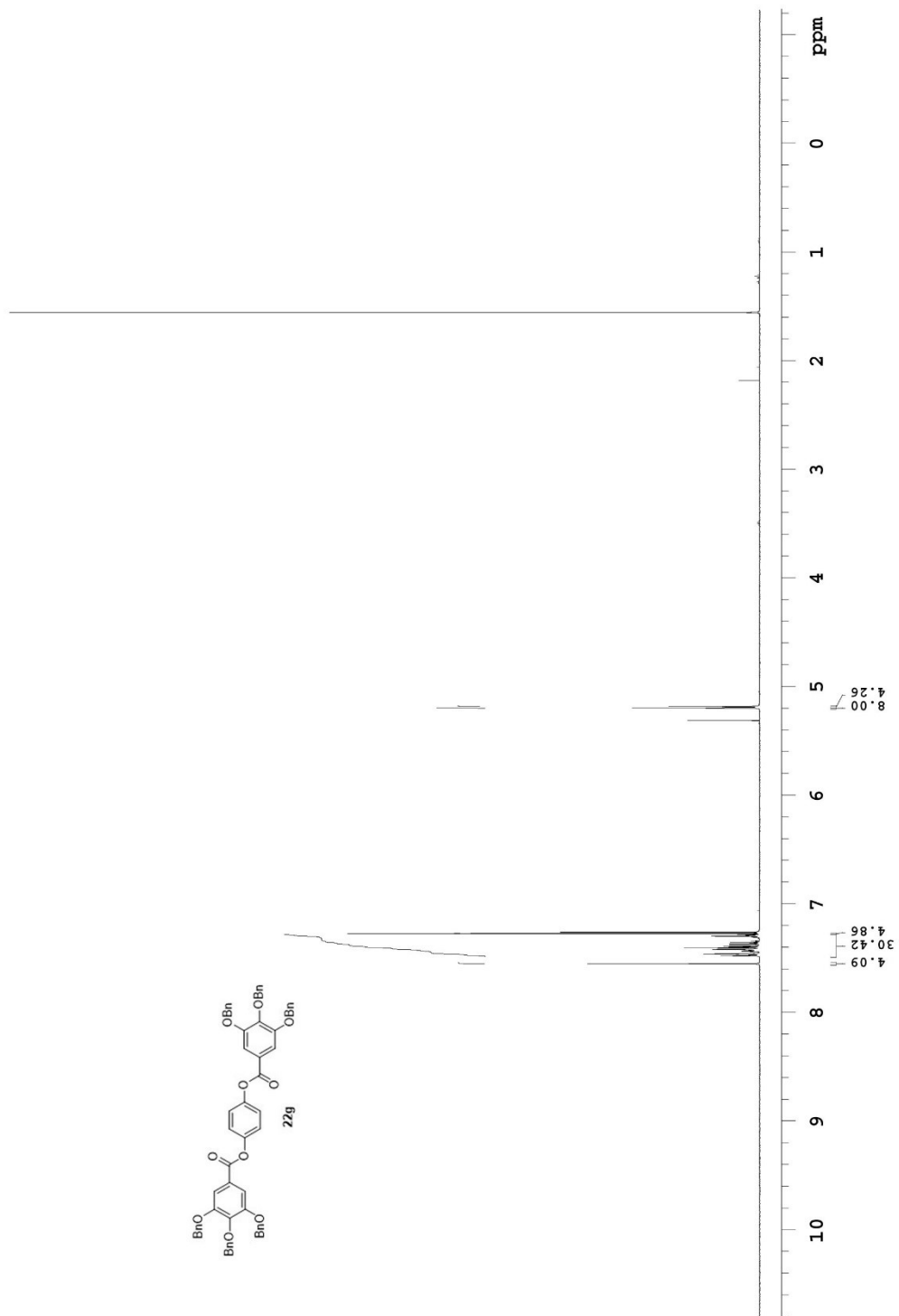
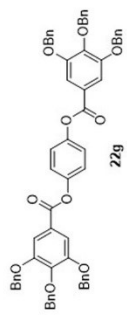




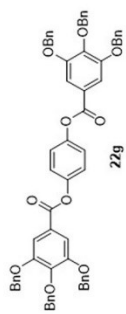
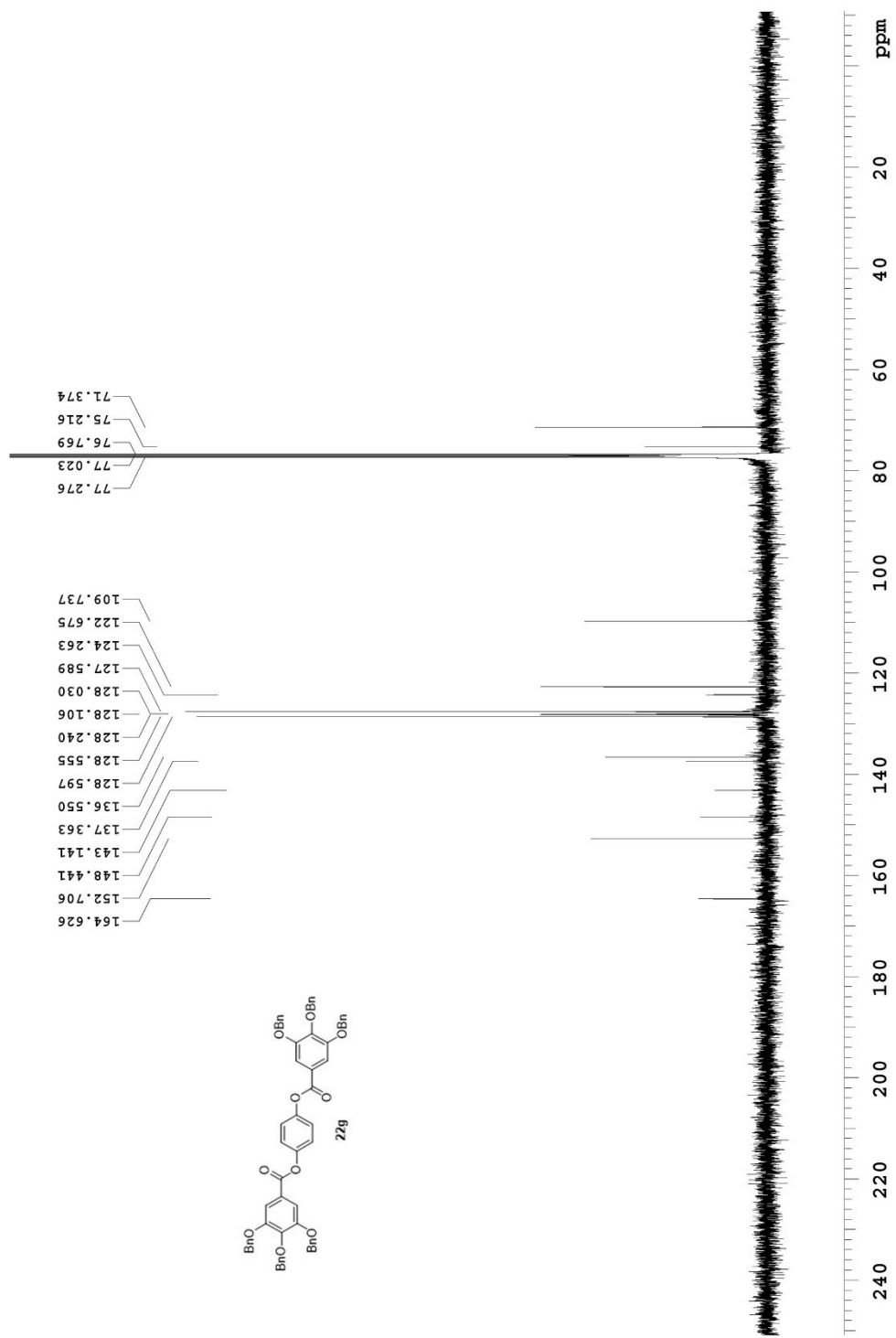
125.691 MHz C<sup>13</sup>[H<sup>1</sup>] 1D in cdcl<sub>3</sub> (ref. to CDCl<sub>3</sub> @ 77.06 ppm), temp 27.7 C -> actual temp = 27.0 C, coldludal probe



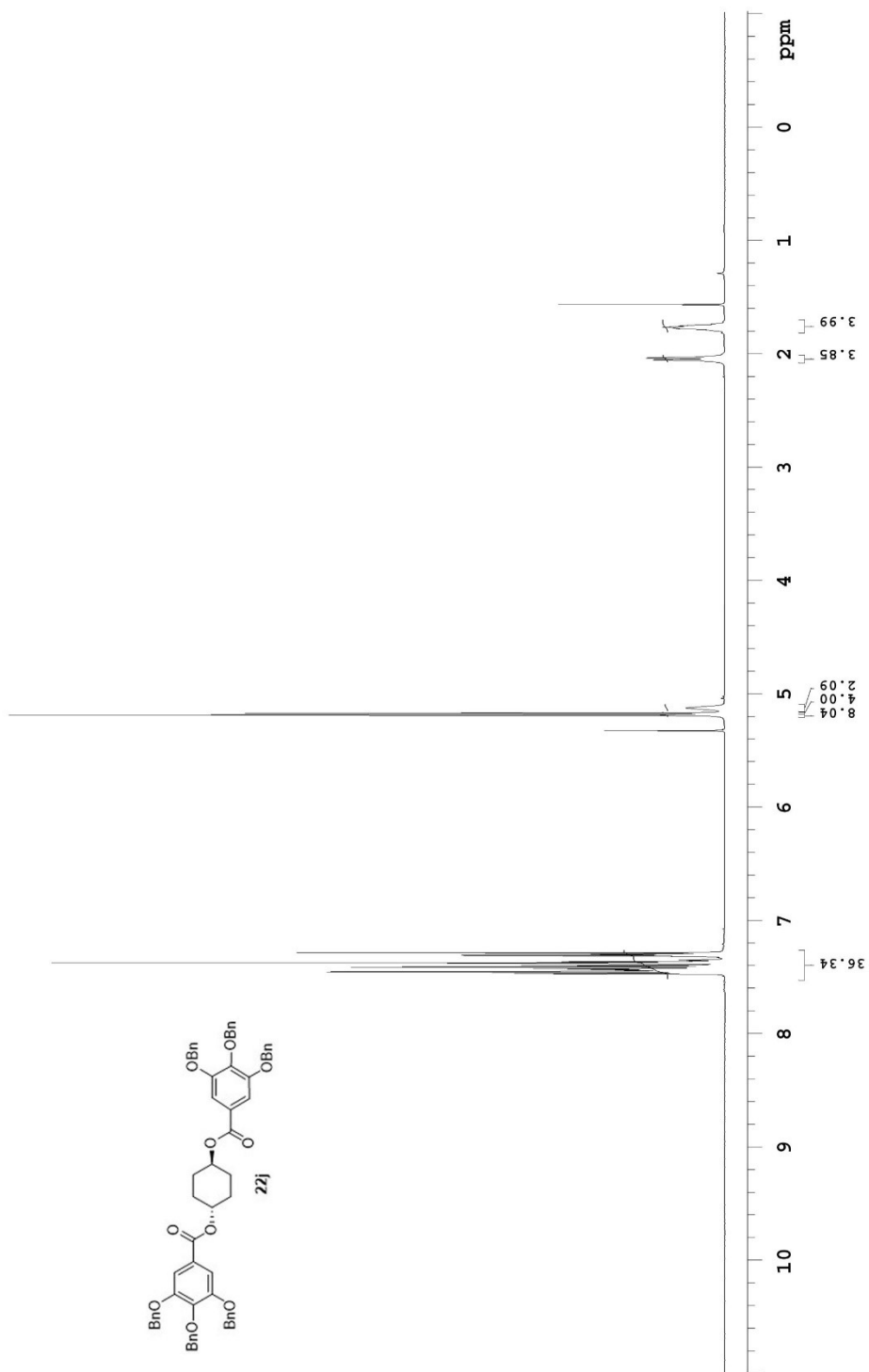
498.118 MHz H1 1D in cdcl3 (ref. to CDCl3 @ 7.26 ppm), temp 26.4 C -> actual temp = 27.0 C, autotxdtb probe



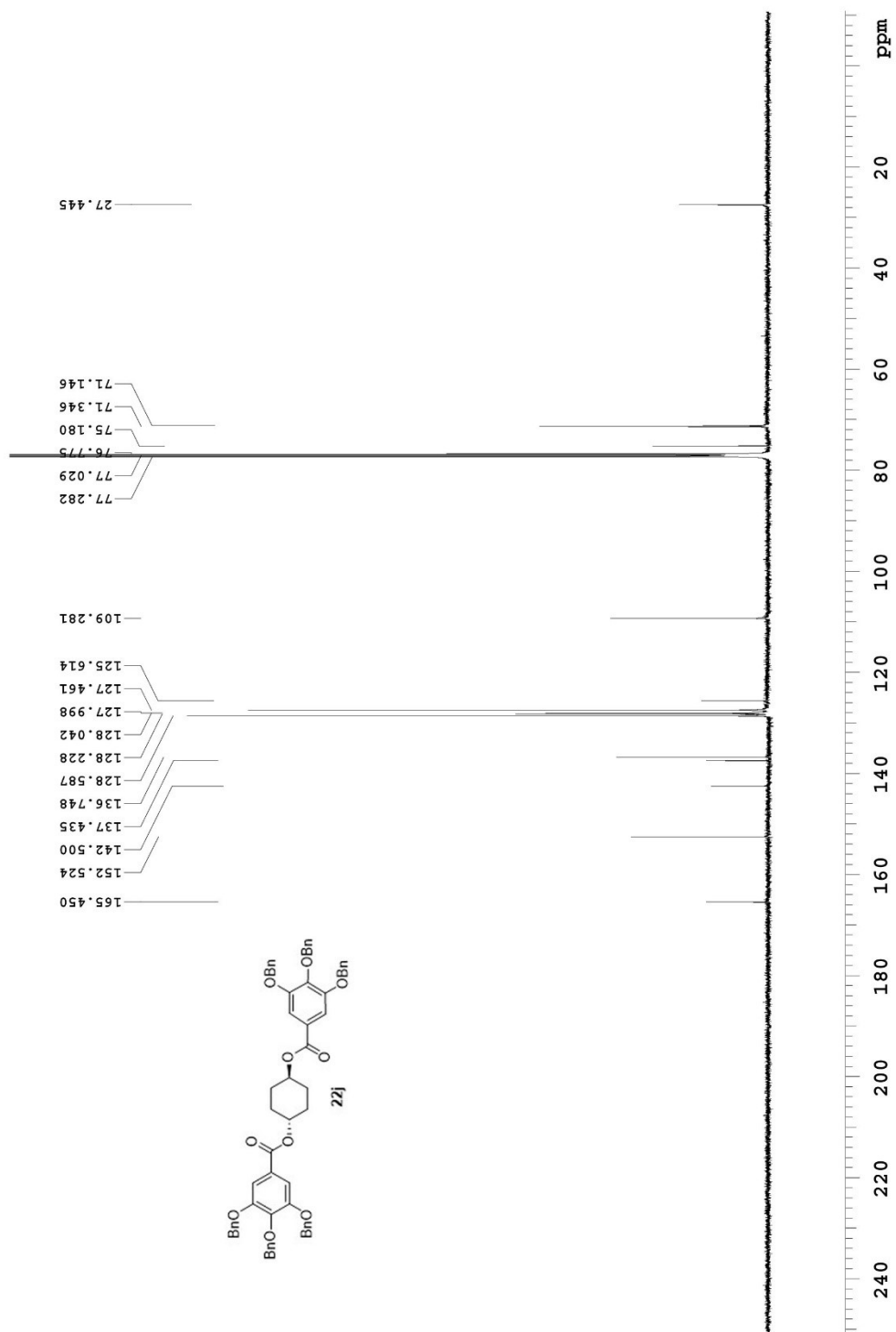
125.891 MHz C13{H1} 1D in cdc13 (ref. to CDC13 @ 77.06 ppm), temp 27.7 C -> actual temp = 27.0 C, coaddual probe



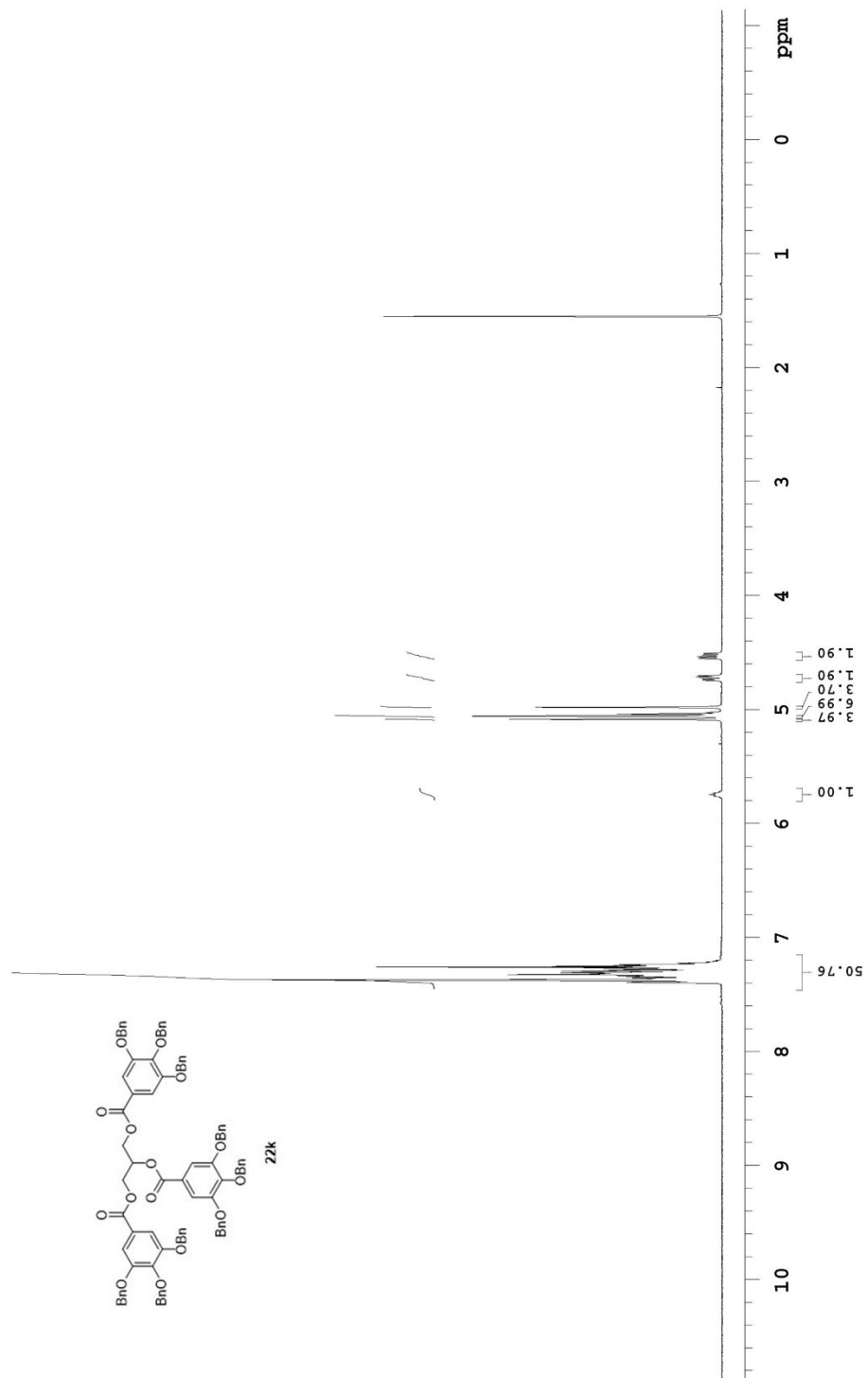
499.806 MHz, H1 PRESAT in cdcl3 (ref. to CDCl3 @ 7.26 ppm), temp 27.7 C -> actual temp = 27.0 C, coldidial probe



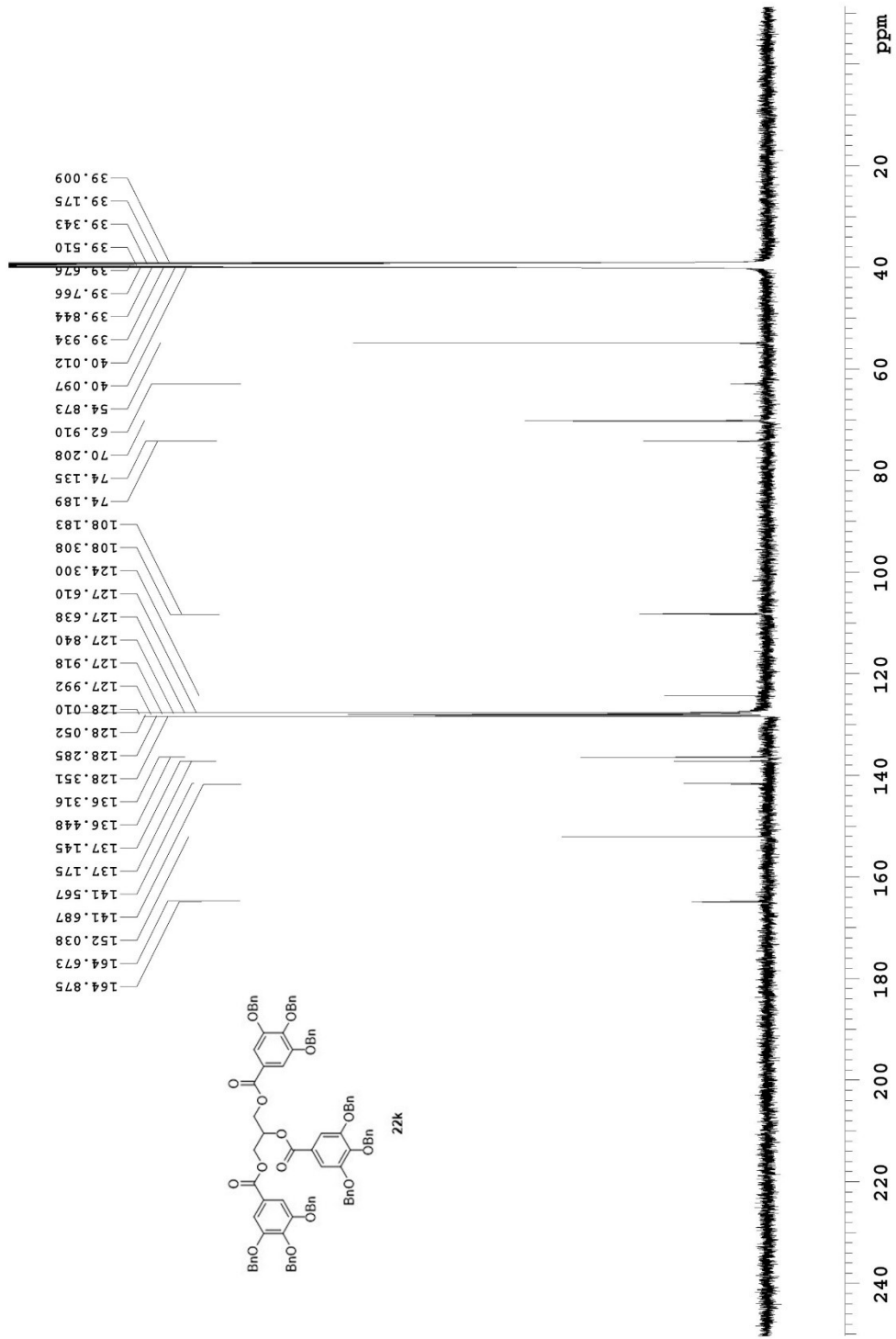
125.691 MHz C13[H1] 1D in cdcl3 (ref. to CDCl3 @ 77.06 ppm), temp 27.7 C -> actual temp = 27.0 C, coldlual probe



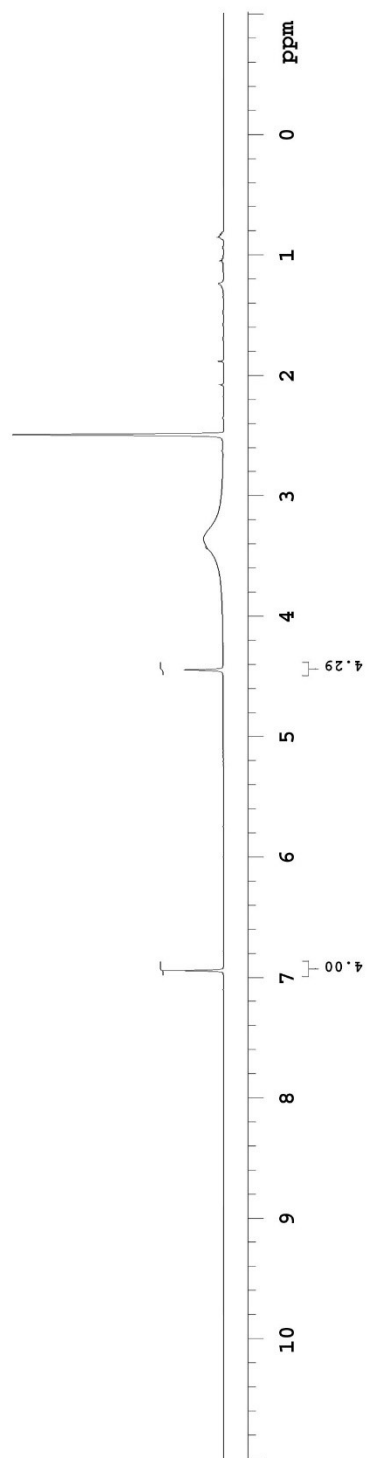
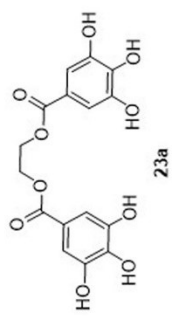
399.984 MHz H1 1D in cdcl3 (ref. to cdcl3 @ 7.26 ppm), temp 25.9 C -> actual temp = 27.0 C, onenmr probe



125.691 MHz C13[H1] 1D in dmso (ref. to DMSO @ 39.5 ppm), temp 27.7 C -> actual temp = 27.0 C, coldidial probe

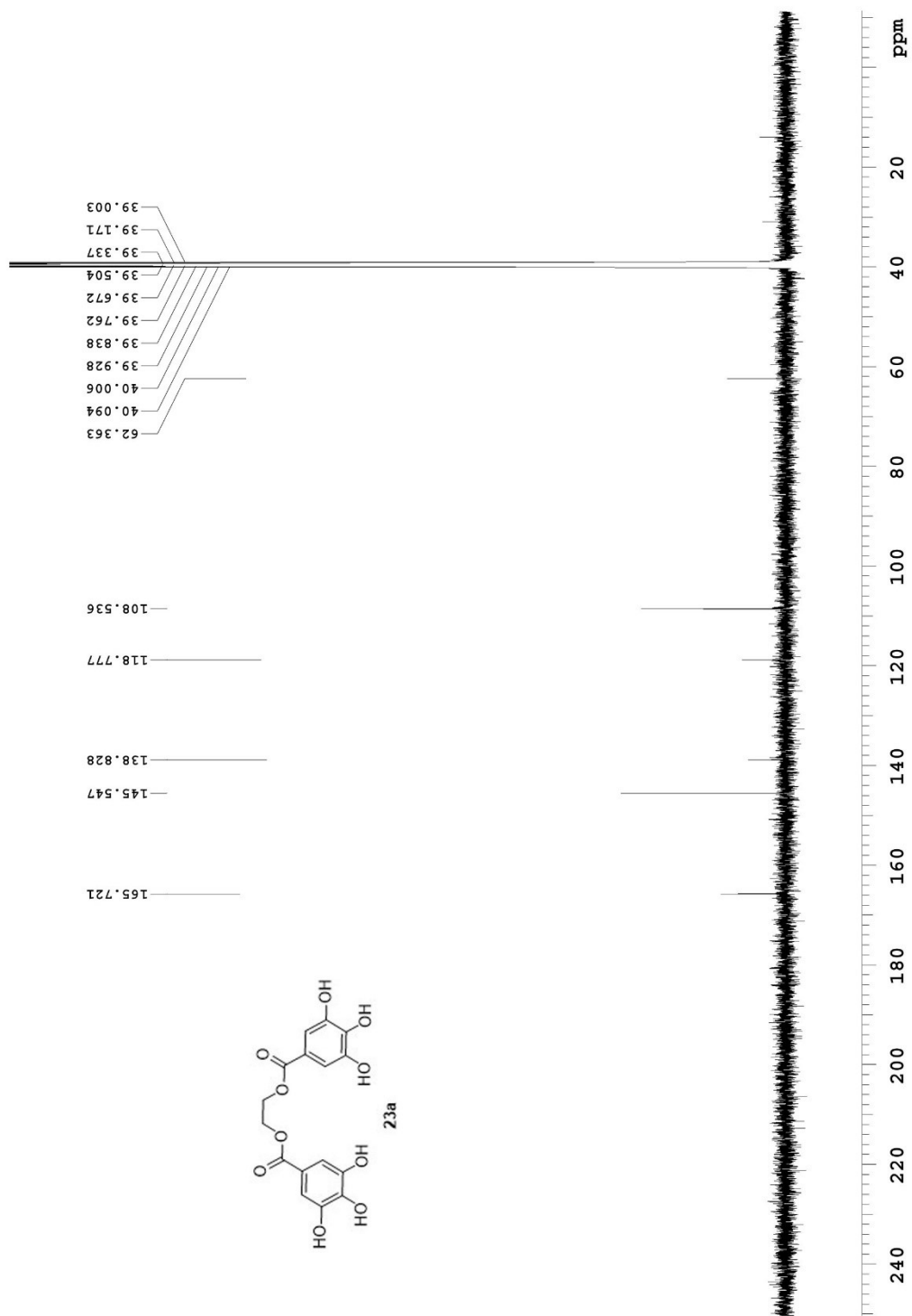


499.809 MHz H1 PRESAT in dmso (ref. to DMSO @ 2.49 ppm), temp 27.7 C -> actual temp = 27.0 C, coldidial probe

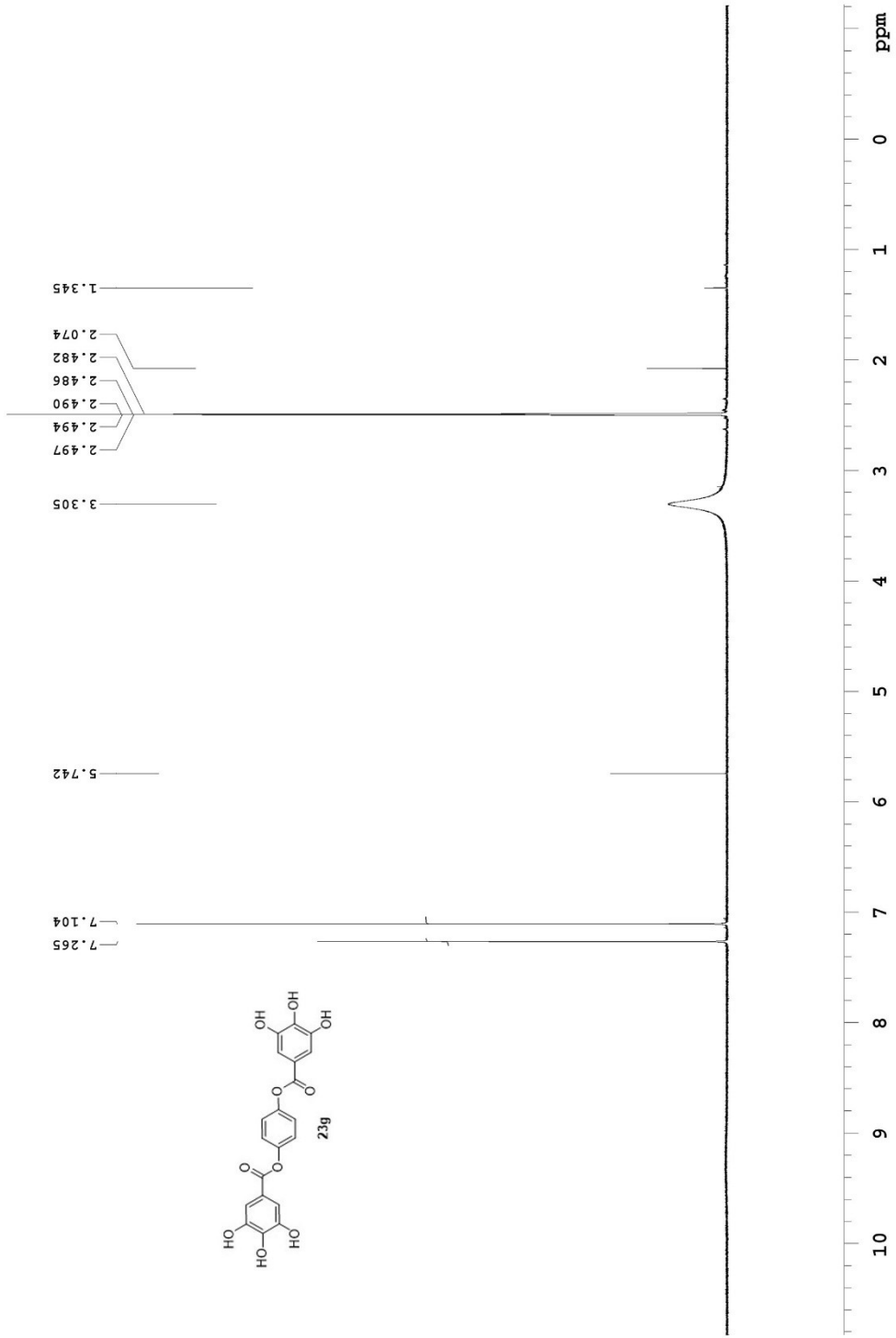




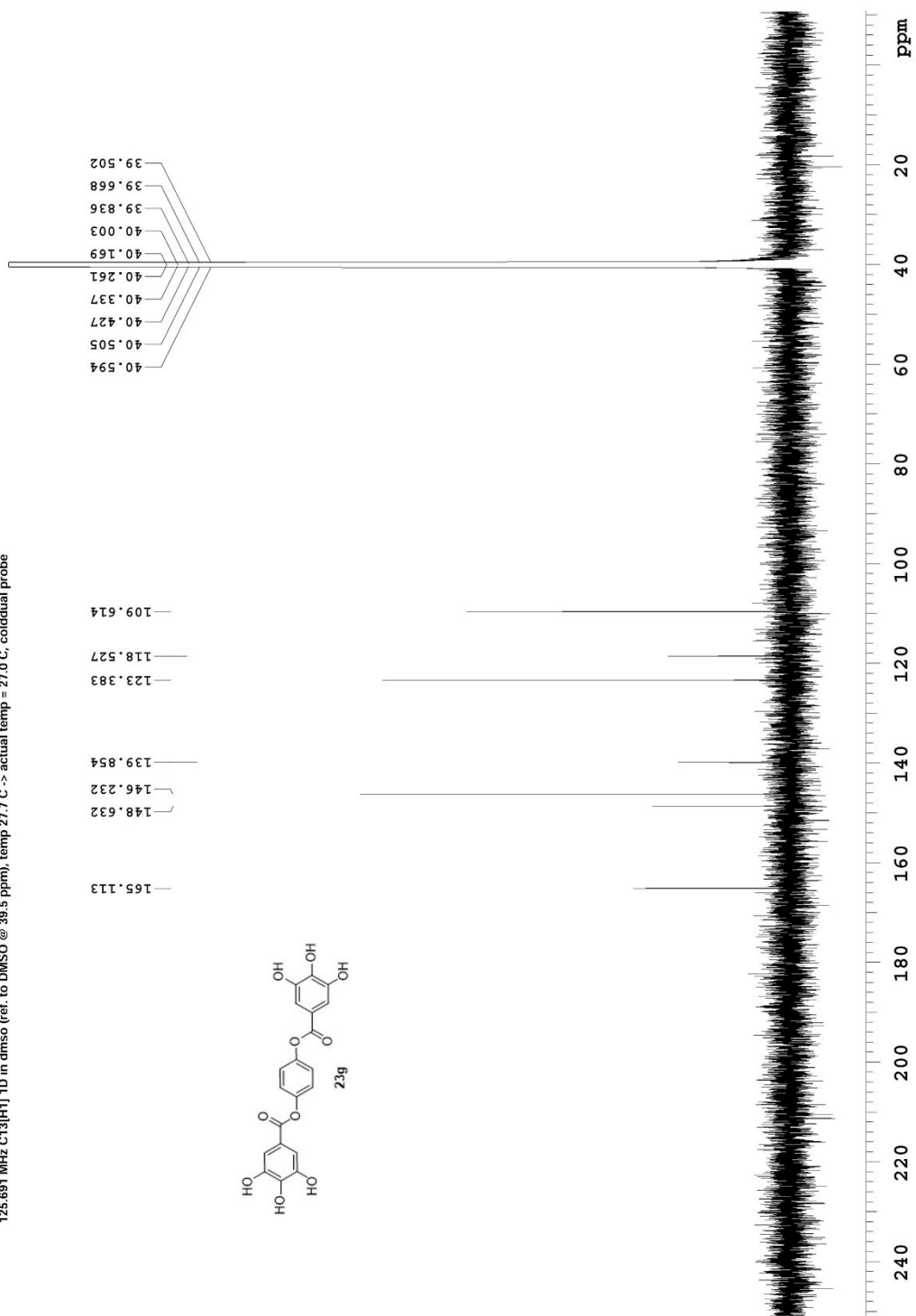
125.691 MHz C13[H1] 1D in dmsd (ref. to DMSO @ 39.5 ppm), temp 27.7 C -> actual temp = 27.0 C, coldltdal probe



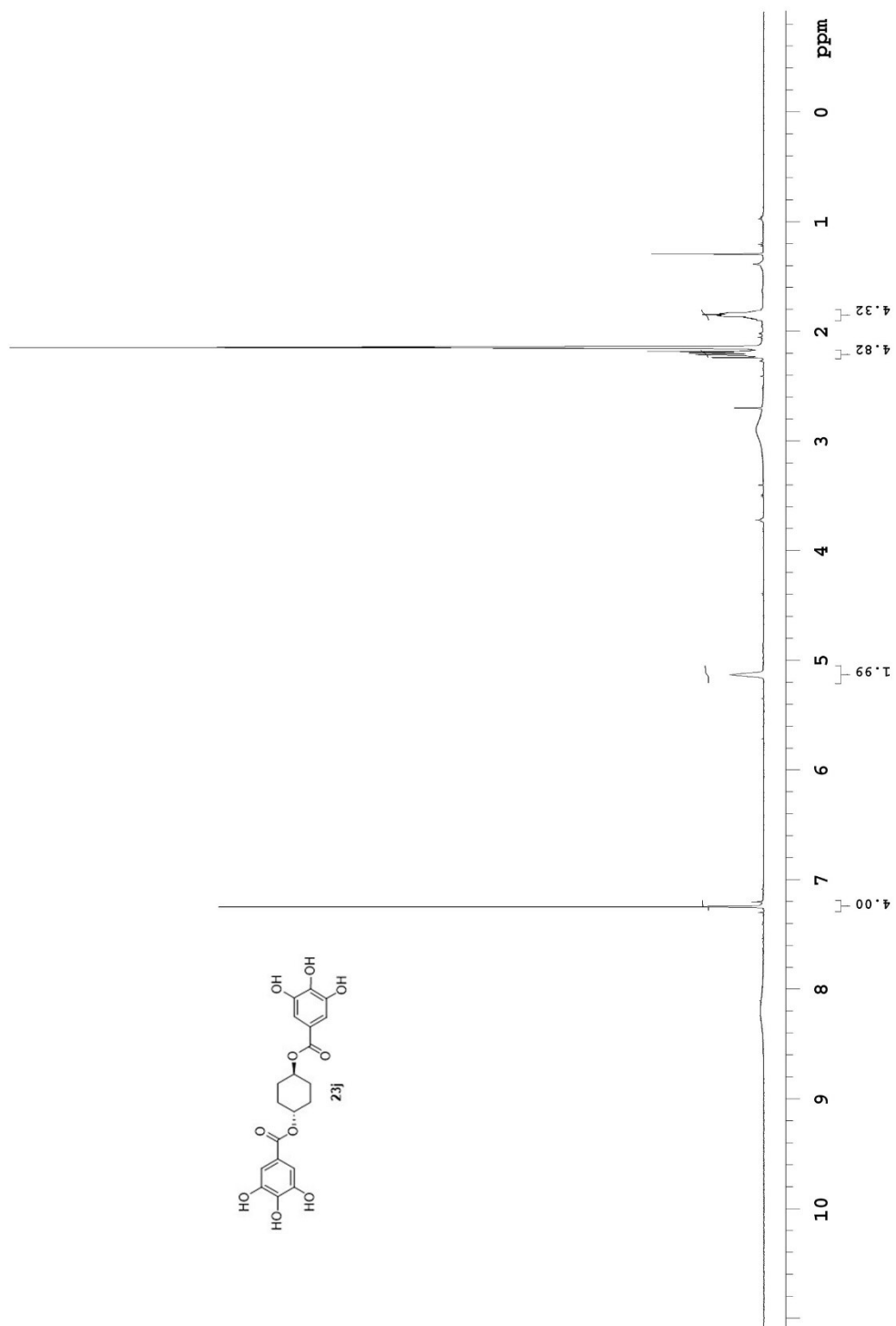
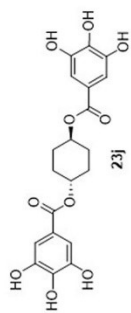
498.120 MHz H1 TD in dmsd (ref. to DMSO @ 2.49 ppm), temp 26.4 C -> actual temp = 27.0 C, autotdb probe



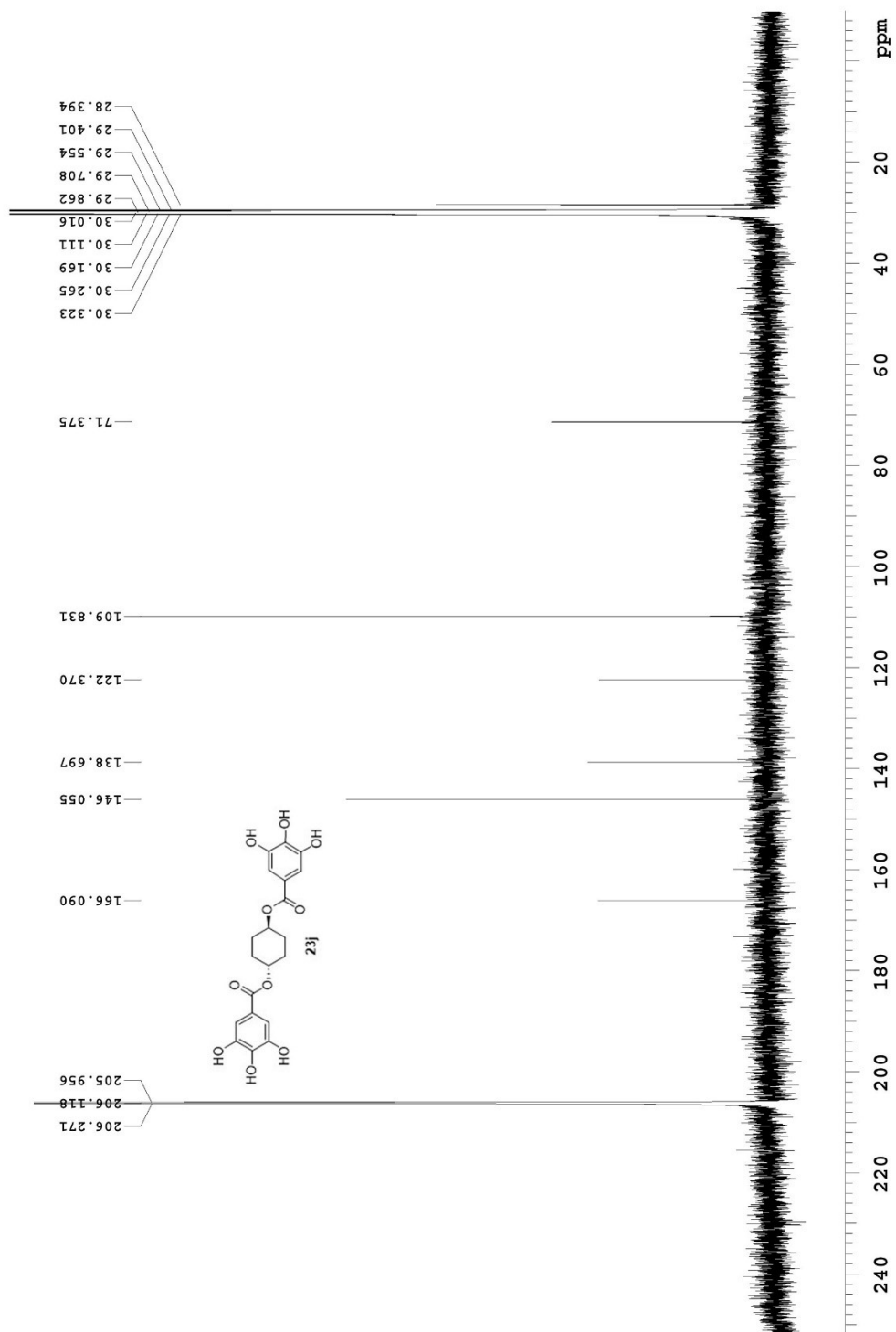
125.691 MHz C13[H1] 1D in dmsc (ref. to DMSO @ 39.5 ppm), temp 27.7 C -> actual temp = 27.0 C, coldlual probe



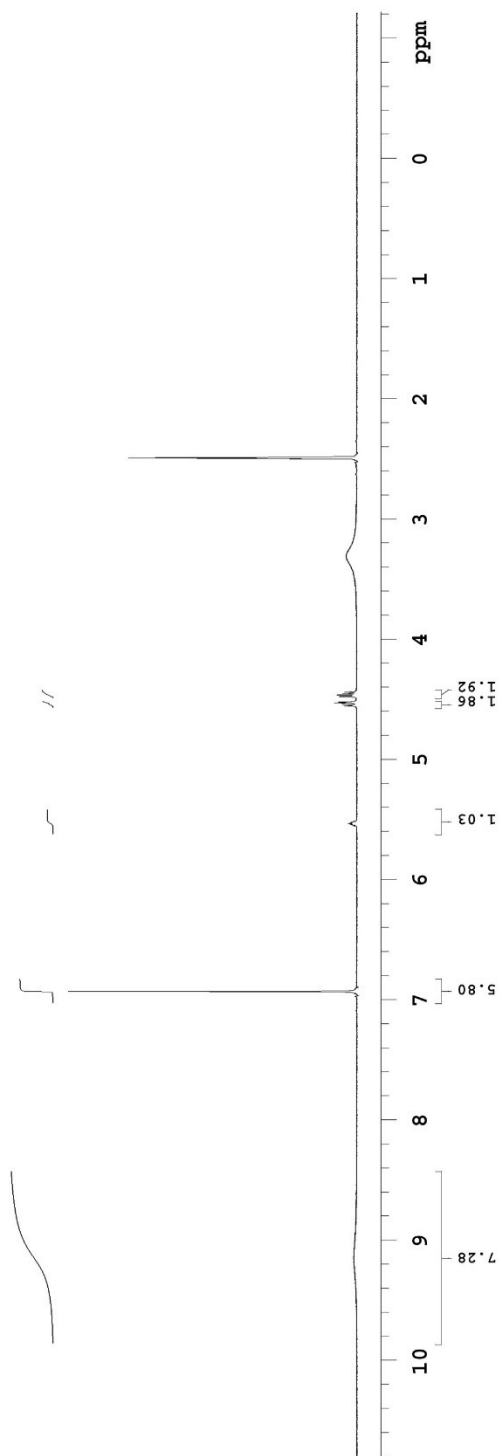
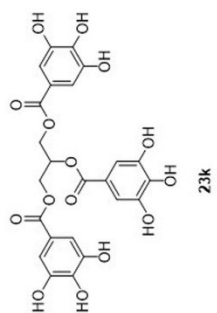
499.809 MHz <sup>1</sup>H PRESAT in acetone (ref. to acetone @ 2.04 ppm), temp 27.7 C -> actual temp = 27.0 C, coldidial probe



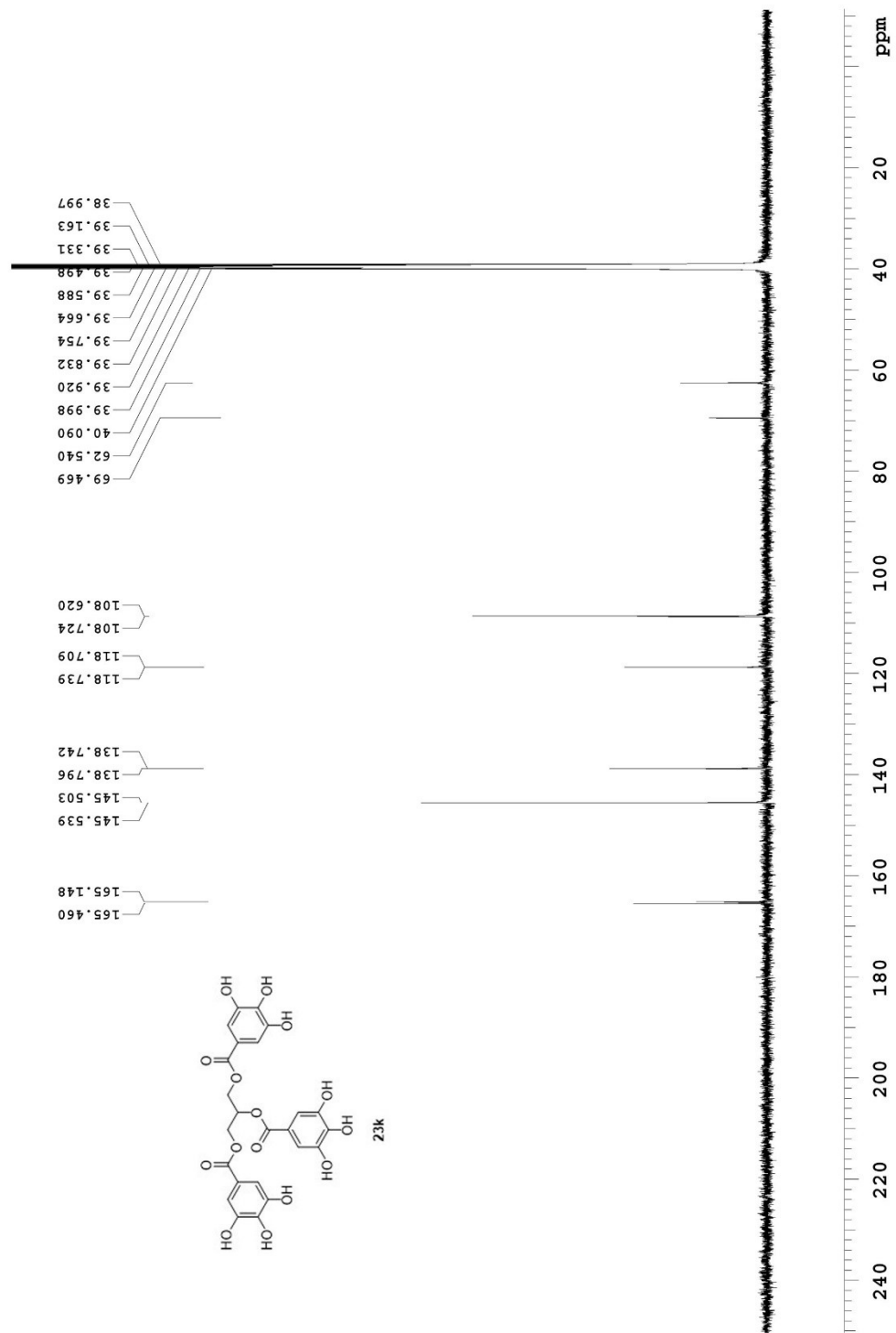
125.692 MHz C13[H1] 1D in acetone (ref. to acetone @ 29.8 ppm), temp 27.7 C -> actual temp = 27.0 C, cold dual probe



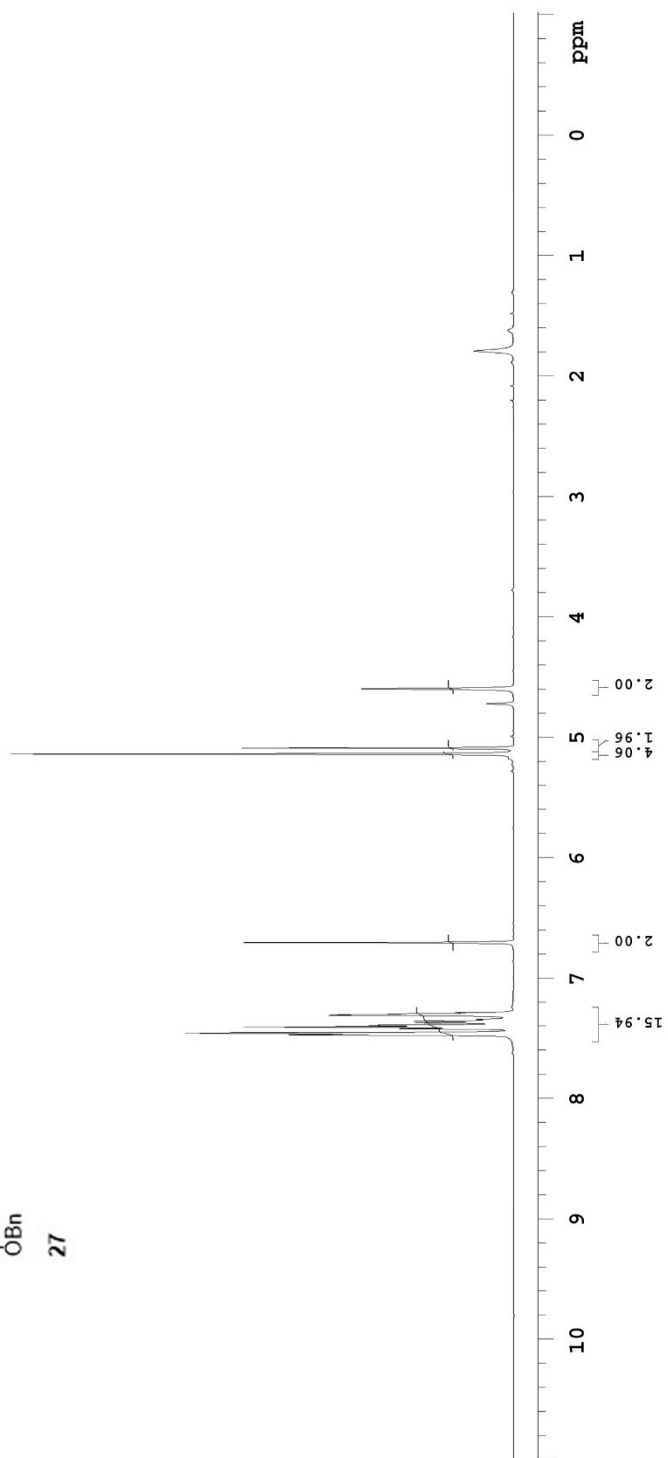
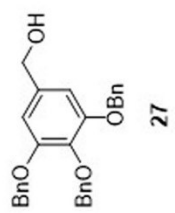
498.120 MHz <sup>1</sup>H 1D in dmsco (ref. to DMSO @ 2.49 ppm), temp 26.4 C -> actual temp = 27.0 C, autotxldb probe



125.691 MHz C13[H1] 1D in dmso (ref. to DMSO @ 39.5 ppm), temp 27.7 C -> actual temp = 27.0 C, coldlual probe

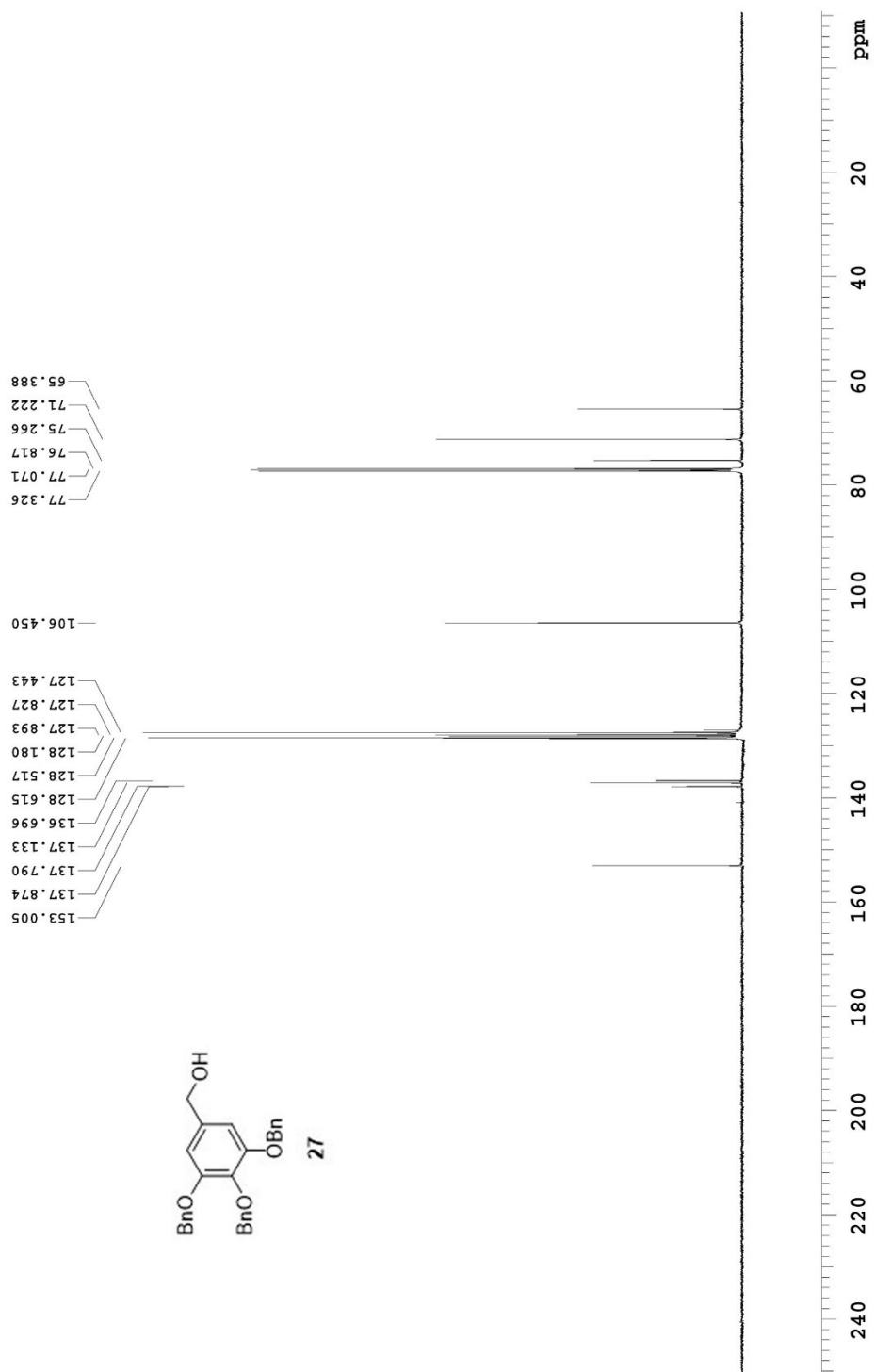


499.806 MHz H1 PRESAT in cdcl3 (ref. to cdcl3 @ 7.26 ppm), temp 27.7 C -> actual temp = 27.0 C, coldddual probe

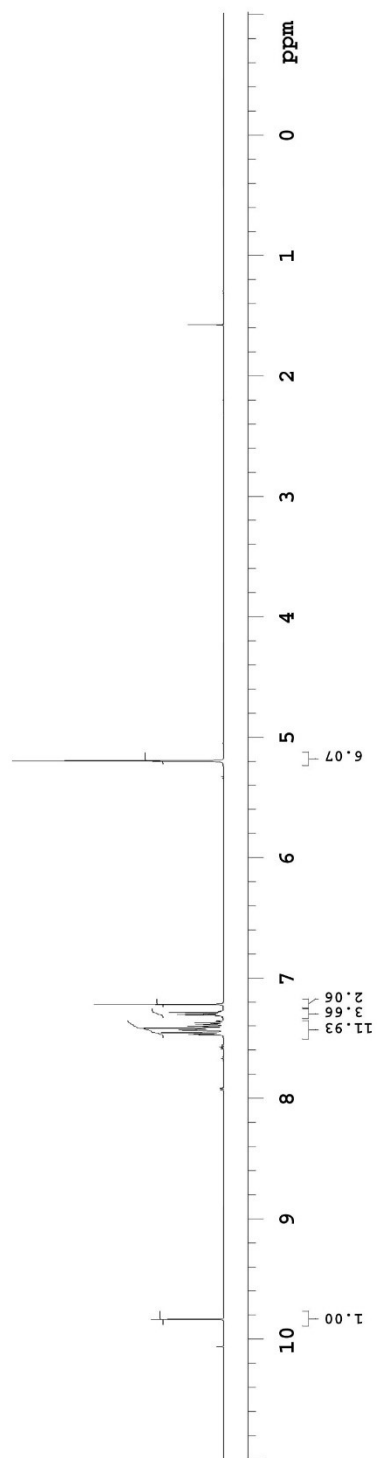
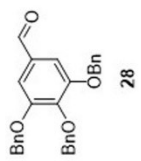




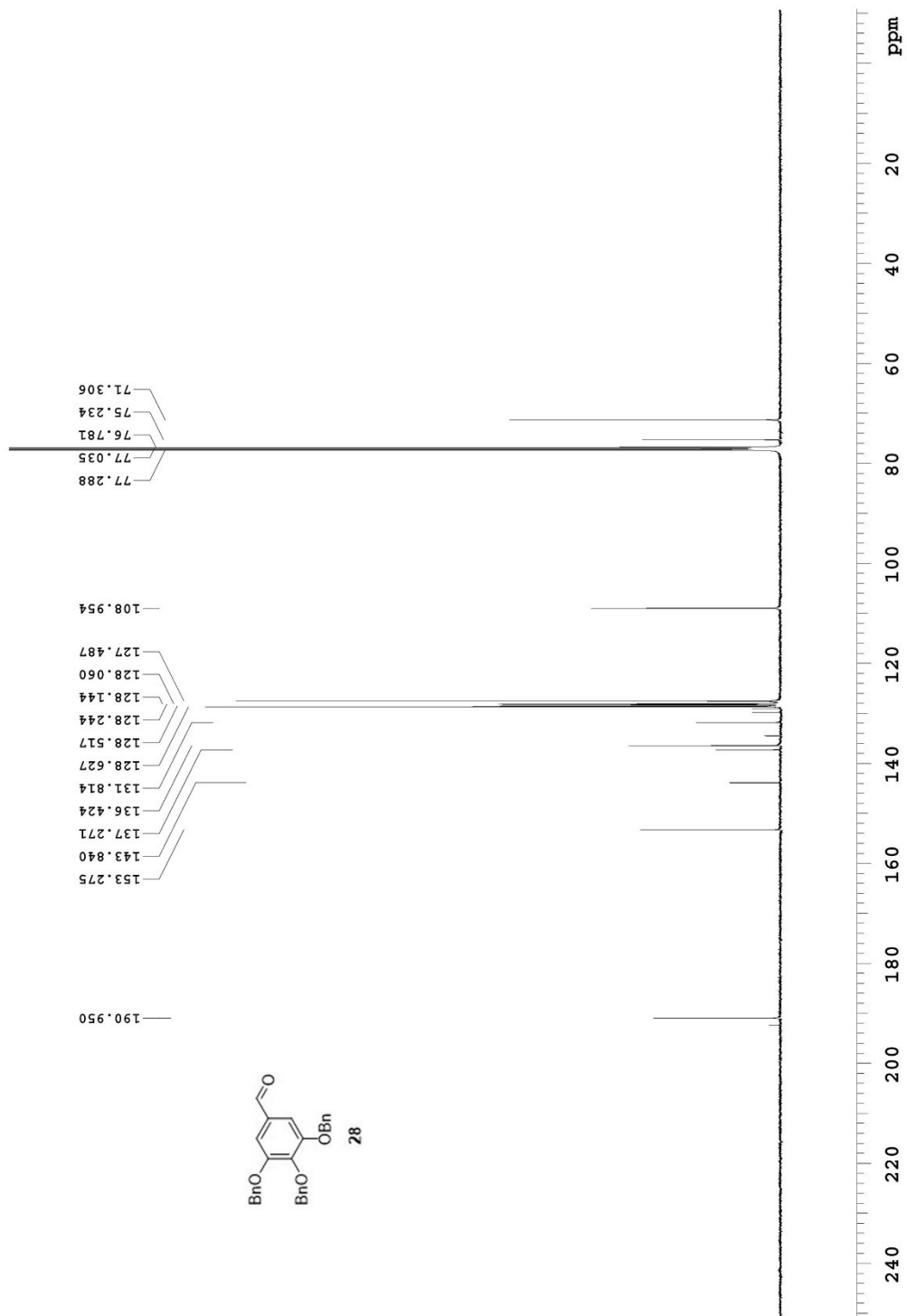
125.691 MHz <sup>13</sup>C{<sup>1</sup>H} 1D in cdcl<sub>3</sub> (ref. to CDCl<sub>3</sub> @ 77.06 ppm), temp 27.7 C -> actual temp = 27.0 C, coldlual probe



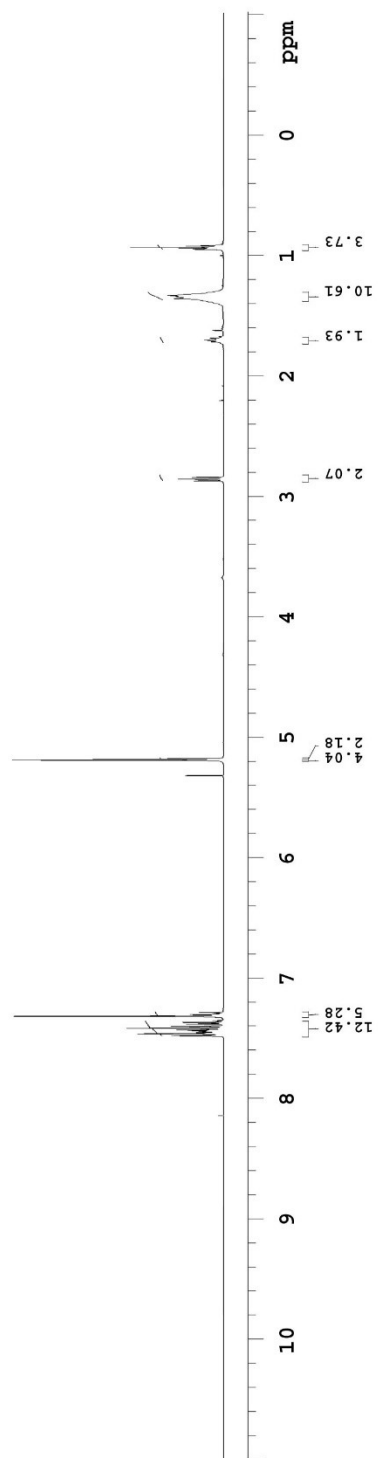
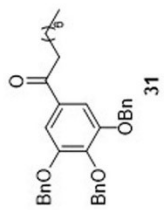
499.806 MHz <sup>1</sup>H PRESAT in cdcl3 (ref. to CDCl3 @ 7.26 ppm), temp 27.7 C -> actual temp = 27.0 C, cold dual probe



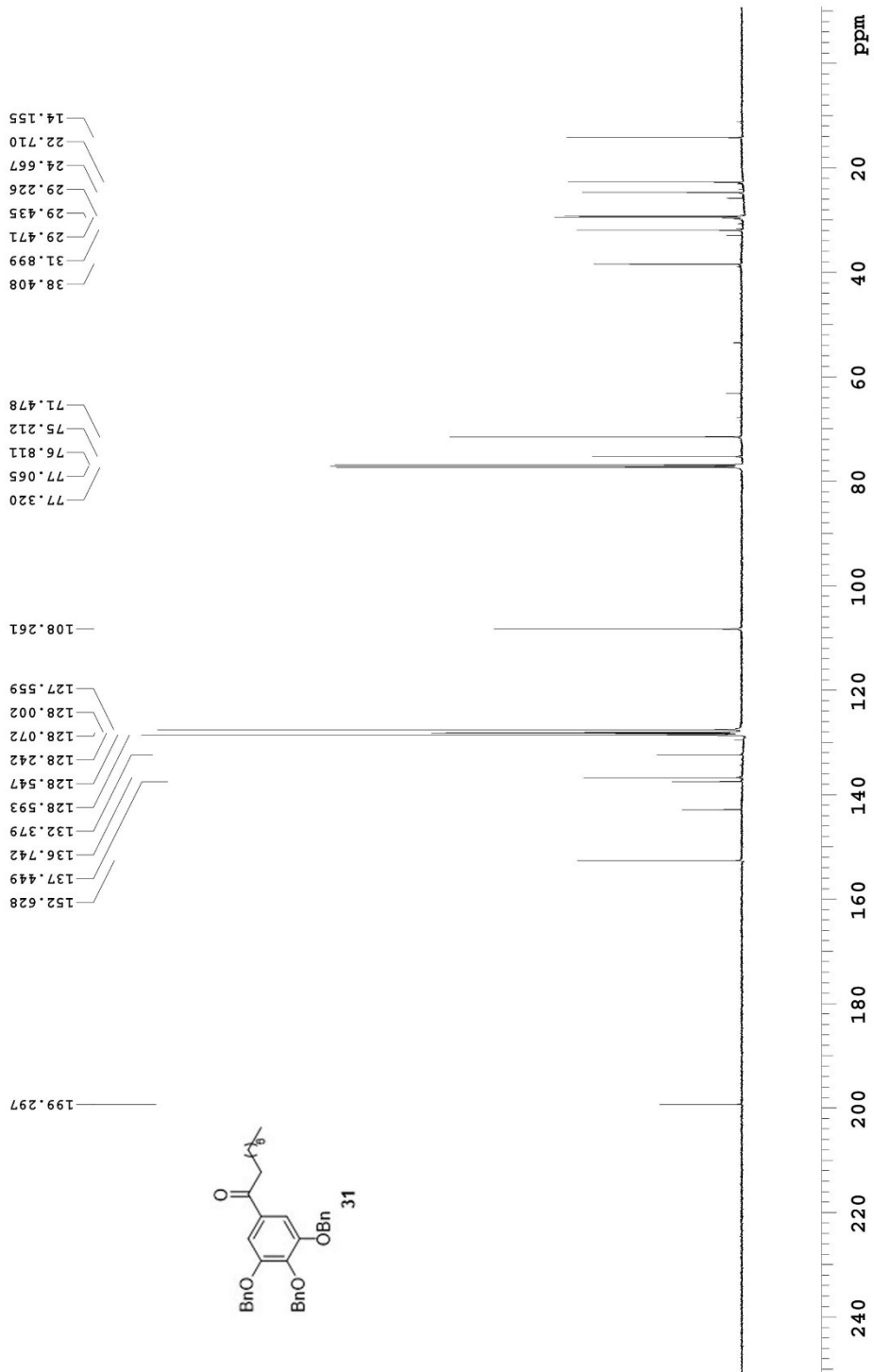
125.691 MHz C13{H1} 1D in cdcl3 (ref. to CDCl3 @ 77.06 ppm), temp 27.7 C -> actual temp = 27.0 C, cold dual probe



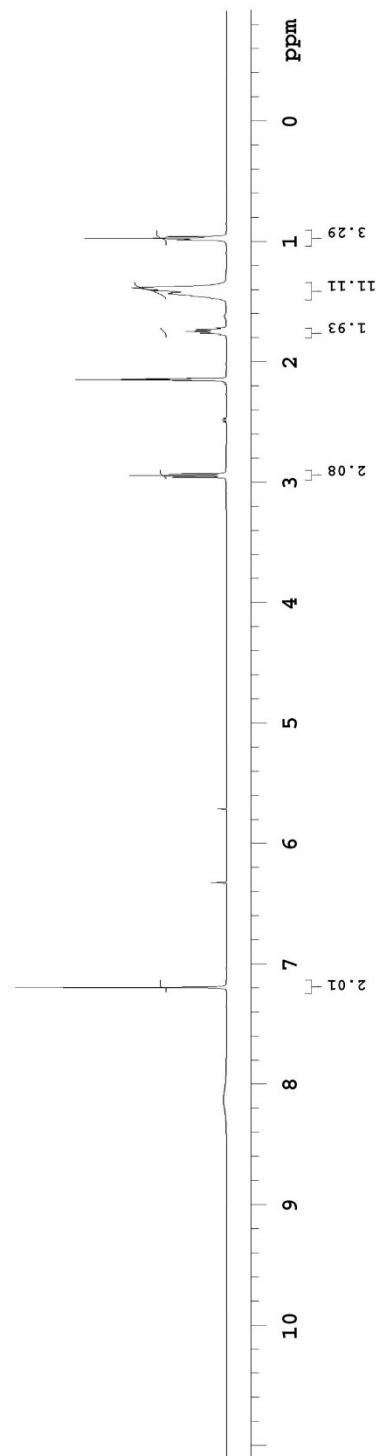
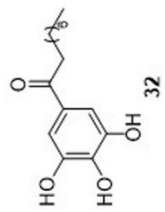
499.806 MHz, H1 PRESAT in cdcl3 (ref. to CDCl3 @ 7.26 ppm), temp 27.7 C -> actual temp = 27.0 C, coldluid probe



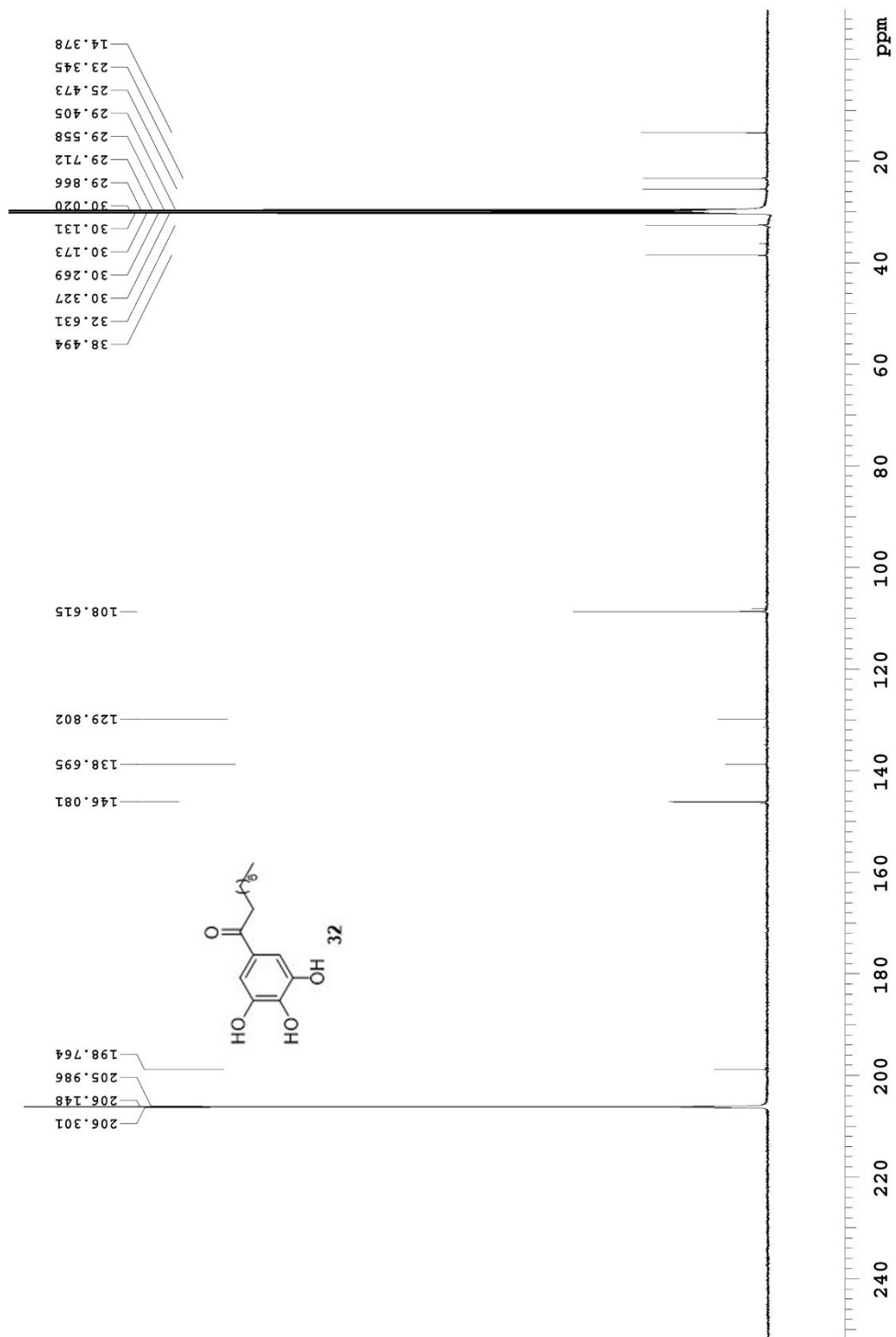
125.691 MHz C13[H1] 1D in cdcl3 (ref. to CDCl3 @ 77.06 ppm), temp 27.7 C -> actual temp = 27.0 C, coldludal probe



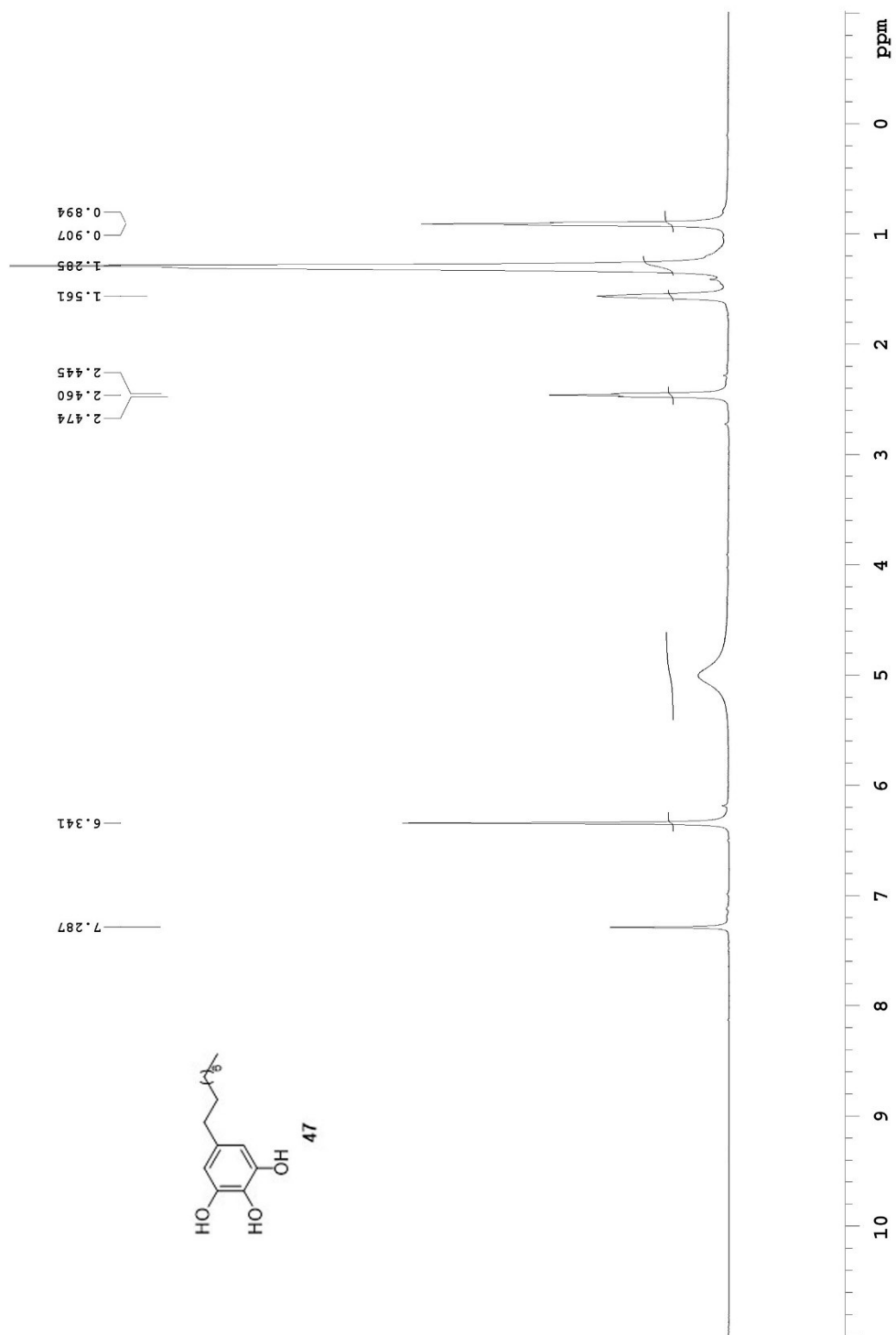
499.809 MHz, H1 PRESAT in acetone (ref. to acetone @ 2.04 ppm), temp 27.7 C -> actual temp = 27.0 C, coldidual probe



125.692 MHz C13[H1] 1D in acetone (ref. to acetone @ 29.8 ppm), temp 27.7 C -> actual temp = 27.0 C, coldlual probe

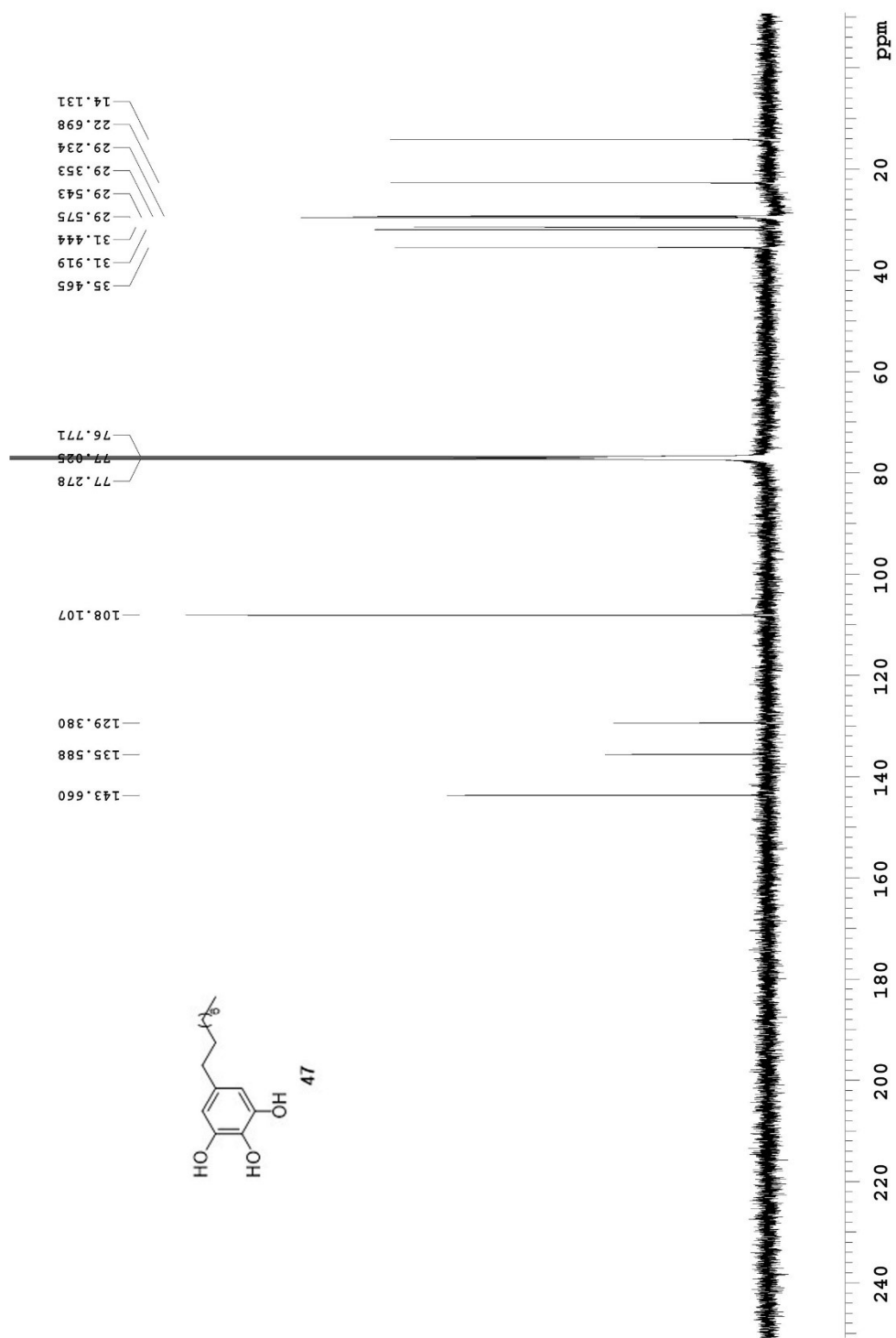


499.806 MHz H1 PRESAT in cdcl3 (ref. to CDC13 @ 7.26 ppm), temp 27.7 C -> actual temp = 27.0 C, coldludal probe





125.691 MHz C13{H1} 1D in cdcl3 (ref. to cdcl3 @ 77.06 ppm), temp 27.7 C.-> actual temp = 27.0 C, coldlual probe



## **Appendix IV: X-ray Crystallographic Data for Compounds 61b (Chapter 3)**

## STRUCTURE REPORT

**XCL Code:** FGW1317

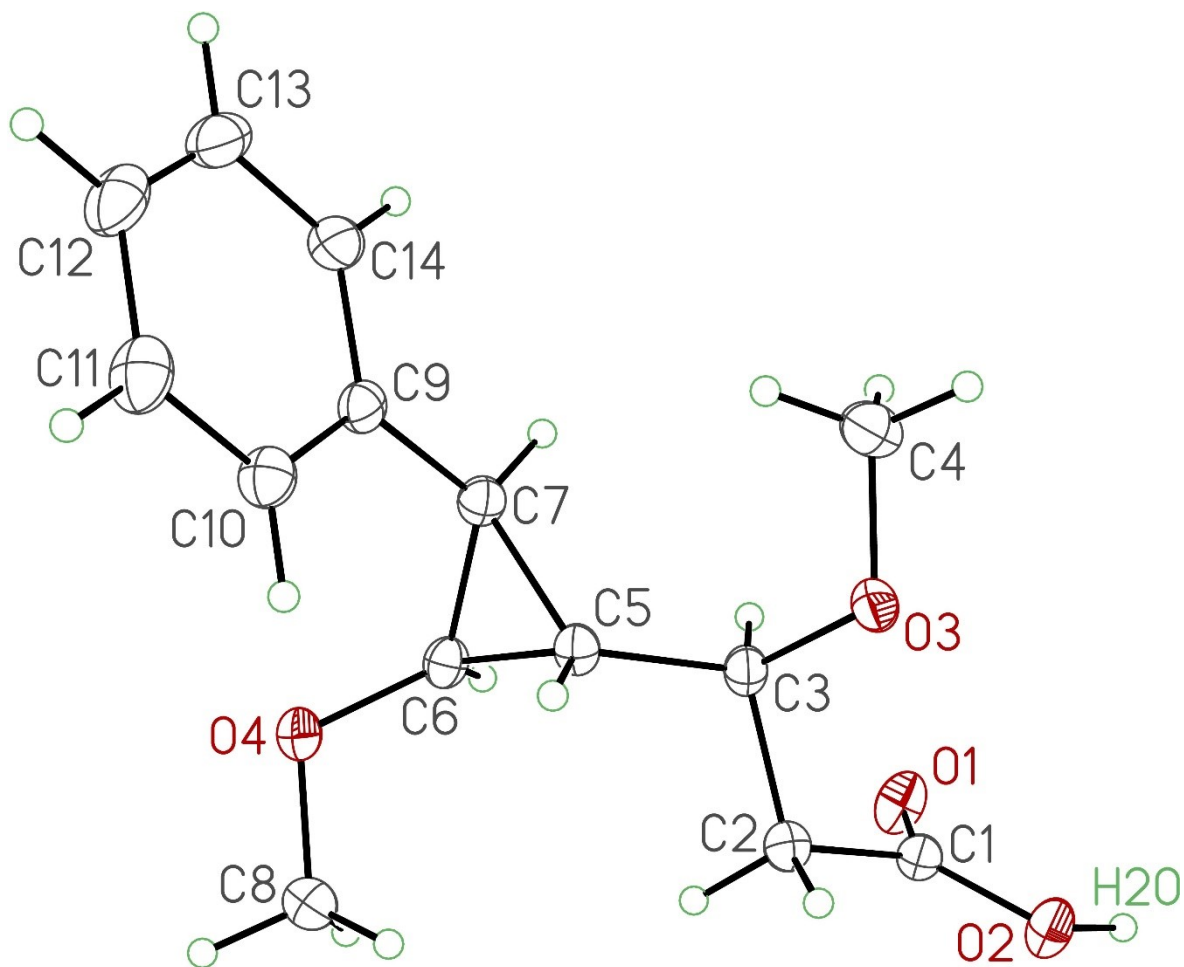
**Date:** 30 September 2013

**Compound:** C<sub>14</sub>H<sub>18</sub>O<sub>4</sub>

**Formula:** C<sub>14</sub>H<sub>18</sub>O<sub>4</sub>

**Supervisor:** F. G. West

**Crystallographer:** R. McDonald



Compounds **61b**